

*McGraw-Hill*  
ELECTRICAL AND ELECTRONIC  
ENGINEERING SERIES

FREDERICK EMMONS TERMAN, *Consulting Editor*

ELECTRON-TUBE CIRCUITS

# McGraw-Hill Electrical and Electronic Engineering Series

FREDERICK EMMONS TERMAN, *Consulting Editor*

---

- BAILEY AND GAULT · Alternating-current Machinery  
CAGE · Theory and Application of Industrial Electronics  
CUCCIA · Harmonics, Sidebands, and Transients in Communication Engineering  
EASTMAN · Fundamentals of Vacuum Tubes  
FITZGERALD AND KINGSLEY · Electric Machinery  
GEPPERT · Basic Electron Tubes  
HESSLER AND CAREY · Fundamentals of Electrical Engineering  
HILL · Electronics in Engineering  
JOHNSON · Transmission Lines and Networks  
KRAUS · Antennas  
LEPAGE · Analysis of Alternating-current Circuits  
LEPAGE AND SEELY · General Network Analysis  
MILLMAN AND SEELY · Electronics  
RÜDENBERG · Transient Performance of Electric Power Systems  
SEELY · Electron-tube Circuits  
SISKIND · Direct-current Machinery  
SKILLING · Electric Transmission Lines  
SKILLING · Transient Electric Currents  
SPANGENBERG · Vacuum Tubes  
TERMAN · Radio Engineering  
TERMAN AND PETTIT · Electronic Measurements

# ELECTRON-TUBE CIRCUITS

BY

SAMUEL SEELY, PH.D.

Professor of Electrical Engineering  
Syracuse University

FIRST EDITION  
FOURTH IMPRESSION

NEW YORK TORONTO LONDON  
McGRAW-HILL BOOK COMPANY, INC.

1950

## ELECTRON-TUBE CIRCUITS

Copyright, 1950, by the McGraw-Hill Book Company, Inc. Printed in the United States of America. All rights reserved. This book, or parts thereof, may not be reproduced in any form without permission of the publishers.

THE MAPLE PRESS COMPANY, YORK, PA.

---

## PREFACE

This book is the outgrowth of several courses that were organized by the author on electron-tube circuits and applications and that covered many of the important circuits in widespread use during the Second World War. It seeks to achieve the following: (1) to develop in the student a clear analytical method in the study of electron-tube circuits; (2) to present and study the various classes of circuits which find widespread application; (3) to indicate with examples how one proceeds to combine circuits of various types to achieve either one or a multiplicity of operations. It is not intended to include either a comprehensive discussion of all aspects of any given field or all possible circuits or methods for achieving a given result. It is hoped that representative circuits have been included and studied and that the reader may find some suggestions that will be of assistance to him in a particular development.

The choice of material to be included and the detail of coverage were the subject of much thought. The principle adopted was to present a coordinated account of each broad field of application, with the main emphasis on the operation of many of the significant circuits. No claim is made to completeness of coverage, nor are the fine points of any given field discussed in detail. Where general practice has favored a given type of circuit, the major emphasis is on these.

Approximately one-half the content is of a radio-engineering character, the remaining material being extensively used in radar, television, pulse communication, and general electronic control. Sufficient material is contained for a course in radio-engineering circuits and for one in non-radio electronic circuits. Sufficient diversity exists for the instructor to choose topics to satisfy almost any course requirements. It has been assumed that the student has completed his basic studies in a-c circuit theory and in basic electronics before undertaking a study of the text.

The order of presentation of the material has been dictated by the character of the analysis rather than by the application. Because of this, circuits of diverse application may be found in a given chapter. However, the book divides itself quite naturally into a number of major sections. The first part of the volume is devoted to a review of the fundamental properties of electron tubes and their basic circuit applications. The next part of the volume includes a discussion of a variety of amplifiers of the untuned variety. This includes circuits in which the

tube is operated as a linear device and other circuits in which the non-linear capabilities of the tube are employed. The former include simple voltage amplifiers, video amplifiers, power amplifiers, and electronic computing circuits. The latter include circuits which utilize the tube as a switch. The third part of the book contains a discussion of circuits of the tuned variety and discusses such topics as tuned voltage amplifiers, tuned power amplifiers, and oscillators. A comprehensive treatment of power rectifiers, filters, and regulators is followed by a discussion of amplitude modulation and demodulation and frequency modulation and detection. The latter part of the text includes a treatment of circuits that have been largely extended by developments in radar applications during the course of the war. This discussion is considerably more detailed and more extensive than has heretofore appeared in any general text.

An effort has been made to include sufficient analysis of the operation of the circuits to indicate clearly the operation and the various factors on which the operation depends. This has a twofold purpose, one of which is to indicate the procedure that must be adopted in effecting an analysis and the second of which is to indicate the factors on which the operation depends. This is considered to be very important, since in some instances the tube plays a direct part in the operation of the circuit, whereas in others it may serve simply in the capacity of a switch. However, the mathematical developments are only a part of the analysis, since the discussion attempts to introduce the physical aspects of the problem and then to incorporate the mathematical results into the complete analysis.

A rather regrettable situation will be found to exist in the matter of notation. This arises from the author's desire to conform to the Institute of Radio Engineers standards on vacuum-tube notation. However, such single-subscript notation in electron-tube circuits is often inadequate, and double-subscript notation is employed, except for those particular cases where no confusion is likely to arise. The result is a mixed single-subscript and double-subscript system of notation, the single-subscript terms generally conforming to the IRE notation.

A controversial matter is also to be noted. Throughout the text the symbols *a-c* and *d-c* are used as adjectives. Purists might object that the word *current* in *a-c current* is redundant and that the phrase *a-c voltage* is fundamentally meaningless. However, the use of the symbols *a-c* and *d-c* as descriptive adjectives is becoming increasingly widespread and does provide a clear and convenient abbreviation.

A number of problems have been included at the end of each chapter. These have been formulated in a way that requires an understanding of the subject matter. As a result, all text assignments may be supple-

mented by problem assignments. Problems which entail nothing more difficult than the substitution of numbers into equations have been kept to a minimum. Wherever possible, the problems are based on practical data in order to familiarize the student with such practical details.

To provide proper acknowledgment of the source of much of this material proves to be an impossible task. Much of the material that is principally of a radio-engineering character has appeared in one form or another in a wide variety of sources over many years, and the significant original sources seem to have been generally neglected. The principal source of many of the circuits which were extended for use in radar applications was the M.I.T. Radiation Laboratory, of which the author was a staff member during the war. However, it is known that many of these circuits were adapted from existing circuits of diverse origin, whereas some were developed at other laboratories, including British laboratories. In only a few cases is the identity of the groups who did some of this work known.

Special mention must be made of the freedom with which the author drew on his earlier text, "Electronics" (by J. Millman and S. Seely, McGraw-Hill Book Company, Inc., New York, 1941). Certain of the material closely parallels that in the earlier book.

The author wishes to acknowledge many helpful discussions with a number of his colleagues. He is particularly indebted to Professors David K. Cheng and Glenn M. Glasford, both for such discussions and for their assistance in proofreading portions of the text. Thanks are also due to the General Electric Co. and the RCA Manufacturing Co. for freely supplying many photographs and tube characteristics.

SAMUEL SEELY

SYRACUSE, N. Y.  
*November, 1949*



---

## CONTENTS

PREFACE . . . . .	v
CHAPTER 1—INTRODUCTION . . . . .	1
2—CHARACTERISTICS OF ELECTRON TUBES . . . . .	9
3—VACUUM TUBES AS CIRCUIT ELEMENTS . . . . .	39
4—BASIC AMPLIFIER PRINCIPLES . . . . .	52
5—UNTUNED VOLTAGE AMPLIFIERS . . . . .	68
6—UNTUNED VOLTAGE AMPLIFIERS— <i>Continued</i> . . . . .	95
7—SPECIAL AMPLIFIER CIRCUITS . . . . .	123
8—ELECTRONIC COMPUTING CIRCUITS . . . . .	146
9—UNTUNED POWER AMPLIFIERS . . . . .	167
10—TUNED VOLTAGE AMPLIFIERS . . . . .	192
11—TUNED POWER AMPLIFIERS . . . . .	213
12—OSCILLATORS . . . . .	244
13—RECTIFIERS . . . . .	271
14—RECTIFIER FILTERS AND REGULATORS . . . . .	292
15—AMPLITUDE MODULATION . . . . .	320
16—DEMODULATION . . . . .	343
17—FREQUENCY MODULATION AND DETECTION . . . . .	363
18—RELAXATION OSCILLATORS . . . . .	395
19—HEAVILY BIASED RELAXATION CIRCUITS . . . . .	414
20—SWEEP GENERATORS . . . . .	442
21—SPECIAL SWEEP GENERATORS . . . . .	460
22—ELECTRONIC INSTRUMENTS . . . . .	473
APPENDIX A—MILLMAN THEOREM . . . . .	489
B—PLATE CHARACTERISTICS OF RECEIVING-TYPE TUBES . . . . .	491
C—CHARACTERISTICS OF TRANSMITTING TUBES . . . . .	508
D—TABLE OF BESSEL FUNCTIONS OF THE FIRST KIND . . . . .	511
INDEX . . . . .	513



---

## CHAPTER 1

### INTRODUCTION

**B**EFORE one undertakes a study of circuits that incorporate electron tubes, it might be well to examine, even superficially, certain of the fundamental physical principles which govern the operation of these tubes. There are two important basic questions that relate to such tubes. One relates to the actual source of the electrons and their liberation, and the second relates to the control of the electron beam. A brief discussion of these matters will be included.

According to modern theory, all matter is electrical in nature. The atom, which is one of the fundamental building blocks of all matter, consists of a central core or nucleus which is positively charged and which carries nearly all the mass of the atom. Enough negatively charged electrons surround the nucleus so that the atom is electrically neutral in its normal state. Since all chemical substances consist of groups of these atoms which are bound to each other, then all matter, whether it is in the solid, the liquid, or the gaseous state, is a potential source of electrons. All three states of matter do, in fact, serve as sources of electrons. A number of different processes serve to effect the release of electrons, those which are of importance in electron tubes being (1) thermionic emission, (2) secondary emission, (3) photoelectric emission, (4) high field emission, and (5) ionization. These processes will be considered in some detail in what follows.

With the release of the electrons, a means for their control must be provided. Such control is effected by means of externally controlled electric or magnetic fields, or both. These fields perform one or both of the following functions: (1) control of the number of electrons that leave the region near the emitter; (2) control of the paths of the electrons after they leave the emitter. Control method 1 is the more common, and such a control method is incorporated in almost all electron tubes, except those of the field-deflected variety. The cathode-ray tube is a very important example of a field-deflected tube. However, even in this latter case, a control of type 1 is incorporated to control the electron-tube current, even though the subsequent motion is controlled by means of an electric or a magnetic field, or both.

**1-1. Thermionic Emission.** Consider matter in the metallic state. Metals are most generally employed in the form of a wire or ribbon filament. If such a filament contains electrons and if these are relatively free to move about in the metal (and this is the case since the application of a small potential difference between the ends of the wire will result in a current flow), it might be expected that some electrons might "leak" out of the metal of their own accord. This does not occur, however.

Consider what happens to an electron as it seeks to escape from a metal. The escaping, negatively charged electron will induce a positive charge on the metal. There will then be a force of attraction between the induced charge and the electron. Unless the escaping electron possesses sufficient energy to carry it out of the region of influence of this image force of attraction, it will be returned to the metal. The minimum amount of energy that is required to release the electron against this attractive force is known as the *work function* of the metal. This requisite minimum amount of energy may be supplied by any one of a number of different methods. One of the most important methods is to heat the metal to a high temperature. In this way, some of the thermal energy supplied to the metal is transferred from the lattice of the heated metal crystals into kinetic energy of the electrons.

An explicit expression relating the thermionic-emission current density and the temperature of the metal can be derived.<sup>1,\*</sup> The expression so derived has the form

$$J_{th} = A_0 T^2 e^{-\frac{b_0}{T}} \quad (1-1)$$

where  $A_0$  is a constant for all metals and has the value of  $120 \times 10^4$  amp/(m<sup>2</sup>)(°K<sup>2</sup>) and  $b_0$  is a constant that is characteristic of the metal. The quantity  $b_0$  is related to the work function  $E_w$  of the metal by

$$b_0 = 11,600 E_w \quad \text{°K} \quad (1-2)$$

It has been found experimentally that Eq. (1-1) does represent the form of the variation of current with temperature for most metals, although the value obtained for  $A_0$  may differ materially from the theoretical value of  $120 \times 10^4$  amp/(m<sup>2</sup>)(°K<sup>2</sup>).

It follows from Eq. (1-1) that metals that have a low work function will provide copious emission at moderately low temperatures. Unfortunately, however, the low-work-function metals melt in some cases and boil in others, at the temperatures necessary for appreciable thermionic emission. The important emitters in present day use are pure tungsten, thoriated-tungsten, and oxide-coated cathodes. The thermionic-emission constants of these emitters are contained in Table 1-1.

\* Superior numbers refer to references at the end of each chapter.

TABLE 1-1

## THE IMPORTANT THERMIONIC EMITTERS AND THE THERMIONIC-EMISSION CONSTANTS

Emitter	$A_0$ , amp/(m <sup>2</sup> )(°K <sup>2</sup> )	$E_w$ , volts
Tungsten.....	$60 \times 10^4$	4.52
Thoriated-tungsten.....	$3 \times 10^4$	2.63
Oxide-coated.....	$0.01 \times 10^4$	1

Tungsten is used extensively for thermionic filaments despite its relatively high work function. In fact, this material is particularly important because it is virtually the only material that can be used successfully as the filament in high-voltage tubes. It is used in high-voltage X-ray tubes, in high-voltage rectifier tubes, and in the large power-amplifier tubes that are used in radio and communication applications. It has the disadvantage that the *cathode emission efficiency*, defined as the ratio of the emission current in milliamperes to the heating power in watts, is small. Despite this, it can be operated at a sufficiently high temperature, between 2600 and 2800°K, to provide an adequate emission.

It has been found that the application of a very thin layer of low-work-function material on filaments of tungsten will materially reduce the work function of the resulting surface. A thoriated-tungsten filament is obtained by adding a small amount of thorium oxide to the tungsten before it is drawn. Such filaments, when properly activated, will yield an efficient emitter at about 1800°K. It is found desirable to *carbonize* such an emitter, since the rate of evaporation of the thorium layer from the filament is thus reduced by about a factor of 6. Thoriated-tungsten filaments are limited in application to tubes that operate at intermediate voltages, say 10,000 volts or less. Higher voltage tubes use pure tungsten filaments.

The oxide-coated cathode is very efficient (about twenty times as efficient as tungsten) and provides a high emission current at the relatively low temperature of 1000°K. It consists of a metal sleeve of konal (an alloy of nickel, cobalt, iron, and titanium) or some other metal, which is coated with the oxides of barium and strontium. These cathodes are limited for a number of reasons to use in the lower voltage tubes, say about 1,000 volts or less. They are used almost exclusively in receiving-type tubes and provide efficient operation with long life.

Curves showing the relative cathode efficiencies of tungsten, thoriated-tungsten, and oxide-coated cathodes are illustrated in Fig. 1-1. It will be seen that tungsten has a considerably lower efficiency than either of the other two emitters.

The thermionic emitters in their practical form in electron tubes may be of the directly heated, or filamentary, type or of the indirectly heated type, and in the case of gas and vapor tubes the cathode may be of the

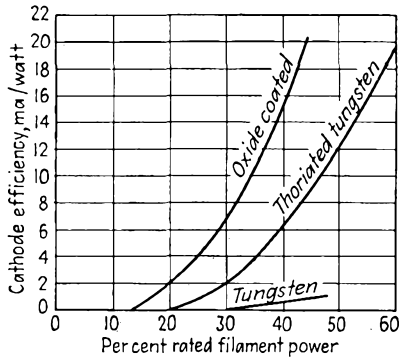


FIG. 1-1. Cathode efficiency curves of an oxide-coated, a thoriated-tungsten, and a pure tungsten filament.

heat-shielded type. Typical filamentary cathodes are illustrated in Fig. 1-2. These filamentary cathodes may be of the pure tungsten, thoriated-tungsten, or oxide-coated type.

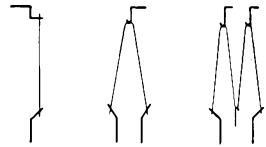


FIG. 1-2. Typical directly heated cathodes.

The indirectly heated cathode for use in vacuum tubes is illustrated in Fig. 1-3. The heater wire is contained in a ceramic insulator which is enclosed by the metal sleeve on which the oxide coating is placed. A cathode assembly of this type has such a high heat capacity that its tem-

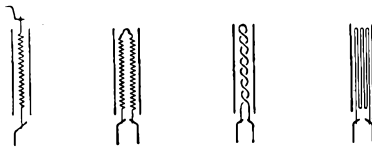


FIG. 1-3. Typical indirectly heated cathodes.

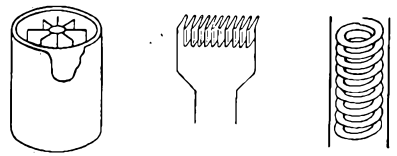


FIG. 1-4. Different types of heat-shielded cathodes.

perature does not change with instantaneous variation in heater current when alternating current is used.

Heat-shielded cathodes, which can be used only in gas-filled electron tubes for reasons to be discussed in Chap. 2, are designed in such a way as to reduce the radiation of heat energy from the cathode. This materially increases the efficiency of the cathode. Several different types of heat-shielded cathodes are illustrated in Fig. 1-4.

**1-2. Photoelectric Emission.** The energy that is required to release an electron from a metal surface may be supplied by illuminating the surface with light. There are certain restrictions on the nature of the surface and the frequency of the impinging light for such electron emission to take place. That is, electron emission is possible only if the frequency

of the impinging light exceeds a certain *threshold* value that depends on the work function  $E_w$  of the surface according to the equation

$$f_c = \frac{eE_w}{h} \tag{1-3}$$

where  $e$  is the charge of the electron and  $h$  is Planck's constant. The corresponding *threshold wave length* beyond which photoelectric emission cannot take place is given by

$$\lambda_c = \frac{ch}{eE_w} = \frac{12,400 \text{ A}}{E_w} \tag{1-4}$$

where A is the angstrom unit ( $10^{-8}$  cm). For response over the entire visible region, 4000 to 8000 A, the work function of the photosensitive surface must be less than 1.54 volts.

The essential elements of a phototube are the photosensitive cathode surface and a collecting electrode, contained in a glass envelope that either is evacuated or contains an inert gas at low pressure. A photograph of such a phototube is shown in Fig. 1-5.

The number of photoelectrons per square millimeter of area of a photocathode is small, and it is customary to use photocathodes of large area, as shown.

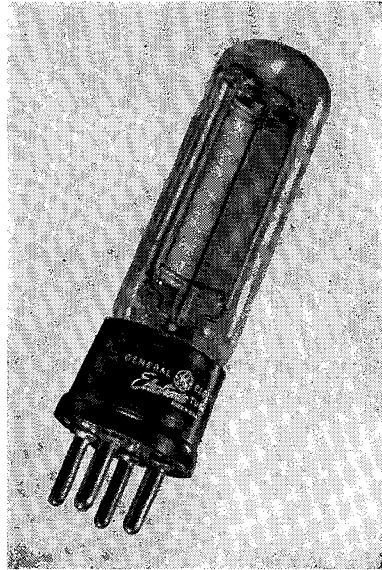


FIG. 1-5. A typical phototube.

The current characteristics of such phototubes for different collecting potentials between the cathode and the collecting anode, with light

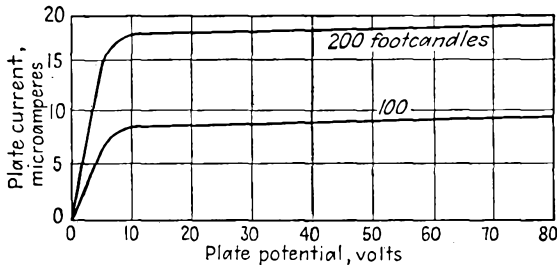


FIG. 1-6. The volt-ampere characteristics of a type PJ-22 vacuum phototube, with light intensity as a parameter.

intensity as a parameter, are illustrated. Figure 1-6 shows the curves of a vacuum phototube with light intensity as a parameter. Note that the

current reaches near saturation values for very low values of applied potential.

The presence in the glass envelope of an inert gas, such as neon or argon, at low pressure materially alters the volt-ampere curves. A set of characteristic curves for a gas phototube are given in Fig. 1-7. The presence of the gas in a phototube increases the sensitivity of the phototube, the

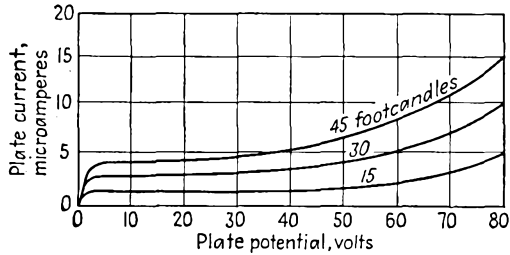


FIG. 1-7. The volt-ampere characteristics of a type PJ-23 gas-filled phototube, with light intensity as a parameter.

current output for a given light intensity increasing with increased plate potential, whereas the output remains sensibly constant in the vacuum phototube.

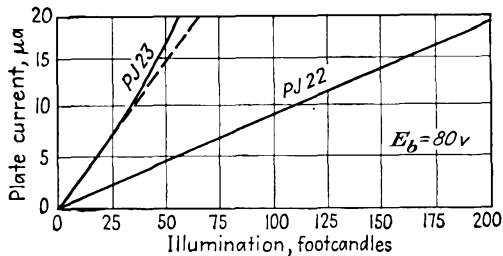


FIG. 1-8. Photocurrent as a function of illumination for a PJ-22 vacuum phototube, and a PJ-23 gas-filled cell.

A significant comparison of the output from two phototubes, one of the vacuum type and the other of the gas-filled type, other characteristics of the tubes being the same, is contained in Fig. 1-8. Note that the photocurrent for the vacuum phototube is a linear function of the illumination, whereas that for the gas-filled cell shows deviations from the linear at the higher illuminations. However, the greater sensitivity of the gas-filled cell is clearly evident.

**1-3. Secondary Emission.** It is possible for a particle, either an electron or a positive ion, to strike a metallic surface and transfer all or a part of its kinetic energy in this collision to one or more of the internal

electrons. If the energy of the incident particle is sufficiently high, some of the internal electrons may be emitted. Several tubes have been designed which incorporate secondary-emission surfaces as part of the device, and highly sensitive phototubes have such auxiliary elements in them. Frequently the secondary emission that exists is of a deleterious nature. This matter will be discussed in explaining certain features of the characteristics of tetrodes.

**1-4. High Field Emission.** The presence of a very strong electric field at the surface of a metal will cause electron emission. Ordinarily the field in the average electron tube is too small to induce such electron emission. This process has been suggested to account for the electron emission from a mercury-pool cathode in a mercury rectifier.

**1-5. Ionization.** The process in which an atom loses an electron is known as *ionization*. The atom that has lost the electron is called a *positive ion*. The process of ionization may occur in several ways.

*Electron Bombardment.* Consider a free electron, which might have been released from the envelope or from any of the electrodes within the tube by any of the processes discussed above. Suppose that this free electron has acquired enough energy from an applied field so that upon collision with a neutral atom, it removes an electron. Following this action, two electrons and a positive ion exist. Since there are now two electrons available, both may collide with gas particles and thus induce further ionization. Such a process as this may become cumulative, with consequent large electron release. This process is very important and accounts for the successful operation of gas- and vapor-filled rectifier tubes. It is also the basis of the gas amplification in gas-filled phototubes.

*Photoelectric Emission.* If the gas is exposed to light of the proper frequency, then this radiant energy may be absorbed by the atom, with resulting electron emission. This process is important in initiating certain discharges.

*Positive-ion Bombardment.* The collision between a positive ion and a neutral gas particle may result in electron release, in much the same manner as by electron bombardment. This process is very inefficient and is usually insignificant in normal gas tubes.

*Thermal Emission.* If the temperature of the gas is high enough, some electrons may become dislodged from the gas particles. However, the gas temperature in electron tubes is generally low, and this process is normally unimportant.

#### REFERENCE

1. Millman, J., and S. Seely, "Electronics," Chap. V, McGraw-Hill Book Company, Inc., New York, 1941.

## PROBLEMS

1-1. A tungsten filament, 0.0085 in. diameter,  $3\frac{1}{16}$  in. long, is operated at 2650°K. What is the temperature-limited current? If the temperature is increased by 50°K, by what percentage does the emission current increase?

1-2. The filament of an FP-400 tungsten-filament tube is 1.25 in. long and 0.005 in. in diameter. If the total emission current is 30 ma, at what temperature is the filament operating?

1-3. A simple inverted-V oxide-coated cathode is made of tungsten ribbon 0.125 by 0.020 in. and is 1.4 in. long. It is maintained at a temperature of 1100°K. What is the thermionic-emission current?

1-4. An oxide-coated emitter is operating at 1100°K. Calculate the relative thermionic-emission currents if  $b_0$  has the value 12,000; the value 11,000.

1-5. At what temperature will a thoriated-tungsten filament give as much current as a tungsten filament of the same dimensions which is maintained at 2650°K?

1-6. At what temperature will an oxide-coated cathode give the same emission as a thoriated-tungsten filament of the same physical dimensions which is maintained at 1750°K?

1-7. Monochromatic light of wave length 5893 Å falls on the following surfaces:

a. Cesium, with a work function 1.8 volts.

b. Platinum, with a work function 5.3 volts.

Is photoelectric emission possible in both cases? Explain.

1-8. A PJ-22 vacuum photocell is to be used to sound an alarm when the light at a given region of a room falls below 40 ft-c or increases above 120 ft-c. What are the corresponding photocurrents? A collecting potential of 45 volts is used.

---

## CHAPTER 2

### CHARACTERISTICS OF ELECTRON TUBES<sup>1</sup>

CONSIDER an isolated thermionic source situated in a vacuum. This cathode will emit electrons, most of which have very little energy when they emerge. Those electrons that first escape will diffuse throughout the space within the envelope. An equilibrium condition will soon be reached when, because of the mutual repulsion between electrons, the free electrons in the space will prevent any additional electrons from leaving the cathode. The equilibrium state will be reached when the space charge of the electron cloud produces a strong enough electric field to prevent any subsequent emission.

The inclusion of a collecting plate near the thermionic cathode will allow the collection of electrons from the space charge when this plate is maintained at a positive potential with respect to the cathode; the higher the potential, the higher the current. Of course, if the thermionic emission is limited, then the maximum current possible is the temperature-saturated value.

In addition to such a simple two-element device, which is the diode, grids may be interposed between the cathode and plate. If a single grid is interposed, the tube is a triode. If two grids are present, the tube is a tetrode; three grids yields a pentode, etc. Details of the characteristics and operation of such devices will be considered in some detail in the following pages.

#### THE HIGH-VACUUM DIODE

**2-1. The Potential Distribution between the Electrodes.** Consider a simple diode consisting of a plane cathode and a collecting plate, or anode, which is parallel to it. It is supposed that the cathode can be heated to any desired temperature and that the potential between the cathode and anode may be set at any desired value. It is desired to examine the potential distribution between the tube elements for various cathode temperatures and fixed anode-cathode applied potential.

Suppose that the temperature of the cathode is high enough to allow some electrons to be emitted. An electron space-charge cloud will be formed in the envelope. The density of the electrons and the potential

at any point in the interelectrode space are related by Poisson's equation

$$\frac{d^2E}{dx^2} = \frac{\rho}{\epsilon_0} \quad (2-1)$$

where  $E$  is the potential in volts,  $\rho$  is the magnitude of the electronic-charge density, in coulombs per cubic meter, and  $\epsilon = 10^{-9}/36\pi$  is the permittivity of space. A study of this expression will yield significant information.

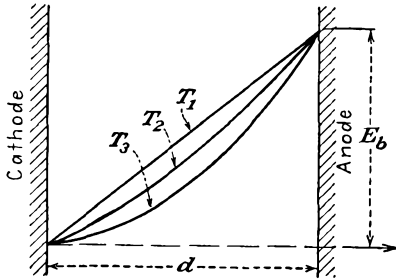


FIG. 2-1. The potential distribution between plane-parallel electrodes, for several values of cathode temperature.

It is supposed that the electrons that are emitted from the cathode have zero initial velocities. Under these conditions, the general character of the results will have the forms illustrated in Fig. 2-1. At the temperature  $T_1$ , which is too low for any emission, the potential distribution is a linear function of the distance from the cathode to the anode.

This follows from Eq. (2-1), since, for zero-charge density,

$$\frac{d^2E}{dx^2} = 0 \quad \text{or} \quad \frac{dE}{dx} = \text{const}$$

This is the equation of a straight line.

At the higher temperature  $T_2$ , the charge density  $\rho$  is not zero. Clearly, the anode-cathode potential, which is externally controlled, will be independent of the temperature, and all curves must pass through the fixed end points. Suppose that the potential distribution is somewhat as illustrated by the curve marked  $T_2$ . All curves must be concave upward, since Eq. (2-1), which may be interpreted as a measure of the curvature, is positive. A positive curvature means that the change in slope  $dE/dx$  between two adjacent points must be positive. Moreover, the curvature is greater for larger values of  $\rho$ , corresponding to the higher temperatures. It is possible to justify that the maximum current that can be drawn from the diode for a fixed plate voltage and any temperature is obtained under the condition of zero electric field at the surface of the cathode. Under these optimum conditions

$$-\frac{dE}{dx} = 0 \quad \text{at} \quad x = 0 \quad (2-2)$$

This condition is valid under the assumption of zero initial velocities of emission of the electrons.

**2-2. Equations of Space Charge.** An explicit relation between the current collected and the potential that is applied between the anode and cathode is possible. In general, the current density is a measure of the rate at which the electrons pass through unit area per unit time in the direction of the field. If  $v$  denotes the drift velocity in meters per second,  $N$  is the electron density in electrons per cubic meter, and  $e$  is the electronic charge in coulombs, then the current density in amperes per square meter is

$$J = Nev = \rho v \tag{2-3}$$

Also, neglecting the initial velocity, the velocity of the electron at any point in the interelectrode space is related to the potential through which it has fallen by the following expression, which is based on the conservation of energy:

$$\frac{1}{2}mv^2 = eE \tag{2-4}$$

By combining the foregoing expressions, there results

$$\frac{d^2E}{dx^2} = \frac{JE^{-\frac{1}{2}}}{\epsilon_0(2e/m)^{\frac{1}{2}}} \tag{2-5}$$

This is a differential equation in  $E$  as a function of  $x$ . The solution of it is given by

$$J = \frac{\epsilon_0}{2.25} \sqrt{2 \frac{e}{m} \frac{E^{\frac{3}{2}}}{x^2}} \quad \text{amp/m}^2 \tag{2-6}$$

For electrons, and in terms of the boundary conditions, there results

$$J = 2.33 \times 10^{-6} \frac{E_b^{\frac{3}{2}}}{d^2} \quad \text{amp/m}^2 \tag{2-7}$$

This equation is known as the *Langmuir-Childs* or *three-halves-power law*. It relates the current density, and so the current, with the applied potential and the geometry of the tube. It shows that the space-charge current is independent of the temperature and the work function of the cathode. Thus, no matter how many electrons a cathode may be able to supply, the geometry of the tube and the applied potential will determine the maximum current that can be collected by the anode. If the electron supply from the cathode is restricted, the current may be less than the value predicted by Eq. (2-7). The conditions are somewhat as represented graphically in Fig. 2-2.

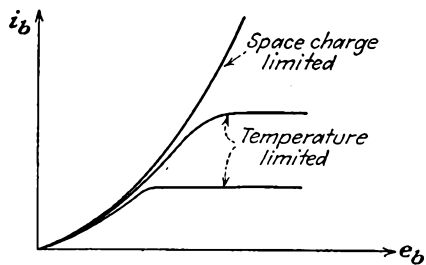


FIG. 2-2. The volt-ampere characteristics of a typical diode.

If the electron supply from the cathode is restricted, the current may be less than the value predicted by Eq. (2-7). The conditions are somewhat as represented graphically in Fig. 2-2.

For the case of a tube that possesses cylindrical symmetry, a similar analysis is possible. The results of such a calculation lead to the following expression for the current,

$$I_b = 14.6 \times 10^{-6} \frac{l}{r_a} \frac{E_b^{3/2}}{\beta^2} \quad \text{amp} \quad (2-8)$$

where  $l$  is the active length of the tube and  $\beta^2$  is a quantity that is determined from the ratio  $r_a/r_k$ , the ratio of anode to cathode radius. For ratios  $r_a/r_k$  of 8 or more,  $\beta^2$  may be taken as unity.

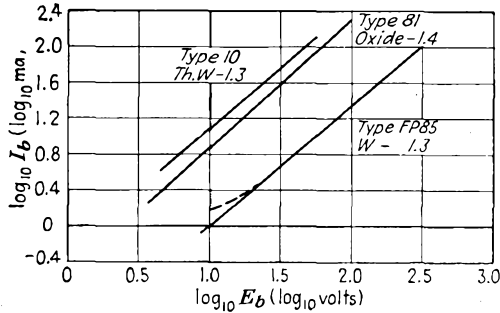


FIG. 2-3. Experimental results to verify the three-halves power law for tubes with oxide-coated, thoriated tungsten, and pure tungsten filaments.

Attention is called to the fact that the plate current depends upon the three-halves power of the plate potential both for the plane parallel and also for a diode possessing cylindrical symmetry. This is a general relationship, and it is possible to demonstrate that an expression of the form  $I_b = kE_b^{3/2}$  applies for any geometry, provided only that the same restrictions as imposed in the above developments are true. The specific value of the constant  $k$  that exists in this expression cannot be analytically determined unless the geometry of the system is specified.

The dependence of the current on the potential for any tube may be determined by plotting the results obtained experimentally on a logarithmic scale. Theoretically one should find, if the expression  $I_b = kE_b^{3/2}$  is valid, that

$$\log_{10} I_b = \log_{10} k + \frac{3}{2} \log_{10} E_b \quad (2-9)$$

The logarithmic plots for three commercial tubes are shown in Fig. 2-3. The type 10 tube is a triode and was converted into a diode by connecting grid and plate together. The other tubes are diodes. It will be observed that the logarithmic plots are straight lines, although the slopes of these lines are all slightly less than the theoretical 1.5.

**2-3. Rating of Vacuum Diodes.** The current and potential ratings of a diode, *i.e.*, the maximum current that the tube may carry and the maxi-

imum potential difference that may be applied between anode and cathode, are influenced by a number of factors.

1. A limit is set to the tube current by the cathode efficiency of the emitter. Thus, for a given input power to the filament, a maximum current is specified.

2. There is a maximum temperature limit to which the glass envelope of the tube may be safely allowed to rise. This is the temperature to which the tube was raised during the outgassing process. This is about 400°C for soft glass and about 600°C for pyrex. For higher temperatures, the gases adsorbed by the glass walls may be liberated. Owing to this limitation, glass bulbs are seldom used for vacuum tubes of more than about 1 kw capacity.

3. A very important limitation is set by the temperature to which the anode may rise. In addition to the fraction of the heat radiated by the cathode that is intercepted by the anode, the anode is also heated by the energy carried by the anode current. The instantaneous power carried by the anode current and supplied to the anode is given by  $e_a i_a$ , where  $e_a$  is the anode-cathode potential and  $i_a$  is the anode current. The temperature to which the anode rises will depend upon the area of the anode and the material of its construction.

The most common metals used for anodes are nickel and iron for receiving tubes and tantalum, molybdenum, and graphite for transmitting tubes. The surfaces are often roughened or blackened in order to increase the thermal emissivity. The anodes of many transmitting tubes may be operated at a cherry-red heat without excessive gas emission. To allow for forced cooling of the anode, cooling coils may be provided, or the tube may be immersed in oil. The newer type of transmitting tubes are frequently provided with radiator fins for forced-air cooling. Several different types of transmitting tubes are illustrated in Fig. 2-4.

4. The voltage limitation of a high-vacuum diode is also dependent on the type of its construction. If the filament and anode leads are brought out side by side through the same glass press, some conduction may take place between these leads through the glass. This effect is particularly marked if the glass is hot, and the resulting electrolysis will cause the glass to deteriorate and eventually to leak. The highest voltage permissible between adjacent leads in glass depends upon the spacing and upon the type of glass but is generally kept below 1,000 volts. Higher voltage tubes are usually provided with filament leads at one end of the glass envelope, with the anode at the other end.

The glass envelope must be long enough so that flashover on the outside of the tube will not occur. In a diode as a rectifier, no current will flow during the time that the anode is negative with respect to the cathode.

The maximum safe rating of a rectifying diode is known as the *peak inverse voltage rating*.

Commercial vacuum diodes are made which will rectify current at high voltages, up to 200,000 volts. Such units are used with X-ray equipment, with high-voltage cable-testing equipment, and with the high-

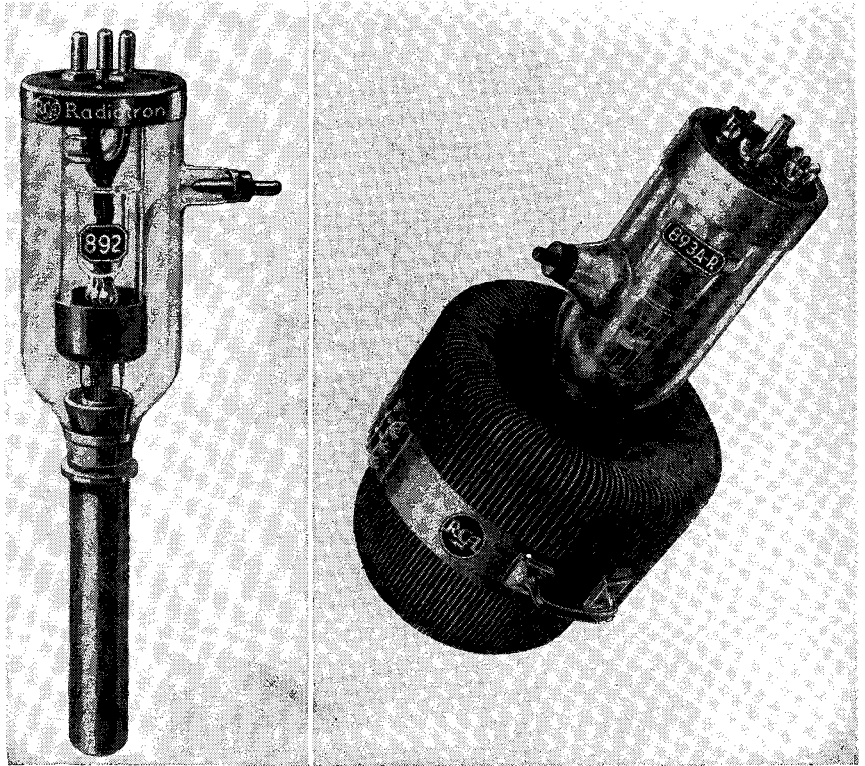


FIG. 2-4. Photographs of two transmitting tubes. (RCA Mfg. Co.)

voltage equipment for nuclear-physics research. The dimensions and shape of the glass envelope will depend upon the current capacity of the tube and the type of cooling to be used, oil-cooled tubes being generally smaller than air-cooled types.

## THE TRIODE

**2-4. The Grid.** The introduction of a third element between the cathode and plate of the diode by DeForest in 1907 was the start of the extensive developments involving vacuum tubes. This new electrode, called the *control grid*, consists of a wire mesh, or screen, which surrounds the cathode and is situated close to it. The potential applied

to the grid in such a tube is usually several volts negative relative to the cathode, whereas the plate is usually maintained several hundred volts positive with respect to the cathode. Clearly, the electric field resulting from the potential of the grid tends to maintain a large space-charge cloud, whereas the field of the plate tends to reduce the space charge. However, owing to its proximity to the cathode, a given potential on the grid will exercise a greater effect on the space charge than the same potential on the plate. This would seem to imply that a strict proportionality should exist between the relative effectiveness of the grid and plate potentials on the space charge and that the plate current should be represented approximately by the equation

$$i_b = k \left( e_c + \frac{e_b}{\mu} \right)^{3/2} \quad (2-10)$$

where  $e_b$  is the plate-cathode potential,  $e_c$  is the grid-cathode potential, and the factor  $\mu$  is a measure of the relative grid-plate potential effectiveness on the tube current. The factor  $\mu$  is known as the *amplification factor* of the grid.

The validity of Eq. (2-10), which is simply a natural extension of the three-halves-power space-charge equation of the diode, has been verified experimentally for many triodes. No simple, rigorous theoretical derivation of this equation is possible, even for a triode of relatively simple geometry. However, the value of the amplification factor  $\mu$  can be calculated with a fair degree of accuracy from equations that are based on electrostatic considerations.

By maintaining the grid at some negative potential with respect to the cathode, it will repel electrons and will, in part, neutralize the attractive field of the anode, thus reducing the anode current. If the grid potential is made positive, the electron stream will increase because of the combined action of both the grid and the plate potentials. But, with a positive potential on the grid, some of the space charge will be attracted to it, and a current in the grid will result. The grid structure must be designed to dissipate the grid power if the grid potential is to be maintained positive; otherwise the grid structure may be seriously damaged. Generally the grid is maintained negative, although positive-grid triodes for power-amplifier applications are available.

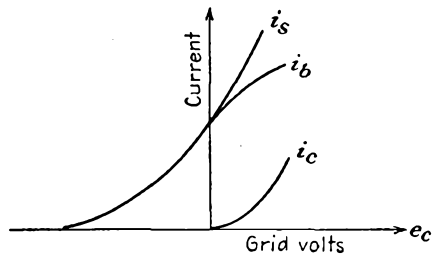


FIG. 2-5. Total space, plate, and grid current in a triode, as a function of grid voltage, with fixed plate voltage.

The variations of the plate and grid currents with variations of grid

potential are illustrated in Fig. 2-5. In this diagram, the plate potential is maintained constant. For sufficiently negative grid potential, cutoff of the plate current occurs. As the grid potential is made less negative, the plate current follows a smooth curve, the variation being expressed analytically by Eq. (2-10). As the grid potential is made positive, grid current flows, the magnitude of this current increasing rapidly with increasing grid potential.

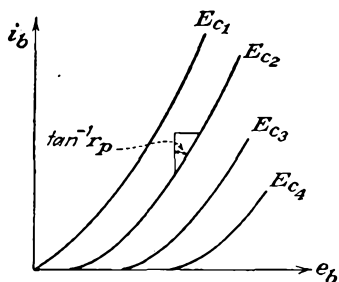


FIG. 2-6. The plate characteristics of a triode.

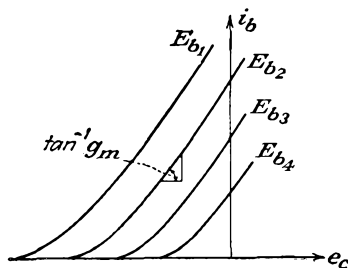


FIG. 2-7. The transfer characteristics of a triode.

For positive grid potentials, and with the consequent grid current, Eq. (2-10) no longer represents the plate current, although it does give a good representation of the total space current. With increasing grid potentials, the grid current increases, and the plate current decreases.

**2-5. Triode Parameters.** In view of Eq. (2-10), the dependence of the plate current on the plate and the grid potentials may be expressed functionally by the expression

$$i_b = f(e_b, e_c) \tag{2-11}$$

Of course the plate current also depends upon the heater temperature, but as the heater current is usually maintained at rated value (this is such

as to provide perhaps five to ten times the normal required current), this term usually does not enter into the functional relationship. If Eq. (2-11) is plotted on a three-dimensional system of axes, a space diagram representing the function  $f(i_b, e_b, e_c) = 0$  is obtained. The projections of these surfaces on the three coordinate planes give three families of characteristic curves. These curves are given in Figs. 2-6, 2-7, and 2-8.

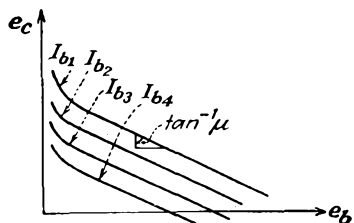


FIG. 2-8. The constant-current characteristics of a triode.

The curves of Fig. 2-6 are known as the *plate characteristics* since they show the variation of the plate current with plate voltage for various

values of grid bias. The main effect of making the grid more negative is to shift the curves to the right, without changing the slopes appreciably. This is in accord with what would be expected from consideration of Eq. (2-10).

If the grid potential is made the independent variable, the *mutual*, or *transfer*, characteristics of Fig. 2-7 result. The effect of making the plate potential less positive is to shift the curves to the right, the slopes again remaining substantially unchanged.

The simultaneous variation of both the plate and the grid potentials so that the plate current remains constant gives rise to a third group of characteristics illustrated in Fig. 2-8. These show the relative effects of the plate and grid potentials on the plate current of the tube. But from the discussion of Sec. 2-4 it is the amplification factor that relates these two effects. Consequently, the amplification factor is defined as the ratio of the change in plate voltage to the change in grid voltage for a constant plate current. Mathematically,  $\mu$  is given by the relation

$$\mu = - \left( \frac{\partial e_b}{\partial e_c} \right)_{i_b} \quad (2-12)$$

The negative sign takes account of the fact that a decreasing grid potential must accompany an increasing plate potential if the plate current is to remain unchanged.

Consider the variation in the plate current. This is obtained by expanding Eq. (2-11) in a Taylor's expansion. But it is here assumed that the variation is small and that it is adequately represented by the first two terms of the expansion. Subject to this limitation, the expression has the form

$$\Delta i_b = \left( \frac{\partial i_b}{\partial e_b} \right)_{E_c} \Delta e_b + \left( \frac{\partial i_b}{\partial e_c} \right)_{E_b} \Delta e_c \quad (2-13)$$

This expression indicates simply that changes both in the plate voltage  $\Delta e_b$  and in the grid voltage  $\Delta e_c$  will cause changes in the plate current.

The quantity  $(\partial e_b / \partial i_b)_{E_c}$  expresses the ratio of an increment of plate potential to the corresponding increment of plate current, for constant  $E_c$ . This ratio has the units of resistance, is known as the *plate resistance* of the tube, and is designated by the symbol  $r_p$ . Clearly,  $r_p$  is the slope of the plate characteristics of Fig. 2-6 and has been indicated there.

The quantity  $(\partial i_b / \partial e_c)_{E_b}$ , which gives the ratio of an increment of plate current to the corresponding increment of grid potential for constant plate potential  $E_b$ , has units of conductance. It is known as the *plate-grid transconductance* or *mutual conductance* and is designated by the symbol  $g_m$ . The mutual conductance  $g_m$  is the slope of the mutual-, or transfer-, characteristic curves of Fig. 2-7.

To summarize, the triode coefficients have the forms

$$\left. \begin{aligned} \left( \frac{\partial e_b}{\partial i_b} \right)_{E_c} &\equiv r_p && \text{plate resistance} \\ \left( \frac{\partial i_b}{\partial e_c} \right)_{E_b} &\equiv g_m && \text{mutual conductance} \\ - \left( \frac{\partial e_b}{\partial e_c} \right)_{I_b} &\equiv \mu && \text{amplification factor} \end{aligned} \right\} \quad (2-14)$$

It is easy to show that  $\mu$  is related to  $r_p$  and  $g_m$  by the expression

$$\mu = r_p g_m \quad (2-15)$$

This is obtained by setting  $\Delta i_b = 0$  in Eq. (2-13) and then using the definitions of Eq. (2-14).

The variations of these parameters for a fixed value of plate potential for the 6C5 tube are shown in Fig. 2-9. It is noticed that the plate

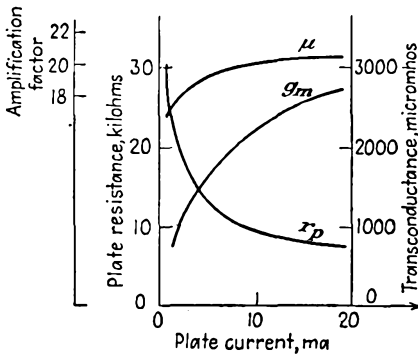


FIG. 2-9. The parameters  $\mu$ ,  $r_p$ , and  $g_m$  of a 6C5 triode as a function of plate current.

resistance varies over rather wide limits, being very high at zero plate current, and approaches a constant value at the higher plate currents. The transconductance varies from a very small value at zero plate current and tends toward a constant value at the higher plate currents. The amplification factor remains reasonably constant over a wide range of currents, although it falls off rapidly at the low currents. The corresponding values for other

values of  $E_b$  may differ numerically, but the general variations will be similar.

High-power triodes are used extensively in transmitters. The grid of such a tube is driven positive with respect to the cathode during part of the cycle, and the current is cut off during part of the cycle. The characteristics of importance of such tubes are the plate curves and the constant-current curves. The variations over normal operating limits are as illustrated in Figs. 2-10 and 2-11 for a type 889A tube.

## MULTIELECTRODE TUBES

**2-6. Tetrodes.** In the tetrode a fourth electrode is interposed between the grid and the plate. This new electrode is known as the *screen grid*, or *grid 2*, in order to distinguish it from the "control" grid of the triode.

AVERAGE PLATE CHARACTERISTICS

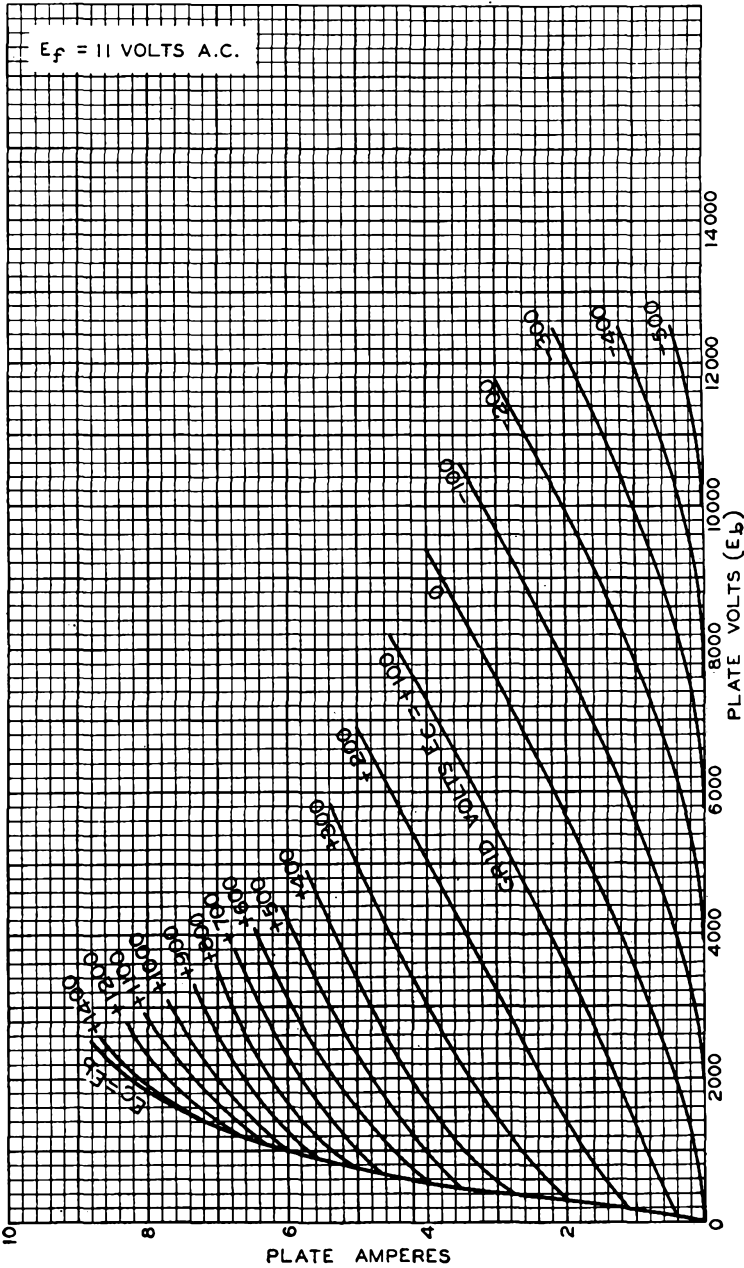


FIG. 2-10. The plate characteristics of a power-triode type 889A.

## AVERAGE CONSTANT-CURRENT CHARACTERISTICS

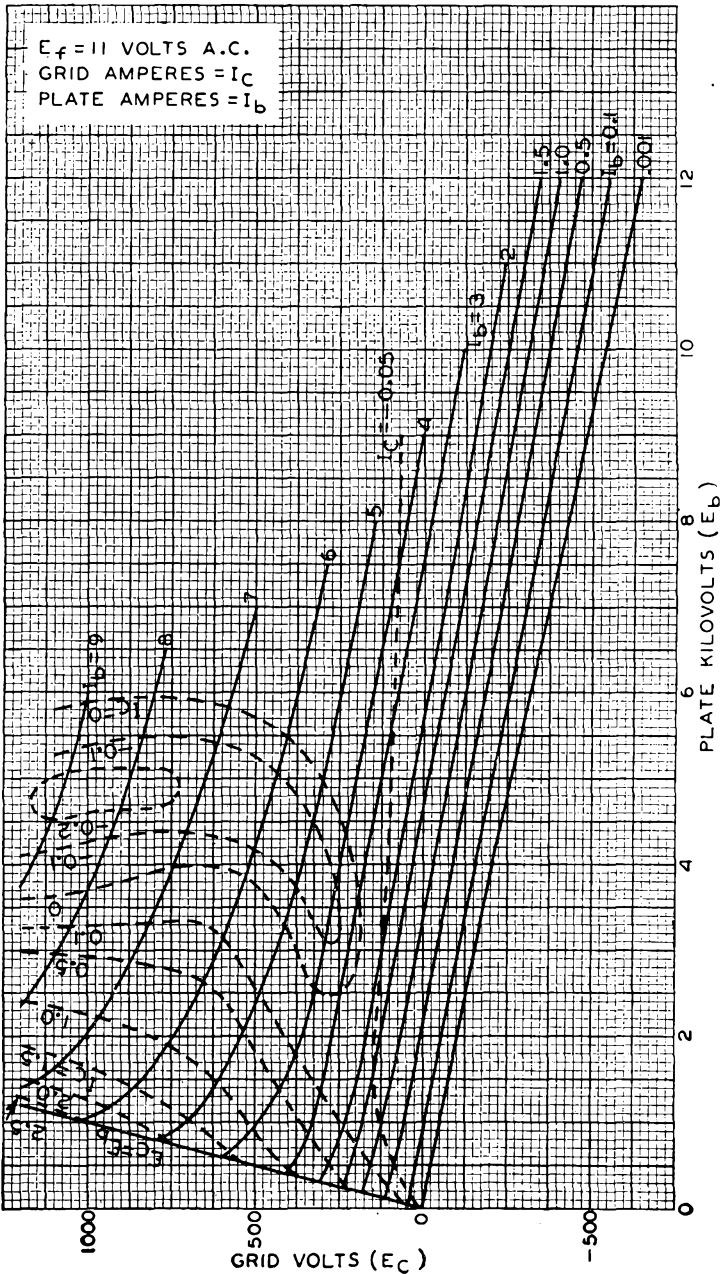


Fig. 2-11. The constant-current characteristics of the power triode of Fig. 2-10.

Physically, it almost entirely encloses the plate. Because of its design and disposition, the screen grid affords very complete electrostatic shielding between the plate and the control grid. This shielding is such that the grid-plate capacitance is reduced by a factor of about 1,000 or more. However, the screen mesh does not interfere appreciably with the electron flow. The reduction of the grid-plate capacitance is a very important improvement over the triode, and this matter will be considered in some detail in Chap. 3.

Because of the electrostatic shielding of the plate by the screen, the potential of the plate has almost no effect in producing an electric field at the cathode. Since the total space current is determined almost wholly by the field near the cathode surface, the plate exerts little or no effect on the total space charge drawn from the cathode. There is, therefore, a significant difference between the triode and the tetrode. In a triode, the plate performs two distinct functions, that of controlling the total space current, and that of collecting the plate current. In a tetrode, the plate serves only to collect those electrons that have passed through the screen.

The passive character of the plate makes the tetrode a much better voltage amplifier than the triode. This follows from the fact that in the triode with a resistance load an increase in load current is accompanied by a decreased plate-cathode potential, which results in a decreased space current. In the tetrode, the decreased plate-cathode potential still exists, but owing to the secondary role of the plate the space current is not materially affected.

The disposition of the cathode and the control grid is nearly the same in both the tetrode and the triode, and therefore the grid-plate transconductance is nearly the same in both tubes. Also, the plate resistance of the tetrode is considerably higher than that of the triode. This follows from the fact that the plate voltage has very little effect on the plate current. Thus, with the high plate resistance and with a  $g_m$  that is about the same as for the triode, the tetrode amplification factor is very high.

**2-7. Tetrode Characteristics.** In the tetrode with fixed control-grid and screen-grid potentials, the total space current is practically constant. Hence, that portion of the space current which is not collected by the plate must be collected by the screen; where the plate current is large, the screen current must be small, and vice versa. The general character of the results is illustrated in Fig. 2-12.

Although the plate potential does not affect the total space current to a very great extent (although a slight effect is noted in the curve at the lower plate potentials), it does determine the division of the space current between plate and screen. At zero plate potential, few of the electrons

have sufficient energy to reach the anode, and the plate current should be small. As the plate potential is increased, a rapid rise occurs in the plate current, with a corresponding reduction of the screen current. When the plate potential is larger than the screen potential, the plate collects almost the entire space current and the screen current approaches zero or a very small value.

An inspection of the curves of Fig. 2-12 shows that the plate current rises very rapidly with increasing plate potential, but this increase is

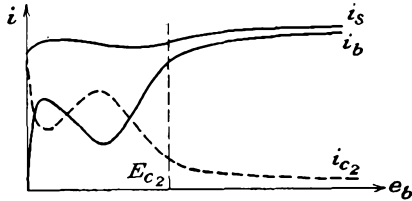


FIG. 2-12. Curves of total space current, plate current, and screen current, in a tetrode.

followed by a region of plate-potential variation in which the plate current decreases with increasing plate potential. This region is one of negative plate resistance, since an increasing plate potential is accompanied by a decreasing plate current. The kinks, or folds, in the curves are caused by the emission of electrons from the plate by the

process of secondary emission. This results from the impact of the primary electrons with the plate. That is, secondary electrons will be released from the anode, and if this is the electrode with the highest positive potential, the electrons will be collected by the anode, without any noticeable effect. If, however, secondary electrons are liberated from the anode, and if these electrons are collected by some other electrode, then the anode current will decrease, whereas the current to the collecting electrode will increase. It is this latter situation which exists in the tetrode when the plate potential is low and the screen is at a high potential.

When the plate potential is higher than the screen potential, the secondary electrons from the plate are drawn back, without appreciable effect. If under these potential conditions secondary electrons are liberated from the screen, these will be collected by the anode. The corresponding plate current will be greater than that in the absence of secondary emission from the screen.

**2-8. Transfer Characteristics.** Since the plate of a tetrode has no appreciable influence on the space current, it is expected that the cathode, the control grid, and the screen grid should possess characteristics not unlike those of a triode. This is actually the case, as illustrated in Fig. 2-13. These curves show the effect of varia-

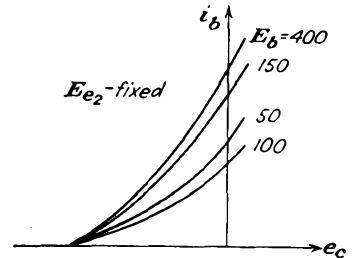


FIG. 2-13. The transfer characteristics of a tetrode, for a fixed screen potential, and with the plate potential as a parameter.

tions of plate potential on plate current, for fixed  $E_{c2}$ . Because of the slight influence of the plate, the transfer curves are bunched together. These curves should be compared with those of the triode in Fig. 2-7, where the transfer curves are widely separated.

The transfer curves for plate voltages below the screen potential, and this is the region of operation which is generally avoided in practice, become separated. In fact, the transfer characteristic for  $E_b = 100$  volts actually falls below that for  $E_b = 50$  volts. This anomalous behavior is directly the result of the secondary-emission effects discussed above.

**2-9. Tube Parameters.** It is expected, on the basis of the foregoing discussion, that the plate current may be expressed as a function of the potential of the various electrodes by an expression of the form

$$i_b = f(e_b, e_{c1}, e_{c2}) \tag{2-16}$$

where  $e_{c1}$  is the potential of the first, or control, grid,  $e_{c2}$  is the potential of the second, or screen, grid, and  $e_b$  is the potential of the plate, all with respect to the cathode. This functional relationship is just a natural extension of that which applies for triodes. In fact, an approximate explicit form of the dependence is possible. This form, which is an extension of Eq. (2-10), may be written as

$$i_b = k \left( e_{c1} + \frac{e_b}{\mu_1} + \frac{e_{c2}}{\mu_2} \right)^{3/2} \tag{2-17}$$

where  $\mu_1$  and  $\mu_2$  are the control-grid and screen-grid amplification factors, respectively.

The variation in the plate current, second- and higher-order terms in the Taylor expansion being neglected, is given by

$$\Delta i_b = \left( \frac{\partial i_b}{\partial e_b} \right)_{E_{c1}, E_{c2}} \Delta e_b + \left( \frac{\partial i_b}{\partial e_{c1}} \right)_{E_b, E_{c2}} \Delta e_{c1} + \left( \frac{\partial i_b}{\partial e_{c2}} \right)_{E_b, E_{c1}} \Delta e_{c2} \tag{2-18}$$

Generally, the screen potential is maintained constant at some appropriate value, and hence  $\Delta e_{c2} = 0$ . The third term in the expansion may be omitted under these conditions. The partial-differential coefficients appearing in this expression furnish the basis for the definitions of the tube parameters. These are

$$\left. \begin{aligned} \left( \frac{\partial e_b}{\partial i_b} \right)_{E_{c1}, E_{c2}} &\equiv r_p && \text{plate resistance} \\ \left( \frac{\partial i_b}{\partial e_{c1}} \right)_{E_b, E_{c2}} &\equiv g_m && \text{mutual conductance} \\ - \left( \frac{\partial e_b}{\partial e_{c1}} \right)_{I_b, E_{c2}} &\equiv \mu && \text{amplification factor} \end{aligned} \right\} \tag{2-19}$$

The two subscripts associated with each term indicate the parameters that are maintained constant during the partial differentiation. It can be shown that here too the relation  $\mu = r_p g_m$  is valid. Nominal values for the various parameters that appear in this relationship are  $r_p = 10^5$  to  $2 \times 10^6$  ohms,  $g_m = 500$  to  $3,000$   $\mu$ mhos, and  $\mu = 100$  to  $1,200$ .

**2-10. Pentodes.** Although the insertion of the screen grid between the control grid and the anode in a triode serves to isolate the plate circuit from the grid circuit, the range of operation of the tube is limited owing to the effects of secondary emission. This limitation results from the fact that, if the plate-potential swing is made too large, the instantaneous plate potential may extend into the region of rapidly falling plate current, with a resulting marked distortion in the output.

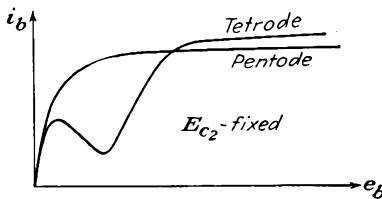


FIG. 2-14. The characteristics of a tube when connected as a tetrode and as a pentode.

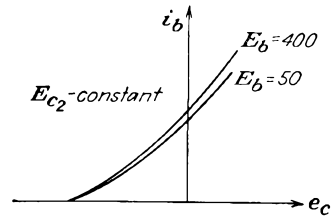


FIG. 2-15. The transfer curves of a pentode for a fixed screen potential and with the plate potential as a parameter.

The kinks, or folds, that appear in the plate-characteristic curves and that limit the range of operation of the tetrode may be removed by inserting a coarse *suppressor-grid* structure between the screen grid and the plate of the tetrode. Tubes that are provided with this extra grid are known as *pentodes*. The suppressor grid must be maintained at a lower potential than the instantaneous potential reached by the plate at any time in its potential excursions. Usually the suppressor is connected to the cathode, either externally or internally. Now since both the screen and the anode are positive with respect to the suppressor grid, secondary electrons from either electrode will be returned to the emitting electrode. The main electron stream will not be materially affected by the presence of the suppressor grid. The effects of the insertion of the suppressor grid are shown graphically in Fig. 2-14.

The pentode has displaced the tetrode in radio-frequency (r-f) voltage amplifiers, because it permits a somewhat higher voltage amplification at moderate values of plate potential. Likewise it permits a greater plate-voltage excursion without distortion. Tetrodes are used extensively in high-power tuned amplifiers.

The transfer curves of a pentode are shown in Fig. 2-15. It is noted that the curves are almost independent of the plate voltage.

**2-11. Remote-cutoff Tubes.** If in a pentode the grid-cathode spacing, the spacing between grid wires, or the diameter of the grid wires is not uniform along the entire length of the control-grid structure, the various portions of the grid will possess different degrees of electrostatic control over the plate current. That is, one portion of the grid may cause electron-flow cutoff, whereas an appreciable current might pass through a more widely spaced section of the grid. As a result, the plate-current control by the grid is considerably less effective than in a conventional pentode. The general character of the results is illustrated in Fig. 2-16. Owing to its construction, a given grid-voltage increment results in a plate-current change that is a function of the bias. This means that the mutual conductance is a function of the bias. For this reason, these tubes are called *variable-mu* tubes. They are also known as *remote-cutoff* and *supercontrol* tubes. They have applications in radio receivers and may be used in f-m transmitters. These applications will be considered in later chapters.

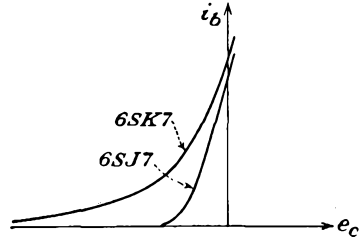


FIG. 2-16. The transfer curves of a 6SJ7 sharp-cutoff pentode and a 6SK7 remote-cutoff pentode.

**2-12. Hexodes, Heptodes.** A number of special-purpose tubes containing more grid elements than the pentode are used extensively. These tubes possess a wide variety of characteristics, depending upon the grids to which fixed potentials are applied and those to which signals might be applied. These tubes are used extensively as converters in superheterodyne receivers and find f-m transmitter and other applications. More will be said about these in the sections having to do with such applications.

**2-13. Beam Power Tubes.** The suppressor grid is introduced into the pentode in order to extend the range of operation of these tubes beyond that of the tetrode. These tubes are quite satisfactory over wide limits, and the range of operation is limited when the instantaneous plate potential falls to the rapidly falling plate-current region at low potentials. This rapid change in plate current for small changes in plate potential in the region of low plate voltage results from the overeffectiveness of the suppressor grid at these low plate potentials.

Because of this, the shape of the suppressor grid in some modern pentodes has been so dimensioned that the effects of secondary emission are just suppressed or only admitted slightly at the low anode voltages. This results in an improved plate characteristic and is manifested by a sharper break in the plate characteristic.

The pentode or tetrode beam power tube was designed with these considerations specifically in mind, and the plate characteristics are illustrated in Fig. 2-17. The essential features of the beam power tube are illustrated in the schematic view of Fig. 2-18. One feature of the design of this tube is that each spiral turn of the screen is aligned with a spiral turn of the control grid. This serves to keep the screen current small and hence leaves the plate current virtually unchanged. Other features are the flattened cathode, the beam-forming side plates (maintained at zero potential), the shape of the plate, the curvature of the

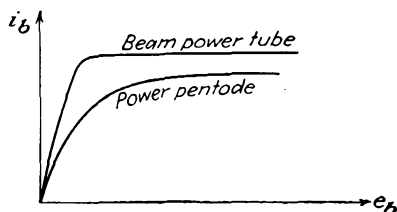


FIG. 2-17. The plate characteristic of a beam power tube and a power pentode.

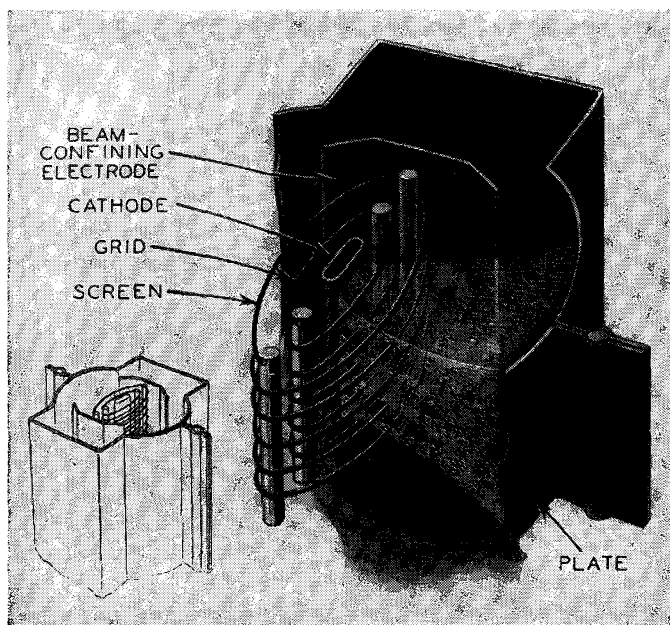


FIG. 2-18. Schematic view of the shapes and arrangement of the electrodes in a beam power tube. (RCA Mfg. Co.)

grids, and the spacing of the various elements. As a result of these design characteristics, the electrons flow between the grid wires toward the plate in sheets, or beams.

The region between the screen and the plate possesses features which are somewhat analogous to those which exist in the space-charge-limited diode. That is, there is a flow of charge between two electrodes. How-

ever, the electrons, when they enter this region do so with an appreciable velocity. For such a case as this, the considerations of Sec. 2-1 would have to be modified to take account of the initial velocity. If this is done, it is found that a potential minimum will exist in the region between the two electrodes. This potential minimum acts as a virtual suppressor grid, and any secondary electrons that are emitted from either the plate or the screen are returned to the emitting electrode.

The actual potential distribution in the screen-plate region will depend on the instantaneous plate potential and the plate current, for a constant screen potential. The resulting variable suppressor action proves to be superior to that possible with a mechanical grid structure, as illustrated.

## GAS TUBES

**2-14. Electrical Discharge in Gases.** There are two important types of discharge in gases that play roles in electron tubes. One of these is the *glow* discharge, and the second is the *arc* discharge. The glow discharge utilizes a cold cathode and is characterized by a fairly high tube drop and a low-current-carrying capacity. The voltage drop across the tube over the operating range is fairly constant and independent of the current. The arc discharge is characterized by a low voltage drop and a high current capacity. For an arc tube with a thermionic cathode, the temperature-limited cathode emission may be drawn with a tube drop approximately equal to the ionization potential of the gas. For a mercury-pool cathode, extremely high current densities exist (of the order of  $5 \times 10^8$  amp/m<sup>2</sup>), with high currents possible and a tube drop approximately equal to the ionization potential of the mercury atom.

Consider a gas tube which consists of a cold cathode and a collecting anode, between which is connected a source of potential through a current-limiting resistor, and an indicating ammeter.

The volt-ampere characteristic of such a tube has the form illustrated in Fig. 2-19. This curve shows that breakdown occurs at a potential which is somewhat higher than the maintaining potential but that there is a region where the tube drop remains substantially constant over an appreciable range of currents. Visually, the discharge is characterized by a colored luminous region, the color being a function of the gas present in the tube.

It is desired to explain the mechanism of operation of these tubes. Consider, therefore, that a free electron exists within the tube; such an

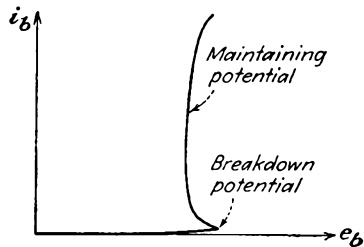


FIG. 2-19. Volt-ampere characteristic of a glow discharge.

electron might have been released by ionization due to collision between a gas molecule and a cosmic ray or by photoelectric emission. With the application of the potential between the electrodes, the electron will drift toward the anode. If the field is large enough, the electron may acquire enough energy to ionize a molecule when it collides with it. Now two electrons will be present, the original one and also the electron that has been liberated by the process of ionization, and a positive ion. The two electrons and the positive ion will move in the applied field, the electrons moving toward the anode, and the positive ion toward the cathode. If the field is large enough, the resulting cumulative ionization may continue until *breakdown* occurs. Once breakdown occurs, the potential distribution within the tube is markedly modified, and most of the region of the discharge becomes virtually equipotential or force-free, containing as many positive as negative charges. This is the plasma of the discharge. Almost the entire potential change occurs in the very narrow region near the cathode. Normal values for cathode-fall voltage range between about 59 volts (a potassium surface and helium gas) and 350 volts. The presence of a low-work-function coating on the cathode will result in a low cathode fall with any gas. Also, the use of one of the inert gases (helium, neon, argon, etc.) results in a low cathode fall with any cathode material. The cathode fall adjusts itself to such a value that each positive ion, when it falls through this field, will release an electron from the cathode by secondary emission. The positive ion combines with this electron and thus becomes neutralized.

Another feature of a normal glow discharge is that the current density of the cathode remains sensibly constant. For higher currents, a greater portion of the cathode is covered with glow, the area of the glow on the cathode increasing directly with the magnitude of the current. Once the cathode is completely covered with glow, any further current through the tube depends on an excess of secondary emission from the cathode over that required to neutralize the positive ions. This is accompanied by a rising cathode fall. This is the "abnormal" glow and is generally of small practical importance.

The dividing line between an arc and a glow discharge is rather indistinct. The arc discharge allows for the passage of large currents at low voltage, the current density at the cathode being high. Nevertheless each discharge has associated with it the cathode fall, the plasma, and the anode fall (which is of minor significance in both types of discharge). The discharges differ in respect to the mechanism by which the electrons are supplied from the cathode. In the glow discharge, as discussed, the electrons are emitted from the cathode by the process of secondary emission resulting from positive-ion bombardment of the cathode. In the arc discharge, the emission of the electrons from the cathode occurs

through the operation of a supplementary mechanism other than by positive-ion bombardment. In the thermionic arc, the electrons are supplied by a cathode that is heated to a high temperature, either by the discharge or externally by means of an auxiliary heating circuit. The mechanism for electron release is not fully understood in the arcs that employ a mercury-pool cathode or an arc between metal surfaces. However, in the discharges the primary function of the gas is to supply a sufficient positive-ion density to neutralize the electron space charge. Because of this, the normal potential drop across an arc tube will be of the order of the ionization potential of the gas.

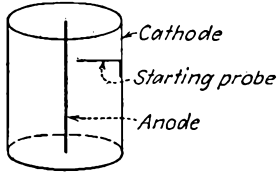


FIG. 2-20. Electrode structure in a VR tube.

**2-15. Glow Tube.** A glow tube is a cold-cathode gas-discharge tube which operates in the normal glow-discharge region. The voltage drop across the tube over the operating range is fairly constant and independent of the current. When the tube is connected in a circuit, a current-limiting resistor must be used if serious damage to the tube is to be avoided.

One commercial type of tube consists of a central anode wire which is coaxial with a cylindrical cathode, as illustrated in Fig. 2-20. The elec-

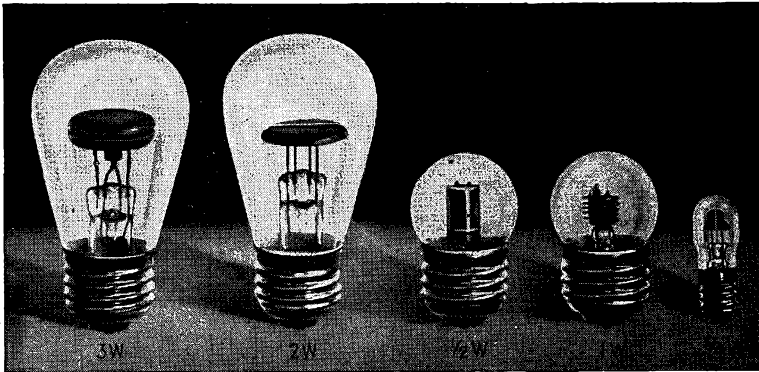


FIG. 2-21. Photographs of several low-capacity glow lamps. (General Electric Co.)

trodes are of nickel, the inner surface of the cathode being oxide-coated. The cathode fall is sometimes lowered by sputtering some misch metal (an alloy of cerium, lanthanum, and didymium) on the cathode. The gases that are commonly used are neon, argon, and helium. The tubes containing neon or helium usually contain a small amount of argon. The presence of the argon lowers the starting voltage. These tubes are available with normal output potentials of 75, 90, 105, and 150 volts and bear the designations VR-75, VR-90, etc. The normal maximum current

is 30 ma. The starting probe that is attached to the cathode, as illustrated in Fig. 2-20, serves to lower the breakdown voltage of the tube.

Glow lamps are also available for pilot, marker, and test-lamp service. Such tubes are available in several sizes from  $\frac{1}{25}$  to 3 watts capacity. Photographs of these are given in Fig. 2-21.

**2-16. Cold-cathode Triodes.** A cold-cathode triode, or *grid-glow tube*, contains three elements, the cathode, the anode, and a starter, or control, anode. The control electrode is placed close to the cathode. The spacing of the electrodes is such that a discharge takes place from the cathode to the control electrode at a lower potential than is required for a discharge from the cathode to the anode. Once the control gap has been broken down, however, it is possible for the discharge to transfer to the main anode. The cathode-anode voltage that is required for this transfer to occur is a function of the transfer current, the current in the control electrode-cathode circuit.

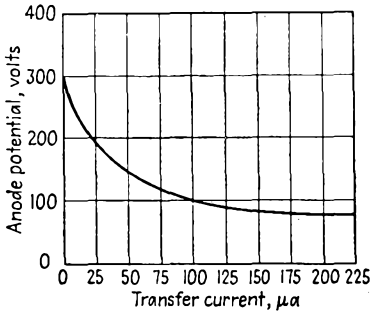


FIG. 2-22. Transfer characteristic of an RCA OA4G cold-cathode triode.

Such a "transfer," or "transition," characteristic is given in Fig. 2-22.

For zero transfer current, which means that the control electrode is not connected in the circuit, the anode voltage is equal to the breakdown voltage between cathode and anode. It is observed from the curve that the required anode-cathode voltage falls rapidly as the transfer current is increased. An increased transfer current indicates the presence of greater ionization. Regardless of the magnitude of the transfer current, however, the anode-cathode voltage can never fall below the maintaining voltage for this gap. The transfer characteristic approaches this sustaining voltage asymptotically.

**2-17. Hot-cathode Gas-filled Diodes.** These tubes are thermionic cathode diodes in which there is an inert gas at low pressure or in which mercury vapor is added. In the latter case a few drops of mercury are added to the tube after evacuation. The pressure in the tube is then a

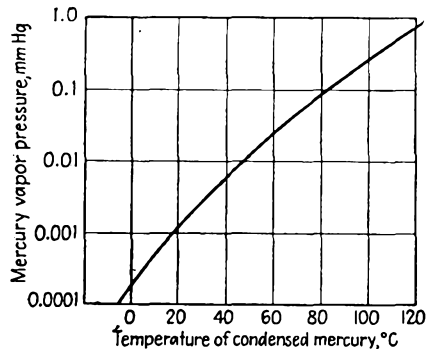


FIG. 2-23. Mercury-vapor pressure as a function of condensation temperature.

function of the mercury-vapor condensation temperature. The relationship between the pressure and the temperature is shown in Fig. 2-23. Under normal operating conditions, the temperature of the tube will be 15 to 20°C above that of the surroundings (ambient temperature).

As already discussed, the sole function of the gas in these tubes is to provide ions for the neutralization of space charge, thus permitting the current to be obtained at much lower voltages than are necessary in

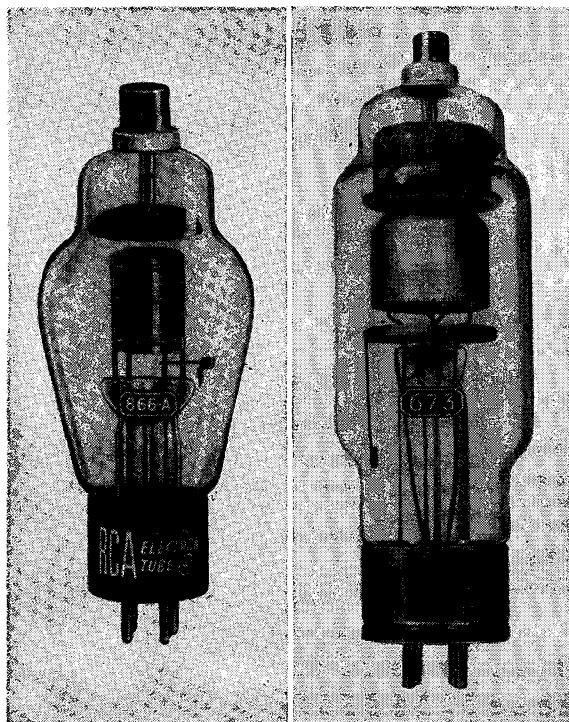


FIG. 2-24. Commercial mercury-vapor diodes of different capacity. (RCA Mfg. Co.)

vacuum tubes. If more than saturation current is demanded by the circuit, then gas amplification, resulting from positive-ion bombardment of the cathode, will occur. Under these circumstances the cathode fall increases. The tube drop should not be permitted to exceed the disintegration voltage of the cathode (about 22 volts for a mercury diode with either oxide-coated or thoriated-tungsten cathodes); otherwise the cathode may be seriously damaged by the positive-ion bombardment.

Two typical commercial mercury-vapor-filled diodes are illustrated in Fig. 2-24.

**2-18. High-pressure Gas Diodes.** Diodes are available which contain argon or a mixture of argon and mercury at a pressure of about 5 cm.

The cathodes in such tubes consist of a short, heavy thoriated-tungsten or oxide-coated filament and are located close to heavy graphite anodes. These tubes, which are known as *tungar* or *rectigon* tubes, are used extensively in chargers for storage batteries.

The presence of the fairly high pressure gas serves a twofold purpose. One is to provide the positive ions for reducing the space charge. The second is to prevent the evaporation of the thorium or the coating from the filament. This second factor is extremely important since the filament is operated at higher than normal temperature in order to provide the large currents from such a simple cathode structure. The high-pressure gas in such a tube imposes a limitation on these tubes, and they are limited to low-voltage operation.

**2-19. The Thyatron.** The thyatron is a three-electrode tube which comprises the cathode, the anode, and a massive grid structure between them. The grid structure is so designed as to provide almost complete electrostatic shielding between the cathode and the anode. In such a tube as this, the initiation of the arc is controlled by controlling the potential of the grid. The grid usually consists of a cylindrical structure which surrounds both the anode and the cathode, a baffle or a series of baffles containing small holes being inserted between the anode and the cathode. The electrode structure of such a tube is illustrated in Fig. 2-25. The shielding by the grid is so complete that the application of a small grid potential before conduction is started is adequate to overcome the field at the cathode resulting from the application of a large anode potential.

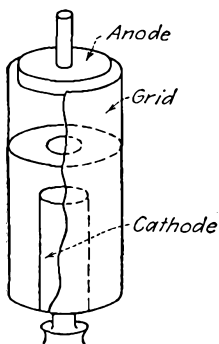


FIG. 2-25. The electrode structure of a negative control thyatron.

Once the arc has been initiated, the grid loses complete control over the arc. Grid control is reestablished only when the anode potential is reduced to a value less than that necessary to maintain the arc. Once the arc has been extinguished by lowering the plate voltage, the grid once more becomes the controlling factor which determines when conduction will again be initiated. That is, if the grid potential is more positive than that necessary for the controlling action to prevail, conduction will take place; if more negative, no conduction will occur. The curve that relates the grid ignition potential with the potential of the anode for conduction just to begin is known as the *critical grid curve*. In fact, a knowledge of this static curve is all that is required to determine completely the behavior of a thyatron in a circuit.

Typical starting characteristic curves of mercury-vapor thyatrons are given in Fig. 2-26. Two distinct types of characteristics are illustrated,

*viz.*, those in which the grid potential must always be positive, and those in which the grid is generally negative, except for very low plate potentials. The physical distinction between these positive and negative control tubes lies essentially in the more complete shielding by the grid in positive control tubes.

In the negative control tube where the shielding is far less complete than in the positive control type, the effect of the plate voltage is clearly

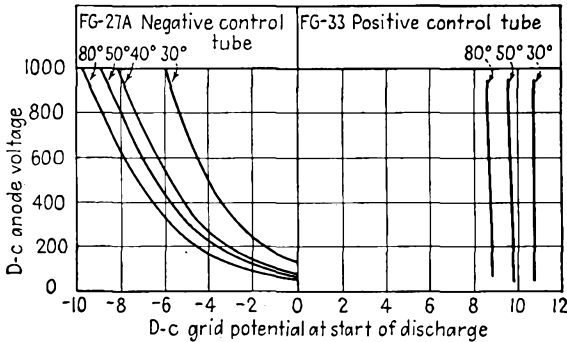


FIG. 2-26. Critical grid characteristics of a positive and a negative control thyatron for different temperatures.

seen; the higher the plate potential, the more negative must the grid potential be in order to prevent conduction from taking place. For low plate potentials, positive grid potentials must be applied before ionization, and hence conduction, can begin. If the plate potential is reduced still more, even below the potential necessary for ionization, breakdown can still be obtained by making the grid sufficiently positive. Now, however, the function of the tube may be destroyed, since the arc may take place between the cathode and the grid, with very little current to the plate. The thyatron will be converted into a gas diode under these conditions, the plate acting as a dummy electrode, the cylindrical grid now serving as the anode. It is because of this that a large current-limiting resistor is connected in the grid circuit, as it is unwise to draw a large grid current.

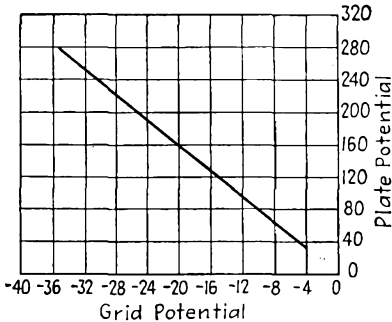


FIG. 2-27. Critical grid characteristic of an 884 argon-filled thyatron.

In addition to the mercury-vapor- and gas-filled thyatrons of moderate current capacity, small argon-filled low-current-capacity tubes are available. The shielding between the cathode and the anode is not so complete in these tubes as in the higher current units. Also, the critical

grid curves are independent of temperature, since the number of gas molecules in the glass envelope remains constant. A typical critical grid curve for an 884 is given in Fig. 2-27.

**2-20. Shield-grid Thyratrons.** Before breakdown of the tube occurs, the current to the grid of a thyatron such as the FG-27A is a few tenths of a microampere. Although this current is entirely negligible for many applications, it will cause trouble in circuits that require very high grid

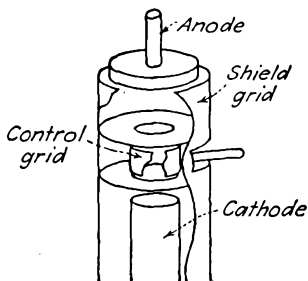


FIG. 2-28. Electrode structure of the FG-98 shield-grid thyatron.

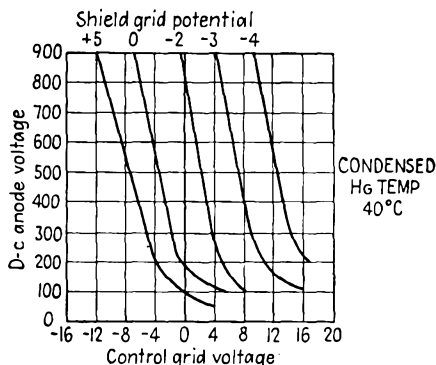


FIG. 2-29. Control characteristics of an FG-98 shield-grid thyatron.

impedances. This is especially true in circuits that employ phototubes. For this reason, a fourth electrode, or shield grid, has been added to the thyatron. Such a shield-grid thyatron structure is illustrated in Fig. 2-28. The massive cylindrical shield-grid structure encloses the cathode, control grid, and anode. Owing to the shielding, the grid current is reduced to a small fraction of its original value, the preignition current being of the order of  $10^{-3}$   $\mu$ amp.

The critical grid starting characteristics of such a tube are shown in Fig. 2-29. It will be observed that these characteristics are functions of the shield-grid voltage.

**2-21. The Ignitron.** The ignitron is a mercury-pool cathode diode which is provided with a third electrode for initiating the discharge between the cathode and anode. The third electrode, or ignitor rod, is made of a suitable refractory material (such as silicon carbide, boron carbide, and carborundum) which projects into the mercury-pool cathode. Such a tube is illustrated in Fig. 2-30.

With an a-c potential applied between the cathode and the anode of the pool-cathode diode, the arc would be extinguished once each alternate half cycle, provided that the arc could be initiated regularly. The application of a potential to the ignitor rod at the appropriate point in the cycle will permit the regular ignition of the arc.

There is a fundamental difference between the control action in a thyatron and that of the ignitor rod in an ignitron. In thyatrons, the grid prevents the formation of an arc, whereas the ignitor initiates the arc. In the former case the electrons already exist in the tube, owing to the presence of an externally heated cathode, but the grid electrostatically prevents the electrons from flowing to the anode until a critical

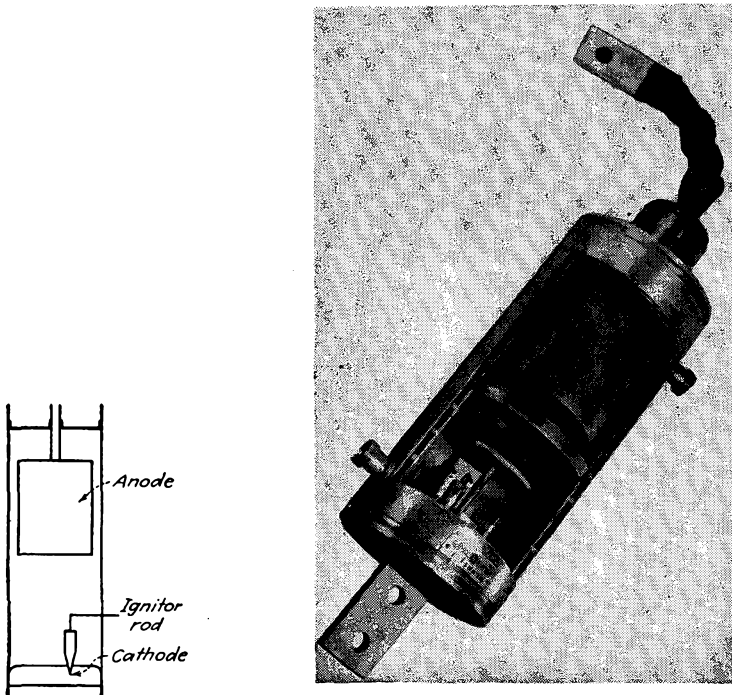


FIG. 2-30. Sketch and photograph of a water-cooled metal ignitron. (*General Electric Co.*)

voltage is reached. In the ignitron, the tube is in a nonconducting state until the ignitor circuit is energized, when conduction is forced.

**2-22. Tube Ratings—Current, Voltage, Temperature.** Gas- and vapor-filled tubes are given average rather than rms current ratings. This rating specifies the maximum current that the tube may carry continuously without excessive heating of any of the parts. The time over which the average is to be taken is also specified by the manufacturer. That the average current is important in such a tube follows from the fact that the instantaneous power to the plate of the tube is given by the product of the instantaneous anode current and the instantaneous tube voltage. Since the voltage is substantially constant and independent of the tube current, the average power is the product of the tube drop and

the average tube current. The tubes are also given peak-current ratings, this rating specifying the maximum current that the tube should be permitted to reach in each conducting cycle.

Such tubes are also given peak-inverse-voltage ratings. This is the largest safe instantaneous negative potential that may be applied to the tube without the possibility of conduction in the inverse direction arising because of breakdown of the gas in the tube. This potential is also referred to as the *flash-back* voltage. The variation of the inverse peak voltage with temperature for an 866 diode is shown in Fig. 2-31.

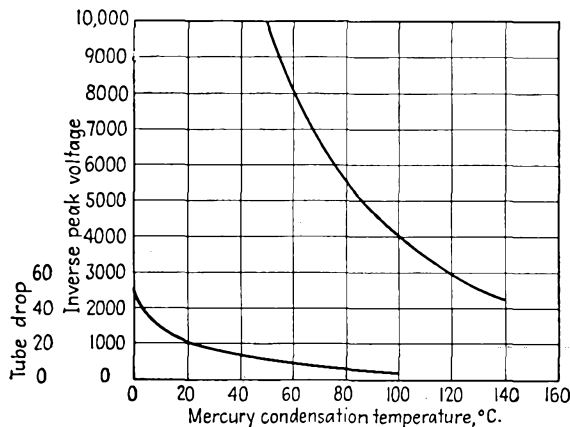


FIG. 2-31. Peak inverse voltage and tube drop of an 866 diode as a function of temperature.

The maximum peak forward voltage is a quantity that is significant only for thyratrons. It specifies the largest positive potential that may be applied to the anode before the grid loses its arc-initiating ability. That is, for potentials higher than this, a glow discharge may occur between anode and grid, which will immediately initiate the cathode-anode arc.

The condensed-mercury temperature limits are specified for the safe and efficient operation of mercury-vapor tubes. The range usually extends from about 30 to 80°C. The upper temperature limit is determined by the allowable peak inverse voltage. The lower limit is set by the allowable tube drop, which increases with decreasing temperature and which may cause serious cathode disintegration, as well as a decreased efficiency.

**2-23. Deionization and Ionization Times.** The ionization time of a tube specifies the time required for conduction to be established once the potentials have been applied. It seldom exceeds 10  $\mu$ seconds and is approximately 0.01  $\mu$ seconds for the 884 thyatron.

The deionization time is a measure of the minimum time that is required after removal of the anode potential before the grid of a thyatron again regains control. It represents the time that is required for the positive ions to diffuse away from the grid and recombine with electrons to form neutral molecules. The deionization time depends on many factors, such as gas pressure, electrode spacing, and exposed areas. For commercial tubes that are operated under rated conditions, it varies between 100 and 1,000  $\mu$ seconds. This is considerably longer than the ionization time and may offer a serious limitation to the use of such tubes in many applications.

#### REFERENCE

1. For more details, see Millman, J., and S. Seely, "Electronics," Chap. VII, McGraw-Hill Book Company, Inc., New York, 1941.

#### PROBLEMS

**2-1.** Plot  $I_b$  vs.  $E_b$  of the 6H6 diode (see Appendix B) on log paper. From this plot determine the quantities  $k$  and  $n$  in the expression  $I_b = kE_b^n$ .

**2-2.** The anode current in a type 5U4G diode with 54 volts applied between the plate and cathode is 200 ma. What is the required potential for a current of 100 ma? The tube operates under space-charge conditions.

**2-3.** Suppose that the FP-400 tube is operating under rated filament power input (see Prob. 1-2). The operating temperature is 2700°K; anode diameter = 0.50 in.

a. Calculate the saturation current.

b. At what potential will the current become temperature saturated?

**2-4.** Plot  $I_b$  vs.  $E_b + \mu E_c$  on log paper of the 6J5 triode (see Appendix B). From this curve, find the quantities  $k$  and  $n$  in the expression  $I_b = k(E_b + \mu E_c)^n$ .

**2-5.** The 6J5 triode is operated with  $E_b = 135$  volts. Determine and plot curves of  $\mu$ ,  $g_m$ , and  $r_p$  as a function of  $E_c$ .

**2-6.** The rating of a certain triode is given by

$$I_b = 130 \times 10^{-6} (E_c + 0.125E_b)^{1.58}$$

With  $E_{cc} = -20$  volts,  $E_{bb} = 350$  volts, find  $I_b$ ,  $r_p$ ,  $g_m$ ,  $\mu$ .

**2-7.** The plate and grid characteristics of a type 851 power triode are given in Appendix C. Plot  $I_s = I_b + I_c$  vs.  $E_b + \mu E_c$  on log paper, and find the quantities  $k$  and  $n$  in the expression  $I_s = k(E_b + \mu E_c)^n$ .

**2-8.** The current in a 6J5 triode for which  $\mu = 20$  and which is operating with  $E_c = -8$  volts,  $E_b = 250$  volts is 8.7 ma. Estimate the current when  $E_b = 200$  volts and  $E_c = -6$  volts.

**2-9.** A 6J5 triode for which  $\mu = 20$  is operating with  $E_b = 250$  volts. What grid voltage is required to reduce the current to zero?

**2-10.** Evaluate the value of  $\mu$ ,  $g_m$ , and  $r_p$  of the 6SJ7 pentode for  $E_c = -3$ ,  $E_{cc2} = 100$ ,  $E_b = 150$  volts.

**2-11.** Evaluate the values of  $\mu$ ,  $g_m$ ,  $r_p$  of the 6SK7 supercontrol pentode for  $E_{cc2} = 100$ ,  $E_b = 250$  volts, with  $E_{cc1} = -2$  volts; with  $E_{cc1} = -10$  volts.

**2-12.** Plot a curve of  $g_m$  vs.  $E_{c1}$  of a 6SK7 with  $E_{cc2} = 100$ ,  $E_b = 250$  volts.

**2-13.** Use the plate characteristics of the 6SJ7 and the 6SK7 pentodes to construct mutual characteristics on the same sheet, with  $E_b = 200$  volts for each tube. Determine the maximum and minimum values of  $g_m$  for each tube in the range of your sketch.

**2-14.** Plot a curve of  $g_m$  vs.  $E_{c3}$  of a 6L7, with  $E_{cc1} = -6$ ,  $E_{cc2} = 150$  volts.

**2-15.** Refer to Sec. 2-7 for a discussion of secondary emission caused by electron impact. What happens to the secondary electrons that are produced by the impact of the primary current on the anode in a diode? In a triode?

## CHAPTER 3

### VACUUM TUBES AS CIRCUIT ELEMENTS

THE analysis of the behavior of a vacuum tube in a circuit may be accomplished by two different methods, both of which are to be examined in some detail. In one method, use is made of the static characteristics of the tube. The second method achieves two forms. In one, the tube is replaced by a constant-voltage generator, the potential of which depends upon the input signal and the internal resistance of which depends on the tube that is used. In the other, the tube is replaced by a constant-current generator, the magnitude of the current depending on the input signal, the generator being shunted by a resistance which is a function of the tube. Owing to the approximations that are made in the second methods, they are inherently less accurate than the direct use of the static characteristics. However, these methods allow a clearer insight into the operation of the circuit. Because of this feature, the equivalent-circuit methods of analysis are considerably more important than that involving the tube characteristics. Moreover, it is possible to estimate the inaccuracies in the method, thus allowing a complete understanding of the operation of the circuit.

The introduction of the methods will be made in terms of the operation of a triode and will later be extended to the operation of the other types of tubes.

#### 3-1. Symbols and Terminology.

The simplest triode amplifier is illustrated in Fig. 3-1. Before proceeding with the analysis, it is necessary to discuss the meaning of the symbols and the general terminology of vacuum-tube circuits.

The input circuit of the amplifier usually refers to all the elements of the circuit that exist between the grid and the cathode terminals of the tube. Similarly, the output, or plate, circuit usually refers to the elements that are connected between the cathode and the plate terminals. In the circuit illustrated, the input circuit comprises the input voltage source  $e_g$ , the grid resistor  $R_g$ , and the bias battery  $E_{cc}$ . The plate circuit

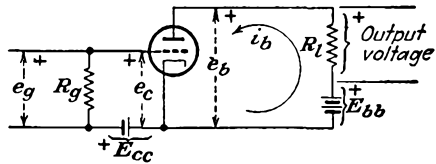


FIG. 3-1. The basic circuit of a triode amplifier.

consists of the load resistor  $R_l$  and the plate supply battery  $E_{bb}$ . In many applications, the input signal  $e_g$  is a sinusoidally varying potential, although the wave shape may be nonsinusoidal, and is frequently very carefully chosen for a particular application.

A variety of potentials, both d-c and varying, are involved simultaneously in a vacuum-tube circuit, making it necessary that a precise method of labeling such sources be established. In what follows, lower-case letters will be used to designate instantaneous values, and capital letters will denote either d-c or rms values of sinusoids. The subscripts  $c$  and  $g$  will refer to the grid circuit, and the subscripts  $b$  and  $p$  will refer to the plate circuit. Examples of the notation follow:

$E_{cc}$  = d-c grid, or C bias

$E_{bb}$  = d-c plate supply, or B supply

$E_g$  = rms value of the a-c input excitation voltage if this excitation is sinusoidal

$E_p$  = rms value of the a-c output potential for a sinusoidal output

$e_g$  = instantaneous input signal; measured with respect to the input terminals

$e_c$  = instantaneous signal that appears between the grid and cathode of the tube

$e_p$  = instantaneous signal that appears across the output element of the circuit

$e_b$  = instantaneous potential between the plate and cathode of the tube

$i_p$  = instantaneous signal component of plate current; positive in the direction from the cathode to the plate through the load

$i_b$  = instantaneous total plate current; positive in the direction from the cathode to the plate through the load

$I_b$  = average or d-c current in the plate circuit

$E_b$  = average or d-c potential from plate to cathode

Figure 3-1 illustrates the reference positive polarities and the reference direction of current.

As a specific illustration of the notation, suppose that the input signal voltage to the amplifier of Fig. 3-1 is

$$e_g = \sqrt{2} E_g \sin \omega t$$

Then the instantaneous grid-cathode potential is

$$e_c = E_{cc} + \sqrt{2} E_g \sin \omega t$$

Circuits will be discussed in which no such simple relation between grid driving signal and grid-cathode potential exists, owing to an involved interconnection of circuit elements among the tube elements.

**3-2. Graphical Analysis.** Refer to Fig. 3-1, and suppose that the grid input signal  $e_g = 0$ . Owing to the d-c sources  $E_{cc}$  and  $E_{bb}$ , it will be

supposed that there is a current in the plate circuit. This is true only if the plate supply  $E_{bb}$  and the grid supply  $E_{cc}$  are properly chosen. The value of this current may be found graphically. In fact, it is essential that a graphical solution be used. This follows from the fact that the plate circuit of Fig. 3-1 yields the relation

$$e_b = E_{bb} - i_b R_l \quad (3-1)$$

However, this one equation is not sufficient to determine the current corresponding to the potential  $E_{bb}$ , since there are two unknown quantities in the expression,  $e_b$  and  $i_b$ .

A second relation between  $e_b$  and  $i_b$  is given by the plate characteristics of the triode. The simultaneous solution of Eq. (3-1) and the plate characteristics will yield the desired current. This is accomplished by drawing Eq. (3-1) on the plate characteristics, in the manner illustrated in Fig. 3-2. The line that passes through the points

$$\begin{aligned} i_b &= 0 & e_b &= E_{bb} \\ i_b &= \frac{E_{bb}}{R_l} & e_b &= 0 \end{aligned}$$

is known as the *load line*. It is obviously independent of the tube characteristics, for it depends only upon elements external to the tube. The intersection of this line with the curve for  $e_c = E_{cc}$  is called the *operating* or *quiescent* point  $Q$ . The grid-bias supply  $E_{cc}$  is usually such as to maintain the grid negative relative to the cathode. The  $Q$  current in the external circuit is  $I_b$ , and the corresponding plate-cathode potential is  $E_b$ .

Suppose that the grid-cathode potential is

$$e_c = E_{cc} + \sqrt{2} E_g \sin \omega t$$

The maximum and minimum values of  $e_c$  will be  $E_{cc} + \sqrt{2} E_g$  and  $E_{cc} - \sqrt{2} E_g$ , respectively. The plate current and the plate voltage will vary about the values of  $I_b$  and  $E_b$ . The graphical construction of Fig. 3-3 shows the details of the variations. The values of  $e_b$  and  $i_b$  for any given value of  $e_c$  are obtained from the intersection of the load line and the  $i_b$ - $e_b$  curve for the specified  $e_c$ . The points  $a'$ ,  $b'$ ,  $c'$ , etc., of the output current and the points  $a''$ ,  $b''$ ,  $c''$ , etc., of the output-voltage wave correspond, respectively, to the points  $A$ ,  $B$ ,  $C$ , etc., of the input-grid-signal wave form.

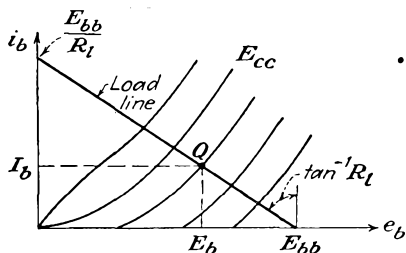


FIG. 3-2. The operating point  $Q$  is located at the intersection of the load line and the plate characteristic for  $e_c = -E_{cc}$ .

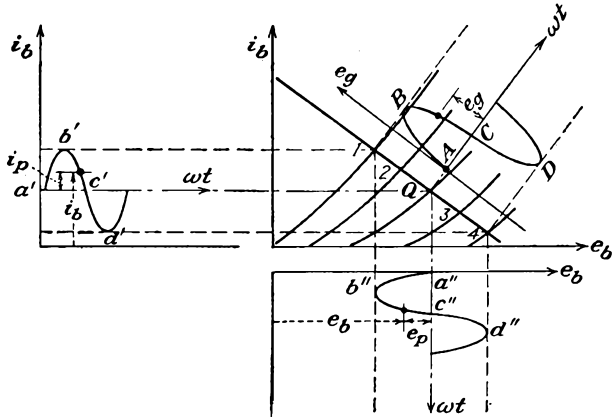


FIG. 3-3. The output current and voltage wave forms for a given input grid signal.

It is instructive to show the several wave shapes in their proper phase relation. This is done in Fig. 3-4. It should be noted in particular that the variations about the quiescent values have been labeled. The quantities so labeled are

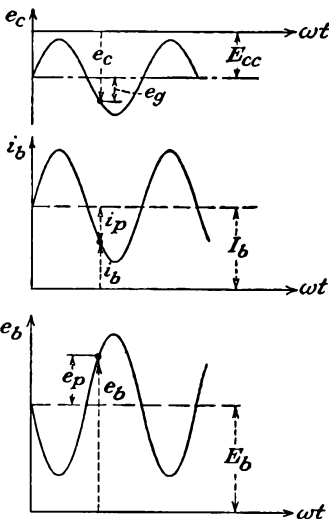


FIG. 3-4. The input grid wave shape, and the corresponding output current and voltage wave shapes.

$$\left. \begin{aligned} e_g &= e_c - E_{cc} \\ e_p &= e_b - E_b \\ i_p &= i_b - I_b \end{aligned} \right\} \quad (3-2)$$

These quantities give a measure of the amplification property of the amplifier, as it is a direct measure of the a-c output variations for a given a-c input variation.

The curves of Fig. 3-4 indicate the following very significant results: If the current  $i_p$  is sinusoidal, then  $i_p$  and  $e_p$  are 180 deg out of phase with each other. Also, the grid driving voltage  $e_g$  and the plate current  $i_p$  are in phase with each other. This simply states that, when a positive-going signal is applied to the grid, the tube current increases. Moreover, with an increased current in the plate circuit, the potential of the plate falls.

A curve of the intersection of the load line with the static-characteristic curves, which is a measure of the current  $i_b$  as a function of  $e_c$  for the specified  $E_b$  and load  $R_L$ , is important. It is known as the "dynamic" characteristic of the tube circuit and yields directly the output current

for a given input signal. The construction is directly related to the construction of Fig. 3-3, and is given in Fig. 3-5. The corresponding points on both curves are similarly marked.

**3-3. Voltage-source Equivalent Circuit of a Triode.** Ordinarily one is interested in the "a-c response" of the circuit, rather than in obtaining the total instantaneous variation of the potentials and currents. That is, the value of  $i_p$  and of  $e_p$  for a given  $e_g$  are ordinarily desired. It will be found possible to obtain this information by an analytic method, without direct recourse to the graphical solution of the foregoing section.

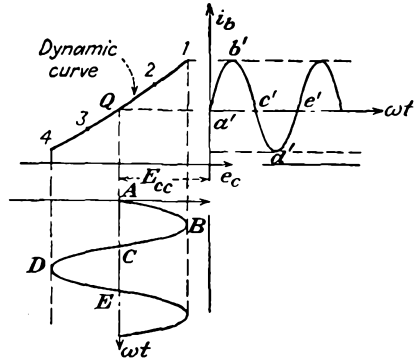


FIG. 3-5. The dynamic curve, and its use in determining the output wave shape for a given input signal.

To this end, again consider certain of the results of Sec. 2-5. According to Eqs. (2-13) and (2-14), the variation in current about the quiescent point is given as

$$\Delta i_b = \left( \frac{\partial i_b}{\partial e_b} \right)_{E_c} \Delta e_b + \left( \frac{\partial i_b}{\partial e_c} \right)_{E_b} \Delta e_c \tag{3-3}$$

This may be written as

$$\Delta i_b = \frac{1}{r_p} \Delta e_b + g_m \Delta e_c \tag{3-4}$$

But as the changes about the quiescent values are, respectively,

$$\left. \begin{aligned} \Delta i_b &= i_b - I_b = i_p \\ \Delta e_c &= e_c - E_{cc} = e_g \\ \Delta e_b &= e_b - E_{bb} = e_p \end{aligned} \right\} \tag{3-5}$$

then Eq. (3-4) becomes

$$i_p = \frac{1}{r_p} e_p + g_m e_g \tag{3-6}$$

or

$$e_p = -\mu e_g + i_p r_p \tag{3-7}$$

This expression shows that the voltage  $e_p$  comprises two components; one is a generated emf which is  $\mu$  times as large as the grid-cathode voltage, and the second is a voltage across the tube resistance  $r_p$  resulting from the current  $i_p$  through it.

These results are illustrated graphically in Fig. 3-6. The tube is replaced by a fictitious generator, with a generated emf  $\mu e_g$  and an internal resistance  $r_p$ . Confusion sometimes arises because of the failure to

appreciate fully the polarities and the potentials in the circuit. Figure 3-6 is redrawn in a manner to stress this matter. This figure, when compared with the original circuit of Fig. 3-1, shows that the equivalent circuit is substantially like the original circuit, except that the tube, *relative to the tube pins*, is replaced by the equivalent voltage generator  $\mu e_{gk}$ , the polarity of which is opposite to that associated with the grid driving potential  $e_{gk}$  and an internal resistor  $r_p$ . Since the equivalent circuits of Figs. 3-6 and 3-7 give a measure of the variation about the  $Q$  point, no d-c quantities appear in the figure.

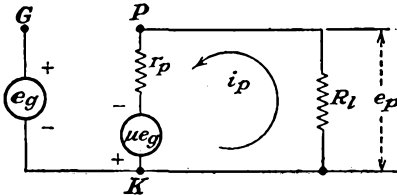


FIG. 3-6. The equivalent circuit of a triode.

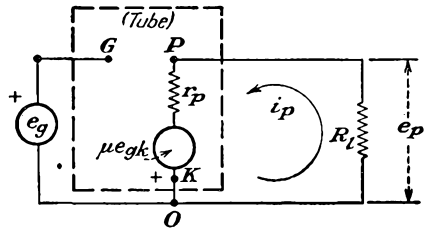


FIG. 3-7. The circuit of Fig. 3-6 redrawn in a manner to show the elements that replace the tube, and the associated potentials.

The equivalent circuit was derived without consideration of the character of the load. Consequently, it is valid for any type of load. The only restriction is that the parameters  $\mu$ ,  $r_p$ , and  $g_m$  must remain substantially constant over the operating range.

The technique of drawing the equivalent circuit of any tube circuit is a straightforward process, although care must be exercised in carrying this process out. To avoid error, the following simple rules will be found helpful.

1. Draw the actual circuit diagram neatly.
2. Mark the points  $G$ ,  $P$ , and  $K$  on this diagram. Locate these points as the start of the equivalent circuit. Maintain the same relative position as in the original circuit.
3. Between points  $P$  and  $K$  include a resistor  $r_p$  and a generator of potential  $\mu e_{gk}$ , where  $e_{gk}$  is the grid-cathode potential. The cathode of this generator is marked  $+$ .
4. Omit the tube and all d-c sources from the diagram, but transfer all circuit elements from the actual circuit to the equivalent circuit without altering the relative positions of these elements.

The point of special importance is that, quite apart from the points of application of the input signal, the equivalent fictitious generator must *always* be  $\mu e_{gk}$ , where  $e_{gk}$  is the total grid-cathode potential.

Once the equivalent circuit has been drawn, it is no longer necessary to

refer to the original circuit. Moreover, since the equivalent circuit will contain only generators and passive circuit elements (resistances, inductances, and capacitances), the usual methods of a-c circuit analysis are employed to calculate the desired quantities.

**3-4. Measurement of Triode Coefficients.** As several specific illustrations of the methods of analysis just discussed, the circuits for obtain-

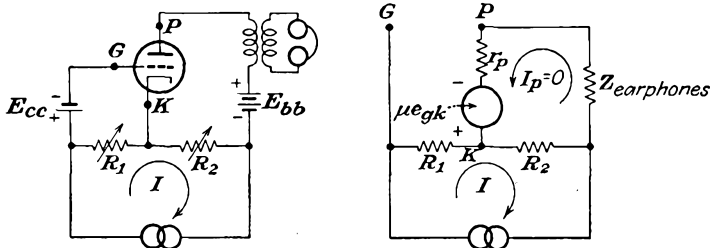


FIG. 3-8. The Miller bridge and its equivalent circuit, for determining the amplification factor of a triode under operating conditions.

ing the values of  $\mu$ ,  $r_p$ , and  $g_m$  of a triode will be analyzed. It should be recalled that the triode coefficients, first discussed in Sec. 2-5, were shown to be related to the slope of the static-characteristic curves, according to Figs. 2-5 to 2-7. However, the accuracy with which these quantities can be measured in this way is not high. Not only do the methods now to be discussed yield results which are made under dynamic conditions, but the results are usually more accurate.

The amplification factor  $\mu$  is readily determined by means of the circuit given in Fig. 3-8. The operations involved in balancing the bridge consist simply in varying  $R_1$  and  $R_2$  until no signal from the oscillator is heard in the earphones. When this condition prevails, the plate current  $I_p = 0$ . Then the potential  $E_{\theta k} = IR_1$ . By applying Kirchhoff's law to the plate circuit,

$$-\mu E_{\theta k} + IR_2 = 0$$

or

$$+\mu E_{\theta k} = IR_2 = \mu IR_1$$

It follows from this that

$$\mu = \frac{R_2}{R_1} \tag{3-8}$$

This measurement may be effected for any desired d-c current in the tube simply by adjusting the grid bias  $E_{cc}$ .

The transconductance  $g_m$  is measured by means of a bridge circuit that is a slight modification of Fig. 3-8. The addition of a resistor  $R_3$  between the plate and cathode makes this measurement possible. The schematic

and equivalent circuits of this bridge network are given in Figs. 3-9. The measurement is accomplished by adjusting the resistors until no signal is heard in the earphones.

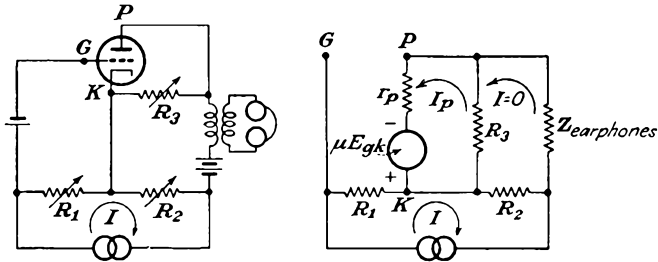


FIG. 3-9. The Miller bridge from determining the transconductance of a triode under operating conditions.

By applying Kirchoff's law to the several meshes there results

$$I_p R_3 + I_p r_p - \mu E_{gk} = 0$$

But the potential  $E_{gk}$  is

$$E_{gk} = IR_1$$

Then

$$I_p(R_3 + r_p) = \mu IR_1 \quad (3-9)$$

Also, it follows that

$$IR_2 - I_p R_3 = 0$$

or

$$IR_2 = I_p R_3 \quad (3-10)$$

The ratio of Eq. (3-9) to Eq. (3-10) is

$$\frac{R_3 + r_p}{R_3} = \mu \frac{R_1}{R_2}$$

from which

$$r_p = R_3 \left( \mu \frac{R_1}{R_2} - 1 \right) \quad (3-11)$$

Although this bridge may be used to evaluate  $r_p$ , the result would be dependent on the measurement of  $\mu$ . If, however,  $R_1$  is chosen in such a way that  $\mu R_1/R_2 \gg 1$ , then approximately

$$r_p \doteq \mu \frac{R_3 R_1}{R_2}$$

or

$$g_m = \frac{\mu}{r_p} = \frac{R_2}{R_3 R_1} \quad (3-12)$$

The plate resistance  $r_p$  of the tube can be measured directly by incor-

porating the plate circuit of the tube as the fourth arm of a Wheatstone bridge, as shown in Fig. 3-10. When the bridge is balanced,

$$r_p = \frac{R_2 R_3}{R_1} \tag{3-13}$$

The above circuits do not yield perfect balance owing to the capacitive effects of the tube, and it is sometimes necessary to provide a means for balancing these effects. Basically, however, the circuits are those given.

**3-5. Current-source Equivalent Circuit.** The current-source equivalent circuit differs from the voltage-source equivalent circuit discussed in Sec. 3-3 principally in replacing the tube by a current generator which supplies a current  $g_m e_{gk}$  in the direction from plate-cathode within the tube, and with the plate resistance  $r_p$  across the generator terminals. The result, illustrated in Fig. 3-11, follows directly from Eq. (3-6),

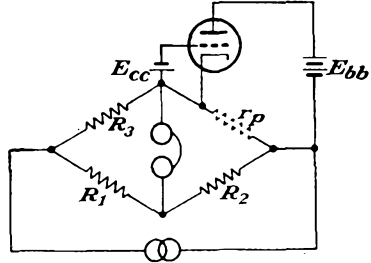


FIG. 3-10. A Wheatstone bridge for determining the plate resistance of a triode under operating conditions.

$$g_m e_g = i_p - \frac{e_p}{r_p} \tag{3-14}$$

or in more complete notation

$$g_m e_{gk} = i_p - \frac{e_{pk}}{r_p} \tag{3-15}$$

Equation (3-15) is interpreted to mean that the tube acts as a generator that supplies a current  $g_m e_{gk}$ . This current divides between  $r_p$  and the

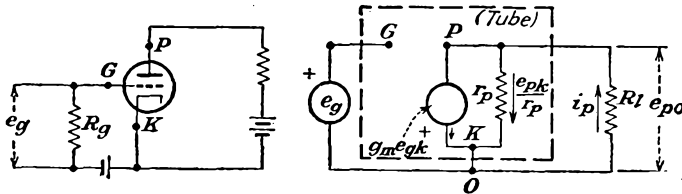


FIG. 3-11. The schematic and current-source equivalent circuit of a simple triode amplifier.

load current  $i_p$ . Note that, if the load impedance is small compared with the plate resistance, then, clearly, the load current may be considered to be substantially constant and equal to  $g_m e_{gk}$ . It will be shown later that this condition applies for a pentode.

**3-6. Harmonic Generation in a Tube.** The analysis of Sec. 3-3 usually permits an adequate solution of an amplifier circuit when the limitations of the method are not exceeded or if relatively slight differences are considered of no importance. There are occasions when it is desirable to examine critically the effects of the assumptions.

The assumption of linear operation, which is implied in Eq. (3-3) and which assumed that higher-order terms in the Taylor expansion of the current  $i_b(e_b, e_c)$  are negligible, is not always valid. This assumption, which allowed the graphical solution of Fig. 3-5 to be replaced by the analytical one of Fig. 3-6, requires that the dynamic characteristic of the amplifier circuit be linear over the range of operation. Actually, the dynamic characteristic is not linear in general but contains a slight curvature. This nonlinear characteristic arises because the  $i_b$ - $e_b$  static characteristics (see Fig. 3-3) are not equidistant lines for constant  $e_c$  intervals over the range of operation. The effect of this nonlinear dynamic characteristic is a nonsinusoidal output wave shape when the input wave is sinusoidal. Such an effect is known as *nonlinear* or *amplitude* distortion.

It is possible to obtain a measure of the degree of nonlinearity that results from the existence of the nonlinear dynamic curve. To do this, it is observed that the dynamic curve with respect to the  $Q$  point may be expressed by a power series of the form

$$i_p = a_1 e_q + a_2 e_q^2 + a_3 e_q^3 + \dots \quad (3-16)$$

Clearly, if all terms in this series vanish except the first, then the linear assumptions of the equivalent-circuit concept result. It will be found that triodes, when operated under normal conditions, may be adequately expressed by retaining the first two terms in the expansion. When a triode is operated with such a large signal that the instantaneous grid-cathode potential becomes positive, or if the triode is operated with such a bias that the very curved portions of the plate characteristics must be employed, more than two terms must be retained in the expansion. Likewise, it is found that the parabolic approximation is not adequate to represent the dynamic curve of a tetrode or a pentode under normal operating conditions. If the dynamic curve contains an extreme curvature or if the operation is over an extreme range, it is sometimes found preferable to devise special methods of analysis. Such special methods will be used in the analysis of a tuned class C amplifier in Chap. 11.

Suppose that the dynamic curve may be represented as in Eq. (3-16), and consider that the input wave is a simple cosine function of time, of the form

$$e_q = E_{qm} \cos \omega t \quad (3-17)$$

By combining this expression with Eq. (3-16) and expanding the higher-order powers of the cosine that appear in the resulting series, the result may be shown to have the form

$$i_b = I_b + B_0 + B_1 \cos \omega t + B_2 \cos 2\omega t + B_3 \cos 3\omega t + \dots \quad (3-18)$$

If it is assumed that the excitation voltage is a sine function of the time instead of the cosine form chosen, the resulting Fourier series representing

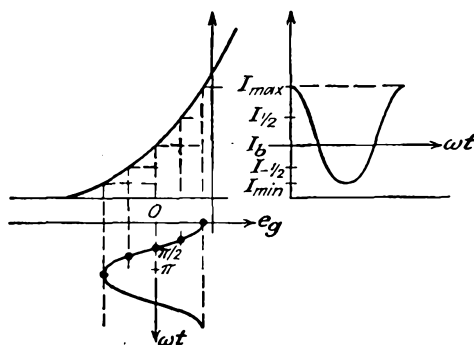


FIG. 3-12. The construction for obtaining the plate-current values to be used in the five-point schedule for determining the Fourier coefficients.

the output current will be found to contain odd sine components and even cosine components.

A number of different methods exist for obtaining the coefficients  $B_0$ ,  $B_1$ ,  $B_2$ , etc. One of the more common methods is best discussed by reference to Fig. 3-12. It will be assumed for convenience that only five terms,  $B_0$ ,  $B_1$ ,  $B_2$ ,  $B_3$ ,  $B_4$ , exist in the resulting Fourier series. In order to evaluate these five coefficients, the values of the current at five different values of  $e_g$  are required. The values chosen are  $I_{max}$ ,  $I_{1/2}$ ,  $I_b$ ,  $I_{-1/2}$ , and  $I_{min}$  and correspond, respectively, to the following values of  $e_g$ : the maximum positive value; one-half the maximum positive value; zero; one-half the maximum negative value; the maximum negative value.

It is evident from the figure that the currents are those chosen as shown at the angles

$$\left. \begin{aligned} \omega t = 0 & & i_b = I_{max} \\ \omega t = \frac{\pi}{3} & & i_b = I_{1/2} \\ \omega t = \frac{\pi}{2} & & i_b = I_b \\ \omega t = \frac{2\pi}{3} & & i_b = I_{-1/2} \\ \omega t = \pi & & i_b = I_{min} \end{aligned} \right\} \quad (3-19)$$

By combining these results with Eq. (3-18), five equations containing five

unknowns are obtained. The simultaneous solution of these equations yields

$$\left. \begin{aligned} B_0 &= \frac{1}{6} (I_{\max} + 2I_{\frac{1}{2}} + 2I_{-\frac{1}{2}} + I_{\min}) - I_b \\ B_1 &= \frac{1}{3} (I_{\max} + I_{\frac{1}{2}} - I_{-\frac{1}{2}} - I_{\min}) \\ B_2 &= \frac{1}{4} (I_{\max} - 2I_b + I_{\min}) \\ B_3 &= \frac{1}{6} (I_{\max} - 2I_{\frac{1}{2}} + 2I_{-\frac{1}{2}} - I_{\min}) \\ B_4 &= \frac{1}{12} (I_{\max} - 4I_{\frac{1}{2}} + 6I_b - 4I_{-\frac{1}{2}} + I_{\min}) \end{aligned} \right\} \quad (3-20)$$

The percentage of harmonic distortion is defined as

$$D_2 = \frac{B_2}{B_1} \times 100\% \quad D_3 = \frac{B_3}{B_1} \times 100\% \quad D_4 = \frac{B_4}{B_1} \times 100\% \quad (3-21)$$

where  $D_s$  ( $s = 2, 3, 4, \dots$ ) represents the per cent distortion of the  $s$ th harmonic and the total distortion is defined as

$$D = \sqrt{D_2^2 + D_3^2 + D_4^2 + \dots} \quad (3-22)$$

For the case where a three-point schedule is sufficient, and, as already indicated, this would apply for a triode under normal operating conditions, the analysis yields the expressions

$$\left. \begin{aligned} B_1 &= \frac{1}{2} (I_{\max} - I_{\min}) \\ B_2 = B_0 &= \frac{1}{4} (I_{\max} - 2I_b + I_{\min}) \end{aligned} \right\} \quad (3-23)$$

### PROBLEMS

**3-1.** A 6C5 triode is used in the circuit of Fig. 3-1, the plate characteristics of which are given in Appendix B.

- With  $E_{bb} = 300$  volts,  $E_{cc} = -8$  volts,  $R_l = 20\text{k}$ , draw the load line, and locate the operating point. Plot the dynamic characteristic.
- If  $e_g = 6 \sin 10,000t$ , determine graphically the output current, and plot the curve as a function of  $\omega t$ .
- From these curves, determine and plot the instantaneous plate voltage for the same interval. Check the phase relation between a-c components of grid voltage, plate current, and plate voltage.

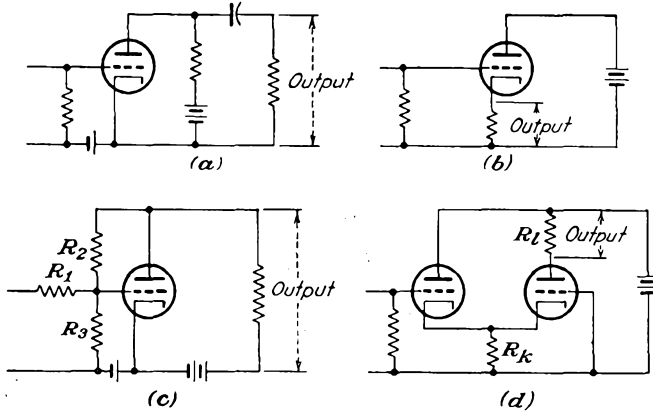
**3-2.** The characteristics of a given triode may be represented by the expression

$$I_b = 8.8 \times 10^{-3} (E_b + 16E_c)^{1.5} \quad \text{ma}$$

It is to be operated at a plate potential  $E_b = 250$  volts and a grid-bias voltage  $E_c = -9$  volts.

- Calculate the plate resistance of the tube.
- If this tube is used in the circuit of Fig. 3-1 with a load resistor  $R_l = 10\text{k}$ , determine the plate-supply voltage necessary for the tube to be operating under the specified conditions.
- Suppose that the grid driving source applies a voltage  $e_g = 8 \sin \omega t$  to the grid. Determine the a-c potential across the load resistor.

3-3. Draw the voltage-source equivalent circuits of the electron-tube circuits in the accompanying diagram.



3-4. A type 6A3 triode is used in an amplifier circuit to supply power to a 3,000-ohm resistor. In this circuit  $E_{cc} = -45$  volts,  $E_{bb} = 350$  volts. A 45-volt peak a-c signal is applied to the grid.

- Plot the dynamic curve of the tube.
- Assume that only the fundamental and a second harmonic exist in the output. Determine the magnitudes of each.
- Plot a curve showing the output current for the sinusoidal input. On the same sheet, plot the corresponding results from the calculations in part b.

3-5. It is possible to obtain a five-point schedule for determining the coefficients  $B_0, B_1, B_2, B_3, B_4$  by almost any sensible choice of angle. Determine the five-point schedule for determining the coefficients  $B$  in terms of  $I_{max}, I_{0.707}, I_b, I_{-0.707}, I_{min}$ .

---

## CHAPTER 4

### BASIC AMPLIFIER PRINCIPLES

THE classification of an amplifier is usually somewhat involved, owing to the fact that a complete classification must include information about the tubes that are used, the conditions of the bias, the character of the circuit elements connected to the tubes, the function of the circuit, and the range of operation. Certain of these factors will be discussed here, but many will be deferred for later discussion.

**4-1. Classification of Tubes and Amplifiers.** Apart from the wide variety of vacuum tubes of the diode, triode, tetrode, pentode, beam, hexode, heptode, and multiunit types and the varied power capacities of each type, it is possible to classify the tubes according to their principal applications. Tubes may be classified roughly into five groups, *viz.*, voltage-amplifier tubes, power-amplifier tubes, current-amplifier tubes, general-purpose tubes, and special-purpose tubes.

1. Voltage-amplifier tubes have a relatively high amplification factor and are used where the primary consideration is one of high voltage gain. Such tubes usually operate into a high impedance load, either tuned or untuned.

2. Power-amplifier tubes are those which have relatively low values of amplification factor and fairly low values of plate resistance. They are capable of controlling appreciable currents at reasonably high plate potentials.

3. Current-amplifier tubes are those which are designed to give a large change of plate current for a small grid potential; *i.e.*, they possess a high transconductance. These tubes may be required to carry fairly large plate currents. Such tubes find application as both voltage and power amplifiers, depending on the tube capacity.

4. General-purpose amplifier tubes are those whose characteristics are intermediate between the voltage- and the power-amplifier tubes. They must have a reasonably high amplification factor and yet must be able to supply some power.

5. Special-purpose tubes include a wide variety of types. The hexode, heptode, and multiunit tubes are of this type.

Amplifiers are classified according to their frequency range, the method of tube operation, and the method of interstage coupling. For example,

they may be classed as direct-coupled amplifiers, audio-frequency (a-f) amplifiers, video amplifiers, or tuned r-f amplifiers if some indication of the frequency of operation is desired. Also, the position of the quiescent point and the extent of the tube characteristic that is being used will

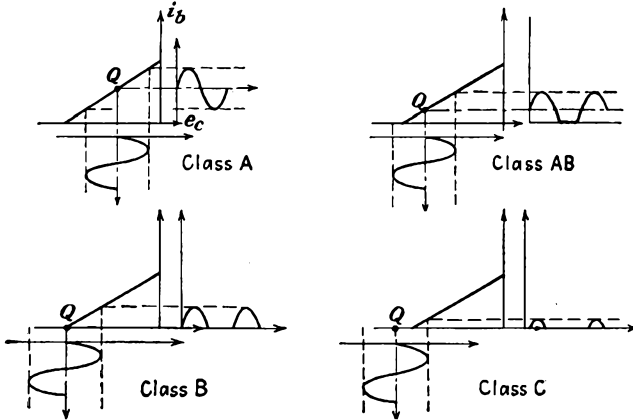


FIG. 4-1. Amplifier classification in terms of the position of the quiescent point of the tubes.

determine the method of tube operation. This will specify whether the tube is being operated in class A, class AB, class B, or class C. These definitions are illustrated graphically in Fig. 4-1.

1. A class A amplifier is an amplifier in which the grid bias and the a-c grid potentials are such that plate current flows in the tube at all times.

2. A class AB amplifier is one in which the grid bias and the a-c grid potentials are such that plate current flows in the tube for appreciably more than half but less than the entire electrical cycle.

3. A class B amplifier is one in which the grid bias is approximately equal to the cutoff value of the tube, so that the plate current is approximately zero when no exciting grid potential is applied, and such that plate current flows for approximately one-half of each cycle when an a-c grid voltage is applied.

4. A class C amplifier is one in which the grid bias is appreciably greater than the cutoff value, so that the plate current in each tube is zero when no a-c grid voltage is applied, and such that plate current flows for appreciably less than one-half of each cycle when an a-c grid potential is applied.

To indicate that grid current does not flow during any part of the input cycle, the suffix 1 is frequently added to the letter or letters of the class identification. The suffix 2 is added to denote that grid current does flow during some part of the cycle. For example, the designation class

$AB_1$  indicates that the amplifier operates under class AB conditions and that no grid current flows during any part of the input cycle.

Voltage amplifiers, whether tuned or untuned, generally operate in class A. Low-power audio amplifiers may be operated under class A and, with special connections, under class AB or class B conditions. Tuned r-f power amplifiers are operated either under class B or under class C conditions. Oscillators usually operate under class C conditions. A detailed discussion is deferred until the appropriate point in the text. When a tube is used essentially as a switch, no classification is ordinarily specified.

**4-2. Distortion in Amplifiers.** The application of a sinusoidal signal to the grid of an ideal class A amplifier will be accompanied by a sinusoidal output wave. Frequently the output wave form is not an exact replica of the input signal wave form because of distortion that results either within the tube or from the influence of the associated circuit. The distortions that may exist either separately or simultaneously are nonlinear distortion, frequency distortion, and delay distortion. These are defined as follows:

1. Nonlinear distortion is that form of distortion which occurs when the ratio of voltage to current is a function of the magnitude of either.

2. Frequency distortion is that form of distortion in which the change is in the relative magnitudes of the different frequency components of a wave, provided that the change is not caused by nonlinear distortion.

3. Delay distortion is that form of distortion which occurs when the phase angle of the transfer impedance with respect to two chosen pairs of terminals is not linear with frequency within a desired range, the time of transmission, or delay, varying with frequency in that range.

In accordance with definition 1, nonlinear distortion results when new frequencies appear in the output which are not present in the input signal. These new frequencies arise from the existence of a nonlinear dynamic curve and are discussed in Sec. 3-6.

Frequency distortion arises when the components of different frequency are amplified by different amounts. This distortion is usually a function of the character of the circuits associated with the amplifier. If the gain vs. frequency characteristic of the amplifier is not a horizontal straight line over the range of frequencies under consideration, the circuit is said to exhibit frequency distortion over this range.

Delay distortion, also called *phase-shift distortion*, results from the fact that the phase shift of waves of different frequency in the amplifier is different. Such distortion is not of importance in amplifiers of the a-f type, since delay distortion is not perceptible to the ear. It is very objectionable in systems that depend on wave shape for their operation, as, for example, in television or facsimile systems. If the phase shift is

proportional to the frequency, a time delay will occur although no distortion is introduced. To see this, suppose that the input signal to the amplifier has the form

$$e_g = E_{m1} \sin(\omega t + \theta_1) + E_{m2} \sin(2\omega t + \theta_2) + \dots \quad (4-1)$$

If the gain  $K$  is constant in magnitude but possesses a phase shift that is proportional to the frequency, the output will be of the form

$$e_p = KE_{m1} \sin(\omega t + \theta_1 + \psi) + KE_{m2} \sin(2\omega t + \theta_2 + 2\psi) + \dots$$

This output voltage has the same wave shape as the input signal, but a time delay between these two waves exists. By writing

$$\omega t' = \omega t + \psi$$

then

$$e_p = KE_{m1} \sin(\omega t' + \theta_1) + KE_{m2} \sin(2\omega t' + \theta_2) + \dots \quad (4-2)$$

This is simply the expression given by Eq. (4-1), except that it is referred to a new time scale  $t'$ . Delay distortion, like frequency distortion, arises from the frequency characteristics of the circuit associated with the vacuum tube.

**4-3. The Decibel; Power Sensitivity.** In many problems where two power levels are to be compared, it is found very convenient to compare the relative powers on a logarithmic rather than on a direct scale. The unit of this logarithmic scale is called the *bel*. A *decibel*, which is abbreviated db, is  $\frac{1}{10}$  bel. By definition, two power sources are in the ratio of  $N$  bels, according to

$$\left. \begin{aligned} \text{Number of bels} &= \log_{10} \frac{P_2}{P_1} \\ \text{Number of db} &= 10 \log_{10} \frac{P_2}{P_1} \end{aligned} \right\} \quad (4-3)$$

It should be emphasized that the bel or the decibel denotes a power ratio. Consequently the specification of a certain power in decibels is meaningless unless a reference level is implied or is explicitly specified. In communication applications it is usual practice to specify 6 mw as the zero reference level. However, any power may be designated as the zero reference level in any particular problem.

Suppose that these considerations are applied to a power amplifier, with  $P_2$  the output power and  $P_1$  the input power. This assumes that the input circuit to the amplifier absorbs power. If the grid circuit does not absorb an appreciable power, then the term *decibel gain* of the amplifier means nothing. Under such conditions, it is customary to speak of *power sensitivity*, which is defined as the ratio of the power output to the

square of the input signal voltage. Thus

$$\text{Power sensitivity} \equiv \frac{P}{E_o^2} \quad \text{mhos} \quad (4-4)$$

where  $P$  is the power output in watts and  $E_o$  is the input signal rms volts.

If the input and output impedances are equal resistances, then  $P_2 = E_2^2/R$  and  $P_1 = E_1^2/R$ , where  $E_2$  and  $E_1$  are the output and input potentials. Under this condition, Eq. (4-3) reduces to

$$\text{Number of db} = 20 \log_{10} \frac{E_2}{E_1} \quad (4-5)$$

In general, the input and output resistances are not equal. Despite this, this expression is adopted as a convenient definition of the decibel voltage gain of an amplifier. It is essential, however, when the gain of an amplifier is discussed, that it be clearly stated whether one is referring to voltage gain or power gain, as these two figures will be different, in general.

Many of the considerations of the foregoing sections are best illustrated by several examples.

**Example 1:** Calculate the gain of the amplifier circuit of Fig. 4-2.

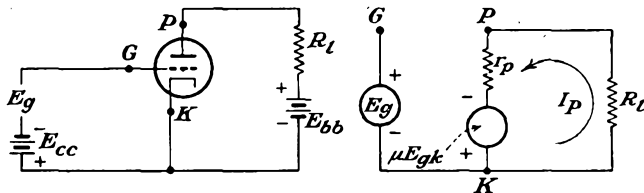


FIG. 4-2. Schematic and equivalent circuits of a simple amplifier.

*Solution:* The equivalent circuit of the amplifier is drawn according to the rules of Sec. 3-3 and is that of Fig. 4-2b. The application of the Kirchoff voltage law to the equivalent circuit yields

$$I_p(R_l + r_p) - \mu E_{gk} = 0$$

But the potential difference  $E_{gk}$  is simply  $E_g$ . The output current is then

$$I_p = \frac{\mu E_g}{R_l + r_p} \quad (4-6)$$

and the corresponding output potential is

$$E_{pk} = -I_p R_l = \frac{-\mu E_g R_l}{R_l + r_p} \quad (4-7)$$

The gain, or voltage amplification, of the amplifier is the ratio of the output to the input potentials and is

$$K = \frac{E_{pk}}{E_{gk}} = \frac{-\mu R_l}{R_l + r_p} = -\frac{\mu}{1 + r_p/R_l} \quad (4-8)$$

A plot of this expression as a function of the load resistance is given in Fig. 4-3. Note that the maximum possible gain is  $\mu$  although this gain cannot be achieved with finite values of  $R_L$ . However, the gain  $K$  increases rapidly with  $R_L$ , and an amplifier with significant gain is easily achieved.

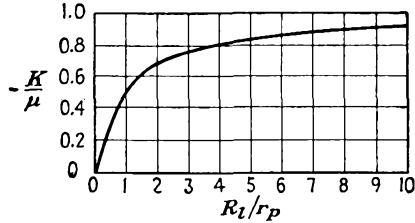
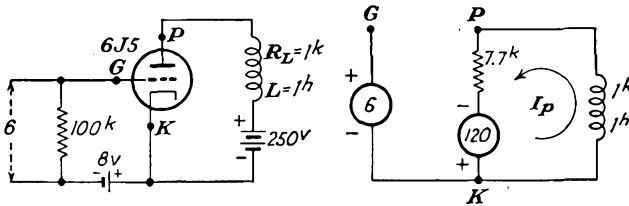


FIG. 4-3. The gain of the amplifier of Fig. 4-2 as a function of load resistance.

**Example 2:** A type 6J5 triode for which  $\mu = 20$ ,  $r_p = 7,700$  ohms is employed in an amplifier, the load of which consists of an inductance for which  $R_L = 1,000$  ohms and  $L = 1$  henry. Calculate the gain and phase shift of the amplifier at  $\omega = 2,000$  rad/sec and  $\omega = 10,000$  rad/sec. Draw the complete voltage sinor\* diagram of the system. The input signal is 6 volts rms.

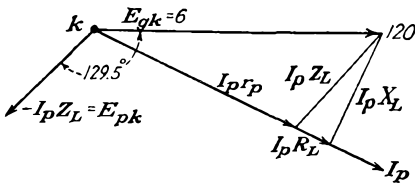
*Solution:* The schematic and equivalent circuits are shown in the accompanying diagram. At  $\omega = 2,000$  rad/sec,



$$I_p = \frac{120 + j0}{7,700 + (1,000 + j2,000)} = 13.1 - j3.01 \text{ ma}$$

The output potential is

$$E_{pk} = -(1,000 + j2,000)(13.1 - j3.01) \times 10^{-3} \\ = -(19.1 + j23.2) = 30.1 / -129.5^\circ$$



The gain is given by

$$K = \frac{E_{pk}}{E_{vk}} = \frac{30.1 / -129.5^\circ}{6 / 0} = 5.01 / -129.5^\circ$$

The voltage sinor diagram has the form shown in the sketch. At  $\omega = 10,000$

rad/sec,

$$I_p = \frac{120 + j0}{7,700 + (1,000 + j10,000)} = 5.94 - j6.83 \text{ ma}$$

\* A number of different terms have been used to describe the rotating line segment, the projection of which generates a sinusoid. The term *sinor* is used in this text. Other terms that appear in the literature are: *vector*, *complex vector*, *complexor*, and *phasor*.

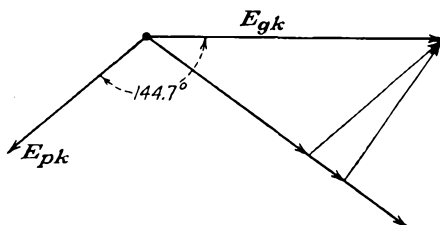
The output voltage is

$$\begin{aligned} E_{pk} &= -(1,000 + j10,000)(5.94 - j6.83) \times 10^{-3} \\ &= -(74.2 + j52.6) \\ &= 90.8 \angle -144.7^\circ \end{aligned}$$

The gain is given by

$$K = \frac{90.8 \angle -144.7^\circ}{6 \angle 0} = 15.1 \angle -144.7^\circ$$

The voltage sinor diagram has the form of the accompanying diagram.



The results are tabulated for convenience. An examination of the results indicates the presence of frequency distortion, since the gain at  $\omega = 2,000$  rad/sec is different from that at  $\omega = 10,000$  rad/sec. Also, phase-shift distortion exists in this amplifier.

$\omega$	Gain and phase	Voltage db gain
2,000	5.01 $\angle -129.5^\circ$	14 db
10,000	15.1 $\angle -144.7^\circ$	23.6 db

**4-4. Interelectrode Capacitances in a Triode.** It was assumed in the foregoing discussions that, with a negative bias on the grid, the grid driving-source current was negligible. This is generally true if one examines only the current intercepted by the grid because of its location within the region of the electron stream. Actually though, owing to the physical proximity of the elements of the tube, interelectrode capacitances between pairs of elements exist. These capacitances are important in the behavior of the circuit, as charging currents do exist.

Owing to the capacitance that exists between the plate and the grid, it is not true that the grid circuit is completely independent of the plate circuit. Since the capacitance between plate and grid is small, the approximation that the plate circuit is independent of the grid circuit is valid at the lower frequencies. However, at the higher frequencies, interelectrode capacitances may seriously affect the operation.

A more complete schematic diagram and its equivalent circuit are given in Fig. 4-4. In this circuit,  $C_{gp}$  denotes the capacitance between the grid

and the plate,  $C_{gk}$  is the grid-cathode capacitance, and  $C_{pk}$  is the capacitance between the plate and the cathode. The solution for the gain of this circuit is readily effected with the aid of the Millman theorem (see Appendix A). The point  $O'$  in Eq. (A-1) corresponds to the plate terminal  $P$ , and the point  $O$  is the cathode terminal  $K$ . Four branches must be considered between these points: the load impedance with zero potential; the

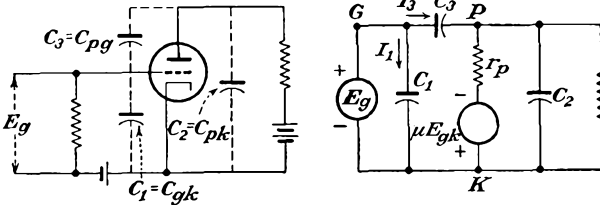


FIG. 4-4. Schematic and equivalent circuits of an amplifier, including the inter-electrode capacitances.

capacitor  $C_2$  with zero potential; the potential rise  $\mu E_g$  in series with  $r_p$ ; the potential  $E_g$  in series with  $C_3$ . The capacitor  $C_1$  which exists across the input  $E_g$  does not appear in the equation. This latter follows from the fact that the exact circuit connections between points 0, 1, 2, and 3 of Fig. A-1 need not be specified. The result is

$$E_{pk} = \frac{-\mu E_g Y_p + E_g Y_3}{Y_p + Y_l + Y_2 + Y_3} \tag{4-9}$$

- where  $Y_p = 1/r_p$  is the admittance corresponding to  $r_p$
- $Y_2 = j\omega C_2$  is the admittance corresponding to  $C_2$
- $Y_3 = j\omega C_3$  is the admittance corresponding to  $C_3$
- $Y_l = 1/Z_l$  is the admittance corresponding to  $Z_l$
- $E_{pk}$  = potential difference between  $P$  and  $K$ , or the voltage across the load impedance

The vector voltage gain is given by

$$K = \frac{\text{output voltage}}{\text{input voltage}} = \frac{E_{pk}}{E_{gk}} = \frac{E_{pk}}{E_g}$$

and may be written in the form

$$K = \frac{Y_3 - g_m}{Y_p + Y_l + Y_2 + Y_3} \tag{4-10}$$

In this expression, use has been made of the fact that  $g_m = \mu/r_p$ .

In this analysis, a number of factors have been neglected. It has been assumed that no conduction or leakage currents exist between tube terminals. Such leakage current will depend upon many variable factors—the spacing between electrodes, the material of the base, the conditions of the surface of the glass and the tube base, and perhaps the surface

leakage between connecting wires. Ordinarily the error is small in neglecting the effects of this surface leakage. If this assumption is not true, the effect can be taken into account by writing for each interelectrode admittance  $g_s + j\omega C_s$  instead of  $j\omega C_s$ , where  $g_s$  takes account of the leakage current and also dielectric losses. Interwiring and stray capacitances must be taken into account. This may be done by considering them to be in parallel with  $C_1$ ,  $C_2$ , and  $C_3$ .

The error made in the calculation of the gain by neglecting the interelectrode capacitances is very small over the a-f spectrum. These interelectrode capacitances are usually 10  $\mu\mu\text{f}$  or less, which corresponds to an admittance of less than 2  $\mu\text{mhos}$  at 20,000 cps. This is to be compared with the mutual conductance of the tube of, say, 1,500  $\mu\text{mhos}$  at the normal operating point. Likewise  $Y_2 + Y_3$  is usually negligible compared with  $Y_p + Y_v$ . Under these conditions, the expression for the gain [Eq. (4-10)] reduces to Eq. (4-8).

**4-5. Input Admittance of a Triode.** Owing to the presence of the interelectrode capacitances, the grid circuit is no longer isolated from the plate circuit. In fact, with a positive-going signal on the grid and with the consequent negative-going potential on the plate, an appreciable change of potential appears across the capacitance  $C_{gp}$ , with a consequent appreciable current flow. Also, the potential change across the capacitance  $C_{pk}$  is accompanied by a current flow. Clearly, therefore, the input signal source must supply these currents. To calculate this current, it is noted from the diagram that

$$I_1 = E_g Y_1$$

and

$$I_3 = E_{gp} Y_3 = (E_g - E_{pk}) Y_3$$

But from the fact that

$$E_{pk} = K E_{gp} = K E_g$$

then the total input current is

$$I_i = I_1 + I_3 = [Y_1 + (1 - K)Y_3]E_g$$

The input admittance, given by the ratio  $Y_i = I_i/E_g$ , is

$$Y_i = Y_1 + (1 - K)Y_3 \quad (4-11)$$

If  $Y_i$  is to be zero, evidently both  $Y_1$  and  $Y_3$  must be zero, since  $K$  cannot, in general, be  $1/0$  deg. Thus, for the system to possess a negligible input admittance over a wide range of frequencies, the grid-cathode and the grid-plate capacitances must be negligible.

Consider a triode with a pure resistance load. At the lower frequencies, the gain is given by the simple expression [Eq. (4-8)]

$$K = \frac{-\mu R_l}{R_l + r_p}$$

In this case, Eq. (4-11) becomes

$$Y_i = j\omega \left[ C_1 + \left( 1 + \frac{\mu R_l}{R_l + r_p} \right) C_3 \right] \tag{4-12}$$

Thus the input admittance is that from a capacitor between grid and cathode of magnitude

$$C_i = C_1 + \left( 1 + \frac{\mu R_l}{R_l + r_p} \right) C_3 \tag{4-13}$$

Owing to the magnitude of the gain, the input capacitance is considerably higher than any of the interelectrode capacitances. The presence of this capacitance will be found to affect the operation of the amplifier.

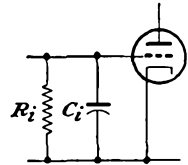


FIG. 4-5. The equivalent input circuit of a triode.

For the general case when the gain of the amplifier  $K$  is a complex quantity, the input admittance will consist of two terms, a resistive and a reactive term. For the case of an inductive load, the gain  $K$  may be written in the form (see Sec. 4-3, Example 2)

$$K = -(k_1 + jk_2) \tag{4-14}$$

and Eq. (4-11) becomes

$$Y_i = -\omega C_3 k_2 + j\omega [C_1 + (1 + k_1)C_3] \tag{4-15}$$

This expression indicates that the equivalent input circuit comprises a resistance (which is negative in this particular case, although it will be positive for a capacitive load) in parallel with a capacitance  $C_i$ , as shown in Fig. 4-5. The equivalent elements have the form

$$R_i = -\frac{1}{\omega C_3 k_2} \tag{4-16}$$

and the capacitor

$$C_i = C_1 + (1 + k_1)C_3 \tag{4-17}$$

As indicated in the above development, it is possible for the term  $k_2$  to be negative (with an inductive load). Under these circumstances the effective input resistance will be negative. Physically, this means that power is being fed back from the output circuit into the grid circuit through the coupling provided by the grid-plate capacitance. If this feedback reaches an extreme stage, the amplifier will oscillate. These

feed-back effects in an amplifier will be examined in some detail in Sec. 5-8.

**4-6. Input Admittance of a Tetrode.** The basic equivalent circuit of the tetrode is essentially that of the triode, even though a screen grid exists in the tetrode. A schematic diagram of a simple amplifier circuit employing a tetrode is given in Fig. 4-6. In drawing the equivalent circuit, the rules given in Sec. 3-3 have been appropriately extended and

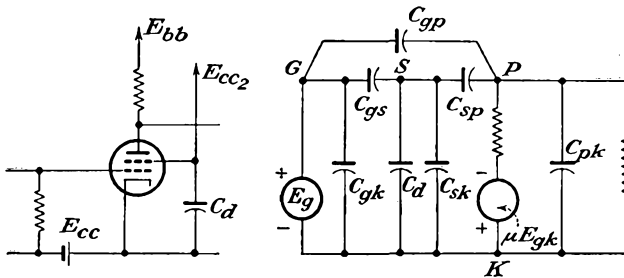


FIG. 4-6. Schematic and equivalent circuits of a tetrode in an amplifier circuit.

employed. This requires the introduction of a point *S*, the screen terminal, in addition to the points *K*, *G*, and *P*.

Notice that the screen potential is maintained at a fixed d-c potential with respect to cathode and is at zero potential in so far as a-c variations about the *Q* point is concerned. As indicated in the figure, this effectively places a short circuit across  $C_{ks}$  and puts  $C_{gk}$  and  $C_{gs}$  in parallel. This parallel combination is denoted  $C_1$ .

The capacitance  $C_{ps}$  now appears from plate to cathode and is effectively in parallel with  $C_{pk}$ . This parallel combination is denoted  $C_2$ . Also, from the discussion in Sec. 2-6, the shielding action of the screen is such that the capacitance  $C_{pg}$  between grid and plate is very small. If this capacitance is assumed to be negligible, and it is less than  $0.001 \mu\text{mf}$  in the average voltage tetrode, then Fig. 4-6b may be redrawn in the form shown in Fig. 4-7. In this figure, the capacitances have the values

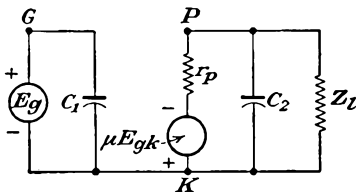


FIG. 4-7. The ideal equivalent circuit of a tetrode amplifier.

$$\left. \begin{aligned} C_1 &= C_{gk} + C_{gs} \\ C_2 &= C_{ps} + C_{pk} \end{aligned} \right\} \quad (4-18)$$

The input admittance of the tube is then

$$Y_i = j\omega C_1 \quad (4-19)$$

The mere substitution of a tetrode for a triode may not result in a very

marked improvement in the amplifier response. This follows from the fact that the stray and wiring capacitances external to the tube may allow significant grid-plate coupling. It is necessary that care be exercised in order that plate and grid circuits be shielded or widely separated from each other in order to utilize the inherent possibilities of the tube.

**4-7. Input Admittance of a Pentode.** The discussion in Sec. 2-6 showed that, even though the tetrode had a significantly smaller grid-plate capacitance than the triode, the presence of the screen grid was accompanied by the effects of secondary emission from the plate when the instantaneous plate potential fell below the screen potential. As

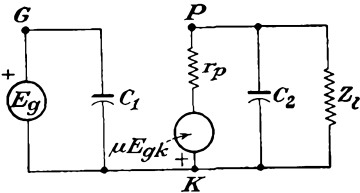


FIG. 4-8. The equivalent circuit of a pentode amplifier.

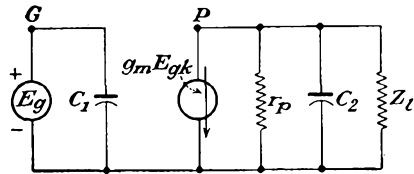


FIG. 4-9. The current source equivalent circuit of the pentode amplifier.

discussed, the effect of this is overcome by the insertion of a suppressor grid between the screen grid and the plate.

When used in a circuit as a voltage amplifier, the pentode is connected in the circuit exactly like the tetrode with the addition that the suppressor grid is connected to the cathode. By drawing the complete equivalent circuit of the pentode amplifier, by appropriately extending the rules of Sec. 3-3, and by including all tube capacitances, it is easy to show that the equivalent circuit reduces to that shown in Fig. 4-8. In this diagram

$$\left. \begin{aligned} C_1 &= C_{gk} + C_{gs} \\ C_2 &= C_{pk} + C_{ps} + C_{p3} \end{aligned} \right\} \quad (4-20)$$

where  $C_{p3}$  is the plate-grid No. 3 capacitance.

The plate load impedance  $Z_l$  is frequently much smaller than the plate resistance of the tube, and it is convenient to use the current-source equivalent circuit representation of the tube, as shown. For the range of frequencies over which the input and output capacitances  $C_1$  and  $C_2$  are negligible, and with  $r_p \gg Z_l$ , the total generator current passes through  $Z_l$ . Under these circumstances the output potential is

$$E_{pk} = -g_m E_g Z_l$$

and the gain is given by the simple form

$$K = -g_m Z_l \quad (4-21)$$

If the assumed conditions are not valid, then the gain becomes

$$K = -g_m Z \quad (4-22)$$

where  $Z$  is the combined parallel impedance in the output circuit.

**4-8. Voltage Sources for Amplifiers.** A number of different potential sources are required in an amplifier. These are the following: the filament, or A, supply; the plate, or B, supply  $E_{bb}$ ; the grid-bias, or C, supply  $E_{cc}$ ; the screen supply  $E_{cc2}$ . These potentials are supplied in different ways.

*The Filament, or A, Supply.* The most common method of heating the cathodes of indirectly heated tubes is from a low-voltage winding on a transformer which operates from the a-c supply lines. Storage batteries may be used if d-c heating is necessary, but this is ordinarily not necessary except in special applications. Special low-drain tubes are available for use in portable radio sets and are fed from dry batteries.

*The Plate, or B, Supply  $E_{bb}$ .* Most equipments involving the use of electron tubes are operated from the a-c supply mains, and the d-c plate supply is then secured by means of a rectifier and filter unit (see Chaps. 13 and 14 for details). For applications with severe requirements on regulation or low ripple, the power supply must be electronically regulated. For low-drain requirements, dry batteries may be used.

*The Grid, or C, Supply  $E_{cc}$ .* The grid circuit of most amplifiers ordinarily requires very little current, and hence low-power dry batteries may be used. In most cases, however, self-bias is used (although this is restricted to class A and class AB amplifiers). Self-bias is achieved by including a resistor  $R_k$  in the cathode of the amplifier tube and shunting this resistor with a capacitor  $C_k$ , the reactance of which is small compared with  $R_k$  over the operating frequency range. The quiescent current  $I_b$  flows through this resistor, and the potential difference provides the grid bias. The correct self-biasing resistor  $R_k = E_{cc}/I_b$ .

The capacitor  $C_k$  serves to by-pass any a-c components in the plate current, so that no a-c component appears across the resistor  $R_k$ . If such an a-c component, or varying bias, does exist, then clearly there is a reaction between the plate circuit and the input circuit. Such a "feedback" effect will receive detailed consideration in Sec. 5-7. If this effect is to be avoided, large-capacitance condensers may be required, particularly if the frequency is low. High-capacitance low-voltage electrolytic capacitors are available for this specific service and are quite small physically.

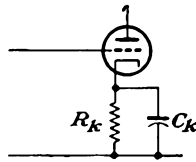


FIG. 4-10. Obtaining self-bias by means of a cathode resistor.

*The Screen Supply  $E_{cc2}$ .* The screen supply is ordinarily obtained from the plate-supply source. In most cases the screen potential is lower than the plate supply, and it is usual practice to connect the screen to the plate supply through a resistor. The resistor is chosen of such a size that the potential drop across it due to the screen current will set the screen at the desired potential. A capacitor is then connected from the screen to the cathode so as to maintain this potential constant and independent of B-supply variations or variations in the screen current.

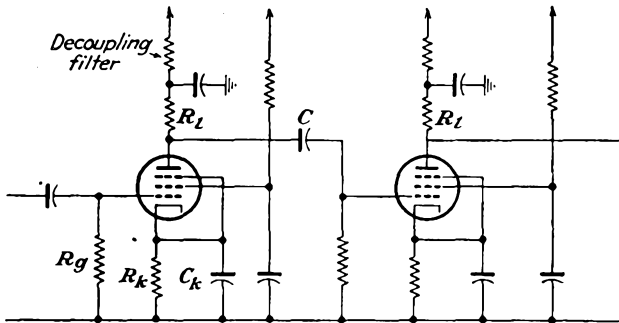


FIG. 4-11. Resistance-capacitance coupled amplifier, with self-bias, decoupling filters, and screen dropping resistors.

It is customary to use a common B supply for all tubes of a given amplifier circuit. Because of this, the possibility for interactions among the stages through this common plate supply does exist and might be troublesome unless the effective output impedance of the power-supply unit is very small. It is necessary in some applications to include  $RC$  combinations known as *decoupling filters* so as to avoid this interaction.

A typical resistance-capacitance coupled-amplifier circuit which is provided with self-bias, decoupling filters, and screen dropping resistors is illustrated in Fig. 4-11.

### PROBLEMS

4-1. Two waves, one of amplitude 10 volts and frequency 1,000 cps, the second of amplitude 5 volts and frequency 3,000 cps, are applied to the input of a certain network. The two waves are so phased that they both pass through zero in the positive-going direction together.

- a. Sketch the resulting input voltage.
  - b. Suppose that the fundamental component suffers a phase delay of 10 deg on the fundamental scale and that the third-harmonic component suffers a 50-deg delay on the third-harmonic scale, although neither amplitude is effected. Sketch the output wave.
- ✓ 4-2. a. The output potential of a given amplifier is 18 volts, when the input voltage is 0.2 volt at 5,000 cps. What is the decibel voltage gain of the amplifier?

b. The output voltage is 7 volts when the input voltage is 0.2 volt at 18,000 cps. By how many decibels is the response of the amplifier at 18 kc below that at 5 kc?

4-3. Prepare a table giving the power sensitivity of the following tubes (assume that the output power and the grid excitation are those specified in the tube manual): 6A3, 6F6, 6V6, 6L6, 6AG7.

4-4. An a-c excitation potential of 5 volts rms at a frequency of 2,000 cps is applied to a 6J5 tube for which  $\mu = 20$ ,  $r_p = 7,700$  ohms. The load is a pure resistance of 15,000 ohms. Calculate the following:

- The a-c current in the plate circuit.
- The a-c output voltage.
- The gain of the amplifier.
- The a-c power in the load resistor.

4-5. Repeat Prob. 4-4 if the load is an inductive reactance of 15,000 ohms.

4-6. A type 6SF5 high- $\mu$  triode is operated as a simple amplifier under specified conditions at 30,000 cps. The important factors are

$$\mu = 100 \quad r_p = 66,000 \text{ ohms} \quad C_{gp} = 2.4 \mu\text{f} \quad C_{ok} = 4.0 \mu\text{f} \\ C_{pk} = 3.6 \mu\text{f}$$

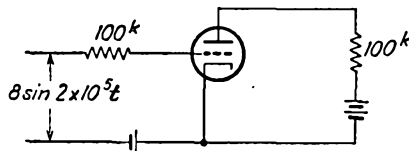
- Calculate the input capacitance and the input resistance of the tube alone when the load is a resistor  $R_l = 100^k$ .
- Repeat when the load impedance is of the form  $60,000 + j60,000$  ohms.

4-7. A type 6J5 triode is operated as a simple amplifier under specified conditions at 22,000 cps. The important factors are

$$\mu = 20 \quad r_p = 7,700 \text{ ohms} \quad C_{gp} = 3.4 \mu\text{f} \quad C_{ok} = 3.4 \mu\text{f} \\ C_{pk} = 3.6 \mu\text{f}$$

- Calculate the input capacitance and the input resistance of the tube when the load is a resistor  $R_l = 20^k$ .
- Repeat when the load is an impedance of the form  $10,000 + j10,000$ .

4-8. A type 6J5 tube is operated in the circuit of the accompanying diagram. Calculate the output voltage. (See Prob. 4-7 for the important factors of the tube.)



4-9. Show that Fig. 4-8 does represent the complete equivalent circuit of the pentode.

4-10. A type 6SJ7 pentode is operated as a simple amplifier under specified conditions.

*a.* When connected as a pentode, with  $R_l = 25k$ , the important factors are

$$g_m = 1,575 \mu\text{mhos} \quad r_p = 0.7 \text{ megohms} \quad C_{op} = 0.005 \mu\text{mf} \quad C_{\text{input}} = 6.0 \mu\text{mf}$$

$$C_{\text{output}} = 7.0 \mu\text{mf}$$

Calculate the input capacitance of the amplifier.

*b.* When this tube is reconnected as a triode, the factors become

$$\mu = 19 \quad r_p = 8,000 \text{ ohms} \quad C_{op} = 2.8 \mu\text{mf} \quad C_{ok} = 3.4 \mu\text{mf} \quad C_{pk} = 11 \mu\text{mf}$$

Calculate the input capacitance with  $R_l = 25k$  and compare with the results of part *b*.

✓ **4-11.** A 6AC7 pentode is to be used as a class A amplifier with  $E_b = 250$  volts. Determine the value of the self-biasing cathode resistor to set  $E_{c1} = -2$  volts; the screen dropping resistor to set  $E_{c2}$  at 150 volts if  $E_{bb} = 350$ .

## CHAPTER 5

### UNTUNED VOLTAGE AMPLIFIERS

IT is frequently necessary to achieve a higher gain in an amplifier than is possible with a single stage. Amplifier stages may be cascaded to achieve this higher gain, the output voltage from one stage serving as the input voltage to the next stage. Ordinarily, however, two or three stages in cascade serving a common function is about the limit for stable opera-

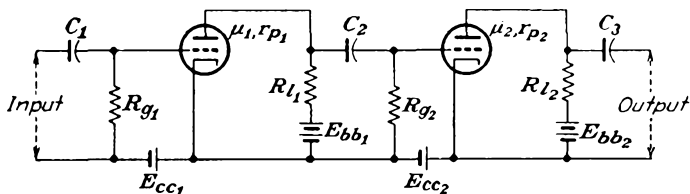


FIG. 5-1. Schematic diagram of a two-stage RC coupled amplifier.

tion, although six- and nine-stage amplifiers are common in radar-receiver practice. Extreme caution is required in the design of such multistage amplifiers.

To calculate the over-all gain and frequency response of such a multistage amplified, the equivalent circuit of the amplifier must be drawn. The rules for accomplishing this are given in Sec. 3-3. The resultant equivalent network is then analyzed as a conventional problem in a-c circuit analysis.

A variety of coupling networks between the cascaded stages are possible, and a few have become very common, either by virtue of their simplicity or because of some especially desirable characteristic. A number of the more common types will be considered in some detail.

**5-1. Resistance-Capacitance (RC) Coupled Amplifier.** The resistance-capacitance (RC) coupled amplifier, illustrated in Fig. 5-1, is one of the more common and more important amplifier circuits. This amplifier circuit is used when a sensibly constant amplification over a wide range of frequencies is desired. By the use of tubes with high amplification factors, it is possible to achieve a gain of 50 or more per stage. It will be found that high-gain triodes possess certain inherent disadvantages, and it is frequently desirable to use pentodes instead. If pentodes

are used, the screen potential must remain constant; otherwise the following analysis will no longer be valid.

The capacitors  $C_1$ ,  $C_2$ , and  $C_3$  in this schematic diagram are known as *coupling* or *blocking* capacitors and serve to prevent any d-c potentials that are present in one stage from appearing in another stage. That is, capacitor  $C_1$  serves to prevent any d-c potential in the input from appearing across the grid resistor  $R_{g1}$  and thus changing the d-c operating level of the amplifier. Capacitor  $C_2$  serves a similar function in coupling stage 1 to stage 2. The value of the coupling capacitors is determined primarily by the l-f amplification. They ordinarily range from about 0.001 to 0.1  $\mu$ f for conventional a-f stages. The resistor  $R_g$ , which is

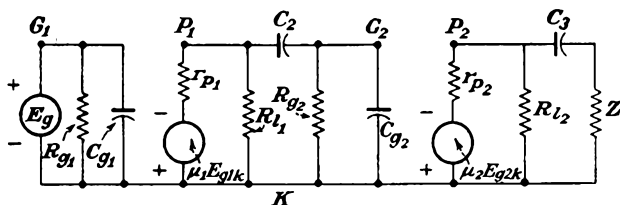


FIG. 5-2. The equivalent circuit of the RC amplifier of Fig. 5-1.

known as the *grid resistor*, furnishes a path by which the grid-bias supply is applied to the grid. It also serves as a leak path through which any electrons that may be collected by the grid from the electron stream within the tube may be returned to the cathode. If such a leak path were not provided, the grid would acquire a negative potential with the collection of the electrons, thus influencing the operation of the tube. A negative bias-supply potential is ordinarily used, and the grid current is usually very small. This permits the use of relatively large resistors for  $R_g$ , say from  $50^k$  to  $2^M$ . Large values of  $R_g$  are desirable in achieving a wide frequency response. The load resistor  $R_l$  is determined principally by the gain and the frequency band width that is desired.

The equivalent circuit of the amplifier of Fig. 5-1 is shown in Fig. 5-2. This circuit is valid for triodes, tetrodes, or pentodes provided that the screen potential of the latter two is maintained constant. In this circuit  $E_g$  denotes the a-c input voltage applied to the grid of the first stage. This potential appears across the parallel combination consisting of the resistor  $R_g$  in parallel with the input impedance to the amplifier. The input impedance of the stage is considered to be a resistor (and assumed positive) in parallel with the input capacitance. However, it is supposed that the impedance of the driving source is low and that the loading by the total input impedance of the first stage does not affect the input potential. The output circuit of the first stage consists of the load resistor, the coupling capacitor  $C_2$ , and the total input impedance of the

second stage. This is denoted as  $R_o$  and  $C_o$  for the total resistive and capacitive components. The output of the amplifier is the potential difference across the output impedance, which is denoted by the symbol  $Z$ . This impedance cannot be specified more completely until the nature of the output circuit is known.

The coupling between the grid and the plate of the tubes through the interelectrode capacitances can be neglected over a wide frequency range with pentodes and over the a-f range with triodes. Consequently each stage may be considered as independent of the following stage, but the output of one stage is the input to the next stage. As a result, it follows that since

$$K_1 = \frac{E_{g2k}}{E_{g1k}} = \frac{\text{output voltage of 1st stage}}{\text{input voltage to 1st stage}}$$

and

$$K_2 = \frac{E_{g3k}}{E_{g2k}} = \frac{\text{output voltage of 2d stage}}{\text{input voltage to 2d stage}} = \frac{\text{output voltage of 2d stage}}{\text{output voltage of 1st stage}}$$

then the resultant over-all gain is

$$K = \frac{E_{g3k}}{E_{g1k}} = \frac{\text{output voltage of 2d stage}}{\text{input voltage to 1st stage}}$$

It follows from these expressions that

$$K = K_1 K_2 \quad (5-1)$$

By taking twenty times the logarithm of the magnitude of this expression,

$$20 \log_{10} K = 20 \log_{10} K_1 + 20 \log_{10} K_2 \quad (5-2)$$

It follows from this that the total decibel voltage gain of the multistage amplifier is the sum of the decibel voltage gains of the separate stages. This fact is independent of the type of interstage coupling.

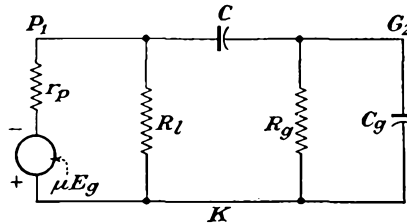


FIG. 5-3. A typical stage of an  $RC$  coupled amplifier.

**5-2. Analysis of  $RC$  Coupled Amplifier.** A typical stage of the  $RC$  coupled amplifier is considered in detail. This stage might represent any of the amplifier chain, except perhaps the output stage.

Representative subscripts have been omitted. The circuit is given in Fig. 5-3.

This circuit may be analyzed with the aid of the Millman theorem. A direct application of the results of this theorem between the points  $G_2$

and  $K$  yields the expression

$$E_{g2k} = \frac{E_{p1k} Y_c}{Y_c + Y_{R_g} + Y_{C_g}} \tag{5-3}$$

where  $Y_c = j\omega C$ ,  $Y_{R_g} = 1/R_g$ , and  $Y_{C_g} = j\omega C_g$ . An application of this theorem between the points  $P_1$  and  $K$  yields the following expression,

$$E_{p1k} = \frac{-\mu E_g Y_p + E_{g2k} Y_c}{Y_p + Y_l + Y_c} \tag{5-4}$$

where  $Y_p = 1/r_p$  and  $Y_l = 1/R_l$ . By combining Eqs. (5-3) with (5-4) and solving for the gain  $K = E_{g2K}/E_g$ , there results

$$K = \frac{-\mu Y_p Y_c}{(Y_c + Y_{R_g} + Y_{C_g})(Y_p + Y_l) + Y_c(Y_{R_g} + Y_{C_g})} \tag{5-5}$$

This is the complete expression for the voltage gain of such an amplifier stage. If the constants of the circuit are known, the gain and phase-shift characteristics as a function of frequency may be calculated. However, by making suitable approximations, it is possible to study the behavior of the circuit for various limiting conditions of frequency.

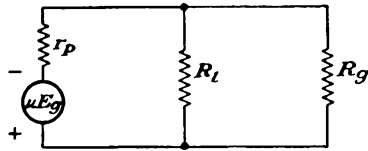


FIG. 5-4. The mid-frequency equivalent circuit of the RC amplifier.

*Intermediate Frequencies.* The intermediate frequencies, or mid-frequencies, are those for which  $Y_c$  is large and  $Y_{C_g}$  is small. Subject to these conditions, the equivalent circuit of Fig. 5-3 reduces to that shown in Fig. 5-4. For the range of frequencies over which this equivalent circuit is valid, the expression for the gain reduces to

$$K = K_0 = \frac{-\mu Y_p}{Y_p + Y_l + Y_{R_g}} \tag{5-6}$$

This expression for the gain is independent of the frequency, since no reactive elements appear in the circuit. Since each of the elements is resistive, the phase angle between input and output voltages is constant and equal to 180 deg.

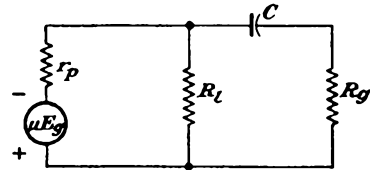


FIG. 5-5. The l-f equivalent circuit of the RC amplifier.

*L-F Region.* At the low frequencies the effect of  $C_g$  is negligible, and  $Y_{C_g}$  may be made zero. The effect of the coupling capacitor  $C$  becomes very important.

The equivalent circuit under these conditions has the form shown in Fig. 5-5. The general expression for the gain [(5-5)] reduces to

$$K = K_1 = \frac{-\mu Y_p Y_c}{Y_c(Y_p + Y_l + Y_{R_o}) + Y_{R_o}(Y_p + Y_l)} \quad (5-7)$$

It is found convenient to examine the l-f gain relative to the mid-frequency gain. The ratio  $K_1/K_0$  becomes

$$\frac{K_1}{K_0} = \frac{1}{1 + \frac{Y_{R_o}(Y_p + Y_l)}{Y_c(Y_p + Y_l + Y_{R_o})}} \quad (5-8)$$

This may be written in the simple form, for any frequency  $f$ ,

$$\frac{K_1}{K_0} = \frac{1}{1 - j(f_1/f)} \quad (5-9)$$

where

$$f_1 \equiv \frac{Y_{R_o}(Y_p + Y_l)}{2\pi C(Y_p + Y_l + Y_{R_o})} \quad (5-10)$$

If the load is a pure resistance, then  $f_1$  is a real number and the magnitude of the relative gain becomes

$$\left| \frac{K_1}{K_0} \right| = \frac{1}{\sqrt{1 + (f_1/f)^2}} \quad (5-11)$$

This shows that the parameter  $f_1$  represents the frequency at which the gain falls to  $1/\sqrt{2}$ , or 70.7 per cent of its mid-frequency value. This frequency is usually referred to as the l-f cutoff frequency of the amplifier. The relative phase angle  $\theta_1$  is given by

$$\tan \theta_1 = \frac{f_1}{f} \quad (5-12)$$

This approaches 90 deg as the frequency approaches zero.

It should be noted that the l-f cutoff value [(5-10)] depends, among other terms, on the size of the coupling capacitor  $C$ . Since the value of  $C$  appears in the denominator of the expression for  $f_1$ , then for a decreased l-f cutoff, larger values of  $C$  must be chosen. Of course, the gain must ultimately fall to zero at zero frequency.

There are several practical limitations to the size of the coupling capacitor that may be used. The capacitor must be of high quality so that any leakage current will be small. Otherwise a conduction path from the plate of one stage to the grid of the next stage may exist. But good-quality capacitors in sizes larger than 0.1  $\mu\text{f}$  are physically large and are relatively expensive. Also, if the coupling capacitor is large, a phenomenon known as blocking may result. This arises when the time constant  $CR_o$  is much larger than the period of the highest frequency to be passed by the amplifier. Thus if an appreciable charge flows into the capacitor

with the application of the input signal and if this cannot leak off quickly enough, a charge will build up. This may bias the tube highly negatively, perhaps even beyond cutoff. The amplifier then becomes inoperative until the capacitor discharges. This condition is sometimes desirable in special electron-tube circuits, and will be the subject of a detailed discussion in Chap. 7. However, it is a condition that must be avoided in an amplifier that is to reproduce the input signal in an amplified form.

The grid resistor  $R_g$  must be made high to keep the gain high, since  $R_g$  of one stage represents a loading across the plate resistor  $R_l$  of the previous stage. The upper limit to this value is set by the grid current. Ordinarily the grid current is small, particularly when the grid bias is negative. But if the grid resistor is made too high, and several megohms is the usual limit, the voltage across this resistor will act as a spurious bias on the tube. While

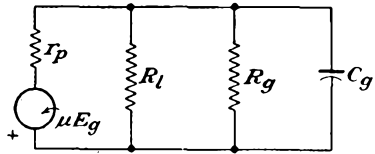


FIG. 5-6. The h-f equivalent circuit of the RC amplifier.

special low-grid-current tubes are available, these are designed for special operations and would not ordinarily be used in conventional circuits.

*H-F Region.* At the high frequencies, the admittance of  $C$  is very large, and the admittance of  $C_g$  becomes important. The equivalent circuit corresponding to these conditions becomes that shown in Fig. 5-6. The general expression for the gain reduces to

$$K = K_2 = \frac{-\mu Y_p}{Y_p + Y_l + Y_{R_g} + Y_{C_g}} \tag{5-13}$$

The gain ratio  $K_2/K_0$  becomes

$$\frac{K_2}{K_0} = \frac{1}{1 + \frac{Y_{C_g}}{Y_p + Y_l + Y_{R_g}}} \tag{5-14}$$

This expression may be written in a form similar to Eq. (5-9) for the l-f case. It becomes

$$\frac{K_2}{K_0} = \frac{1}{1 + j(f/f_2)} \tag{5-15}$$

where

$$f_2 \equiv \frac{Y_p + Y_l + Y_{R_g}}{2\pi C_g} \tag{5-16}$$

In this expression  $C_g$  denotes the total capacitance from grid to cathode and comprises the input capacitance of the following stage, the output wiring, and the output tube capacitance.

If the load is a pure resistance, then  $f_2$  is a real number and the magnitude of the relative gain becomes

$$\left| \frac{K_2}{K_0} \right| = \sqrt{\frac{1}{1 + (f/f_2)^2}} \quad (5-17)$$

It follows from this that  $f_2$  represents that frequency at which the h-f gain falls to  $1/\sqrt{2}$ , or 70.7 per cent, of its mid-frequency value. This frequency is usually referred to as the *h-f cutoff* of the amplifier. The relative phase angle  $\theta_2$  is given by

$$\tan \theta_2 = -\frac{f}{f_2} \quad (5-18)$$

This angle approaches  $-90$  deg as the frequency becomes very large compared with  $f_2$ .

Note from Eq. (5-16) that the h-f cutoff value depends on the value of  $C_p$ , among other factors. Since the value of  $C_p$  appears in the denominator of the expression, then clearly a high h-f cutoff requires a small value of  $C_p$ . Moreover, since the input capacitance of a pentode is appreciably less than that of a triode, the pentode possesses inherently better possibilities for a broad frequency response than does the triode. It will be found in Sec. 6-5, in the discussion of the cathode-follower amplifier, that triodes with cathode-follower coupling stages also possess broad-band capabilities, although this is accomplished at the expense of a tube. Note above that the h-f cutoff is improved by the use of large  $Y_p$ ,  $Y_l$ , and  $Y_{R_p}$ , which implies the use of small values of resistance and a tube with a small plate resistance.

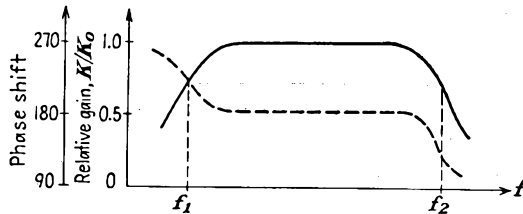


FIG. 5-7. A typical frequency response and phase characteristic of an  $RC$  coupled amplifier.

**5-3. Universal Amplification Curves for  $RC$  Amplifiers.**<sup>1</sup> The foregoing analysis shows that the gain of an  $RC$  coupled amplifier is substantially constant over a range of frequencies and falls off at both the high and the low frequencies. A typical frequency-response curve has the form sketched in Fig. 5-7.

Since the relative gain and the relative phase-shift characteristics depend only upon the two parameters  $f_1$  and  $f_2$ , it is possible to construct

curves which are applicable to any such amplifier. Such universal curves are given in Fig. 5-8.

The frequency-response characteristics of any *RC* coupled amplifier can easily be obtained with the aid of these curves. The first step in the analysis is to calculate the values of the parameters  $f_1$  and  $f_2$  from Eqs.

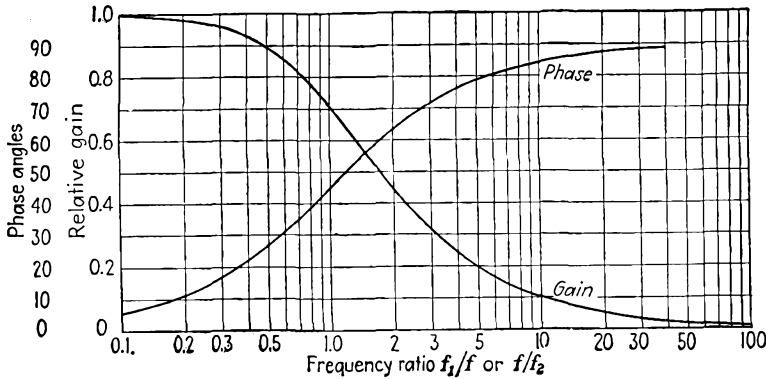


FIG. 5-8. Universal gain and phase-shift curves for an *RC* coupled amplifier.

(5-10) and (5-16). Then the values of the relative gain and the relative phase angle are obtained from the curves for a number of values of the ratio  $f_1/f$  and  $f/f_2$ . These are plotted as a function of  $f$ . It must be remembered in using Fig. 5-8 that the ordinate is  $K_1/K_0$  or  $\theta_1$  when the abscissa is  $f_1/f$ . Also, the ordinate is  $K_2/K_0$  or  $\theta_2$  when the abscissa is  $f/f_2$ .

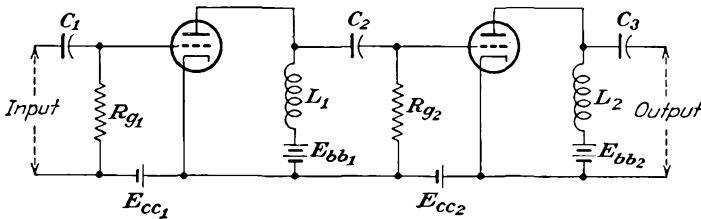


FIG. 5-9. Schematic diagram of an inductance-capacitance coupled amplifier.

**5-4. Impedance-Capacitance (LC) Coupled Amplifier.** The circuit of the impedance-capacitance coupled amplifier differs from that of the resistance-capacitance coupled amplifier only in the use of an inductance plate load instead of a plate resistor. The schematic diagram of the amplifier is given in Fig. 5-9. The use of an inductance instead of a resistance in the plate circuit makes possible the use of a smaller plate-supply voltage for a particular tube operating condition, since the d-c resistance of the inductor is small and the d-c voltage drop across this inductor is also small.

The equivalent circuit of one stage of this amplifier is given in Fig. 5-10. Observe that this circuit differs from the corresponding equivalent circuit of Fig. 5-3 only in the plate-circuit impedance. Consequently the analysis leading to Eq. (5-5) is valid in the present case provided that the plate-circuit admittance is interpreted to be

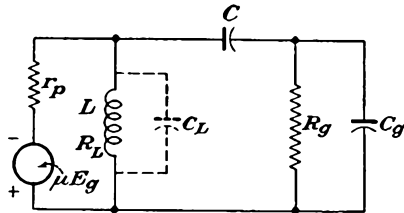


FIG. 5-10. The equivalent circuit of a typical stage of an  $LC$  coupled amplifier.

$$Y_l = j\omega C_L + \frac{1}{R_L + j\omega L} \quad (5-19)$$

Here  $C_L$  is the distributed winding capacitance, which has been assumed to shunt the inductance, and  $R_L$  is the resistance of the inductor.

The frequency-response characteristic of this amplifier may be examined in the same way as that for the  $RC$  system. The analysis shows that the response is generally similar to that for the  $RC$  amplifier, except that the sensibly flat region is narrower, although the mid-frequency gain is somewhat higher. The gain drops off more rapidly than for the  $RC$

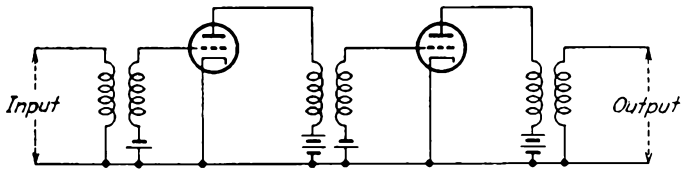


FIG. 5-11. Schematic diagram of a transformer-coupled amplifier.

amplifier at the low frequencies owing to the low reactance of  $L$  in addition to the high reactance of  $C$ . The gain drops off more rapidly than for the  $RC$  amplifier at the high frequencies because of the shunting effects of both  $C_L$  and  $C_g$ . The mid-frequency gain is higher than for the  $RC$  amplifier provided that the impedance of the inductor at these frequencies is higher than the resistance of the plate load of the  $RC$  amplifier.

The  $LC$  coupled amplifier is seldom used as a voltage amplifier owing to the narrow frequency band and the cost of the inductor. This type of coupling, which is also referred to as *shunt-* or *parallel-feed* coupling, is frequently used in power amplifiers.

**5-5. Transformer-coupled Amplifiers.** The circuit of a transformer-coupled amplifier is given in Fig. 5-11. The transformer as a coupling device possesses several desirable features. Owing to the step-up character of the transformer, a total amplification per stage greater than the  $\mu$  of the tube can be achieved. Also, the d-c isolation provided by the transformer automatically removes the requirement for a blocking

capacitor. High-quality interstage transformers generally have voltage ratios of 1:3 or less. Higher transformation ratios usually are accompanied by distributed winding capacitances and by interwinding capacitances that are excessive. The effects of these capacitances will be considered below.

The equivalent circuit of a typical transformer-coupled stage is given in Fig. 5-12.

*Mid-frequency Response.* An approximate expression for the gain per stage may readily be found if it is assumed that the transformer is ideal.

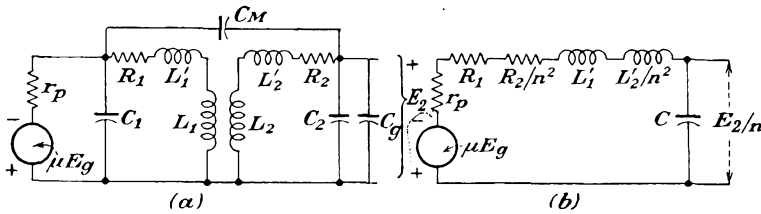


FIG. 5-12. The equivalent circuit of a typical transformer-coupled stage.

An ideal transformer is one for which unity coupling exists between primary and secondary windings and in which the losses and stray capacitances are negligible. If it is assumed that the secondary of the transformer, which feeds the grid of the following stage, is essentially open-circuited, then the plate-circuit impedance is infinite. Consequently the full effective voltage  $\mu E_g$  of the stage appears across the transformer primary. The corresponding output voltage at the secondary terminals is  $n\mu E_g$ , where  $n$  is the transformation ratio of the transformer. The gain of the stage is then simply

$$K = K_0 = n\mu \tag{5-20}$$

a constant, independent of the frequency.

*L-F Region.* The foregoing considerations are only approximate, owing

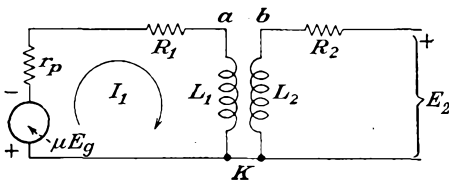


FIG. 5-13. The l-f equivalent circuit of a transformer-coupled amplifier.

to the character of the assumptions that were made. To examine the response at the lower frequencies, the effective distributed winding capacitances and leakage inductances may be neglected. The

corresponding equivalent circuit has the form shown in Fig. 5-13. The resistance of the primary winding is denoted as  $R_1$ , and its inductance is  $L_1$ . Similarly,  $R_2$  and  $L_2$  represent the secondary resistance and inductance, respectively.

It is evident from this diagram that the primary current is

$$I_1 = \frac{\mu E_o}{r_p + R_1 + j\omega L_1}$$

The potential difference across the primary inductance is

$$E_{ak} = \frac{-\mu E_o}{1 - j\left(\frac{r_p + R_1}{\omega L_1}\right)} \quad (5-21)$$

But the potential that appears across the secondary winding  $E_{bk}$  is  $n$  times as large as  $E_{ak}$ . The secondary voltage may be in phase or 180 deg out of phase with  $E_{ak}$  and depends upon the relative winding direction of the primary and secondary windings. The gain of the transformer-coupled stage is then

$$K_1 = \frac{E_{bk}}{E_o} = \pm \frac{n\mu}{1 - j\left(\frac{r_p + R_1}{\omega L_1}\right)} \quad (5-22)$$

The ratio of l-f to mid-frequency gain is then

$$\frac{K_1}{K_0} = \pm \frac{1}{1 - j\left(\frac{r_p + R_1}{\omega L_1}\right)} \quad (5-23)$$

which may be written in the form

$$\frac{K_1}{K_0} = \pm \frac{1}{1 - j(f_1/f)} \quad (5-24)$$

where

$$f_1 = \frac{r_p + R_1}{2\pi L_1} \quad (5-25)$$

Observe that the gain ratio has the same general form as for the  $RC$  coupled amplifier. Now the gain drops off at the lower frequencies because the reactance of the primary winding decreases and no longer will be large compared with the total resistance of the primary circuit  $r_p + R_1$ .

Equation (5-25) contains an explanation why high-gain tubes, which inherently possess high plate resistances, are not employed in transformer-coupled amplifiers. If such high-gain tubes were used, then the l-f response would be very poor. If an attempt were made to improve the l-f response by designing the transformer to have a very high primary inductance, the associated distributed capacitances would become excessive. The alternative method of obtaining high primary inductance through the use of core material of very high permeability has led to the development of high-permeability alloys such as permalloy and hiperm.

*H-F Region.* At the high frequencies the shunting effects of the primary and secondary windings may be neglected. However, the effects

of the leakage inductances, and also the interwinding and distributed capacitances, are important. The circuit of Fig. 5-12 appears in Fig. 5-14a with the transformer replaced by its T-equivalent, and referred to the primary. At the high frequencies the circuit reduces to that of Fig. 5-14b, in which the winding, interwinding, interelectrode, and stray wiring capacitances are lumped into an equivalent capacitance  $C$  across the primary of the transformer.

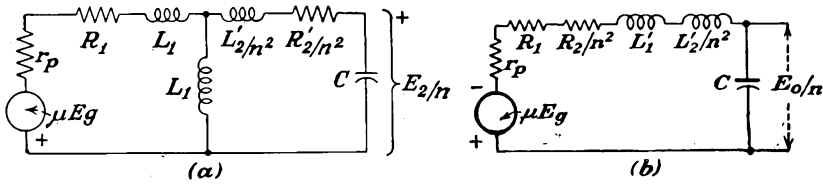


FIG. 5-14. The complete and approximate h-f equivalent circuit of a transformer-coupled stage.

The total effective shunting capacitance is related to the several components by the approximate expression

$$C = [(1 \pm n)^2 C_m + n^2 C_2] + n^2 C_0 \tag{5-26}$$

The  $\pm$  sign depends on the relative disposition and connection of the primary and secondary coils. When properly connected, the minus sign usually applies. To justify this expression, examine Fig. 5-14a. If the voltage across the input terminals is  $E_1$ , and that across the output terminals is  $E_2$ , the difference of potential across  $C_m$  is

$$E_{C_m} = E_1 \pm E_2 \doteq E_1(1 \pm n)$$

where  $n = N_2/N_1$ . The energy stored in this capacitance per cycle is

$$W = \frac{C_m E_{C_m}^2}{2} = \frac{C_m}{2} (1 \pm n)^2 E_1^2$$

The equivalent capacitance across the primary terminals which will store the same energy per cycle will be  $(1 \pm n)^2 C_m$ . The other capacitances in the secondary are reflected into the primary as  $n^2(C_2 + C_0)$ . The total shunting capacitance is that given in Eq. (5-26).

An analysis of the approximate equivalent circuit yields for the gain of the amplifier the expression

$$K_2 = \pm \frac{j n \mu X_C}{R + j(X_L - X_C)} \tag{5-27}$$

where  $R = r_p + R_1 + R_2/n^2$ ;  $L = L'_1 + L'_2/n^2$ ;  $X_L = \omega L$ ;  $X_C = 1/\omega C$ . The primary leakage inductance is  $L'_1$ , and the secondary leakage inductance is  $L'_2$ . The gain ratio may be written in the form

$$\frac{K_2}{K_0} = \pm \frac{j X_C}{R + j(X_L - X_C)} \tag{5-28}$$

The magnitude of the gain ratio is

$$\left| \frac{K_2}{K_0} \right| = \frac{X_c}{\sqrt{R^2 + (X_L - X_c)^2}} \tag{5-29}$$

At the lower end of the region of frequencies where this analysis is valid,  $X_L$  is small and  $X_c$  is large, so that the gain ratio approaches unity, as it should. At the higher frequencies,  $X_c$  is small,  $X_L$  is large, and the gain falls to zero. Notice, however, that the secondary circuit may pass through a maximum, owing to a resonance condition that exists. The maximum is found to occur when

$$X_c = \frac{2X_L^2 + R^2}{2X_L}$$

Usually  $R$  will be much smaller than  $X_L$ , and the maximum occurs when  $X_c = X_L$ , the condition for series resonance. But as the frequency at which this resonance occurs is

$$\omega_0 = \frac{1}{\sqrt{LC}}$$

then the corresponding value of the gain is

$$\left( \frac{K_2}{K_0} \right)_{\max} = \frac{1}{\omega_0 CR} = \frac{1}{R} \sqrt{\frac{L}{C}} \tag{5-30}$$

A typical frequency-response curve, the dependence on the primary inductance  $L_1$ , and the total leakage inductance  $L$  are illustrated in Fig. 5-15.

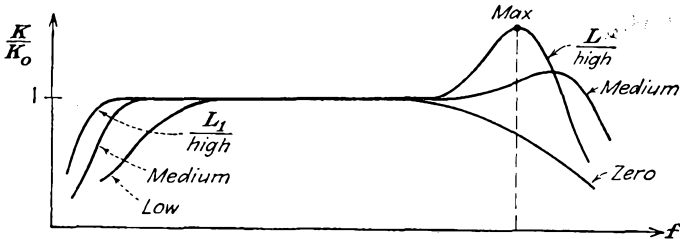


FIG. 5-15. A typical frequency-response characteristic of a transformer-coupled amplifier.

The peaking of the transformer-coupled-amplifier frequency-response curve may be suppressed to a considerable extent by several methods. The simplest way consists in shunting the secondary of the transformer with an appropriately chosen resistance. This reduces the height of the resonant peak, although it also causes the mid-frequency gain to be less than  $n\mu$ . Another method for improving the response characteristic is in the design of the transformer. In modern transformers the shunt

capacitance is decreased by decreasing the contributing factors. The use of a grounded shield between windings reduces the interwinding capacitance. The design of the windings reduces the distributing capacitances. Further, the leakage inductance is reduced, so that the peaking will occur at frequencies beyond the normal operating range of the amplifier. This reduction has been accomplished both by proper design of the windings and by use of suitable high-permeability-core materials. Also, the use of a high-resistance secondary winding tends to suppress the resonant peak. A high-resistance primary winding is to be avoided owing to the adverse effect on the l-f response. High-quality transformers are available that are flat with 1 db over a range of frequencies from approximately 20 to 10,000 cps. The peaking may also be reduced materially through the use of inverse feedback in the amplifier, as will be shown below.

Transformers are seldom used as interstage coupling devices merely to obtain higher gain. This follows because the use of a pentode in an  $RC$  coupled amplifier will ordinarily provide a higher gain than is possible with a triode with a step-up transformer. Furthermore, the  $RC$  coupled stage requires less space and makes use of relatively inexpensive equipment. The principal uses of transformers are as the coupling stage between the driver and a push-pull amplifier, so as to provide the required two voltages that are 180 deg apart in phase (although this application is largely being supplanted by tube circuits), and also as the output transformer in a power amplifier. Here the principal function is one of impedance matching and permits the matching of low impedance loads to high-internal-resistance tubes. These applications will be discussed in some detail in Chap. 9.

**5-6. Feedback in Amplifiers.**<sup>2</sup> When a part of the output signal is combined with the input signal, feedback is said to exist. If the net effect of the feedback is to increase the effective input signal, the feedback is called *positive, direct, or regenerative*. If the resultant input signal is reduced by the feed-back voltage, the feedback is called *negative, inverse, or degenerative*.

The application of negative feedback to an amplifier results in a number of characteristics that are highly desirable in the amplifier. It tends to flatten the frequency-response characteristic and to extend the range of uniform response.<sup>3</sup> It materially reduces nonlinear and phase distortion. It improves the stability of the amplifier, making the gain less dependent on the operating voltages or on variations of the tube characteristics. Also, it tends to make the gain less dependent on the load, so that load variations do not seriously influence the operating characteristics of the amplifier. The use of feed-back networks of special design will provide selective attenuation, thus permitting a frequency response of desired characteristics.

The application of positive feedback has the opposite effects. Thus positive feedback tends to sharpen the frequency-response curve and to decrease the range of uniform response. This permits an increased gain and selectivity. Positive feedback in an amplifier is critical of adjustment. Too much regenerative feedback in any system may result in oscillation. Ordinarily, negative feedback is more common than positive feedback in amplifiers.

The action of a feed-back path depends upon the frequency of operation. That is, the feedback may remain regenerative or degenerative

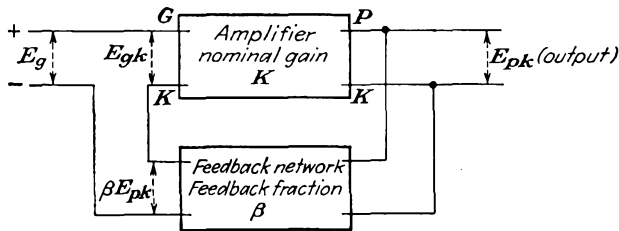


FIG. 5-16. The principle of feedback in amplifiers.

throughout the range of operation of the circuit, although the magnitude and phase angle of the feed-back signal may vary with frequency. It is also possible for the feedback to be positive over a certain range of frequencies and negative over another range.

The principle of feedback is illustrated in the schematic diagram of Fig. 5-16. For simplicity, series injection is shown at the input, but other forms of network coupling may be employed. In the diagram shown, a voltage  $E_g$  is applied to the input terminals of the amplifier, with the polarity as shown. Suppose that the resultant voltage at the output terminals is  $E_{pk}$ . Suppose that a fraction  $\beta$  of this output is fed back in series with the input signal in such a way that the resultant signal that appears between the grid-cathode terminals has the form

$$E_{gk} = E_g + \beta E_{pk} \quad (5-31)$$

But since the nominal gain of the amplifier is, by definition,

$$K \equiv \frac{\text{output potential}}{\text{input potential between grid and cathode}} = \frac{E_{pk}}{E_{gk}}$$

then

$$E_{pk} = K E_{gk} \quad (5-32)$$

By combining this with Eq. (5-31), there results

$$E_{pk} = K E_g + K \beta E_{pk}$$

from which it follows that

$$E_{pk} = \frac{K E_g}{1 - K \beta} \quad (5-33)$$

But the resultant gain of the amplifier including the effects of feedback is defined as

$$K_r \equiv \frac{\text{output potential}}{\text{input-signal potential}} = \frac{E_{pk}}{E_g}$$

Therefore it follows that

$$K_r = \frac{K}{1 - K\beta} \quad (5-34)$$

This equation expresses the resultant gain of the amplifier with feedback in terms of the nominal gain  $K$  of the amplifier without feedback, and the feed-back fraction  $\beta$ . It should be noted that the three quantities  $K_r$ ,  $K$ , and  $\beta$ , which appear in this equation, may be complex quantities.

Suppose that the feedback is negative and that the feed-back factor  $K\beta$  is made large compared with unity. The resultant gain equation (5-34) becomes

$$K_r \doteq \frac{K}{K\beta} = \frac{1}{\beta} \quad (5-35)$$

This means that when  $|K\beta| \gg 1$ , the actual amplification with negative feedback is a function of the characteristics of the feed-back network only. In particular, if  $\beta$  is independent of frequency, then the over-all gain will be independent of the frequency. This permits a substantial reduction of the frequency and phase distortion of the amplifier. In fact, by the proper choice of feed-back network, it is possible to achieve almost any desired frequency characteristic.

Note that if  $K\beta \gg 1$ , then  $K_r \doteq K/K\beta \ll K$ , so that the over-all gain of the amplifier with inverse feedback is less than the nominal gain without feedback. This is the price that must be paid to secure the advantages of negative feedback. This is not a serious price to pay, since the loss in gain can be overcome by the use of additional tubes.

Clearly, if  $K\beta$  is greater than unity, then Eq. (5-35) shows that the over-all gain will not change with tube replacements or with variations in battery potentials, since  $\beta$  is independent of the tube. Even if Eq. (5-35) is not completely valid, a substantial improvement results in general stability. This follows from the fact that a change in the nominal gain  $dK$  for whatever reason results in a change  $dK_r$  in the resultant gain by an amount

$$\frac{dK_r}{K_r} = \frac{1}{|1 - K\beta|} \frac{dK}{K} \quad (5-36)$$

where  $|1 - K\beta|$  represents the magnitude of the quantity  $1 - K\beta$ . This equation is the logarithmic derivative of Eq. (5-34). In this expression,  $dK_r/K_r$  gives the fractional change in  $K_r$ , and  $dK/K$  gives the

fractional change in  $K$ . If, for example, the quantity  $|1 - K\beta| = 5$  in a particular feed-back amplifier, then the variation in any parameter that might cause a 5 per cent change in the nominal gain will result in a change of only 1 per cent in the resultant gain of the amplifier.

One effect was omitted in the above considerations. It was implicitly assumed that the dynamic curve was linear and that the output voltage was of the same wave shape as the input. If an appreciable nonlinear distortion exists, then the output contains harmonic components in addition to the signal of fundamental frequency. Suppose, for simplicity, that only a second-harmonic component  $B_2$  is generated within the tube when a large signal voltage is impressed on the input. Because of the feedback, the second-harmonic component  $B'_2$  that appears in the output is different from that generated within the tube. To find the relationship that exists between  $B'_2$  and  $B_2$ , the procedure parallels that for the gain considerations. Thus, for a second harmonic  $B'_2$  in the output, a fraction  $\beta B'_2$  is supplied to the input. As a result, the output actually must contain two components of second-harmonic frequency, the component  $B_2$  that is generated within the tube and the component  $K\beta B'_2$  that arises from the signal that is fed back to the input. This requires that

$$K\beta B'_2 + B_2 = B'_2$$

or

$$B'_2 = \frac{B_2}{1 - K\beta} \quad (5-37)$$

Note that since both  $K$  and  $\beta$  are functions of the frequency, in general, the appropriate values that appear in this equation must be evaluated at the second-harmonic frequency.

It should be pointed out that this derivation has assumed that the harmonic distortion generated within the tube depends only upon the grid swing of the fundamental signal voltage. The small amount of additional distortion that might arise because a fraction of the second-harmonic component is returned to the input has been neglected. Ordinarily this procedure will lead to little error, although a more exact calculation taking these successive effects into account is readily possible.<sup>3</sup>

Another feature of Eq. (5-37) should be noted. According to this expression, if  $|1 - K\beta| = 10$ , then the second-harmonic distortion with feedback is only one-tenth its value without feedback. This is the situation when the total output-voltage swing is the same in each case; otherwise the harmonic generation within the tube could not be directly compared. This requires that the signal, when feedback is applied, must be  $|1 - K\beta|$  times that in the absence of feedback. As a practical consideration, since appreciable nonlinear distortion is generated only when the signal voltage is large, then the full benefit of the feed-back

amplifier in reducing nonlinear distortion is obtained by applying negative feedback to the large-signal stages.

**5-7. Feed-back Circuits.** The voltage fed back from the output of the amplifier may be proportional either to the voltage across the load or to the current through the load. In the first case the feedback is called

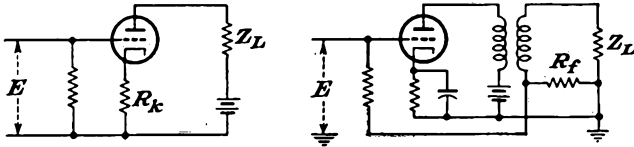


FIG. 5-17. Circuits employing current feedback.

*voltage feedback*; in the second case, *current feedback*. In either case, the feedback may be positive or negative, depending upon the connection. An amplifier may possess any combination of voltage and current feedback.

Two examples of amplifiers with current feedback are shown in Fig. 5-17. In the circuit of Fig. 5-17a, the feedback is effected through the resistor in the cathode of the amplifier and is frequently referred to as *cathode degeneration*. In the circuit of Fig. 5-17b, the feedback is effected through a resistor in the load circuit, the total feed-back potential depending on the feed-back resistor  $R_f$ .

The feedback fraction is of the same form in both circuits and is  $R_k/Z$  in the first circuit and  $R_f/Z$  in the second circuit. To find the expressions for the gain, it is noted that the equivalent circuits for both circuits have the same form, as shown in Fig. 5-18.

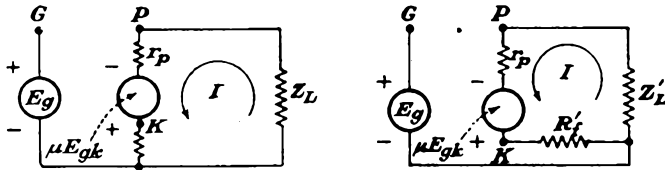


FIG. 5-18. The equivalent circuits corresponding to the current-feed-back circuits of Figs. 5-17.

Two methods of analysis exist. One method effects the solution by direct application of the general principles of electron-tube circuit analysis. The second method makes use of the feedback considerations implied by the general equation of the feedback amplifier [Eq. (5-34)]. The solution by both methods will be given.

According to the general principles of electron-tube circuit analysis, the output potential is readily found. Thus the current is given by

$$I = \frac{\mu E_{gk}}{r_p + R_k + Z_L} \tag{5-38}$$

But the potential  $E_{gk}$  is given by

$$E_{gk} = -IR_k + E_g \tag{5-39}$$

Combining these two expressions gives

$$I = \frac{\mu E_g}{r_p + (\mu + 1)R_k + Z_l} \tag{5-40}$$

The output potential  $E_{pk}$  is then

$$E_{pk} = -IZ_l = \frac{-\mu Z_l E_g}{r_p + (\mu + 1)R_k + Z_l} \tag{5-41}$$

and the gain becomes

$$K_r = \frac{-\mu Z_l}{r_p + (\mu + 1)R_k + Z_l} \tag{5-42}$$

To apply the feed-back method, it is noted that the feed-back fraction is

$$\beta = \frac{R_k}{Z_l} \tag{5-43}$$

Also, the current is

$$I = \frac{\mu E_{gk}}{r_p + R_k + Z_l} \tag{5-44}$$

so that the nominal gain  $K$  is

$$K = \frac{E_{pk}}{E_{gk}} = \frac{-\mu Z_l}{r_p + R_k + Z_l} \tag{5-45}$$

The resultant gain is then

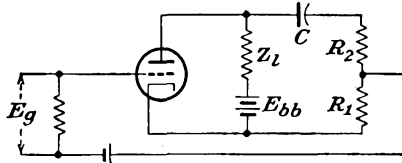
$$K_r = \frac{K}{1 - K\beta} = \frac{\frac{-\mu Z_l}{r_p + Z_l + R_k}}{1 - \frac{R_k}{Z_l} \left( \frac{-\mu Z_l}{r_p + R_k + Z_l} \right)} = \frac{-\mu Z_l}{r_p + (\mu + 1)R_k + Z_l} \tag{5-46}$$

which is the same as above.

Refer to Eq. (5-40) for the current in the plate circuit. This may be interpreted to show that the effect of the negative feedback is to increase the effective internal resistance of the tube from  $r_p$  without feedback to the value

$$r_p + (\mu + 1)R_k.$$

FIG. 5-19. Circuit employing voltage feedback.



This means, of course, that, if the effective internal impedance of the tube is high compared with the impedance of the external load, the current is effectively independent of variation of load impedance.

A circuit for achieving voltage feedback is given in Fig. 5-19. In this

circuit, the resistor combination  $R_1 + R_2$  which shunts the output is made large compared with the load impedance  $Z_l$ . The capacitor  $C$  has a reactance that is negligible compared with  $R_1 + R_2$  at the frequencies to be employed. Its sole purpose is to block the d-c potential from the plate circuit from appearing in the grid circuit.

To obtain an expression for the resultant gain of the amplifier, the feedback method will be employed. By neglecting the shunting effect of the feedback resistor on the load impedance, it follows that the nominal gain of the amplifier is given by

$$K = \frac{-\mu Z_l}{r_p + Z_l} \quad (5-47)$$

Also

$$\beta = \frac{R_1}{R_1 + R_2} \quad (5-48)$$

Then the resultant gain with feedback is

$$K_r = \frac{K}{1 - K\beta} = \frac{-\mu Z_l}{r_p + Z_l + \beta\mu Z_l} \quad (5-49)$$

This expression may be transformed to the form

$$K_r = \frac{-\mu' Z_l}{r'_p + Z_l} \quad (5-50)$$

where

$$\mu' = \frac{\mu}{1 + \mu\beta} \quad r'_p = \frac{r_p}{1 + \mu\beta} \quad (5-51)$$

This is the gain that would be obtained from a tube whose amplification factor is  $\mu'$ , whose plate resistance is  $r'_p$ , and which feeds an external load  $Z_l$ . These results show that the effective amplification factor of the tube is reduced in the same ratio as the plate resistance of the tube. This feature will permit an impedance match between a tube with a high plate resistance and a low impedance load. This is accomplished, of course, at the expense of effectively converting the tube into a triode, with low  $\mu$  and low  $r_p$ .

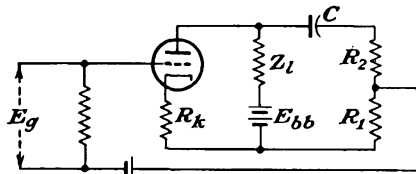


FIG. 5-20. Circuit employing compound feedback.

The combination of current and voltage feedback in an amplifier is frequently called *compound* or *bridge feedback*. The circuit of such an amplifier is given in Fig. 5-20. The feed-back fraction is readily found to be

$$\beta = \frac{R_1}{R_1 + R_2} + \frac{R_k}{Z_l} = \beta_1 + \beta_2 \quad (5-52)$$

As in the analysis of Fig. 5-19, it is assumed that the resistance combination  $R_1 + R_2 \gg Z_l$  and that the reactance of the capacitor is negligible over the frequency range of operation. The resultant gain of the amplifier has the form

$$K_r = \frac{-\mu Z_l}{r_p + (\mu + 1)R_k + (1 + \mu\beta_1)Z_l} \quad (5-53)$$

This may be written in the form

$$K_r'' = \frac{-\mu'' Z_l}{r_p'' + Z_l} \quad (5-54)$$

where

$$\left. \begin{aligned} \mu'' &= \frac{\mu}{1 + \mu\beta_1} \\ r_p'' &= \frac{r_p + (\mu + 1)R_k}{1 + \mu\beta_1} \end{aligned} \right\} \quad (5-55)$$

The effect of the feedback is seen to reflect itself as a change in effective  $\mu$  and  $r_p$  of the tube. Moreover, owing to the form of the expression for  $r_p''$ , this quantity may be made greater than, equal to, or less than its value without feedback.

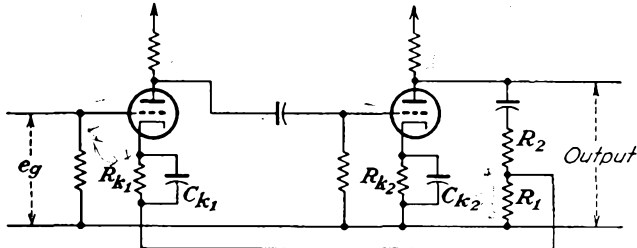


FIG. 5-21. A two-stage  $RC$  coupled amplifier with current feedback in the first stage and voltage feedback between stages.

Feedback can be effected over several stages and need not be confined to a stage-by-stage practice. A two-stage  $RC$  coupled amplifier employing current degeneration in the first stage through resistor  $R_1$  and voltage feedback between stages is illustrated in Fig. 5-21. A careful consideration of the application of the potentials will show that both types of feedback are negative.

### 5-8. Effect of Feedback on the Output Impedance of an Amplifier.

The discussion in the foregoing sections has shown that the application of negative feedback in an amplifier is accompanied by an equivalent tube resistance which varies according to the type of feedback that is employed. As a consequence of this, the output terminal impedance of the amplifier likewise depends on the type of feedback that is employed.

A general relationship between the output terminal impedance without feedback and that with feedback is possible. To find this, suppose that the input terminals are shorted, and that a generator is applied to the output terminals. The ratio of the applied potential to the current is the output impedance. Consider Fig. 5-22, which is Fig. 5-16, a circuit with voltage feedback, which has been modified for the determination of output impedance. Note that a voltage appears in the input through the feedback network even though the input terminals are shorted.

If the applied voltage to the output terminals is  $E_0$ , a voltage  $\beta E_0$  will appear at the input terminals to the tube. The equivalent voltage that appears in the output or plate circuit is  $K\beta E_0$ . The nominal output impedance of the amplifier is designated  $Z'_0$ . The current in the output circuit is seen to be

$$I = \frac{E_0 - K\beta E_0}{Z'_0}$$

The effective output impedance is

$$Z_0 = \frac{E_0}{I} = \frac{Z'_0}{1 - K\beta} \quad (5-56)$$

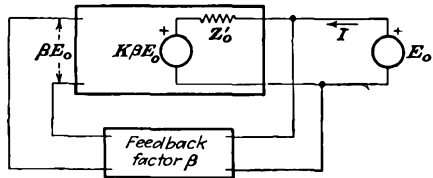


FIG. 5-22. The modifications of the general feed-back circuit for calculating the output impedance of the amplifier.

This expression shows that the output impedance is reduced by the same factor as the voltage gain, when voltage feedback is applied.

A calculation for a circuit provided with current feedback yields the expression (see Prob. 5-17)

$$Z_0 = Z'_0 \frac{(1 - KZ_f/Z'_0)}{(1 - KZ_f/Z_L)} \quad (5-57)$$

where  $Z_f$  is the feedback impedance, and  $Z_L$  is the load impedance. In general, for current feedback,  $Z_0$  is greater than  $Z'_0$ . For compound feedback, the output impedance will depend on the relative fraction of voltage and current feedback, and may be higher or lower than that without feedback.

**5-9. Feedback and Stability.** A great deal of information about the stability of an amplifier can be obtained from an analysis of the factor  $1 - K\beta$  that appears in the general gain expression [Eq. (5-33)]. This is best analyzed through the use of the polar plot of the expression  $K\beta$ . Since  $K\beta$  is a function of the frequency, points in the complex plane are obtained for the values of  $K\beta$  corresponding to all values of  $f$  from 0 to  $\infty$ . The locus of all of these points forms a closed curve.

As a particular example, suppose that the locus of  $K\beta$  in the complex

plane is drawn for the amplifier illustrated in Fig. 5-19. To do this, the complete expression for the nominal gain, including the effect of the feedback circuit, must be written, rather than the simple form given in Eq. (5-46). Also, the value of  $\beta$  must include the effects of the blocking

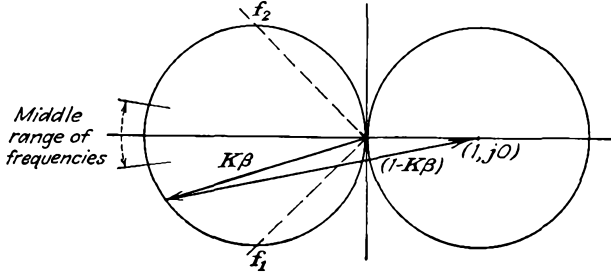


FIG. 5-23. The locus in the complex plane of  $K\beta$  for the circuit of Fig. 5-19.

capacitor  $C$ . Certain of the features of the response are known. At the mid-frequencies, the gain is substantially constant and has a phase of 180 deg. For the low and high frequencies, the gain falls to zero, and the phase approaches  $\pm 90$  deg. At the l-f and h-f cutoff values, the phase is  $\pm 135$  deg. It may be shown that the general locus of  $K\beta$  for all frequencies is a circle. The result is shown in Fig. 5-23. A vector drawn from the polar locus to the point  $(+1, j0)$  is  $1 - K\beta$ . For this particular circuit its magnitude is greater than unity for all frequencies, and it has its maximum magnitude at the middle range of frequencies. Moreover, since the resultant gain varies inversely with  $1 - K\beta$ , then the effect of the feedback is to cause a general flattening of the frequency-response characteristic.

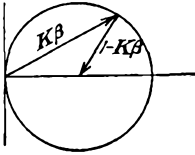


FIG. 5-24. A plot of  $|1 - K\beta| = 1$  in the complex plane.

The criterion for positive and negative feedback is evident on the complex plane. First note that the quantity  $|1 - K\beta| = 1$  represents a circle of unit radius with its center at the point  $(1, j0)$ , as illustrated. Clearly, if for a given amplifier  $|1 - K\beta| > 1$ , then the feedback is negative, with an over-all reduction of gain. Likewise, if  $|1 - K\beta| < 1$ , there is an over-all increase in gain, and the feedback is positive. These considerations show that, if  $K\beta$  extends outside of the unit circle for any frequency, then the feedback is positive at that frequency. If  $K\beta$  lies within the unit circle, then the feedback is negative. If  $K\beta$  passes through the point  $(1, j0)$  then  $1 - K\beta = 0$ , and, as will later be shown, the amplifier becomes an oscillator. A more general analysis by Nyquist<sup>4,2</sup> has shown that the amplifier will oscillate if the curve of  $K\beta$  encloses the point  $(1, j0)$  and is stable if the curve does not enclose this point.

Clearly, therefore, if the magnitude of  $K\beta$  is less than unity when its phase angle is zero, no oscillations are possible.

As a specific example for discussion, suppose that the plot of a given amplifier is that illustrated in Fig. 5-25. The feedback is negative for this amplifier in the frequency range from 0 to  $f_1$ . Positive feedback exists in the frequency range from  $f_1$  to  $\infty$ . Note, however, that, since the locus of  $K\beta$  does not enclose the point  $(1, j0)$ , then, according to the Nyquist criterion, oscillations will not occur.

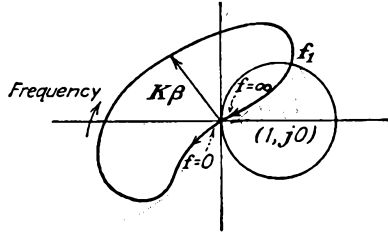


FIG. 5-25. The polar plot of an amplifier.

REFERENCES

1. Terman, F. E., *Electronics*, **10**, 34 (June, 1937).
2. Black, H. S., *Elec. Eng.*, **53**, 114 (1934).  
Peterson, E., J. G. Kreer, L. A. Ware, *Bell System Tech. J.*, **13**, 680 (1934).
3. Feldkeller, R., *Teleg. fernsp. Tech.*, **25**, 217 (1936).
4. Nyquist, H., *Bell System Tech. J.*, **11**, 126 (1932).

PROBLEMS

5-1. The important constants of one of a chain of RC-coupled-amplifier stages employing pentodes (see Fig. 5-3) are

$$R_i = 75^k \quad r_p = 10^6 \quad g_m = 1,600 \text{ } \mu\text{mhos} \quad C = 0.01 \text{ } \mu\text{f} \quad C_{pk} = 11 \text{ } \mu\mu\text{f}$$

$$C_{pk} = 8 \text{ } \mu\mu\text{f} \quad R_o = 500^k$$

- a. Calculate the mid-frequency gain and the upper and lower cutoff frequencies.
- b. Between what frequencies is the amplifier-stage phase  $180 \pm 15$  deg?

5-2. The frequency response of a three-stage cascaded RC amplifier employing pentodes is to be constant within 0.5 db up to 18 kc. Calculate the h-f cutoff of each stage.

5-3. The LC coupled amplifier of Fig. 5-9 uses a triode. The important factors are

$$r_p = 10^k \quad g_m = 2,000 \text{ } \mu\text{mhos} \quad R_o = 10^6 \quad C = 0.01 \text{ } \mu\text{f} \quad L = 40^k$$

$$\text{Distributed capacitance} = 200 \text{ } \mu\mu\text{f}$$

Determine the upper and lower cutoff frequencies and the maximum gain.

5-4. A transformer-coupled amplifier is to be constant within 3 db over the frequency range from 100 to 8,400 cps.

- a. Specify the required values of primary inductance, leakage inductance (reduced to unity-turns ratio), and frequency of secondary resonance. The tube is a 6J5 with  $r_p = 7,700$  ohms. Neglect the winding resistance in the calculations.
- b. If the turns ratio is 3 and the total input and wiring capacitance of the next

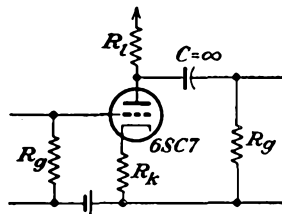
tube is  $25 \mu\mu f$ , what is the permissible equivalent capacitance across the secondary of the transformer?

5-5. An amplifier has a gain  $3,000/0$ . When negative feedback is applied, the gain is reduced to  $2,000/0$ . Determine the feed-back network.

5-6. An amplifier without feedback gives an output of 46 volts with 8 per cent second-harmonic distortion when the input is 0.16 volt.

- If 1 per cent of the output is fed back into the input in a degenerative circuit, what is the output voltage?
- If an output of 46 volts with 1 per cent second-harmonic distortion is permissible, what is the input voltage?

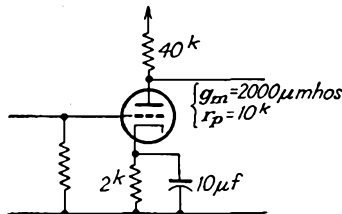
5-7. Given the amplifier stage with cathode degeneration shown in the accompanying diagram,



$$\begin{aligned} E_{bb} &= 250 \text{ volts} & R_L &= 100^k \\ g_m &= 1,200 \mu\text{mhos} & \mu &= 70 \\ R_g &= 1^M \end{aligned}$$

- What should be the value of  $R_k$  to give an over-all gain of 8?
- What is the value of  $E_{cc}$ , and the largest value of  $e_o$  to yield an output without distortion?

5-8. Plot the gain as a function of frequency of the simple amplifier shown in the accompanying figure. Also plot on the same sheet the gain of the stage when fixed bias is used.



5-9. The first stage of the circuit of Fig. 5-21 uses a 6SJ7 pentode with

$$E_b = 250 \text{ volts} \quad E_{cc1} = -3 \quad E_{cc2} = 100 \quad I_b = 3 \text{ ma}$$

The second stage is a 6C5, with  $E_b = 250$ ,  $E_{cc1} = -8$ ,  $I_b = 8 \text{ ma}$ .

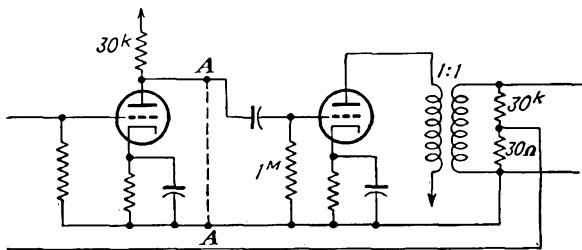
The other factors are

$$R_{i1} = 100^k \quad R_g = 250^k \quad R_{i2} = 25^k \quad C = 0.04 \mu f \quad C_{k1} = 10 \mu f$$

$$C_{k2} = 2.5 \mu f \quad C_d = 0.1 \mu f \quad R_1 = 200\Omega \quad R_2 = 150^k$$

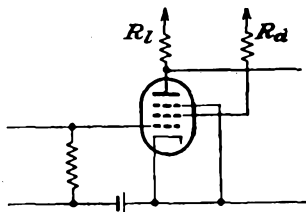
- Specify the values of  $R_{k1}$ ,  $R_{k2}$ ,  $E_{bb}$ .
- Draw the complete mid-frequency equivalent circuit.
- The total shunting capacitance across  $R_{g2}$  is  $80 \mu f$ . Calculate and plot a gain-frequency-response curve over the range from 20 to 50,000 cps.
- Repeat (c) if  $R_1 = 0$ ,  $R_2 = 150^k$ .

5-10. Given the two-stage circuit which is provided with negative voltage feedback. The tubes have  $r_p = 10^6$  ohms,  $g_m = 1,200 \mu mhos$ .



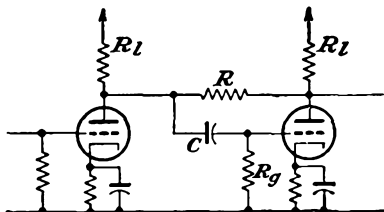
- Calculate the output impedance.
- Calculate the impedance between points AA.

5-11. Given a simple pentode amplifier stage as illustrated, the screen by-pass being omitted. Derive an expression for the gain of the amplifier stage. Assume



that  $I_b$  is independent of  $E_b$ , and that  $\mu_{sg}$  of the screen grid relative to control grid is the same relative to plate and to screen currents.

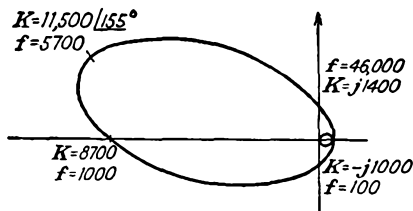
5-12. Calculate the gain of the inverse feed-back pair.\* Assume that the tubes are identical and that  $R_g \gg R_L$ .



\* Mezger, G. R., *Electronics*, 17, 126 (April, 1944).

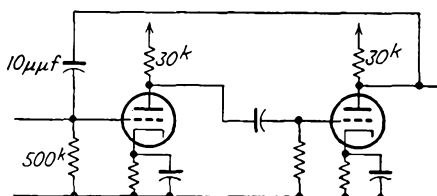
5-13. Given a three-stage  $RC$  coupled amplifier, each stage of which has an l-f cutoff of 20 cps, an h-f cutoff of 84 kc, and a gain of 220. Plot the locus of the complex voltage amplification.

5-14. The locus of the complex voltage amplification of a certain amplifier is illustrated. If 1 per cent negative feedback is applied, determine the value of the

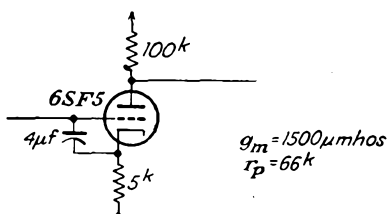


gain  $K$  at the frequencies 100, 10 kc, 40 kc. Assume that  $\beta$  is independent of frequency and that the voltage fed back is in phase with the output voltage.

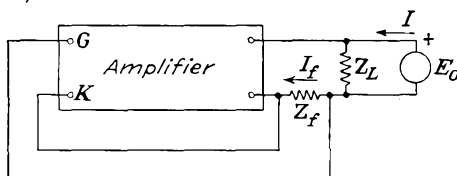
5-15. Calculate the effective input impedance at 10 kc of the circuit in the accompanying figure. Each tube has the value  $g_m = 2,000 \mu\text{mhos}$ ,  $r_p = 10^k$ . Neglect all tube and wiring capacitances.



5-16. Calculate the effective input impedance of the circuit in the accompanying diagram.



5-17. The general current feedback circuit, as viewed from the output terminals for output impedance measurements, is illustrated. Analyze this circuit, and verify Eq. (5-57).



5-18. Apply Eq. (5-57) to Fig. 5-17. Show that the results so obtained yield the expected results.

## CHAPTER 6

### UNTUNED VOLTAGE AMPLIFIERS—*Continued*

THE untuned voltage amplifiers that are discussed in the foregoing chapter possess flat frequency-response characteristics over a range of frequencies. Frequently, however, the region of uniform amplification must be wider than is possible with the simple circuits. For example, radar receivers may require a uniform response from 2 to 8 megacycles,

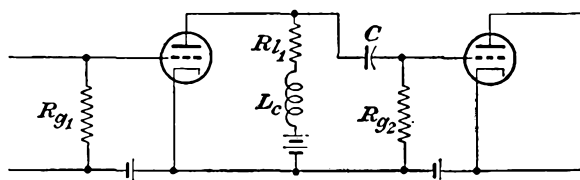


FIG. 6-1. A shunt-peak video amplifier stage.

depending upon the service, although the l-f response in these is not too critical. Television receivers require a sensibly uniform amplification over the range from about 30 cps to 4.5 megacycles. These broad-band amplifiers may be accomplished by compensating the simple amplifier at both the l-f and the h-f ends of the frequency scale; by the use of tubes as coupling devices, these being connected ordinarily as cathode followers; or by the use of circuits operating with certain of the elements which normally cause the droop in the frequency-response characteristic eliminated from the circuit.

**6-1. Compensated Broad-band Amplifiers.** It is possible to compensate for the drooping of the frequency-response characteristic of a resistance-capacitance coupled amplifier at both the h-f and the l-f ends of the curve. Several methods exist for accomplishing this result, and these will be considered below in some detail. However, it is advisable to examine roughly what occurs in these several methods of compensation before undertaking a complete analysis.

In the shunt-peaked method of h-f compensation, an inductance is inserted in series with the plate resistance. The circuit has the form illustrated in Fig. 6-1. The inductance  $L_c$  is chosen of such a value that it resonates with the effective input capacitance of the following tube in the neighborhood of the frequency at which the response would otherwise

begin to fall appreciably. In this way, the h-f end of the response curve can be appreciably extended. The choice of the value of  $L_c$  is critical; otherwise a peak in the response curve may occur. Such overcompensation must be avoided in most applications.

The l-f end of the response curve may be improved by the use of a capacitor across a portion of the load resistor, as illustrated in Fig. 6-2.

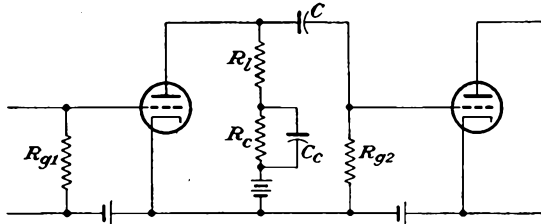


FIG. 6-2. L-F compensation by use of a capacitor across a portion of the load.

In this method, the load resistance is effectively  $R_l$  at the high frequencies, owing to the shunting action of the capacitance  $C_c$  across  $R_c$ . At the low frequencies, the shunting effect of  $C_c$  is negligible, and the load resistance is effectively  $R_l + R_c$ . The increased gain of the stage resulting from the increased effective load impedance thus compensates for the loss of

gain resulting from the voltage-divider action of the coupling capacitor and the grid resistor. In this case, as for the h-f compensation, care must be exercised in the choice of circuit constants.

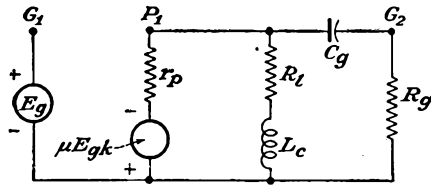


FIG. 6-3. The equivalent circuit of an RC amplifier with an inductance in series with the plate resistor for h-f compensation.

**6-2. H-F Compensation.** To study the gain characteristics of an amplifier that is provided with a shunt compensating circuit, the equivalent circuit of Fig. 6-1 is drawn.

As the series inductance  $L_c$  is small (20 to 50  $\mu$ h), its presence does not in any way affect the l-f or mid-frequency gains of the amplifier. Consequently for this amplifier, Eq. (5-6) for the mid-frequency gain and Eqs. (5-11) and (5-12) for the l-f gain are still valid. These expressions are rewritten here for convenience.

$$\left. \begin{aligned} K_0 &= \frac{-\mu Y_p}{Y_p + Y_l + Y_{R_g}} \\ \frac{K_1}{K_0} &= \frac{1}{\sqrt{1 + (f_1/f)^2}} \frac{\tan^{-1} f_1/f}{\phantom{\sqrt{1 + (f_1/f)^2}}} \end{aligned} \right\} \quad (6-1)$$

Broad-band amplifiers usually employ pentodes with relatively small plate-load resistances. Because of this, the discussion here will be confined to amplifiers of this type. For pentodes

$$\left. \begin{aligned} r_p &\gg R_l \\ R_{g2} &\gg R_l \end{aligned} \right\} \quad (6-2)$$

and the equivalent circuit of Fig. 6-3 reduces to the form of Fig. 6-4. It follows directly from this that the mid-frequency gain is

$$K_0 = -g_m R_l \quad (6-3)$$

and the h-f gain becomes

$$K_2 = \frac{-\mu Y_p}{Y_p + Y_l + Y_{R_g} + Y_{C_g}} \doteq \frac{-g_m}{Y_l + Y_{C_g}} \quad (6-4)$$

The h-f- to mid-frequency-gain ratio is

$$\frac{K_2}{K_0} = \frac{1}{R_l(Y_l + Y_{C_g})} \quad (6-5)$$

But the half-power frequency without compensation is, from Eq. (5-16),

$$f_2 = \frac{Y_p + Y_l + Y_{R_g}}{2\pi C_g} \doteq \frac{1}{2\pi R_l C_g} \quad (6-6)$$

Also, it is convenient to define the quantity  $Q_2$  as

$$Q_2 = \frac{L_c}{R_l^2 C_g} = \frac{\omega_2 L_c}{R_l} \quad (6-7)$$

Equation (6-5) may then be written in the form

$$\frac{K_2}{K_0} = \frac{1}{1 + j(\omega/\omega_2)Q_2 + j(\omega/\omega_2)} \quad (6-8)$$

This expression is expanded, thus,

$$\frac{K_2}{K_0} = \frac{1 + j(\omega/\omega_2)Q_2}{[1 - (\omega/\omega_2)^2 Q_2] + j(\omega/\omega_2)}$$

which may be written as

$$\frac{K_2}{K_0} = \sqrt{\frac{1 + (\omega/\omega_2)^2 Q_2^2}{[1 - (\omega/\omega_2)^2 Q_2]^2 + (\omega/\omega_2)^2}} \angle \left[ \tan^{-1} \frac{\omega}{\omega_2} Q_2 - \tan^{-1} \frac{\omega/\omega_2}{1 - (\omega/\omega_2)^2 Q_2} \right] \quad (6-9)$$

The significance of this equation is best understood by examining curves

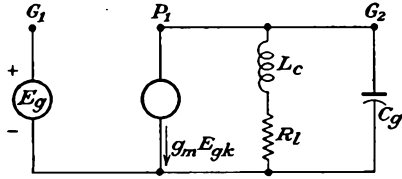


FIG. 6-4. The approximate equivalent circuit of Fig. 6-3 at the mid- and high-frequencies.

of gain and phase shift for various values of  $Q_2$ . A set of gain curves is given in Fig. 6-5.

It is ordinarily desired that the voltage gain be practically constant up to a certain designated high frequency. An inspection of Fig. 6-5 shows that this is best achieved by choosing  $Q_2$  to have a value approximately

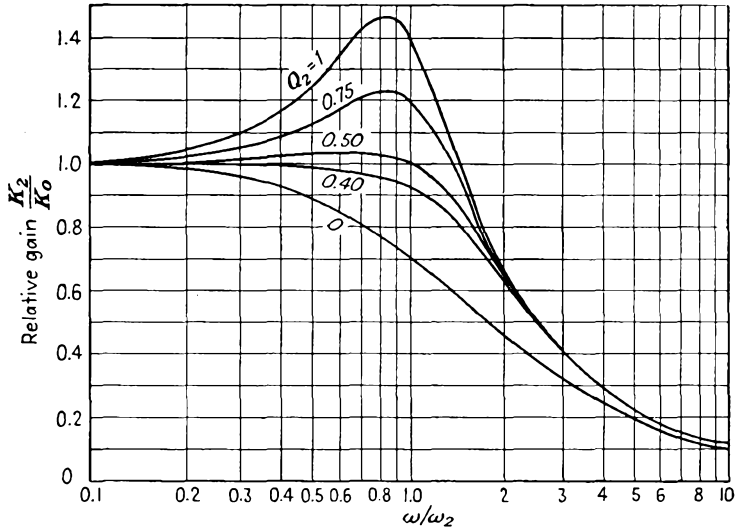


FIG. 6-5. Dimensionless relative gain curves for the shunt-compensated amplifier. (Adapted from Bedford and Fredendall.<sup>1</sup>)

0.45. Actually the optimum value for  $Q_2$  is 0.414, under which conditions  $dK/df = d^2K/df^2 = 0$  at  $f_2$ , which yields the maximum flatness. From Eqs. (6-6) and (6-7), this requires approximately that

$$\left. \begin{aligned} R_l &\doteq \frac{1}{\omega_2 C_g} \\ \omega_2 L_c &\doteq \frac{R_l}{2} \end{aligned} \right\} \quad (6-10)$$

That is, approximately constant gain is achieved when the load resistance is approximately equal to the reactance of the effective shunt capacitance and when the inductive reactance is equal approximately to one-half the load resistance at that frequency.

In order to preserve the wave form of the signal in an amplifier, not only must the relative amplitudes of the various frequency components be maintained, but also their phase relations must be held constant. If this is not so, then phase distortion results. The phase shift through the amplifier is contained in Eq. (6-9), which is

$$\left. \begin{aligned} \text{or } \varphi &= 180 + \left[ \tan^{-1} \frac{\omega}{\omega_2} Q_2 - \tan^{-1} \frac{\omega/\omega_2}{1 - (\omega/\omega_2)^2 Q_2} \right] \\ \varphi &= 180 - \tan^{-1} \frac{\omega}{\omega_2} \left[ 1 - Q_2 + \left( \frac{\omega Q_2}{\omega_2} \right)^2 \right] = 180 - \theta \end{aligned} \right\} \quad (6-11)$$

Evidently, for the wave form to be preserved, either the phase shift of the various components through the amplifier must be zero, or else the phase of all the frequency components must be changed by the same amount in time and the relative phase relations among the harmonics in

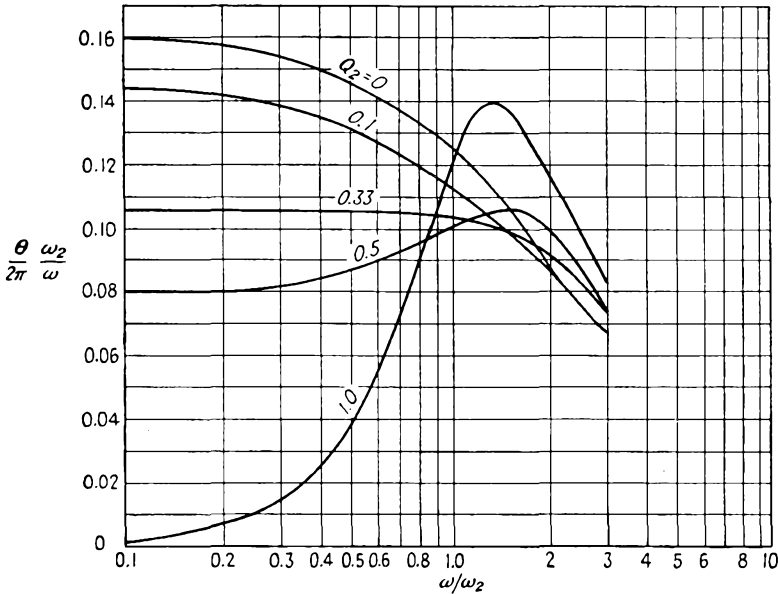


FIG. 6-6. Dimensionless curves of  $\theta/\omega$  as a function of  $\omega/\omega_2$  for shunt-compensated amplifiers.

the wave form must be preserved. Clearly, a criterion for zero phase distortion is that  $\theta/\omega$  be a constant. A plot of  $\theta\omega_2/2\pi\omega$  vs.  $\omega/\omega_2$  is contained in Fig. 6-6.

Figure 6-6 shows a family of dimensionless curves which apply to any amplifier. With  $\omega/\omega_2$  and  $Q_2$  given, the phase shift at any frequency is readily determined. It will be observed that the curve for  $Q_2 = 0.34$  shows the least variation of  $\theta/\omega$  and so introduces the least phase distortion or time delay. On the other hand, the curve for  $Q_2 = 0.414$  shows the least variation in gain. In general, therefore, it would appear that the value of  $Q_2$  should lie in the range from 0.34 to 0.41. Frequently a value of  $Q_2$  of 0.5 is used, for the following reasons.

The curve for  $Q_2 = 0.5$  yields a relatively uniform amplification over

as wide a frequency range as for any value of  $Q_2$ . For this case, the relative gain increases by about 3 per cent ( $=0.3$  db) at  $\omega/\omega_2 = 0.70$ . This is frequently a tolerable increase if only a few stages are used. Moreover, the time-delay errors of the individual stages are additive and would be tolerable in many applications. If many stages are to be used, then the situation changes. For example, a 10-stage amplifier designed with  $Q_2 = 0.50$  would have a 3-db (41 per cent) bump in the gain curve,

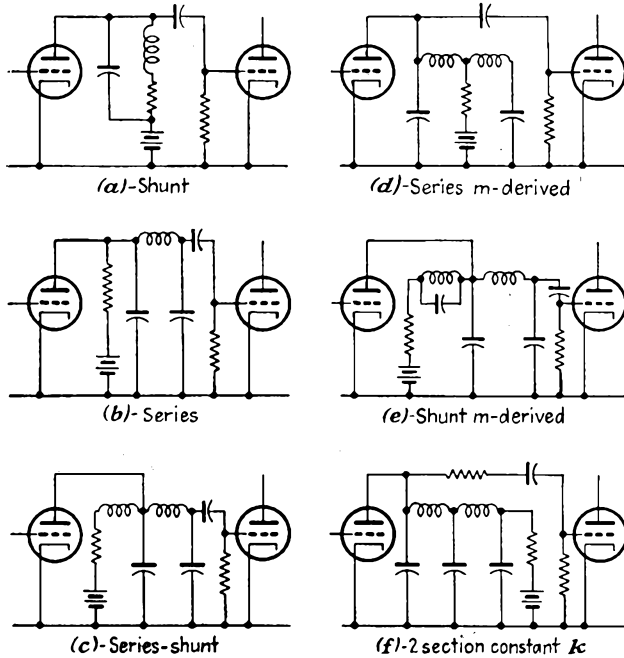


FIG. 6-7. Various h-f-compensating coupling circuits. (D. L. Jaffee, *Electronics*, April, 1942.)

with a corresponding serious time-delay error. Such characteristics might not be tolerable, and a value of  $Q_2$  of 0.41 would then be used.

Clearly, therefore, the acceptable value of  $Q_2$  will be determined by the maximum allowable variation in gain and the tolerable time-delay error. If one can tolerate the resulting variation in gain, then a given number of stages with  $Q_2 = 0.50$  will provide a given gain with a broader band width than is possible with  $Q_2 = 0.41$ . This means that the requirement for maximum flatness sacrifices band width for a more uniform amplification curve and less time-delay or phase distortion.

It should perhaps be emphasized that the inclusion of an inductance as a compensating network has resulted in a rather remarkable improvement in response. That such a simple correcting network does not provide both optimum gain and constant-phase characteristics for the

same conditions should not be surprising or unexpected. More elaborate h-f compensating networks that provide better gain characteristics have been devised. A number of these are illustrated in Fig. 6-7.

The transient response of these more elaborate networks is generally inferior to that of the simple shunt-peaking compensation.<sup>1</sup> This results from the fact that the amplification and phase-shift characteristics do not deteriorate so rapidly in the shunt-peaked circuit as in other h-f compensating systems having the same h-f limit. Consequently the apparent advantage of these circuits is largely eliminated.

**6-3. L-F Compensation.** A circuit that compensates for the droop in the low-frequency response characteristics of an  $RC$  amplifier is given in Fig. 6-2. A

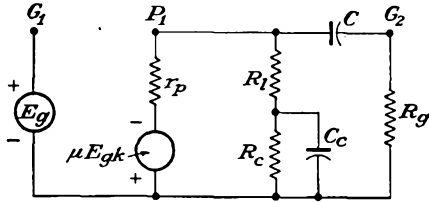


FIG. 6-8. The equivalent circuit of an l-f-compensated  $RC$  amplifier.

physical explanation of the operation of the l-f compensating network is given on page 96. An analytical study is to be made of the performance of this circuit, in order to obtain a more complete description of its behavior.

The equivalent circuit, given in Fig. 6-8, is to be analyzed. Use is again made of the fact that pentodes are generally used in video amplifiers, whence  $r_p$  is greater than the combined output load impedance  $Z$ . Also in general, the grid resistor of the following stage  $R_g$  is large compared with the load resistor  $R_l$ .

The mid-frequency gain assumes that the reactances of  $C_c$  and  $C$  are small compared with  $R_l$  and  $R_g$ , respectively. The gain expression is then simply

$$K_0 = -g_m R_l \tag{6-12}$$

The low-frequency gain is readily obtained from an examination of Fig. 6-8. The expression is

$$K_1 = -g_m Z \frac{R_g}{R_g + \frac{1}{j\omega C}} \tag{6-13}$$

where  $Z$  is the total effective impedance of the output network at the low frequencies. By inserting the known value of  $Z$  in Eq. (6-13), and combining with Eq. (6-12), there results

$$\frac{K_1}{K_0} = \frac{1}{R_l \left( \frac{1}{R_l + \frac{1}{\frac{1}{R_c} + j\omega C_c}} + \frac{1}{R_g + \frac{1}{j\omega C}} \right)} \frac{R_g}{R_g + \frac{1}{j\omega C}} \tag{6-14}$$

or

$$\frac{K_1}{K_0} = \frac{1}{\frac{1}{R_c} + \frac{j\omega CR_l}{1 + j\omega CR_g}} \frac{1}{1 + \frac{1}{j\omega CR_g}}$$

or

$$\frac{K_1}{K_0} = \frac{1}{\frac{R_l + j\omega C_c R_c R_l}{R_l + R_c + j\omega C_c R_c R_l} + \frac{j\omega CR_l}{1 + j\omega CR_g}} \frac{1}{j\omega CR_g}$$

which is

$$\frac{K_1}{K_0} = \frac{1}{\frac{R_l}{R_g} + \left( \frac{R_l + j\omega C_c R_c R_l}{R_l + R_c + j\omega C_c R_c R_l} \right) \left( \frac{1 + j\omega CR_g}{j\omega CR_g} \right)} \quad (6-15)$$

But ordinarily the ratio  $R_l/R_g \ll 1$ , and Eq. (6-15) becomes

$$\frac{K_1}{K_0} = \frac{1}{\frac{R_l}{R_l + R_c} \frac{1 + j\omega C_c R_c}{1 + j\omega C_c \frac{R_c R_l}{R_c + R_l}} \frac{1 + j\omega CR_g}{j\omega CR_g}} \quad (6-16)$$

Three time constants appear in this expression, *viz.*,

$$R_c C_c \quad C_c \frac{R_c R_l}{R_c + R_l} \quad R_g C$$

By choosing the parameters such that

$$X CR_g = C_c \frac{R_c R_l}{R_c + R_l} \quad (6-17)$$

then Eq. (6-16) becomes

$$\frac{K_1}{K_0} = \frac{1}{\frac{R_l}{R_l + R_c} \frac{1 + j\omega C_c R_c}{1 + j\omega CR_g} \frac{1 + j\omega CR_g}{j\omega CR_g}}$$

which is

$$\frac{K_1}{K_0} = \frac{1}{(1 + j\omega C_c R_c) \frac{R_l}{j\omega C_c R_c R_l}} = \frac{1}{1 - j \frac{1}{\omega C_c R_c}} \quad (6-18)$$

This may be written in the form

$$\frac{K_1}{K_0} = \frac{1}{\sqrt{1 + (X_{c_c}/R_c)^2}} / \tan^{-1} X_{c_c}/R_c \quad (6-19)$$

It is noted that this choice of parameters yields exactly the same form for the l-f response for the compensated case as that of the uncompensated amplifier, except that the l-f response is now controlled by the time constant  $R_c C_c$  rather than by the output time constant  $R_g C$ .

**6-4. The Cathode Follower.<sup>2</sup>** The foregoing sections show that, to achieve a uniform frequency response of an  $RC$  amplifier over a wide

frequency band, it is necessary that the effective output impedance of each stage be low and the effective input capacitance be small. The small effective input capacitance can be attained by the use of pentodes. However, the output impedance of a pentode is high unless the load resistance is small, in which case distortion may result. Considerable

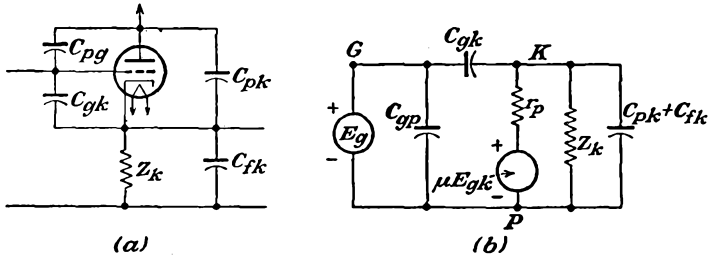


FIG. 6-9. The basic circuit (a) and the equivalent plate circuit (b) of the cathode follower.

improvement results from the use of two or more high-gain stages, preferably using pentodes, which are coupled by a triode which is connected to provide a low input capacitance and a low output impedance. Although such a coupling tube may contribute nothing to the over-all gain of the system, it does make possible a uniform amplification over a wider frequency range than with the conventional coupled amplifier. The use of a cathode follower as the coupling stage is particularly suitable because it possesses a low effective input capacitance, high input impedance, low output impedance, and low nonlinear distortion. Such a stage does possess a gain that is less than unity, although this is not a serious limitation.

The basic circuit and the corresponding equivalent circuit of the cathode follower are given in Figs. 6-9. To find an expression for the gain of the amplifier, it is noted that

$$E_{pk} = \frac{-E_g Y_{C_{gk}} - \mu E_{gk} Y_p}{Y_{C_{gk}} + Y_p + Y_{C_{pk}+C_{fk}} + Y_{Z_k}} = \frac{-Y_{C_{gk}} E_{gp} - \mu E_{gk} Y_p}{Y_{C_{gk}} + Y_p + Y_{C_{pk}+C_{fk}} + Y_{Z_k}} \tag{6-20}$$

But it follows that

$$E_{gk} = E_{gp} + E_{pk}$$

and Eq. (6-20) becomes

$$E_{pk} = \frac{-j\omega C_{gk} E_{gp} - \mu Y_p (E_{gp} + E_{pk})}{j\omega (C_{gk} + C_{pk} + C_{fk}) + \frac{1}{r_p} + \frac{1}{Z_k}} \tag{6-21}$$

Solving for the gain  $K$ , which is given by

$$K \equiv \frac{E_{kp}}{E_{gp}} \tag{6-22}$$

there results

$$K = \frac{(j\omega r_p C_{gk} + \mu)Z_k}{j\omega r_p Z_k (C_{gk} + C_{pk} + C_{fk}) + r_p + (\mu + 1)Z_k} \tag{6-23}$$

For those values of  $Z_k$  which are normally used, the effect of the inter-electrode and wiring capacitances on the voltage amplification is negligible for frequencies below about 1 megacycle. Equation (6-23) reduces, for these lower frequencies, to

$$K \doteq \frac{\mu Z_k}{r_p + (\mu + 1)Z_k} \tag{6-24}$$

Examination of this expression shows that the gain  $K$  approaches the limiting value  $\mu/(\mu + 1)$  as the ratio of  $Z_k/r_p$  approaches infinity. For the values of  $Z_k$  and  $r_p$  found in normal cases,  $K$  is of the order of 0.9.

The limits of linear operation of the cathode follower are determined by the grid current and cutoff characteristics of the tube. These limits can be obtained readily. It is assumed that the voltage  $E_{gk} = E_{gp} - E_{kp}$  has the limits zero (for zero grid current) and  $E_0$  (at cutoff). If the region of a-c operation is so chosen that the operating point is midway between these limits and also that the grid-cathode signal reaches these limits at the peaks, then the maximum output is given by

$$\frac{E_{kp,\max}}{E_{gk,\max}} = \frac{K}{1 - K}$$

But

$$E_{gk,\max} = \frac{E_0 - 0}{2\sqrt{2}}$$

and

$$E_0 \doteq \frac{E_b}{\mu}$$

then

$$E_{kp,\max} = \frac{E_0}{2\sqrt{2}} \frac{K}{1 - K} = \frac{E_0\mu}{2\sqrt{2}\left(1 + \frac{r_p}{Z_k}\right)} = \frac{E_b}{2\sqrt{2}\left(1 + \frac{r_p}{Z_k}\right)} \tag{6-25}$$

The value of  $E_b$  to be used in this expression will be dependent on the character of the load. For example, if the load is inductive, then  $E_b$  will be a value less than  $E_{bb}$ , owing to the elliptical load curve.

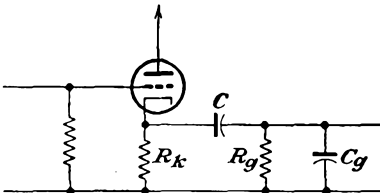


FIG. 6-10. An RC coupled cathode-follower stage.

**6-5. The Cathode-follower Amplifier.** When used as a coupling amplifier between stages, the cathode-follower circuit becomes essentially that illustrated in Fig. 6-10. In this cir-

circuit,  $C_o$  is the sum of the effective output capacitance of the cathode follower and the effective input capacitance of the next stage.

The gain of this amplifier will be examined for the various frequency ranges. These follow directly from Eq. (6-24) with the proper interpretation of  $Z_k$ .

*Mid-frequency Gain.* The inter-electrode capacitances are negligible over the mid-frequency band, whence  $C_o$  may be neglected. Also the coupling capacitor  $C$  is assumed sufficiently large so that its reactance is negligible. The resulting circuit becomes that of Fig. 6-11. The mid-frequency gain becomes

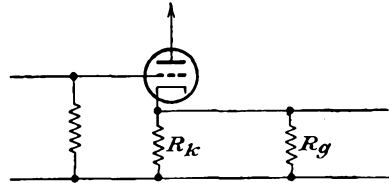


FIG. 6-11. The mid-frequency cathode-follower circuit.

$$K_0 = \frac{\mu Z'_k}{r_p + (\mu + 1)Z'_k} = \frac{\mu}{(\mu + 1) + (r_p/Z'_k)} \tag{6-26}$$

where

$$\frac{1}{Z'_k} = \frac{1}{R_k} + \frac{1}{R_g} \tag{6-27}$$

*H-F Gain.* At the h-f end of the response curve, the coupling capacitor may be omitted, although the effect of  $C_o$  becomes important. The equivalent circuit has the form shown in Fig. 6-12. The gain equation [Eq. (6-24)] now becomes

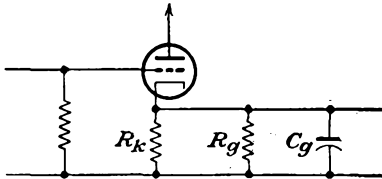


FIG. 6-12. The h-f circuit of the cathode follower.

$$K_2 = \frac{\mu}{(\mu + 1) + (r_p/Z'_k)} \tag{6-28}$$

where

$$\frac{1}{Z'_k} = \frac{1}{R_k} + \frac{1}{R_g} + j\omega C_o \tag{6-29}$$

The gain ratio  $K_2/K_0$  becomes

$$\frac{K_2}{K_0} = \frac{1}{1 + \frac{j\omega C_o r_p}{(\mu + 1) + (r_p/Z'_k)}}$$

which is

$$\frac{K_2}{K_0} = \frac{1}{1 + j\omega r'_p C_o} = \frac{1}{1 + j(f/f_2)} \tag{6-30}$$

where

$$r'_p = \frac{r_p}{(\mu + 1) + (r_p/Z'_k)} \quad f_2 = \frac{1}{2\pi r'_p C_o} \tag{6-31}$$

It should be noted that this expression has substantially the same form as Eq. (5-15) for the conventional RC circuit. However, since the prod-

uct  $r'_p C_\theta$  for the cathode follower is much smaller than  $r_p C_\theta$  of the  $RC$  amplifier, then the upper frequency limit of uniform response is much greater for the cathode follower than for the conventional  $RC$  stage. Because of this, it is possible to achieve a high h-f limit even when the

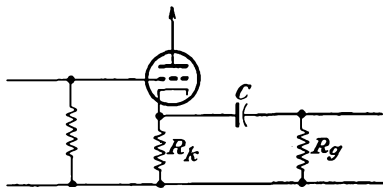


FIG. 6-13. The l-f circuit of the cathode-follower amplifier.

cathode follower is followed by a stage having a high input capacitance. This means that a rather wide frequency response is possible under these conditions even with a following triode stage.

*L-F Gain.* At the low frequencies,  $C_\theta$  may be neglected, and the effect of the coupling capacitor becomes very important. Equation (6-24) appropriately modified becomes

$$K_1 = \frac{\mu}{(\mu + 1) + (r_p/Z'_k)} \frac{R_g}{R_g + (1/j\omega C)} \quad (6-32)$$

This expression may be written in the form

$$K_1 = \frac{\mu}{(\mu + 1) + \frac{r_p}{Z'_k} - \frac{r_p}{R_g(1 + j\omega CR_g)}} \frac{j\omega CR_g}{1 + j\omega CR_g} \quad (6-33)$$

where use has been made of the fact that

$$\frac{1}{Z'_k} = \frac{1}{R_k} + \frac{1}{R_g + \frac{1}{j\omega C}} = \frac{1}{Z'_k} - \frac{1}{R_g(1 + j\omega CR_g)} \quad (6-34)$$

The gain ratio becomes

$$\frac{K_1}{K_0} = \frac{1}{(\mu + 1) + \frac{r_p}{Z'_k} - \frac{r_p}{R_g(1 + j\omega CR_g)}} \frac{j\omega CR_g}{1 + j\omega CR_g} \left[ (\mu + 1) + \frac{r_p}{Z'_k} \right]$$

which reduces to the form

$$\left. \begin{aligned} \frac{K_1}{K_0} &= \frac{1}{1 - j(1/\omega CR_1)} = \frac{1}{1 - j(f_1/f)} \\ \text{where} \quad R_1 &= \frac{R_g}{1 - \frac{r_p/R_g}{(\mu + 1) + (r_p/Z'_k)}} \quad f_1 = \frac{1}{2\pi CR_1} \end{aligned} \right\} \quad (6-35)$$

This expression has substantially the same form as Eq. (5-9) for the l-f gain of the  $RC$  amplifier except that it may be shown that under typical operating conditions the value of  $f_1$  is much lower for the cathode follower.

**6-6. Input Capacitance and Output Impedance of the Cathode Follower.** To find an expression for the input capacitance of the cathode follower, refer to Fig. 6-9b. It is seen that the current flowing through the source comprises two components. One of these is the current through the capacitance  $C_{gp}$  and is

$$I_1 = j\omega C_{gp} E_{gp} \tag{6-36}$$

The second is the current through the capacitance  $C_{gk}$ . This is

$$I_2 = j\omega C_{gk} E_{gk} \tag{6-37}$$

But as  $E_{gk} = E_{gp} + E_{pk}$  and  $K = E_{kp}/E_{gp}$ , then

$$I_2 = j\omega C_{gk}(1 - K)E_{gp} \tag{6-38}$$

The total current is

$$I = I_1 + I_2 = j\omega[C_{gp}E_{gp} + (1 - K)C_{gk}E_{gp}]$$

and the effective input capacitance is

$$C_i = C_{gp} + (1 - K)C_{gk} \tag{6-39}$$

Since in many circuits  $K$  is approximately 0.9, then  $C_i$  has the approximate value

$$C_i \doteq C_{gp} + 0.1C_{gk} \tag{6-40}$$

A comparison of this expression with the corresponding form given by Eq. (4-13) shows a roughly similar dependence on the tube capacitances, although the numerical value for the cathode follower is considerably smaller than for the conventional amplifier stage.

The effective output impedance can be determined by finding the current that flows as a result of the application of an a-c potential to the output terminals of Fig. 6-9. The grid exciting potential is made zero, and the grid generator is replaced by its internal impedance—according to the superposition theorem. The equivalent circuit may then be drawn in the form of Fig. 6-14. The effective output admittance of the tube alone is

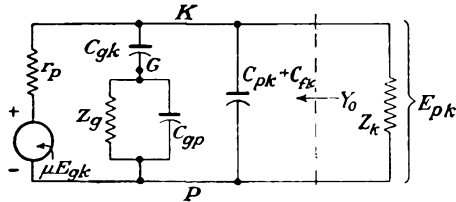


FIG. 6-14. The equivalent output circuit of the cathode follower.

$$Y_0 = \frac{1}{E_{pk}} \left( \frac{E_{pk} + \mu E_{gk}}{r_p} + \frac{E_{pk}}{\frac{1}{Y_{c_{gk}}} + \frac{1}{Y_g + Y_{c_{gp}}}} \right) \tag{6-41}$$

But from the diagram it is seen that

$$E_{gk} = \frac{Z_{c_{ok}}}{\frac{1}{Y_{z_g} + Y_{c_{gp}}} + Z_{c_{ok}}} E_{pk} = \frac{1}{1 + \frac{Y_{c_{ok}}}{Y_{z_g} + Y_{c_{gp}}}} E_{pk} \quad (6-42)$$

Ordinarily  $Z_k$  is a resistor which is  $10^k$  or less, and the reactances of  $C_{gk}$  and  $C_{gp}$  are approximately  $20^k$  at 1 megacycle (for capacitances of  $10 \mu\text{f}$ ). Under most conditions Eq. (6-42) becomes

$$E_{gk} \doteq E_{pk}$$

and the output admittance reduces to the approximate form

$$Y_0 \doteq \frac{1 + \mu}{r_p} \quad (6-43)$$

This expression shows that the output terminal admittance of the tube is somewhat greater than the transconductance of the tube. But for the actual values of transconductance of available tubes, the output terminal

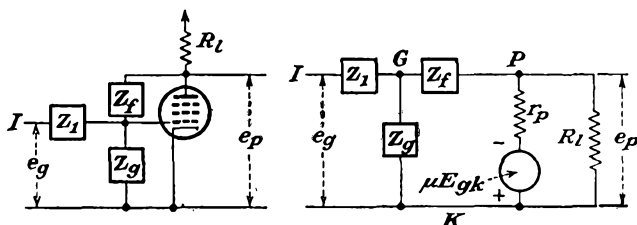


Fig. 6-15. A general feed-back circuit, and its equivalent circuit.

impedance  $Z_0$  may be less than 150 ohms and would seldom exceed 1,000 ohms with single tubes, under the assumptions made in the derivation of Eq. (6-43). In many applications the impedance of the coupled load is much larger than the output impedance of the tube and so will have very little effect on the resultant output impedance. A double-cathode-follower circuit has been devised which has a greatly reduced output impedance.<sup>3</sup>

**6-7. The Anode Follower.** A circuit which possesses roughly the same properties as the cathode follower but which also provides for phase inversion is called an *anode follower*. This may be a desirable property in certain applications. The circuit of such an anode follower is given in Fig. 6-15. Actually, the circuit of Fig. 6-15 is that of a general feed-back circuit and will be shown in Chap. 8 to have many applications. It is a simple amplifier which is provided with voltage feedback through the impedance  $Z_f$ .

An analysis of the equivalent circuit is readily carried out. An application of the Millman network theorem between the points  $K$  and  $G$  yields

$$E_{kg} = \frac{E_{kl}Y_1 + E_{kp}Y_f}{Y_1 + Y_f + Y_g} \tag{6-44}$$

When applied between *K* and *P*, the network theorem yields

$$E_{kp} = \frac{E_{kg}Y_f + \mu E_{gk}Y_p}{Y_f + Y_p + Y_l} = \frac{E_{kg}(Y_f - g_m)}{Y_f + Y_p + Y_l} \tag{6-45}$$

By combining these expressions, there results

$$E_{kp} = \frac{Y_f - g_m}{Y_f + Y_p + Y_l} \frac{E_{kl}Y_1 + E_{kp}Y_f}{Y_1 + Y_g + Y_f} \tag{6-46}$$

By solving for the gain, the result is

$$K_r = \frac{E_{kp}}{E_{kl}} = \frac{Y_1(Y_f - g_m)}{(Y_f + Y_p + Y_l)(Y_1 + Y_f + Y_g) - Y_f(Y_f - g_m)}$$

which may be written in the form

$$K_r = \frac{Y_1(Y_f - g_m)}{(Y_1 + Y_f + Y_g)(Y_p + Y_l) + Y_f(Y_1 + Y_g + g_m)} \tag{6-47}$$

To obtain an expression for the output impedance of this general feed-back circuit, the procedure followed is substantially that used in Sec. 6-6. In the present case, the equivalent circuit for this calculation becomes as shown in Fig. 6-16. The output admittance is given by

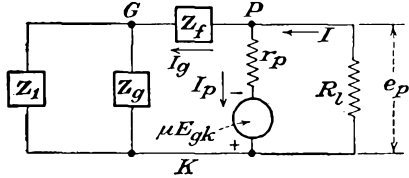


FIG. 6-16. The equivalent circuit for calculating the output impedance of the feed-back circuit of Fig. 6-15.

$$Y_0 = \frac{I}{E_{pk}} = \frac{I_p + I_g}{E_{pk}} \tag{6-48}$$

This may be written in the form

$$Y_0 = \frac{1}{E_{pk}} \left[ \frac{E_{pk} + \mu E_{gk}}{r_p} + E_{gk}(Y_g + Y_1) \right]$$

which is

$$Y_0 = \frac{1}{E_{pk}} [(Y_1 + Y_g + g_m)E_{gk} + Y_p E_{pk}] \tag{6-49}$$

But from the diagram

$$E_{gk} = \frac{Y_f}{Y_1 + Y_f + Y_g} E_{pk} \tag{6-50}$$

and the expression for the output admittance becomes

$$Y_0 = Y_p + Y_f \left( \frac{Y_1 + Y_g + g_m}{Y_1 + Y_f + Y_g} \right) \tag{6-51}$$

An expression for the input impedance is readily obtained. It follows directly from the circuit that

$$E_{l_0} + E_{o_k} + E_{k_l} = 0$$

The input admittance is given by

$$Y_i = \frac{I}{E_{l_k}} = Y_1 \left( 1 - \frac{E_{o_k}}{E_{l_k}} \right) \quad (6-52)$$

But by Eqs. (6-44) and (6-47)

$$E_{k_o} = \frac{E_{k_l} Y_1 + K_r E_{k_l} Y_f}{Y_1 + Y_o + Y_f} = E_{k_l} \frac{Y_1 + K_r Y_f}{Y_1 + Y_o + Y_f} \quad (6-53)$$

Then

$$Y_i = Y_1 \left( 1 - \frac{Y_1 + K_r Y_f}{Y_1 + Y_o + Y_f} \right)$$

which may be written in the form

$$Y_i = \frac{Y_1}{Y_1 + Y_o + Y_f} [Y_o + (1 - K_r) Y_f] \quad (6-54)$$

If it is supposed that a pentode is used in the circuit, and with the following choice of circuit elements,

$$\begin{aligned} Y_p &\sim 10^{-6} \\ g_m &\sim 2,000 \times 10^{-6} \\ Y_1 = Y_f &= 2 \times 10^{-6} \quad \text{for } R_1 = R_f = 0.5M \\ Y_o &= 0.2 \times 10^{-6} \quad \text{for } R_o = 5M \end{aligned}$$

the several important results are as follows:

1. The expression for the gain [Eq. (6-47)]

$$K_r \doteq \frac{-Y_1 g_m}{2Y_1 Y_l + Y_1 g_m} = -\frac{1}{1 + (2/R_l g_m)} \doteq -1 \quad (6-55)$$

2. The output impedance, given by Eq. (6-51), reduces to

$$Z_o \doteq \frac{2}{g_m} \quad (6-56)$$

3. The input impedance becomes, approximately,

$$Y_i \doteq \frac{1 - K_r}{2} Y_1 \doteq Y_1 \quad (6-57)$$

A comparison of these results with those for a cathode follower is interesting. This comparison is contained in Table 6-1. It is observed that the gains of the two circuits are both approximately unity; the cathode-follower output impedance is approximately one-half that of the

anode follower; the input impedance of the cathode follower may be considerably higher than that of the anode follower.

TABLE 6-1  
COMPARISON OF THE CATHODE AND ANODE FOLLOWER

	Gain	Output impedance	Input impedance
Anode follower.....	$-\frac{1}{1 + \frac{2}{g_m R_l}}$	$\frac{2}{g_m}$	$R_l$
Cathode follower.....	$+\frac{1}{1 + \frac{1}{g_m R_k}}$	$\frac{1}{g_m}$	$R_o$

**6-8. Direct-coupled Amplifier.**<sup>4</sup> It is possible to build a type of cascaded amplifier without reactive elements and, in principle at least, secure a very broad band amplifier. The voltage gain of such an amplifier does not depend on the frequency, at least to a first approximation, except for the effect of tube and wiring capacitances at the higher frequencies. It might appear that such amplifiers would find very widespread use because of these desirable characteristics. However, such amplifiers do possess certain disadvantages, and their use is limited, though they find extensive use in applications as d-c amplifiers and as amplifiers for very slowly varying inputs.

A battery-coupled cascade-amplifier circuit of basic design, together with the equivalent plate circuit for small changes in voltage and current, is shown in Fig. 6-17. The gain of such an amplifier stage is readily found to be

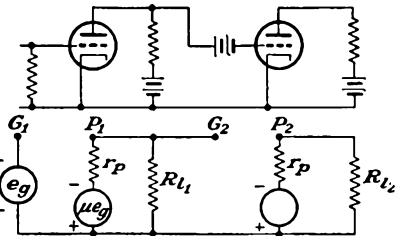


FIG. 6-17. Basic battery-coupled amplifier circuit.

$$K = \frac{-\mu R_l}{r_p + R_l} \tag{6-58}$$

It will be observed that the circuits are quite like the RC coupled amplifier except that the coupling (blocking) capacitors are absent. Because of the fact that the grid of one stage is directly connected to the plate circuit of the previous stage, it is necessary to include d-c sources in the various critical points in the circuit in order that the quiescent conditions be those of class A operation.

The battery-coupled amplifier has the outstanding feature that it will amplify a steady component in the input voltage, but it suffers from three main disadvantages. The first is the cost of the relatively high voltage grid-bias batteries. These are required when a common plate and a common filament supply are used. In an alternative arrangement, indirectly heated cathodes having different potentials are used, thus obviating the necessity for large grid-bias voltages. However, separate plate supplies are required in this case.

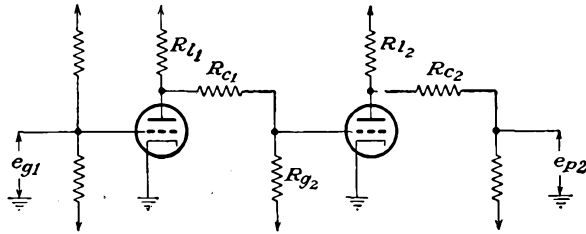


FIG. 6-18. A resistance-coupled amplifier.

The second disadvantage of the direct-coupled amplifier is the inherent instability associated with the direct coupling. The characteristics of the tubes in the circuit change slightly with time; the battery voltages, or the a-c line-operated rectified power supplies, likewise change with time. Since such changes are amplified, the d-c amplifier is not feasible unless precautions can be taken which tend to overcome this instability. For

this reason, balanced circuits and circuits with degenerative feedback are used, since they tend to minimize this difficulty.

The third disadvantage arises from the capacitance between the grid-bias batteries and the cathodes. This, plus the interelectrode capacitances, stray wiring capacitance, and stray inductance, influences the transient-response time and materially affects the rapidity with which the amplifier output responds to rapid changes of input voltage. In consequence, even though the amplifier is direct-coupled, precautions must be taken to ensure a broad h-f response in order to provide a short response time.

It is possible to build a direct-coupled amplifier that uses a positive plate supply, a negative bias supply, and resistance coupling networks. This overcomes disadvantage 1. The circuit of such an amplifier is illustrated in Fig. 6-18. The equivalent circuit of a typical stage of this amplifier is given in Fig. 6-19. The gain of such an amplifier is readily

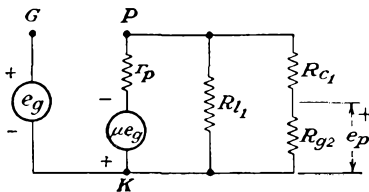


FIG. 6-19. The equivalent circuit of a typical stage of the resistance-coupled amplifier of Fig. 6-18.

found to be

$$K = - \frac{\mu \frac{R_{g2}}{R_{g2} + R_{c1}} \frac{R_{l1}(R_{c1} + R_{g2})}{R_{l1} + R_{c1} + R_{g2}}}{r_p + \frac{R_{l1}(R_{c1} + R_{g2})}{R_{l1} + R_{c1} + R_{g2}}} \tag{6-59}$$

For an appreciable voltage gain, the parallel combination of  $R_{l1}$  and  $R_{c1} + R_{g2}$  should be large compared with  $r_p$ , and  $R_{g2}$  should be large compared with  $R_{c1}$ . This will necessitate the use of a large bias voltage.

Direct-coupled amplifiers are used extensively as the amplifier in a circuit, the grid exciting source of which has a very high internal resistance or which is capable of supplying only a very small current. In this case, the grid current must be very small. In particular, the grid current is significant when the grid-cathode resistance of the tube, though high,

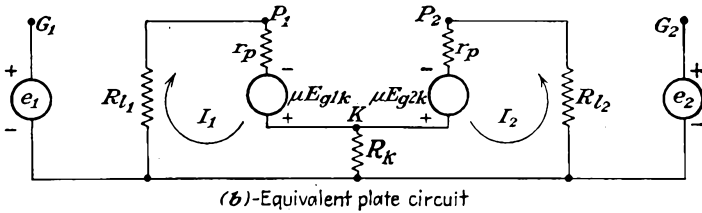
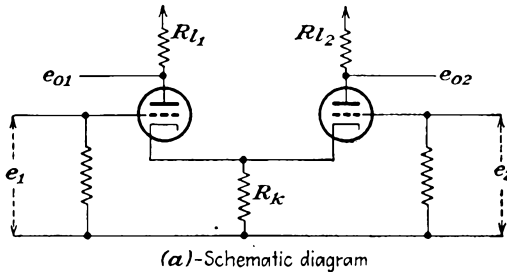


FIG. 6-20. Schematic and equivalent plate circuit of the difference amplifier.

might not be large in comparison with the resistance of the circuit that supplies the grid signal voltage. Special electrometer tubes in which the grid current is of the order of  $10^{-15}$  amp are available for such applications. The grid current of the typical negative-grid tube is of the order of  $10^{-8}$  amp with normal rated voltages applied to the tube electrodes. With the electrode voltages at very low values, the grid current may be reduced as low as  $10^{-12}$  amp. More will be said about the applications of such amplifiers in Chap. 22.

**6-9. The Difference Amplifier.** A two-tube amplifier which is used extensively as a d-c amplifier is illustrated in Fig. 6-20. This circuit

overcomes disadvantage 1 of the previous section and permits the use of common battery supplies for all stages. Also, the amplifier possesses some very desirable features and as a result finds applications in various services. The analysis below will indicate the reason for the descriptive name of this amplifier circuit.

To analyze the operation of the circuit, Kirchhoff's law is applied around each circuit. This yields the equations

$$\left. \begin{aligned} I_1(R_{l1} + r_p + R_k) + I_2R_k &= \mu E_{g1k} \\ I_1R_k + I_2(R_{l2} + r_p + R_k) &= \mu E_{g2k} \end{aligned} \right\} \quad (6-60)$$

But the potential difference between grid and cathode of each tube is related to the circuit parameters by the equations

$$\left. \begin{aligned} E_{g1k} &= e_1 - (I_1 + I_2)R_k \\ E_{g2k} &= e_2 - (I_1 + I_2)R_k \end{aligned} \right\} \quad (6-61)$$

By combining these expressions with Eqs. (6-60) there result

$$\left. \begin{aligned} I_1(R_{l1} + r_p + R_k) + I_2R_k &= \mu[e_1 - (I_1 + I_2)R_k] \\ I_1R_k + I_2(R_{l2} + r_p + R_k) &= \mu[e_2 - (I_1 + I_2)R_k] \end{aligned} \right\}$$

which may be written in the form

$$\left. \begin{aligned} I_1[R_{l1} + r_p + (\mu + 1)R_k] + I_2(\mu + 1)R_k &= \mu e_1 \\ I_1(\mu + 1)R_k + I_2[R_{l2} + r_p + (\mu + 1)R_k] &= \mu e_2 \end{aligned} \right\} \quad (6-62)$$

A solution of this set of equations for the currents yields, for  $I_1$ ,

$$I_1 = \frac{+\mu \left[ \left( \frac{R_{l2} + r_p}{\mu + 1} + R_k \right) e_1 - R_k e_2 \right]}{\frac{(R_{l1} + r_p)(R_{l2} + r_p)}{\mu + 1} + R_k(R_{l1} + R_{l2} + 2r_p)} \quad (6-63)$$

and, for the current  $I_2$ ,

$$I_2 = \frac{-\mu \left[ R_k e_1 - \left( \frac{R_{l1} + r_p}{\mu + 1} + R_k \right) e_2 \right]}{\frac{(R_{l1} + r_p)(R_{l2} + r_p)}{\mu + 1} + R_k(R_{l1} + R_{l2} + 2r_p)} \quad (6-64)$$

It follows from these that the output potentials are, respectively,

$$e_{o1} = -I_1R_{l1} = \frac{-\mu R_{l1} \left[ \left( \frac{R_{l2} + r_p}{\mu + 1} + R_k \right) e_1 - R_k e_2 \right]}{\frac{(R_{l1} + r_p)(R_{l2} + r_p)}{\mu + 1} + R_k(R_{l1} + R_{l2} + 2r_p)} \quad (6-65)$$

and

$$e_{02} = -I_2 R_{l2} = \frac{+\mu R_{l2} \left[ R_k e_1 - \left( \frac{R_{l1} + r_p}{\mu + 1} + R_k \right) e_2 \right]}{(R_{l1} + r_p)(R_{l2} + r_p) + R_k(R_{l1} + R_{l2} + 2r_p)} \quad (6-66)$$

Under ordinary conditions of operation of tubes, the ratio  $(R_l + r_p)/(\mu + 1) \ll R_k$ . Under these conditions Eqs. (6-65) and (6-66) reduce to

$$e_{01} = \frac{-\mu R_{l1}}{R_{l1} + R_{l2} + 2r_p} (e_1 - e_2) \quad (6-67)$$

$$e_{02} = \frac{+\mu R_{l2}}{R_{l1} + R_{l2} + 2r_p} (e_1 - e_2) \quad (6-68)$$

It will be observed from these equations that the output voltages are given in terms of an amplified difference between the two input potentials.

Special cases of these equations are extremely important. Four such cases will be examined: (a) when the plate resistors are equal; (b) when one plate resistor is zero; (c) when one grid is grounded and one plate resistor is zero; (d) when the plate resistors are equal, with one grid grounded.

*Equal Plate Resistors.* In this case, it is supposed that the plate resistors are the same,  $R_{l1} = R_{l2} = R_l$ . Equations (6-67) and (6-68) reduce to

$$e_{01} = \frac{-\mu R_l}{2(R_l + r_p)} (e_1 - e_2) \quad (6-69)$$

$$e_{02} = \frac{+\mu R_l}{2(R_l + r_p)} (e_1 - e_2) \quad (6-70)$$

These expressions show that the two output potentials are of equal magnitude but of opposite polarity. Also, appreciable amplification is provided by the circuit. Note also that the difference between the two output voltages is

$$e_{01} - e_{02} = \frac{-\mu R_l}{R_l + r_p} (e_1 - e_2) \quad (6-71)$$

Although this expression was obtained from expressions that are only approximate, this result is actually exact. That this is so may be verified by using Eqs. (6-65) and (6-66) directly, and not the approximate forms, Eqs. (6-67) and (6-68).

Evidently, the difference amplifier may be used to indicate the exact point of balance between two d-c potentials. In fact, such a balancing circuit, with a center-reading voltmeter connected between the plates of the two tubes, is frequently drawn as a bridge circuit in the manner illustrated in Fig. 6-21. In this circuit, when there is no input signal and when the tubes are properly matched, the indicating center-reading volt-

meter is at zero. When a signal is applied, an amplified signal results, a measure of the signal strength being indicated on the voltmeter.

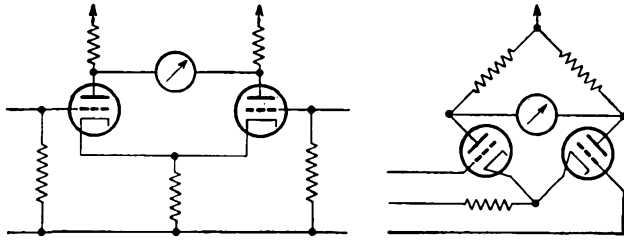


FIG. 6-21. A difference amplifier in conventional form, and also drawn in a manner to indicate the equivalent bridge character of the circuit.

*One Plate Resistor Zero.* Suppose that the plate resistor  $R_{11} = 0$ . It follows from Eqs. (6-67) and (6-68) that

$$\left. \begin{aligned} e_{01} &= 0 \\ e_{02} &= \frac{\mu R_l}{R_l + 2r_p} (e_1 - e_2) \end{aligned} \right\} \quad (6-72)$$

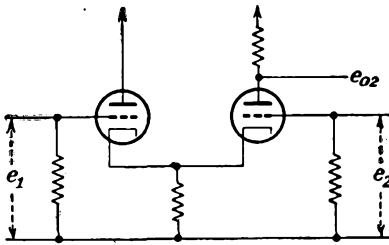


FIG. 6-22. The difference amplifier with one plate resistor at zero.

*One Grid Grounded, One Plate Resistor Zero.* In this case, it will be supposed that  $e_2 = 0$ , and  $R_{11} = 0$ . Under these conditions, Eqs. (6-67) and (6-68) reduce to

$$\left. \begin{aligned} e_{01} &= 0 \\ e_{02} &= \frac{\mu R_l}{R_l + 2r_p} e_1 \end{aligned} \right\} \quad (6-73)$$

With this arrangement, an amplified output voltage  $e_{02}$  results for an input signal  $e_1$ . In effect, therefore, two tubes are used to perform the same function as a single tube in a conventional type of circuit. As discussed above, however, it is now

This circuit yields an amplified output that is the difference between the signals to the two grids. If only a single output signal is required, the present connection provides slightly higher gain than the connection of Fig. 6-21, without the output from a single plate.

*One Grid Grounded, One Plate*

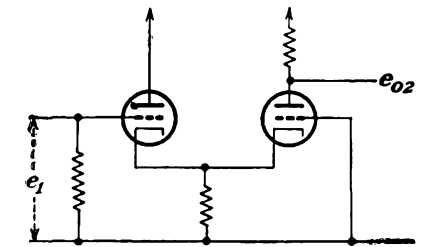


FIG. 6-23. The difference amplifier connected to provide a single output from a single input.

possible to use a common set of voltage supplies. A typical circuit showing a cascade amplifier of difference amplifiers is given in Fig. 6-24.

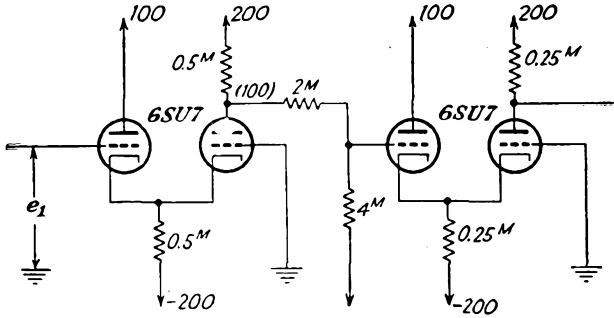


FIG. 6-24. A multistage d-c amplifier employing difference amplifiers.

*Equal Plate Resistors, One Grid Grounded.* In this case, the two plate resistors are equal, and one grid is grounded. Consequently, this circuit produces two potentials from a single input voltage, and from Eqs. (6-67) and (6-68) the results are

$$\left. \begin{aligned} e_{o1} &= \frac{-\mu R_l}{2(R_l + r_p)} e_1 \\ e_{o2} &= \frac{+\mu R_l}{2(R_l + r_p)} e_1 \end{aligned} \right\} \quad (6-74)$$

This circuit is known as a *cathode-coupled paraphase amplifier* and is used extensively to provide push-pull signals from a single source of potential. It is used to provide a virtually balanced set of push-pull potentials for the deflection plates of a cathode-ray oscilloscope and is also used as the driver of a push-pull power amplifier.

An examination of the complete expressions, Eqs. (6-67) and (6-68), will show that the output potentials are exactly balanced only if  $R_k = \infty$ . Ordinarily the amount of unbalance is not serious, but if completely balanced voltages are required, the self-balancing paraphase inverter (see Sec. 9-11) may be used.

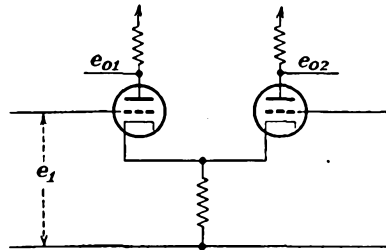


FIG. 6-25. A cathode-coupled paraphase amplifier.

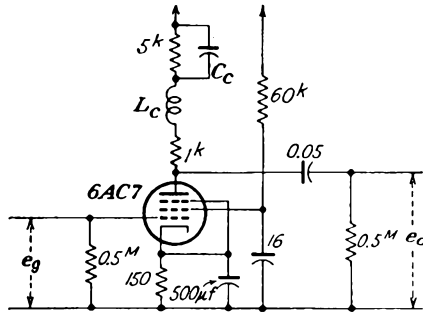
REFERENCES

1. For a detailed discussion of the transient characteristics of video amplifiers, see Bedford, A. V., and G. L. Fredendall, *Proc. IRE*, **27**, 277 (1939).  
Kallman, H. E., R. E. Spencer, and C. P. Singer, *Proc. IRE*, **33**, 169, 482 (1945).

- Arguimbau, L. B., "Vacuum Tube Circuits," Chap. IV, John Wiley & Sons, Inc., New York, 1948.
2. Reich, H. J., "Theory and Application of Electron Tubes," 2d ed., Sec. 6-11, McGraw-Hill Book Company, Inc., New York, 1944.
- Reich, H. J., *Proc. IRE*, **35**, 573 (1947).
- Kraus, H. L., *Electronics*, **20**, 116 (January, 1947).
- Schlesinger, K., *Electronics*, **21**, 103 (February, 1948).
3. Hammock, C., *M.I.T. Radiation Lab. Rept.* 469, 1943.
4. Artzt, M., *Electronics*, **18**, 112 (August, 1945).

### PROBLEMS

**6-1.** A 6AC7 tube is used as one of a chain in a video amplifier that is shunt-compensated at the high frequencies and is also l-f-compensated. The circuit of this amplifier is shown in the accompanying diagram. Calculate the value of



$L_c$  that will yield the same gain at the upper frequency  $f_2$  as at the mid-band. Assuming the stray wiring capacitances to be  $20 \mu\text{mf}$ , the tube capacitances of the 6AC7 are  $C_{gp} = 0.015 \mu\text{mf}$ ,  $C_{pk} = 5 \mu\text{mf}$ ,  $C_{ek} = 11 \mu\text{mf}$ . Calculate also  $f_1$  under the optimum conditions for the l-f compensation.

**6-2.** A video amplifier stage is constructed using a 6AC7. An experimental test shows that the voltage amplification drops to 0.707 of the mid-frequency gain at  $f_2 = 1$  megacycle with  $R_i = 6^k$ .

- For what value of  $R_i$  will the h-f cutoff value be 3 megacycles?
- What value of  $L_c$  is required for flattest gain under conditions of (a)?
- What value of  $L_c$  is required for "compromise" gain?
- What is the mid-frequency gain?
- What is the phase angle for flattest gain when  $f = 0.8f_2$ ?

**6-3.** A video amplifier using 6AC7 tubes is to provide an over-all gain of 20,000 with a 3-megacycle over-all band width. If the total stage shunt capacitance is  $25 \mu\text{mf}$  and with  $g_m = 9,000 \mu\text{mhos}$

- Calculate the number of stages required, for  $Q_2 = 0.414$ .
- If 6SJ7 tubes are used ( $g_m = 1,600 \mu\text{mhos}$ ), how many stages are required?

**6-4.** A five-stage shunt-peaked video amplifier is to be built.

- a. If the amplification must not rise more than 1 db above the mid-frequency gain, estimate the value of  $Q_2$  to be used. All stages are identical.
- b. If the time delay at the h-f cutoff point is to be within 10 per cent of the midfrequency value, what range of  $Q_2$  is permissible?

6-5. Calculate and plot as a function of frequency on semilog paper the gain, output impedance, and input impedance of the cathode-follower amplifier of Fig. 6-10 at the following values of  $\omega$ : 250, 2,500, 25,000, 250,000,  $2.5 \times 10^6$ ,  $5 \times 10^6$  rad/sec. Choose a 6J5 tube for which

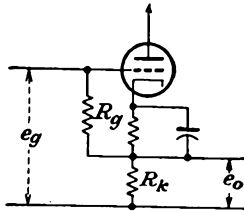
$$r_p = 7,700 \quad \mu = 20 \quad C_{op} = 3.4 \mu\mu f \quad C_{ok} = 3.4 \mu\mu f \quad C_{pk} = 3.6 \mu\mu f$$

Also choose

$$R_k = 10^4 \quad R_g = 200^4 \quad C = 0.01 \mu f \quad C_o = 40 \mu\mu f$$

6-6. What must be the value of  $R_k$  in Fig. 6-9 if  $Z_o = 300$  ohms at 1,000 cps? A 6J5 tube is used.

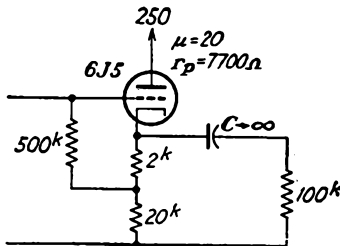
6-7. Given the cathode-follower circuit with the grid resistor  $R_g$  tied from grid to cathode, as shown in the accompanying figure. Derive an expression for the



input impedance and the output impedance of this circuit, neglecting the tube capacitances.

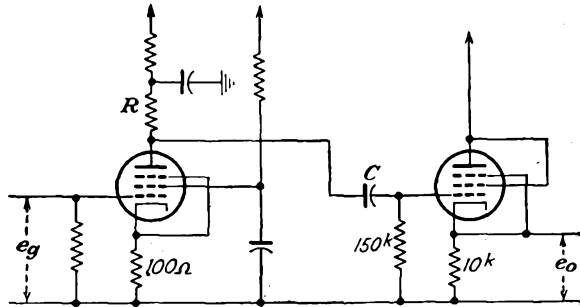
6-8. In the circuit shown in the accompanying diagram, determine

- a. Positive signal which will drive  $e_c$  to zero.
- b. Negative signal to drive the tube to cutoff.
- c. Mid-frequency gain.
- d. Input admittance when  $C_{op} = 3.4 \mu\mu f$ ,  $C_{ok} = 4 \mu\mu f$ .

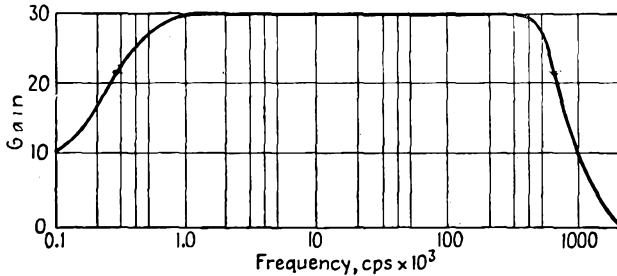


6-9. Repeat (c) and (d) of Prob. 6-8 when the tube is changed to a 6AC7, assuming that the tube operates in its linear region.

6-10. A video amplifier is coupled to a cathode follower, as shown in the figure.

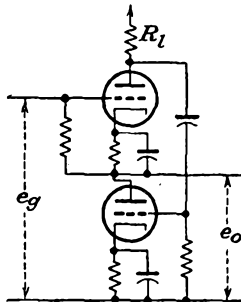


The frequency-response curve of this amplifier is also sketched. Assume that the transconductance  $g_m = 9,000 \mu\text{mhos}$ .



- a. Calculate the approximate value of the coupling capacitor between the two stages.
- b. Calculate the approximate value of the total shunt capacitance.

6-11. The essentials of a double cathode follower<sup>3</sup> are illustrated.



a. Show that the expression for the gain is

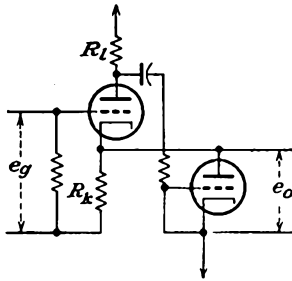
$$K = \frac{\mu^2 + \mu r_p / R_l}{(\mu^2 + \mu + 1) + (\mu + 2)r_p / R_l}$$

b. Show that the output admittance is

$$Y_o = \frac{\mu + 1}{r_p + R_l} + \frac{1 + \frac{\mu(\mu + 1)}{1 + r_p/R_l}}{r_p}$$

$$\cong \mu g_m$$

6-12. Repeat Prob. 6-11 for the double cathode follower in the diagram.



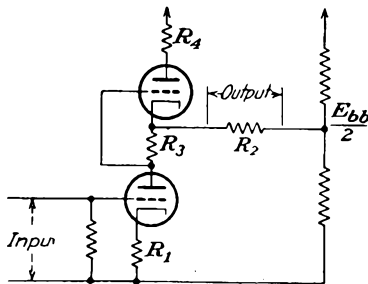
6-13. Show that the h-f cutoff of the anode-follower amplifier is approximately one-half that of the cathode follower. Show also that the l-f cutoff is approximately the same as that of the cathode-follower amplifier, for  $Z_1 = R_g$  in Circuit Fig. 6-10.

6-14. Refer to Fig. 6-18 showing a resistance-coupled amplifier. The circuit constants are

$$R_{l1} = 250^k \quad R_{g2} = 500^k \quad R_{c1} = 500^k$$

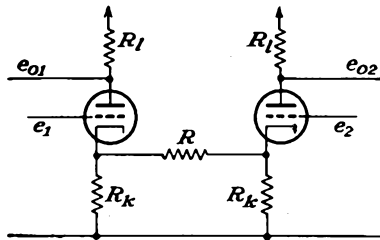
If  $I_{b1} = 0.5$  ma,  $E_{bb} = 300$  volts, what must be the value of  $E_{c2}$  if  $E_c$  of T2 is to be  $-8$  volts?

6-15. Calculate the gain of the series balanced d-c amplifier shown in the diagram.



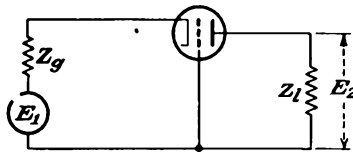
6-16. Calculate the input admittance and the output impedance of the difference amplifier when connected as shown in Fig. 6-23. Neglect tube and wiring capacitances.

6-17. Obtain an expression for the output voltages of the cathode-coupled two-tube circuit shown in the figure, and compare with Eqs. (6-67) and (6-68).

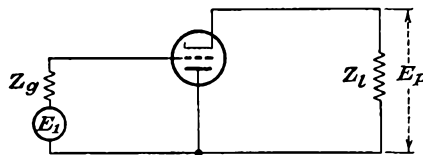


6-18. The circuit of a grounded-grid amplifier is shown. (Batteries have been omitted for convenience.) Determine the following:

- The gain.
- Input impedance.
- Ratio of output to input power if  $Z_o$  and  $Z_i$  are resistors.



6-19. Repeat the calculations of Prob. 6-18 for the inverted amplifier of the accompanying figure.



## CHAPTER 7

### SPECIAL AMPLIFIER CIRCUITS

A WIDE variety of special amplifier circuits have been devised. Among those to be studied are limiting and clipping amplifiers, peaking circuits, and clamping circuits.

**7-1. Limiting and Clipping Amplifiers.** In addition to the various amplifiers that are intended to reproduce a given wave form with a minimum of distortion, there are other forms of circuits which are designed to alter the wave shape of an input wave in some predetermined manner.

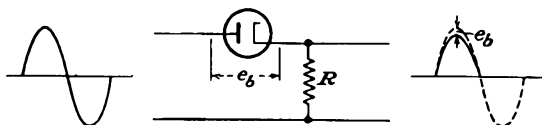


FIG. 7-1. A series diode used to limit negative signals.

Limiting or clipping circuits are designed to remove by electronic means one or the other extremity of an input wave.

A limiter is used when it is desired to square off the extremities of an applied signal. For example, it is used as one stage in a chain to obtain a substantially rectangular wave form from a sine-wave signal. A limiter may also be used to eliminate either the positive or the negative portion of a wave. Such circuits also find application in f-m receivers to limit to a constant value the amplitude of the signal that is applied to the detection system. This application is discussed in Sec. 17-14.

Limiting and clipping may be accomplished with the aid of diodes, triodes, or multielectrode tubes. For triodes and multielectrode tubes, the limiting may be accomplished either in the grid or in the plate circuits. The general features of a number of such limiting circuits will be examined below.

*Series-diode Limiting.* The circuit of the series-diode limiter is given in Fig. 7-1. It will be observed that this circuit is precisely that of a diode as used in a rectifier circuit. Since the tube conducts only when the plate is at a positive potential with respect to the cathode, then only the positive portion of the applied wave will pass through the tube, the negative portion of the wave being eliminated. By neglecting the relatively small drop across the tube during conduction, the output wave

form is simply the positive portion of the applied wave form. If the diode connections are reversed, then the positive portion of the wave will be eliminated and only the negative portion of the wave will pass through to the output.

The series-diode circuits possess the feature that they tend to isolate the driving circuit from the following circuit and thus prevent feedback.

*Shunt-diode Limiting.* A diode may be connected in shunt across the load for limiting action. In such cases, the diode may be looked upon as an infinite impedance for polarities opposite to that necessary for conduction and as a virtual short circuit for the polarity in the conducting direction. The diode is then acting as a switch which will short-circuit a given load for a certain polarity and amplitude of the applied potential.

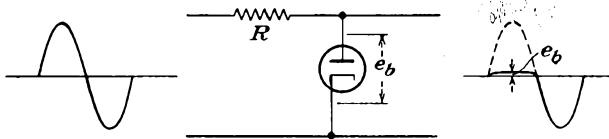


FIG. 7-2. A shunt-diode positive limiting circuit.

The connections of a shunt diode for limiting the positive signals at approximately ground potential are shown in Fig. 7-2. With the cathode maintained at ground potential, the diode conducts throughout the entire positive half cycle. During the portion of the cycle when the diode is conducting, the current passes through the series resistor  $R$ . With  $R$  large compared with the drop across the tube, practically the entire input voltage is developed across  $R$ , and the output voltage is only the small drop across the diode. On the negative portion of the input voltage, the diode does not conduct, and the voltage that appears across the output is then determined by the resistor  $R$  and the resistance of the load.

If the connections to the diode are reversed, with the anode held at ground potential, the tube will conduct only when the input potential is negative with respect to ground. As a result, the negative potential will appear across the series resistor, except for the small tube drop, which may ordinarily be neglected.

An input voltage can be limited to any desired positive or negative value by maintaining the proper diode electrode at the desired potential. Two circuits for limiting about a desired potential are shown in Figs. 7-3.

In the circuit of Fig. 7-3a for positive limiting, it is observed that the cathode is maintained at a fixed potential  $E$  above the input. As a result, the diode does not conduct until the positive potential on the anode exceeds  $E$ , when the action becomes exactly like that of Fig. 7-2. The input voltage during the conducting portion of the cycle is lost in the series resistor  $R$ .

The operation of the circuit of Fig. 7-3b is essentially like that of Fig. 7-3a except that conduction of the diode occurs when the cathode falls below the value  $-E$ . The input portion of the voltage during conduction appears across the resistor  $R$ .

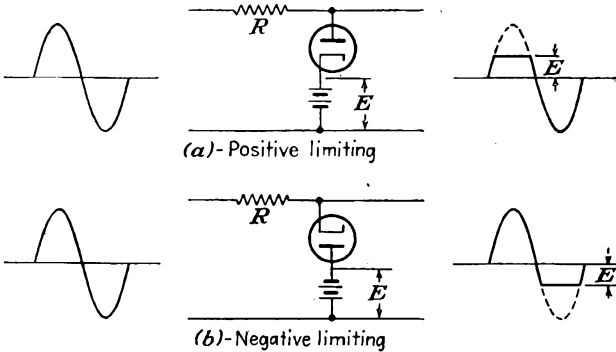


FIG. 7-3. Positive and negative limiting above and below ground.

*Series-Shunt Limiting.* Somewhat improved limiting action is possible by combining both the series and shunt limiting circuits into a single circuit. The possible combinations are illustrated in Fig. 7-4. In the form shown, the circuits limit completely all signals of a given polarity. Of course, if biasing potentials are applied, as in Fig. 7-3, the limiting point would be placed at the discrete level determined by the bias voltage  $E$ .

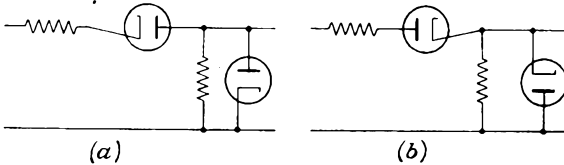


FIG. 7-4. Double-diode limiters for removing (a) all positive-going potentials; (b) all negative-going potentials.

This circuit, as for the simple series-diode limiting circuits, isolates the driving circuit from the following circuit and thus prevents feedback through the circuit.

*Double-diode Limiting.* It is possible to limit both amplitude extremities of a wave form at any desired levels by placing two diodes in the circuit, one of which acts to limit the positive peaks, and the other of which acts to limit the negative peaks. The circuit for such double-diode operation is given in Fig. 7-5. In this circuit the diode  $T1$  conducts whenever the input voltage exceeds the positive value  $E_1$ . The diode  $T2$  conducts when the input voltages falls more negative than the potential  $-E_2$ .

*Grid-circuit Limiting.* Limiting in the grid circuit of a triode, tetrode, or pentode is possible in exactly the same way as in the plate-cathode circuit of the diode circuit of Fig. 7-2. The series resistor  $R$  in the grid

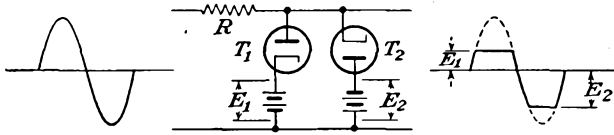


FIG. 7-5. Double-diode limiting circuit.

circuit is large compared with the grid-cathode resistance when the grid is drawing current. The circuit is given in Fig. 7-6.

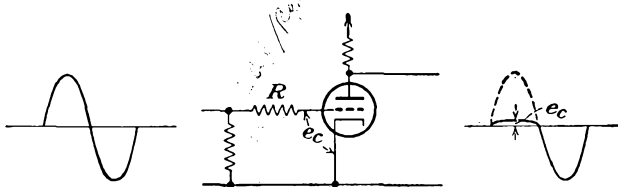


FIG. 7-6. Grid-circuit limiter.

If a bias voltage is used, as in Fig. 7-7, limiting occurs about the bias level, precisely as in the manner of the circuit of Fig. 7-3a. It is

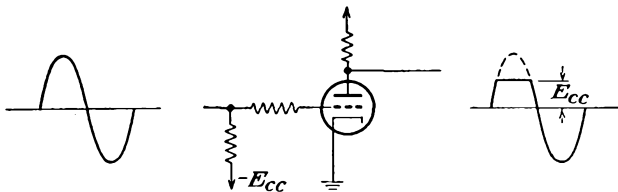


FIG. 7-7. Grid-circuit limiting about a fixed potential level.

possible to use self-bias instead of fixed bias for setting the potential level about which the positive portion of the wave is limited. The basic circuit of such a limiter is given in Fig. 7-8.

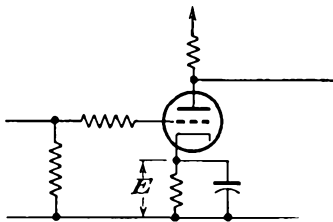


FIG. 7-8. A self-biased grid-circuit limiter.

*Saturation Limiting.* Limiting action may also be obtained in the plate circuit of an amplifier by employing a large load resistor in conjunction with a low value of plate voltage. Such limiting arises from the fact that, with a highly positive signal on the grid, the maximum tube current is limited because of the low plate potential  $E_{bb}$ . The minimum output potential is  $E_{bb} - E_b$ . Since these limits, for small  $E_{bb}$ , are reached

Since these limits, for small  $E_{bb}$ , are reached

with small signals, clipping occurs for values greater than these limits. These results are made evident by an examination of the plate characteristics of the tube as illustrated in Fig. 7-9. The circuit and the results using a pentode for saturation limiting as employed in a receiver for f-m signals are given in Sec. 17-14.

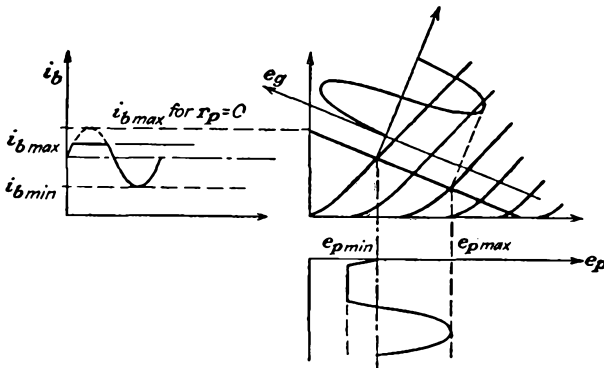


FIG. 7-9. Saturation limiting in a triode.

*Cutoff Limiting.* If a tube is operated in the class B region by setting the bias so that the current in the tube is nominally near cutoff, then the application of a sine-wave grid signal will give rise to an output current that possesses features not unlike the current from a diode rectifier. This results from the fact that a small negative potential will drive the

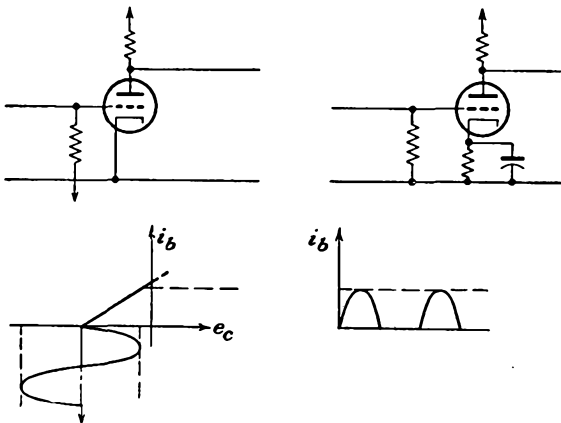


FIG. 7-10. Cutoff limiting in a strongly biased amplifier.

tube beyond cutoff and that no current will flow for any potential below this value. The operation is made evident by an examination of the dynamic characteristic of the tube as illustrated in Fig. 7-10.

*Combination of Limiting Actions.* A combination of grid limiting and cutoff limiting may be employed in an amplifier to produce a substantially

square wave from a sine wave or other comparable wave shape. The action is illustrated in Fig. 7-11. During the positive portion of the swing, the grid-circuit limiting is effective; the plate current reaches its

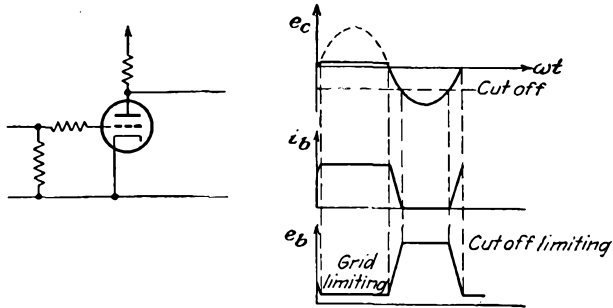


FIG. 7-11. Formation of a square wave by grid-circuit and cutoff limiting.

maximum, and the output potential reaches its minimum. During the negative portion of the grid swing, the tube is cut off, whence the plate current falls to zero and the plate potential is at its maximum.

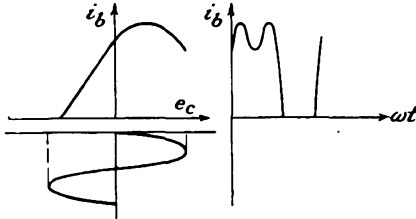


FIG. 7-12. Formation of a square wave by saturation and cutoff limiting. The overdriven amplifier.

A combination of saturation limiting and cutoff limiting in a tube is called an *overdriven amplifier*. The operation is substantially like that of the circuit with grid-circuit limiting, except that the grid circuit limits by virtue of the high grid potential, which causes a high grid current and hence a small grid-cathode resistance. The operation is illustrated in Fig. 7-12.

**7-2. Peaking Circuits.** Electronic control systems frequently require the accurate synchronization of one event or a multiplicity of events relative to each other. Often this synchronization is accomplished by generating triggering pulses in the proper time sequence and having each triggering pulse initiate the operation of some portion of the total circuit in the proper order. As a rule these triggering pulses should be of short duration and should have an extremely sharp leading edge. Such pulses can be generated in specially designed pulse-forming circuits, and a number of these will be examined in Chap. 19. It is also possible to produce them in a *peaking circuit*. Such a circuit is capable of distorting an input signal wave in such a way as to produce an output wave form in which the time duration is shortened and in which the leading edge is made as nearly vertical as possible.

The choice of peaking circuit used will depend primarily upon the input wave shape. One of the common methods is to use sufficient limiting

and amplification so that a substantially rectangular wave is available and then apply this square wave to an  $RC$  differentiating circuit. Although a number of such differentiating circuits exist, the requirements imposed by this application are not very stringent in general, and simple forms of so-called *differentiating circuits* may be used.

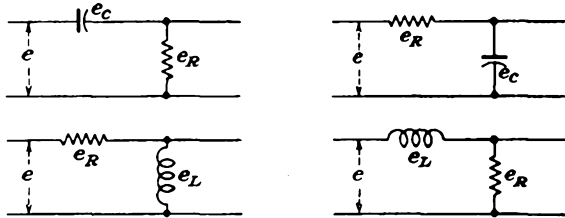


FIG. 7-13. Several differentiating and integrating networks.

The forms of circuit in common use for differentiation and integration are shown in Fig. 7-13. In the  $RC$  network, the instantaneous behavior for an applied potential  $e$  is governed by the equations

$$\left. \begin{aligned} e_r &= iR = RC \frac{de_c}{dt} \\ e_c &= \frac{1}{C} \int i dt = \frac{1}{RC} \int e_r dt \end{aligned} \right\} \quad (7-1)$$

The corresponding equations for the  $LR$  circuits are

$$\left. \begin{aligned} e_L &= L \frac{di}{dt} = \frac{L}{R} \frac{de_r}{dt} \\ e_r &= iR = \frac{R}{L} \int e_L dt \end{aligned} \right\} \quad (7-2)$$

But the sum of the potentials appearing across the capacitance and the resistance in series must be equal, at every instant, to the applied potential. If  $e_c$  is very small compared with  $e_r$ , then  $e_r$  must be approximately equal to the applied potential. It therefore follows that (1)  $e_c$  is approximately proportional to the time integral of the applied potential when  $e_c/e_r$  is small and (2)  $e_r$  is approximately proportional to the time derivative of the applied potential when  $e_r/e_c$  is small.

If a perfect differentiating and integrating network were used, then the output potential may be specified directly. Thus it follows that

Input	Differentiation	Integration
Square.....	Vertical lines above and below base line	Triangular
Saw-tooth.....	Horizontal line on one side of base line spike	Parabolic
Triangular.....	Square	Parabolic half cycles

The behavior of the circuits for an applied d-c potential is governed respectively by the equations

a. For  $RC$  Circuit

$$\left. \begin{aligned} i &= \frac{E_0}{R} e^{-\frac{t}{RC}} \\ e_R &= E_0 e^{-\frac{t}{RC}} \\ e_C &= E_0(1 - e^{-\frac{t}{RC}}) \\ e &= e_R + e_C \end{aligned} \right\} (7-3a)$$

b. For  $RL$  Circuit

$$\left. \begin{aligned} i &= \frac{E_0}{R} (1 - e^{-\frac{Rt}{L}}) \\ e_L &= E_0 e^{-\frac{Rt}{L}} \\ e_R &= E_0(1 - e^{-\frac{Rt}{L}}) \\ e &= e_L + e_R \end{aligned} \right\} (7-3b)$$

A plot of the general characteristics of these equations is given in Fig. 7-14.

An examination of these equations reveals the following very important facts: In the  $RC$  circuit, the current through the capacitor may change instantaneously, although the voltage across it cannot change suddenly.

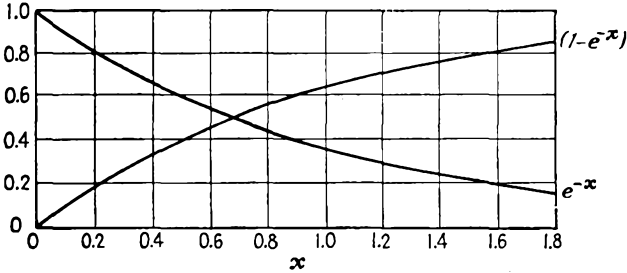


Fig. 7-14. The exponential characteristics of the transient solutions of Eqs. (7-3a) and (7-3b).

That is, a capacitor acts like a short circuit for sudden changes in potential. In the  $RL$  circuit, the current through the inductance cannot change suddenly, although the voltage across it may change instantaneously.

If, instead of a steady d-c potential, a recurring square wave is applied to the circuit, the potential across each element will begin to rise according to the time constant of the circuit and will begin to decay when the applied potential reverses. Curves showing the character of the increase, with the ratio  $f/f_0$  as a parameter, where  $f$  is the frequency of the applied square wave and  $f_0 = 1/(2\pi RC)$  is the quantity defined by the time constant of the circuit, are given in Fig. 7-15. These curves are essentially a plot of the function

$$e_C = E_0(1 - e^{-\frac{t}{RC}})$$

or

$$\frac{e_C}{E_0} = 1 - e^{-2\pi \left(\frac{f_0}{f}\right) \frac{t}{T}} \quad (7-5)$$

For example, if the quantity  $f_0$  of the circuit is 3,000 cps and a 1,000-cps square wave is applied,  $f/f_0$  is  $\frac{1}{3}$  and the capacitor voltage will rise in accordance with the curve marked  $\frac{1}{3}$  and will reach 90 per cent of its full value in about 0.13 cycle.

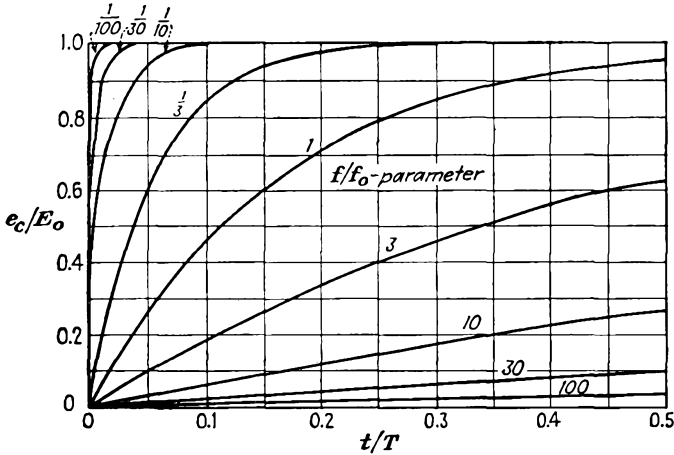


FIG. 7-15. The potential across the capacitor as a function of time, with  $f/f_0$  as a parameter.

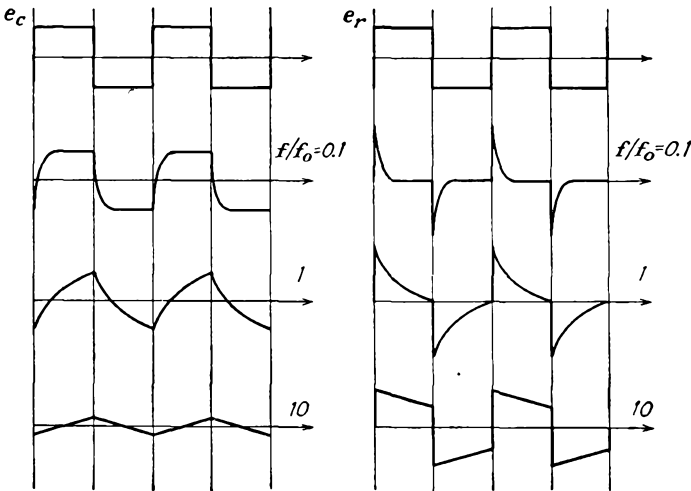


FIG. 7-16. The voltage forms  $e_c$  and  $e_r$  for an applied square wave on a differentiating circuit, with  $f/f_0$  as parameter.

To obtain the complete response for a given applied square wave, a careful application of the curves of Fig. 7-15 must be made. This gives the form for  $e_c$ . The set of curves for  $e_r$  is obtained from the fact that  $e_r = e - e_c$ . The results have the form illustrated in Fig. 7-16.

Theoretically it is of no consequence whether the circuit is composed of inductance and resistance or resistance and capacitance. Apart from the higher cost, it is ordinarily inadvisable to use an inductive differentiating circuit if it can be avoided, because the effective resistance of the coil is usually large enough to change the output character of the results. When an  $RC$  differentiating circuit is used, the series capacitance should

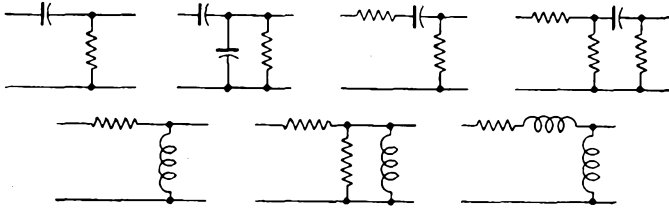


FIG. 7-17. Differentiation circuits with similar response characteristics.

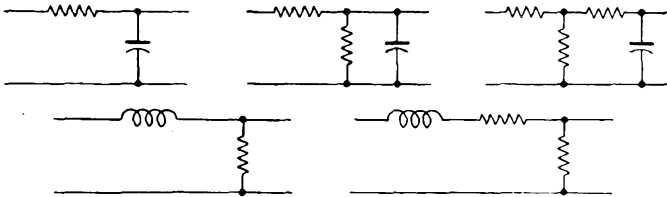


FIG. 7-18. Integrating circuits with similar response characteristics.

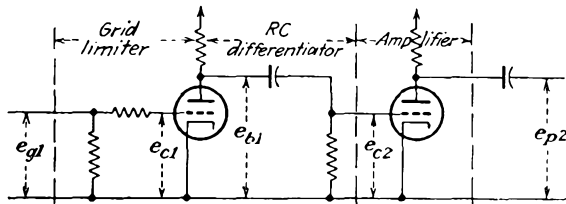


FIG. 7-19. A typical application of an  $RC$  differentiator as a peaker.

be large compared with any distributed capacitances that may exist in the circuit. In particular, if the output of such a differentiating circuit is to be used to feed the grid of a tube, the series capacitance should be large compared with the input capacitance of the tube in order that the time constant will not be altered by an indefinite amount.

A number of circuits exist which give transient-response curves that are similar to those represented by Eqs. (7-3a) and (7-3b). The circuits of Fig. 7-17 give transient-response curves similar to those represented by Eqs. (7-3a), and the circuits of Fig. 7-18 give results similar to those of Eqs. (7-3b).

The circuit of Fig. 7-19 illustrates a practical application of an  $RC$

differentiator as a peaker circuit. The general character of the wave shapes at several points in the circuit are illustrated in Fig. 7-20.

Care must be exercised in analyzing the actions in such a circuit, particularly if the grid of any tube is driven positive. In particular, the grid-cathode resistance  $r_c$  when the grid is conducting is low and is of the order of 1,000 ohms. When a tube is conducting, the average tube resistance, or beam resistance,  $r_b$  (the ratio  $e_b/i_b$ ) is low. When the tube is cut off, the grid-cathode resistance may be taken as infinite; and the beam resistance is also infinite. Thus, for the circuit of Fig. 7-19, the equivalent circuit during the time that  $T1$  is cut off has the form shown in Fig. 7-21. The equivalent circuit during the time that  $T1$  is conducting is as shown in Fig. 7-22.

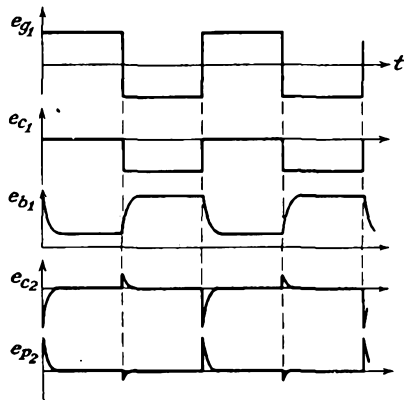


FIG. 7-20. The wave shapes at several points in the circuit of Fig. 7-19.

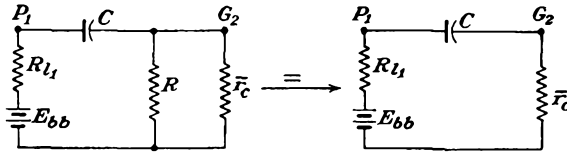


FIG. 7-21. The equivalent circuit of Fig. 7-19 during the time that  $T1$  is cut off.

**7-3. Clamping Circuits.** Because no conductive path exists whenever any asymmetrical wave form is passed through a capacitor or a transformer, the average ordinate of the wave form must assume a zero potential.

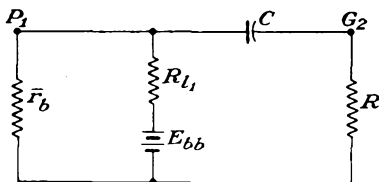


FIG. 7-22. The equivalent circuit of Fig. 7-19 during the time that  $T1$  is conducting.

This is another way of saying that the d-c component of a wave form that is passed through a capacitor or a transformer must necessarily be zero since neither device will pass a d-c current. This fact is a source of difficulty whenever the average ordinate of a wave form must assume a

potential other than zero. Thus the passage of a saw-tooth or other asymmetrical voltage through a capacitor or the passage of a saw-tooth current through a transformer will cause the zero of the wave to be at some level other than its base. The effect of the average ordinate not being at

the base in a cathode-ray oscilloscope is to displace the sweep to one side. The results are illustrated graphically in Fig. 7-23.

It is possible to bring the sweep back to its proper position by applying a bias voltage which is equal to the average ordinate displacement from the base. This is equivalent to restoring to the wave the d-c component

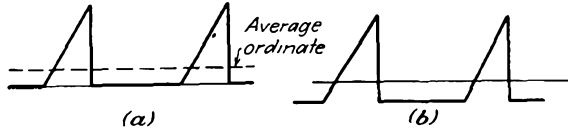


FIG. 7-23. (a) A saw-tooth deflecting voltage. (b) The saw-tooth voltage after passing through an element without a conductive path.

which was eliminated by the capacitor. This method, referred to as *d-c restoration*, is acceptable if an invariable wave form is employed. If, however, some dimension of the wave is changed, such as its amplitude or the duration of the voltage rise, the average value will change and the amount of d-c restoration required will be different.

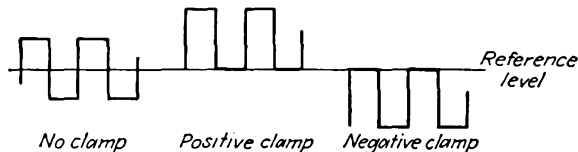


FIG. 7-24. A voltage variation with respect to a definite reference potential.

Simple electronic circuits exist which will hold either amplitude extreme of a wave form to a given level of potential. Such circuits are known as *clamping* circuits and are divided roughly into two classes, *continuously acting* and *synchronized* types. The continuously acting diode and grid clamping circuits clamp either amplitude extreme and allow the wave form to extend in only one direction from the reference potential. Figure 7-24 illustrates the effect of such clamps. One type of synchronized

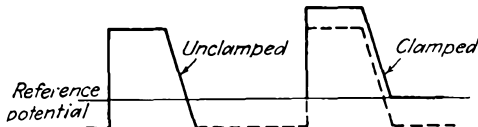


FIG. 7-25. A synchronized clamp that introduces a d-c reference level.

clamp maintains the output potential at a fixed invariable level until a synchronizing pulse is applied, when the output potential is allowed to follow the input. At the end of the synchronizing pulse, the output voltage is returned immediately to the reference level. The general action is illustrated in Fig. 7-25. In a type of synchronized clamp that is extensively used in television receivers, the output potential is reset

during the synchronizing period to a fixed reference level, and the clamp is then opened to allow the output to follow the input for a fixed period of time before the level is again reset.

**7-4. Continuously Acting Clamps.** *Diode Clamp.* The simplest type of clamping circuit utilizes a diode in conjunction with the ordinary  $RC$  circuit, as illustrated in Fig. 7-26. The action of this circuit depends on

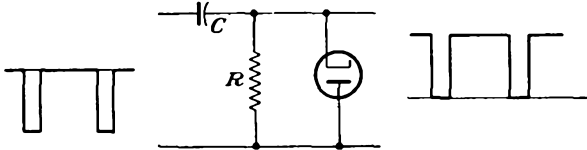


FIG. 7-26. A positive clamping circuit.

the fact that, when the cathode of the diode is made negative with respect to the anode, current will flow and the circuit acts as if a low resistance has been connected across the terminals. When the cathode is positive with respect to the anode, no current will flow and there is, in effect, a high resistance across the terminals. The "closed" impedance is usually between 300 and 3,000 ohms for most diode and triode clamps, and the "open" impedance is several megohms.

To examine the operation of the positive clamping circuit in greater detail, suppose that the wave form of Fig. 7-27a is applied to the input of the circuit of Fig. 7-26. The resulting output wave form is shown in Fig. 7-27b.

During the time interval from  $A$  to  $B$ , the input voltage is zero, and the output voltage is likewise zero. At the point  $B$ , the input voltage drops suddenly to  $-100$  volts, to the point  $C$ . Since the capacitor cannot change its charge instantaneously, the potential across  $R$  also drops suddenly to  $-100$  volts. But the cathode of the diode is now 100 volts negative with respect to the anode, and the tube will conduct heavily, charging the capacitor very rapidly through the short time-constant  $RC$  path (the  $R$  being the beam resistance of the diode), until the capacitor voltage becomes equal to the applied voltage. At this time the output voltage has returned to zero, and the diode becomes nonconducting. Moreover, during the interval until  $D$  is reached, the output voltage remains at zero potential.

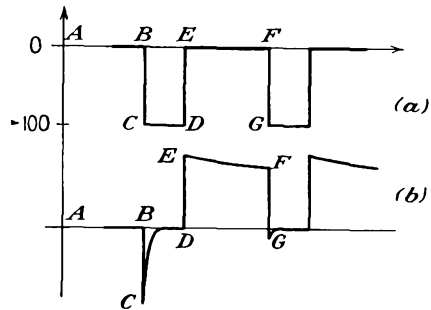


FIG. 7-27. The applied negative-going voltage applied to a diode clamp, and the corresponding clamped output.

At point  $D$  the input voltage changes back to zero, a 100-volt change

in the positive-going direction. This rise appears across  $R$ . Now, however, the capacitor discharges slowly through  $R$ , as the diode is nonconducting (and  $R$  is now a high resistance). The voltage across  $R$  decays

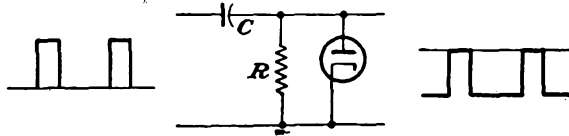


FIG. 7-28. A negative clamping circuit.

slowly, in accordance with the time constant  $RC$  of the circuit, until the point  $F$  is reached, when the input voltage drops to  $-100$  volts. Instantaneously the output across  $R$  falls to a value that is 100 volts below

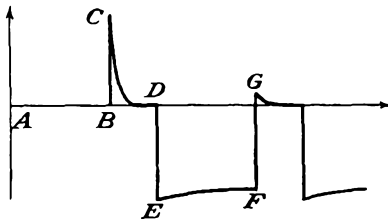


FIG. 7-29. The output wave form from a negative clamping circuit for an applied positive gate pulse.

its value at the instant that point  $F$  is reached. The diode conducts, quickly reduces the output to zero, and returns the charge on the capacitor. Note that no portion of the wave form is lost after the first cycle.

If the situation is as illustrated in Fig. 7-28 for a negative clamping circuit, the corresponding output wave form for an applied positive gate voltage will be of the form shown in Fig. 7-29.

*Grid Clamping.* The function of clamping may be performed at the grid of a triode, since if the grid is made positive with respect to the

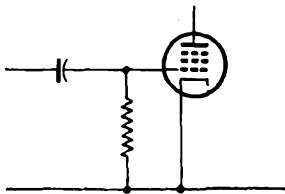


FIG. 7-30. A grid clamping circuit.

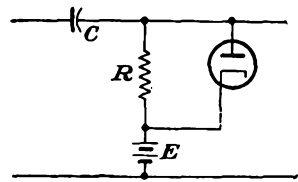


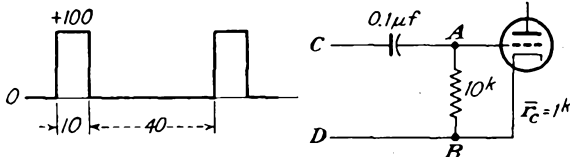
FIG. 7-31. Clamping circuit which establishes the reference voltage  $E$  volts.

cathode, an electron current flows and the cathode-grid resistance is very low, whereas when the grid is made negative with respect to the cathode, no grid current flows and the circuit is essentially open. Hence the grid of a triode or a multielectrode tube when connected according to the circuit of Fig. 7-30 will act as the plate of a diode and produce the same clamping action. In fact, the open and closed impedances of the grid clamp are roughly comparable with those of the diode.

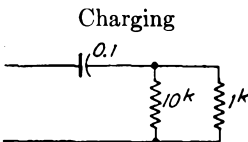
*Clamping Above or Below Ground Potential.* It is not necessary that a clamping circuit tie one extremity of the input signal to zero potential. The reference potential can be made almost any desired value by introducing the necessary fixed reference potential. In the circuit of Fig. 7-31, clamping is established with reference to the fixed potential  $E$ .

The operation of a simple clamp and also the effects of the clamp impedance are made more evident by a specific example.

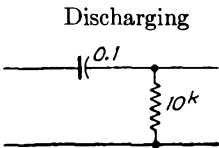
**Example 1:** The circuit and the applied voltage wave form are illustrated in the sketch. Assume that the effective grid-cathode resistance during grid conduction is 1,000 ohms.



a. Estimate the reading of a d-c voltmeter which draws negligible current when connected between points C and A in the circuit in the sketch.



Time const  
 $T = 91 \mu\text{sec}$



Time const  
 $T = 1,000 \mu\text{sec}$

b. What would the voltmeter read when connected between C and D?

c. What would the voltmeter read when connected between A and B?

*Solution:* The equivalent circuits during the charging and discharging periods are shown in the accompanying diagrams.

The potential differences at various points in the circuit are illustrated in the

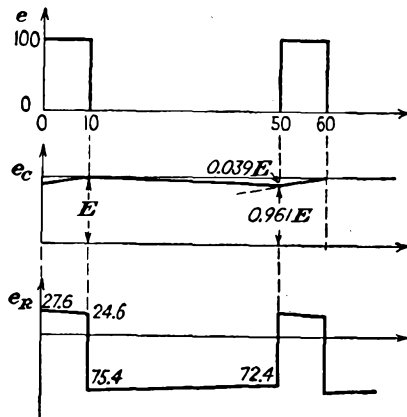


figure. These sketches show the potential variations across the capacitor and across the grid-cathode resistor after steady-state conditions have been reached.

The potential across the capacitor at the end of the charging cycle ( $10 \mu\text{sec}$ ) is denoted as  $E$ . During the discharge portion of the cycle, the capacitor potential falls from the value  $E$  to the value  $E(e^{-\frac{40}{1,000}}) = 0.961E$ . During the charge portion of the cycle, the potential across the capacitor increases from  $0.961E$  to  $E$  according to the charging curve  $(100 - 0.961E)(1 - e^{-196t})$ . For an equilibrium condition to be established, it is required that

$$(100 - 0.961E)0.104 = 0.039E$$

or

$$E = 75.4 \text{ volts}$$

$$(a) E_{CA} = \bar{e}_C = 0.98 \times 75.4 = 73.9 \text{ volts}$$

$$(b) E_{CD} = 100 \times \frac{10}{40 + 10} = 20 \text{ volts}$$

$$(c) E_{AB} = \bar{e}_R = \frac{\frac{1}{2}(27.6 + 24.6) - \frac{1}{2}(75.4 + 72.4)}{50} = -54.1 \text{ volts}$$

Owing to the approximations made,  $E_{CD} = E_{CA} + E_{AB}$  is not exactly verified.

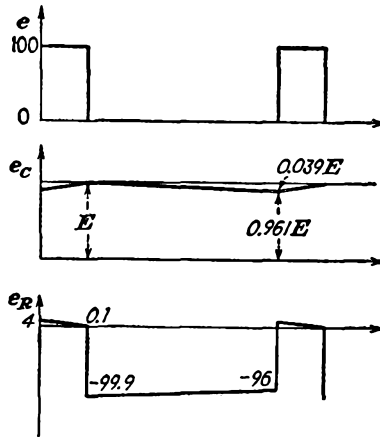
**Example 2:** Repeat the foregoing example for the case where the circuit constants are changed to read  $C = 0.001 \mu\text{f}$ ,  $R = 10^6$  ohms.

*Solution:* The charging and discharging circuits, with the corresponding time constants, are

$$\text{Charging: } T = 1,000 \times 0.001 \times 10^{-6} = 1 \mu\text{sec}$$

$$\text{Discharging: } T = 10^6 \times 10^{-9} = 1,000 \mu\text{sec}$$

The important wave forms are illustrated in the accompanying figure.



A comparison of the above examples shows that, the lower the clamp impedance relative to the circuit impedance, the "tighter" the clamp

becomes. In particular, if a zero-impedance clamp were possible, then perfect clamping would result.

**7-5. Switched Clamps.** It is sometimes necessary to open or to close a clamp at regular intervals which may or may not be directly related to the signals. If the clamp can conduct in only one direction when closed, it is called a *one-way*, or *single-sided*, clamp. If the clamp can conduct in both directions when closed, it is a *two-way*, or *double-sided*, clamp.

*Switched Clamps—Single-sided.* The clamping circuits discussed in Sec. 7-4 are essentially single-sided, and if provision is made to cause the diodes or triodes that cause the clamping action to turn off during a certain prescribed period, the clamp then becomes a switched single-sided clamp. The modification that is necessary in order to convert the biased clamp of Fig. 7-31 into a switched clamp is illustrated in Fig. 7-32. Here the diode is switched out of the circuit

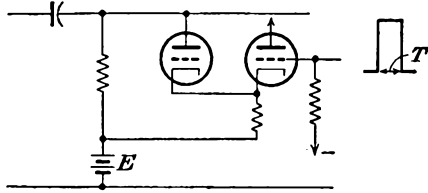


FIG. 7-32. A switched diode clamp that is open for a time  $T$ .

by the application of a square pulse for a time  $T$  to the grid of the cathode follower. Clearly, for the switching to operate, the amplitude of the signal at the cathode of the cathode follower must exceed the bias potential  $E$ . The other clamping circuits can be modified in generally similar ways.

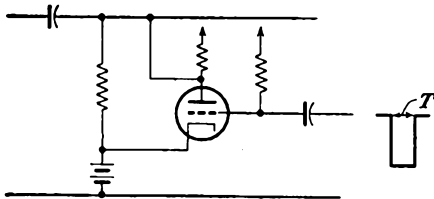


FIG. 7-33. A one-way clamp using a single triode.

A somewhat comparable circuit that utilizes a triode is given in Fig. 7-33. In this circuit the clamping is done through the beam resistance of the tube, but since the clamp impedance is rather large, the clamp is correspondingly quite "loose."

*Switched Clamps—Double-sided.* Several different types of switched double-sided clamps exist. One type of synchronized clamp is so arranged that the output may follow the input during the time that the synchronizing pulse is applied but is then returned to the reference potential when the synchronizing pulse is removed. The elements of such a circuit are illustrated in Fig. 7-34.

Suppose that the synchronizing pulse is applied as a negative rectangular gate which drives  $T1$  and  $T2$  beyond cutoff for the desired length of time. With tubes  $T1$  and  $T2$  cut off, the grid of  $T3$  is free to follow any changes in the input voltage amplitude. Since capacitor  $C_1$  has no discharge path, the voltage is transferred to the grid of  $T3$ , which then follows this voltage variation. At the end of the synchronizing period,

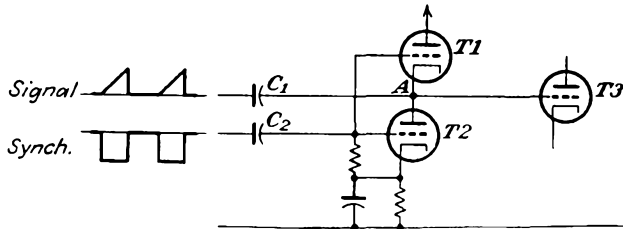


FIG. 7-34. A switched double-sided clamping circuit.

tubes  $T1$  and  $T2$  again conduct, and the grid potential of  $T3$  is returned to the reference potential determined by  $T1$  and  $T2$  in series.

If for any reason a signal appears on the grid of  $T3$  without a synchronizing potential on the clamping triodes, the effect of  $T1$  and  $T2$  is to prevent the grid potential on  $T3$  to change. This self-compensating effect arises because a slight increase in the potential at the point  $A$  causes  $T2$  to conduct more current, which reflects itself as an increase in the bias of  $T1$ . This tends to reduce the current through  $T1$ , which thus counteracts the impressed potential. In a similar manner, if the signal tends to decrease the current through  $T2$ , the grid bias of  $T1$  decreases, with a resulting increase in current. Hence, so long as  $T1$  and  $T2$  conduct, the voltage at the grid of  $T3$  is held constant and no input signal will reflect itself as a variation in the output of  $T3$ .

This clamping circuit operates quite satisfactorily and is satisfactory for many applications. However, owing to the existence of interelectrode and distributed capacitances to the signal line, a slight dimple might appear

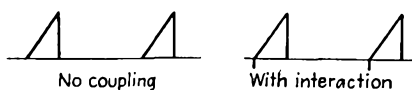


FIG. 7-35. The character of the effect on the output signal by the synchronizing pulse acting through the interelectrode and distributed capacitances to the signal line.

on the signal, somewhat as illustrated in Fig. 7-35, owing to the interaction of the synchronizing pulse on the signal line. This effect is quite tolerable in some applications but is objectionable in television circuits, where such an extraneous signal might affect the

actual signal pattern. This effect is overcome by using two synchronizing pulses of opposite polarity in appropriate circuits.

A clamping circuit of importance in television practice,<sup>1</sup> provides for

establishing an arbitrary reference potential at fixed and regular intervals on some chosen circuit element in the picture amplifier. The clamping is applied during the period that the television picture is blanked during the retrace period. A diagram of such a clamping circuit is given in Fig. 7-36.

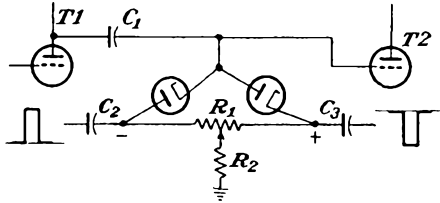


FIG. 7-36. A double-sided switched clamp.

The reference potential is that which exists at the mid-point of  $R_1$ . This may be deduced as follows: During the keying-pulse intervals, both diodes conduct, and both terminals of  $R_1$  are at the same potential. Because of this conduction, the equal coupling capacitors  $C_2$  and  $C_3$  are oppositely charged. During the intervals when the diodes are not conducting, a current flows in  $R_1$ , thus discharging these capacitors. Since both the circuit and the keying signals are balanced, the diodes always reach the same potential during the pulse intervals, this potential being that at the mid-point of  $R_1$  during the intervals between pulses. The time constant  $C_2R_1 = C_3R_1$  is made large compared with the period of the pulses, so that the current in  $R_1$  is small and the charges on  $C_2$  and  $C_3$  remain substantially constant.

If  $R_1$  is connected as shown, the reference potential may be shifted with respect to ground. However, if the circuit is seriously unbalanced, some difficulty may be experienced in maintaining the pulse shape. To minimize this, the resistor  $R_2$  may be inserted in the ground connection. The current through this resistor is very small, and even with large  $R_2$  there is no serious disturbance of the reference potential.

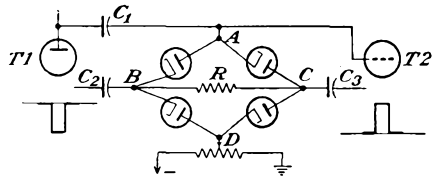


FIG. 7-37. A self-balancing clamp circuit.

The coupling capacitor  $C_1$  must charge through the clamp circuit, in the absence of grid current in  $T_2$ . During the open-circuit intervals in the clamp circuit, the charge on  $C_1$  cannot change. Consequently the l-f response of the coupling circuit between  $T_1$  and  $T_2$  is not seriously affected.

A clamping circuit that is essentially self-balancing is illustrated in Fig. 7-37. If it is assumed that the four diodes are identical, then upon

the application of the keying pulses the points *A* and *D* are at the same potential.

Both the foregoing clamping circuits require that the keying pulses be larger than the amplitude of the picture signal at the point where the clamp operates. Otherwise conduction from the signal line through the clamp may occur and thus affect the level. Usually the amplitude of the keying pulses is made about twice the amplitude of the picture signal.

### REFERENCES

1. Roe, J. H., *Proc. IRE*, **12**, 1532 (1947).
2. As a general reference, consult "Principles of Radar," 2d ed., M.I.T. Radar School Staff, McGraw-Hill Book Company, Inc., New York, 1946.

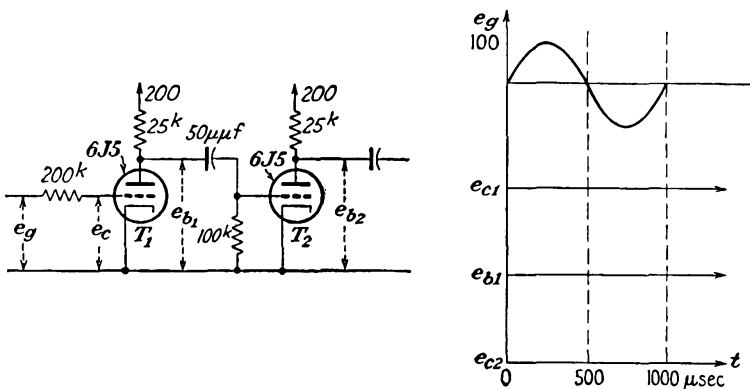
### PROBLEMS

*General Note:* The solution of many of the following problems may require direct reference to a tube manual for additional tube information.

**7-1.** The double-diode limiting circuit of Fig. 7-5 is used to clip a sine-wave input  $100 \sin 5,000t$ . In the circuit  $R = 100k$ , and  $E_1 = E_2 = 5$  volts. 6H6 tubes are used.

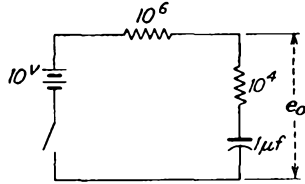
- Plot the output voltage  $e_2$  as a function of time.
- Suppose that the output  $e_2$  is amplified to a 200-volt peak-peak voltage and is passed through a second identical clipper. Plot the output as a function of time. Indicate the total rise time on the diagram.

**7-2.** Consider the circuit in the accompanying figures. Determine the wave

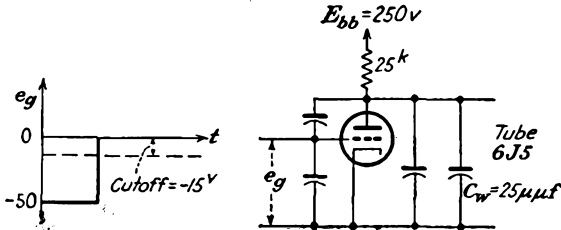


shapes at the several points indicated, and sketch these in the manner shown. Neglect interelectrode and wiring capacitances. Assume  $r_c = 500$  ohms when grid current is drawn.

- ✓ **7-3.** Write an expression for the output voltage as a function of time after closing the switch (see the figure for this problem).

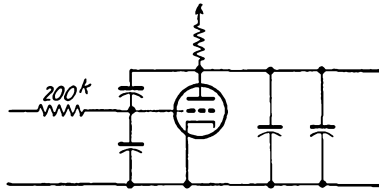


7-4. The interelectrode and wiring capacitances will affect the shape of the output wave form for a given input wave form. Refer to the circuit in the accompanying diagram.

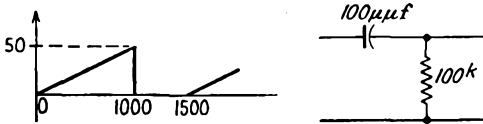


- Draw the equivalent circuit of this amplifier when the tube is conducting; when the tube is nonconducting.
- Determine the output wave shape for the designated input wave.

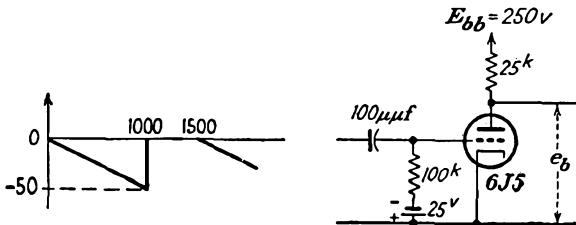
7-5. Repeat Prob. 7-4 when the circuit is modified as shown in the accompanying figure.



7-6. A saw-tooth voltage is applied to the circuit shown in the diagram for this problem. Calculate and sketch the output voltage during one complete period.

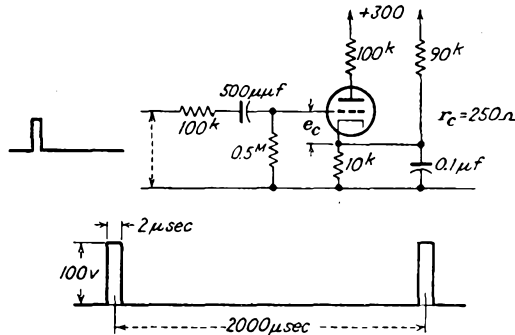


7-7. The input voltage to the amplifier is as shown (see the figure).



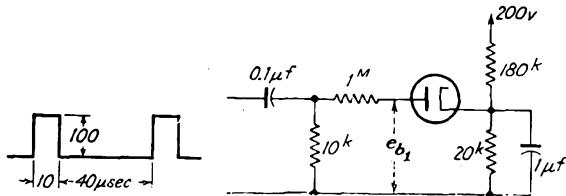
- Calculate and sketch  $e_c$  during one complete period. Neglect tube and wiring capacitances.
- Calculate and sketch the output voltage during the period.

**7-8.** Given the circuit shown in the diagram. The generator has negligible internal resistance and produces 100-volt rectangular pulses of 2  $\mu$ sec duration.



- Draw a simplified equivalent circuit for the generator and its load during the 2- $\mu$ sec pulse interval.
- Draw the simplified equivalent circuit for the generator and its load during the interval between the pulses.
- From the equivalent circuits, determine the principal function of the 500- $\mu$ f capacitor. Is any appreciable signal bias developed? If so, how much?
- Sketch the grid voltage  $e_c$  approximately to scale.

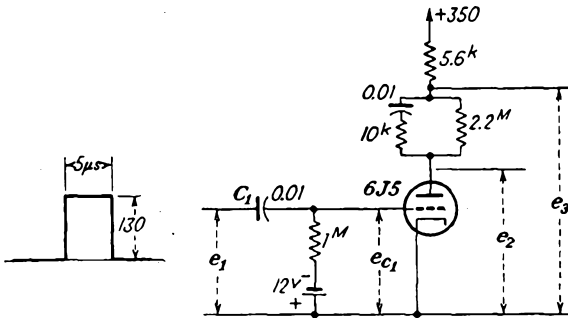
**7-9.** Refer to the circuit in the figure.



- What is the maximum value of  $e_{b1}$ ?
- What is the approximate value of the voltage across the 0.1- $\mu$ f capacitor?
- Sketch the wave form  $e_{b1}$ .

**7-10.** Given the circuit shown in the figure. The input to the circuit is the rectangular pulses shown, with a pulse-recurrence frequency of 82.6 per second. Choose the following values:

$$\begin{aligned} r_c &= 500 \text{ ohms when the grid exceeds } +10 \text{ volts} \\ r_b &= 1,000 \text{ ohms when the grid exceeds } +10 \text{ volts} \\ e_{c1} \text{ at the beginning of the pulse} &= -27.5 \text{ volts} \end{aligned}$$



- Draw the equivalent circuit for the charging of  $C_1$  during each pulse, and determine the voltage across  $C_1$  at the end of the pulse.
- Determine the grid voltage  $e_{c1}$  at the end of the pulse.
- Sketch the voltage across  $C_1$  and  $e_{c1}$ .
- Calculate the average d-c value of  $e_{c1}$ .
- Calculate and sketch the voltage  $e_2$ .
- Calculate and sketch the voltage  $e_3$ .

## CHAPTER 8

### ELECTRONIC COMPUTING CIRCUITS

CIRCUITS of the type to be considered here are particularly important in what are known as *analogue computers*. In these computers, electrical quantities, usually voltages, which can be varied and measured conveniently are made to obey differential equations which are identical in form with those of the system under survey. This permits the use of purely electrical principles and components to yield information concerning the behavior of a wide variety of physical problems.

Several other basic methods are used in computer design. Some are entirely mechanical in character and operation, some are electromechanical, and others are essentially electrical. The electrical types are divided into two general classes, the digital and the analogue types. The circuits of importance in the analogue type are to be examined.

Among the circuits to be examined are those which perform such basic mathematical operations as addition, subtraction, differentiation, and integration. In some cases these circuits depend for their operation on the special shapes of the tube characteristics. In other cases, feedback

is applied in special ways to achieve the desired results. Certain operations are performed by combination of circuits.

#### 8-1. Difference Amplifiers.

Several circuits exist in which the output voltage is the difference between two input signals. One of these was discussed in detail in Sec. 6-9, and the circuit is redrawn

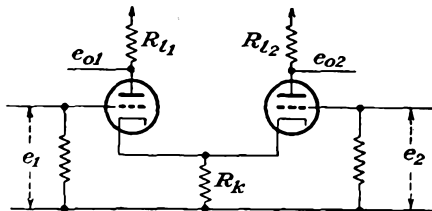


FIG. 8-1. The common cathode difference amplifier.

as Fig. 8-1. The results of an analysis of the operation of this circuit are contained in the equations

$$\left. \begin{aligned} e_{o1} &= \frac{-\mu R_{l1}}{2(R_l + r_p)} (e_1 - e_2) \\ e_{o2} &= \frac{+\mu R_{l2}}{2(R_l + r_p)} (e_1 - e_2) \end{aligned} \right\} \quad (8-1)$$

If a single output is desired, the circuit may be modified to the form shown

in Fig. 8-2. The output from this circuit is given by Eq. (6-72) and is

$$e_{o2} = \frac{\mu R_l}{R_l + 2r_p} (e_1 - e_2) \tag{8-2}$$

It should be noted that no restrictions have been placed on the input voltages  $e_1$  and  $e_2$ , and the results are therefore independent of the wave shapes and amplitudes, except that the amplitudes must not be so large as to vitiate the linear equivalent circuit of the tubes.

A second, though generally less desirable, form of difference amplifier is illustrated in Fig. 8-3. Note that one of the input potentials is isolated from ground. This may introduce a complication in many cases.

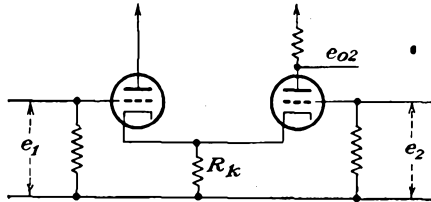


FIG. 8-2. A modification of Fig. 8-1 to yield a single output.

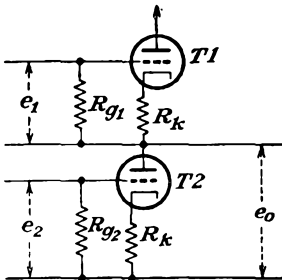


FIG. 8-3. A series or "cascode" type of difference amplifier.

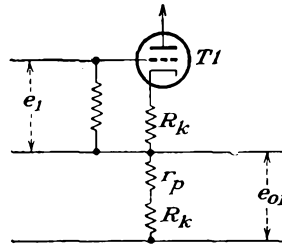


FIG. 8-4. The operating circuit of tube  $T_1$ .

The operation of the circuit can be analyzed by the usual methods involving the equivalent plate circuit theorem. For diversity of analysis,

use is made of the superposition theorem. When the circuit of tube  $T_1$  is considered,  $e_2$  is set equal to zero. The equivalent circuit for  $T_1$  then becomes that shown. The output voltage from the circuit is readily calculated to be

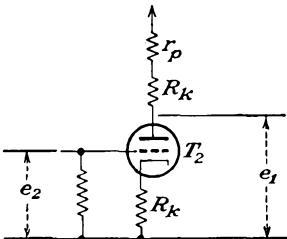


FIG. 8-5. The operating circuit of tube  $T_2$ .

$$e_{o1} = \frac{\mu(R_k + r_p)}{(\mu + 2)R_k + 2r_p} \tag{8-3}$$

Similarly, when the circuit of tube  $T_2$  is considered, the input to  $T_1$  is set equal to zero. The equivalent circuit of  $T_2$  then becomes that illustrated in Fig. 8-5. The output voltage from this circuit is found to be

$$e_{02} = \frac{-\mu(R_k + r_p)}{(\mu + 2)R_k + 2r_p} \quad (8-4)$$

The total output voltage is given by

$$e_0 = e_{01} + e_{02} = \frac{\mu(R_k + r_p)}{(\mu + 2)R_k + 2r_p} (e_1 - e_2) \quad (8-5)$$

For the case where the following conditions are satisfied,

$$R_k \gg 2r_p$$

the output voltage becomes

$$e_0 \doteq \frac{\mu}{\mu + 2} (e_1 - e_2) \quad (8-6)$$

which shows that the output voltage appears without gain.

Owing to the need for an isolated input potential, a requirement that can be met if the input is an a-c potential of nominal frequency by the use of an isolating transformer, and the fact that the output is achieved without amplifier gain, the circuit of Fig. 8-2 is generally to be preferred.

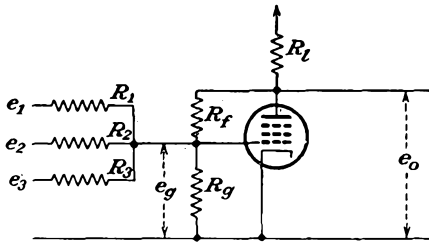


FIG. 8-6. A feed-back summing amplifier.

**8-2. Adding Circuits.** Suppose that it is desired to add a number of voltages of arbitrary phase, amplitude, and frequency. A number of circuits exist for effecting

this addition. The addition may be effected in the grid circuit, the cathode circuit, or the plate circuit of appropriately connected tubes.

A simple feed-back summing amplifier is illustrated in Fig. 8-6. To show that the output potential is very nearly the sum of the input voltages, one may proceed as follows: A direct application of Kirchoff's current law yields the expression

$$\frac{e_1 - e_g}{R_1} + \frac{e_2 - e_g}{R_2} + \cdots + \frac{e_n - e_g}{R_n} + \frac{e_0 - e_g}{R_f} = \frac{e_g}{R_g} \quad (8-7)$$

from which

$$\frac{e_1}{R_1} + \frac{e_2}{R_2} + \cdots + \frac{e_n}{R_n} = e_g \left( \frac{1}{R_g} + \frac{1}{R_f} + \frac{1}{R_1} + \cdots + \frac{1}{R_n} \right) - \frac{e_0}{R_f}$$

If the resistors are chosen to be

$$R_1 = R_2 = \cdots = R_n = R_f = R$$

and with

$$R_g \gg R$$

then the above equation becomes

$$\frac{1}{R} \sum_n e_n = -\frac{e_0}{K} \frac{n+1}{R} - \frac{e_0}{R} \tag{8-8}$$

where  $K$  is the gain of the tube. Note that a distinction is being made between the gain of the tube  $K$  and the resultant gain of the amplifier  $K_r$ . In fact, a comparison of Fig. 8-6 with Fig. 6-15 of the anode follower would lead one to expect a resultant gain of the circuit of Fig. 8-6 to be

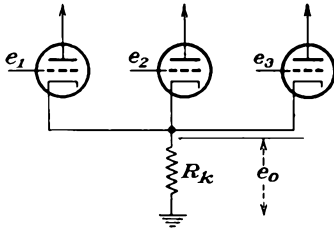


FIG. 8-7. A common cathode summing chain.

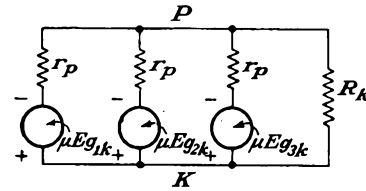


FIG. 8-8. The equivalent circuit of Fig. 8-7.

low and of the order of unity. However, the gain of the stage as measured between the grid and plate terminals will be high, particularly if a pentode is used. For the case of a pentode, Eq. (8-8) reduces to the approximate form

$$\frac{1}{R} \sum_n e_n \doteq -\frac{e_0}{R}$$

which is

$$e_0 = -\sum e_n \tag{8-9}$$

A circuit for the addition of voltages in the cathode circuit of a chain of stages is shown in Fig. 8-7. An analysis of this circuit is readily effected if it is assumed that identical tubes are used. In this case the equivalent circuit attains the form shown in Fig. 8-8. An application of the Millman theorem yields

$$E_{kp} = \frac{\mu E_{g1k} Y_p + \mu E_{g2k} Y_p + \dots + \mu E_{g nk} Y_p}{n Y_p + Y_k}$$

$$E_{kp} = \frac{\mu Y_p}{n Y_p + Y_k} (E_{g1k} + \dots + E_{g2k}) \tag{8-10}$$

But the grid-cathode potentials are

$$\left. \begin{aligned} E_{g1k} &= e_1 + E_{pk} = e_1 - E_{kp} \\ &\vdots \\ &\vdots \\ &\vdots \\ E_{g nk} &= e_n + E_{pk} = e_n - E_{kp} \end{aligned} \right\} \tag{8-11}$$

which leads to

$$E_{kp} = \frac{\mu Y_p}{nY_p + Y_k} (e_1 + \dots + e_n - nE_{kp})$$

or

$$E_{kp} = \frac{\mu Y_p}{n(\mu + 1)Y_p + Y_k} \sum e_n \tag{8-12}$$

which is given, with good approximation, by

$$E_{kp} \doteq \frac{\mu}{n(\mu + 1)} \sum e_n \tag{8-13}$$

This circuit allows for voltage summation with very small interaction among the sources of voltage, owing to the large input impedance to each stage. However, it does so at the expense of one tube for each source voltage. For this reason, the circuit of Fig. 8-6 with large series resistors is to be preferred.

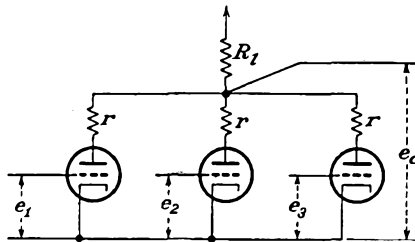


FIG. 8-9. A common plate summing chain.

Addition is also possible by connecting a chain of tubes through a common plate resistor, as illustrated in Fig. 8-9. The resistors  $r$  in the plate lead of each tube are small suppressor resistors. It may

be shown that the output voltage from such a plate summing chain has the form

$$e_o = \frac{-\mu R_i}{r_p + \mu R_i} 3 \sum_n e_n \tag{8-14}$$

Here, as in the case of the common cathode summing chain, a tube is required for each voltage to be included in the adding group, although some over-all gain is effected by the circuit.

**8-3. Squaring Circuits.** A squaring circuit is one in which the output voltage is proportional to the square of the input voltage. Such a circuit makes use of the curvature of the tube characteristics of two tubes to accomplish the squaring operation. The schematic diagram of the circuit is given in Fig. 8-10. It will be observed that the circuit consists of a single-tube paraphase amplifier (refer to Sec. 9-11 for a detailed discussion of this amplifier circuit) which provides two signals that differ by 180 deg in phase. These signals are applied to the grids of two amplifier stages which are so connected that the odd-harmonic terms cancel in the output. This stage should be compared with a normal push-pull amplifier in which the even-harmonic terms are canceled in the output.

As a result of its connection, the even-harmonic terms become the important ones in the output.

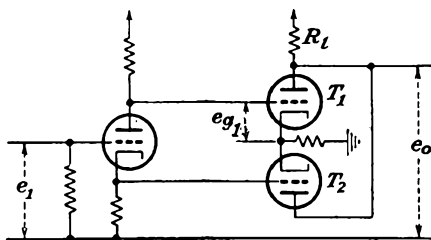


FIG. 8-10. A squaring amplifier.

It is assumed that the plate current in tube  $T1$  may be represented by a series of the form

$$i_{p1} = a_1 e_{g1} + a_2 e_{g1}^2 + a_3 e_{g1}^3 + \dots \quad (8-15)$$

Likewise, the plate current in tube  $T2$  will then be given by the series

$$i_{p2} = a_1(-e_{g1}) + a_2(-e_{g1})^2 + a_3(-e_{g1})^3 + \dots \quad (8-16)$$

The total plate current

$$i_p = i_{p1} + i_{p2}$$

becomes, if it is assumed that the first three terms of the series representation adequately represent the output,

$$i_p = 2a_2 e_{g1}^2 \quad (8-17)$$

and the output voltage is then of the form

$$e_0 = i_p R_L = 2a_2 R_L e_{g1}^2$$

An explicit expression for the amplitude factor  $a_2$  appearing in this equation is possible in terms of the tube characteristics. If use is made of the Taylor expansion of the current in terms of the grid potential, *viz.*,

$$i_p = g_m e_g + \frac{1}{2!} \frac{\partial g_m}{\partial e_g} e_g^2 + \frac{1}{3!} \frac{\partial^2 g_m}{\partial e_g^2} e_g^3 + \dots \quad (8-18)$$

then clearly the coefficient  $a_2$  is related to  $\partial g_m / \partial e_g$  and the output voltage is given by the form

$$e_0 = R_L \frac{\partial g_m}{\partial e_g} e_g^2 \quad (8-19)$$

But since the gain of the paraphase amplifier is approximately unity [see Eq. (9-41)], then finally

$$e_0 \doteq R_L \frac{\partial g_m}{\partial e_g} e_1^2 \quad (8-20)$$

This expression shows that, for the output to be proportional to the square of the input voltage, it is essential that the coefficient  $\partial g_m / \partial e_g$  remain constant over the range of operation of the tube. This condition requires that the composite characteristic of the amplifier must be of the square-law type.

A number of tubes have been examined in order to ascertain which yield satisfactory characteristics for such squaring operations. It has been found that the 6B8 and the 6SK7 tubes are satisfactory when grid-driven and the 6U7G and the 6D6 are quite satisfactory when screen-driven.

A second circuit for squaring is included in the next section as a special application of the multiplying circuit considered there.

**8-4. Multiplying Circuits.** A variety of multiplying circuits have been devised for use in radio-circuit applications and have been extensively used for modulation and demodulation. Thus it is the function of the modulator to multiply the carrier and the modulating signals to yield a modulated carrier wave. Likewise, in the demodulating circuits, the modulated wave must be combined with the carrier wave to yield the modulating signal. While such circuits are suitable for these applications, they are not suitable in general as simple multiplying circuits. This is so because of the wide variety of other multiplication products that appear in the output, owing to the nonlinear characteristics, although these are suppressed in modulation and demodulation applications by the use of tuned circuits in the output.

A solution is more nearly approached through the use of a tube circuit, the voltage gain of which may be controlled by means of the potential on one grid, while the signal output depends directly on the signal applied to a second grid. That is, if the gain of the amplifier  $K$  is proportional to a voltage  $e_3$ , then

$$K = ke_3$$

If the output voltage  $e_0$  is directly proportional to the input signal  $e_1$ , according to the relation

$$e_0 = Ke_1$$

then the application of the two signals  $e_1$  and  $e_3$  simultaneously will yield an output

$$e_0 = ke_3e_1 \tag{8-21}$$

A number of tubes possess characteristics which would permit their use as part of a multiplying circuit. In Fig. 8-11 are illustrated the mutual-conductance curves of a 6L7 multielectrode tube as it depends on the voltage applied to grid 3. It will be noted that  $g_m$  is a linear function of the voltage applied to grid 3 over a wide range of potential variation. Equation (8-21) is satisfied over this linear range. Of course, if grids 1

and 3 are connected together and a single input voltage is applied, the output voltage will be proportional to the square of the input voltage.

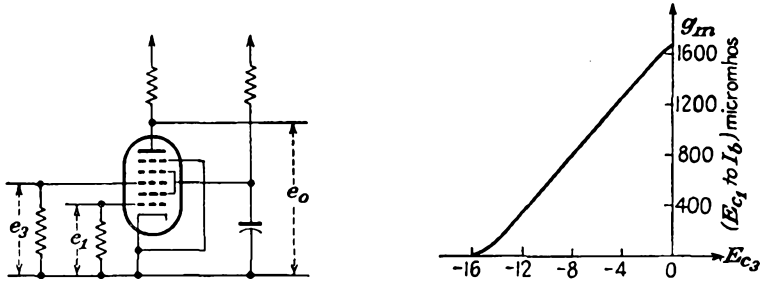


FIG. 8-11. The connections and  $g_m$  of a 6L7 tube for use in a multiplying circuit.

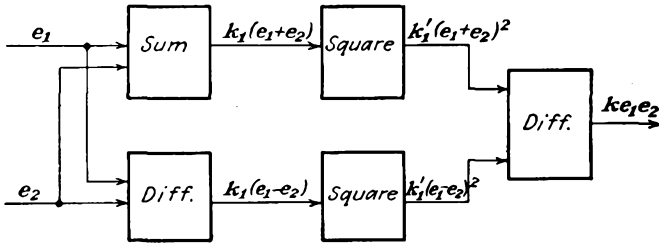


FIG. 8-12. The "quarter-square" method of performing the multiplication of two quantities.

A second method for multiplying two quantities makes use of what might be called the "quarter-square" method. This depends on the fact that the product of two quantities may be expressed by an equation of the form

$$e_1e_2 = \frac{(e_1 + e_2)^2}{4} - \frac{(e_1 - e_2)^2}{4}$$

The block diagram of Fig. 8-12 shows the elements required for yielding the desired results.

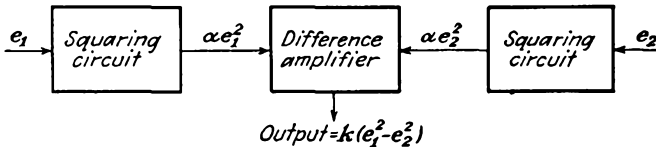


FIG. 8-13. Circuit for obtaining the difference of squares.

**8-5. Difference of Squares.** It is possible to combine several of the foregoing circuits to yield a number of circuits for performing other mathematical operations. For example, the combination of two squaring circuits and a difference amplifier, according to the block diagram of Fig. 8-13, will yield an output that is the difference of the squares of the

input signals. This circuit is a simple combination of the basic circuits that are required to perform the separated indicated operations.

**8-6. Square-root Circuit.** A block diagram showing the elements for yielding the square root of a given voltage is illustrated in Fig. 8-14.

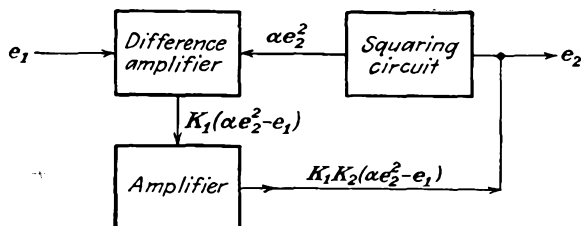


FIG. 8-14. A square-root circuit.

The input to the circuit is  $e_1$ , which is applied to one input of a difference amplifier of the type illustrated in Fig. 8-2. Likewise, it is supposed that a voltage  $e_2$  appears at the input of a squaring circuit, the output of which is applied to the second input to the difference amplifier. The output from the difference amplifier, which is the input to a simple amplifier of gain  $K_2$ , is then  $K_1(\alpha e_2^2 - e_1)$ . But the output from the amplifier is actually the source of the voltage  $e_2$  which appears at the input to the squaring circuit. This requires, therefore, that

$$K_1 K_2 (\alpha e_2^2 - e_1) = e_2$$

But for large amplifier gain  $K_2$ ,

$$\frac{e_2}{K_1 K_2} \doteq 0$$

which requires therefore that

$$\alpha e_2^2 - e_1 = 0$$

It follows from this that the output voltage  $e_2$  is then related to the input voltage by the relation

$$e_2 = \sqrt{\frac{e_1}{\alpha}} \quad (8-22)$$

**8-7. Dividing Circuit.** A block diagram showing the elements of a circuit for yielding an output which is proportional to the ratio of two given voltages is given in Fig. 8-15. In this circuit the two input voltages are  $e_1$  and  $e_2$ , one of which is applied to the difference amplifier, the second of which is applied to a multiplying circuit. An examination of the circuit shows that the output from the amplifier, which provides the output and which also furnishes one input to the multiplying circuit, is

$$e_3 = KA(e_1 - ke_2e_3)$$

If the amplifier provides a high gain, then it follows that

$$\frac{e_3}{KA} \doteq 0$$

from which

$$e_1 - ke_2e_3 \doteq 0$$

or finally

$$e_3 = k' \frac{e_1}{e_2} \tag{8-23}$$

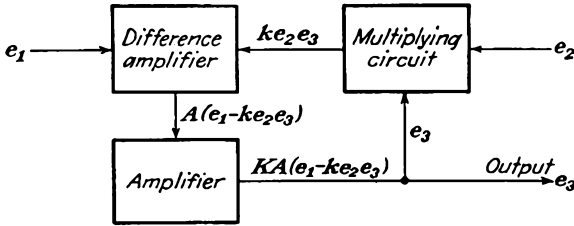


FIG. 8-15. A circuit which divides two voltages.

**8-8. General Feed-back Circuit—Approximate Analysis.**<sup>1</sup> A number of computing circuits utilize feedback in special ways in order to achieve the desired results. A circuit that is used extensively in such applications is given in Fig. 8-16, together with the equivalent circuit.

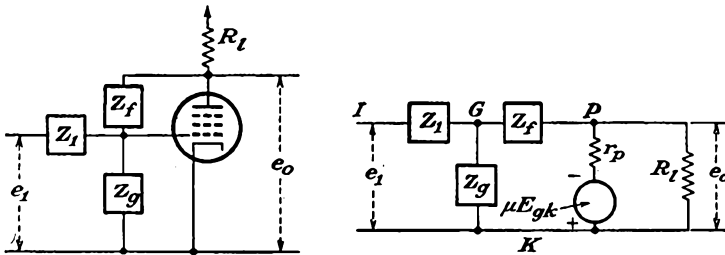


FIG. 8-16. A general feed-back circuit and its plate-circuit equivalent.

This circuit was examined in Sec. 6-7 in connection with its application as an anode follower. An exact analysis of this circuit is included in Sec. 6-7. However, an approximate analysis yields important information, and this will be examined before the exact analysis is discussed.

In this connection, an application of the Millman network theorem yields directly

$$E_{kg} = \frac{E_{kl}Y_1 + E_{kp}Y_f}{Y_1 + Y_f + Y_g} \tag{8-24}$$

This is rewritten in the form

$$E_{kp} = \frac{Y_1 + Y_f + Y_g}{Y_f} E_{kg} - \frac{Y_1}{Y_f} E_{kl} \tag{8-25}$$

But the gain of the tube is, by definition,

$$K \equiv \frac{E_{pk}}{E_{gk}} \quad (8-26)$$

and the amplifier resultant gain is

$$K_r = \frac{E_{pk}}{E_{ik}} \quad (8-27)$$

Then Eq. (8-25) becomes

$$K_r = \frac{Y_1 + Y_f + Y_g}{Y_f} \frac{E_{kg}}{E_{kl}} - \frac{Y_1}{Y_f} \quad (8-28)$$

or

$$K_r = \frac{Y_1 + Y_f + Y_g}{Y_f} \frac{K_r}{K} - \frac{Y_1}{Y_f}$$

Solving for  $K_r$  yields

$$K_r \left( 1 - \frac{Y_1 + Y_f + Y_g}{Y_f} \frac{1}{K} \right) = - \frac{Y_1}{Y_f} \quad (8-29)$$

This becomes

$$K_r = - \frac{Y_1}{Y_f} \frac{1}{1 - \frac{1}{K} - \frac{Y_1 + Y_g}{Y_f} \frac{1}{K}} \quad (8-30)$$

or equivalently

$$K_r = - \frac{Z_f}{Z_1} \frac{1}{1 - \frac{1}{K} - Z_f \frac{Z_1 + Z_g}{Z_1 Z_g} \frac{1}{K}} \quad (8-31)$$

Some important results can be obtained from this expression. As an approximate analysis, suppose that the grid impedance  $Z_g \gg Z_1$ . Equation (8-31) becomes

$$K_r \doteq \frac{Z_f}{Z_1} \frac{1}{1 - \frac{1}{K} - \frac{Z_f}{Z_1} \frac{1}{K}} \quad (8-32)$$

If one defines, for convenience,

$$K_r' \equiv \frac{Z_f}{Z_1} \quad (8-33)$$

then

$$K_r = -K_r' \frac{1}{1 - \frac{1}{K} - \frac{K_r'}{K}} \quad (8-34)$$

This expression shows that the resultant gain of the amplifier is slightly less than the quantity  $K_r'$  defined in Eq. (8-33). Moreover, if it is assumed that the gain of the tube as defined in Eq. (8-26) is large, and this is generally true for a pentode, then Eq. (8-34) becomes approximately

$$K_r \doteq -K_r' \quad (8-35)$$

Consequently, a great deal of insight into the circuit operation is possible by an examination of  $K'_r$ , the network ratio, without having to perform a detailed calculation of a complex circuit. In fact, noting that

$$K_r = -K'_r = -Z_f Y_1 \doteq \frac{E_{pk}}{E_{Ik}}$$

then

$$E_{pk} \doteq -[Z_f Y_1] E_{Ik} \tag{8-36}$$

Consequently, if one considers  $[Z_f Y_1]$  as an operator, then Eq. (8-36) may be interpreted as an operational expression. That is, one might consider  $[Z_f Y_1]$  as an operator which, when acting on  $E_{Ik}$ , yields the output voltage  $E_{pk}$ .

It is sometimes found very convenient to draw an approximate equivalent circuit of the above diagram. Such an approximate equivalent circuit is shown in Fig. 8-17. The presence of the virtual ground in the diagram is used to emphasize that, owing to the large gain of the tube, the change in potential at the grid for a given output potential is so small that it can be assumed as a first approximation that the grid potential does not vary.

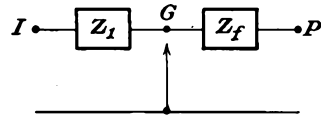
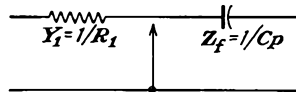


FIG. 8-17. An approximate equivalent circuit of Fig. 8-16.

A number of special applications of this circuit will be considered, and the corresponding more detailed analyses of several of these applications will be carried out below. Among the direct applications of this circuit are circuits for integration and differentiation.

*Integrating Circuit.* If the impedance elements in the circuit of Fig.



8-17 are chosen as shown in the accompanying diagram, then Eq. (8-36) becomes

$$E_{pk} = -\frac{1}{R_1 C_p} E_{Ik} = -\frac{1}{R_1 C} \int E_{Ik} dt \tag{8-37}$$

which shows that the output potential is related to the integral of the input voltage.

For the particular case in which the input voltage is sinusoidal and of the form

$$E_{Ik} = E_m \sin \omega t$$

then

$$E_{pk} = -\frac{1}{R_1 C} \int E_m \sin \omega t dt = \frac{E_m}{R_1 C} \cos \omega t + k$$

If the constants are adjusted to be

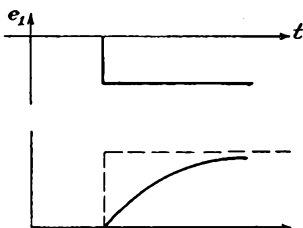
$$R_1C = \frac{1}{\omega}$$

then the output voltage is

$$E_{pk} = E_m \cos \omega t = E_m \sin (\omega t + 90)$$

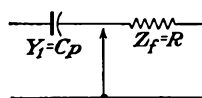
This permits an output voltage which is the same amplitude and shifted 90 deg with respect to the input voltage. Such circuits may be adjusted to yield the 90-deg phase shift to within 10 min or less.

If the input voltage is a square wave, then the output is a linear function of time and has the form illustrated in the accompanying figure.



Actually it will be found that the variation follows an exponential variation, the start of which is a linear function of time. The output wave form will be somewhat as illustrated.

*Differentiating Circuits.* If the circuit impedances are chosen and con-



nected as shown in the accompanying diagram, then Eq. (8-36) becomes

$$E_{pk} = -CRpE_{Ik} = -CR \frac{dE_{Ik}}{dt} \tag{8-38}$$

This expression shows that the output voltage is the time derivative of the input potential.

**8-9. The Integrating Circuit.** The equations of Sec. 6-7 permit an exact analysis to be made of the integrating circuit. The circuit of such a common integrating circuit is shown in Fig. 8-18. The general expression for the output is given by Eq. (6-46);

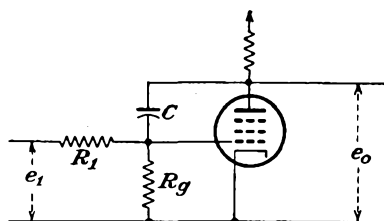


FIG. 8-18. A common integrating circuit.

it becomes for this case, since

$$\begin{aligned} Z_1 &= R_1 \\ Z_g &= R_g \\ Y_f &= Cp \end{aligned}$$

where the operator  $p(\equiv d/dt)$  is the usual time-derivative operator of circuit analysis, and for a pentode circuit,

$$K_r \doteq \frac{Y_1(Cp - g_m)}{(Y_1 + Y_g + Cp)Y_l + Cpg_m} \quad (8-39)$$

This expression may be written in the form

$$K_r = \frac{Y_1(Cp - g_m)}{C(g_m + Y_l)p + (Y_1 + Y_g)Y_l} = \frac{Y_1\left(p - \frac{g_m}{C}\right)}{(g_m + Y_l)\left[p + \frac{(Y_1 + Y_g)Y_l}{C(g_m + Y_l)}\right]} \quad (8-40)$$

from which it follows that the output is related to the input voltage by

$$e_o = A \frac{p - a}{p + b} e_1 \quad (8-41)$$

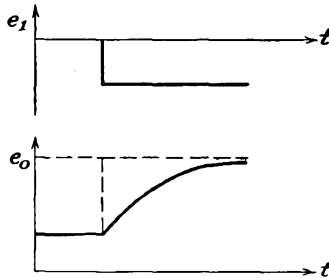
where

$$\left. \begin{aligned} a &= \frac{g_m}{C} \\ b &= \left(\frac{Y_1 + Y_g}{g_m + Y_l}\right) \frac{Y_l}{C} \\ A &= \frac{Y_1}{g_m + Y_l} \end{aligned} \right\} \quad (8-42)$$

\*For the application of a step function  $e_1$ , the results are expressed analytically by the expression

$$e_o = A \left[ e^{-bt} - \frac{a}{b} (1 - e^{-bt}) \right] \quad (8-43)$$

which has the form illustrated in the accompanying figure. If the con-



stant  $b$  is small, a condition that is readily achieved, then Eq. (8-43) reduces to the approximate expression

$$e_o \doteq A[1 - (a + b)t] \quad (8-44)$$

The output impedance of this circuit is of some interest. Equation (6-51) becomes for the present case

$$Y_0 \doteq \left( Y_p + \frac{Cp g_m}{Y_1 + Y_o + Cp} \right) \doteq \frac{C g_m p}{Y_1 + Y_o + Cp}$$

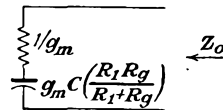
or

$$Z_0 = \frac{Y_1 + Y_o + Cp}{g_m Cp} = \frac{1}{g_m} + \frac{Y_1 + Y_o}{g_m Cp} \quad (8-45)$$

This expression becomes, for an applied a-c voltage,

$$Z_0 = \frac{1}{g_m} + \frac{R_1 + R_o}{j\omega C g_m R_1 R_o} \quad (8-46)$$

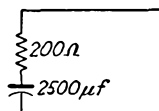
But the circuit that gives rise to an expression of this form is that illus-



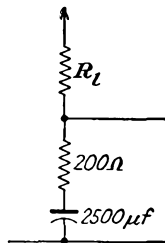
trated in the accompanying figure. This circuit consists of a relatively low series resistance  $1/g_m$ , which would ordinarily be of the order of several thousand ohms or less, and a capacitor, the value of which can be made very large. For example, suppose that the tube and circuit constants are the following:

$$\begin{aligned} g_m &= 5,000 \times 10^{-6} \text{ mho} \\ C &= 1 \mu\text{f} \\ R_1 &= R_o = 1^M \end{aligned}$$

The equivalent circuit then becomes as shown, and the complete output



circuit of the amplifier has the form sketched. Such a circuit as this



may be used as a voltage stabilizer, since, owing to the very large effective capacitance across the output, a ripple of almost any frequency that appears in  $E_{bb}$  is eliminated in the output of the circuit.

Such a circuit as this finds extensive application as the reactance-tube modulator of an f-m transmitter and depends on the fact that the effective output capacitance of the circuit varies directly with  $g_m$  of the tube, a quantity that can be controlled by an input signal. This application is discussed in detail in Sec. 17-7.

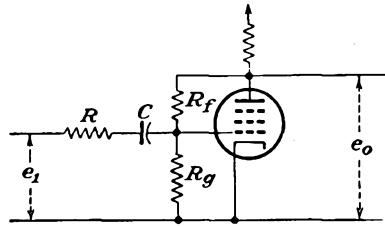


FIG. 8-19. A differentiating circuit.

**8-10. Differentiating Circuit.** The basic differentiating circuit is illustrated in Fig. 8-19. This is substantially the circuit discussed in Sec. 8-8 (page 158), except for the presence of the series input resistor  $R$ . The respective impedance elements contained in Eq. (6-46) are chosen to be

$$Z_1 = R + \frac{1}{Cp} \quad Y_1 = \frac{1}{R} \frac{p}{p + a} \quad a = \frac{1}{RC}$$

$$Z_f = R_f$$

$$Z_g = R_g$$

There results, subject to the approximations of a pentode tube,

$$e_0 \doteq \frac{-Y_1 g_m}{(Y_1 + Y_f + Y_g) Y_l + Y_f (Y_1 + g_m)} e_1$$

$$= \frac{-Y_1 g_m}{Y_1 (Y_l + Y_f) + Y_f (Y_l + g_m) + Y_g Y_l} e_1$$

$$= \frac{-g_m p}{p(Y_l + Y_f) + R(p + a)[Y_f (Y_l + g_m) + Y_g Y_l]} e_1$$

$$= \frac{g_m p}{p[Y_l + Y_f + R(Y_f Y_l + Y_f g_m + Y_g Y_l)] + aR[Y_f (Y_l + g_m) + Y_g Y_l]} e_1 \tag{8-47}$$

This may be written in the form

$$e_0 = A \frac{p}{p + b} e_1 \tag{8-48}$$

where

and

$$A = \frac{-g_m}{Y_l + Y_f + R(Y_f Y_l + Y_f g_m + Y_g Y_l)}$$

$$b = \frac{1}{C} \frac{Y_f Y_l + Y_f g_m + Y_g Y_l}{(Y_l + Y_f) + R(Y_f Y_l + Y_f g_m + Y_g Y_l)}$$

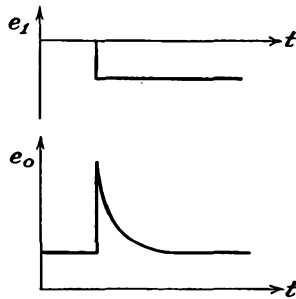
$$= \frac{1/C}{R + \frac{Y_l + Y_f}{Y_f Y_l + Y_f g_m + Y_g Y_l}}$$

$$\left. \begin{matrix} A = \dots \\ b = \dots \end{matrix} \right\} \tag{8-49}$$

The application of a step function to the input yields the expected result, viz.,

$$e_0 = A e^{-bt}$$

which has the form sketched.

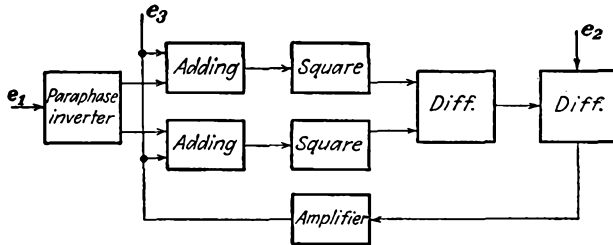


REFERENCES

1. Williams, F. C., F. J. U. Ritson, and T. Kilburn, *J. IEE*, **93**, 1275 (1946).
2. As general references, consult I. A. Greenwood, Jr., J. V. Holdam, Jr., and D. MacRae, Jr., "Electronic Instruments," M.I.T. Radiation Laboratory Series, vol. 21, McGraw-Hill Book Company, Inc., New York, 1948.  
 Korn, G. A., *Electronics*, **21**, 122 (April, 1948).  
 Ragazinni, J. R., R. H. Randall, and F. A. Russell, *Proc. IRE*, **35**, 444 (1947).  
 Mynall, D. J., *Electronic Eng.*, June, 1947, p. 178; July, 1947, p. 214; August, 1947, p. 259; September, 1947, p. 283.

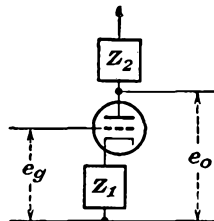
PROBLEMS

- 8-1. Derive Eq. (8-14) for the common plate summing chain.
- 8-2. Show that the output of the circuit  $e_3$  in the diagram is proportional to the ratio  $e_2/e_1$ .

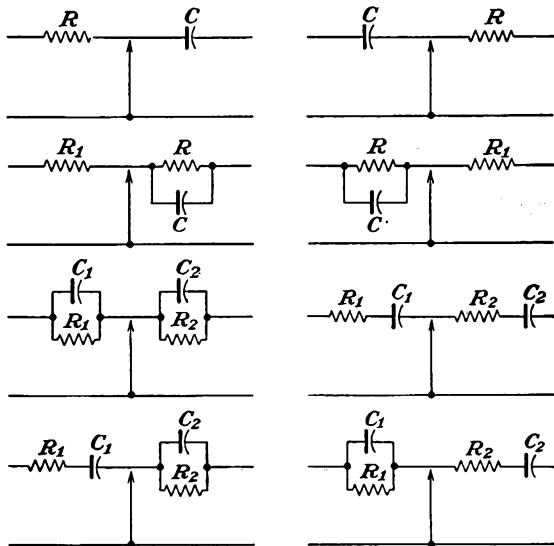


- 8-3. Show that the output of the circuit shown has the form

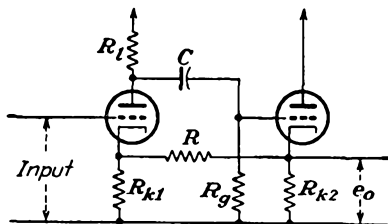
$$e_o = -[Z_2 Y_1] e_g$$



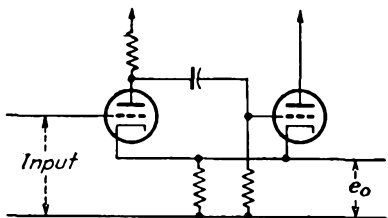
8-4. Determine the character of the mathematical operation performed by each of the feed-back circuits shown in the figure.



8-5. Analyze the differentiating circuit shown in the figure.\*

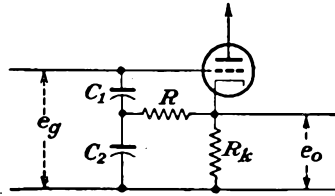


8-6. Analyze the differentiating circuit shown in the diagram.

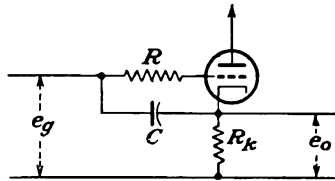


\* Schmitt, O. H. and W. E. Tolles, *Rev. Sci. Instruments*, **13**, 115 (1942).

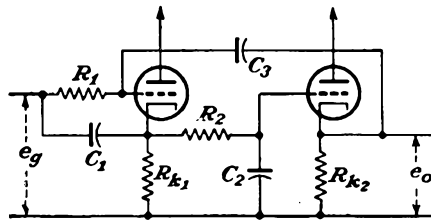
8-7. Analyze the integrating circuit shown in the figure for this problem.



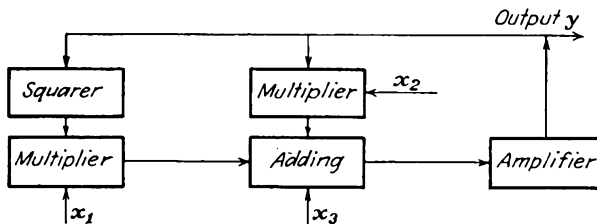
8-8. Analyze the integrating circuit in the diagram.



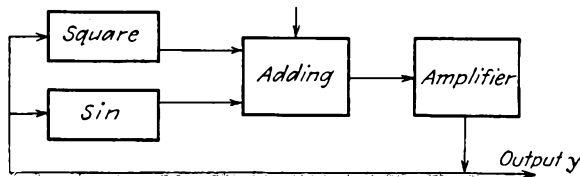
8-9. Analyze the integrating circuit shown in the accompanying figure.



8-10. What equation does the computer in the figure solve?



8-11. What equation does the computer in the diagram solve?



8-12. Sketch the block diagrams of computers that will solve the following equations:

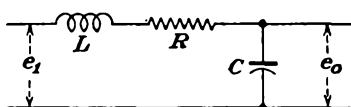
$$(a) x_1^2 + x_2 = y$$

$$(b) x_1^3 + x_1^2 = y$$

$$(c) x_1 x_2 + \frac{x_2}{x_1} = y$$

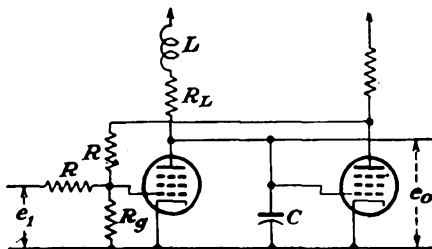
8-13. Show that in the indicated network the output voltage is related to the input voltage by the equation

$$e_1 = e_0 + RC \frac{de_0}{dt} + LC \frac{d^2 e_0}{dt^2}$$

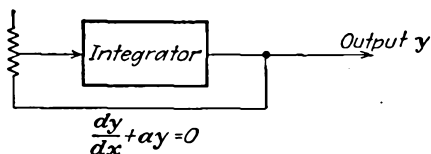


8-14. Show that in the circuit shown the output voltage is related to the input voltage by the expression

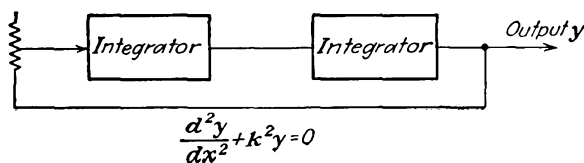
$$e_0 = e_1 + R_L C \frac{de_1}{dt} + LC \frac{d^2 e_1}{dt^2}$$



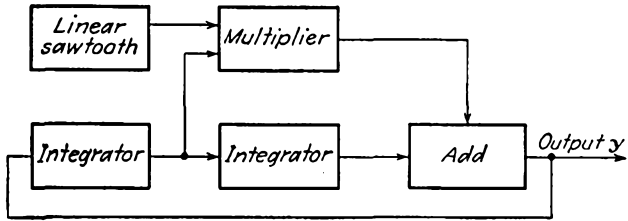
8-15. Show that the computer sketched yields a solution of the differential equation indicated.



8-16. Show that the computer sketched yields a solution of the equation indicated.



8-17. Determine the differential equation that is solved by the computer sketched.



## CHAPTER 9

### UNTUNED POWER AMPLIFIERS

THE voltage amplifiers discussed in Chaps. 5 and 6 are designed to increase a voltage signal from a low level to one which is adequate for operating some low-power circuit. Such amplifiers are generally operated in class A since the amplification is to be accomplished without distortion.

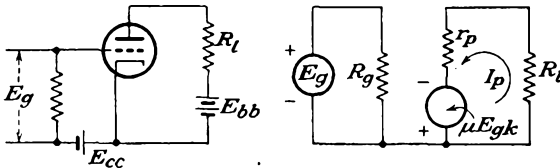


FIG. 9-1. The schematic and equivalent circuits of a simple series-fed power amplifier.

A power amplifier serves to supply an appreciable amount of power to some power-absorbing circuit, although in general it must be accomplished under very low grid driving-power demands. Power amplifiers may be operated as class A, B, or C or at any point between these limits, the choice of operating conditions being determined by the ultimate purpose of the amplifier. If the amplifier is to reproduce the audio spectrum without distortion, then the amplifier must be operated in class A if a single tube is used. If two tubes are used in a push-pull circuit, then the amplifier may be operated in class AB or class B. If the amplifier is to reproduce the input wave shape over a very narrow range of frequencies, tuned class B or tuned class C amplifiers may be used. Only a-f amplifiers will be considered in this chapter.

**9-1. Class A Triode Power Amplifiers.** The basic schematic diagram of a typical series-fed power amplifier and its equivalent circuit are given in Fig. 9-1. It is observed that this circuit is identical with that of Fig. 5-1 for the simple voltage amplifier.

If it is assumed that the dynamic curve is linear over the entire range of operation, then the plate current is given by

$$I_p = \frac{\mu E_g}{R_L + r_p} \quad (9-1)$$

and the power supplied to the load is

$$P = I_p^2 R_l = \frac{\mu^2 E_g^2}{4r_p} \frac{4}{\left(1 + \frac{R_l}{r_p}\right)^2} \frac{R_l}{r_p} \tag{9-2}$$

A sketch showing the variation of the output power as a function of  $R_l/r_p$  is given in Fig. 9-2. It can be seen that the power curve reaches a maximum at the point at which  $R_l/r_p = 1$ , although this maximum is quite broad.  $P$  is a slowly varying function of  $R_l$  in the neighborhood of the maximum, and the power is at least 88 per cent of its maximum value for values of  $R_l/r_p$  ranging from 0.5 to 2.0. This condition shows that the power loss is less than 2.25 db for all values of  $R$  between  $0.5r_p$  and  $2r_p$ .

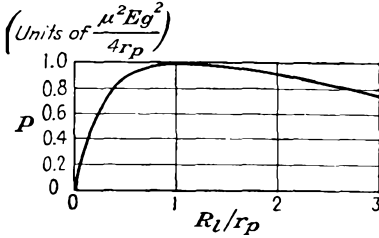


FIG. 9-2. Variation of power output as a function of resistance ratio  $R_l/r_p$ .

Since the maximum power transfer occurs when the load resistor equals the internal plate resistance of the tube, it is necessary to use tubes with low values of  $r_p$  in order to obtain reasonable amounts of power with nominal values of plate-supply voltage. Since the  $g_m$  of a tube cannot be designed over very wide limits, then tubes with low  $r_p$  also possess low values of  $\mu$ . As a result, large grid excitation voltages are required for appreciable amounts of power output. Note from Eq. (9-2) for a given value of  $E_g$  that tubes which possess large values of

$$\frac{\mu^2}{r_p} = g_m \mu$$

possess high output power capacity. In fact, the power sensitivity which was defined by Eq. (4-4) becomes, under the conditions of maximum power transfer, simply  $\mu g_m/4$ .

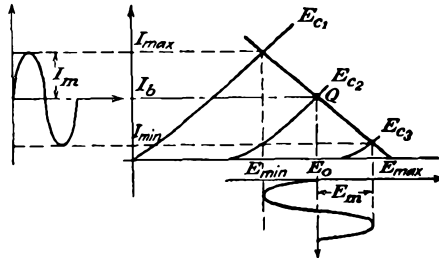


FIG. 9-3. The output current and voltage wave forms in a triode power amplifier.

To determine the power output directly from the static plate characteristic of the tube, it is necessary only to draw the appropriate load line on

these characteristics and read the significant information from the diagram. Thus, by referring to Fig. 9-3, it follows that

$$\left. \begin{aligned} I_p &= \frac{I_m}{\sqrt{2}} = \frac{I_{\max} - I_{\min}}{2\sqrt{2}} \\ E_p &= \frac{E_m}{\sqrt{2}} = \frac{E_{\max} - E_{\min}}{2\sqrt{2}} \end{aligned} \right\} \quad (9-3)$$

The power output is

$$P = \frac{E_m I_m}{2} = \frac{I_m^2 R_l}{2}$$

which may be written in the form

$$P = \frac{(E_{\max} - E_{\min})(I_{\max} - I_{\min})}{8} \quad (9-4)$$

If distortion is not negligible, the harmonic components must be evaluated according to Eqs. (3-22). The total power output is then

$$P = (B_1^2 + B_2^2 + B_3^2 + \dots) \frac{R_l}{2}$$

This may be written as

$$P = \left[ 1 + \left( \frac{B_2}{B_1} \right)^2 + \left( \frac{B_3}{B_1} \right)^2 + \dots \right] \frac{B_1^2}{2} R_l$$

which becomes, by Eq. (3-21),

$$P = (1 + D_2^2 + D_3^2 + \dots) P_1$$

or

$$P = (1 + D^2) P_1 \quad (9-5)$$

where  $D$  is the total distortion. Notice, however, that if the total distortion is high, say 10 per cent, then  $P = 1.01P_1$ . That is, a 10 per cent distortion represents a power of only 1 per cent of the fundamental. Thus, with little error, the output power is approximately that of the fundamental frequency component only.

**9-2. Output Circuits.** It is not always feasible, nor is it generally desirable, to connect the load directly in the plate lead, as shown in Fig. 9-1. Among the reasons for this are that the quiescent current through the load resistor represents a considerable waste of power, as it does not contribute to the a-c component of power, and that the quiescent current may cause a serious polarization of the output. For example, it is inadvisable to pass a large d-c current through the voice coil of a loud-speaker. For these reasons, the transformer-coupled load is used extensively, although the parallel-feed system may be used.

The circuit of the parallel-feed system is illustrated in Fig. 9-4. It is clear that this is just the impedance-capacitance coupled system discussed in Chap. 5. In this system the plate supply is connected to the plate of the tube through a high inductance  $L$ , the load resistor being connected across the output through a blocking capacitor  $C$ . The inductor  $L$  must be so chosen that  $\omega L \gg R_L$ , and  $C$  must be so chosen that  $1/\omega C \ll R_L$  over the operating range of frequencies.

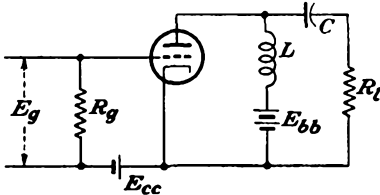


FIG. 9-4. A parallel or shunt-fed power amplifier.

The voltage and current relations for the parallel-feed system are illustrated in Fig. 9-5. Observe that the quiescent current through the tube is determined by  $R_L$ , the resistance of the inductor, although the "dynamic" resistance into which the tube is working is  $R_L$ . Since the static resistance of the choke or the transformer winding is usually small, the static load line is almost vertical.

The voltage and current relations for the parallel-feed system are illustrated in Fig. 9-5. Observe that the quiescent current through the tube is determined by  $R_L$ , the resistance of the inductor, although the "dynamic" resistance into which the tube is working is  $R_L$ . Since the static resistance of the choke or the transformer winding is usually small, the static load line is almost vertical.

Since the static resistance of the choke or the transformer winding is usually small, the static load line is almost vertical.

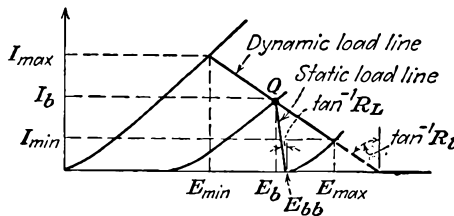


FIG. 9-5. The dynamic and static load lines of a shunt-feed or transformer-coupled amplifier.

Suppose that the load resistance into which the tube works is small; for example, the resistance of the voice coil of a dynamic speaker usually ranges from about 5 to 15 ohms. If such a low resistance load were used in either the series- or the shunt-feed circuits, only a very small power output would be possible, most of the power being lost within the tube resistance. In this case, and in fact in any case in which the load resistance does not properly match the tube resistance, the use of a transformer as an impedance matching device will permit optimum power transfer. Such a system is illustrated in Fig. 9-6.

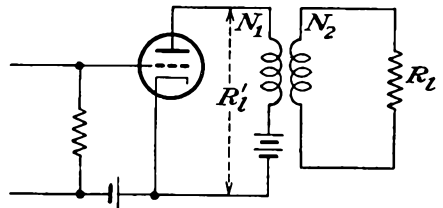


FIG. 9-6. A simple transformer-coupled load in a power amplifier.

The impedance-transforming property of an ideal transformer follows

The impedance-transforming property of an ideal transformer follows

from the simple transformer relations

$$\text{and } \left. \begin{aligned} E_1 &= \frac{N_1}{N_2} E_2 \\ I_1 &= \frac{N_2}{N_1} I_2 \end{aligned} \right\} \quad (9-6)$$

where  $E_1$  and  $E_2$  are the primary and secondary potentials, respectively, and  $I_1$  and  $I_2$  are the primary and secondary currents. The ratio of the above yields

$$\frac{E_1}{I_1} = \left( \frac{N_1}{N_2} \right)^2 \frac{E_2}{I_2}$$

which may be written as

$$R'_l = \left( \frac{N_1}{N_2} \right)^2 R_l = \frac{1}{n^2} R_l \quad (9-7)$$

since  $E_1/I_1$  and  $E_2/I_2$  represent the effective input and output impedances. When the turns ratio  $N_1/N_2$  is greater than unity, the transformer is called a *step-down* transformer; with the ratio  $N_1/N_2$  less than unity, it is a *step-up* transformer.

Equation (9-7) is true for an ideal transformer. In general, however, the coupling is not perfect, the primary and secondary resistances are not negligible, and the core losses cannot be neglected. By taking these factors into account, the input impedance is given by

$$Z'_l = \left( R_1 + \frac{R_2}{n^2} \right) + j\omega \left( L'_1 + \frac{L'_2}{n^2} \right) + \frac{Z_l}{n^2} \quad (9-8)$$

where  $R_1$  and  $R_2$  are the primary and secondary winding resistances,  $L'_1$  and  $L'_2$  are the primary and secondary leakage inductances, and  $Z_l$  is the load impedance.

The same distinction between the static and dynamic load lines must be made for transformer-coupled loads as for the shunt-feed circuit, and, as noted, Fig. 9-5 applies for both circuits. But for the reasons discussed in Sec. 5-5 the frequency response of the transformer is not flat for all frequencies. However, the effects are less severe than for a transformer interstage coupling, since over the audio range the transformer capacitances, tube capacitances, and stray capacitances appear across a relatively low plate-resistance tube or across the low-output load resistance.

**9-3. Maximum Undistorted Power.** The foregoing analyses, which are based on the linear equivalent plate circuit, are not completely valid owing to the curvature of the dynamic characteristic, particularly in the region of small plate currents. In order to obtain the maximum possible power output without making the instantaneous plate current too small

during the most negative part of the applied signal, and without driving the grid positive at the positive peak of the applied signal, it is necessary to maintain a careful balance among the grid bias, load impedance, plate supply voltage, and plate resistance.

To find the expression for the output power under these conditions, and also to determine the appropriate conditions in order to achieve the present results, refer to the graphical construction of Fig. 9-7. Since the distortion that results at small plate currents arises from the curvature

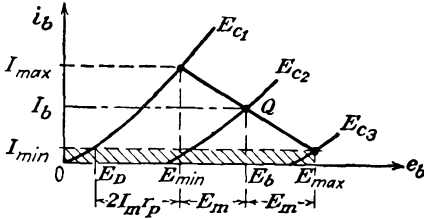


FIG. 9-7. Graphical construction for determining the operating conditions and maximum undistorted power output from an amplifier.

of the static characteristics, this region is eliminated by setting  $I_{min}$  at an appropriate value. This is the crosshatched area of the diagram. Thus the grid is allowed to swing from any point  $Q$ , corresponding to the potential  $E_b$  (which would be  $E_{bb}$  if an ideal shunt-fed or transformer-coupled load were used) between zero grid bias and to that bias which corresponds to  $I_{min}$ . It will be assumed

that the distortion is negligible in this region. The characteristics are essentially linear in the operating region, with a slope corresponding to  $r_p$ .

To find the value of load resistance for which the power will be a maximum, refer to Fig. 9-7. It is noted that

$$E_b = E_D + 2I_m r_p + E_m$$

But since

$$E_m = R_l I_m$$

then it follows that

$$\begin{aligned} E_b &= E_D + 2I_m r_p + I_m R_l \\ &= E_D + I_m (R_l + 2r_p) \end{aligned}$$

Solving this expression for  $I_m$ , there results

$$I_m = \frac{E_b - E_D}{R_l + 2r_p} \tag{9-9}$$

The power to the load is then given by the expression

$$P = \frac{I_m^2 R_l}{2} = \frac{(E_b - E_D)^2}{16r_p} \frac{4R_l/2r_p}{(1 + R_l/2r_p)^2} \tag{9-10}$$

A sketch showing the variation of the output power as a function of  $R/r_p$  is given in Fig. 9-8. This curve, like that of Fig. 9-2, reaches a maximum, but in this case at the point at which  $R_l = 2r_p$ , although the variation is not rapid in the region of the maximum. The power remains at least 88

per cent of its maximum value for load resistances  $R_l$  ranging from  $r_p$  to  $4r_p$ .

To find the appropriate bias for these conditions, combine Eq. (9-9) with the fact that the current changes from  $I_b$  to  $I_m$  when the signal voltage  $E_o$  is equal to  $E_c$ . Thus

$$I_m = \frac{\mu E_c}{R_l + r_p} \quad (9-11)$$

The result, by equating Eq. (9-9) to (9-11) yields

$$E_c = \frac{3}{4\mu} (E_b - E_D) \quad (9-12)$$

in which  $R_l$  has been set equal to  $2r_p$ . The value of  $E_D$  is obtained directly from the curves.

The maximum undistorted power output becomes from Eqs. (9-10) and (9-12)

$$P_{\max} = \frac{\mu^2 E_c^2}{9r_p}$$

Further, since  $E_c = E_{gm}$ , this becomes

$$P_{\max} = \frac{\mu^2 E_{gm}^2}{9r_p} = \frac{2}{9} \mu g_m E_o^2 \quad (9-13)$$

and the power sensitivity at optimum power output is

$$\text{Power sensitivity} = \frac{P}{E_o^2} = \frac{2}{9} \mu g_m \quad \text{mhos} \quad (9-14)$$

which is slightly less than that for the conditions of Sec. 9-1.

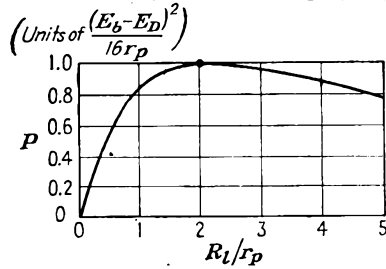


FIG. 9-8. Variation of output power as a function of load  $R_l$ .

The results showing the power output and second-harmonic distortion as a function of  $R_l$  of a type 6A3 triode are illustrated in Fig. 9-9. Optimum output is obtained at about  $R_l = 2,500$  ohms, which is approximately three times the plate resistance  $r_p$  of the tube. Although the second-harmonic distortion is not negligible at this point, a 5 per cent distortion is usually tolerable.

The above analysis is based on the use of a plate-supply source of so-called nominal value (about 300 volts).

If it is assumed that a plate source of any voltage is available, then with increases in the value of  $E_b$ , the ulti-

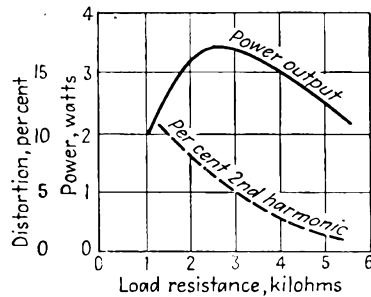


FIG. 9-9. Power output and second-harmonic distortion of a type 6A3 triode as a function of load resistance.

mate limitation will be imposed by the allowable plate dissipation. Under these circumstances, it is found that the circuit should be operated with a value of  $R_l$  that greatly exceeds  $2r_p$ .<sup>1</sup>

**9-4. Plate-circuit Efficiency.** The foregoing discussion indicates the methods for calculating the output power of a power amplifier. The a-c power so obtained is converted from the d-c plate supply by the vacuum tube. The ratio of these quantities is called the *plate-circuit efficiency* of the amplifier. Thus

$$\eta_p = \frac{\text{a-c power output to the load}}{\text{d-c power input to the plate circuit}} \times 100\% \quad (9-15)$$

Suppose that  $P_p$  denotes the average power dissipated by the plate. Then by the principle of the conservation of energy

$$E_{bb}I_b = I_b^2R_1 + E_pI_p + P_p$$

where  $R_1$  is the static load resistance. By solving for  $P_p$ , there obtains

$$P_p = E_{bb}I_b - I_b^2R_1 - E_pI_p$$

But as

$$E_{bb} = E_b + I_bR_1$$

then  $P_p$  has the form

$$P_p = E_bI_b - E_pI_p \quad (9-16)$$

This equation expresses the amount of power that must be dissipated by the plate and represents the kinetic energy of the electrons that is converted into heat at the plate. Notice in particular that the heating of the anode is reduced by the amount of the a-c power that the tube supplies to the load. Hence, a tube is cooler when delivering power to a load than when there is no such a-c power transfer. This is a very important factor in the operation of high-power r-f transmitting tubes, since such tubes are ordinarily operated close to the rated allowed plate dissipation. If for any reason the output circuit becomes slightly detuned, with a consequent decrease in output power, the plate power may become dangerously high.

The plate-circuit efficiency may be written in several different forms. From Eq. (9-15),

$$\eta_p = \frac{E_pI_p}{E_{bb}I_b} \times 100\% \quad (9-17)$$

This may also be written as

$$\eta_p = \frac{P_o}{P_o + P_p + I_b^2R_1} \times 100\% \quad (9-18)$$

Clearly, a large value of  $\eta_p$  means a small value of  $P_p$  for a given output.

This means that a smaller tube with a smaller plate-supply source may be used.

It is possible to obtain an approximate expression for the theoretical value of  $\eta_p$  for the series-fed and the shunt-fed circuits. Consider that

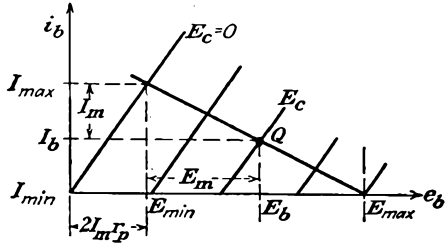


FIG. 9-10. The plate characteristics of an ideal tube.

an ideal tube is used in an amplifier circuit. The plate characteristics of such a tube would have the form illustrated in Fig. 9-10. Suppose that the grid does not swing beyond  $E_c = 0$  and may swing to give zero current. Then, by the proper choice of  $E_c$ ,

$$I_b = I_m$$

and

$$\eta_p = \frac{E_p I_p}{E_{bb} I_b} = \frac{E_m I_m}{2E_{bb} I_m} = 50 \frac{E_m}{E_{bb}} \quad \% \tag{9-19}$$

For the series-fed circuit, the point marked  $E_{max} = E_{tb}$ , and from the diagram,

$$E_{max} = E_{bb} = 2E_m + 2I_m r_p$$

Hence Eq. (9-19) becomes

$$\eta_p = 50 \frac{E_m}{2(E_m + I_m r_p)} = \frac{25}{1 + (I_m r_p / E_m)} \quad \%$$

from which, since

$$E_m = I_m R_l$$

then

$$\eta_p = \frac{25}{1 + r_p / R_l} \quad \% \tag{9-20}$$

The theoretical maximum plate-circuit efficiency for the series-fed amplifier is 25 per cent. For the conditions of maximum power output, when  $R = r_p$ ,  $\eta_p = 12.5$  per cent. Actually, owing to the limited range of operation without distortion,  $\eta_p$  seldom exceeds 10 per cent in practice. Evidently, the linear vacuum-tube amplifier is an inefficient device for converting d-c into a-c power.

In the shunt-fed system a means has been devised for eliminating the d-c power loss in the load. This results in an improved plate efficiency.

If the static resistance is assumed negligible, then

$$E_{bb} = E_b = E_m + 2I_m r_p$$

and

$$\eta_p = 50 \frac{E_m}{E_{bb}} = 50 \frac{E_m}{E_m + 2I_m r_p} \quad \%$$

This reduces to the form

$$\eta_p = \frac{50}{1 + 2r_p/R_l} \quad \% \tag{9-21}$$

The theoretical maximum plate-circuit efficiency of the shunt-fed or transformer-fed amplifier is 50 per cent. Thus the elimination of the static power loss in the load reflects itself as an improved plate efficiency. For the conditions of maximum output power, when  $R = 2r_p$ ,  $\eta_p = 25$  per cent. However, since the static resistance is not negligible and since the current  $I_{min}$  cannot be taken as zero if distortion is to be avoided, the actual plate-circuit efficiency will be less than the 25 per cent figure.

**9-5. Power Pentodes and Beam Power Tubes.** The plate characteristics of the power pentode are markedly different from those of a triode,

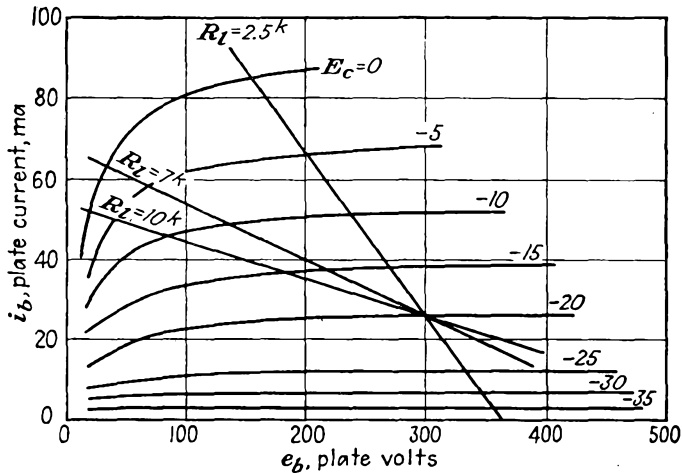


FIG. 9-11. Plate characteristics of a 6F6 power pentode.

and the graphical analyses given above are not valid for pentodes. Since the characteristics of the beam power tubes are similar to those of the power pentode, the discussion to follow applies for both the power pentode and the beam power tube.

Power pentodes differ from triodes principally in the character of the dynamic curve with increasing load resistances. In the triode, the dis-

tortion decreases as the magnitude of the load resistance increases. This follows from the fact that the dynamic curve becomes increasingly linear as the load resistance becomes higher. In the power pentode, the dynamic characteristic is critically dependent on the load resistance, with excessive curvature at both the high and the low values of load resistance. Moreover, the critical load resistance to be used cannot be related analytically with the plate resistance of the tube. This resistance is

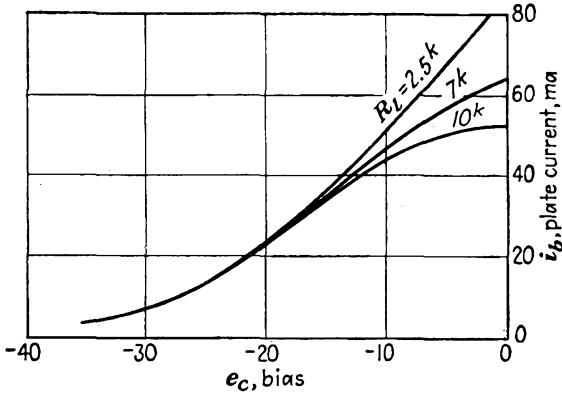


FIG. 9-12. Dynamic characteristics of a 6F6 for three values of plate load resistance.

always less than the plate resistance of the tube. It might appear therefore that the output power capacity of the tube would be too low to make the tube feasible. Actually, owing to the large  $\mu g_m$  product, even with the appropriate  $R_L$  the power output is usually higher than with the tube connected as a triode, and this with a smaller grid driving-voltage amplitude.

To examine the matter in somewhat greater detail, refer to Fig. 9-11, which gives the plate characteristics of a 6F6 power pentode. It will be supposed that the load is transformer-coupled to the tube and that the plate potential is maintained at 300 volts. Three load lines are shown, 2,500, 7,000, and 10,000 ohms. The corresponding dynamic curves are given in Fig. 9-12. The following example will help clarify the situation.

**Example:** Calculate the output power, the plate-circuit efficiency, and the second, third, and fourth harmonics for the 6F6 that supplies power to a loud-speaker, the effective resistance of which is changed to have values of 2.5 $\times 10^3$ , 7 $\times 10^3$ , and 10 $\times 10^3$  ohms. A 300-volt source is available, and the tube is biased at -20 volts.

**Solution:** The important data from Figs. 9-11 and 9-12 are included in the tabulation. The general character of the results is given graphically in Fig. 9-13. Notice that optimum power transfer occurs somewhat above 10 $\times 10^3$ , which is very small compared with the tube resistance of 78,000 ohms.

$R_l \backslash I$	2.5k	7k	10k
$I_{max}$	86	64	53
$I_{1/2}$	52	49	46
$I_b$	25	25	25
$I_{-1/2}$	6	6	6
$I_{min}$	1	1	1

$R_l \backslash B$	2.5k	7k	10k
$B_0$	9	4	1
$B_1$	44	35	31
$B_2$	9	4	1
$B_3$	-1	-4	-5
$B_4$	+1/2	-1/2	

$R_l \backslash D$	2.5k	7k	10k
$D_2$	20.5	11.5	3.2
$D_3$	-2.3	-11.5	-16
$D_4$	+1	-1.4	

$R_l \backslash$	2.5k	7k	10k
$I_{a-c}$	45.0	35.5	31
$P_{a-c}$	2.5	4.4	4.8
$I_{d-c}$	34	29	26
$P_{d-c}$	10.2	8.7	7.8
$\eta_p$	24.5	50.6	61.6

**9-6. Push-pull Amplifiers.** The use of two tubes in parallel provides

twice the output power of a single tube with the same distortion. A push-pull amplifier circuit is a much more desirable connection for two tubes. In this circuit, the two tubes are arranged as shown in Fig. 9-14. The excitation voltages to the grids of the two tubes must be of equal magnitude, but of opposite phase. In the circuit shown, a center-tapped transformer is used to provide the two equal voltages that differ by 180 deg. A number of vacuum-tube circuits are possible for achieving these results, and several of these will be examined below.

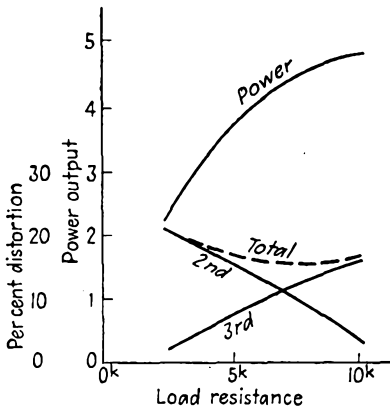


FIG. 9-13. Operating characteristics of a 6F6 pentode as a function of load resistance.

To examine certain of the features of such an amplifier, suppose that the input grid voltage to one tube is of the form

$$e_{g1} = E_{gm} \cos \omega t$$

The plate current of this tube will be represented in general by the expression (see Sec. 3-6)

$$i_{b1} = B_0 + B_1 \cos \omega t + B_2 \cos 2\omega t + B_3 \cos 3\omega t + \dots \quad (9-22)$$

The corresponding signal to the second tube is

$$e_{g2} = -E_{gm} \cos \omega t = E_{gm} \cos (\omega t + \pi)$$

and the output plate current is

$$i_{b2} = B_0 + B_1 \cos (\omega t + \pi) + B_2 \cos 2 (\omega t + \pi) + B_3 \cos 3 (\omega t + \pi) + \dots$$

which has the form

$$i_{b2} = B_0 - B_1 \cos \omega t + B_2 \cos 2\omega t - B_3 \cos 3\omega t + \dots \quad (9-23)$$

But, from Fig. 9-14, the currents are in opposite directions through the output transformer windings. The total output is then proportional to the difference between the plate currents in the two tubes. This is

$$i = k(i_{b1} - i_{b2}) = 2(B_1 \cos \omega t + B_3 \cos 3\omega t + \dots) \quad (9-24)$$

This expression shows that the push-pull circuit balances out all even harmonics in the output and leaves the third-harmonic term as the principal source of distortion.

Another feature of importance in the push-pull system is evident from the circuit of Fig. 9-14. It is observed that the steady components of the plate currents flow in opposite directions in the windings,

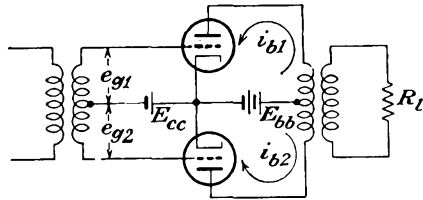


FIG. 9-14. The basic push-pull circuit.

thus opposing each other magnetically in the transformer core. This eliminates any tendency toward core saturation and the resulting distortion that might arise from the magnetization of the transformer core.

The effects of ripple voltages that may be contained in the power supply owing to inadequate filtering will be balanced out in the push-pull circuit. This is so because the currents that are produced by this ripple voltage are in opposition in the output transformer and hence will not appear in the load. Of course, the effects of the ripple voltage that appear on the grids of the amplifier will not be balanced out and will be noticeable with the signal.

Another feature of this amplifier is that, under self-biased conditions, there is no need for a by-pass capacitor across the cathode resistor. This follows from the fact that the voltage which appears across the self-bias resistor  $R_k$  is  $(i_{b1} + i_{b2})R_k$ . But this is, from Eqs. (9-22) and (9-23),

$$(i_{b1} + i_{b2})R_k = 2R_k(I_b + B_0 + B_2 \cos 2\omega t + B_4 \cos 4\omega t + \dots)$$

But for tubes operating in class A the harmonic amplitudes are very small and are therefore not significant.

One of the particularly significant features of the push-pull amplifier

is that the output power possible with the two tubes for a given total distortion is higher than twice that of the single tube. This results from the fact that, with the automatic cancellation of even harmonics in

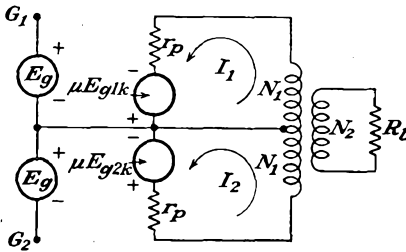


FIG. 9-15. Equivalent circuit of the class A push-pull amplifier of Fig. 9-14.

the output, the tubes may be driven harder until the third-harmonic terms become significant. Note also that, with the increased grid drive, the rectification component  $2B_0R_k$  becomes significant and adds to the bias  $2I_bR_k$ , if self-bias is used. As a result, the effective bias increases, with consequent reduction of output power. This means that the output power of a push-pull

amplifier under otherwise similar conditions will be higher with fixed bias than with self-bias.

**9-7. Equivalent Circuit of a Class A Push-pull Amplifier.** Suppose that both tubes of the push-pull amplifier are identical and that  $\mu$  and  $r_p$  are constant over the range of operation. The equivalent circuit of the system then has the form given in Fig. 9-15. Observe that the connection between the cathode terminals and the mid-point of the output transformer does not carry a fundamental frequency component of current, owing to the cancellation that occurs. This connection may be omitted from the diagram without influencing the operation. The resulting circuit then has the form given in Fig. 9-16. In this diagram

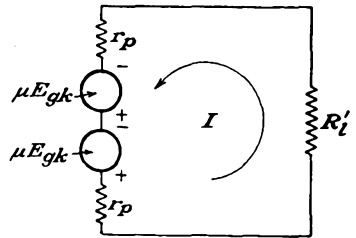


FIG. 9-16. The simplified equivalent circuit of the class A push-pull amplifier.

$$R'_l = \left(\frac{2N_1}{N_2}\right)^2 R_l \tag{9-25}$$

The resultant current is given by

$$I = \frac{2\mu E_g}{2r_p + R'_l} \tag{9-26}$$

which may be written in the form

$$I = \frac{\mu E_g}{r_p + (R'_l/2)} \tag{9-27}$$

The total power delivered to the load is then

$$P = I^2 R'_l = 2 \left( \frac{\mu E_g}{r_p + \frac{R'_l}{2}} \right)^2 \frac{R'_l}{2} \tag{9-28}$$

This expression may be interpreted to mean that the total output power is twice the power of each tube considered to be working into the equivalent load resistance  $R'_l/2$ .

A more significant expression results by writing Eq. (9-28) in the form

$$P = \left( \frac{\mu E_g}{(r_p/2) + (R'_l/4)} \right)^2 \frac{R'_l}{4} \tag{9-29}$$

This may be interpreted to show that the class A push-pull amplifier may be represented by a single composite generator which has emf  $\mu E_g$ , with an internal resistance  $r_p/2$ , and which works into a load resistance equal to  $R'_l/4$ . It is possible, in fact, to derive a set of static characteristics of the composite tube from the tube plate characteristics and to obtain significant operating information from this.

**9-8. Composite Static-characteristic Curves.** The composite static characteristics of the push-pull amplifier may be obtained from the plate

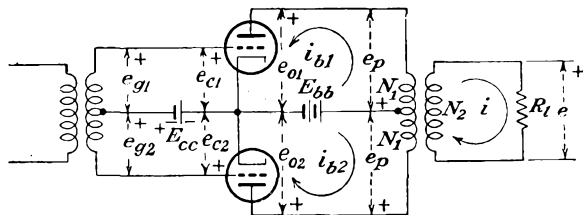


FIG. 9-17. The potentials in the push-pull amplifier.

characteristics of the individual tube by a graphical construction.<sup>2</sup> It is assumed that the output transformer is ideal, whence the voltages across each half of the transformer are equal. The situation is illustrated in Fig. 9-17. The load voltage is given by

$$e = \frac{N_2}{N_1} e_p \tag{9-30}$$

Also, in the ideal transformer, the net primary ampere turns are equal to the secondary ampere turns, from which

$$N_1 i_{b1} - N_1 i_{b2} = N_2 i \tag{9-31}$$

Thus the load voltage is

$$e = i R_L = (i_{b1} - i_{b2}) \frac{N_1}{N_2} R_L \tag{9-32}$$

By combining Eqs. (9-30) and (9-32) there results

$$e_p = (i_{b1} - i_{b2}) \left( \frac{N_1}{N_2} \right)^2 R_l \tag{9-33}$$

which may be written in the form

$$e_p = (i_{b1} - i_{b2}) \frac{R'_l}{4} \tag{9-34}$$

where  $R'_l$  is the plate-plate resistance.

The following relationships are evident from an inspection of the diagram of Fig. 9-17:

$$\left. \begin{aligned} e_{b1} &= E_b - e_p \\ e_{b2} &= E_b + e_p \\ e_{c1} &= E_{cc} + e_g \\ e_{c2} &= E_{cc} - e_g \end{aligned} \right\} \tag{9-35}$$

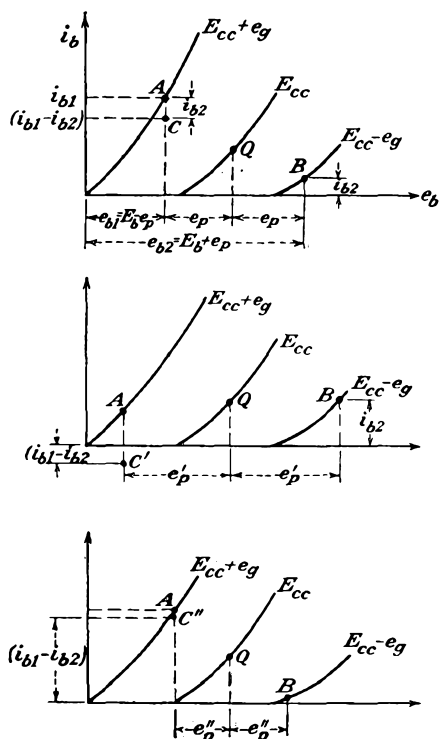


FIG. 9-18. To construct the composite static characteristics of a push-pull amplifier from the plate characteristic.

It follows from these equations that, when the plate-cathode potential  $e_{b1}$  of tube  $T1$  decreases from the quiescent-point value  $E_b$  by an amount  $e_p$ , then the corresponding potential  $e_{b2}$  of tube  $T2$  increases beyond  $E_b$

by a like amount. Also, when the grid-cathode potential  $e_{c1}$  increases beyond  $E_{cc}$  by the signal voltage  $e_g$ , the corresponding value of  $e_{c2}$  decreases below  $E_{cc}$  by  $e_g$ . These conditions are shown in Fig. 9-18 for three different values of  $e_p$ . In these diagrams point  $A$  corresponds to conditions  $e_{b1} = E_b - e_p$ ,  $e_{c1} = E_{cc} + e_g$ , the tube current being  $i_{b1}$ . Point  $B$  is that for  $e_{b2} = E_b + e_p$ ,  $e_{c2} = E_{cc} - e_g$ , and the tube current is  $i_{b2}$ . Point  $C$  has the ordinate  $i_{b1} - i_{b2}$  for the chosen value of  $e_p$ .

The composite static characteristics are the family of curves of  $i_{b1} - i_{b2}$  vs.  $e_b$ , with grid signal voltage as a parameter. Clearly, point  $C$  is one point on the composite static curve for the signal voltage  $e_g$ . Other points on this characteristic are found by maintaining  $e_g$  constant and by varying  $e_p$ . The construction for two other values  $e'_p$  and  $e''_p$  are given in Figs. 9-18b and 9-18c. These locate two other points  $C'$  and  $C''$  on the composite static characteristic. The complete composite static is given in Fig. 9-19.

Several significant features are evident from Fig. 9-19. The composite static characteristic extends above and below the zero current axis.

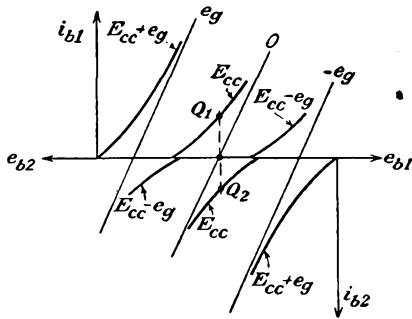


FIG. 9-20. The Thompson method of obtaining the composite static characteristics of a push-pull amplifier.

Also, the composite static curve is much more linear than the plate characteristics of the individual tube. An alternative method for obtaining the composite static characteristics was described by Thompson.<sup>3</sup> According to this method, the plate characteristics of the tube are plotted in the usual way. The curves are also plotted in an inverted manner, with the voltage scale shifted so that the voltages  $E_b$  of both sets of curves coincide with each other. This construction is shown in Fig. 9-20. The inverted curves represent the plate family of tube  $T_2$ . The two methods are essentially equivalent.

The foregoing discussion of the graphical construction is general and applies to any type of tube under operation under class A, AB, or B conditions. Although the illustrations are for triodes, the curves for other

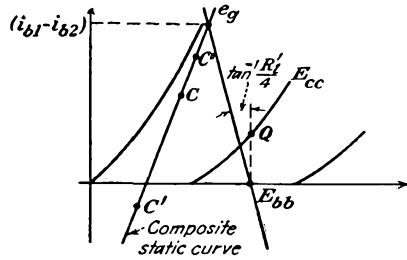


FIG. 9-19. The composite static curve derived from the constructions of Fig. 9-18.

These locate two other points  $C'$  and  $C''$  on the composite static characteristic. The complete composite static is given in Fig. 9-19.

Several significant features are evident from Fig. 9-19. The composite static characteristic extends above and below the zero current axis. Also, the composite static curve is much more linear than the plate characteristics of the individual tube.

An alternative method for obtaining the composite static characteristics was described by Thompson.<sup>3</sup> According to this method, the plate characteristics of the tube are plotted in the usual way. The curves are also plotted in an inverted manner, with the voltage scale shifted so that the voltages  $E_b$  of both sets of curves coincide with each other.

This construction is shown in Fig. 9-20. The inverted curves represent the plate family of tube  $T_2$ . The two methods are essentially equivalent.

The foregoing discussion of the graphical construction is general and applies to any type of tube under operation under class A, AB, or B conditions. Although the illustrations are for triodes, the curves for other

tube types are obtained in the same way. In fact, owing to their shape, the composite static characteristics for pentode-type tubes are more easily obtained than the triode curves. The simplification results because the current  $i_{b2}$  remains substantially constant for large variations in  $e_b$ . The composite static characteristics for the 6F6 pentode are shown in Fig. 9-21.

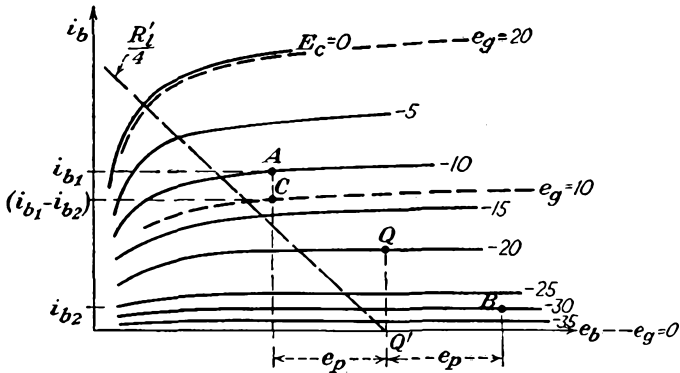


FIG. 9-21. Composite static characteristics of a 6F6 pentode push-pull amplifier.

**9-9. Composite Dynamic Characteristic.** The composite dynamic characteristic of a push-pull amplifier is obtained from the composite static characteristics in precisely the same way that the dynamic curve is obtained from the plate characteristics of a single-tube amplifier. This

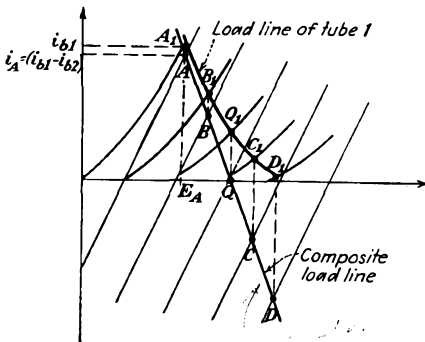


FIG. 9-22. The load line of the composite circuit, and the load line of one tube of the push-pull amplifier.

requires drawing the effective composite load line on the composite static curves and noting the points of intersection of the two, which are points on the composite dynamic curve. This construction also permits obtaining the load line into which each tube is working and hence also the dynamic characteristic of the individual tubes. The construction is shown in Fig. 9-22. Clearly, the intersection of the push-pull load line with the composite plate characteristics gives points on the composite dynamic characteristic. That is, points A, B, C, D are points on the composite dynamic curve. These points are replotted in Fig. 9-23 to give the composite dynamic curve.

To find the dynamic characteristic of each tube, the procedure is essentially the reverse of that of Sec. 9-8. In particular, consider the

requires drawing the effective composite load line on the composite static curves and noting the points of intersection of the two, which are points on the composite dynamic curve. This construction also permits obtaining the load line into which each tube is working and hence also the dynamic characteristic of the individual tubes. The construction is shown in Fig. 9-22. Clearly, the intersection of the push-pull load line with the composite plate characteristics gives points on the composite dynamic characteristic. That is, points A, B, C, D are points on the composite dynamic curve. These points are replotted in Fig. 9-23 to give the composite dynamic curve.

point *B* in Fig. 9-22. This point is a representation of  $i_{b1} - i_{b2}$  corresponding to the appropriately chosen value of  $e_p$ . But the point  $i_{b1}$  lies vertically above this point, by an amount  $i_{b2}$ , and must lie on the plate characteristic of the tube. This defines the point  $A_1$ . The other points are obtained in a similar way, and the results are shown in Fig. 9-22. These points are plotted also in Fig. 9-23. The points  $A_2, B_2, C_2, D_2$  for tube *T2* are obtained by symmetry from the corresponding points of tube *T1*.

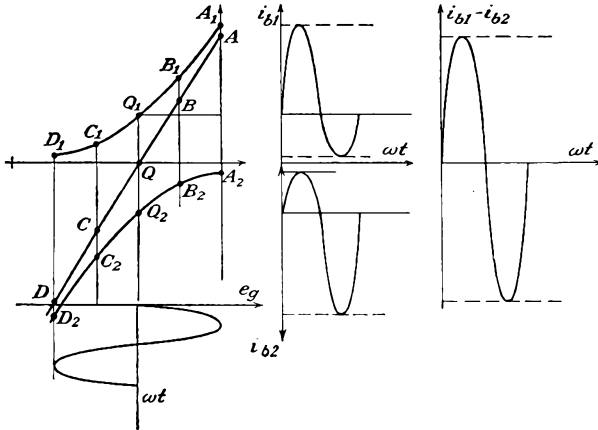


FIG. 9-23. The single-tube dynamic characteristics and the composite dynamic curve of the push-pull amplifier. The wave shape in each tube and in the output are also shown.

It is interesting to note that the composite dynamic curve is practically a straight line, although the individual tube dynamic curves are markedly curved. Thus, for a sinusoidal input, the total output current is closely sinusoidal, although the current in each tube is not sinusoidal, in general.

If only the output current is desired, there is no requirement for the individual tube dynamics. If the plate-circuit efficiency is required, the individual tube dynamics are required in order to calculate the value of  $I_b$  and the d-c component  $B_0$  that results from the partial rectification due to the curvature of the dynamic. The total d-c power input to the amplifier is  $2E_{bb}(I_b + B_0)$ .

**9-10. Power Output and Distortion in Push-pull Amplifiers.** Owing to the fact that the dynamic curve must be an odd function, by virtue of the manner of its construction, then for the composite circuit

$$\left. \begin{aligned} I_b &= 0 \\ I_{\max} &= -I_{\min} \\ I_{1/2} &= -I_{-1/2} \end{aligned} \right\} \quad (9-36)$$

Under these circumstances the five-point schedule of Eq. (3-20) reduces to

$$\left. \begin{aligned} B_0 &= B_2 = B_4 = 0 \\ B_1 &= \frac{2}{3}(I_{\max} + I_{\frac{1}{2}}) \\ B_3 &= \frac{1}{3}(I_{\max} - 2I_{\frac{1}{2}}) \end{aligned} \right\} \quad (9-37)$$

The fundamental power output is given by the expression

$$P_1 = \left( \frac{B_1}{\sqrt{2}} \right)^2 \frac{R'_l}{4} = \frac{B_1^2 R'_l}{8} \quad (9-38)$$

By neglecting the harmonic components of power, the total power is given by

$$P_1 = \frac{E_m I_m}{2} \quad (9-39)$$

where  $E_m$  and  $I_m$  denote the peak values of the a-c output voltage and current, respectively. These values are obtained directly from the curves of Fig. 9-22, since  $I_m = I_A$  and  $E_m = E_b - E_A$ , whence

$$P = \frac{(E_b - E_A) I_A}{2} \quad (9-40)$$

To find the maximum output power in the push-pull class A system utilizing triodes, use is made of the fact that the load resistance should equal the internal resistance of the equivalent or composite generator. This follows from Eq. (9-29) for the class A amplifier and requires that  $R'_l/4 = r_p/2$ . This requires that the slope of the effective load line must be equal to the reciprocal of the composite static characteristic, which has a value of  $r_p/2$ .

Suppose that the tubes are operated in push-pull class B. Now, since the tubes are biased to cutoff, then either one or the other of the two tubes will be supplying current to the circuit and each contributes power for one-half of each cycle. Consequently, the equivalent generator will be one with an internal resistance equal to  $r_p$  of the tube. The maximum power under these conditions will be obtained for  $R'_l/4 = r_p$ . It is reasonable to expect that the internal resistance of the equivalent source of a push-pull class AB amplifier will lie between the value for the class A circuit  $r_p/2$  and that for the class B circuit  $r_p$ . In all cases, however, recourse should be had to the composite static characteristics, and then  $R'_l/4$  should be set equal to the reciprocal of the slope of these lines.

The situation for pentodes is different from that discussed above for triodes and follows roughly the reasoning of Sec. 9-5. The optimum load is that which yields the maximum power with low distortion. The optimum load line is drawn through the point  $Q'$  so that it intersects the peak

composite grid-voltage curve in the neighborhood of the knee of the curve. This is illustrated in Fig. 9-21 for the 6F6 tube.

**9-11. Driver Stages for Push-pull Amplifiers.** The driver may be considered to comprise the circuit that supplies the two voltages of equal magnitude but in phase opposition to the grids of the push-pull power amplifier. A variety of suitable circuits exist, the most direct of which is illustrated in Fig. 9-24. This circuit consists of a simple amplifier with a transformer in the output, the secondary of which is center-tapped.

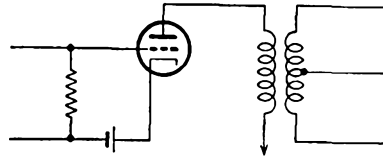


Fig. 9-24. A simple driver circuit for a push-pull amplifier.

The characteristics of this stage are determined by the grid driving-power requirements of the power amplifier. If the push-pull circuit requires substantially no driving power, then there are no serious requirements imposed on the driver stage. If the driver stage is called upon to supply power, and this would seldom exceed 15 per cent of the output of the push-pull stage, although it is ordinarily less than this amount, the driver stage must have a relatively low internal resistance if no distortion is to be introduced into the grid circuit of the push-pull amplifier. It is advisable in such cases that a step-down transformer be used to couple the driver stage to the push-pull input in order to reduce the effective resistance in the grid circuit.

If the power requirements are low, then any one of a wide variety of "paraphase" circuits may be used. A paraphase circuit is one which provides two equal output potentials which are 180 deg apart in phase from a single signal source.

*Single-tube Paraphase Amplifier.* A single-tube amplifier in which the plate resistor is divided equally between the plate and cathode circuits is the simplest form of paraphase amplifier. The circuit is given in Fig. 9-25. The resistors  $R_l$  and  $R_k$  have the same value, whence the amplitude of the voltage developed across each is the same, since the same current flows through each. The polarity is opposite because the cathode output is taken from the more positive end of  $R_k$  and the plate output is taken from the less positive end of  $R_l$ . An analysis of this circuit will show that the gain of the stage is less than unity and is given by the expression

$$K = \frac{\mu}{\mu + 2} \tag{9-41}$$

*Two-tube Paraphase Amplifiers.* In the two-tube paraphase amplifier, one tube is used as a conventional amplifier, and a second tube is used as a phase-inverter amplifier. Figure 9-26 illustrates such a circuit. The

resistors  $R_1$  and  $R_2$  comprise a voltage divider across the output of a conventional amplifier, the ratio of the resistances being chosen so that the gain from the anode of  $T_1$  to the anode of  $T_2$  is unity. Also, the operating conditions of the tubes are carefully chosen to allow the curvature of the characteristic of  $T_2$  to compensate for the curvature of  $T_1$ . Thus the output potentials relative to ground are both slightly distorted

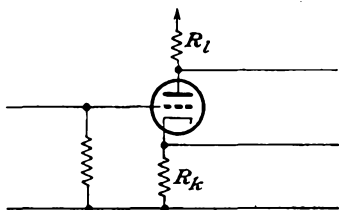


FIG. 9-25. A single-tube paraphase amplifier.

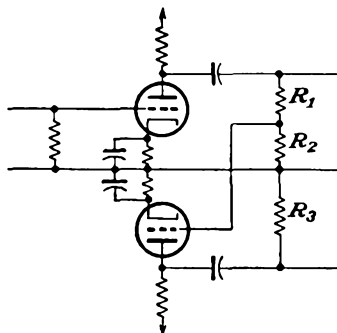


FIG. 9-26. A two-tube paraphase amplifier.

to provide a comparatively undistorted potential difference between the output terminals. This method is difficult to apply in practice because the adjustments necessary to reduce distortion to a minimum are critical.

A second form of two-tube paraphase amplifier employs the differential voltage between the outputs of two tubes as the input signal to the phase-inverter section. This circuit, which is also referred to as the *floating paraphase* amplifier, is illustrated in two versions in Fig. 9-27.

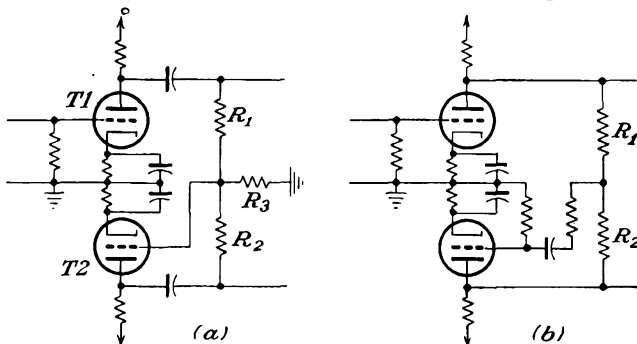


FIG. 9-27. Two forms of floating paraphase amplifiers.

In the circuit of Fig. 9-27a tube  $T_1$  is an amplifier to increase the amplitude of the applied wave form. The cathode resistors  $R_k$ , if not by-passed, will provide some degeneration, which will help to reduce distortion. The output from  $T_1$  is coupled through  $C_1$  to  $R_1$  and  $R_3$ , both of which have

the same value as  $R_2$ . The voltage which appears across  $R_3$  is applied to the grid of  $T_2$ . The output of  $T_2$  is passed through  $C_2$  and is applied across  $R_2$  and  $R_3$ . Thus half the output of both  $T_1$  and  $T_2$  appears across  $R_3$ . Since these potentials are of opposite polarity, the resultant voltage across  $R_3$  is the difference between these two. The output of  $T_1$  is larger than the output of  $T_2$ , and in order that this difference should be kept as small as possible, pentodes are used, so as to take advantage of their high amplification.

The feature of the circuit of Fig. 9-27b is that the difference between the output voltages is taken care of in the choice of the resistors  $R_1$  and  $R_2$  so that the output voltages have the same amplitude. To do this requires that the following conditions be satisfied,

$$\left. \begin{aligned} R_g \gg R_2 \quad \mu R_g \gg r_p \\ \frac{R_1}{R_2} = \frac{K - 1}{K + 1} \end{aligned} \right\} \quad (9-42)$$

where  $K$  is the gain of the stage.

The cathode-coupled paraphase amplifier was discussed in some detail in Sec. 6-9. This circuit is used extensively to provide push-pull deflection potentials for the plates of a cathode-ray tube. It may also be used as the driver of a push-pull amplifier. The circuit is redrawn in Fig. 9-28 for convenience.

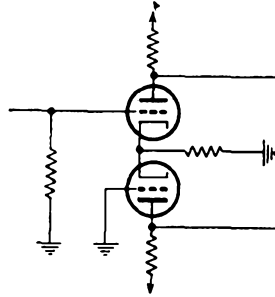


FIG. 9-28. A cathode-coupled paraphase amplifier.

#### REFERENCES

1. Nottingham, W. B., *Proc. IRE*, **29**, 620 (1941).
2. Millman, J., and S. Seely, "Electronics," Chap. XX, McGraw-Hill Book Company, Inc., New York, 1941.
3. Thompson, B. J., *Proc. IRE*, **21**, 591 (1933).

#### PROBLEMS

9-1. A 6F6 tube is operated as a triode and supplies power to a 4,000-ohm load. With  $E_{bb} = 300$ ,  $E_{cc} = -25$  volts and with a peak signal of 25 volts, calculate the following:

- a. Output power.
- b. Plate-circuit efficiency.
- c. Per cent second-harmonic distortion.
- d. Plate dissipation.

9-2. Repeat Prob. 9-1 when the load is transformer-coupled to the tube.

**9-3.** It is supposed that the plate dissipation at the operating point is kept constant. Prove that for class A operation the plate load is made larger with increasing values of  $E_{bb}$  and the plate efficiency increases.

**9-4.** A 6V6 is operated with  $E_{bb} = E_{c2} = 250$  volts and with  $E_{cc} = -12.5$  volts. The grid signal is sinusoidal, with a peak value of 12.5 volts. Calculate the following for a shunt-fed load of 5,000 ohms:

- a. Output power.
- b. Total distortion.
- c. Plate dissipation.
- d. Plate-circuit efficiency.

**9-5.** Repeat Prob. 9-4 if the load is 2,000 ohms; 8,000 ohms.

**9-6.** Two 6F6 tubes are connected as triodes and are operated in push-pull class A from a 350-volt plate source, with a grid bias of  $-30$  volts. A 30-volt peak signal is used.

- a. Draw the composite static characteristics.
- b. From this, determine the plate-plate resistance for maximum output power.
- c. Calculate the power output, third-harmonic distortion, and plate-circuit efficiency.

**9-7.** Two 6F6 tubes are connected as pentodes and are operated in push-pull class AB from a 350-volt plate source, with a grid bias of  $-25$  volts. The screen potentials are maintained at 250 volts.

- a. Draw the composite static characteristics.
- b. Plot the composite dynamic and the dynamic characteristic of each tube.
- c. Calculate the output power, third-harmonic distortion, and plate-circuit efficiency for a plate-plate resistance of 10,000 ohms. The peak grid signal is 40 volts.

**9-8.** Two 2A3 triodes are operated in push-pull with  $E_{bb} = 300$ ,  $E_{cc} = -60$  volts.

- a. Draw the composite static characteristic.
- b. From this, determine the plate-plate resistance for maximum power output
- c. Calculate the power output under these conditions.
- d. Repeat c for  $\frac{1}{2}$  and 2 times the optimum value.
- e. Construct the paths of operation for the individual tubes.

**9-9.** A 6N7 zero-bias tube is connected as a class B push-pull audio amplifier and is to furnish 10 watts into a dynamic speaker, the voice coil of which has a resistance of 8 ohms. A 35:1 step-down transformer is used. The plate supply is 325 volts. Determine the following:

- a. D-c plate current.
- b. Grid driving voltage.

**9-10.** The typical operating characteristics of a 6L6 beam power tube when used in push-pull class A are shown below. Values shown are for two-tube unless otherwise specified.

Plate supply.....	270 volts
Screen supply.....	270 volts
Cathode resistor.....	125 ohms
Zero-signal plate current.....	134 ma
Maximum-signal plate current.....	145 ma
Zero-signal plate current.....	11 ma
Maximum-signal screen current.....	17 ma
Plate resistance.....	23,500 ohms
Transconductance.....	5,700 $\mu$ mhos
Effective load resistance (plate to plate).....	5,000 ohms
Maximum-signal power output.....	18.5 watts

The 6L6 tubes are to supply the 18.5 watts to the grids of a pair of 806 triodes which are operating in class B push-pull. The required peak grid driving voltage is 660 volts.

- a. Calculate the turns ratio of the output transformer.
- b. What is the peak a-c plate voltage on each tube?
- c. What is the peak a-c grid-voltage swing on each tube?
- d. Does grid current flow during any part of the input cycle?
- e. Calculate the plate-circuit efficiency.

**9-11.** Verify Eq. (9-41).

**9-12.** Verify the conditions (9-42) imposed on the floating paraphase amplifier for balanced output voltages. What conditions are imposed on  $R_3$ ?

**9-13.** It is suggested that the paraphase principle be combined with a push-pull amplifier to yield push-pull operation without a separate driving source. The push-pull amplifier feeds a dynamic speaker. Discuss the suggested operation from the point of view of class of operation possible; of distortion.

## CHAPTER 10

### TUNED VOLTAGE AMPLIFIERS

**T**UNED voltage amplifiers are used in those cases in which it is desired to amplify a relatively narrow band of frequencies centered about some designated mean or carrier frequency. Voltages whose frequencies lie outside of this range are undesirable and should be rejected. The use of tuned networks accomplishes this, as it is possible to adjust the tuned network so that the impedance falls steeply to low values outside of the

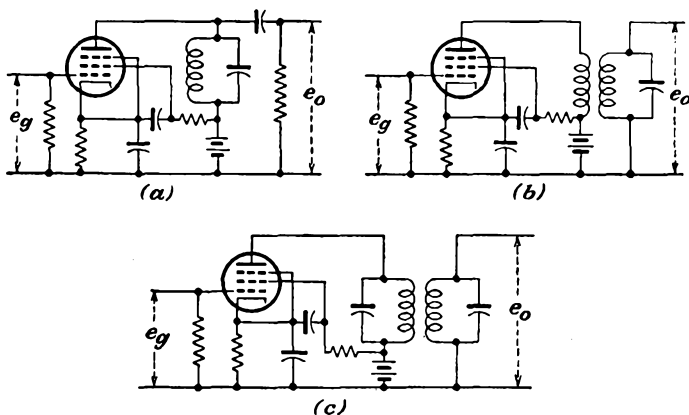


FIG. 10-1. The three basic tuned-amplifier circuits: (a) single-tuned, direct coupling; (b) single-tuned, transformer coupling; (c) double-tuned.

desired frequency band, with the consequent reduction in amplifier gain to negligibly low values. The resulting nonlinear distortion that is produced in these amplifiers is very small, both because the stage is operated under class A conditions and because the tuned plate-circuit impedance may be very low for any harmonic frequencies that might be generated.

There are three basic tuned-amplifier circuits, and these are illustrated in Fig. 10-1. Pentodes are ordinarily used in such amplifiers, and the circuits are drawn showing such tubes. In two of these types, a single resonant circuit is used, which may be included directly in the plate circuit (direct-coupled) or which may be inductively coupled to the plate circuit (transformer-coupled). In the third type, a double-tuned band-

pass arrangement is used, both the primary and secondary circuits being tuned. An analysis of the operation of each of these amplifier circuits will be given.

**10-1. Single-tuned Direct-coupled Amplifier.** The equivalent circuit of a typical single-tuned direct-coupled stage is given in Fig. 10-2.

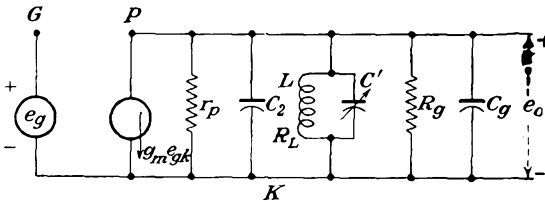


FIG. 10-2. The equivalent circuit of a single-tuned direct-coupled class A amplifier.

Included in this diagram are the output tube capacitances  $C$  [see Eq. (4-20)] and the input and wiring capacitances to the following stage. The coupling capacitor may be neglected, as its capacitance is presumed to be large.

In accordance with the discussion of Sec. 4-7, the gain of the amplifier can be written directly as

$$K = -g_m Z \tag{10-1}$$

where  $Z$  is the total load impedance. This impedance has the form

$$\frac{1}{Z} = \frac{1}{r_p} + \frac{1}{R_g} + \frac{1}{Z_t} \tag{10-2}$$

where  $Z_t$  is the impedance of the antiresonant circuit, and comprises the inductor  $L$  and the sum of the various capacitances  $C_t = C_2 + C_g + C'$  where  $C_2$  is defined as in Eq. (4-20).

The impedance  $Z_t$  has the form

$$C_t = C_{pk} + C_{p2} + C_{p3}$$

$$Z_t = \frac{-j \frac{1}{\omega C} (R_L + j\omega L)}{R_L + j \left( \omega L - \frac{1}{\omega C} \right)} \tag{10-3}$$

which may be written in the form

$$Z_t = \frac{\frac{L}{C} \left( 1 - j \frac{R_L}{\omega L} \right)}{R_L \left[ 1 + j \frac{\omega L}{R_L} \left( 1 - \frac{1}{\omega^2 LC} \right) \right]} \tag{10-4}$$

By writing

$$\left. \begin{aligned} \omega_0 &= \frac{1}{\sqrt{LC}} \\ \delta &= \frac{\omega}{\omega_0} - 1 \\ Q &= \frac{\omega_0 L}{R_L} = \frac{1}{\omega_0 C R_L} = \frac{1}{R_L} \sqrt{\frac{L}{C}} \end{aligned} \right\} \quad (10-5)$$

the impedance function becomes

$$\begin{aligned} Z_t &= \frac{R_L Q^2 \left( 1 - j \frac{1}{Q} \frac{\omega_0}{\omega} \right)}{\left[ 1 + jQ \left( \frac{\omega}{\omega_0} - \frac{\omega_0}{\omega} \right) \right]} \\ &= \frac{R_L Q^2 \left[ (1 + \delta) - j \frac{1}{Q} \right]}{(1 + \delta) + jQ\delta(2 + \delta)} \end{aligned} \quad (10-6)$$

At resonance  $\omega = \omega_0$ , and  $\delta = 0$ . Then

$$Z_t = R_L Q^2 \left( 1 - j \frac{1}{Q} \right) \quad (10-7)$$

Since  $Q$  for the circuit used is usually high, that is,  $Q \geq 10$ , then with good approximation

$$Z_t = R_0 \doteq R_L Q^2 \quad (10-8)$$

This result shows that the shunt impedance  $R_0$  of the antiresonant circuit is essentially resistive, for circuits with  $Q > 10$ , and at the resonant frequency.

By combining Eq. (10-8) with Eq. (10-2), the gain at resonance becomes

$$K_{\text{res}} = \frac{-g_m}{\frac{1}{r_p} + \frac{1}{R_g} + \frac{1}{R_L Q^2}} = \frac{-g_m \omega_0 L Q}{1 + \frac{\omega_0 L Q}{r_p} + \frac{\omega_0 L Q}{R_g}} \quad (10-9)$$

This expression may be written in the form

$$K_{\text{res}} = -g_m \omega_0 L Q_e \quad (10-10)$$

where  $Q_e$ , the effective  $Q$  of the amplifier, is

$$Q_e = \frac{Q}{1 + \frac{\omega_0 L Q}{r_p} + \frac{\omega_0 L Q}{R_g}} \quad (10-11)$$

This is the equivalent  $Q$  of the resonance curve of the tuned amplifier and is the  $Q$  of the actual resonant circuit as modified by the shunting resistances  $R_g$  and  $r_p$ .

To find the gain of the amplifier when the input frequency and the resonant frequency of the tuned circuit are slightly different from each other, it is supposed that  $\omega \doteq \omega_0$ , whence  $\delta$  is small. Then, from Eq. (10-6), it follows that

$$Z_i = R_L Q^2 \frac{1 - j \frac{1}{Q}}{1 + 2j\delta Q} \doteq \frac{R_L Q^2}{1 + 2j\delta Q} \quad (10-12)$$

The corresponding value of the gain, given by Eq. (10-9), is

$$K = - \frac{g_m}{\frac{1}{r_p} + \frac{1}{R_g} + \frac{1 + 2j\delta Q}{R_L Q^2}} \quad (10-13)$$

The gain ratio  $K/K_{\text{res}}$  is then

$$\frac{K}{K_{\text{res}}} = \frac{1}{1 + j2\delta Q_e} \quad (10-14)$$

from which the amplitude ratio is

$$\left| \frac{K}{K_{\text{res}}} \right| = \frac{1}{\sqrt{1 + (2\delta Q_e)^2}} \quad (10-15)$$

A plot of these results is given in Fig. 10-3. This is essentially the "universal resonance" curve. Note from Eq. (10-15) that when

$$2\delta Q_e = 1$$

then

$$\left| \frac{K}{K_{\text{res}}} \right| = \frac{1}{\sqrt{2}}$$

But since the band width of the circuit is the frequency width between the 3-db power points,

$$B = 2(f_{3\text{db}} - f_0) = \frac{2(f - f_0)f_0}{f_0}$$

or

$$B = 2\delta f_0 = \frac{f_0}{Q_e} \quad (10-16)$$

In order that the voltage gain at resonance be large, the resonant impedance of the tuned circuit, and the grid resistor  $R_g$ , must be large compared with  $r_p$ . Note, however, from Eqs. (10-5) and (10-8) that an increase of  $Z_i$  at resonance by increasing the  $L/C$  ratio is accompanied by a decreased  $Q_e$ , with a corresponding increase of band width or decreased frequency selectivity. This is an undesirable condition if a narrow band

width is desired, but it is an important consideration in wide-band tuned amplifiers. Note also that if the circuit  $Q$  of the tuned circuit is increased at fixed values of  $\omega_0$  and  $L/C$  ratio, then the effective  $Q_e$  of the amplifier

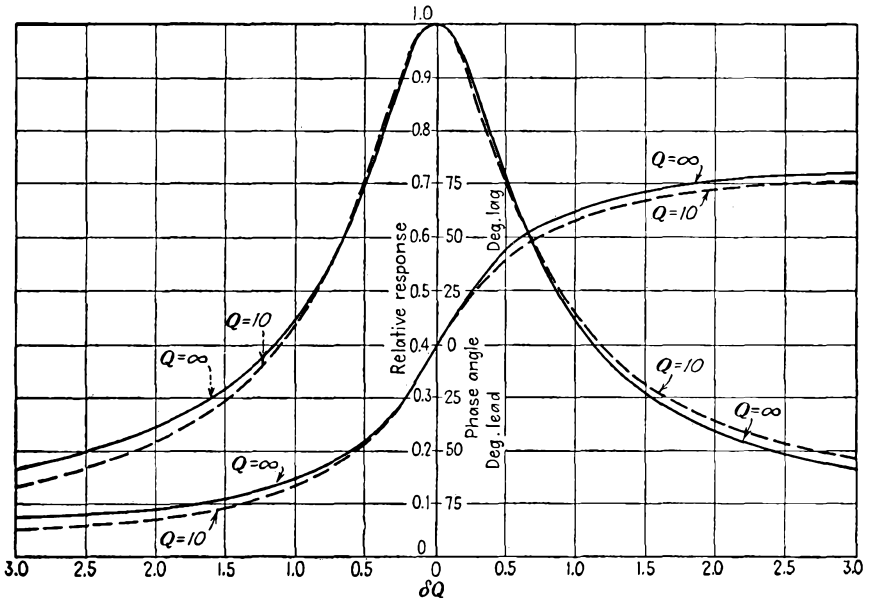


FIG. 10-3. Plots showing the amplitude  $K/K_{res}$  and phase of the output of the single-tuned direct-coupled amplifier. (From Terman, F. E., *Radio Engineering*, 3d ed., McGraw-Hill Book Company, Inc., New York, 1947.)

is increased, with a corresponding increase of frequency selectivity or decreased band width.

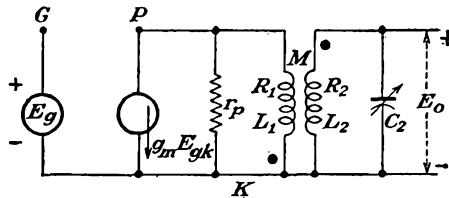


FIG. 10-4. The equivalent circuit of the single-tuned transformer-coupled voltage amplifier.

**10-2. Single-tuned Transformer-coupled Amplifier.** The general behavior of the single-tuned transformer-coupled amplifier is quite similar to that of the direct-coupled circuit. To examine the operation of the circuit in some detail, refer to Fig. 10-4, which gives the equivalent circuit of this amplifier. An approximate expression for the voltage gain of the amplifier is readily obtained. If it is noted that  $r_p$  is usually large

compared with  $R_1$  and  $L_1$ , then the voltage induced in the secondary of the transformer is given by

$$E_{\text{ind}} = j\omega M(g_m E_{gk}) = j\omega M(g_m E_g) \quad (10-17)$$

The output voltage, which is the potential across the capacitor  $C_2$ , is then seen to be

$$E_o = \frac{j\omega M(g_m E_g)}{R_2 + j\left(\omega L_2 - \frac{1}{\omega C_2}\right) + \frac{(\omega M)^2}{r_p}} \frac{1}{j\omega C_2} \quad (10-18)$$

where  $(\omega M)^2/r_p$  is the reflected impedance of the primary into the secondary circuit. The expression for the gain then becomes

$$K = \frac{E_o}{E_g} = \frac{\mu M/C_2}{r_p \left[ R_2 + j\left(\omega L_2 - \frac{1}{\omega C_2}\right) \right] + \omega^2 M^2} \quad (10-19)$$

The corresponding expression for the voltage gain at resonance is

$$K_{\text{res}} = \frac{\mu(M/C_2)}{r_p R_2 + \omega_0^2 M^2} \quad (10-20)$$

This result may also be expressed in terms of  $Q_2 = \omega_0 L_2/R_2 = 1/\omega_0 C_2 R_2$  and is

$$K_{\text{res}} = g_m \frac{\omega_0 M Q_2}{1 + (\omega_0^2 M^2/r_p R_2)} \quad (10-21)$$

which may be written as

$$K_{\text{res}} = g_m \omega_0 M Q_e \quad (10-22)$$

where the effective value  $Q_e$  is

$$Q_e = \frac{Q_2}{1 + (\omega_0^2 M^2/r_p R_2)} \quad (10-23)$$

A comparison of this expression with Eq. (10-10) shows that transformer coupling modifies the amplification by the ratio  $M/L$ . This provides a means for controlling the gain of the stage and still retaining the high  $Q$  required for selectivity. It might appear that there are no limits on the gain, and that it continues to increase with increasing values of  $M$ . This is not so, owing to the appearance of  $M$  in the denominator of Eq. (10-20). An optimum value of gain exists, and this occurs when  $M$  has the value required to make  $\partial K/\partial M = 0$ . This yields, for the optimum value of  $M$ ,

$$\frac{\partial K}{\partial M} = \frac{\mu/C_2}{r_p R_2 + \omega_0^2 M^2} - \frac{\frac{\mu M}{C_2} (2\omega_0^2 M)}{(r_p R_2 + \omega_0^2 M^2)^2} = 0$$

or

$$M_{\text{opt}} = \frac{\sqrt{r_p R_2}}{\omega_0} \quad (10-24)$$

Equation (10-21) becomes

$$\begin{aligned} K_{\text{res, opt}} &= g_m \frac{\sqrt{r_p R_2} Q_2}{2} \\ &= \frac{\mu Q_2}{2} \sqrt{\frac{R_2}{r_p}} \end{aligned} \quad (10-25)$$

To find the band width of the amplifier, consider the general expression for the gain given by Eq. (10-19). By writing, as before,

$$\left. \begin{aligned} \omega_0 &= \frac{1}{\sqrt{LC}} \\ \delta &= \frac{\omega}{\omega_0} - 1 \\ Q_2 &= \frac{\omega_0 L_2}{R_2} = \frac{1}{\omega_0 C_2 R_2} = \frac{1}{R_2} \sqrt{\frac{L_2}{C_2}} \end{aligned} \right\} \quad (10-26)$$

and noting that in the neighborhood of resonance

$$\begin{aligned} \omega L_2 - \frac{1}{\omega C_2} &= \sqrt{\frac{L_2}{C_2}} \left( \frac{\omega}{\omega_0} - \frac{\omega_0}{\omega} \right) \\ &\doteq 2\delta \sqrt{\frac{L_2}{C_2}} = 2\delta R_2 Q_2 \end{aligned} \quad (10-27)$$

Eq. (10-19) becomes

$$K = \frac{\mu M / C_2}{r_p R_2 \left( 1 + j \frac{1}{R_2} 2\delta \sqrt{\frac{L_2}{C_2}} \right) + \omega^2 M^2} \quad (10-28)$$

The gain ratio [Eqs. (10-28) to (10-20)] then becomes

$$\frac{K}{K_{\text{res}}} = \frac{1}{1 + j2\delta Q_e} \quad (10-29)$$

which has the same form as for the direct-coupled connection [Eq. (10-14)]. The band width of this amplifier is, following the same reasoning as that which led to Eq. (10-16),

$$B = \frac{f_0}{Q_e} \quad (10-30)$$

The optimum value of  $M$  is not of much importance, owing to practical limitations. This follows from Eq. (10-24), which shows that for pentodes, with the corresponding large values of  $r_p$ , the value of  $M$  would be large. In fact, to achieve these values of  $M$ , the distributed capacitances of the windings may become excessive, and the self-resonant frequency

may be so low as to make the coils useless. Owing to this, the mutual inductance is usually chosen far below the optimum value in the pentode amplifier.

**10-3. The Double-tuned Amplifier.** Both the single-tuned direct-coupled amplifier and the double-tuned amplifier are extensively used in radar, television, and communication receivers. For the i-f amplifiers of both a-m and f-m types, the double-tuned amplifier is commonly

used. This is so because such an amplifier can provide substantially constant amplification over a band of frequencies and the gain falls more sharply outside of this band than does the single-tuned stage.

To examine the operation of the circuit, refer to the equivalent circuit of this amplifier. This circuit can be further simplified by applying Thévenin's theorem to the portion of the circuit to the left of the points *aa*. The equivalent generator has the potential

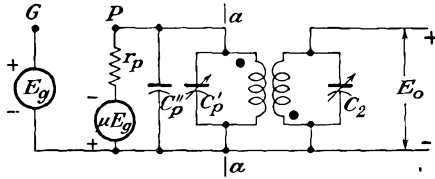


FIG. 10-5. The equivalent circuit of a double-tuned amplifier.

$$E = \frac{\mu E_g (1/j\omega C_1)}{r_p + (1/j\omega C_1)} \tag{10-31}$$

where  $C_1 = C'_p + C''_p$ . But since  $r_p > 1/\omega C_1$  for the pentode, then with good approximation

$$E \doteq \frac{\mu E_g}{j\omega r_p C_1} = \frac{g_m E_g}{j\omega C_1} \tag{10-32}$$

The internal impedance of the equivalent generator will have the value

$$Z = \frac{r_p (1/j\omega C_1)}{r_p + (1/j\omega C_1)}$$

which is, to the same approximation as above,

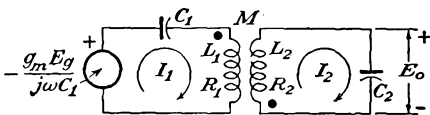


FIG. 10-6. The equivalent series form of Fig. 10-5.

$$Z \doteq \frac{1}{j\omega C_1} \tag{10-33}$$

Then the equivalent circuit of Fig. 10-5 reduces to the form of Fig. 10-6.

This circuit is analyzed by the standard methods of network analysis. Accordingly, if one writes

$$\left. \begin{aligned} E &= Z_{11}I_1 + Z_{12}I_2 \\ 0 &= Z_{12}I_1 + Z_{22}I_2 \end{aligned} \right\} \tag{10-34}$$

then the current in the secondary is

$$I_2 = - \frac{EZ_{12}}{Z_{11}Z_{22} - Z_{12}^2} \quad (10-35)$$

where

$$\left. \begin{aligned} Z_{11} &= R_1 + j \left( \omega L_1 - \frac{1}{\omega C_1} \right) \\ Z_{12} &= j\omega M \\ Z_{22} &= R_2 + j \left( \omega L_2 - \frac{1}{\omega C_2} \right) \end{aligned} \right\} \quad (10-36)$$

The gain of the amplifier becomes

$$K = \frac{E_0}{E_g} = \frac{(g_m/j\omega C_1)(1/j\omega C_2)j\omega M}{Z_{11}Z_{22} - Z_{12}^2} \quad (10-37)$$

But it must be noted that both circuits are tuned to the same resonant frequency. Thus

$$\left. \begin{aligned} \omega_0 &= \frac{1}{\sqrt{L_1 C_1}} = \frac{1}{\sqrt{L_2 C_2}} \\ Q_1 &= \frac{\omega_0 L_1}{R_1} = \frac{1}{\omega_0 C_1 R_1} \\ Q_2 &= \frac{\omega_0 L_2}{R_2} = \frac{1}{\omega_0 C_2 R_2^*} \\ a &= \frac{\omega_0 M}{\sqrt{R_1 R_2}} = k \sqrt{Q_1 Q_2} \end{aligned} \right\} \quad (10-38)$$

and write

Then, by Eq. (10-27),

$$\left. \begin{aligned} Z_{11} &= R_1 + j \left( \omega L_1 - \frac{1}{\omega C_1} \right) = R_1(1 + j2\delta Q_1) \\ \text{Similarly} \quad Z_{22} &= R_2(1 + j2\delta Q_2) \\ \text{and} \quad Z_{12} &= j\omega M \end{aligned} \right\} \quad (10-39)$$

The expression for the gain [Eq. (10-37)] then becomes for frequencies near resonance

$$\begin{aligned} K &= \frac{-jg_m(M/\omega_0 C_1 C_2)}{R_1 R_2 (1 + j2\delta Q_1)(1 + j2\delta Q_2) + \omega_0^2 M^2} \\ K &= \frac{-jg_m \frac{\omega_0 M}{\sqrt{R_1 R_2}} Q_1 Q_2 \sqrt{R_1 R_2}}{\left( 1 + \frac{\omega_0^2 M^2}{R_1 R_2} \right) + 2j\delta(Q_1 + Q_2) - 4\delta^2 Q_1 Q_2} \end{aligned}$$

\* If the amplifier is one of a chain, the loading effect of the following stage should be included in  $Q_2$ .

or finally

$$K = \frac{-jag_m Q_1 Q_2 \sqrt{R_1 R_2}}{1 + a^2 + j2\delta(Q_1 + Q_2) - 4\delta^2 Q_1 Q_2} \tag{10-40}$$

The gain at resonance is obtained by setting  $\delta = 0$  in this expression. There results

$$K_{res} = \frac{-jag_m Q_1 Q_2 \sqrt{R_1 R_2}}{1 + a^2} \tag{10-41}$$

The gain ratio at frequencies slightly different from resonance is given by

$$\frac{K}{K_{res}} = \frac{1}{\left(1 - \frac{4\delta^2 Q_1 Q_2}{1 + a^2}\right) + j \frac{2\delta(Q_1 + Q_2)}{1 + a^2}} \tag{10-42}$$

The exact shape of the response curve of the double-tuned system depends upon the parameter  $a$ , or, correspondingly, on  $k$ , the coefficient of coupling between the primary and secondary coils. The resonant gain

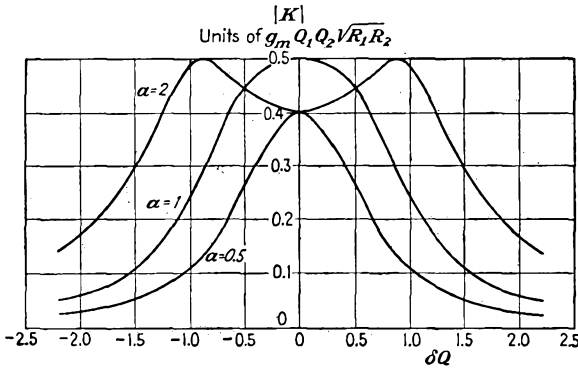


FIG. 10-7. The response characteristics of a double-tuned amplifier for various values of coupling.

is a maximum when  $a = 1$ , as may be verified by examining  $dK/da = 0$ . Moreover, if the primary and secondary  $Q$  values are the same and  $a = 1$ , the response curve has the maximum possible flatness in the vicinity of resonance. This is the condition for critical coupling  $k_c$ . A value of  $a$  greater than unity (overcoupling) results in double peaks, whereas a value of  $a$  less than unity (undercoupling) causes the response to be rounded on the top. If the circuit is considerably undercoupled, then the gain may be less than that at resonance. The situation discussed is illustrated graphically in Fig. 10-7.

An analytic expression for the positions of the peaks in the overcoupled circuit is readily possible. These are given, of course, by the values of

frequency at which Eq. (10-40) is a maximum. To find these values, it is noted that the gain is a maximum without regard to the phase. Thus the square of the absolute value of Eq. (10-40) is differentiated with respect to  $\delta$  and maximized. The results are

$$|K|^2 = (g_m Q_1 Q_2 \sqrt{R_1 R_2})^2 \frac{a^2}{(1 + a^2 - 4\delta^2 Q_1 Q_2)^2 + [2\delta(Q_1 + Q_2)]^2} \quad (10-43)$$

and the derivative  $\partial |K|^2 / \partial \delta = 0$  yields

$$1 + a^2 - 4\delta^2 Q_1 Q_2 = \frac{(Q_1 + Q_2)^2}{2Q_1 Q_2}$$

from which

$$\delta = \pm \frac{1}{2} \sqrt{k^2 + \frac{1}{Q_1 Q_2} - \frac{1}{2} \left( \frac{Q_1 + Q_2}{Q_1 Q_2} \right)^2}. \quad (10-44)$$

Frequently the circuits are designed with  $Q_1 = Q_2$ . Even if this condition is not true, ordinarily  $Q_1$  does not differ too markedly from  $Q_2$ , and it is possible to assume that

$$\sqrt{Q_1 Q_2} \doteq \frac{Q_1 + Q_2}{2}$$

Subject to this approximation, Eq. (10-44) becomes

$$\delta = \pm \frac{1}{2} \sqrt{k^2 - \frac{1}{Q_1 Q_2}} \quad (10-45)$$

which becomes, in the manner of representation of Fig. 10-7, simply

$$\delta \sqrt{Q_1 Q_2} = \pm \frac{1}{2} \sqrt{a^2 - 1} \quad (10-46)$$

The value of the gain at either peak  $K_{\max}$  is obtained by combining Eq. (10-46) with (10-40). The result is

$$K_{\max} = -j(g_m Q_1 Q_2 \sqrt{R_1 R_2}) \frac{a}{2(1 + j\sqrt{a^2 - 1})}$$

or

$$|K_{\max}| = \frac{1}{2}(g_m Q_1 Q_2 \sqrt{R_1 R_2}) \quad (10-47)$$

This shows that for the overcoupled case the maximum gain is the same as that for critical coupling  $a = 1$ , and at resonance  $\delta = 0$ .

The gain at the dip, or the frequency  $\omega_0$ , can be found readily by setting  $\delta = 0$  in Eq. (10-40). The result is

$$K_{\min} = -j(g_m Q_1 Q_2 \sqrt{R_1 R_2}) \frac{a}{1 + a^2}$$

or

$$|K_{\min}| = (g_m Q_1 Q_2 \sqrt{R_1 R_2}) \frac{a}{1 + a^2} \quad (10-48)$$

For the case where the primary and secondary  $Q$  values are not the same, the flattest selectivity curve may be shown to occur when

$$a^2 = \frac{1}{2} \left( \frac{Q_1}{Q_2} + \frac{Q_2}{Q_1} \right) \quad (10-49)$$

although the mid-band gain is not a maximum under these conditions. When Eq. (10-49) is satisfied, the circuit is said to be *transitionally* coupled. The transitional value of coupling coefficient is, by Eqs. (10-49) and (10-38),

$$k_t = \sqrt{\frac{1}{2} \left( \frac{1}{Q_1^2} + \frac{1}{Q_2^2} \right)} \quad (10-50)$$

For a coupling coefficient larger than this value, the selectivity curve divides into two peaks. For values less than this, the curve has a single peak.

It follows from Eqs. (10-46) and (10-47) that increased coupling increases the frequency separation of the two peaks, but does not change their amplitudes. If the coupling is very large, then the approximation made in Eq. (10-40) is no longer valid. The effect of the factor  $\omega/\omega_0$  in this equation is to increase the lower frequency maximum and decrease the higher frequency maximum.

It is interesting to compare the gain of the double-tuned circuit with a single-tuned circuit having the same  $Q$ . The gain of the two circuits at resonance are given by Eqs. (10-10), and (10-41) for optimum value of  $a$ , and are

Single-tuned direct-coupled:  $K_{res} = -g_m \omega_0 L Q_e$

Double tuned (with  $a = 1$  and identical coils):

$$K_{res} = -j0.5g_m Q^2 R = -j0.5g_m \omega_0 L Q$$

It is observed that for critical coupling the gains at resonance of the two amplifiers are identical if it is assumed that the tuning capacitance of the individual tuned circuit in the double-tuned circuit is one-half the tuning capacitance for the single-tuned case.

Despite the fact that the response characteristics are optimum under critical coupling conditions, the transformers in narrow-band double-tuned amplifiers are usually undercoupled slightly. This is done in order that the frequency alignment of the tuned circuits may be made easier, since, with undercoupled stages, each stage can be adjusted separately to give maximum response at the specified frequency. If overcoupled circuits exist, owing to the interactions between coils and the

resulting double peak, this alignment is more critical. The critical coupling case is likewise difficult to align.

The band width of the amplifier, under optimum conditions  $a = 1$  and with equal primary and secondary values of  $Q$ , is readily calculated. Under these conditions Eq. (10-42) becomes

$$\frac{K}{K_{\text{res}}} = \frac{1}{(1 - 2\delta^2 Q^2) + j2\delta Q} \quad (10-51)$$

and the magnitude becomes

$$\left| \frac{K}{K_{\text{res}}} \right| = \frac{1}{\sqrt{1 + 4\delta^4 Q^4}} \quad (10-52)$$

Since, by definition, the band width gives a measure of the frequency spread over which the gain remains within 3 db of the maximum value, then

$$4\delta^4 Q^4 = 1$$

from which it follows that the band width is

$$B = 2\delta f_0 = \sqrt{2} \frac{f_0}{Q} \quad (10-53)$$

A comparison of this result with Eq. (10-16) for the single-tuned stage shows that the 3-db band width of the double-tuned circuit is 1.414 times that of the single-tuned stage.

**10-4. Cascaded Tuned Amplifiers.** It is frequently necessary to incorporate more than one stage of amplification in a given amplifier. Although such a practice provides a higher gain, this higher gain is accompanied by a narrower band width than for the single stage. Analytic expressions for the effect of cascading identical amplifiers are readily possible.

Consider first  $n$  single-tuned stages in cascade. The gain of such an  $n$ -stage amplifier becomes, from Eq. (10-15),

$$\left| \frac{K}{K_{\text{res}}} \right|^n = \frac{1}{[1 + (2\delta Q_e)^2]^{\frac{n}{2}}} \quad (10-54)$$

To find the corresponding band width, it is noted that

$$[1 + (2\delta Q_e)^2]^{\frac{n}{2}} = \sqrt{2}$$

from which

$$1 + (2\delta Q_e)^2 = 2^{\frac{1}{n}}$$

so that

$$2\delta Q_e = \sqrt{2^{\frac{1}{n}} - 1}$$

But the band width is given by

$$B_{1n} = 2\delta f_0 = \frac{\sqrt{2^{\frac{1}{n}} - 1}}{Q_c/f_0} \quad (10-55)$$

This may be expressed in terms of the band width of the single stage  $B_1$ , in the form

$$B_{1n} = B_1 \sqrt{2^{\frac{1}{n}} - 1} \quad (10-56)$$

Table 10-1 gives the band-width reduction function  $\sqrt{2^{\frac{1}{n}} - 1}$ . It is seen, for example, that two stages in cascade have a band width that is

TABLE 10-1

THE SINGLE-TUNED-AMPLIFIER BAND-WIDTH REDUCTION FACTOR

$n$	$\sqrt{2^{\frac{1}{n}} - 1}$
1	1.0
2	0.643
3	0.510
4	0.435
5	0.387
6	0.350
7	0.323
8	0.301

only 0.64 times that of a single stage. To maintain a given band width, it is accordingly necessary that the  $Q$  of the individual stages be decreased as the number of stages is increased.

A corresponding expression is possible for the double-tuned amplifier. For such an  $n$ -stage amplifier, with critical coupling  $a = 1$  and equal primary and secondary values of  $Q$ , the relative gain becomes, from Eq. (10-52),

$$\left| \frac{K}{K_{res}} \right|^n = \frac{1}{(1 + 4\delta^4 Q^4)^{\frac{n}{2}}}$$

It follows from this that

$$\delta Q = \sqrt[4]{\frac{2^{\frac{1}{n}} - 1}{4}}$$

The band width of the  $n$ -stage amplifier then has the form

$$B_{2n} = 2\delta f_0 = 2 \sqrt[4]{\frac{2^{\frac{1}{n}} - 1}{4}} \frac{f_0}{Q}$$

which may be written in terms of one-stage band width as

$$B_{2n} = B_2 \sqrt[4]{2^{\frac{1}{n}} - 1} \quad (10-57)$$

The band-width reduction factor is tabulated in Table 10-2. For a two-stage double-tuned amplifier with the coils critically coupled, the band width is 0.802 times that of the single-stage amplifier. Note that

TABLE 10-2  
THE DOUBLE-TUNED-AMPLIFIER BAND-WIDTH REDUCTION FACTOR  
FOR  $a = 1$

$n$	$\sqrt[4]{\frac{1}{2^n} - 1}$
1	1.00
2	0.802
3	0.713
4	0.659
5	0.622
6	0.592
7	0.568
8	0.548

this reduction is considerably less than the corresponding reduction of the two-stage single-tuned amplifier. This arises from the fact that the amplification or selectivity curve of the double-tuned amplifier has steeper sides than that of the single-tuned circuit and with successive stages drops away less rapidly than for the single-tuned case. In particular, an ideal amplifier with a rectangular response curve would show no band-width reduction with the addition of successive stages.

**10-5. Gain-Band Width Product.** It is of interest to tabulate the gain at resonance of the three amplifier circuits that have been studied. These follow:

$$\begin{aligned} \text{Single-tuned direct-coupled:} & \quad K_{\text{res}} = -g_m \omega_0 L Q_e \\ \text{Single-tuned transformer-coupled:} & \quad K_{\text{res}} = g_m \omega_0 M Q_c \\ \text{Double-tuned:} & \quad K_{\text{res}} = -j0.5 g_m Q_1 Q_2 \sqrt{R_1 R_2} \end{aligned}$$

These expressions may be interpreted as showing that the gain in each case has the form

$$K_{\text{res}} = g_m |Z| \quad (10-58)$$

where  $g_m$  is the transconductance of the tube and  $|Z|$  is the effective impedance of the load. Moreover, the foregoing analyses for these amplifiers show that the band width in each case varies inversely with the effective  $Q$  of the tuned circuit. Clearly, therefore, the higher gains are accompanied by a decreasing band width. Consequently a specification of the impedance or the gain at resonance of the tuned circuit is not in itself a very good measure of the excellence of the amplifier.

It might appear that the product of the gain and the band width would be a significant quantity. Such is actually the case, and this product may be considered to represent the area under a perfect band-pass amplifier having a constant gain over the full band width. Consider first the

gain-band width product of the single-tuned direct-coupled amplifier. Combining Eq. (10-10) with (10-16), there results

$$K_{res}B = -g_m \omega_0 L Q_e \frac{f_0}{Q_e} = -g \frac{\omega_0^2 L}{2\pi}$$

which may be written in the form

$$K_{res}B = -\frac{g_m}{2\pi C} = -\frac{g_m}{2\pi(C_{in} + C_{out})} \quad (10-59)$$

Notice that this product is independent of the resonant frequency or of the band width and depends only on the transconductance of the tube and on the total tuning capacitance. If in an amplifier the tuning capacitance is determined by the tube capacitance, then the gain-band width product is a measure of the *merit* of the tube. What is desired is a large transconductance in proportion to the input plus output electrode capacitances. The 6AK5 and the 6AC7 tubes are both highly satisfactory in this respect, the 6AK5 being slightly better than the 6AC7. An average 6AK5 has a gain-band width product of approximately 55 megacycles/sec, an average 6AC7 having a corresponding value of 50 megacycles/sec when allowance is made for socket and wiring capacitance.

The gain-band width product of the double-tuned amplifier is found by combining Eq. (10-41) with (10-53) and is

$$\begin{aligned} K_{res}B &= -j \frac{g_m}{2} Q_1 Q_2 \sqrt{R_1 R_2} \sqrt{2} \frac{f_0}{\sqrt{Q_1 Q_2}} \\ &= -j \frac{1}{\sqrt{2}} g_m \sqrt{Q_1 Q_2 R_1 R_2} \frac{\omega_0}{2\pi} \\ &= -j \frac{g_m}{2\pi} \frac{1}{\sqrt{2} \sqrt{C_1 C_2}} \end{aligned} \quad (10-60)$$

This expression shows that the gain-band width product of the double-tuned amplifier is  $\sqrt{2}$  as great as that for single-tuned circuits. That is, by splitting the tube input and output capacitances by the use of the double-tuned circuit, there is an increase in the gain-band width product.

**10-6. Stagger Tuning.**<sup>1</sup> If it is desired to build a wide-band high-gain amplifier, one procedure is to use either single-tuned or double-tuned circuits which have been heavily loaded so as to increase the band width. The gain per stage is correspondingly reduced, by virtue of the constant gain-band width product. The use of a cascade chain will provide for the desired gain. For example, a particular amplifier comprising nine cascaded single-tuned stages, each of 6 megacycles/sec band width, has an over-all band width of 1.7 megacycles. A nine-cascaded double-tuned amplifier, each also of 6 megacycles band width, yields an over-all band

width of 3.2 megacycles. However, double-tuned stages are difficult to align and also are more sensitive to variations in tube capacitance and coil inductance than that of the single-tuned circuits.

A means is available for achieving large band width and other characteristics of double-tuned circuits by using single-tuned circuits. This consists in taking two single-tuned circuits of a certain band width and staggering their resonance peaks by an amount equal to their band width. The result will have a band width that is  $\sqrt{2}$  times as great as that of

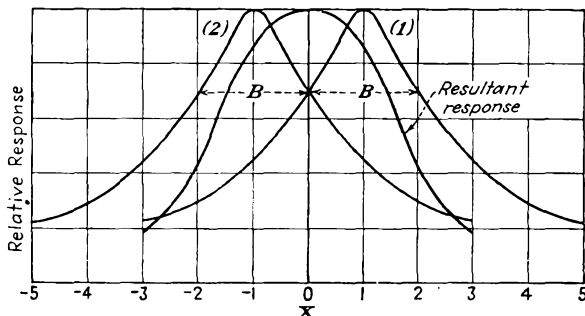


FIG. 10-8. The adjustments of frequency of a stagger-tuned pair.

each of the individual circuits; the over-all selectivity function will be identical with the corresponding single-stage double-tuned system. The general situation is illustrated in Fig. 10-8.

An analytic expression is readily obtained for the over-all characteristics of the stagger-tuned pair. If it is noted that the general selectivity function of the single-tuned direct-coupled circuit is, from Eq. (10-14),

$$\frac{K}{K_{\text{res}}} = \frac{1}{1 + j2\delta Q_e} = \frac{1}{1 + jx}$$

and the band width between the 3-db points is, from Eq. (10-16),

$$B = 2\delta f_0 = \frac{f_0}{Q_e}$$

then the corresponding selectivity functions of the two circuits are, respectively,

$$\left(\frac{K}{K_{\text{res}}}\right)_1 = \frac{1}{1 + j(x + 1)}$$

and

$$\left(\frac{K}{K_{\text{res}}}\right)_2 = \frac{1}{1 + j(x - 1)}$$

By multiplying the selectivity functions together, there results

$$\left(\frac{K}{K_{\text{res}}}\right)_1 \left(\frac{K}{K_{\text{res}}}\right)_2 = \frac{1}{2 - x^2 + j2x}$$

which becomes, on considering the magnitude of the resulting function,

$$\left| \frac{K}{K_{res}} \right|_1 \left| \frac{K}{K_{res}} \right|_2 = \frac{1}{\sqrt{4+x^4}} = \frac{1}{2} \frac{1}{\sqrt{1+4\delta_0^4 Q^4}} \quad (10-61)$$

where  $\delta_0$  is the value of  $\delta$  referred to the new frequency  $\omega_0$ , and where  $Q$  is the value of  $Q_e$  for each circuit referred to  $\omega_0$ . A comparison of this expression with Eq. (10-52) for the double-tuned circuit shows that the forms of the variation are identical.

A calculation shows that the gain-band width product of the stagger pair is 1.10 times that of two synchronously tuned stages. However, the stagger pair is smaller than two double tuned stages by the factor 1.60.

The principle of stagger tuning can be extended, and staggered triples are in fairly common use in radar receivers. In this case a centered single-tuned circuit of relative band width 2 and relative resonant gain  $\frac{1}{2}$  is combined with two single-tuned circuits, each of relative band width 1 and relative gain 1, staggered such that their resonance peaks are  $\pm \sqrt{3}/2$  from the band center. The resultant sensitivity function is of the form

$$\left| \frac{K}{K_{res}} \right| = \frac{1}{\sqrt{1+x^6}} \quad (10-62)$$

This sensitivity function has the same form as that for a triple-tuned circuit.

The advantage of stagger-tuned amplifiers, and the principle may be extended to  $n$ -uples, lies in the fact that simple single-tuned circuits are used throughout. This makes the alignment of the stages very easy, as they are independent of each other.

#### REFERENCES

1. Wallman, H., *M.I.T. Radiation Lab. Rept.* 524, Feb. 23, 1944.  
Wallman, H., *Electronics*, **21**, 100 (May, 1948).
2. As a general reference, consult Sturley, K. R., "Radio Receiver Design," Part I, John Wiley & Sons, Inc., New York, 1943.

#### PROBLEMS

✓ 10.1. A 6SJ7 pentode is used in a certain class A r-f amplifier, with  $E_{bb} = 250$  volts,  $E_{cc2} = 100$  volts, and  $E_{cc1} = -3$  volts. At these conditions the tube parameters are approximately  $g_m = 1,600 \mu\text{mhos}$ ,  $r_p = 1.2 \times 10^6$  ohms. A single-tuned load consists of a 1-mh coil in parallel with a 100- $\mu\text{mf}$  capacitor. The resonant  $Q$  of the load is 200.

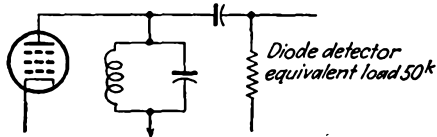
- a. Determine the voltage gain of the stage at the resonant frequency.
- b. Determine the voltage gain of the stage 10 kc above and below resonance.

10.2. In a single-tuned direct-coupled amplifier stage using a 6SJ7 tube that is tuned to 1,100 kc, it is found that the band width is 18 kc. Determine the  $Q$  of the circuit.

10-3. It is discussed in the text that the response of the single-tuned direct-coupled or transformer-coupled amplifier for small deviation  $\delta$  and high  $Q$  is given by either Eq. (10-14) or Eq. (10-29).

- a. Calculate the error in each case for  $Q = 3$ ,  $\delta$  very small.
- b. Repeat for  $Q$  large,  $\delta = 0.1$ .

10-4. A single-tuned circuit employing a 6SK7 tube feeds a diode detector.



The equivalent output circuit is illustrated. The tank is tuned to  $f_0 = 1$  megacycle,  $L = 0.5$  mh,  $Q = 60$ . Assume for the 6SK7 that  $r_p = 10^6$ ,  $g_m = 2,000$   $\mu$ mhos. Determine

- a. Gain at resonance.
- b. Gain at resonance if detector is removed.
- c. Band width with and without the detector circuit.

10-5. A direct-coupled single-tuned amplifier has a band width of 150 kc and a resonant shunt impedance of  $50^k$ . What must be the value of the shunting resistance across the tank if the gain is to be constant within 10 per cent over the 150-kc band?

10-6. A direct-coupled single-tuned amplifier has a band width of 50 kc, when  $C = 25$   $\mu$ mf. Calculate the band width if  $C$  is increased to 100  $\mu$ mf, and

- a. If the resonant frequency is kept constant.
- b. If  $L$  is maintained constant.

10-7. A single-tuned direct-coupled stage has a  $Q = 100$  when tuned to 800 kc. Two equal signals are fed to the grid, one of which is 50 cps off resonance and the other of which is 5,000 cps off resonance. What will the amplitude ratio be in the output of the amplifier?

10-8. A direct-coupled single-tuned amplifier is to have a band width of 200 kc at 4.7 megacycles. If the total capacitance is 25  $\mu$ mf,

- a. Calculate the maximum impedance and the value of  $L$ .
- b. Over what frequency band is the total phase shift through this amplifier less than 30 deg?

10-9. Repeat Prob. 10-8 for the transformer-coupled single-tuned amplifier, for optimum coupling.

10-10. A double-tuned circuit with  $C = 12$   $\mu$ mf has a band width of 1 megacycle at 10 megacycles for the critically coupled stage. Determine the value of  $L$  and  $Q$  if both primary and secondary windings are identical.

10-11. A single-stage double-tuned amplifier using a 6SK7 tube is critically

coupled. It operates at 455 kc and has a band width of 12 kc. The total primary  $C$  and total secondary  $C$  are each  $26 \mu\text{mf}$ . The coils and loading are the same.

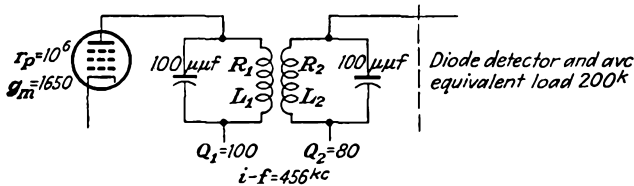
- a. Calculate the values of shunt resistance of each circuit,  $L$  and  $M$ .
- b. Calculate the mid-frequency gain. Choose  $g_m = 1,500 \mu\text{mhos}$ .

**10-12.** A 6SK7 double-tuned circuit comprises two identical  $200\text{-}\mu\text{h}$  coils, with  $Q = 80$ , which are tuned to 500 kc.

- a. Calculate the critical coefficient of coupling.
- b. Calculate and plot the gain of the stage as the mutual inductance is varied from zero to twice the critical value.

**10-13.** Determine the proper design for the winding of an i-f transformer with  $L_1 = L_2$  and each winding tuned to resonance by a capacitance of  $100 \mu\text{mf}$ . The secondary voltage is not to fall below 0.88 of the peak value in a 10-kc band, centered at 465 kc. Find  $k$ ,  $L_1$ ,  $L_2$ ,  $Q_1$ ,  $Q_2$  and the secondary voltage, with 1 volt, 465 kc to the primary. Assume critical coupling.

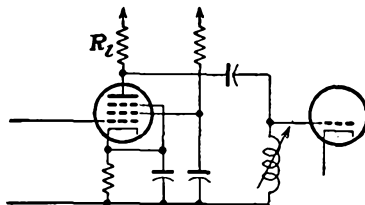
**10-14.** A 6SJ7 is used in a double-tuned circuit which feeds a diode detector and automatic-volume-control circuit. The significant portion of the circuit is shown.



The rms potential across the secondary feeding the detector-automatic-volume-control circuits must be 10 volts.

- a. What is the coefficient of coupling?
- b. What is the value of  $e_o$  to give the required output?

**10-15.** The i-f amplifier section in a radar receiver consists of four identical stages, each of the form illustrated. The maximum over-all gain of the four



stages is 10,000, and the gain at 28.5 and 31.5 megacycles is 7,070. 6AC7 tubes are used, with  $g_m = 9,000 \mu\text{mhos}$ ,  $C_i = 11 \mu\text{mf}$ ,  $C_o = 5 \mu\text{mf}$ .

- a. Calculate the value of the plate-load resistor.
- b. Calculate the wiring capacitance.
- c. Calculate the value of the inductance of the coil.

**10-16.** A six-stage single-tuned i-f amplifier using 6AC7 tubes has a maximum over-all gain of 4,100 and an over-all band width of 6.0 megacycles. If the over-all gain had to be obtained from four stages instead of six stages, what would have been the band width?

**10-17.** A six-stage single-tuned amplifier using 6AC7 tubes has a maximum over-all gain of 530,000 and an over-all band width of 2 megacycles.

- a. If it is found that the over-all band width need not be greater than 1.5 megacycles, what would be the corresponding over-all gain by an appropriate change in the value of the effective shunt resistance of each stage?
- b. If the original over-all gain of 530,000 had been obtained from four stages instead of six, calculate the over-all band width that would result.

**10-18.** Suppose that three identical stages having the characteristics of Prob. 10-2 are connected in cascade. Calculate and plot a curve of relative gain in decibels vs. frequency. Carry out the calculations to frequencies at which the gain is down at least 75 db below the optimum value.

**10-19.** A three-stage direct-coupled single-tuned amplifier is used in a broadcast receiver. A three-ganged 165- $\mu\text{mf}$  capacitor is used to tune the receiver over the range from 550 to 1,650 kc. The loading is chosen to give a minimum band width of 10 kc.

- a. Determine the variation of band width as the receiver is tuned over the entire range, assuming that  $Q$  remains constant.
- b. Repeat for the case where  $C$  is fixed at 100  $\mu\text{mf}$  and  $L$  is varied.

**10-20.** Refer to a tube manual, and prepare a table of the *merit* of the following tubes: 6AB7, 6AC7, 6AG7, 6AK5, 6C5, 6K7, 6L6, 6SF5, 6SJ7, 6SK7, 6V6, 6Y6.

**10-21.** A two-stage direct-coupled single-tuned amplifier using 6AC7 tubes operates at 60 megacycles, and is to have a 2-megacycle band width.

- a. What gain is possible if both stages are tuned to the same frequency? Assume that the shunt capacitance is 25  $\mu\text{mf}$ .
- b. If the stages are to be stagger-tuned to be critically flat, what gain is possible?

**10-22.** Show that, by choosing the three single-tuned stages in the manner discussed in the text to yield a staggered triple, the relative response function has the form given by Eq. (10-62). Sketch the individual response characteristics and that of the resultant staggered triple.

## CHAPTER 11

### TUNED POWER AMPLIFIERS

THE basic circuit of a tuned power amplifier is substantially that of the single-tuned direct-coupled type discussed in Sec. 10-1. The essential differences are in the magnitude of the grid-bias supply voltage  $E_{cc}$ , the corresponding value of the grid input signal  $e_g$ , and the amount of power involved. A schematic diagram of a tuned power amplifier is given in Fig. 11-1.

Owing to the negative bias on the tube, which is adjusted approximately to plate-current cutoff in the class B amplifier and which is adjusted beyond plate-current cutoff in the class C amplifier, harmonic currents are generated in the plate which are comparable in amplitude with the fundamental component. However, if the  $Q$  of the tuned plate circuit has a value of 10 or more, the impedance of the tank circuit to the second or higher harmonics will be very low. As a result, the higher harmonic potentials across the tank will be very small compared with the fundamental potential. That is, the effect of the harmonic generation in the tube plate current is largely suppressed by the tuned plate load.

But the requirement that the  $Q$  of the tank circuit must be high in order to suppress harmonics in the output imposes a limitation on the frequency-response characteristics of the amplifier, since the gain is constant over a very narrow band of frequencies. Consequently such amplifiers are confined in their operation to narrow frequency bands. In fact, the class B amplifier may be used to amplify a narrow band of frequencies of differing amplitudes, whereas the class C amplifier is confined to a narrow band of frequencies of constant amplitudes. Despite these severe restrictions, both classes of amplifier are extensively used in restricted applications, the class B amplifier to amplify an a-m r-f carrier wave, the class C amplifier as a frequency multiplier or as a source for the production of an a-m carrier wave.

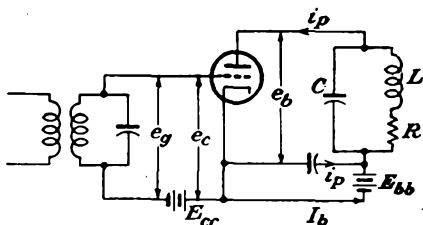


FIG. 11-1. Schematic diagram of a tuned power amplifier.

**11-1. Properties of the Tank Circuit.** The tuned plate load in the diagram of Fig. 11-1 is drawn as a simple parallel resonant circuit. Ordinarily the load is coupled inductively to the plate tank, and a more typical coupling network is that shown in Fig. 11-2. The capacitor  $C_2$

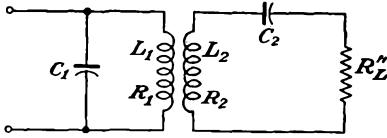


FIG. 11-2. A typical tuned-amplifier tank circuit.

is assumed to be so adjusted that  $1/2\pi \sqrt{L_2 C_2}$ , the resonant frequency of the secondary circuit, is equal to the operating frequency of the amplifier. Because of the resonance in the secondary circuit, only a resistive component  $R'_L = (\omega M)^2 / (R'_L + R_2)$

is reflected into the primary of the tuned circuit. The equivalent circuit then becomes that shown in Fig. 11-3.

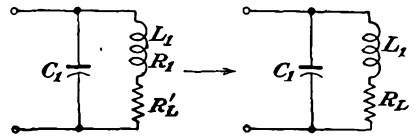


FIG. 11-3. The equivalent circuits of Fig. 11-2.

If the characteristics of the tank circuit were ideal, the impedance at resonance would be resistive and equal to the shunt resistance  $R_0$  of the resulting network. The impedance would be zero at any of the harmonic frequencies. That is, the impedance would be

$$\left. \begin{aligned} Z(\omega_0) &= R_0 \\ Z(n\omega_0) &= 0 \quad n = 2, 3, 4, \dots \end{aligned} \right\} \quad (11-1)$$

These ideal conditions do not prevail in practice, although it is possible to achieve relatively low impedance for  $Z(n\omega_0)$ . To examine this, refer to Eq. (10-6) for the impedance function of the simple tuned circuit.

$$Z = R_L Q^2 \frac{(1 + \delta) - j(1/Q)}{(1 + \delta) + jQ\delta(2 + \delta)} \quad (11-2)$$

At resonance  $\omega = \omega_0$ , and  $\delta = 0$ . Equation (11-2) reduces to

$$Z(\omega_0) = R_L Q^2 \left( 1 - j \frac{1}{Q} \right) = R_L Q^2 \sqrt{1 + \frac{1}{Q^2}} \angle \tan^{-1} \frac{1}{Q}$$

Note, however, that, if  $Q = 10$ , then

$$Z(\omega_0) = R_L Q^2 \times 1.005 \angle -5.7^\circ$$

which shows that the impedance of the tank circuit is essentially resistive and is given by

$$Z(\omega_0) = R_0 \doteq R_L Q^2 \quad (11-3)$$

Under these conditions it follows that

$$R_0 = R_L Q^2 = \omega_0 L_1 Q = \frac{L_1}{R_L C_1} = Q \sqrt{\frac{L_1}{C_1}} \tag{11-4}$$

Now consider the situation at the second-harmonic frequency. When  $\omega = 2\omega_0$ ,  $\delta = 1$  and Eq. (11-2) reduces to

$$Z(2\omega_0) = R_L Q^2 \frac{1 - j \frac{1}{2Q}}{1 + j 1.5Q} = R_L Q^2 \frac{0.25 - j \left( \frac{1}{2Q} + 1.5Q \right)}{1 + 2.25Q^2} \tag{11-5}$$

For  $Q = 10$  this reduces to

$$Z(2\omega_0) \doteq R_L Q^2 \frac{1}{j 1.5Q} = -j \frac{1}{1.5} \sqrt{\frac{L_1}{C_1}} \tag{11-6}$$

The ratio of the second harmonic to the fundamental frequency impedance is then

$$\left| \frac{Z(2\omega_0)}{Z(\omega_0)} \right| = \frac{R_L Q^2 (1/1.5Q)}{R_L Q^2} = \frac{1}{1.5Q}$$

In fact, under the extreme conditions when  $I_{p2} = I_{p1}$ , the relative power ratio is

$$\frac{P_{L1}}{P_{L2}} = \frac{I_{p1}^2 \Re Z(\omega_0)}{I_{p2}^2 \Re Z(2\omega_0)} = \frac{R_L Q^2 I_{p1}^2}{\left[ \frac{R_L Q^2 I_{p2}^2}{4(1 + 2.25Q^2)} \right]} = 4(1 + 2.25Q^2)$$

where  $\Re$  denotes "the real part of." With  $Q = 10$ , this reduces to

$$\frac{P_{L1}}{P_{L2}} = 900$$

Clearly, therefore, the second-harmonic power is negligible under these conditions.

Obviously, there will be losses in the tank circuit owing to the resistive component of the coils, and perhaps the capacitor. The power delivered to the effective load is

$$P'_L = (Q I_{p1})^2 \frac{(\omega M)^2}{R'_L + R_2} \frac{R'_L}{R'_L + R_2} \tag{11-7}$$

and the power lost in the tank circuit is

$$P_T = (Q I_{p1})^2 \left[ R_1 + \frac{(\omega M)^2}{R'_L + R_2} \frac{R_2}{R'_L + R_2} \right] \tag{11-8}$$

The circuit transfer efficiency, which is defined as the ratio of the power delivered to the load to that supplied to the tank circuit, is given by

$$\eta = \frac{P'_L}{P'_L + P'_T} \times 100\% = \frac{P'_L - P_T}{P'_L} \times 100\%$$

$$\eta = \frac{R_L - \left[ R_1 + \frac{(\omega M)^2 R_2}{(R'_L + R_2)^2} \right]}{R_L} \quad (11-9)$$

By defining a quantity  $Q_u$ , as in Eq. (11-10), and this is the  $Q$  of the circuit when the coupled load is removed, and writing the loaded  $Q$  of the circuit as  $Q_L$ , then

$$Q_u = \frac{\omega_0 L_1}{R_1 + \frac{(\omega M)^2 R_2}{(R'_L + R_2)^2}} \quad Q_L = \frac{\omega_0 L_1}{R_L} \quad (11-10)$$

and the transfer efficiency may be written in the form

$$\eta = \frac{(1/Q_L) - (1/Q_u)}{1/Q_L} = 1 - \frac{Q_L}{Q_u} \quad (11-11)$$

Thus, for high tank-circuit efficiency,  $Q_L$  should be low, and  $Q_u$  should be high. However, since  $Q_L$  must be 10 or greater in order to provide for a low harmonic content in the output, then it is important that the value of  $Q_u$  be high. The values of  $Q_u$  that are possible in practice will vary with the power output, the character of construction of the coil, and the frequency of operation. Typical values for coils of conventional design vary somewhat as follows for frequencies in the range from 500 to 1,500 kc:

$$Q_u \sim 100 \text{ to } 200 \quad \text{for low-power coils}$$

$$Q_u \sim 500 \text{ to } 800 \quad \text{for high-power coils.}$$

**11-2. Class B Tuned Amplifier.** Under class B operation, the grid-bias supply voltage  $E_{cc}$  in Fig. 11-1 is made negative by an amount

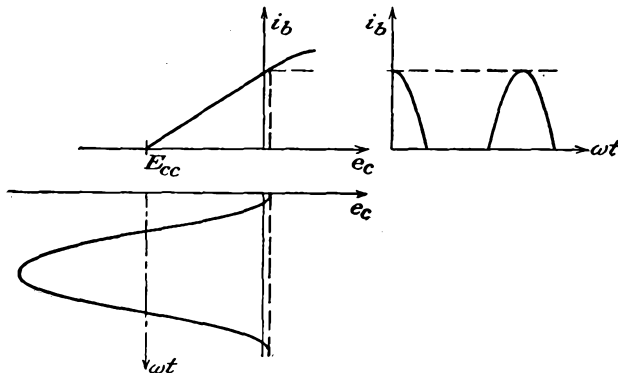


FIG. 11-4. The output wave shape from a class B stage, with a linear dynamic curve.

sufficient to reduce the plate current to zero for zero signal voltage  $e_g$ . If the dynamic characteristic of the amplifier is linear over the range of

operation, then for sinusoidal input signal voltage the current will consist of half-wave rectified pulses. The construction for deducing the output wave shape is sketched in Fig. 11-4.

It is important that it be recognized that Fig. 11-4 represents an idealized picture, which depends upon a linear dynamic curve. This is not completely true, although, in the analysis to follow, it will be assumed that the linear relation does apply. If the dynamic curve is not linear, then a graphical solution must be used in order to determine the shape of the plate-current curve and the linear class B analysis is not valid.

To find the operating path of an amplifier with a tuned load, a special construction is required, since the conditions are different from those of

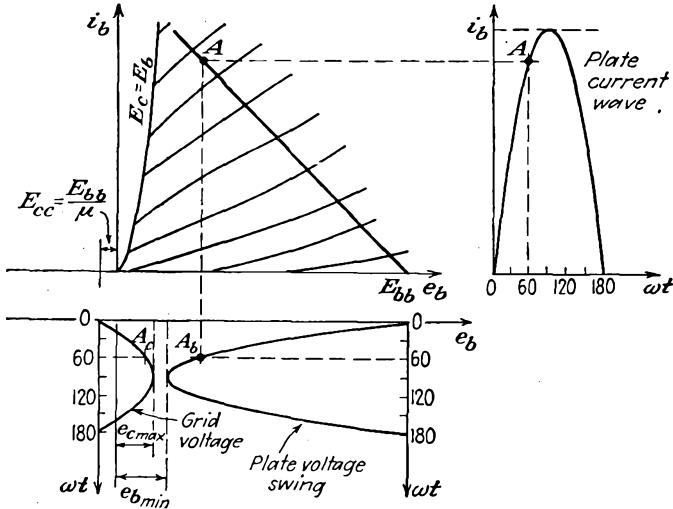


FIG. 11-5. The construction for determining the plate-current wave shape graphically from the plate characteristics.

an amplifier with a pure resistance load. This is so because of the interrelation of a number of factors and the different manner of operation of the circuit. Among the important factors that must be considered are the allowable plate dissipation of the tube, the  $Q$  of the circuit, the effective shunt resistance of the tank circuit, the grid driving potential, the shape of the plate-current wave, and the corresponding harmonic components in the plate current. Ordinarily a method of successive approximations is necessary, in which a given set of conditions is assumed and a calculation is made. If a consistent solution is not found, a second trial must be made. This procedure must be continued until a consistent solution is found.

Although the determination of the operating path is not essential for the linear analytical solution to follow, the method will be discussed here,

since it will permit a check on the validity of the linear assumptions. Moreover, it is a general method and will also be used later in the discussion of the tuned class C amplifier. The details of the construction are illustrated in Fig. 11-5.

To find the operating path, it is assumed that the plate-voltage swing is sinusoidal when the grid input signal is sinusoidal. Also, as a starting

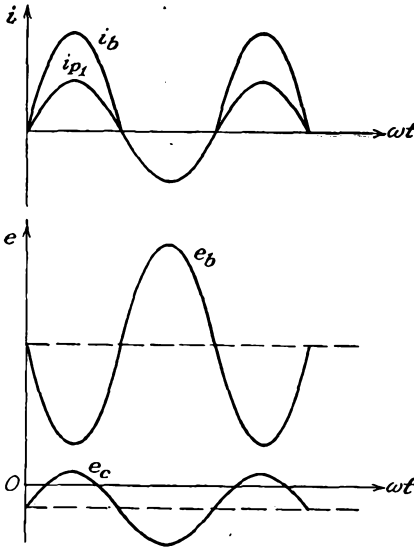


FIG. 11.6. The important wave shapes in a class B tuned amplifier.

point, it is assumed that  $e_{b\min}$  is approximately 10 per cent of  $E_{bb}$ . The value of  $e_{c\max}$  must not be allowed to reach an instantaneous positive potential that is higher than the plate potential  $e_{b\min}$ ; otherwise the current to the grid will increase very rapidly. This may cause serious damage to the tube. Even if no damage results, the increasing grid current is accompanied by a decreasing plate current, and in consequence the analysis will no longer be valid owing to the resulting nonlinearity of the dynamic curve. With this choice of conditions, the analysis can be completed, and a calculation can be made of the following: the d-c power from the plate-supply source, the

a-c power output to the load, and the plate dissipation. If the plate dissipation is within the rating of the tube, then the resulting calculations will indicate the adjustments of the circuit parameters that are necessary to achieve the indicated results.

The specific procedure is the following (refer to Fig. 11-5): Select any particular instantaneous grid potential  $e_c$ , such as that corresponding to the point  $A_c$ . Determine the corresponding instantaneous plate potential  $e_b$  by locating the point  $A_b$  at the same phase angle in the operating cycle. By projecting  $A_b$  up to its intersection with the curve for the selected grid potential, the point  $A$  on the operating path will be located. Other points are determined in a similar manner. For class B operation, the operating path should be approximately linear and should intersect the plate-voltage axis at  $E_{bb}$ , approximately.

To determine the shape of the plate-current pulse as a function of the phase angle, the current corresponding to each point  $A$  on the operating path is plotted as a function of the appropriate phase angle. The corresponding plate-current pulse is plotted in the above diagram.

The curves of Fig. 11-6 illustrate the important wave shapes of the amplifier.

**11-3. Analytic Solution of Tuned Class B Amplifier.**<sup>1</sup> An analytic solution of the tuned class B amplifier is based on finding an analytic form for the tube characteristics. From Eq. (2-10), the general relationship between the plate current and the plate and grid potentials is of the form

$$i_b = k \left( e_c + \frac{e_b}{\mu} \right)^\alpha \quad \left( e_c + \frac{e_b}{\mu} \right) > 0$$

Actually, it is found that for power triodes over a wide range of parameters the plate current is of the form

$$i_b = k \left( e_c + \frac{e_b}{\mu} \right)$$

which may be written in the more complete form

$$i_b = g_m \left( e_c + \frac{e_b}{\mu} \right) \quad (11-12)$$

This is, of course, simply the first term in the Taylor expansion for the current.

The instantaneous potentials are of the form

$$\left. \begin{aligned} e_c &= E_{cc} + E_{gm} \cos \omega t \\ e_b &= E_{bb} - E_{p1m} \cos \omega t \end{aligned} \right\} \quad (11-13)$$

But since the current is zero when the grid signal is zero, then, for  $i_b = 0$ ,

$$e_c + \frac{e_b}{\mu} = 0$$

which requires that

$$E_{cc} + \frac{E_{bb}}{\mu} = 0$$

or, for cutoff,

$$E_{cc} = - \frac{E_{bb}}{\mu} \quad (11-14)$$

By combining Eqs. (11-12) and (11-13), the expression for plate current becomes

$$\begin{aligned} i_b &= g_m \left( E_{cc} + E_{gm} \cos \omega t + \frac{E_{bb}}{\mu} - \frac{E_{p1m}}{\mu} \cos \omega t \right) \\ &= g_m \left( E_{gm} \cos \omega t - \frac{E_{p1m}}{\mu} \cos \omega t \right) \\ &= g_m \left( E_{gm} - \frac{E_{p1m}}{\mu} \right) \cos \omega t \end{aligned} \quad (11-15)$$

which is written in the form

$$\left. \begin{aligned} i_b &= I_{bm} \cos \omega t & -\frac{\pi}{2} < \omega t < \frac{\pi}{2} \\ i_b &= 0 & \frac{\pi}{2} < \omega t < \frac{3\pi}{2} \end{aligned} \right\} \quad (11-16)$$

where

$$I_{bm} = g_m \left( E_{gm} - \frac{E_{p1m}}{\mu} \right) \quad (11-17)$$

The average value of the plate current is

$$I_b = \frac{1}{2\pi} \int_0^{2\pi} i_b d(\omega t) \quad (11-18)$$

or

$$I_b = \frac{2}{2\pi} \int_0^{\frac{\pi}{2}} I_{bm} \cos \omega t d(\omega t) = \frac{I_{bm}}{\pi} \quad (11-19)$$

Also, by Fourier analysis, the amplitude of the fundamental component of the plate current is

$$I_{p1m} = \frac{1}{\pi} \int_0^{2\pi} i_b \cos \omega t d(\omega t) \quad (11-20)$$

or

$$I_{p1m} = \frac{2}{\pi} \int_0^{\frac{\pi}{2}} I_{bm} \cos^2 \omega t d(\omega t) = \frac{I_{bm}}{2} \quad (11-21)$$

But at resonance  $Z(\omega_0) = R_0$  is resistive, and the fundamental-frequency potential difference across the load is

$$E_{p1m} = I_{p1m} R_0 \quad (11-22)$$

Combining Eq. (11-22) with (11-21) and (11-17),

$$E_{p1m} = \frac{R_0 I_{bm}}{2} = \frac{R_0}{2} g_m \left( E_{gm} - \frac{E_{p1m}}{\mu} \right)$$

It follows from this that

$$E_{p1m} + \frac{R_0}{2} g_m \frac{E_{p1m}}{\mu} = \frac{R_0}{2} g_m E_{gm}$$

or

$$\boxed{E_{p1m} = R_0 \frac{\mu E_{gm}}{R_0 + 2r_p}} \quad (11-23)$$

which yields, for the rms value of the fundamental-frequency component of current, the expression

$$I_{p1} = \frac{\mu E_g}{2r_p + R_0} \quad (11-24)$$

Also, from Eqs. (11-21) and (11-24), and  $(11-19)$ ,  $I_{p1m} = \sqrt{2} I_{p1}$   $I_{p1} = \frac{I_{p1m}}{\sqrt{2}}$

$$I_b = \frac{I_{bm}}{\pi} = \frac{2\sqrt{2} I_{p1}}{\pi} = \frac{2\sqrt{2}}{\pi} \frac{\mu E_g}{2r_p + R_0} \quad (11-25)$$

The gain of the amplifier is given in Eq. (11-23) and is

$$K = - \frac{\mu R_0}{2r_p + R_0} \quad (11-26)$$

The d-c power input to the plate circuit, which is equal to the average power furnished by the plate supply when the d-c power dissipated in the plate load resistance is negligible, is given by

$$P_{bb} = \frac{1}{2\pi} \int_0^{2\pi} E_{bb} i_b d(\omega t)$$

This becomes

$$P_{bb} = E_{bb} \frac{1}{2\pi} \int_0^{2\pi} i_b d(\omega t) = E_{bb} I_b \quad (11-27)$$

The a-c power output of importance is that at the fundamental frequency and is given by

$$P_L = \frac{1}{2\pi} \int_0^{2\pi} e_L i_p d(\omega t)$$

which becomes

$$P_L = \frac{1}{2\pi} \int_0^{2\pi} E_{p1m} \cos \omega t I_{p1m} \cos \omega t d(\omega t)$$

$$\boxed{P_L = E_{p1} I_{p1} = I_{p1}^2 R_0} \quad (11-28)$$

The plate-circuit efficiency, which is the ratio of  $P_{ac}$  to  $P_{bb}$ , is

$$\eta_p = \frac{P_L}{P_{bb}} \times 100\% = \frac{E_{p1} I_{p1}}{E_{bb} I_b} \times 100\%$$

$$\eta_p = \frac{E_{p1} I_{p1}}{E_{bb} (2\sqrt{2}/\pi) I_{p1}} = \frac{\pi}{2\sqrt{2}} \frac{E_{p1}}{E_{bb}} = \frac{\pi}{4} \frac{E_{p1m}}{E_{bb}}$$

$$\eta_p = 78.5 \times \frac{E_{p1m}}{E_{bb}} \% \quad (11-29)$$

The plate dissipation is given by

$$P_p = \frac{1}{2\pi} \int_0^{2\pi} e_b i_b d(\omega t)$$

or

$$P_p = \frac{1}{2\pi} \int_0^{2\pi} (E_{bb} - e_L) i_b d(\omega t) = \boxed{E_{bb} I_b - P_L} \quad (11-30)$$

which becomes, by virtue of Eqs. (11-27) to (11-29),

$$\boxed{P_p = (1 - \eta_p) P_{bb}} \quad (11-31)$$

It is of some interest to calculate the results corresponding to the optimum conditions  $e_{c\max} = e_{b\min}$ . For this condition

$$\left. \begin{aligned} e_{c\max} &= E_{cc} + E_{gm} \\ e_{b\min} &= E_{bb} - E_{p1m} \end{aligned} \right\} \quad (11-32)$$

from which

$$E_{gm} + E_{p1m} = E_{bb} - E_{cc}$$

By Eqs. (11-14) and (11-23), this yields

$$E_{gm} + E_{gm} \frac{\mu R_0}{2r_p + R_0} = E_{bb} + \frac{E_{bb}}{\mu}$$

or

$$E_{gm} = E_{bb} \frac{\mu + 1}{\mu} \frac{2r_p + R_0}{2r_p + (\mu + 1)R_0} \quad (11-33)$$

The corresponding expressions for the fundamental-frequency component and the d-c components of current are, respectively,

$$I_{p1} = \frac{E_{bb}(\mu + 1)}{\sqrt{2}} \frac{1}{2r_p + (\mu + 1)R_0} \quad (11-34)$$

and

$$I_b = \frac{2}{\pi} E_{bb}(\mu + 1) \frac{1}{2r_p + (\mu + 1)R_0} \quad (11-35)$$

The corresponding values of the optimum  $P_{bb}$ ,  $P_{ac}$ , and  $\eta_p$  are readily calculated from these expressions for  $I_{p1}$  and  $I_b$ . The expression for the plate-circuit efficiency is found to be

$$\eta_p = \frac{I_{p1}^2 R_0}{E_{bb} I_b} = \frac{\left( \frac{E_{bb}(\mu + 1)}{\sqrt{2}} \frac{1}{2r_p + (\mu + 1)R_0} \right)^2 R_0}{\frac{2}{\pi} E_{bb}^2 (\mu + 1) \frac{1}{2r_p + (\mu + 1)R_0}}$$

which reduces to

$$\eta_p = 78.5 \times \frac{R_0(\mu + 1)}{2r_p + R_0(\mu + 1)} \quad \% \quad (11-36)$$

Ordinarily the plate dissipation is the limiting factor on the output power. The appropriate value of  $R_0$  is then specified, since all aspects of the circuit may be expressed in terms of it. To examine this, note that

$$P_p = E_{bb} I_b - I_{p1}^2 R_0$$

which may be written as

$$P_p = E_{bb}^2 \frac{2}{\pi} (\mu + 1) \frac{1}{2r_p + (\mu + 1)R_0} - \left( \frac{E_{bb}}{\sqrt{2}} (\mu + 1) \frac{1}{2r_p + (\mu + 1)R_0} \right)^2 R_0$$

This expression may be rearranged and yields the following quadratic

expression for  $R_0$ , from which  $R_0$  may be evaluated:

$$R_0^2 + \left[ \frac{4r_p}{\mu + 1} - \frac{E_{bb}^2}{P_p} \left( \frac{2}{\pi} - 1 \right) \right] R_0 + \left[ \frac{4r_p^2}{(\mu + 1)^2} - \frac{E_{bb}^2}{P_p} \frac{4r_p}{(\mu + 1)\pi} \right] = 0 \tag{11-37}$$

**11-4. Semigraphical Analysis of Class C Amplifiers.** An analysis of the operation of the tuned class C amplifier can be made on the basis of the assumption of a linear tube characteristic, essentially as an extension of the method of Sec. 11-3.<sup>2</sup> This analysis is considerably complicated by the fact that  $E_{cc}$  is no longer the single value chosen to yield a zero

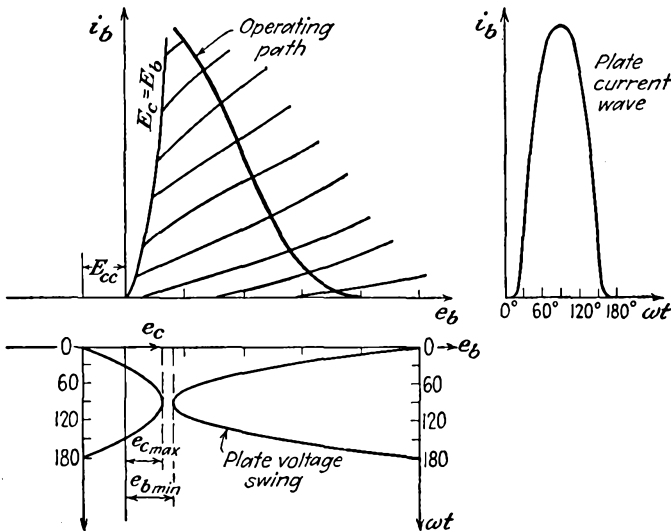


FIG. 11-7. The construction for determining the plate-current pulses in a class C amplifier.

current for zero excitation but is now a parameter. Moreover, it is no longer valid to assume that the operating characteristic is linear. Hence, although such a linear-tube-characteristic analysis is possible, it is a poor approximation. It does have the advantage over other methods of giving an explicit solution for the optimum operating conditions. Owing to its approximate nature, other methods are preferred.

To see that the operating path is not linear, the construction of Fig. 11-5 is again employed. The only differences that exist arise because the grid bias  $E_{cc}$  is adjusted beyond the cutoff value. With such values of  $E_{cc}$  and with the appropriately increased value of grid driving potential, the results have the form illustrated in Fig. 11-7. The curves of Fig. 11-8 illustrate the important wave shapes in such an amplifier.

A comparison of these curves with those of Fig. 11-6 indicates that in the class C amplifier the plate current consists of pulses, the duration of which is less than 180 deg of the cycle. Also, it is not possible, in general, to derive easily an analytic expression for the shape of the plate-current pulse.

In the case of class C operation there will be no output for small grid signals since the plate current is zero. Consequently the output voltage

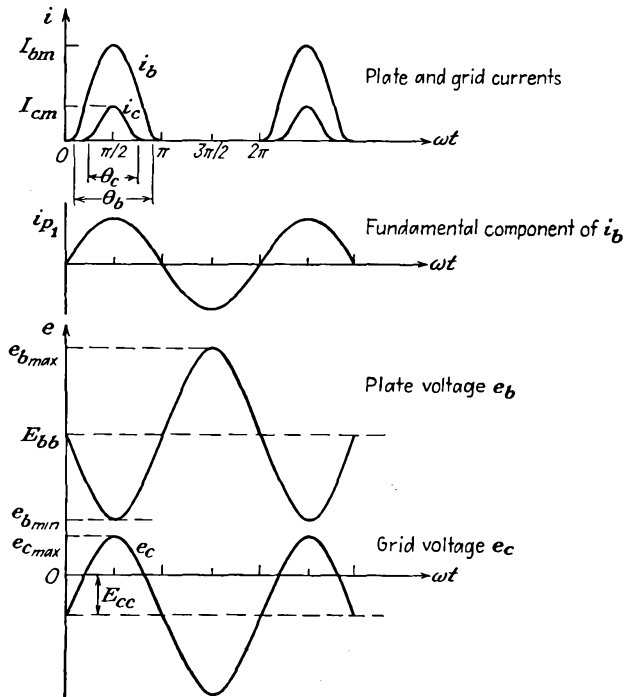


FIG. 11-8. The wave shapes at various points in the tuned amplifier.

is not proportional to the input voltage, and these amplifiers cannot be used where such a linear relation must be maintained. They are used extensively for amplifying a signal of fixed amplitude. They are also used extensively in radio communication as either low-level or high-level modulation stages. This latter application will be examined in detail in Chap. 15. When the amplifier is biased to class B operation, a linear relation between the output and input voltages does exist and such amplifiers find extensive use in those applications requiring this characteristic. The most important application is to increase the power level of a modulated carrier wave.

A second method of obtaining the operating path of a tuned power amplifier is possible. This makes use of the fact that the operating line

appears as a straight line on the constant-current ( $e_b, e_c$ ) characteristics of the tube. These constant-current tube characteristics are available for transmitting-type tubes and are provided for this particular purpose.

To verify that the dynamic characteristic is a straight line on the constant-current characteristics, use is made of Eqs. (11-13) for the grid and plate potentials, *viz.*,

$$\left. \begin{aligned} e_c &= E_{cc} + E_{gm} \cos \omega t \\ e_b &= E_{bb} - E_{p1m} \cos \omega t \end{aligned} \right\} \quad (11-38)$$

This latter expression is valid when the  $Q$  of the tank circuit is 10 or greater. Now combine these expressions by writing

$$\begin{aligned} \frac{e_c}{E_{gm}} &= \frac{E_{cc}}{E_{gm}} + \cos \omega t \\ \frac{e_b}{E_{p1m}} &= \frac{E_{bb}}{E_{p1m}} - \cos \omega t \end{aligned}$$

Adding these expressions gives

$$\frac{e_c}{E_{gm}} + \frac{e_b}{E_{p1m}} = \frac{E_{cc}}{E_{gm}} + \frac{E_{bb}}{E_{p1m}}$$

This may be written in the form

$$e_c = - \frac{E_{gm}}{E_{p1m}} e_b + \left( E_{cc} + \frac{E_{gm}}{E_{p1m}} E_{bb} \right) \quad (11-39)$$

which is the slope-intercept form of the equation of a straight line. The results are illustrated in Fig. 11-9.

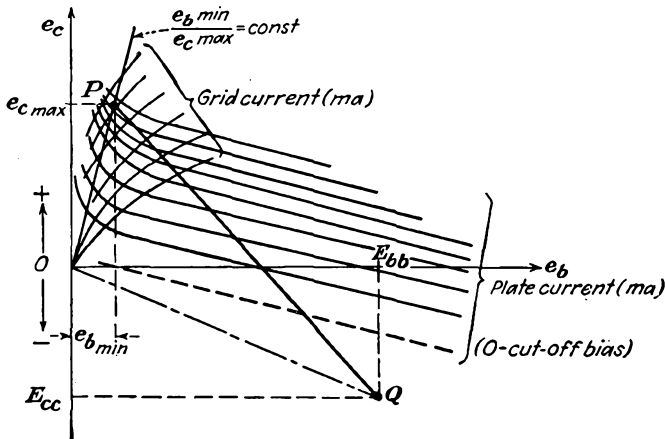


FIG. 11-9. The operating line on the constant-current curves of a power tube.

In order to establish the range of operation, it is necessary to specify the end points of the region of operation. Ordinarily this is done by

specifying  $E_{bb}$ ,  $e_{bmin}$ ,  $e_{cmax}$ , quantities which are determined from considerations of economy, power output desired, efficiency, and tube ratings. The manner of this dependence will be investigated below. With these factors specified, the operating characteristics of the amplifier are obtained from the curves in the manner illustrated in Fig. 11-10.

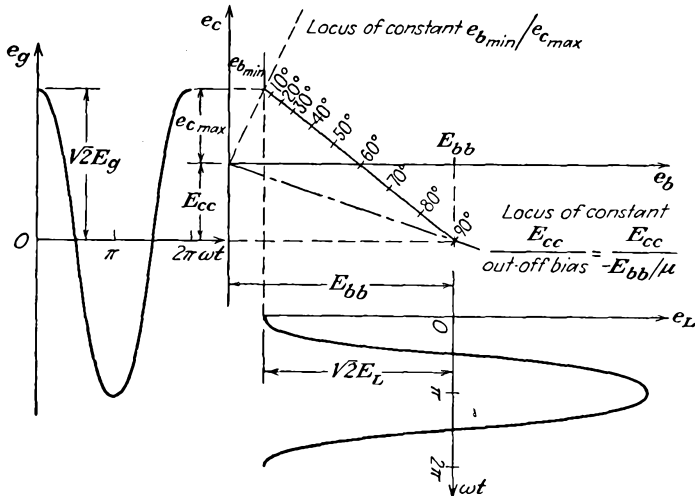


FIG. 11-10. The operating characteristics of a class C amplifier.

**11-5. Grid and Plate Currents in Class C Amplifiers.**<sup>3</sup> In order to obtain a numerical solution of the operational features of the amplifier, such as power output, efficiency, grid driving power, and plate dissipation, the average and rms values of the grid and plate currents are required. These must be deduced from the plate- and grid-current pulses as obtained from the curves, as discussed above. It is well to examine this matter before considering a detailed analysis of the amplifier operation.

An inspection of Figs. 11-7 and 11-8 shows that the plate- and grid-current pulses possess zero-axis symmetry. Consequently, these recurring waves may be represented by a Fourier series involving only cosine terms. In particular, the plate- and grid-current pulses may be represented analytically by series of the form

$$\left. \begin{aligned} i_b &= I_b + I_{p1m} \cos \omega t + I_{p2m} \cos 2\omega t + \dots \\ i_c &= I_c + I_{g1m} \cos \omega t + I_{g2m} \cos 2\omega t + \dots \end{aligned} \right\} \quad (11-40)$$

The average or d-c value of the plate current is given by the integral

$$I_b = \frac{1}{2\pi} \int_0^{2\pi} i_b d(\omega t)$$

which becomes, by virtue of the zero-axis symmetry and the fact that conduction proceeds over the angle  $\theta_b$ ,

$$I_b = \frac{1}{\pi} \int_0^{\frac{\theta_b}{2}} i_b d(\omega t) \tag{11-41}$$

This integral expresses the area under the plate-current pulse. Since, however, an analytic expression for the current pulse is not available, recourse is had to any of the available methods of numerical integration, *e.g.*, through the use of a planimeter; by dividing the base of the wave into equal parts, approximating the mean ordinates of the resulting rectangles,

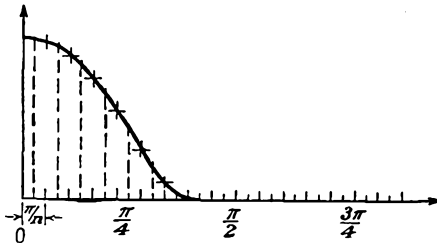


FIG. 11-11. Current wave form and its approximate representation.

and then summing the areas of these rectangles; or through the use of other methods devised for numerical integration.

The details of the second method are given. Suppose that Fig. 11-11 is the current wave form, certain features of which are to be examined. Suppose that the half recurrence period is divided into  $n$  equal parts; hence each division is  $\pi/n = 180/n$  deg long. Since the current flow will proceed for less than 90 deg in each half period, and taking account of the symmetry, the integral for  $I_b$  is then given with good approximation by the expression

$$I_b \doteq \frac{1}{n} \left[ \frac{i_b(O)}{2} + \sum_{k=1,2,3,\dots} i_b \left( \frac{k\pi}{n} \right) \right] \tag{11-42}$$

The average value of the grid current is found in a similar manner from the graph of the grid-current pulse. It is

$$I_c = \frac{1}{2\pi} \int_0^{2\pi} i_c d(\omega t)$$

which has the form

$$I_c = \frac{1}{\pi} \int_0^{\frac{\theta_c}{2}} i_c d(\omega t) \tag{11-43}$$

where  $\theta_c$  denotes the grid-current conduction angle. In terms of the

approximate calculation, this becomes

$$I_c \doteq \frac{1}{n} \left[ \frac{i_c(O)}{2} + \sum_{k=1,2,3,\dots} i_c \left( \frac{k\pi}{n} \right) \right] \quad (11-44)$$

The amplitude of the fundamental-harmonic component of the plate current is obtained from considerations of the general Fourier series representation of the current. This leads to the form

$$I_{p1m} = \frac{1}{\pi} \int_0^{2\pi} i_b \cos \omega t \, d(\omega t)$$

which may be written, in view of the existing symmetry, in the form

$$I_{p1m} = \frac{2}{\pi} \int_0^{\frac{\theta_b}{2}} i_b \cos \omega t \, d(\omega t) \quad (11-45)$$

This integral may be expressed as a summation by the approximate methods that have been employed above. This becomes

$$I_{p1m} \doteq \frac{2}{n} \left[ \frac{i_b(O) \cos O}{2} + \sum_k i_b \left( \frac{k\pi}{n} \right) \cos \frac{k\pi}{n} \right] \quad (11-46)$$

The amplitude of the fundamental-harmonic component of the grid current is obtained in the same way as the corresponding component of plate current. It is given by

$$I_{g1m} = \frac{1}{\pi} \int_0^{2\pi} i_c \cos \omega t \, d(\omega t)$$

which reduces to the form

$$I_{g1m} = \frac{2}{\pi} \int_0^{\frac{\theta_c}{2}} i_c \cos \omega t \, d(\omega t) \quad (11-47)$$

In general, the grid current flows for a relatively small portion of the cycle in the neighborhood of  $\theta_c = 0$ . But the value of  $\cos \omega t$  does not appreciably differ from unity during this interval. Then approximately

$$I_{g1m} \doteq \frac{2}{\pi} \int_0^{\frac{\theta_c}{2}} i_c \, d(\omega t)$$

from which it follows that

$$I_{g1m} \doteq 2I_c \quad (11-48)$$

In general, it is not necessary to plot the grid- and plate-current wave forms, since the information may be taken directly from the curve of Fig. 11-10 and combined in a table like Table 11-1 to yield the desired results.

TABLE 11-1  
ANALYSIS OF CLASS B AND CLASS C TUNED AMPLIFIER

Tube \_\_\_\_\_

$E_{bb}$ _____	$E_{cc}$ _____	$E_{om}$ _____	$e_{cmax}$ _____
$e_{bmin}$ _____	$e_{bmin}$ _____	$E_{p1m}$ _____	$i_{bmax}$ _____
$e_{cmax}$ _____	$n$ _____	$k$ _____	$\theta_b$ _____
$i_{cmax}$ _____	$i_b = l = \text{length of line } PQ$ _____		

1	k	0	1	2	3	4	5	6	7	8	9
2	$\theta_k$										
3	$\cos \theta_k$										
4	$l \cos \theta_k$										
5	$i_b(\theta_k)$										
6	$i_c(\theta_k)$										
7	$i_b(\theta_k) \cos \theta_k$										

$$\left\{ \begin{aligned} I_b &= \frac{1}{n} \left[ \frac{i_b(0)}{2} + \sum i_b \left( \frac{k\pi}{n} \right) \right] \\ I_c &= \frac{1}{n} \left[ \frac{i_c(0)}{2} + \sum i_c \left( \frac{k\pi}{n} \right) \right] \\ I_{p1m} &= \frac{2}{n} \left[ \frac{i_b(0) \cos 0}{2} + \sum i_b \left( \frac{k\pi}{n} \right) \cos \left( \frac{k\pi}{n} \right) \right] \end{aligned} \right.$$

**11-6. Power Considerations in Class C Amplifiers.** A number of the results are the same as those considered in Sec. 11-3 for the class B amplifier. Here too the d-c power input to the plate circuit, which is equal to the average power furnished by the plate supply when the d-c power dissipated in the plate load resistance is negligible, is given by

$$P_{bb} = \frac{1}{2\pi} \int_0^{2\pi} E_{bb} i_b d(\omega t) = E_{bb} I_b \tag{11-49}$$

The a-c power output of importance is that at the fundamental frequency and is given by

$$P_L = \frac{1}{2\pi} \int_0^{2\pi} e_L i_p d(\omega t) = \frac{1}{2\pi} \int_0^{2\pi} E_{p1m} \cos \omega t I_{p1m} \cos \omega t d(\omega t)$$

which is

$$P_L = \frac{E_{p1m} I_{p1m}}{2} = E_{p1} I_{p1} \tag{11-50}$$

The plate-circuit efficiency is

$$\eta_p = \frac{P_L}{P_{bb}} \times 100\% = \frac{E_{p1} I_{p1}}{E_{bb} I_b} \times 100\% \tag{11-51}$$

It might be noted that typical values for class C operation are  $\theta_b$  in the range 120 to 150 deg, with corresponding plate-circuit efficiencies approximately from  $\eta_p \sim 80$  to 60 per cent.

The power dissipated in the plate of the tube is given by

$$P_p = \frac{1}{2\pi} \int_0^{2\pi} e_b i_b d(\omega t) = \frac{1}{2\pi} \int_0^{2\pi} (E_{bb} - e_L) i_b d(\omega t)$$

which reduces to

$$P_p = E_{bb} I_b - E_{p1} I_{p1} = P_{bb} - P_L \quad (11-52)$$

By combining this with Eq. (11-51), there results

$$P_p = (1 - \eta_p) P_{bb} \quad (11-53)$$

This expression shows that the plate dissipation decreases as the output power increases, for a given plate power input.

The average grid power supplied by the driving source is given by

$$P_g = \frac{1}{2\pi} \int_0^{2\pi} e_g i_c d(\omega t)$$

This reduces, under the assumption that the grid potential is at its maximum value when the grid current flows and does not vary appreciably during this interval, to

$$P_g \doteq E_{gm} \frac{1}{2\pi} \int_0^{2\pi} i_c d(\omega t)$$

which is

$$P_g \doteq E_{gm} I_c \quad (11-54)$$

The results of Thomas<sup>4</sup> have shown that the grid driving power is given more accurately by the expression

$$P_g = 0.9 E_{gm} I_c \quad (11-55)$$

A somewhat better approximation is given by Maling,<sup>5</sup>

$$\left. \begin{aligned} P_g &= E_{gm} I_c \left( 0.85 + 0.16 \cos \frac{\theta_c}{2} \right) && \text{for triodes} \\ P_g &= E_{gm} I_c \left( 0.81 - 0.20 \cos \frac{\theta_c}{2} \right) && \text{for tetrodes and pentodes} \end{aligned} \right\} \quad (11-56)$$

The average grid dissipation is given by the expression

$$P_c = \frac{1}{2\pi} \int_0^{2\pi} e_c i_c d(\omega t)$$

This may be written as

$$\begin{aligned} P_c &= \frac{1}{2\pi} \int_0^{2\pi} (E_{cc} + e_g) i_c d(\omega t) \\ &= E_{cc} I_c + E_{gm} I_c \end{aligned} \quad (11-57)$$

but the first term gives a measure of the amount of power that the grid battery is absorbing from the input driving source, since

$$P_{cc} = \frac{1}{2\pi} \int_0^{2\pi} E_{cc} i_c d(\omega t) = E_{cc} I_c \tag{11-58}$$

and  $E_{cc}$  is inherently negative. Hence the power dissipated in the grid circuit is

$$P_c = P_g - |P_{cc}| \tag{11-59}$$

**Example:** In order to illustrate the calculations for a typical transmitting tube, consider the following specific problem: A type 806 triode having the constant-

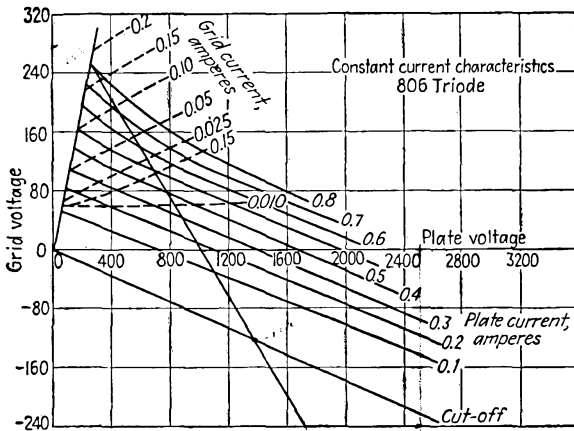


Fig. 11-12. Constant-current characteristics of an 806 triode.

current characteristics shown in Fig. 11-12 is used as a class C amplifier, under the following conditions:

$$\begin{aligned} E_{bt} &= 2,500 \text{ volts} & E_{cc} &= -500 \text{ volts} \\ \frac{e_{bmin}}{e_{cmax}} &= 1.0 & E_{gm} &= 755 \text{ volts} \end{aligned}$$

Determine the following:

- a. Power supplied by the plate power supply.
- b. A-c power output.
- c. Plate-circuit efficiency.
- d. Plate dissipation.
- e. Grid driving power.

(Note: The details of the solution are given in Table 11-2.)

**11-7. Design Considerations for Class C Amplifiers.** The analysis presented above is based on the assumption that the locus of the operating point of the tube characteristic is known. Frequently, however, the engineering design carries with it the requirement for the selection of the tube and the selection of the operating conditions that govern the locus to give a high plate-circuit efficiency, and other specified results. A num-

TABLE 11-2  
ANALYSIS OF CLASS C AMPLIFIER

Tube—806

$E_{bb} = 2,500$	$E_{cc} = -500$	$E_{\phi m} = 755$	$e_{cmax} = 255$
$\frac{e_{bmin}}{e_{cmax}} = 1.0$	$e_{bmin} = 255$	$E_{p1m} = 2,245$	$I_{bmax} = 825 \text{ ma}$
$I_{cmax} = 185 \text{ ma}$	$n = 18$	$k = 9$	$\theta_b = 120^\circ$

Length of line  $PQ = 27.8 \text{ cm}$

1	$k$	0	1	2	3	4	5	6	7	8	9
2	$\theta_k$	0	$10^\circ$	20	30	40	50	$60^\circ$	70	80	90
3	$\cos \theta_k$	1.0	0.985	0.94	0.86	0.76	0.64	0.50	0.34	0.17	0.00
4	$l \cos \theta_k$	27.8	27.4	26.1	24.1	21.3	17.9	13.9	9.5	4.8	0.0
5	$i_b(\theta_k)$	825	800	750	640	410	150	0	0	0	0
6	$i_c(\theta_k)$	185	170	120	55	12	0	0	0	0	0
7	$i_b(\theta_k) \cos \theta_k$	825	788	710	555	314	96	0	0	0	0

$$I_b = \frac{1}{18}(825 \frac{1}{2} + 2,750) = 176 \text{ ma}$$

$$I_c = \frac{1}{18}(185 \frac{1}{2} + 357) = 25 \text{ ma}$$

$$I_{p1m} = \frac{1}{9}(825 \frac{1}{2} + 2,463) = 319 \text{ ma}$$

$$P_{bb} = 2,500 \times 176 = 440 \text{ watts}$$

$$P_L = \frac{2,245 \times 319}{2} = 357 \text{ watts}$$

$$\eta = \frac{357}{440} \times 100\% = 81\%$$

$$P_p = (1 - 0.81) \times 440 = 83.5 \text{ watts}$$

$$P_o = 0.9 \times 755 \times 0.025 = 17 \text{ watts}$$

ber of factors are important in such a design, and it is desirable to examine the influence of these.

The important factors that are involved in the engineering design of a class C amplifier are the following:

1. The peak space current that should be demanded of a given tube. This is usually controlled by the values of  $e_{bmin}$  and  $e_{cmax}$ , since the total peak-space-current demand is given by

$$I_{smax} = I_{bmax} + I_{cmax} \\ = f(e_{bmin}, e_{cmax})$$

2. The minimum potential to which the plate falls,  $e_{bmin}$ .
3. The maximum value of the instantaneous grid potential,  $e_{cmax}$ .
4. The angle of plate-current flow,  $\theta_b$ .
5. The angle of grid-current flow,  $\theta_c$ .

6. The plate supply potential,  $E_{bb}$ .

The influence of each of these factors is considered in some detail.

*Item 1.* In so far as the total space current that may be safely drawn in a vacuum tube is concerned, it is limited by the allowable emission from the cathode, if saturation current may be drawn from the tube. Although it might not be too unreasonable to draw emission saturation current on the current peaks in a tube that is provided with a pure tungsten filament, it is unwise to drive a tube with either a thoriated-tungsten or an oxide-coated cathode to such extremes. Reasonable figures for the average emitter are

Tungsten filament— $I_{smax}$  approximately 100 per cent of total emission current.

Thoriated-tungsten— $I_{smax}$  from 15 to 35 per cent of the total emission current.

Oxide-coated cathode— $I_{smax}$  from 10 to 20 per cent of the total emission current.

*Items 2 and 3.* The optimum values of  $e_{bmin}$  and  $e_{cmax}$  will be such that the total allowable peak space current will not be exceeded. Moreover, their relative values must be so chosen that the maximum plate current occurs at  $\omega t = 0$ . This requires that the tube must not be driven so hard that it operates in the region of rapidly falling plate current. Such a condition is avoided by keeping  $e_{bmin} > e_{cmax}$ . However, high plate-circuit efficiency results when  $e_{bmin} = e_{cmax}$ , although for low grid driving power it is required that  $e_{bmin} > e_{cmax}$ . Typical values of the ratio  $e_{bmin}/e_{cmax}$  usually range from 1 to 2.

*Item 4.* The range over which plate conduction occurs, *i.e.*, the conduction angle  $\theta_b$ , influences both the average current  $I_b$  and the first-harmonic current amplitude  $I_{p1m}$ . For a large value of the first-harmonic current amplitude, it is desirable that  $\theta_b$  be made large. However, in order to provide a high value of plate-circuit efficiency, small values of  $\theta_b$  are indicated. Consequently, it is necessary to compromise between plate efficiency and power output. Typical values for class C operation, as already discussed, are  $\theta_b$  in the range from 120 to 150 deg, with corresponding plate efficiencies  $\eta$  from about 80 to 60 per cent.

With the choice of  $I_s$ ,  $e_{bmin}$ ,  $e_{cmax}$ , and  $\theta_b$  specified, the other operating conditions are established. It is desired, therefore, to examine the relation that expresses the grid bias,  $E_{cc}$ , and also the grid conduction angle  $\theta_c$ , in terms of the fixed parameters. To find an expression for  $E_{cc}$ , it is noted that the plate current becomes zero when  $\omega t = \theta_b/2$ . At this point, the grid signal is given by

$$e_g = E_{gm} \cos \omega t = E_{gm} \cos \frac{\theta_b}{2} \quad (11-60)$$

But at this point it is necessary that  $e_c + e_t/\mu = 0$ . This follows from the fact that the plate current may be written by an expression of the form  $i_b = f(e_c + e_b/\mu)$  and, for  $i_b$  to be zero,  $e_c + e_b/\mu$  must be zero. By virtue of this

$$\left( E_{gm} \cos \frac{\theta_b}{2} + E_{cc} \right) + \frac{1}{\mu} \left( E_{bb} - E_{p1m} \cos \frac{\theta_b}{2} \right) = 0$$

But since

$$\begin{aligned} e_{c\max} &= E_{gm} + E_{cc} \\ e_{b\min} &= E_{bb} - E_{p1m} \end{aligned}$$

it follows that

$$\left[ (e_{c\max} - E_{cc}) \cos \frac{\theta_b}{2} + E_{cc} \right] + \frac{1}{\mu} \left[ E_{bb} - (E_{bb} - e_{b\min}) \cos \frac{\theta_b}{2} \right] = 0$$

from which

$$E_{cc} = \frac{-E_{bb}}{\mu} + \left( e_{c\max} + \frac{e_{b\min}}{\mu} \right) \frac{\cos \frac{\theta_b}{2}}{\cos \frac{\theta_b}{2} - 1} \quad (11-61)$$

The angle of grid flow is readily determined, since the grid current becomes zero when  $\omega t = \theta_c/2$ . At this point

$$e_c = E_{gm} \cos \frac{\theta_c}{2} + E_{cc} = 0$$

from which it follows that

$$\cos \frac{\theta_c}{2} = - \frac{E_{cc}}{E_{gm}} \quad (11-62)$$

where  $E_{cc}$  is obtained from Eq. (11-61).

**11-8. Approximate Analytic Solution.**<sup>6</sup> The foregoing development permits an exact analysis of the performance of a class C amplifier. This analysis requires that the instantaneous plate and grid voltages and currents should be obtained and plotted and then from these curves should be derived such information as the plate loss, the power output, and the grid driving power. This method, while it possesses the virtue of yielding an exact solution, does have the disadvantage of being fairly laborious.

An approximate calculation of the performance can be obtained without recourse to the point-by-point analysis. This approximate calculation takes advantage of the fact that the total space current can be expressed quite accurately by an expression of the form

$$i_s = i_b + i_c = k \left( e_c + \frac{e_b}{\mu} \right)^\alpha \quad \text{for} \left( e_c + \frac{e_b}{\mu} \right) > 0 \quad (11-63)$$

The constant  $\alpha$  ordinarily lies in the range from 1 to  $\frac{3}{2}$ . The accuracy of the results that follow under this approximation will probably be well within the accuracy with which tube circuit conditions are known and within the reasonable variations of individual tubes from the average of the group.

Evidently, when the current is specified by this relationship, the pulses of current have a form that may be analytically expressed. However, the current pulses so specified are for the space current, and not for the plate current. Consequently the method yields information regarding the space-current pulses. By making reasonable assumptions, information is also obtained regarding the grid-current pulses. The difference between these two must then be the plate current. Since the grid current is ordinarily a small fraction of the total space current, then an error in the choice of the grid-current pulse will not introduce a very large error in the resulting plate current.

To examine the situation in some detail, use is made of the known relations for the grid and plate potentials [see Eqs. (11-13)], *viz.*,

$$\begin{aligned} e_c &= E_{cc} + E_{gm} \cos \omega t \\ e_b &= E_{bb} - E_{p1m} \cos \omega t \end{aligned}$$

with

$$\begin{aligned} E_{gm} &= e_{c\max} - E_{cc} \\ E_{p1m} &= E_{bb} - e_{b\min} \end{aligned}$$

Now within the limits of current flow, *i.e.*, within the limits from  $-\theta_b/2$  to  $\theta_b/2$ , the space current may be written in the form

$$i_s = k \left[ (e_{c\max} - E_{cc}) \cos \omega t + E_{cc} + \frac{E_{bb}}{\mu} - \frac{(E_{bb} - e_{b\min})}{\mu} \cos \omega t \right]^\alpha$$

which is

$$i_s = k \left[ \left( e_{c\max} + \frac{e_{b\min}}{\mu} \right) \cos \omega t + \left( E_{cc} + \frac{E_{bb}}{\mu} \right) (1 - \cos \omega t) \right]^\alpha \quad (11-64)$$

But the maximum value of this expression, which occurs when  $\cos \omega t = 1$ , is

$$I_{s\max} = k \left( e_{c\max} + \frac{e_{b\min}}{\mu} \right)^\alpha \quad (11-65)$$

Hence the ratio of the current at any instant to the maximum value is given by

$$\frac{i_s}{I_{s\max}} = \left[ \cos \omega t + \frac{E_{cc} + \frac{E_{bb}}{\mu}}{e_{c\max} + \frac{e_{b\min}}{\mu}} (1 - \cos \omega t) \right]^\alpha \quad (11-66)$$

But the value of the bias voltage to provide for a conduction angle  $\theta_b$  is given by Eq. (11-61). By combining Eqs. (11-61) and (11-66), the current ratio becomes

$$\frac{i_s}{I_{s\max}} = \left[ \cos \omega t + \frac{\cos \frac{\theta_b}{2}}{\cos \frac{\theta_b}{2} - 1} (1 - \cos \omega t) \right]^\alpha$$

which reduces to the form

$$\frac{i_s}{I_{s\max}} = \left( \frac{\cos \frac{\theta_b}{2} - \cos \omega t}{\cos \frac{\theta_b}{2} - 1} \right)^\alpha \quad (11-67)$$

This expression may be used to provide the average or d-c component of the space current and any of the harmonic-component values. In particular, the average or d-c component of the space current is given by the expression

$$\frac{I_s}{I_{s\max}} = \frac{1}{2\pi} \int_0^{2\pi} \left( \frac{i_s}{I_{s\max}} \right) d(\omega t)$$

which reduces to the form

$$\frac{I_s}{I_{s\max}} = \frac{1}{\pi} \int_0^{\frac{\theta_b}{2}} \left( \frac{\cos \frac{\theta_b}{2} - \cos \omega t}{\cos \frac{\theta_b}{2} - 1} \right)^\alpha d(\omega t) \quad (11-68)$$

- In a similar way, the fundamental component has the form

$$\frac{I_{s1m}}{I_{s\max}} = \frac{1}{\pi} \int_0^{2\pi} \left( \frac{i_s}{I_{s\max}} \right) \cos \omega t d(\omega t)$$

which may be written as

$$\frac{I_{s1m}}{I_{s\max}} = \frac{2}{\pi} \int_0^{\frac{\theta_b}{2}} \left( \frac{\cos \frac{\theta_b}{2} - \cos \omega t}{\cos \frac{\theta_b}{2} - 1} \right)^\alpha \cos \omega t d(\omega t) \quad (11-69)$$

These expressions, for given values of  $\alpha$ , are functions of  $\theta_b$ , and they may be conveniently expressed in graphical form. The curves of Fig. 11-13 give the relation of the d-c and fundamental-frequency components of the space-current pulse as a function of the angle of flow  $\theta_b$ , and the peak amplitude  $I_{s\max}$ .

To find the corresponding values of the plate current, the grid current

is approximated by assuming an analytic form for the equation of the grid current. As the grid current is usually a small part of the total space current, a reasonable choice for the grid current will provide good

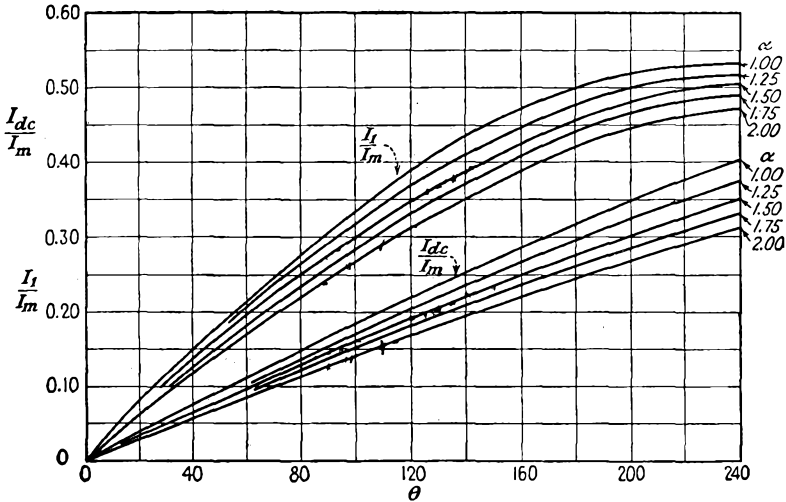


FIG. 11-13. Curves giving the relation of d-c and peak fundamental-frequency component of current as a function of the angle of current flow, and the peak amplitude.

results for the plate current. An expression that represents the grid current with good approximation is\*

$$i_c = k' \left( e_c + \frac{e_b}{\mu} \right)^\alpha \quad \text{for } e_c > 0 \tag{11-70}$$

Consequently, by following a parallel development to that above, there results

$$\frac{i_c}{I_{cmax}} = \left( \frac{\cos \frac{\theta_c}{2} - \cos \omega t}{\cos \frac{\theta_c}{2} - 1} \right)^\alpha \tag{11-71}$$

from which the d-c and fundamental-frequency components become

$$\frac{I_c}{I_{cmax}} = \frac{1}{\pi} \int_0^{\frac{\theta_c}{2}} \left( \frac{\cos \frac{\theta_c}{2} - \cos \omega t}{\cos \frac{\theta_c}{2} - 1} \right)^\alpha d(\omega t) \tag{11-72}$$

\* Maling finds that the exponent 2 is suitable for most triodes, and a value 1.4 seems suitable for most tetrodes and pentodes.

and

$$\frac{I_{c1m}}{I_{cmax}} = \frac{2}{\pi} \int_0^{\frac{\theta_c}{2}} \left( \frac{\cos \frac{\theta_c}{2} - \cos \omega t}{\cos \frac{\theta_c}{2} - 1} \right)^\alpha \cos \omega t d(\omega t) \quad (11-73)$$

These expressions are functions of  $\theta_c$  and have the same graphical form as the space-current components. Consequently the curves of Fig. 11-13 are also a valid representation of the grid-current components.

**Example:** To illustrate the methods of Sec. 11-8, the example on page 231 is repeated according to the methods of Sec. 11-8, and the corresponding results will be compared.

$$\text{Peak space current: } I_{sm} = I_{bmax} + I_{cmax} = 825 + 185 = 1,010 \text{ ma}$$

To find the grid current, choose  $\alpha = 2$ ; then

$$\frac{\theta_c}{2} = \cos^{-1} \frac{500}{755} = 48^\circ \quad \theta_c = 96^\circ$$

and from Fig. 11-13

$$\frac{I_c}{I_{cmax}} = 0.14 \quad \frac{I_{c1m}}{I_{cmax}} = 0.26$$

Hence the currents of importance are

$$\begin{aligned} I_c &= 0.14 \times 185 = 26 \text{ ma} \\ I_{c1m} &= 0.26 \times 185 = 48 \text{ ma} \end{aligned}$$

To find the plate current, the space current must be calculated. To do this, choose  $\alpha = \frac{3}{2}$ , and

$$\frac{\theta_b}{2} = \cos^{-1} \frac{378}{755} = 60^\circ \quad \theta_b = 120^\circ$$

Then, from Fig. 11-13,

$$\frac{I_s}{I_{smax}} = 0.19 \quad \frac{I_{s1m}}{I_{smax}} = 0.35$$

from which it follows that

$$\begin{aligned} I_s &= 0.19 \times 1,010 = 192 \text{ ma} \\ I_{s1m} &= 0.35 \times 1,010 = 353 \text{ ma} \end{aligned}$$

The plate-current components are then

$$\begin{aligned} I_b &= I_s - I_c = 192 - 26 = 166 \text{ ma} \\ I_{p1m} &= 353 - 48 = 305 \text{ ma} \end{aligned}$$

The significant quantities are

$$\begin{aligned} P_{bb} &= 2,500 \times 166 \times 10^{-3} = 415 \text{ watts} \\ P_L &= \frac{1}{2} \times 305 \times 10^{-3} (2,500 - 255) = 342 \text{ watts} \\ P_p &= 415 - 342 = 73 \text{ watts} \\ P_o &= 755 \times 0.26 \times 0.9 = 17.6 \text{ watts} \\ \eta_p &= \frac{342}{415} \times 100 = 82.3\% \end{aligned}$$

A more accurate calculation would require a logarithmic plot of Eq. (11-63) for the particular tube and a determination from this of the exponent  $\alpha$ . However, the use of the approximate methods would not be justified under these circumstances in general since the effort involved would be comparable with that in applying the methods of Sec. 11-5.

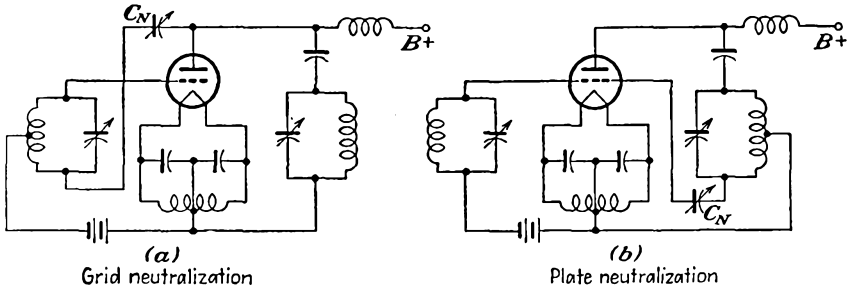


FIG. 11-14. Grid and plate neutralization of a single-ended amplifier.

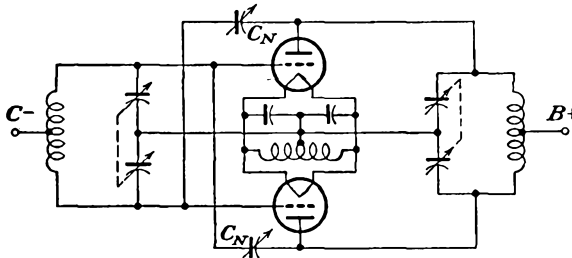


FIG. 11-15. Neutralization of a push-pull tuned amplifier.

**11-9. Neutralization.** When a triode is used as a power amplifier in the circuit of Fig. 11-1, some feedback between the grid circuit and the plate circuit exists through the interelectrode capacitance  $C_{gp}$ . This feedback is usually positive and tends to cause the stage to oscillate. It may be balanced out by one of several methods of *neutralization*. Tetrodes and pentodes usually do not require neutralization, as the capacitance  $C_{gp}$  is usually small enough in these tubes so that the amount of feedback is very small. The principle of neutralization is very simple and consists in providing feedback through external circuits in an amount equal to that through  $C_{gp}$ , but in opposite phase.

Two common methods of neutralization are illustrated in Figs. 11-14. The first is called *grid neutralization*, and the second is called *plate neutralization*. In Fig. 11-14a the plate is connected through the adjustable neutralizing capacitance  $C_n$  to a point in the grid circuit which has a potential of phase opposite to that of the grid. In Fig. 11-14b the grid is connected to a point in the plate circuit at which the potential is of opposite phase to that of the plate. The diagram of Fig. 11-15 shows the simple method of neutralizing a push-pull tuned amplifier.

## REFERENCES

1. Everitt, W. L., "Communication Engineering," 2d ed., pp. 582-590, McGraw-Hill Book Company, Inc., New York, 1937.
2. Everitt, W. L., "Communication Engineering," 2d ed., pp. 565-594, McGraw-Hill Book Company, Inc., New York, 1937.
3. M.I.T. Staff, "Applied Electronics," Chap. X, John Wiley & Sons, Inc., New York, 1943.  
Cruft Laboratory, War Training Staff, "Electronic Circuit and Tubes," Chap. XIV, McGraw-Hill Book Company, Inc., New York, 1947.  
Mourontseff, I. E., and H. N. Kozanowski, *Proc. IRE*, **23**, 752 (1935).
4. Thomas, H. P., *Proc. IRE*, **21**, 1134 (1933).
5. Maling, H. F., private communication.
6. Terman, F. E., and J. H. Ferns, *Proc. IRE*, **22**, 359 (1934).  
Terman, F. E., and W. C. Roake, *Proc. IRE*, **24**, 620 (1936).

## PROBLEMS

11-1. A type 800 tube is to be used in a tuned power amplifier. Find the operating curves for  $E_{bb} = 1,000$  and the following three conditions of grid characteristics:

$$\begin{array}{ll} E_{cc} = -55 \text{ volts} & E_{gm} = 170 \text{ volts peak} \\ = -95 & = 210 \\ = -135 & = 250 \end{array}$$

Would any of the indicated operating conditions yield class B operation? Choose  $e_{b\min} = e_{c\max}$ .

11-2. The type 800 tube is operated as an r-f power amplifier under class B conditions under the following conditions:

D-c plate voltage.....	1,000 volts
D-c grid voltage.....	-55 volts
Peak r-f grid voltage.....	170 volts
$\mu$ .....	15
$r_p$ .....	5,700 ohms

Calculate the following for  $e_{b\min} = 1.5e_{c\max}$ :

- a. Power output.
- b. Plate dissipation.
- c. Plate-circuit efficiency.
- d. The impedance of the tuned circuit at resonance.

11-3. A type 833A triode has the following maximum ratings for operation as a class B r-f amplifier.

D-c plate voltage.....	4,000 volts
D-c grid voltage.....	-120 volts
Peak r-f grid voltage.....	180 volts
Plate dissipation.....	400 watts
$\mu$ .....	35
$g_m$ .....	15,800 micromhos

It is planned to use this tube as a class B amplifier with a grid signal frequency of 16.0 mc, a plate supply of 4,000 volts, and a value of  $e_{b\min}/e_{c\max}$  equal to 2.0. Find the following:

- a. A-c power output.
- b. Current by the plate power supply.
- c. Plate dissipation.
- d. Plate efficiency.
- e. Impedance of tuned circuit at resonance.
- f. The values of  $L$  and  $C$  in the tuned circuit if the loaded resonant  $Q$  is 12.
- g. What value of  $R_0$  should be used if the maximum allowable plate dissipation is 400 watts and  $e_{b\min} = e_{c\max}$ ?

**11-4.** A class C amplifier uses an 851 tube and operates under the following conditions:

D-c plate voltage.....	2,500 volts
D-c grid voltage.....	-250 volts
Peak r-f grid voltage.....	450 volts
Plate dissipation.....	550 watts
Shunt resistance of tank circuit.....	1,550 ohms
D-c grid current.....	0.10 amp

Calculate the following:

- a. A-c plate potential.
- b. Output power.
- c. D-c plate current.
- d. Plate-circuit efficiency.
- e. Grid driving power.
- f. Grid dissipation

Assume that  $e_{b\min} = e_{c\max}$ .

**11-5.** A class C amplifier uses an 852 tube and operates under the following conditions:

D-c plate voltage.....	3,000 volts
D-c grid bias.....	-600 volts
Peak r-f signal.....	850 volts
D-c plate current.....	85 ma
D-c grid current.....	15 ma
Fundamental component of plate current.....	120 ma peak

Calculate the following, assuming  $e_{b\min} = e_{c\max}$ :

- a. Output power.
- b. Plate-circuit efficiency.
- c. Grid driving power.
- d. The amplifier is to operate at 1,500 kc. Specify the elements of the plate tank. Choose  $Q = 23$ .

11-6. The typical operating conditions for the type 893 A-R transmitting triode when used as a class C r-f power amplifier or oscillator are

D-c plate voltage.....	18,000 volts
D-c grid bias.....	-1,000 volts
Peak r-f grid signal.....	1,630 volts
D-c plate current.....	3.6 amp
D-c grid current.....	0.21 amp approx
Grid driving power.....	340 watts approx
Fundamental component of plate current.....	6.25 amp peak
Minimum value of plate voltage $e_{bmin}$ .....	1,000 volts

Calculate the following:

- Power output.
- The inductance required in the tank circuit. Assume that the effective  $Q$  of the tank circuit = 5, resonant frequency = 1 megacycle.
- The required capacity to tune to 1 megacycle.
- The circulating current in the tank circuit.
- The grid driving power. Compare this result with that shown in the tabulation above. Explain any discrepancy.
- The power input to the plate circuit.
- The plate-circuit efficiency.

11-7. A type 851 triode is used as a class C amplifier. The operating conditions are to be

D-c plate voltage.....	2,500 volts
D-c grid voltage.....	-250 volts
Peak r-f grid voltage.....	450
Ratio $e_{bmin}/e_{cmax}$ .....	1

Determine the following:

- D-c plate supply power.
- A-c output power.
- Plate circuit efficiency.
- Plate dissipation.
- Grid driving power.

11-8. Repeat Prob. 11-7 using the semigraphical method of Sec. 11-8.

11-9. A class C amplifier is operated under the following conditions:

D-c plate voltage.....	3,000 volts
D-c grid bias.....	-200 volts
Peak r-f grid voltage.....	360 volts
$e_{bmin}/e_{cmax}$ .....	2
Peak space current.....	2.2 amp
Conduction angle.....	120 deg
Ratio:	
D-c grid current to peak space current.....	0.15
D-c plate current to peak space current.....	0.21

Peak plate a-c current to peak space current.....	0.37
Frequency.....	2 megacycles
Loaded $Q$ .....	12

Calculate the following:

- |                                      |                                     |
|--------------------------------------|-------------------------------------|
| <i>a.</i> D-c plate current.         | <i>e.</i> Grid driving power.       |
| <i>b.</i> Plate-circuit power input. | <i>f.</i> Load impedance.           |
| <i>c.</i> Plate dissipation.         | <i>g.</i> Tank-circuit inductance.  |
| <i>d.</i> Plate efficiency.          | <i>h.</i> Tank-circuit capacitance. |

**11-10.** Show the general character of the construction (like Fig. 11-7) for determining the operating features of a class C frequency doubler. In this circuit the output tank is tuned to a frequency that is twice the frequency of the grid driving source. What can be said about the plate conduction angle?

---

## CHAPTER 12

### OSCILLATORS

THE effects of feedback in amplifiers were examined in Secs. 5-6 and 5-8. It is there shown that positive feedback is to be avoided in an amplifier if stability is to be achieved. On the other hand, if the circuit is provided with a sufficient amount of regenerative feedback, the vacuum-tube circuit will serve as a generator of periodically varying waves. This output may be sinusoidal, with a high degree of purity of wave form; it may be an essentially square wave, hence being of high harmonic content; or it may be of periodically recurring, though nonsinusoidal, shape.

A large variety of feed-back circuits which differ considerably in detail are available for the production of self-sustained oscillations. These possess certain features which are common to all. In each case a feed-back circuit exists through which is fed back into the input circuit a certain fraction of the output and in such a phase and of such an amplitude that self-excitation results. In the usual class of tube, the feedback from the output to the input circuit is accomplished externally to the tube itself by means of coupling networks. In certain special types of tubes, *e.g.*, a klystron of the reflex type and a magnetron of the running-wave type, the feedback is accomplished through the electron beam itself. Nevertheless even these can be represented by equivalent circuits which have features that are common to all feed-back oscillators.

Conventional self-excited oscillators ordinarily operate as class C devices, although class A oscillators are possible and will be discussed below. It is desirable to consider the class C oscillator first before examining the operating features of the class A type. However, it is important to keep clearly in mind the fact that the theory of class C oscillators is of necessity only an approximate one owing to the nonlinear character of the region of operation of such devices. Therefore, this theory, while contributing materially to an understanding of the operation of the device, must be recognized as a limited solution of the oscillator problem. But by supplementing the theory with practical design and operating data a generally satisfactory understanding is possible.

**12-1. Conditions for Self-excitation.**<sup>1</sup> To ascertain the conditions that must be fulfilled for oscillations to be sustained in a vacuum-tube circuit, refer to Fig. 12-1. In Fig. 12-1*a*, the circuit is supposed to be

open at the point *A*, as shown. If a voltage  $E_{\theta k}$  is impressed on the grid of the vacuum tube without regard to the source of this potential, then the output current is given by  $g_m E_{\theta k}$  for an assumed linear operation of the circuit. Now because of the current  $I_p$  to the input of the coupling network a certain voltage will appear across the output terminals of this coupling network. If this voltage is equal in magnitude and phase to the

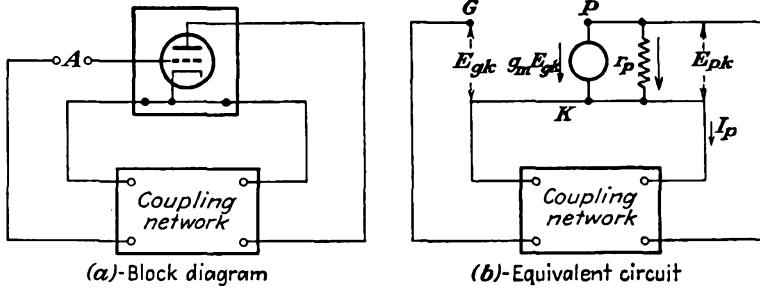


FIG. 12-1. A vacuum-tube circuit with coupling between the output and input circuits.

original voltage  $E_{\theta k}$ , the circuit may be connected at the point *A* and the system will continue to operate.

The transfer impedance of the coupling network is denoted by  $Z_T$  and is defined as the ratio of the output potential to the input current. From the diagram of Fig. 12-1*b*, this is seen to be  $Z_T = E_{\theta k}/I_p$ . Consequently for oscillations to occur it is necessary that

$$\left(g_m E_{\theta k} + \frac{E_{pk}}{r_p}\right) Z_T = E_{k\theta} = -E_{\theta k}$$

or

$$g_m Z_T \left(E_{\theta k} + \frac{E_{pk}}{\mu}\right) = E_{k\theta} = -E_{\theta k}$$

But since the output voltage of the vacuum tube is related to the input voltage by the gain,

$$E_{pk} = K E_{\theta k}$$

and

$$g_m Z_T E_{\theta k} \left(1 + \frac{K}{\mu}\right) = -E_{\theta k}$$

Therefore, for oscillations to be sustained, it is necessary that

$$g_m Z_T \left(1 + \frac{K}{\mu}\right) = -1 \tag{12-1}$$

It should be noted that both the transfer impedance  $Z_T$  and the driving-point impedance of the coupling network  $Z$  are involved in this expression,

the latter impedance appearing in the expression for the gain. Equation (12-1) may be considered as one form of the Barkhausen criterion for oscillations.

A parallel expression for the conditions for sustained oscillations involving only the impedance  $Z$  is readily possible. Thus, noting that the voltage  $E_{kp}$  is given by  $I_p Z$ ,

$$\left( g_m E_{gk} + \frac{E_{pk}}{r_p} \right) Z = E_{kp} = -E_{pk}$$

This becomes

$$\left( g_m E_{gk} + \frac{K E_{gk} g_m}{\mu} \right) Z = -K E_{gk}$$

or

$$g_m Z \left( \frac{1}{K} + \frac{1}{\mu} \right) = -1 \quad (12-2)$$

which may be written in the form

$$\left( \frac{1}{g_m Z} + \frac{1}{\mu} \right) = -\frac{1}{K} \quad (12-3)$$

This is another form of the Barkhausen criterion for oscillations.

Also, if it is noted that the ratio  $E_{gk}/E_{pk}$  is a measure of the fraction of the output voltage that is fed back into the input circuit through the coupling network, and denoting this ratio as  $\beta$ ,

$$\left( \frac{1}{g_m Z} + \frac{1}{\mu} \right) = -\beta \quad (12-4)$$

Note that the feed-back ratio of the network is related to the gain of the amplifier circuit by the simple expression

$$\beta K = 1 \quad (12-5)$$

This condition for oscillation was discussed in Sec. 5-8.

**12-2. Influence of Transconductance  $g_m$ .** The criteria for oscillation given in Eqs. (12-1), (12-3), and (12-4) are valid only for the linear region of the tube characteristics, since it is only for this region that the current-source equivalent circuit is valid. Despite this limitation, the expressions may be extended with significant results over the nonlinear portion of the tube characteristics.

Refer first to Eq. (12-1). Note that the ratio  $K/\mu$  is given in terms of circuit elements external to the tube, and these elements are independent of the voltage and current magnitudes. Clearly,  $g_m$  is the only factor in the expression that might vary and hence must be examined critically. Likewise, in Eqs. (12-3) and (12-4), if it is assumed that  $\mu$  remains sub-

stantially constant over wide excursions of signal amplitude (and this is a reasonable assumption), and since  $K$  involves  $\mu$  and  $r_p$ , or  $g_m$ , then here too  $g_m$  is the only factor that must be examined critically.

The transconductance  $g_m$ , which is the slope of the  $e_c$ - $i_b$  curve, is not constant for large changes of input grid voltage. In fact, it is precisely this variable character of  $g_m$  which accounts for the successful operation of oscillators. For a given set of circuit parameters, the oscillations will build up until the value assumed by  $g_m$  is such that the conditional equations [Eqs. (12-1), (12-3) and (12-4)] are satisfied, when sustained oscillations will result. If  $g_m$  cannot assume a sufficiently large value for these equations to be satisfied, then the voltage fed back from the output to the input circuit is insufficient for maintaining the oscillations and they will die out. If  $g_m$  were too large, the voltage fed back would be greater than that required for the oscillations just to be sustained and the amplitude would continue to increase.

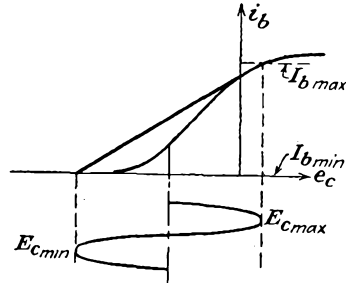


FIG. 12-2. Sketch for defining the average transconductance  $\overline{g_m}$ .

If the average transconductance  $\overline{g_m}$  is defined as the slope of the line connecting the two extreme points on the transfer characteristic appropriate to the input signal, as illustrated in Fig. 12-2,

$$\overline{g_m} = \frac{I_{bmax} - I_{bmin}}{E_{cmax} - E_{cmin}} \tag{12-6}$$

The Barkhausen criteria for sustained oscillations in modified form become

$$\left. \begin{aligned} & -\overline{g_m} Z_T \left( 1 + \frac{K}{\mu} \right) \\ & -\frac{1}{\beta} \left( \frac{1}{\overline{g_m} Z} + \frac{1}{\mu} \right) \\ & -K \left( \frac{1}{\overline{g_m} Z} + \frac{1}{\mu} \right) \end{aligned} \right\} \left\{ \begin{aligned} & < 1, \text{ decaying oscillations} \\ & = 1, \text{ sustained oscillations} \\ & > 1, \text{ growing oscillations} \end{aligned} \right\} \tag{12-7}$$

**12-3. Amplitude and Frequency Conditions.** Since in Eqs. (12-7) the quantities  $K$ ,  $Z$ , and  $Z_T$  are complex in general, the conditions for self-sustained oscillations requires that both the real and the imaginary parts of the expressions separately and simultaneously satisfy the appropriate conditions. Refer specifically to the third equation of (12-7). Here the conditions to be satisfied are

$$\left. \begin{aligned} \Re \left( \frac{1}{g_m Z} + \frac{1}{\mu} \right) &= \Re \left( \frac{1}{K} \right) \\ \Im \left( \frac{1}{g_m Z} + \frac{1}{\mu} \right) &= \Im \left( \frac{1}{K} \right) \end{aligned} \right\} \quad (12-8)$$

where  $\Re$  and  $\Im$  denote the real and imaginary parts, respectively, or the equivalent pair of expressions

$$\left. \begin{aligned} \left| \frac{1}{g_m Z} + \frac{1}{\mu} \right| &= \left| \frac{1}{K} \right| \\ \angle \left( \frac{1}{g_m Z} + \frac{1}{\mu} \right) &= \angle \frac{1}{K} \end{aligned} \right\} \quad (12-9)$$

The first of the two sets of conditions contains a great deal of information concerning the amplitude of the oscillations and specifies, in fact, a value of  $\overline{g_m}$  and in consequence determines the amplitude of the oscillations. The second of the two sets of conditions contains information about the frequency of oscillation.

An examination of the first of Eqs. (12-9) reveals the following general information: Since  $\mu$  appears in the denominator, then for large  $\mu$  there is an almost 1:1 correspondence between  $\overline{g_m}$  and  $K$ . Since, however,  $\overline{g_m}$  will vary over a range from zero to some finite value, then any condition that makes  $Z$  large (and  $K$  therefore reaches a constant value) would permit most easily the production of sustained oscillations. That is, sustained oscillations are favored by circuits for which  $Z > r_p$ . Note also that Eq. (12-5) is very sensitive to the angle of  $K$ . Thus since the angle characteristic of an antiresonant circuit is very sensitive to frequency near resonance, an oscillator with an antiresonant circuit permits sustained oscillations with good frequency stability.

**12-4. Fixed Bias and Starting Characteristics.** Before examining particular types of oscillator circuits, it is well to examine the effect of the grid bias on the operating features of the feed-back circuit. In particular, suppose that the bias of the circuit, as indicated in Fig. 12-2, is set to a value beyond the cutoff value of the tube. A number of possible operating conditions are illustrated in Fig. 12-3. Evidently the initial value of  $\overline{g_m} = \overline{g_{m1}}$  is zero, and Eqs. (12-7) show that oscillations cannot build up since the circuit conditions correspond to decaying oscillations.

Suppose that a voltage  $e_{\theta 2}$  is applied, whether from an external source or produced by a transient phenomenon. If the mean value of  $\overline{g_{m2}}$  is small, the conditions required by Eqs. (12-7) for sustained oscillations may still not be satisfied and the oscillations may die out. If the signal, say  $e_{\theta 3}$ , appears on the grid and if this is sufficiently large for oscillations to grow, the amplitude of  $e_{\theta 3}$  will increase until the conditions for sustained oscillations are fulfilled.

Clearly, for an oscillator biased near to or beyond cutoff, the circuit will not be self-starting. However, as is evident by comparing the results illustrated in Fig. 12-3 with those in Fig. 12-2, the amplitude of the oscillations is larger in the heavily biased oscillator. This results in an increased efficiency, a feature that may be very desirable in a power

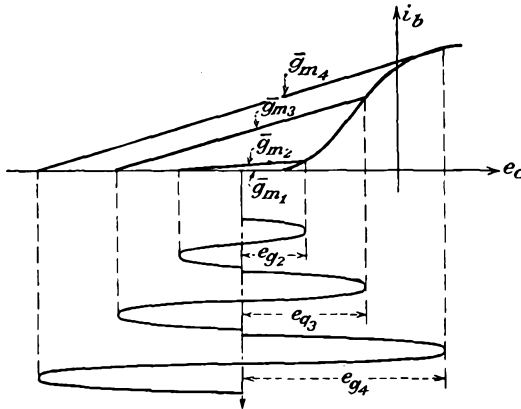


FIG. 12-3. A feed-back oscillator biased to the left of cutoff, and the corresponding secants for determining the average transconductance.

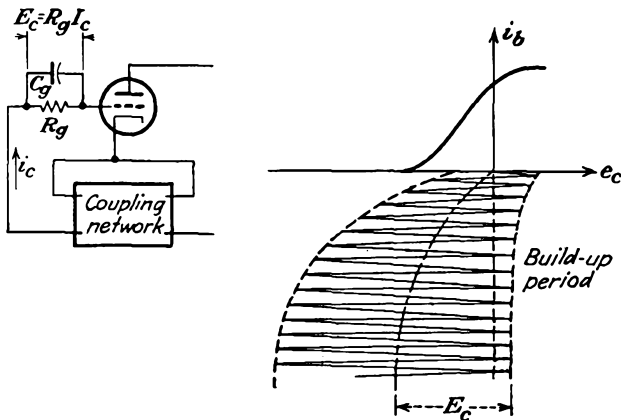


FIG. 12-4. An oscillator with grid resistor and grid-capacitor biasing. The build-up conditions are sketched.

oscillator although it is of small consequence in low-power sources. Also, since it is usually quite easy to induce oscillations, the overbiased condition is not objectionable from this point of view.

**12-5. Grid-resistor-Grid-capacitor Biasing Circuits.** The use of a grid-resistor and grid-capacitor combination, as illustrated in Fig. 12-4, not only allows the self-starting feature but also provides for an operating bias at or beyond cutoff. The operation of the circuit is illustrated in

Fig. 12-4, and is essentially the following: When the circuit is first placed in operation, the grid bias is zero, and the operating point is high on the characteristic, where the value of  $g_m$  is large. The third of the criteria [Eq. (12-7)] applies, and growing oscillations occur and continue to increase in amplitude. On the positive portion of the swing, the grid potential becomes positive, thus charging the capacitor. The time constant of the grid resistor and capacitor is such that a substantially steady bias is maintained. This bias displaces the operating point to the left, as illustrated, with consequent increasing amplitude of oscillations. The amplitude of the oscillations continues to increase until an equilibrium condition is reached between this amplitude and the consequent bias  $E_c$ . The magnitude of the bias may be controlled to any value between zero and  $E_c$  by the proper choice of  $R_g$  and  $C_g$ . The values of  $R_g$  and  $C_g$  are not critical, and they are generally determined experimentally.

As illustrated, the amplitude of oscillation will be such as to allow a small grid current to flow during the positive peaks of the cycle. It is this small grid current which serves to charge the grid capacitor. In fact, the variation in grid current can be used as an indication that oscillations have been established and also as a rough indication of the amplitude.

If the time constant  $R_g C_g$  is too large, the bias voltage across  $C_g$  adjusts itself slowly to sudden changes in the amplitude of oscillation. If this rate of adjustment is so slow that the oscillations can die out before the bias voltage can change appreciably, then with sudden changes in the amplitude the action is very much as though fixed bias were used. As a

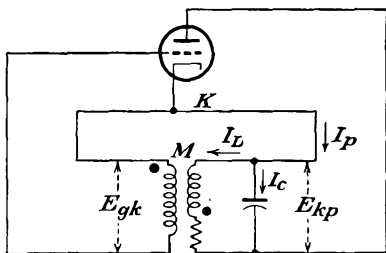


FIG. 12-5. Tuned-plate oscillator.

result, it is possible that the oscillations will die out. Hence a possible condition is one in which the oscillations first build up in amplitude to the equilibrium value. Any slight irregularity that tends to reduce the amplitude of the oscillations will cause the oscillations to die out owing to the substantially steady bias that exists.

Once the grid capacitor discharges through the grid resistor and the bias reduces sufficiently, the oscillations will again build up, until the above process repeats itself. This intermittent operation can be overcome by decreasing the time constant  $R_g C_g$ . For stability to exist, it is necessary that the bias reduce as the amplitude of oscillations decreases.

**12-6. Tuned-plate Oscillator.** The tuned-plate oscillator is one in which an antiresonant circuit is connected directly in the plate circuit

of the vacuum tube, the grid excitation being supplied by inductive coupling to this plate circuit. The complete circuit has the form illustrated in Fig. 12-5. It should be specifically noted that this is just the circuit of a tuned class C amplifier, but with the circuit providing its own grid excitation. Consequently the analyses of Chap. 11 of the tuned class C amplifier apply for the tuned plate oscillator except that the grid driving power reduces the total available power output.

In order to examine certain of the properties of the oscillator the conditional equation for sustained oscillations [Eq. (12-7)] will be examined. For simplicity, it will be assumed that the grid current may be neglected. The grid excitation is then simply

$$E_{gk} = j\omega M I_L \equiv Z_M I_L$$

The transfer impedance is given by the relation

$$Z_T = \frac{E_{kg}}{I_p} = - \frac{Z_M I_L}{I_L + I_c} \tag{12-10}$$

But since  $I_L Z_L = I_c Z_c$ ,

$$Z_T = - \frac{Z_M I_L}{I_L + I_L(Z_L/Z_c)} = - \frac{Z_M Z_c}{Z_L + Z_c} \tag{12-11}$$

Also, the quantity

$$1 + \frac{K}{\mu} = 1 - \frac{Z}{r_p + Z} = \frac{r_p}{r_p + Z} \tag{12-12}$$

where

$$Z = \frac{Z_L Z_c}{Z_L + Z_c} \tag{12-13}$$

The conditional equation for sustained oscillations may then be written in the form

$$\bar{g}_m \frac{Z_M Z_c}{Z_L + Z_c} \frac{r_p}{r_p + (Z_L Z_c / (Z_L + Z_c))} = 1 \tag{12-14}$$

which is

$$\bar{g}_m Z_M Z_c = (Z_L + Z_c) + \frac{Z_L Z_c}{r_p}$$

or

$$\bar{g}_m \frac{M}{C} = R + j \left( \omega L - \frac{1}{\omega C} \right) - j \frac{R}{\omega C r_p} + \frac{L}{C r_p} \tag{12-15}$$

By equating the real and the imaginary terms, there results

$$\left. \begin{aligned} \bar{g}_m \frac{M}{C} &= R + \frac{L}{C r_p} \\ \omega L - \frac{1}{\omega C} - \frac{R}{\omega C r_p} &= 0 \end{aligned} \right\} \tag{12-16}$$

and

The first of these equations may be written in the form

$$\bar{g}_m = \frac{\mu RC}{\mu M - L} \quad (12-17)$$

which specifies the average value of  $\bar{g}_m$  and which thus provides information, at least in principle, concerning the amplitude of the oscillations. The second equation becomes

$$\omega^2 = \frac{1}{LC} \left( 1 + \frac{R}{r_p} \right) \quad (12-18)$$

If the quantity  $\omega_0$  is defined by the relation

$$\omega_0 \equiv \frac{1}{\sqrt{LC}}$$

Eq. (12-18) becomes

$$\omega = \omega_0 \sqrt{1 + \frac{R}{r_p}} \quad (12-19)$$

The amplitude equation (12-17) gives a relation among the circuit constants from which the approximate amplitude of oscillation may be evaluated. To do this, one must refer to the static curves of the tube and determine from these that amplitude for which the value of  $\bar{g}_m$  has the value required by Eqs. (12-7).

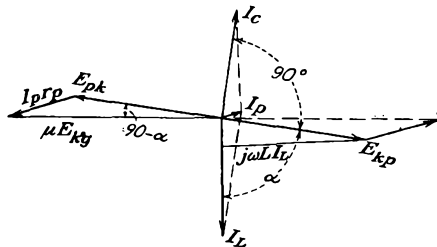


FIG. 12-6. The sinor diagram of a tuned-plate oscillator.

The frequency equation [Eq. (12-19)] shows that the frequency of oscillation will be approximately the resonant frequency of the circuit, the factor involving the ratio  $R/r_p$  being small. However, the frequency of oscillation will always be slightly higher than the resonant value. Clearly, the tube plays only a minor part in determining the frequency of oscillation, the external circuit elements exercising the main control. In fact, the influence of the tube on the frequency becomes less as the shunt resistance of the antiresonant circuit increases or, correspondingly, as the series resistance in the tank decreases. If circuits of very low dissipation are provided, the oscillator has a very high degree of stability.

A sinor diagram of the circuit in its steady oscillating state may be

drawn; this applies for the fundamental frequency. In the diagram (see Fig. 12-6) the sinors are not drawn to scale owing to the different orders of magnitudes that usually exist among the currents and voltages. Also, angles are exaggerated for clarity.

Under most circumstances the angle  $\alpha = \tan^{-1} (\omega L/R) = \tan^{-1} Q$  will be very nearly equal to 90 deg, and the feedback angle  $(90 - \alpha)$ , that is, the angle between  $-E_{pk}$  and  $E_{gk}$ , will be very small. This means that the feedback occurs substantially with 180 deg phase displacement, so that a decreasing plate potential reflects itself as an increasing potential on the grid.

**12-7. Other Oscillator Circuits.** A variety of vacuum-tube feed-back oscillator circuits exist, each of which possesses some special characteristics. The coupling networks of the more important types of oscillators (see Prob. 12-1 for the amplitude and frequency equations) are contained in Fig. 12-7. In each of these circuits the operation is essentially class C, the essential differences among them being in the coupling network.

Each of these circuits provides an antiresonant circuit of some type, with either inductive or conductive coupling between the output and input circuits. This does not imply that only circuits which possess an antiresonant circuit will operate successfully as an oscillator. In fact, circuits in which the feedback is accomplished through resistance and capacitance networks will be examined in some detail. However, the above networks do possess a feature that is common to all feed-back oscillator circuits: they all provide for a 180-deg phase shift between the output and input circuits. This is a necessary condition in order that regenerative feedback exist.

A special word is desirable about the tuned-grid-tuned-plate oscillator. This oscillator depends for its operation on the feedback that will be possible through the grid-plate capacitance  $C_{gp}$ . In this circuit the plate tank circuit will be tuned slightly below that of the grid tank. This causes the plate circuit to be inductive, and a negative input resistance results which overcomes the grid-circuit losses and thus allows oscillations to occur.

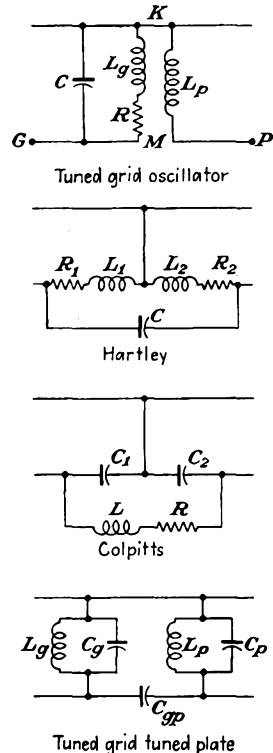


FIG. 12-7. The coupling networks of the more important oscillators.

**12-8. Stabilization of Feed-back Oscillators.**<sup>2</sup> Vacuum-tube oscillators will suffer changes in frequency with variations in any operating characteristic that involves either the tube or the circuit parameters. For example, a change in temperature may cause a change in the inductance and capacitance of the tank elements and may also cause a change in the grid-cathode and the plate-cathode interelectrode capacitances. Also, a change in plate potential will result in changes in the interelectrode capacitances. A change in the coupled load causes a change in the shunt resistance, with a consequent change in frequency. Although these

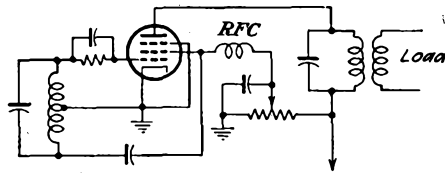


FIG. 12-8. Electron-coupled oscillator.

factors have been neglected in the explicit discussions given above of the various oscillator circuits, they do play a part in determining the frequency, since they will contribute to a variation of the tube or circuit constants of the coupling network.

A number of corrective measures may be taken in order to improve the stability of an oscillator. This would include the careful choice of the inductance and capacitance, either with negligible temperature coefficients or with such temperature variation that a change in one is counteracted by an opposite change in the other. Of course, any changes that might result from changes in the plate potential can be overcome by the use of adequately regulated sources.

The effect of changes in the load impedance on the frequency may be eliminated by using an amplifier to separate the load from the oscillator. This system is called a *master-oscillator power-amplifier arrangement*, usually abbreviated MOPA.

The oscillator and power amplifier can be combined into a single tube, by using a tetrode or a pentode. Such an oscillator is called an *electron-coupled oscillator*. A typical electron-coupled oscillator circuit employing a pentode is illustrated in Fig. 12-8. Here the cathode, grid 1, and grid 2 are operated as a conventional Hartley oscillator, grid 2 acting as the ordinary anode in a triode. The current to grid 2 is small, but it is sufficient to maintain the oscillations. The main part of the space current serves to produce the power in the load impedance. The plate current is controlled by the oscillator portion of the tube, but since the plate current is substantially independent of the plate potential, except

at the very low plate potentials, there is very little reaction between the output circuit and the oscillator section of the tube.

In such electron-coupled oscillators it is found that increasing the plate potential causes the frequency to decrease slightly, whereas increasing the screen potential causes the frequency to increase slightly. Hence, by obtaining the screen potential from a voltage divider, as shown in Fig. 12-8, and by locating the screen tap at the proper point (and this is determined experimentally), it is possible to make the frequency substantially independent of the plate supply voltage.

The effects of a varying plate resistance  $r_p$  on the frequency can be materially reduced through the use of *resistance stabilization*. In this, a resistance  $R_f$  is added between the plate of the tube and the tank circuit. This added resistance serves to make the total effective resistance in the plate circuit so high that changes in the plate resistance of the tube have very little effect on the frequency. The resistance also serves as a convenient means of controlling the feedback and hence the amplitude of the oscillations. It is ordinarily desirable that the resistance be made so high that the oscillations will just barely start.

Llewellyn<sup>2</sup> has shown that the frequency of oscillation can be made to approach the resonant frequency of the tuned circuit by inserting suitable reactances in series with the grid or with the plate, or both. This might be called *impedance stabilization*. It follows from the equivalent circuit of an oscillator shown in Fig. 12-9 that

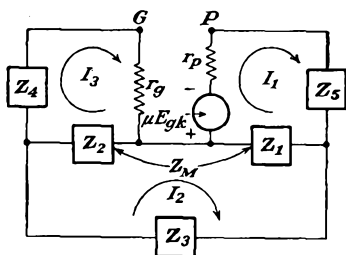


FIG. 12-9. The basic circuit of impedance stabilization.

$$\left. \begin{aligned} \mu E_{gk} &= Z_{11}I_1 + Z_{12}I_2 + Z_{13}I_3 \\ 0 &= Z_{21}I_1 + Z_{22}I_2 + Z_{23}I_3 \\ 0 &= Z_{31}I_1 + Z_{32}I_2 + Z_{33}I_3 \end{aligned} \right\} \quad (12-20)$$

where

$$\left. \begin{aligned} Z_{11} &= r_p + Z_1 + Z_5 & Z_{22} &= Z_0 = Z_1 + Z_2 + Z_3 + 2Z_M \\ Z_{12} &= -Z_1 + Z_M & Z_{23} &= -(Z_2 + Z_M) \\ Z_{13} &= -Z_M & Z_{33} &= r_g + Z_2 + Z_4 \end{aligned} \right\} \quad (12-21)$$

and

$$E_{gk} = I_3 r_g \quad (12-22)$$

The resulting expressions that obtain by equating the real and the imaginary terms are

$$\begin{aligned} X_0[r_p(X_2 + X_4) + r_g(X_1 + X_5)] + \mu r_g(X_1 + X_M)(X_2 + X_M) \\ = X_0 X_M \mu r_g - (X_1 + X_M)^2 r_g + (X_2 + X_M)^2 r_p \end{aligned} \quad (12-23)$$

from the reals and

$$X_0[r_p r_g - (X_1 + X_5)(X_2 + X_4)] - 2X_M(X_1 + X_M)(X_2 + X_M) = -X_0 X_M^2 - (X_1 + X_M)^2(X_2 + X_4) - (X_2 + X_M)^2(X_1 + X_5) \quad (12-24)$$

from the imaginaries. If in Eq. (12-24)  $X_4$  and  $X_5$  have such values as to satisfy the condition

$$2X_M(X_1 + X_M)(X_2 + X_M) = (X_1 + X_M)^2(X_2 + X_4) + (X_2 + X_M)^2(X_1 + X_5)$$

which contains all terms not containing  $Z_0$ , then the resonant frequency is exactly that to cause  $X_0$  to become zero and to remain so independently of  $r_p$ ,  $r_g$ , and  $\mu$ . That is, the frequency of oscillation is exactly the series-resonant frequency of the tuned circuit.

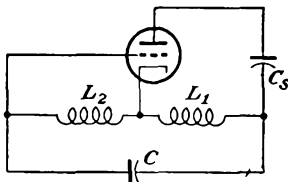


FIG. 12-10. A plate-stabilized Hartley oscillator.

As a particular example, consider a plate-stabilized Hartley oscillator, as shown. The condition for stabilization becomes, by writing  $X_4 = 0$ ,

$$X_5 = 2\omega M \left( \frac{L_1 - M}{L_2 + M} \right) - \omega L_2 \left( \frac{L_1 + M}{L_2 + M} \right)^2 - \omega L_1$$

which requires that  $X_5$  be negative. By setting

$$X_5 = -\frac{1}{\omega C_5}$$

and since, for  $X_0 = 0$ ,

$$\omega^2 = \frac{1}{C(L_1 + L_2 + 2M)}$$

then

$$C_5 = C \frac{L_1 + L_2 + 2M}{L_1 + L_2 \left( \frac{L_1 + M}{L_2 + M} \right)^2 - 2M \left( \frac{L_1 + M}{L_2 + M} \right)}$$

For the ideal case in which the effective tank circuit  $Q$  is extremely high, the compensation is perfect, and the frequency is independent of the tube voltages. In the actual case, the compensating reactances must be adjusted experimentally, and the compensation, although not perfect, represents a substantial improvement in independence of frequency from tube variations.

Several other cases are illustrated in Fig. 12-11.

**12-9. Crystal Oscillators.**<sup>3</sup> The frequency stability of an oscillator can be made very high by utilizing piezoelectric crystals as antiresonant circuits. Such crystals, which are sections cut from a quartz crystal in

such a way that the flat sides are perpendicular to an electrical axis, when stressed or compressed along this axis, are accompanied by the appearance of electric charges on the surface of the crystal. Conversely, when such crystals are placed in an alternating electric field, they are set

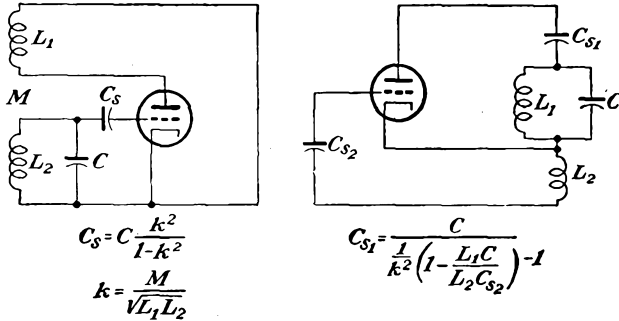


FIG. 12-11. Impedance-stabilized oscillators.

into mechanical vibration. If the applied electrical frequency is very near to that which produces mechanical resonance, the amplitude of the vibrations will be very large.

A vibrating crystal can be replaced by an equivalent electrical circuit, as shown in Fig. 12-12. In this circuit,  $C_m$  represents the capacitance of the crystal, and its mounting when it is not oscillating, the series combination  $L$ ,  $C$ , and  $R$ , represents the electrical equivalent of the vibrational characteristics of the material.  $L$  is the electrical equivalent of the crystal mass that is effective in vibration,  $C$  is the electrical equivalent of the crystal compliance, and  $R$  is the electrical equivalent of the coefficient of friction. The values of  $L$  and  $C$  are in series resonance at the frequency of mechanical resonance.

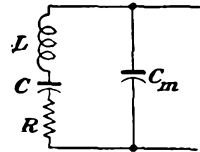


FIG. 12-12. The equivalent electrical network of a vibrating quartz crystal.

One of the most common types of crystal-controlled oscillators is illustrated in Fig. 12-13. When the crystal is replaced by its equivalent circuit, it is seen that the oscillator is essentially of the tuned-plate-tuned-grid type, the crystal making up the tuned-grid circuit. Owing to the extremely high  $Q$  of the equivalent circuit of the crystal, which may be

100 times as high as that of a conventional electrical circuit, the crystal can oscillate only over a very narrow frequency range. As a result, the

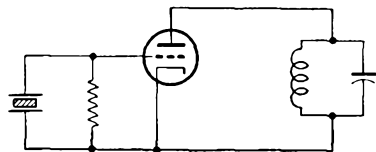


FIG. 12-13. A crystal-controlled oscillator.

frequency stability of such an oscillator is very high. When the temperature of the crystal is maintained constant, the frequency drift may be made less than 1 part in  $10^6$ .

**12-10. Class A Oscillators.**<sup>4</sup> Some stabilization is made possible by operating an oscillator in class A instead of class C, for this eliminates the

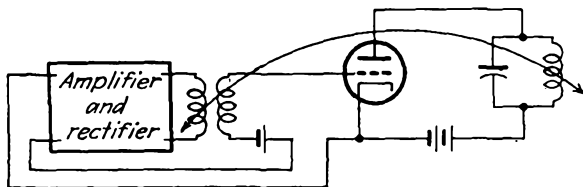


FIG. 12-14. A linear-stabilized oscillator.

grid current and any nonlinear effects resulting from it. Moreover, the output wave shape from a class A oscillator will be sinusoidal, with a high degree of purity of wave form. Owing to the manner of its operation, the oscillating frequency is determined by the resonant elements alone. However, since the self-regulating amplitude-control feature of the non-

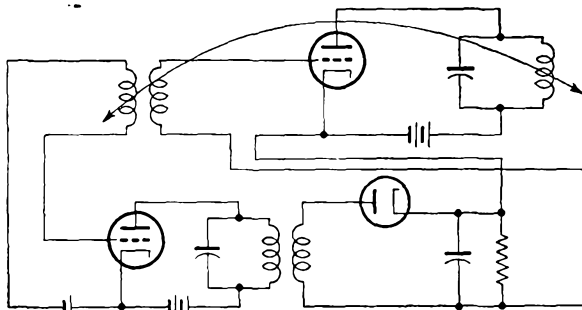


FIG. 12-15. The circuit of a linear-stabilized oscillator.

linear tube characteristic is no longer being employed, other methods must be provided in order to stabilize the amplitude of the output. One way for providing for linear stabilized operation is illustrated in Fig. 12-14. In this circuit, the output is coupled to a rectifier, the output of which is used to control the d-c bias of the oscillator. If the gain of the amplifier before rectification is large, thus yielding a large d-c output, the oscillator will operate as a linear amplifier.

A circuit showing the details of such an amplitude-stabilized oscillator is given in Fig. 12-15.

Amplitude stabilization may be effected by providing an amplitude-sensitive network to control the output of the oscillator. Such a method

is employed in the Wien bridge oscillator, which is described in the next section.

**12-11. Resistance-Capacitance Oscillators.** A form of coupling network that has been used extensively in relatively low frequency oscillators is given in Fig. 12-16. The phase shift through such a network as this is a fairly sensitive function of the frequency, and such RC oscillators are quite stable. However, such a simple network will not provide a large phase shift between the input and output terminals, and

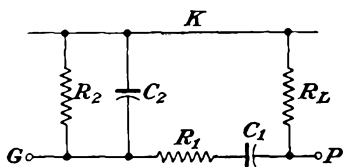


FIG. 12-16. An RC coupling network for an oscillator.

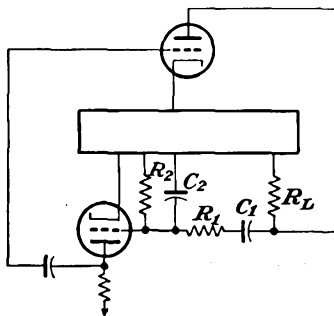


FIG. 12-17. An RC coupled oscillator.

it is necessary to incorporate a second vacuum tube in the circuit in order to provide an additional 180-deg phase shift. The circuit, when drawn in the manner of the previous circuits, is as shown in Fig. 12-17.

This circuit may be analyzed in a direct manner by an application of Eqs. (12-7). Refer to Fig. 12-18, which shows the complete coupling

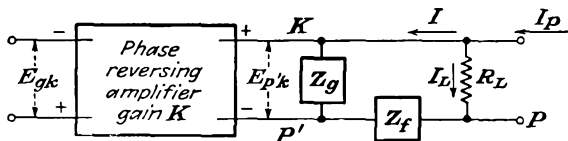


FIG. 12-18. The complete coupling circuit of the RC oscillator.

network, in which the amplifier is replaced by a “black box” which provides a gain  $K$  and a phase shift of 180 deg. An inspection of this diagram shows that

$$E_{gk} = KE_{p'k}$$

This may be written in the form

$$E_{gk} = KIZ_o$$

if it is assumed that the input impedance to the amplifier is very high. The transfer impedance of the network becomes

$$Z_T = \frac{E_{kg}}{I_p} = - \frac{KIZ_o}{I_L + I}$$

But as

$$I(Z_o + Z_f) = I_L R_L$$

then

$$Z_T = -\frac{KI Z_g}{I \frac{Z_g + Z_f}{R_L} + I} = -\frac{KZ_g R_L}{Z_g + Z_f + R_L} \quad (12-25)$$

Also, it is noted that

$$Z = \frac{R_L(Z_g + Z_f)}{R_L + Z_g + Z_f} \quad (12-26)$$

Then the term  $1 + (K/\mu)$ , which appears in Eq. (12-7), becomes

$$1 + \frac{K}{\mu} = \frac{r_p}{r_p + \frac{R_L(Z_g + Z_f)}{R_L + Z_g + Z_f}} \quad (12-27)$$

and Eq. (12-7) for sustained oscillations becomes

$$\overline{g_m K Z_g R_L} \frac{r_p}{r_p(R_L + Z_g + Z_f) + R_L(Z_g + Z_f)} = 1 \quad (12-28)$$

This may be written in the form

$$\overline{g_m K} \left[ Z_g R_L - \frac{R_L}{\mu K} (Z_g + Z_f) \right] = R_L + Z_g + Z_f$$

from which it follows that

$$\overline{g_m K R_L} = \frac{R_L + Z_g + Z_f}{Z_g \left( 1 - \frac{1}{\mu K} \right) - \frac{Z_f}{\mu K}} \quad (12-29)$$

By including in this expression the known values of  $Z_g$  and  $Z_f$ , namely,

$$Z_g = \frac{-j(R_2/\omega C_2)}{R_2 - j(1/\omega C_2)} \quad Z_f = R_1 - j \frac{1}{\omega C_1}$$

and equating the real and the imaginary terms, two expressions result. They are

$$\left. \begin{aligned} -\overline{g_m} \frac{R_L}{\mu} \left( R_1 R_2 - \frac{1}{\omega^2 C_1 C_2} \right) &= R_2 (R_1 + R_L) - \frac{1}{\omega^2 C_1 C_2} \\ \overline{g_m} \frac{R_L}{\mu} \left( \frac{R_2}{C_1} + \frac{R_1}{C_2} - (\mu K - 1) \frac{R_2}{C_2} \right) &= - \left( \frac{R_2}{C_1} + \frac{R_L + R_1}{C_2} + \frac{R_2}{C_2} \right) \end{aligned} \right\} \quad (12-30)$$

The first of these yields for the frequency the expression

$$\omega^2 = \frac{1}{C_1 C_2 \left( R_1 R_2 + \frac{R_2 R_L}{1 + \frac{R_L}{r_p}} \right)} \quad (12-31)$$

Ordinarily  $R_1 = R_2 \gg R_L$ ;  $R_L > r_p$ ; and Eq. (12-31) reduces to

$$\omega^2 \doteq \frac{1}{C_1 C_2 R_1 R_2} \tag{12-32}$$

The amplitude equation leads to the expression

$$\frac{1}{g_m} = \frac{\mu[(R_1 + R_2 + R_L)C_1 + R_2 C_2]}{R_L\{[(\mu K - 1)R_2 - R_1]C_1 - R_2 C_2\}} \tag{12-33}$$

For the special conditions for which

$$\begin{aligned} R_1 &= R_2 = R \\ C_1 &= C_2 = C \end{aligned}$$

then

$$\left. \begin{aligned} \omega &\doteq \frac{1}{CR} \\ \frac{1}{g_m} &\doteq \frac{3\mu}{(\mu K - 3)} \frac{1}{R_L} \doteq \frac{3}{KR_L} \end{aligned} \right\} \tag{12-34}$$

The use of the phase-inverting amplifier stage ordinarily introduces so much gain that a voltage divider must be incorporated in the circuit to control the output.

Ordinarily the circuit is altered slightly, with distinctly superior results. The modifications of the circuit provide for class A rather than class C

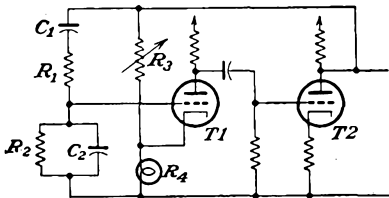


FIG. 12-19. Wien bridge oscillator.

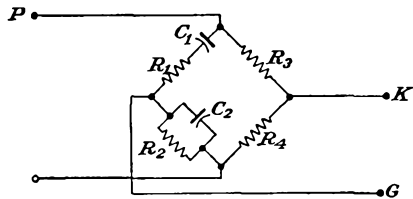


FIG. 12-20. The Wien-bridge-oscillator coupling network.

operation. The altered circuit provides the phase-reversing stage with negative feedback, thus providing for an improved wave form. Also, there is incorporated in the circuit an automatic amplitude control. The practical circuit<sup>5</sup> of such an improved RC oscillator, which is known as a Wien bridge oscillator, is given in Fig. 12-19. The reason for the name is to be found in the form of the coupling network to tube T1. A sketch showing the bridge nature of the network is given in Fig. 12-20.

The resistor  $R_4$  is usually a tungsten filament lamp, which possesses a positive temperature coefficient of resistance; the hotter the filament of the lamp, the higher its resistance. This provides automatic control of the amplitude of the oscillations. If the amplitude of the oscillations

tends to increase, the lamp becomes hotter and  $R_4$  increases. As a result, the grid-cathode potential of  $T1$  is reduced, with a resulting decrease of amplitude. If  $R_3$  is properly adjusted initially, the amplitude of the oscillations is maintained at a substantially constant level, even though the frequency may be varied over very wide limits.

A simple *phase-shift*<sup>6</sup> oscillator is possible which incorporates  $RC$  networks to provide the requisite 180-deg phase between input and output potentials. Consequently, only a single tube is required in the circuit.

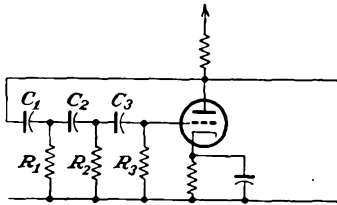


FIG. 12-21. A phase-shift oscillator.

The circuit is illustrated in Fig. 12-21. It may best be understood by supposing that each  $L$  section, consisting of a  $C$  and  $R$  combination, shifts the phase by 60 deg. The use of three such sections will shift the phase of the output by a total of 180 deg relative to the input.

This oscillator operates as a class C device, but the wave form of the output is very nearly sinusoidal if the bias on the tube is adjusted to a value which barely allows oscillations to be maintained. The frequency stability of the circuit is also quite good.

Owing to the fact that the range over which the frequency can be changed is not very great, such phase-shift oscillators are relatively limited in their applications. The frequency can be changed by changing any of the phase-shifting capacitors or resistors. Large frequency changes are not possible unless both  $X_c$  and  $R$  are changed, although the ratio  $X_c/R$  must be maintained in order that the phase-shift of the section remain unchanged.

**12-12. Negative-resistance Oscillators.** One may consider the foregoing analyses of feed-back oscillators as a demonstration of the fact that it is possible to devise circuits containing vacuum tubes in which the power generated is sufficient to overcome the losses of the circuit and also to provide the power that is transferred to an external circuit. If the total loading or dissipation within the circuit is represented by a certain equivalent resistance in the plate circuit, then one might consider the tube as representing a negative resistance of such a magnitude as just to overcome the total dissipative terms. The oscillations in the circuit will then be sustained at the stable level required by the variations of the negative-resistance properties of the circuit.

If one is able to find a device that possesses a negative resistance, *i.e.*, a device in which a positive increment of current through it is accompanied by a negative potential increment across it, then this can be used to neutralize the positive resistance representing the total dissipation.

Such negative-resistance devices do exist, the simple tetrode operating with a plate potential below that of the screen being a common example. The connections of such a device and the plate characteristics which show the region of negative plate resistance are shown in Figs. 12-22.

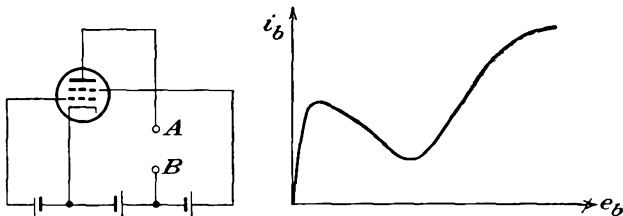


FIG. 12-22. A negative-resistance tetrode circuit, and the plate characteristics, showing the region of negative plate resistance.

A circuit that exhibits an effective negative resistance and at the same time avoids the objectionable features of secondary emission is illustrated in Fig. 12-23. A pentode is operated with a plate potential that is lower than the screen potential, and the suppressor grid is maintained slightly negative relative to the cathode. Since the plate is at a low positive potential, it does not exert much force on the electrons and under these conditions the suppressor grid repels most of the electrons that manage to get past the screen grid, with a resulting higher screen current.

If the suppressor voltage is increased slightly, *i.e.*, is made less negative, then there will be less repelling action by the suppressor and more plate current will flow at the expense of the screen current. The electrons that were previously being repelled by the suppressor and returned to the screen will now pass to the plate, with a consequent reduced screen current. Note that even if the screen potential is increased by the same potential as that applied to the suppressor grid the net effect is still a reduction of the screen-grid current. That is, if the screen current were to increase somewhat with the increase of screen potential, the decrease in screen current owing to the action of the suppressor grid is so much greater that the net effect is a reduction of the screen current. Therefore, with the circuit shown, there is a decrease of current through the terminals *AB* with an increase in potential across these terminals, with a consequent negative resistance.

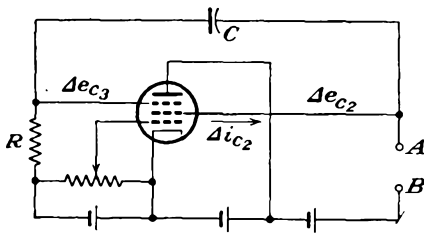


FIG. 12-23. A pentode circuit that exhibits a negative output resistance.

To analyze the circuit analytically,<sup>7</sup> it is assumed that the change in screen current is a linear function of the changes in the suppressor-grid and screen-grid voltages and also that the suppressor-grid current is negligible. That is, it is assumed that

$$\Delta i_{c2} = g_{32} \Delta e_{c3} - \frac{\Delta e_{c2}}{r_{g2}}$$

The factor  $g_{32}$  has the dimensions of a conductance and is such that  $g_{32} \Delta e_{c3}$  gives a measure of the influence of a change in current  $i_{c2}$  due to a change in potential of the suppressor grid. Note from the foregoing discussion that  $g_{32}$  is inherently negative since a positive  $\Delta e_{c3}$  is accompanied by a negative  $\Delta i_{c2}$ . The factor  $r_{g2}$  is a measure of the change in  $i_{c2}$  due to a change in  $e_{c2}$ .

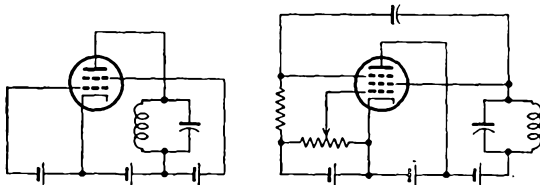


FIG. 12-24. A negative-resistance, or dynatron, and a negative-transconductance, or transatron, oscillator.

If it is assumed that  $g_{32}$  and  $r_{g2}$  remain constant over the range of operation, and by noting that with a large  $C$  and  $R$  a change in voltage  $\Delta e_{c2}$  appears on the suppressor as a change  $\Delta e_{c3}$ , then

$$\Delta i_{c2} = \left( g_{32} + \frac{1}{r_{g2}} \right) \Delta e_{c2}$$

The input resistance between points  $A$  and  $B$  is then

$$r \equiv \frac{\Delta e_{c2}}{\Delta i_{c2}} = \frac{r_{g2}}{1 + g_{32}r_{g2}}$$

which is negative when

$$-g_{32}r_{g2} > 1$$

To examine the operation of the circuit of such negative resistances as part of an oscillator, suppose that a tank circuit is coupled to the terminals  $AB$  of the two circuits shown in Fig. 12-24. These circuits may be drawn in the manner of Fig. 12-1. Since the feed-back voltage is zero, the circuit simplifies to that shown in Fig. 12-25. This may be drawn as a simple coupled circuit, in the form illustrated in Fig. 12-26.

To evaluate the characteristics of the circuit, apply Kirchhoff's law to the two-mesh network. This yields

$$\left. \begin{aligned} \left( rp + \frac{1}{Cp} \right) I_1 - \frac{1}{Cp} I_2 &= 0 \\ -\frac{1}{Cp} I_1 + R + Lp + \frac{1}{Cp} I_2 &= 0 \end{aligned} \right\} \quad (12-35)$$

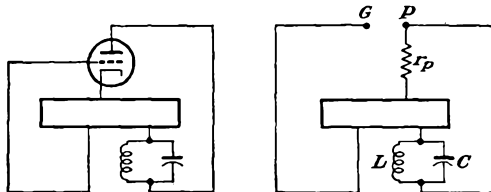


FIG. 12-25. The equivalent and simplified circuit of the negative-resistance oscillator.

To solve for  $I_2$ , the current through the inductance and load, the following differential equation must be evaluated:

$$\frac{d^2 I_2}{dt^2} + \left( \frac{R}{L} + \frac{1}{r_p C} \right) \frac{dI_2}{dt} + \left( \frac{R + r_p}{r_p CL} \right) I_2 = 0 \quad (12-36)$$

If it is assumed that  $r_p$ , which is inherently negative, remains substantially constant over the range of operation, this equation may be solved directly to give, for the oscillatory case,

$$I_2 = A e^{-\frac{1}{2} \left( \frac{R}{L} + \frac{1}{r_p C} \right) t} \sin(\omega t + \theta) \quad (12-37)$$

where  $A$  and  $\theta$  are constants. The expression for  $I_1$  has exactly the same form, although with different values for  $A$  and  $\theta$ . The angular frequency of oscillation is

$$\omega = \sqrt{\left( \frac{R + r_p}{r_p LC} \right) - \frac{1}{4} \left( \frac{R}{L} + \frac{1}{r_p C} \right)^2}$$

or

$$\omega = \sqrt{\frac{1}{LC} \left( \frac{r_p + R}{r_p} \right) - \frac{1}{4} \left( \frac{R}{L} + \frac{1}{r_p C} \right)^2} \quad (12-38)$$

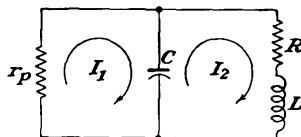


FIG. 12-26. The basic equivalent circuit of a negative-resistance oscillator.

Under the assumed oscillatory conditions, the expression for  $I_2$  indicates that the amplitude of the oscillations may decrease, remain constant, or increase, depending upon the exponential term in the expression. If the term  $(R/L) + (1/r_p C)$  is positive, then the oscillations which might have been started in any manner will ultimately fall to zero. If the quantity  $(R/L) + (1/r_p C)$  is negative, the oscillations will tend to increase in amplitude with time. For the critical case for which the quantity  $(R/L) + (1/r_p C)$  equals zero, the exponential factor is unity and the

amplitude of the oscillations remains constant. For this condition

$$r_p = -\frac{L}{RC} \quad (12-39)$$

and the corresponding frequency is

$$\omega = \sqrt{\frac{1}{LC} \left(1 + \frac{R}{r_p}\right)} = \sqrt{\frac{1}{LC} \left(1 - \frac{R^2C}{L}\right)} \quad (12-40)$$

Such negative-resistance oscillators are self-regulating in much the same manner as the normal feedback oscillators. Thus, owing to the variation of the negative-resistance characteristic of the tube circuit that is used, if the quantity  $(R/L) + (1/r_p C)$  were negative, thus allowing for continually increasing amplitude of oscillations, these oscillations would increase until the region of operation extended to the point where  $r_p = -L/RC$ , when the build-up condition would cease. These conditions are illustrated in Fig. 12-27. It should be noted from the diagram that even with an assumed sinusoidal output potential, and this is not a required condition, the output current will be nonsinusoidal.

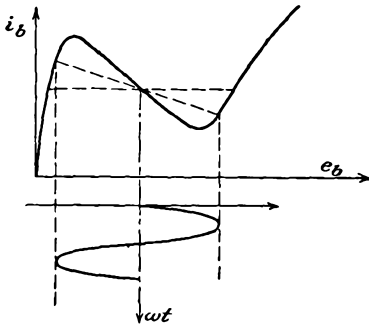


Fig. 12-27. The amplitude of oscillation increases until the value of  $r_p$  assumes the critical value  $L/RC$ .

#### REFERENCES

1. Barkhausen, H., "Lehrbuch der Elektronenrohren," vol. III, S. Hirzel, Leipzig, 1935.  
M.I.T. Staff, "Applied Electronics," Chap. XI, John Wiley & Sons, Inc., New York, 1943.
2. Terman, F. E., *Electronics*, **6**, 190 (1933).  
Llewellyn, F. B., *Proc. IRE*, **19**, 2063 (1931).  
Jefferson, H., *Wireless Eng.*, **22**, 384 (1945).
3. For further details, see Terman, F. E., "Radio Engineering," 3d ed., Sec. 8-3, McGraw-Hill Book Company, Inc., New York, 1947.
4. ARGUIMBAU, L. B., "Vacuum Tube Circuits," p. 320, John Wiley & Sons, Inc., New York, 1948.
5. Terman, F. E., R. R. Buss, W. R. Hewlett, and F. C. Cahill, *Proc. IRE*, **24**, 649 (1939).
6. Ginzton, E. L., and L. M. Hollingsworth, *Proc. IRE*, **29**, 43 (1941).
7. Herold, E. W., *Proc. IRE*, **23**, 1201 (1935).

#### PROBLEMS

12-1. Show that the amplitude and frequency of the oscillators illustrated in Fig. 12-7 are the following:

Tuned grid:

$$\omega = \frac{1}{\sqrt{L_0 C \left( 1 + \frac{RL_p}{r_p L_g} \right)}}$$

$$\bar{g}_m \doteq \frac{\mu RL_0 C}{M(\mu L - M)}$$

Hartley:

$$\omega = \sqrt{\frac{1 + R_2/r_p}{C(L_1 + L_2 + 2M)}}$$

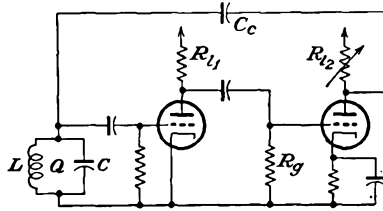
$$\bar{g}_m \doteq \frac{C(R_1 + R_2)(L_1 + L_2 + 2M)}{(L_1 + M)(L_2 + M)}$$

Colpitts:

$$\omega = \sqrt{\frac{1}{L \left( \frac{1}{C_1} + \frac{1}{C_2} + \frac{R}{r_p C_2} \right)}}$$

$$\bar{g}_m \doteq \frac{\mu R(C_1 + C_2)}{L(\mu - C_1/C_2)}$$

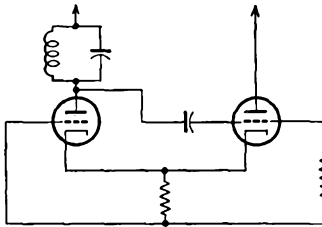
12-2. Two identical triodes are connected in a Franklin oscillator. Determine in terms of the circuit parameters



- a. The expression for the critical value of the resistance  $R_{i2}$  at which oscillations will just begin.
- b. The frequency of oscillation.

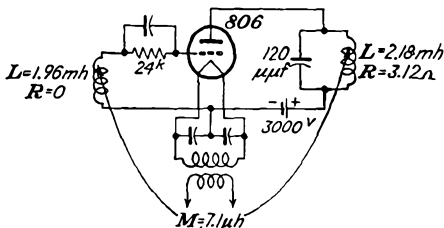
Assume that the power absorbed in the tuned circuit, which determines its  $Q$ , may be represented as that absorbed in a resistance in shunt with the inductance and capacitance.

12-3. Obtain an expression for the operating frequency of the cathode-coupled oscillator shown in the diagram.\*



12-4. Using the 806 tube, whose constant current characteristics are given in Chap. 11, calculate the performance when it is used in the oscillator circuit shown in the figure.

\*Crosby, M. G., *Electronics*, 19, 136 (May, 1946).



12-5. A type 852 triode has the following ratings as an r-f power amplifier and oscillator (key down conditions without modulation per tube):

D-c plate voltage.....	3,000 volts
D-c grid voltage.....	-600 volts
Peak r-f grid voltage.....	850 volts
D-c plate current.....	85 ma
D-c grid current.....	15 ma approx
Driving power.....	12 watts approx
Power output.....	165 watts approx

The tube is operated under rated conditions in a tuned-plate oscillator, operating at a frequency of 1 megacycle. Determine the following:

- Grid dissipation.
- Plate dissipation.
- Power output.
- Oscillator efficiency.
- Resonant impedance of tank circuit.
- Grid leak required.
- Mutual inductance between grid and plate coils.

Assume that the maximum grid voltage is equal to the minimum plate potential. Neglect the leakage inductances and resistances of the grid and plate coils, and assume that the tank circuit has a  $Q = 20$ .

12-6. A type 806 triode when used as an r-f power amplifier has the following ratings:

D-c plate voltage.....	2,500 volts
D-c grid voltage.....	-500 volts
D-c plate current.....	195 ma
D-c grid current.....	25 ma
Driving power.....	17 watts
Grid resistor.....	20,000 ohms
Power output.....	370 watts

This tube is connected as a Hartley oscillator and is operated under the conditions specified. The tank tuning capacitor is  $250 \mu\mu\text{f}$ ; the resonant frequency is 2 megacycles; the loaded  $Q$  is 23.5. Determine the following:

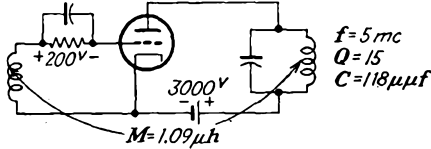
- The inductance, and resistance of the tank circuit.
- The power output.
- How far from the bottom of the tank coil is the cathode connection?
- The oscillator efficiency.

Assume  $e_{cmax} = e_{bmin}$ .

12-7. An 833A transmitting tube has characteristics that may be represented approximately by the equations

$$i_b = 4 \times 10^{-4} (25e_c + e_b) \quad \text{amp} \quad \text{for } (25e_c + e_b) > 0$$

$$i_b = 0 \quad \text{for } (25e_c + e_b) < 0$$



This tube is to be operated as a power oscillator in the circuit shown in the accompanying figure. Assume that  $e_{bmin} = e_{cmax}$ . Calculate the following:

- a. Power input to the plate circuit.
- b. A-c power output.

When calculating the grid signal voltage, neglect the grid driving power.

12-8. Typical constants of a crystal are

$$R = 1,500 \text{ ohms}$$

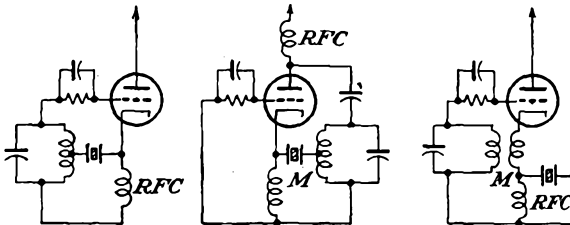
$$L = 250 \text{ h}$$

$$C = 0.04 \text{ } \mu\mu\text{f}$$

$$C_m = 8 \text{ } \mu\mu\text{f}$$

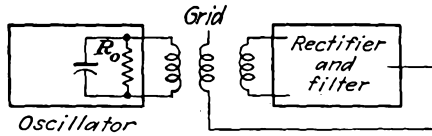
- a. Calculate the  $Q$  of the crystal.
- b. Calculate the series- and parallel-resonant frequencies.
- c. What is the percentage change in the series and parallel frequencies if  $C_m$  is doubled?

12-9. Crystals may be used in what are called series-resonant crystal-controlled oscillators.\* Discuss the operating features of the accompanying figures.



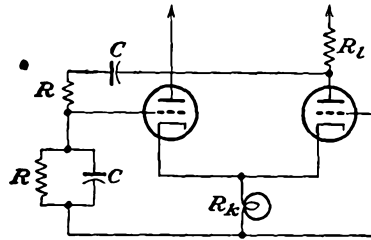
12-10. An amplitude-controlled oscillator uses a 6J5 tube. It operates at 5 megacycles. A measurement of the network and rectifier when the oscillator

\* Butler, F., *Wireless Eng.*, **23**, 157 (1946).



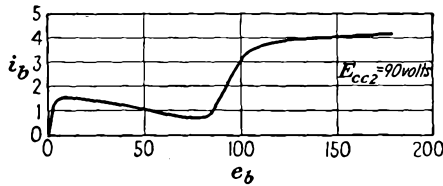
tube is removed indicates that with an input of  $E_p = 8$  volts rms the potentials are  $E_g = 0.4$  volts rms,  $E_{cc} = 11.4$  volts d-c. What is the value of  $R_o$  for the bias to adjust itself to  $-7.5$  volts?

12-11. A cathode-coupled Wien bridge oscillator is shown in the diagram for



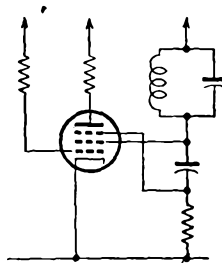
this problem. Determine the critical value of  $R_l$  at which oscillations will just start.

12-12. The plate characteristic of a 24A tube connected as a tetrode is given in the figure. The d-c potential  $E_{bb}$  is adjusted to 45 volts. A parallel-resonant circuit tuned to 1 mc is used, with  $C = 250 \mu\mu f$ .



- Determine the minimum value of  $R$  for which oscillations will be sustained.
- Plot the oscillation amplitude as a function of  $R$ .
- Plot the current wave shape for maximum oscillation amplitude.

12-13. Discuss the operation of the transition oscillator illustrated in the diagram.



## CHAPTER 13

### RECTIFIERS

ANY electrical device having a high resistance to current in one direction and a low resistance to current in the opposite direction possesses the ability to convert an a-c current into a current which contains a d-c component in addition to a-c components. An ideal rectifier would be one with zero resistance in the forward direction and with an infinite resistance in the reverse direction. A number of devices possess nonlinear characteristics, among which are high-vacuum thermionic diodes, gas-filled and

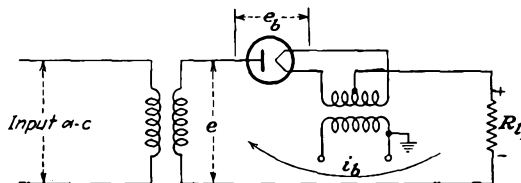


FIG. 13-1. A simple half-wave rectifier circuit.

vapor-filled thermionic diodes, pool-cathode mercury arcs, and certain crystals.

The important rectifiers for power purposes fall into two general groups, depending on their inherent characteristics. The vacuum rectifier possesses an infinite resistance on the inverse cycle, as the tube will not conduct when the plate is negative with respect to the cathode. On the forward, or conducting, portion of the cycle, the vacuum diode is characterized by an almost constant and low value of resistance. The gas or vapor rectifiers also possess an infinite resistance on the inverse cycle, but as discussed in Sec. 2-17, they are characterized by a substantially constant tube drop during conduction. Owing to these differences, the resulting operation in a circuit is slightly different. A detailed discussion is included below.

**13-1. Single-phase Half-wave Vacuum Rectifier.** The basic circuit for half-wave rectification is shown in Fig. 13-1. It is assumed that the load is a pure resistance. Also, it is supposed that the power transformer is ideal, with negligible resistance and leakage reactance.

An application of Kirchoff's law to the load circuit yields

$$e = e_b + i_b R_L \quad (13-1)$$

where  $e$  is the instantaneous value of the applied potential,  $e_b$  is the instantaneous voltage across the diode when the instantaneous current is  $i_b$ , and  $R_l$  is the load resistance. This one equation is not sufficient for the determination of the two unknown quantities  $i_b$  and  $e_b$  that appear in the expression. Here, as for triodes and multielectrode tubes, a second relation is contained in the static plate characteristic of the tube. Consequently a solution is effected by drawing the load line on the plate characteristic.

There is one significant difference between the solution of the diode as a rectifier and that for the other tubes as amplifiers. With the rectifier, an a-c potential is applied from a source, this source supplying the power

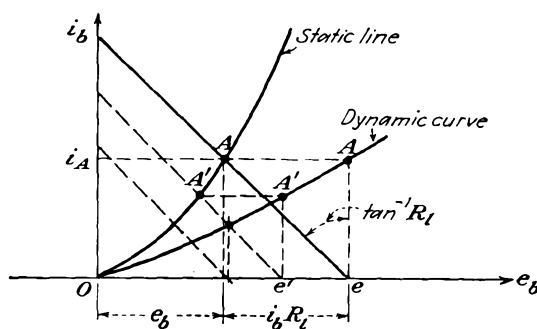


FIG. 13-2. The static and dynamic characteristics of a rectifier.

to the circuit. A vacuum tube as an amplifier converts direct current from the plate supply into alternating current.

The dynamic characteristic for the rectifier is obtained somewhat differently from the corresponding curve for an amplifier. The procedure is illustrated in Fig. 13-2. For an applied potential  $e$ , the current is the intersection of the load line with the static characteristic, say point  $A$ . That is, for the particular circuit, the application of the potential  $e$  results in a current  $A$ . This is one point on the dynamic curve and is drawn vertically above  $e$  in the diagram. The slope of the load line does not vary, although the intersection with the  $e_b$  axis varies with  $e$ . Thus, when the applied potential has the value  $e'$ , the corresponding current is  $A'$ . The resulting curve so generated is the dynamic characteristic.

If the static characteristic of the tube were linear, the dynamic characteristic would also be linear. Note from the construction, however, that there is considerably less curvature in the dynamic curve than there is in the static characteristic. It will be assumed in what follows that the dynamic curve is linear.

To find the wave shape of the current in the output circuit, the pro-

cedure followed is that illustrated in Fig. 13-3. This procedure is very much like that used to find the wave shape in a general amplifier circuit; in fact, the situation here is quite like that of a class B amplifier, except that cutoff of the tube exists at zero input.

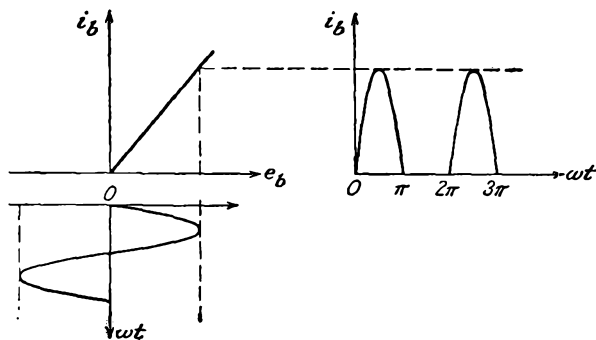


FIG. 13-3. The method of obtaining the output-current wave form from the dynamic characteristic.

If it is assumed that the relation

$$e_b = i_b r_p \tag{13-2}$$

is valid during conduction, and this supposes that the static characteristic is linear, then from Eq. (13-1) it follows that

$$e = e_b + i_b R_l = i_b (r_p + R_l) = E_m \sin \omega t \tag{13-3}$$

or

$$\left. \begin{aligned} i_b &= \frac{E_m}{R_l + r_p} \sin \omega t = I_m \sin \omega t && \text{when } 0 \leq \omega t \leq \pi \\ i_b &= 0 && \text{when } \pi \leq \omega t \leq 2\pi \end{aligned} \right\} \tag{13-4}$$

where

$$I_m = \frac{E_m}{R_l + r_p}$$

The d-c power supplied to the load is defined as the product of the reading of a d-c ammeter in the load circuit and a d-c voltmeter across the load. Thus

$$P_{d-c} \equiv E_{d-c} I_{d-c} \tag{13-5}$$

Clearly, the reading of the d-c ammeter is represented by

$$I_{d-c} = \frac{1}{2\pi} \int_0^{2\pi} i_b d\alpha = \frac{1}{2\pi} \int_0^{\pi} I_m \sin \alpha d\alpha = \frac{I_m}{\pi} \tag{13-6}$$

and so

$$P_{d-c} = I_{d-c}^2 R_l = \left(\frac{1}{\pi}\right)^2 \frac{E_m^2 R_l}{(r_p + R_l)^2} \tag{13-7}$$

The power supplied to the circuit from the a-c source, and this is the power that would be read by a wattmeter with its current coil in the line and with the potential coil across the source, is given by the integral

$$P_i = \frac{1}{2\pi} \int_0^{2\pi} ci_b d\alpha \quad (13-8)$$

This becomes, by Eqs. (13-2) and (13-3),

$$P_i = \frac{1}{2\pi} \int_0^{2\pi} i_b^2 (r_p + R_l) d\alpha \quad (13-9)$$

which may be written in the form

$$P_i = I_{rms}^2 (r_p + R_l) \quad (13-10)$$

where the rms current has the value

$$I_{rms} = \sqrt{\frac{1}{2\pi} \int_0^{2\pi} i_b^2 d\alpha} = \sqrt{\frac{1}{2\pi} \int_0^{\pi} I_m^2 \sin^2 \alpha d\alpha} = \frac{I_m}{2} \quad (13-11)$$

The efficiency of rectification is defined by the relation

$$\eta_r = \frac{P_{d-c}}{P_i} \times 100\% = \frac{I_{d-c}^2 R_l}{I_{rms}^2 (r_p + R_l)} \times 100\%$$

which becomes

$$\eta_r = \left( \frac{I_{d-c}}{I_{rms}} \right)^2 \frac{100}{1 + (r_p/R_l)} \quad (13-12)$$

By combining this with Eqs. (13-6) and (13-11), there results

$$\eta_r = \left( \frac{I_m/\pi}{I_m/2} \right)^2 \frac{100}{1 + (r_p/R_l)} = \frac{40.6}{1 + (r_p/R_l)} \% \quad (13-13)$$

This indicates that the theoretical maximum efficiency of the single-phase half-wave rectifier is 40.6 per cent. But it may be shown that maximum power output occurs when  $R = r_p$ , with a corresponding theoretical plate-circuit efficiency of 20.3 per cent.

There are several features of such a rectifier circuit that warrant special attention. Refer to Fig. 13-1, which shows the complete wiring diagram of the rectifier. On the inverse cycle, *i.e.*, on that part of the cycle during which the tube is not conducting, the maximum potential across the rectifier tube is equal to the transformer maximum value. That is, the peak inverse voltage across the tube is equal to the transformer maximum value.

Note also from the diagram that with the negative terminal of the output connected to ground the full transformer potential exists between the primary and the secondary windings of the filament heating transformer.

This requires that the transformer insulation must be adequate to withstand this potential without rupture. Evidently if the positive terminal is grounded, then the transformer need not have a high insulation strength.

**13-2. Ripple Factor.** Although it is the object of a rectifier to convert a-c into d-c current, the simple circuit considered does not achieve this. Nor, in fact, do any of the more complicated rectifier circuits, either single-phase or polyphase, accomplish this exactly. What is achieved is a unidirectional current, certain periodically fluctuating components still remaining in the output. Filters are ordinarily used in rectifier systems in order to help decrease these fluctuating components. A measure of the fluctuating components is given by the ripple factor  $r$ , which is defined as

$$r = \frac{\text{rms value of the a-c components of the wave}}{\text{avg or d-c value of the wave}}$$

and which may be written as

$$r = \frac{I'_{\text{rms}}}{I_{\text{d-c}}} = \frac{E'_{\text{rms}}}{E_{\text{d-c}}} \quad (13-14)$$

where  $I'_{\text{rms}}$  and  $E'_{\text{rms}}$  denote the rms values of the a-c components only.

An analytical expression for the ripple factor is readily possible. It is noted that the instantaneous a-c component of the current is given by

$$i' = i - I_{\text{d-c}}$$

But by definition

$$I'_{\text{rms}} = \sqrt{\frac{1}{2\pi} \int_0^{2\pi} (i - I_{\text{d-c}})^2 d\alpha} = \sqrt{\frac{1}{2\pi} \int_0^{2\pi} (i^2 - 2iI_{\text{d-c}} + I_{\text{d-c}}^2) d\alpha}$$

This expression is readily interpreted. The first term of the integrand when evaluated yields the square of the rms value of the total wave  $I_{\text{rms}}^2$ . The second term yields

$$\frac{1}{2\pi} \int_0^{2\pi} 2iI_{\text{d-c}} d\alpha = 2I_{\text{d-c}}^2$$

The rms ripple current then becomes

$$I'_{\text{rms}} = \sqrt{I_{\text{rms}}^2 - 2I_{\text{d-c}}^2 + I_{\text{d-c}}^2} = \sqrt{I_{\text{rms}}^2 - I_{\text{d-c}}^2}$$

By combining these results with Eq. (13-13)

$$r = \frac{\sqrt{I_{\text{rms}}^2 - I_{\text{d-c}}^2}}{I_{\text{d-c}}} = \sqrt{\left(\frac{I_{\text{rms}}}{I_{\text{d-c}}}\right)^2 - 1} \quad (13-15)$$

This expression is independent of the current wave shape and applies in general, since the development was not confined to a particular wave

shape In the case of the half-wave single-phase rectifier, the ratio

$$\frac{I_{rms}}{I_{d-c}} = \frac{I_m/2}{I_m/\pi} = \frac{\pi}{2} = 1.57$$

and hence

$$r = \sqrt{1.57^2 - 1} = 1.21 \quad (13-16)$$

It follows from this that the rms value of the ripple voltage exceeds the d-c potential of the output. This merely tends to show that a single-phase half-wave rectifier without filter is a relatively poor device for converting a-c to d-c potential.

**13-3. Single-phase Full-wave Rectifier.** The circuit of the single-phase full-wave rectifier, given in Fig. 13-4, is seen to bear some resemblance to a push-pull circuit. Actually the circuit comprises two half-wave circuits which are so connected that conduction takes place through

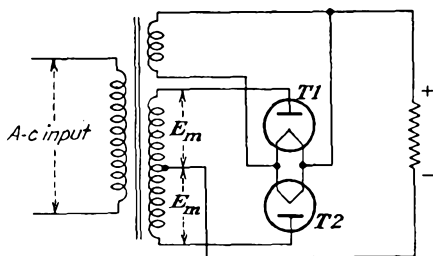


FIG. 13-4. Schematic wiring diagram of a single-phase full-wave rectifier.

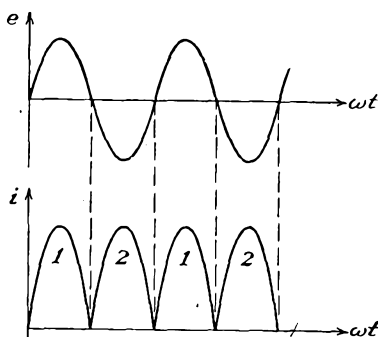


FIG. 13-5. Transformer voltage and output load current in a single-phase full-wave rectifier.

one tube during one-half of the total power cycle and through the other tube during the second half of the power cycle. The output current through the load has the form illustrated, where the portions of the wave marked 1 flow through tube *T1* and the portions of the wave marked 2 flow through tube *T2*.

The d-c and rms values of the load current are found from Eqs. (13-6) and (13-11) to be

$$\left. \begin{aligned} I_{d-c} &= \frac{2I_m}{\pi} \\ I_{rms} &= \frac{I_m}{\sqrt{2}} \end{aligned} \right\} \quad (13-17)$$

where  $I_m$  is the peak value of the current wave. The d-c output power

is then

$$P_{d-c} = I_{d-c}^2 R_l = \left(\frac{2}{\pi}\right)^2 \frac{E_m^2 R_l}{(r_p + R_l)^2} \quad (13-18)$$

By comparing this expression with Eq. (13-7) it is seen that the power delivered to the load is higher by a factor of 4 in the full-wave case. However, the power depends on the circuit parameters in the same way as for the half-wave circuit.

The input power from the a-c source is readily found to have the same form as Eq. (13-10), *viz.*,

$$P_i = I_{rms}^2 (r_p + R_l) \quad (13-19)$$

The efficiency of rectification is

$$\eta_r = \frac{81.2}{1 + (r_p/R_l)} \% \quad (13-20)$$

This expressions shows a theoretical maximum that is twice that of the half-wave rectifier.

The ripple factor is readily found when it is noted that

$$\frac{I_{rms}}{I_{d-c}} = \frac{I_m/\sqrt{2}}{2I_m/\pi} = 1.11$$

From Eq. (13-15),

$$r = \sqrt{1.11^2 - 1} = 0.482 \quad (13-21)$$

Thus the ripple factor has dropped from 1.21 in the half-wave rectifier to 0.482 in the present case. What has been accomplished in the full-wave rectifier therefore is that the rectification process has become more efficient, with a higher percentage of the power supplied to the circuit being converted into the desired d-c power, and with a consequent smaller fraction remaining in a-c form, which, while producing heating of the load, does not contribute to the desired d-c power.

A study of Fig. 13-4 indicates that when one tube is conducting, say *T1*, then tube *T2* is in the nonconducting state. Except for the tube drop  $i_b r_p$  in *T1*, the peak-inverse-potential difference across *T2* is  $2E_m$ , or twice the transformer maximum voltage. The potential stress between windings of the filament transformer is seen to be the full d-c potential, if the negative is grounded, and is sensibly zero if the positive is grounded.

**13-4. Circuits with Gas Diodes.** Gas diodes may be used in the half-wave and full-wave circuits discussed above. Owing to their different plate characteristics, the results are somewhat different. For these tubes a sensibly constant voltage appears across the tube when the tube is conducting, but conduction does not begin until the applied potential exceeds the breakdown potential of the tube. The tube will consequently

conduct for less than 180 deg in each cycle. The situation is illustrated in Fig. 13-6.

The equation of the potential across the load during conduction is, by applying Kirchhoff's law to the plate circuit,

$$e_l = i_b R_l = E_m \sin \alpha - E_0 \quad (13-22)$$

and the corresponding expression for the current is

$$i_b = \frac{E_m \sin \alpha - E_0}{R_l} \quad (13-23)$$

where  $E_0$  is the constant tube drop during conduction.

The d-c plate current is found by taking the average value of the instantaneous current and is

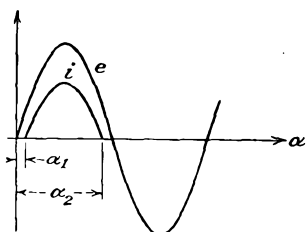


FIG. 13-6. The applied potential and the current wave shape in a half-wave rectifier circuit using a gas diode.

$$I_{d-c} = \frac{1}{2\pi} \int_{\alpha_1}^{\alpha_2} \frac{E_m \sin \alpha - E_0}{R} d\alpha \quad (13-24)$$

where  $\alpha_1$  is the angle at which the tube fires and  $\alpha_2$  is the angle at which conduction ceases. Ordinarily the applied plate potential is much larger than  $E_0$ , and the angles  $\alpha_1$  and  $\pi - \alpha_2$  are very nearly zero. Consequently the limits on the integral of Eq. (13-24) may be changed to 0 and  $\pi$  without appreciable error in the result. When this

is done and the integral is evaluated, it is found that

$$I_{d-c} = \frac{E_m}{\pi R_l} - \frac{E_0}{2R_l} = \frac{E_m}{\pi R_l} \left( 1 - \frac{\pi E_0}{2 E_m} \right) \quad (13-25)$$

The load voltage  $E_{d-c}$  may be written as

$$E_{d-c} = \frac{E_m}{\pi} \left( 1 - \frac{\pi E_0}{2 E_m} \right) \quad (13-26)$$

This equation does not contain the load current. This means, of course, that  $E_{d-c}$  is independent of the load current, with consequent perfect regulation.

To calculate the efficiency of rectification, it is necessary to calculate the input power to the plate circuit. This is given by

$$P_i = \frac{1}{2\pi} \int_0^\pi e i_b d\alpha = \frac{1}{2\pi} \int_0^\pi E_m \sin \alpha \left( \frac{E_m \sin \alpha - E_0}{R_l} \right) d\alpha$$

where the limits are again taken as 0 and  $\pi$ . This expression reduces to

$$P_i = \frac{E_m^2}{4R_l} \left( 1 - \frac{4 E_0}{\pi E_m} \right) \quad (13-27)$$

The efficiency of rectification is then

$$\eta_r = \frac{P_{d-c}}{P_i} = \frac{4}{\pi^2} \frac{\left(1 - \frac{\pi E_0}{2 E_m}\right)^2}{1 - \frac{4 E_0}{\pi E_m}} \quad (13-28)$$

which may be reduced to the form

$$\eta_r = 40.6 \left(1 - 1.87 \frac{E_0}{E_m}\right) \% \quad (13-29)$$

Note that this value is independent of the load current or load resistance. To the same approximation, namely,  $E_m \gg E_0$ , the ripple factor is given by

$$r = 1.21 \left(1 + 0.5 \frac{E_0}{E_m}\right) \quad (13-30)$$

which is slightly higher than the value with the vacuum diode. This increased ripple results because the tube conduction is less than 180 deg.

The corresponding properties of the full-wave circuit with gas tubes will follow a completely parallel development and yield results that bear the same relation to the vacuum-tube case as the foregoing results do toward the corresponding half-wave vacuum-rectifier case.

**13-5. Miscellaneous Single-phase Rectifier Circuits.** A variety of other rectifier circuits exist which find widespread use. Among these are bridge rectifier circuits, voltage-doubling circuits, and voltage-multiplying circuits. The bridge circuit finds extensive use both as a power rectifier and also as the rectifying system in rectifier-type a-c meters. The rectifiers for power use utilize thermionic diodes of both the vacuum and gas varieties, whereas those for instrument use are usually of the copper oxide or crystal types.

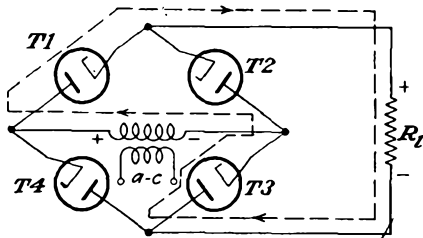


FIG. 13-7. Single-phase full-wave bridge rectifier circuit.

To examine the operation of the bridge circuit, refer to Fig. 13-7. It is observed that two tubes conduct simultaneously during one half of the cycle and the other two tubes conduct during the second half of the cycle. The conduction paths and directions are such that the resulting current through the load is substantially that shown in Fig. 13-5.

The primary features of the bridge circuit are the following: The currents drawn in both the primary and secondary of the plate-supply transformer are sinusoidal. This permits a smaller transformer to be used for

a given output power than is possible with the single-phase full-wave circuit of the two-tube type. Also, the transformer need not have a center tap. Since each tube has only transformer voltage across it on the inverse cycle, the bridge circuit is suitable for high-voltage applications. However, the transformers supplying the heaters of the tubes must be properly insulated for the high voltage.

A rectifier meter is essentially a bridge-rectifier system which utilizes copper oxide elements. The voltage to be measured is applied through a multiplier resistance to two corners of the bridge, a d-c milliammeter being used as an indicating instrument across the other two corners. But as the d-c milliammeter reads average values of current, the scale of the meter is calibrated to give rms values of sinusoidal waves by applying a sinusoidal voltage to the input terminals. The indication on such an instrument is not correct for input signals that contain appreciable harmonics.

A common voltage-doubling circuit is shown in Fig. 13-8. The output<sup>1</sup> from such a circuit is approximately equal to twice the transformer maximum voltage. It operates by alternately charging each of the two capacitors to the transformer peak voltage  $E_m$ , current being continually

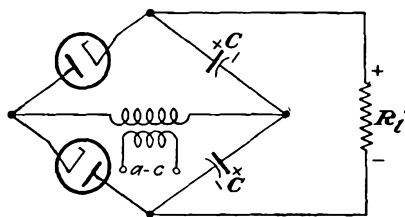


FIG. 13-8. A full-wave voltage-doubling circuit.

drained from the capacitors through the load. This circuit is characterized by poor regulation unless very large capacitors are used. The peak inverse voltage is twice the transformer peak voltage. If ordinary rectifiers are used, two separate filament sources are required. If a relatively low voltage system is built, and these are used extensively in

a-c/d-c radio sets, special tubes such as 25Z5 are available. These tubes are provided with separate indirectly heated cathodes. The cathodes in these tubes are well insulated from the heaters, which are connected in series internally.

An alternative voltage-doubling circuit<sup>2</sup> is shown in Fig. 13-9. The output potential from this circuit, like that from Fig. 13-8, is approximately equal to twice the transformer maximum voltage. It operates by charging capacitor  $C_1$  during one half cycle through tube  $T_1$  to the transformer peak voltage  $E_m$  and during the next half cycle charges  $C_2$  through tube  $T_2$  to the potential determined by that across  $C_1$  and the transformer in series, the peak being approximately  $2E_m$ . The peak inverse voltage across each tube is twice the transformer peak voltage.

This circuit may be extended to a quadrupler by adding two tubes and

two capacitors, as shown in Fig. 13-10. It may be extended to provide  $n$ -fold multiplication, odd or even.

**13-6. Controlled Rectifiers.** It is sometimes necessary to provide a control on the amount of the rectified current in a rectifier. Such controlled currents are required in motor speed control, in certain electric welding operations, in lighting-control installations in theaters, in torque controls of various types, and in a variety of industrial control applica-

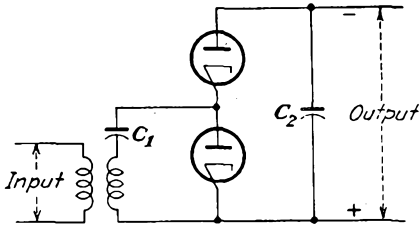


FIG. 13-9. A half-wave voltage-doubling circuit.

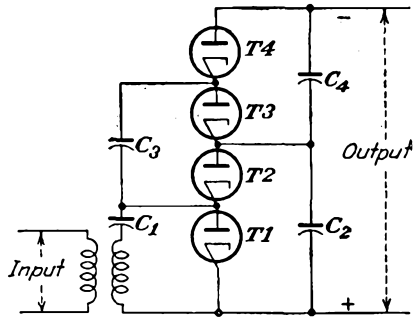


FIG. 13-10. A half-wave voltage-quadrupling circuit.

tions. Such control of the output of a rectifier may be accomplished by controlling the voltage of the power transformer feeding the rectifier, or this might, in some cases, be controlled by inserting a controlling resistor in the output circuit. The first method may require expensive control equipment, and the second would be characterized by poor efficiency. The development of thyratrons and ignitrons has made control a direct and relatively inexpensive process. However, the basic analyses are common to both types of tubes, and no loss of generality is incurred by confining our attention to thyratrons.

In the discussion in Sec. 2-19 it was indicated that the complete electrostatic shielding of the cathode by the massive grid structure in the thyatron provides a means for controlling the initiation of the arc in the tube by controlling the grid potential. Thus since the arc is extinguished once each cycle on each negative half cycle, provided that the arc is initiated regularly, control is possible if the point in each half cycle at which the arc is initiated can be controlled. Such regular control is possible, thus providing a control on the average rectified current.

In order to analyze the action of a thyatron in a controlled circuit, use is made of the critical grid breakdown characteristic of Fig. 2-26. As indicated in Sec. 2-19 a knowledge of this single curve is sufficient to predict the behavior of the thyatron in the control circuit. This curve gives the minimum grid potential required for conduction to occur for

each value of plate potential. Thus if a sinusoidal plate voltage is applied to the tube, the potential on the grid just to permit conduction at each point in the cycle is found from the critical grid curve. The conditions are illustrated in Fig. 13-11. On this diagram, corresponding to any time  $t_1$  in the positive half cycle, the plate potential is  $e_{b1}$ . The corresponding critical grid potential is obtained directly from the critical grid breakdown characteristic and is shown in the figure. This means that, unless the grid potential is more positive than that given by  $e_{cg}$  at the particular instant, conduction will not take place. Of course, once con-

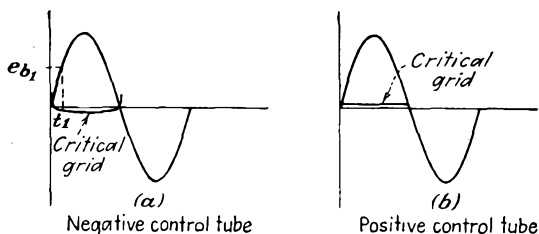


FIG. 13-11. The grid-control curve for an applied sinusoidal plate potential to a thyatron.

duction begins at any point in the cycle, the grid loses control of the arc and cannot again control until the arc is extinguished.

Suppose that the circuit is so arranged that the grid potential exceeds the critical grid breakdown value at some angle, say  $\phi$ . Conduction will start at this point in the cycle. But the voltage drop across the tube

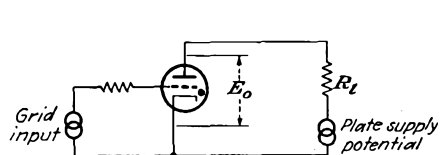


FIG. 13-12. A thyatron circuit with a-c plate and grid excitation.

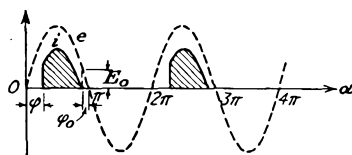


FIG. 13-13. The plate potential and the plate current in a thyatron.

during conduction of the thyatron, like that in any gas arc discharge, remains substantially constant at a low value  $E_0$  that is independent of the current. Consequently the current in the plate circuit of the tube is readily found. Refer to Fig. 13-12, which gives the schematic diagram of a thyatron circuit, and to Fig. 13-13, which shows the voltage and current wave shapes in the thyatron.

If the tube drop after conduction has begun is  $E_0$ , then the current in the plate load of resistance  $R_l$  during the conducting portion of the cycle is

$$i_b = \frac{E_m \sin \alpha - E_0}{R_l} \quad (13-31)$$

where  $E_m$  is the maximum value of the applied potential. Clearly, the current is zero until conduction takes place, after which it assumes the value dictated by Eq. (13-31). The current follows the form of Eq. (13-31) until the supply voltage  $e$  falls below  $E_0$  at the phase  $\pi - \varphi_0$ . The current remains zero until the phase  $\varphi$  is again reached in the next cycle.

The average rectified current, *i.e.*, the value read on a d-c ammeter, is given by the expression

$$I_{a-c} = \frac{1}{2\pi} \int_{\varphi}^{\pi - \varphi_0} i_b d\alpha$$

$$= \frac{E_m}{2\pi R_t} \int_{\varphi}^{\pi - \varphi_0} \left( \sin \alpha - \frac{E_0}{E_m} \right) d\alpha$$

which integrates to

$$I_{a-c} = \frac{E_m}{2\pi R_t} \left[ \cos \varphi + \cos \varphi_0 - \frac{E_0}{E_m} (\pi - \varphi_0 - \varphi) \right] \quad (13-32)$$

where  $\alpha = \omega t$ , and where  $\varphi_0$  is defined by the relation

$$E_0 = E_m \sin \varphi_0 \quad (13-33)$$

If the ratio  $E_0/E_m$  is very small, then  $\varphi_0$  may be taken as zero. Equation (13-32) reduces under this condition to the form

$$I_{a-c} \doteq \frac{E_m}{2\pi R_t} (1 + \cos \varphi) \quad (13-34)$$

The limits of variation of the angle are from 0 to  $\pi$ .

It is clear from this analysis that the average rectified current can be controlled by varying the position in the cycle at which the grid voltage exceeds the critical grid starting value. The maximum current is obtained when the arc is initiated at the beginning of each cycle.

The minimum current is obtained when the arc is not initiated, and this would occur if initiation were adjusted to occur at the end of each cycle. Sketches showing the character of the results are given in Fig. 13-14.

The potential across the thyatron throughout the cycle will vary in the manner illustrated in Fig. 13-15. During the portion of the cycle when

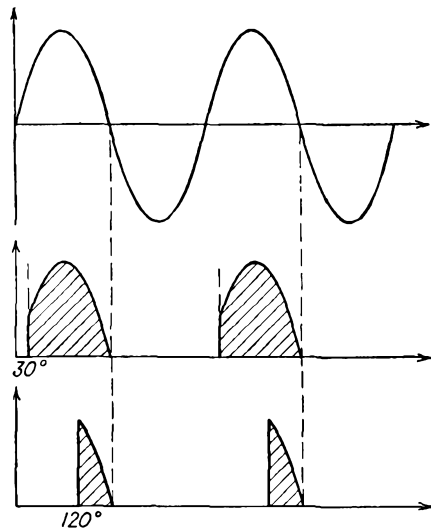


FIG. 13-14. The character of the conduction in a thyatron for various angles of initiation of the arc.

the tube is not conducting current, the full applied potential appears across the tube. During the portion of the cycle when the tube is conducting, the drop across the tube is  $E_0$ , which is assumed constant and independent of the tube current.

The reading of a d-c voltmeter placed across the tube will be

$$E_{d-c} = \frac{1}{2\pi} \int_0^{2\pi} e_b d\alpha$$

This integrates to

$$E_{d-c} = \frac{1}{2\pi} \left( \int_0^\varphi E_m \sin \alpha d\alpha + \int_\varphi^{\pi-\varphi_0} E_0 d\alpha + \int_{\pi-\varphi_0}^{2\pi} E_m \sin \alpha d\alpha \right)$$

If the peak transformer voltage  $E_m \gg E_0$ , this reduces to

$$E_{d-c} \doteq -\frac{E_m}{2\pi} (1 + \cos \varphi) \quad (13-35)$$

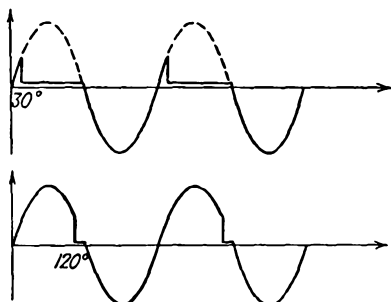


FIG. 13-15. The potential across the thyatron for various current-conduction periods.

The appearance of the negative sign merely means that the cathode is more positive than the plate for most of the cycle. It is to be emphasized that the d-c voltmeter does not read the value  $E_0$  when an a-c potential is applied to the tube.

The readings of d-c and a-c indicating instruments may be calculated in somewhat similar ways.

For example, the reading of an a-c ammeter in the plate lead will be

$$I_{rms} = \sqrt{\frac{1}{2\pi} \int_0^{2\pi} i_b^2 d\alpha}$$

which is

$$I_{rms} = \sqrt{\frac{1}{2\pi} \int_\varphi^{\pi-\varphi_0} \left( \frac{E_m \sin \alpha - E_0}{R_l} \right)^2 d\alpha} \quad (13-36)$$

This integration is readily effected. Similarly, the reading of a wattmeter to indicate the total power supplied to the plate circuit is

$$P = \frac{1}{2\pi} \int_0^{2\pi} e_b i_b d\alpha$$

which is

$$P = \frac{1}{2\pi} \int_\varphi^{\pi-\varphi_0} E_m \sin \alpha \left( \frac{E_m \sin \alpha - E_0}{R_l} \right) d\alpha \quad (13-37)$$

This integration is also readily effected. In particular, it is essential to

set up the basic expression for any quantity before proceeding in its evaluation.

**13-7. Phase-shift Control.** In the phase-shift method of control, the conduction point of the cycle is controlled by controlling the phase angle between the plate and grid potentials. The situation is illustrated in Fig. 13-16. In this figure, the grid-cathode potential  $e_c$  lags the plate-cathode potential  $e_b$  by the angle  $\theta$ , as indicated in the voltage sinor diagram. Note from the figure that the grid potential equals the critical

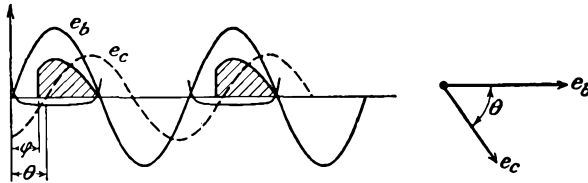


FIG. 13-16. Phase-shift control of a thyatron.

grid breakdown potential at the angle  $\varphi$  and conduction begins at this point in the cycle. The arc is extinguished when the plate potential falls below the value to maintain conduction.

If the applied grid potential is large compared with the critical grid potential at the point of conduction, the angles  $\varphi$  and  $\theta$  are approximately the same. Also, it may be assumed under these conditions that the critical grid curve coincides with the zero-voltage axis. Also, if  $E_m \gg E_0$ , then Eq. (13-34) will give the dependence of d-c load current on the phase angle for all values of  $\varphi$  for which the grid voltage lags behind the plate potential. When the grid potential leads the plate potential by any angle, conduction will occur very nearly at the beginning of each cycle, with full rectification. A sketch showing these results is given in Fig. 13-17. The curve possesses a discontinuity at the 180-deg position, since for an angle slightly larger than 180 deg the plate current is at its full value, whereas for an angle slightly less than 180 deg the plate current is zero.

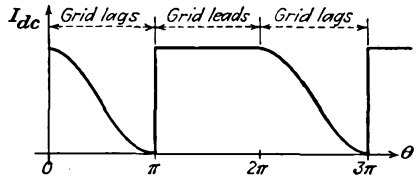


FIG. 13-17. The average load current as a function of phase angle between the grid and plate potentials.

For those cases where a small plate potential or a small grid potential is used, the foregoing simplifications are not valid. However, the analysis follows the same general form, due account being taken of the difference between  $\varphi$  and  $\theta$  and of the angles  $\pi - \varphi_0$  and  $\pi$ .

Circuits for achieving the phase-shift control in a single-phase system are readily analyzed. A common circuit and the voltage sinor diagram

that applies to this circuit are given in Fig. 13-18. The phase between the grid and the plate voltages is controlled by means of the two imped-

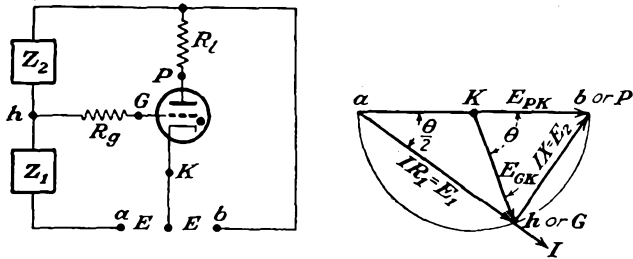


FIG. 13-18. A simple phase-shifting network, and the voltage circle diagram.

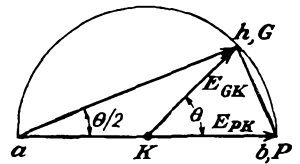
ances  $Z_1$  and  $Z_2$ . It should be noted that the voltage circle diagram in Fig. 13-18 has been drawn under the assumption that

$$Z_1 = R \quad (\text{a resistance}) \quad Z_2 = \omega L \quad (\text{an inductance})$$

Also, the voltage circle diagram applies only during the periods before conduction begins in each cycle. Before conduction begins, there is no current in the load  $R_l$ , and points  $b$  and  $P$  are the same. From the results of the voltage circle diagram, it is clear that the phase  $\theta$  between the plate and grid potentials can be varied over the range from 0 to 180 deg by varying the control resistor  $R$  in the phase-shifting network, with  $\theta$  at 180 deg when  $R = 0$  and with  $\theta$  at 0 deg when  $R = \infty$ . Evidently, the load current will decrease as the resistor  $R$  decreases. The phase angle  $\theta$  is, from inspection of Fig. 13-18,

$$\tan \frac{\theta}{2} = \frac{E_2}{E_1} = \frac{Z_2}{Z_1} \tag{13-38}$$

If the control impedances  $Z_1$  and  $Z_2$  are interchanged, then the sinor diagram that results has the following form, which shows that  $E_{\theta k}$  leads the voltage  $E_{pk}$ . Then, from Fig. 13-17, no control over the plate current is possible, and  $I_{a-c}$  is a constant and equal to its maximum value for all values of  $\theta$ . The use of  $R$  and  $C$  as control impedances is possible and is generally preferred over the use of  $R$  and  $L$ . With an  $RC$  phase-shifting circuit, control is possible for  $Z_1 = X_c$ ,  $Z_2 = R$  but is not possible for  $Z_1 = R$ ,  $Z_2 = X_c$ .



**13-8. D-C Bias Control.** The magnitude of the d-c or average rectified current of a thyratron may be controlled by applying a d-c bias to the grid of the tube and controlling its magnitude. The plate supply must be an a-c potential. The situation is best understood by reference to Fig. 13-19.

The tube will conduct at the point where  $E_0$  intersects the critical grid curve, the angle  $\varphi$  in the diagram. Clearly, if the negative grid potential is too large to intersect the critical grid curve, no conduction will be possible. The optimum bias is that for which the grid-voltage line is tangent to the critical grid curve, and the tube conducts for one-half of the cycle. For less negative bias, the conduction angle  $\varphi$  is less than 90 deg. Control is evidently possible over the range from full conduction to half conduction. The results of Fig. 13-20 show the character of the control.

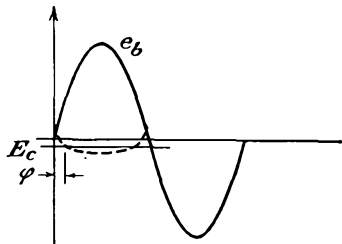


FIG. 13-19. D-c bias control of a thyatron.

**13-9. Bias Phase Control.** The combination of d-c and a-c potentials as a bias yields bias phase control. A circuit for such control is given in Fig. 13-21. The network comprising  $R$  and  $C$  serves to introduce an a-c potential of fixed phase with respect to the plate potential.

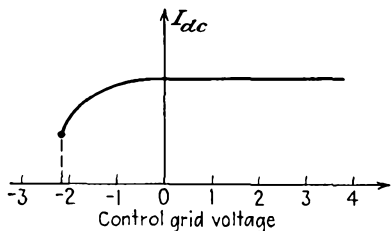


FIG. 13-20. The average plate current in a thyatron as a function of the d-c grid-bias potential.

Suppose, for convenience, that  $R = X_c$ . The a-c grid potential will then lag the plate voltage by 45 deg. The amplitude of the a-c grid potential is 0.707 that of the plate potential. Suppose also that the critical grid potential coincides with the zero axis.

The general features of the operation of this control are illustrated in Fig. 13-22. The conditions corresponding to three different values of  $E_c$  are illustrated. In the first,  $E_c$  is positive; in the second,  $E_c$  is zero; in the third,  $E_c$  is negative. For the circuit shown, the minimum rectified current occurs when  $E_c$  is negative and equal to  $E_{gm}$ . Conduction begins at 135 deg in the cycle and continues until the end of the cycle. If the d-c bias is made more negative than this, no conduction is possible. It is evident from the diagrams that conduction will begin at the start of the cycle when the d-c bias equals 0.707 times  $E_{gm}$ .

**13-10. On-off Control.** A variety of circuits exist which permit on-off control. Such circuits would be used when it is desired to use a thyatron

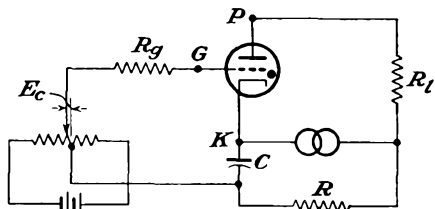


FIG. 13-21. A circuit for bias phase control of a thyatron.

as an arcless switch or contactor. A circuit for on-off control is given in Fig. 13-23. With switch  $S$  open, no conduction occurs since  $E_{cc}$  is so adjusted that it is more negative than the maximum negative critical grid value. When the switch  $S$  is closed, the grid is tied to the cathode and approximately maximum rectified current is delivered. The resistor  $R$  serves to prevent short circuiting of the battery source  $E_{cc}$  when  $S$  is closed.

**13-11. Control of Ignitrons.** As discussed in Sec. 2-21, the ignitron will

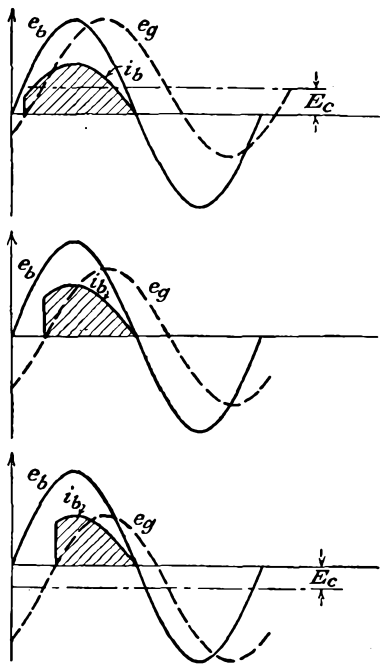


FIG. 13-22. Bias phase control, showing current variations for three different values of d-c component  $E_c$ .

not conduct at any portion of the cycle of an applied a-c potential to the plate unless ignition is caused by applying a potential to the igniter rod. Moreover, since this ignition pulse may be applied at any point in the cycle, control of the average current is afforded by controlling the ignition of the tube. However, the instantaneous power required by the igniter circuit of the ignitron is higher than that required by the grid circuit of a thyatron, and the methods of thyatron control are not applicable to ignitrons. But with control accom-

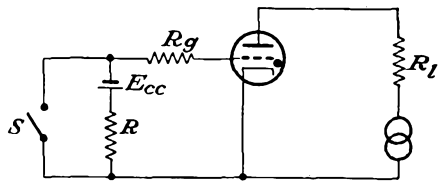


FIG. 13-23. An on-off thyatron control circuit.

plished the general discussion of Sec. 13-6 is applicable, and Eqs. (13-31) to (13-37) express the results for the ignitron as well as for the thyatron.

Several common methods of establishing the point of ignition in each cycle of an ignitron are illustrated in Fig. 13-24. These methods utilize thyatrons for the control of the ignitron. In the first of these diagrams, the ignitron current passes through the load resistor, whereas, in the second, the igniter-rod current does not pass through the load.

Refer to Fig. 13-24*b*, and suppose that the thyatron is not conducting. In this circuit the capacitor  $C$  will be charged to the peak value of the transformer voltage through the rectifier. If the thyatron grid voltage

is adjusted to permit conduction, the capacitor charge will pass through the thyatron and igniter-rod circuits, and the ignitron will conduct provided that the ignitron anode potential is sufficiently positive to maintain the discharge. The current surge through the ignitron-rod circuit

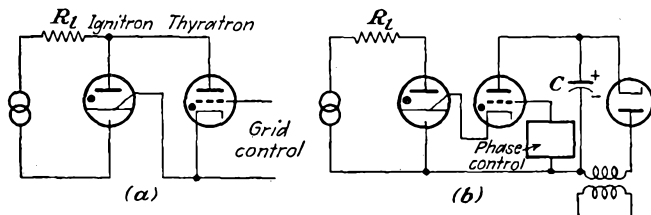


FIG. 13-24. Several ignitron control circuits.

will quickly discharge the capacitor, the thyatron anode potential will fall below that to maintain the arc, and the thyatron igniter-rod circuit current will fall to zero. The capacitor will be recharged through the diode rectifier circuit in time to control the ignition point in the next cycle.

#### REFERENCES

1. For an analysis of the operation, see Waidelich, D. L., *Proc. IRE*, **29**, 554 (1941).
2. Cockcroft, J. D., and E. T. S. Walton, *Proc. Roy. Soc. (London)*, **136**, 619 (1932).  
Waidelich, D. L., *Proc. IRE*, **30**, 534 (1942).  
Mitchell, R. G., *Wireless Eng.*, **22**, 474 (1945).

#### PROBLEMS

**13-1.** A type 5U4G is connected in a half-wave circuit to supply power to a 1,500-ohm load from a 350-volt rms source of potential.

- a. On a plate characteristic of the tube, plot the load line, and from this find the dynamic curve.
- b. Obtain a plot of the output-current wave shape for a sinusoidal applied voltage.
- c. Estimate the value of the plate resistance  $r_p$  from the static characteristic at four different values of current (50, 100, 150, 200 ma). Use the average of these as the  $r_p$  of the tube.
- d. Plot on the curve in part b the value obtained from Eq. (13-4), and compare.

**13-2.** The two sections of a 6X5 diode are connected in parallel and supply power to a 1,000-ohm load from a 325-volt rms source of potential. The effective plate resistance of the parallel combination of diodes is approximately 125 ohms. Calculate the following:

- a. The d-c load current.
- b. The a-c current (rms).
- c. The reading of a d-c voltmeter placed across the diode terminals.
- d. The total input power to the plate circuit.

- e. The efficiency of rectification.
- f. The regulation from no load to the given load.
- g. The ripple factor.

**13-3.** Suppose that a 6X5 tube supplies power to a 1,000-ohm load from a 325-0-325 transformer. Repeat Prob. 13-2 under these conditions.

**13-4.** Show that the input power to a rectifier using gas diodes may be expressed in the form

$$P_i = I_{rms}^2 R_L + E_o I_{d-o}$$

**13-5.** A gas diode for which the breakdown and maintaining voltage is taken to be 10 volts supplies power in a half-wave rectifier circuit to a 1,000-ohm load from a 325-volt rms source. Calculate the following:

- a. The d-c current through the load.
- b. The a-c (rms) current through the load.
- c. The reading of a d-c voltmeter placed across the diode.
- d. The reading of an rms a-c voltmeter across the diode.
- e. The power input to the plate circuit.
- f. The efficiency of rectification.
- g. The ripple factor.

**13-6.** The peak inverse plate voltage rating of a 2X2/879 half-wave high-vacuum rectifier is 12,500 volts. Calculate the maximum d-c voltage possible to a load, without exceeding the peak inverse voltage, when such tubes are used in

- a. A half-wave circuit.
- b. A full-wave circuit.
- c. A full-wave bridge circuit.
- d. A full-wave voltage-doubling circuit.
- e. A half-wave voltage-doubling circuit.
- f. Specify in each case the insulation strength of each filament transformer when the positive terminal is grounded.

**13-7.** Analyze the operation of the voltage-quadrupling circuit of Fig. 13-10. Calculate

- a. The maximum possible voltage across each condenser.
- b. The peak inverse voltage of each tube.
- c. The required insulation strength of each filament transformer.

**13-8.** The arc drop in a certain thyratron is 12 volts. The tube supplies power to a 100-ohm resistor from a 330-volt rms supply. Calculate the reading of a d-c ammeter in the circuit when

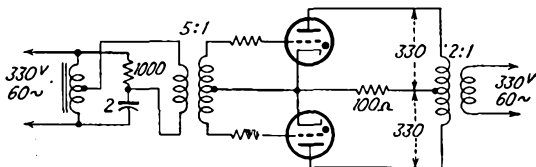
- a. The grid and plate voltages are in phase.
- b. The grid voltage leads the plate voltage by 60 deg.
- c. The grid voltage lags the plate voltage by 60 deg.

Assume a zero critical grid voltage for all values of plate voltage.

**13-9.** The circuit of Fig. 13-18 is used to control the current in a load of 100 ohms. The voltage  $E_{ab} = 330$  volts rms, and the power frequency is 60 cps. A 1,000-ohm resistor and a 2- $\mu$ f capacitor are available.

- Draw a voltage diagram that applies for the case where conduction occurs for less than the full half cycle.
- Calculate the d-c current in the load.
- Calculate the a-c power supplied by the line to the plate circuit.

**13-10.** The full-wave controlled rectifier for a certain application is shown in the accompanying diagram. The resistor in the phase-shift network is adjusted to 1,000 ohms.



- Draw a voltage diagram that applies for the case where conduction continues for less than the full half cycle.
- Calculate the d-c current in the load.
- Calculate the a-c power supplied by the line to the plate circuit.

**13-11.** An FG-27A tube operates at a temperature of 50°C and supplies power to a 100-ohm load from an input potential source of 330 volts rms.

- A d-c bias potential of  $-4$  is applied. Calculate the d-c plate current.
- A 4-volt rms grid potential that lags the plate by 60 deg is applied. Calculate the d-c plate current.
- The two sources in parts *a* and *b* are connected in series. Calculate the d-c plate current.

**13-12.** An ignitron is used in the circuit of Fig. 13-24*b*. The phase of the control circuit of the thyatron is adjusted for conduction to begin 60 deg after the beginning of each cycle. The tube drop during conduction is 20 volts. If the applied voltage is 330 volts rms and the load resistor is 20 ohms, calculate

- The d-c load current.
- The a-c power to the load circuit.
- The power dissipated in the tube.
- The total power dissipated in the load.

---

## CHAPTER 14

### RECTIFIER FILTERS AND REGULATORS

It is usually the requirement of a power supply to provide a relatively ripple-free source of d-c potential from an a-c line. However, as seen in the last chapter, a rectifier actually provides an output which contains a-c components in addition to the d-c term that is desired, the magnitude of the a-c components being specified by the ripple factor. It is customary to include a filter between the rectifier and the output to attenuate these ripple components.

The analysis of the action of such filters is complicated by the fact that the rectifier as a driving source contains nonlinear circuit elements, thus requiring the solution of circuits with nonlinear elements. It is possible to make reasonable assumptions in order to effect a solution. In consequence, the results obtained are only approximate.

**14-1. The Harmonic Components in Rectifier Circuits.** An analytic representation of the output of the single-phase half-wave rectifier is obtained in terms of a Fourier series. This series representation has the form

$$i = b_0 + \sum_{k=1}^{\infty} b_k \cos k\alpha + \sum_{k=1}^{\infty} a_k \sin k\alpha \quad (14-1)$$

where  $\alpha = \omega t$  and where the coefficients that appear in the series are given by the integrals

$$\left. \begin{aligned} b_0 &= \frac{1}{2\pi} \int_0^{2\pi} i \, d\alpha \\ b_k &= \frac{1}{\pi} \int_0^{2\pi} i \cos k\alpha \, d\alpha \\ a_k &= \frac{1}{\pi} \int_0^{2\pi} i \sin k\alpha \, d\alpha \end{aligned} \right\} \quad (14-2)$$

It should be recalled that the constant term  $b_0$  that appears in the Fourier series is the average or d-c value of the current.

The explicit expression for the current in a half-wave rectifier circuit, which is obtained by performing the indicated integrations using Eqs. (13-4) over the two specified intervals, yields

$$i = I_m \left[ \frac{1}{\pi} + \frac{1}{2} \sin \omega t - \frac{2}{\pi} \sum_{k=2,4,6,\dots} \frac{\cos k\omega t}{(k+1)(k-1)} \right] \quad (14-3)$$

where  $I_m = E_m/(r_p + R_l)$  and  $E_m$  is the peak transformer voltage. The lowest angular frequency that is present in this expression is that of the primary source. Also, except for this single term of frequency  $\omega$ , all other harmonic terms that appear in the expression are even-harmonic terms.

The corresponding Fourier series representation of the output of the full-wave rectifier which is illustrated in Fig. 13-5 may be derived from Eq. (14-3). Thus, by recalling that the full-wave circuit comprises two half-wave circuits which are so arranged that one circuit is operating during the interval when the other is not operating, then clearly the currents are functionally related by the expression  $i_2(\alpha) = i_1(\alpha + \pi)$ . The total load current, which is  $i = i_1 + i_2$ , then attains the form

$$i = I_m \left[ \frac{2}{\pi} - \frac{4}{\pi} \sum_{\substack{k \text{ even} \\ k \neq 0}} \frac{\cos k\omega t}{(k+1)(k-1)} \right] \quad (14-4)$$

where  $I_m = E_m/(R_l + r_p)$  and where  $E_m$  is the maximum value of the transformer voltage measured to the center tap.

A comparison of Eqs. (14-3) and (14-4) indicates that the fundamental angular-frequency term has been eliminated in the full-wave circuit, the lowest harmonic term in the output being  $2\omega$ , a second-harmonic term. This will be found to be a distinct advantage in filtering.

The Fourier series representation of the half-wave and full-wave circuits using gas diodes can be obtained in the same way as above, although the form will be more complex. This is so because conduction begins at some small angle  $\varphi_0$  and ceases at the angle  $\pi - \varphi_0$ , when it is assumed that the breakdown and the extinction potentials are equal. But since these angles are usually small under normal operating conditions, it will be assumed that Eqs. (14-3) and (14-4) are applicable for circuits with vacuum or gas diodes. The Fourier series representation of the output of a controlled rectifier is also possible, although the result is quite complex. However, such controlled rectifiers are ordinarily used in services in which the ripple is not of particular concern, and, as a result, no detailed analysis will be undertaken. Some results will be given below covering these rectifiers, however.

**14-2. Inductor Filters.** The operation of an inductor filter depends on the inherent property of the inductance to oppose any change of current that may tend to take place in the circuit. Consequently any sudden changes in current that might otherwise take place in the circuit

without an inductance would have these rapid current changes smoothed out by the inductance.

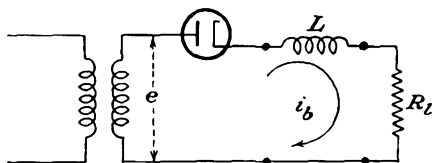


FIG. 14-1. Half-wave rectifier circuit with choke filter.

In particular, suppose that an inductor is connected in series with the load in a single-phase half-wave circuit, as illustrated in Fig. 14-1. For simplicity, suppose that the tube and choke resistances are negligible. Then

the controlling differential equation for the current in the circuit during the time that current flows is

$$L \frac{di_b}{dt} + R_L i_b = E_m \sin \omega t \tag{14-5}$$

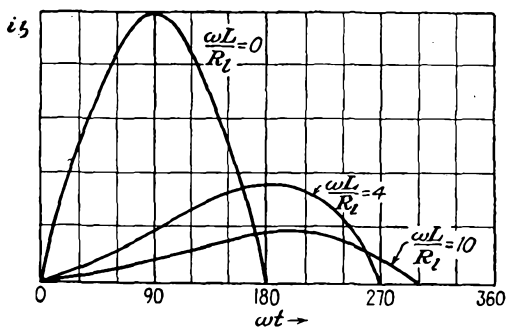


FIG. 14-2. The effect of changing inductance on the wave form of the current in a half-wave rectifier with inductor filter. The load  $R_L$  is assumed constant.

A solution of this differential equation may be effected. This solution is complicated by the fact that current continues over only a portion of the cycle. The general character of the solution is shown graphically in Fig. 14-2, in which is shown the effect of changing the inductance on the wave form of the current. Since a simple inductance choke is seldom used with a half-wave circuit, further details of the analysis will not be given.

Suppose that an inductor filter is applied to the output of a full-wave rectifier. The circuit and a sketch of the output-current wave shape are given in Fig. 14-3. Since no cutout occurs in the current, the analysis

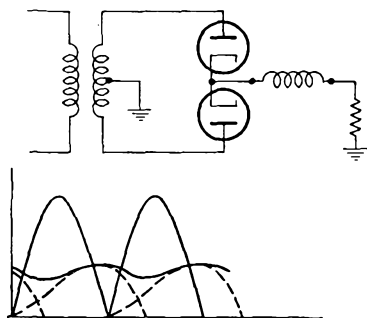


FIG. 14-3. Full-wave rectifier circuit with inductance choke, and the wave shape of the load current.

assumes a different form from that for the half-wave case. Now, instead of considering the circuit differential equation, as in Eq. (14-5), and adjusting the initial conditions to fulfill the required physical conditions, an approximate solution is effected. It is supposed that the equation of the potential that is applied to the filter is given by Eq. (14-4). Moreover, it is noted that the amplitudes of the a-c terms beyond the first, and this is of second-harmonic frequency, are small compared with that of the first term. In particular, the fourth-harmonic frequency term is only 20 per cent of the second-harmonic term. Furthermore, the impedance of the inductance increases with frequency, and better filtering action exists for the higher-harmonic terms. Consequently it is assumed that all higher-order terms may be neglected.

In accordance with the discussion, it is supposed that the input potential to the rectifier and load has the approximate form

$$e = \frac{2E_m}{\pi} - \frac{4E_m}{3\pi} \cos 2\omega t \quad (14-6)$$

The corresponding load current is, in accordance with a-c circuit theory,

$$i_l = \frac{2E_m}{\pi R_l} - \frac{4E_m \cos(2\omega t - \psi)}{3\pi \sqrt{R_l^2 + 4\omega^2 L^2}} \quad (14-7)$$

where

$$\tan \psi = \frac{2\omega L}{R_l} \quad (14-8)$$

The ripple factor, defined in Eq. (13-14), becomes

$$r = \frac{\frac{4E_m}{3\pi} \frac{1}{\sqrt{R_l^2 + 4\omega^2 L^2}}}{\frac{2E_m}{\pi R_l}} = \frac{2R_l}{3\sqrt{2}} \frac{1}{\sqrt{R_l^2 + 4\omega^2 L^2}}$$

which may be expressed in the form

$$r = \frac{2}{3\sqrt{2}} \frac{1}{\sqrt{1 + (4\omega^2 L^2/R_l^2)}} \quad (14-9)$$

If the ratio  $\omega L/R_l$  is large, this reduces to

$$r = \frac{1}{3\sqrt{2}} \frac{R_l}{\omega L} \quad (14-10)$$

This expression shows that the filtering improves with decreased load resistance or, correspondingly, with increased load current. At no load,  $R_l = \infty$ , and the filtering is poorest, with  $r = 2/3\sqrt{2} = 0.47$ . This is also the result which applies when no choke is included in the circuit.

[Compare with result with Eq. (13-21), which gives 0.482. The difference arises from the terms in the Fourier series that have been neglected.] The expression also shows that large inductances are accompanied by decreased ripple.

The d-c output voltage is given by

$$E_{d-c} = I_{d-c}R_l = \frac{2E_m}{\pi} = 0.637E_m = 0.90E_{rms} \quad (14-11)$$

where  $E_{rms}$  is the transformer secondary voltage measured to the center tap. Note that under the assumptions made, *viz.*, negligible power-transformer leakage reactance and negligible transformer resistance, tube resistance, and inductor resistance, the output voltage does not change with load, with consequent perfect regulation. Because the neglected effects are not negligible, the output voltage actually decreases with increased current.

**14-3. Capacitor Filter.** Filtering is frequently effected by shunting the load with a capacitor. During the time that the rectifier output is

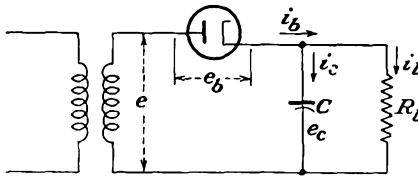


FIG. 14-4. A single-phase half-wave capacitor filtered rectifier.

increasing, the capacitor is charging to the rectifier output potential and energy is stored in the capacitor. During the time that the rectifier potential falls below that of the capacitor, the capacitor delivers energy to the load, thus maintaining the voltage at a high level for a longer period

than without the capacitor. The ripple is therefore considerably decreased. Clearly, the diode acts as a switch, permitting charge to flow into the capacitor when the rectifier voltage exceeds the capacitor voltage, and then acts to disconnect the power source when the potential falls below that of the capacitor.

To examine the operation in some detail, refer to Fig. 14-4, which shows a diagram of the circuit. The tube current during the conducting portion of the cycle is

$$i_b = i_c + i_l \quad (14-12)$$

where

$$i_l = \frac{e_l}{R_l} = \frac{e_c}{R_l} \quad (14-13)$$

and where

$$i_c = \frac{dq_c}{dt} = C \frac{de_c}{dt} \quad (14-14)$$

where  $q_c$  is the capacitor charge. The controlling differential equation

of the charging current through the tube is then

$$i_b = \frac{e_c}{R_1} + C \frac{de_c}{dt} \quad (14-15)$$

But the voltage  $e_c$  during the time that the tube is conducting is simply the transformer voltage, if the tube drop is neglected. Hence the capacitor voltage during this portion of the cycle is sinusoidal and is

$$e_c = e = E_m \sin \omega t$$

The corresponding tube current is

$$i_b = \frac{E_m}{R_1} \sin \omega t + \omega C E_m \cos \omega t$$

This may be written in the equivalent form

$$i_b = E_m \sqrt{\omega^2 C^2 + \frac{1}{R_1^2}} \sin (\omega t + \psi) \quad (14-16)$$

where

$$\psi = \tan^{-1} \omega C R_1 \quad (14-17)$$

A sketch of the current wave is illustrated in Fig. 14-5.

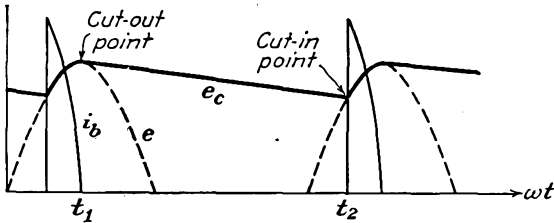


FIG. 14-5. The tube current and the load voltage in a single-phase half-wave capacitor filtered rectifier.

Equation (14-16) shows that the use of large capacitors, in order to improve the filtering, is accompanied by large tube currents. Therefore, if a large capacitor is used for a given load in order to maintain the output voltage more nearly constant, a very peaked current exists. In fact, for a certain required average current demand by the load, the tube-current pulse becomes more and more peaked as the capacitor is made large. This imposes serious duty conditions on the tube, since the average current through the tube may be well within the tube rating and yet the large peak current may injure the cathode. Vacuum diodes would not be appreciably damaged by the high peak-current demands, since temperature-saturated currents may be drawn without seriously injuring the cathode. In the case of gas tubes, however, any attempt to draw higher than temperature-saturated current will usually be accompanied

by severe positive-ion bombardment, with consequent cathode disintegration. It is for this reason that large capacitor input filters should not be used with rectifiers that employ gas diodes.

When the tube stops conducting,  $i_b = 0$  and the controlling differential equation during the nonconducting portion of the cycle is, from Eq. (14-15),

$$C \frac{de_c}{dt} + \frac{e_c}{R_l} = 0 \quad (14-18)$$

The solution of this differential equation is

$$e_c = A e^{-\frac{t}{R_l C}} \quad (14-19)$$

This shows that the capacitor discharges exponentially through the load.

To determine the value of the constant  $A$  that appears in this expression, use is made of the fact that at the time  $t = t_1$ , the cutout time,

$$e_c = e = E_m \sin \omega t_1$$

Combining this result with Eq. (14-19) gives

$$A = E_m \sin \omega t_1 e^{\frac{t_1}{R_l C}} \quad (14-20)$$

and Eq. (14-19) becomes

$$e_c = E_m \sin \omega t_1 e^{-\frac{(t-t_1)}{R_l C}} \quad (14-21)$$

The quantity  $t_1$  that appears in this expression is known, since at  $t = t_1$  the tube current is zero. From Eq. (14-16) this requires

$$\sin(\omega t_1 + \psi) = 0$$

from which it follows that

$$\omega t_1 = \pi - \psi = \pi - \tan^{-1} \omega C R_l \quad (14-22)$$

If  $t_1$  from Eq. (14-22) is substituted in Eq. (14-21), there results

$$e_c = E_m \sin \omega t_1 e^{-\frac{(\omega t + \psi - \pi)}{\omega C R_l}} \quad (14-23)$$

To find the "cutin" point, it is noted that  $e_c$  equals the impressed transformer voltage  $e$  at this point. This requires

$$E_m \sin \omega t_2 = E_m \sin \omega t_1 e^{-\frac{(\omega t_2 - \psi - \pi)}{\omega C R_l}}$$

or

$$\sin \omega t_2 = \sin \omega t_1 e^{-\frac{(\omega t_2 - \psi - \pi)}{\omega C R_l}} \quad (14-24)$$

The evaluation of the cutin time  $t_2$  cannot be solved explicitly, for this is a transcendental equation. Graphical methods can be used effectively in this evaluation. The results are given in Fig. 14-6. Included on this

graph are a plot of Eq. (14-22) for the cutout angle and a plot of Eq. (14-24) for the cutin angle.

The foregoing analysis permits a calculation of the d-c output potential and ripple factor. However, such an analysis is very involved, and it is

expedient to make several reasonable approximations. The character of the approximations is made evident by an inspection of Fig. 14-7, which shows a trace of an oscillogram of the load voltage in a single-phase full-wave capacitor filtered rectifier. The voltage curve may be approximated by two straight-line segments, as shown in Fig. 14-8. If the total capacitor discharge voltage is denoted as  $E_r$ , then, from the diagram, the average value of the voltage is

$$E_{d-c} = E_m - \frac{E_r}{2} \quad (14-25)$$

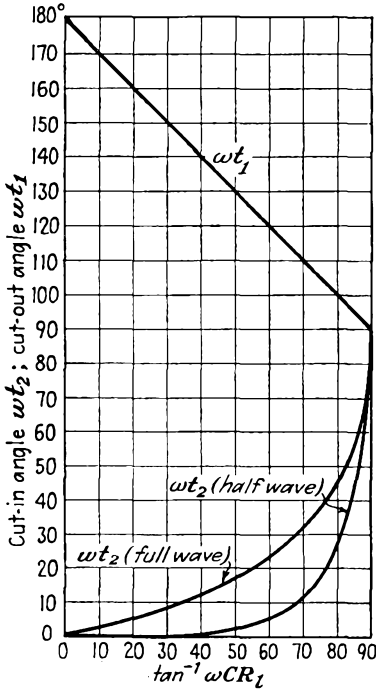


FIG. 14-6. Plot of cutin angle  $\omega t_2$  and cutout angle  $\omega t_1$  vs. circuit parameters for the capacitor filter.

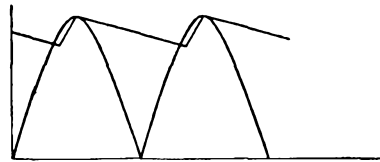


FIG. 14-7. Oscillogram of the load voltage in a single-phase full-wave capacitor filtered rectifier.

Also, the rms value of the triangular ripple voltage may be shown to be

$$E'_{rms} = \frac{E_r}{2\sqrt{3}} \quad (14-26)$$

Also, if it is assumed that the capacitor discharge continues for the full half cycle at a constant rate which is equal to the average load current  $I_{d-c}$ , the fall in potential during this half cycle is  $E_r$ . That is, approximately

$$E_r = \frac{I_{d-c}}{2fC} \quad (14-27)$$

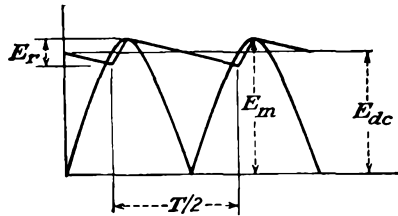


FIG. 14-8. The approximate load-voltage wave form corresponding to the curves of Fig. 14-7.

The ripple factor is then given by

$$r = \frac{E'_{rms}}{E_{d-c}} = \frac{E_r}{2\sqrt{3}E_{d-c}} = \frac{I_{d-c}}{4\sqrt{3}fCE_{d-c}} \quad (14-28)$$

But since  $E_{d-c} = I_{d-c}R_l$ ,

$$r = \frac{1}{4\sqrt{3}fCR_l} \quad (14-29)$$

This expression shows that the ripple factor varies inversely with the load resistance and the filter capacitance. At no load,  $R_l = \infty$ , and the ripple is zero. As  $R_l$  decreases, corresponding to increasing current, the ripple becomes larger. Also, for given  $R_l$ , the ripple is smaller for large capacitances. Actually, Eq. (14-29) is more nearly correct for small values of ripple than for the larger values, the value of ripple being generally larger than that obtained experimentally. The results are adequate for most purposes.

The regulation curve is obtained by combining Eqs. (14-25) and (14-27). This yields

$$E_{d-c} = E_m - \frac{I_{d-c}}{4fC} \quad (14-30)$$

This expression represents a linear fall in potential with d-c output current. Also, it shows that the simple capacitor filter will possess poor regulation unless the capacitance  $C$  is large.

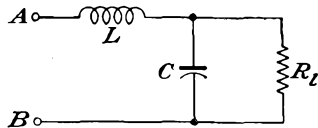


FIG. 14-9. An  $L$ -section filter.

Now refer to the circuit of Fig. 14-4 to ascertain the peak inverse voltage across the tube. It is seen to be twice the transformer peak voltage. For the full-wave case, the peak inverse voltage is also twice

the transformer maximum voltage, as measured from the mid-point to either end. Thus the presence of the capacitor increases the peak inverse voltage in the half-wave circuit from  $E_m$  to  $2E_m$  but does not affect the relatively simple peak inverse voltage in the full-wave circuit.

**14-4. L-section Filter.** An  $L$ -section filter consists of a series inductor and a shunt capacitor, as shown in Fig. 14-9. This filter is so arranged that the inductor offers a high impedance to the harmonic terms, and the capacitor shunts the load, so as to by-pass the harmonic currents. The resulting ripple is markedly reduced over that of the relatively simple filters of Secs. 14-2 and 14-3.

The ripple factor is readily approximated by taking for the voltage applied to the input terminals of the filter the first two terms in the Fourier series representation of the output voltage of the rectifier, *viz.*,

$$e = \frac{2E_m}{\pi} - \frac{4E_m}{3\pi} \cos 2\omega t \quad (14-31)$$

But since the filter elements are chosen to provide a high choke impedance and a very low shunting impedance, certain plausible approximations may be made. Thus, since the choke impedance is high compared with the effective parallel impedance of the capacitor and load resistor, the net impedance between terminals  $AB$  is approximately  $X_L$  and the a-c current through the circuit is

$$I'_{\text{rms}} \doteq \frac{4E_m}{3\sqrt{2}\pi} \frac{1}{X_L} = \frac{\sqrt{2}}{3} E_{\text{d-c}} \frac{1}{X_L} \quad (14-32)$$

Likewise, since the a-c impedance of the capacitor is small compared with  $R_l$ , it may be assumed that all the a-c current passes through the capacitor and none through the resistor. The a-c voltage across the load (the ripple voltage) is the voltage across the capacitor and is

$$E'_{\text{rms}} \doteq \frac{\sqrt{2}}{3} E_{\text{d-c}} \frac{X_C}{X_L} \quad (14-33)$$

The ripple factor is then given by

$$r = \frac{\sqrt{2} X_C}{3 X_L} = \frac{\sqrt{2}}{3} \frac{1}{2\omega C} \frac{1}{2\omega L} \quad (14-34)$$

which may be written, at 60 cps, with  $L$  in henrys and  $C$  in farads,

$$r = \frac{0.830}{LC} \quad (14-35)$$

It should be noted that the effect of combining the decreasing ripple of the inductor filter and the increasing ripple of the simple capacitor filter for increasing loads is a constant ripple circuit, independent of load.

The above analysis assumes that no current cutout exists at any time of the cycle. If it did, the analysis would follow along the lines of Sec. 14-3 and Eq. (14-31) for the potential would not apply. But since with no inductance in the filter cutout will occur, whereas with sufficient inductance there will be no cutout, it would be expected that there would be some minimum inductance for a given current below which cutout would occur, although for larger values than this critical value the conduction would continue for the full cycle. The situation is best illustrated graphically. Figure 14-10 shows the tube current for various amounts of series inductance  $L$ .

If the rectifier is to pass current throughout the entire cycle, the peak current delivered must not exceed the d-c component. But the d-c value is  $E_{\text{d-c}}/R_l$ . Also, the peak a-c current is  $(2E_{\text{d-c}}/3)(1/X_L)$ . Hence for current flow during the full cycle it is necessary that

$$\frac{E_{\text{d-c}}}{R_l} \geq \frac{2E_{\text{d-c}}}{3} \frac{1}{X_L}$$

or

$$X_L \geq \frac{2R_l}{3} \quad (14-36)$$

from which the value for the critical inductance is found to be

$$L_c = \frac{2R_l}{3\omega}$$

which has the value

$$L_c = \frac{R_l}{1,130} \quad (14-37)$$

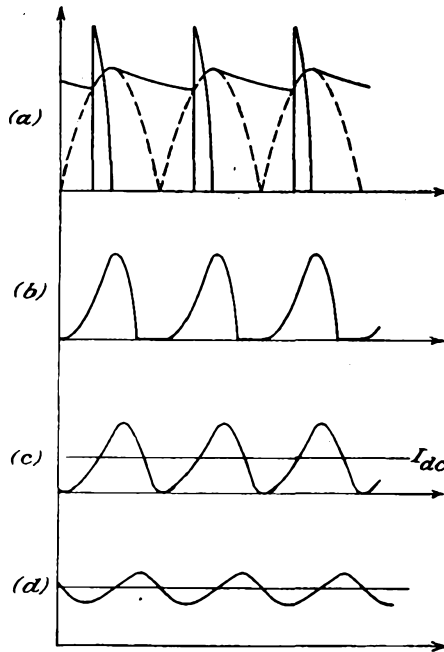


FIG. 14-10. The tube current in the full-wave rectifier with  $L$ -section filter, for (a)  $L = 0$ , (b)  $L$  less than critical inductance  $L_c$ , (c)  $L$  equal to  $L_c$ , (d)  $L$  greater than  $L_c$ .

for a 60-cps power frequency, where  $R_l$  is in ohms and  $L_c$  is in henrys. However, owing to the approximations that have been made in this analysis, it is advisable for conservative design to increase  $L_c$  above that given in Eq. (14-37). A good practical figure is to choose the denominator as 1,000 instead of 1,130.

The effect of the cutout is illustrated in Fig. 14-11, which shows a regulation curve of the system, for constant  $R_l$  and varying series inductance. Clearly, when the series inductance is zero, the filter is of the simple capacitance type and the output voltage is approximately  $E_m$ . With

increasing inductance, the voltage falls, until at  $L = L_c$  the output potential is that corresponding to the simple  $L$  filter with no cutout, or  $0.637E_m$ . For values of  $L$  greater than  $L_c$ , there is no change in potential, except for the effects of the resistances of the various elements of the circuit.

It is not possible to satisfy the conditions of Eq. (14-37) for all values of load, since at no load this would require an infinite inductance. However, when good voltage regulation is desired, it is customary to use a bleeder resistance across the load so as to maintain the conditions of Eq. (14-37) even if the useful load resistance is high.

A more efficient method than using a high bleeder current, with its consequent power dissipation, is to make use of the fact that the inductance of an iron-core reactor depends, among other things, on the amount of d-c current in the winding.

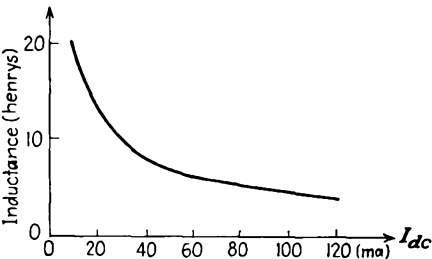


FIG. 14-12. The inductance of a swinging choke as a function of the d-c current through it.

Chokes for which the inductance is high at low values of d-c current and which decrease markedly with increased d-c currents are called "swinging" chokes. A typical curve for such a reactor is illustrated in Fig. 14-12. The advantage of such a choke is that for high  $R_i$ , and therefore low d-c current, the inductance is high. As a result, the conditional equation (14-37) is satisfied over a wider range of  $R_i$ . Clearly, however, when a swinging choke is used, the ripple factor is no longer independent of the load.

The above analysis for the critical inductance of the  $L$ -type filter applies for the full-wave rectifier for which conduction continues for 180 deg in each cycle. Consequently the results so obtained are not applicable when an  $L$ -section filter is used with a controlled rectifier. The analysis for a full-wave controlled rectifier is considerably more complicated than that above, owing to the fact that the amplitude of the harmonics in the Fourier series representation of the output depends on the delay angle, and these are of such amplitude that they cannot be neglected in the analysis. The results of such an analysis are given graphically<sup>1</sup> in

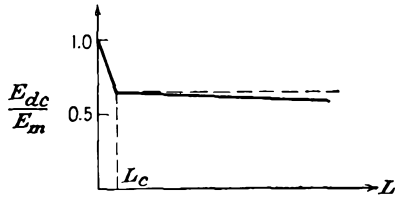


FIG. 14-11. The regulation curve of a rectifier with  $L$ -section filter as a function of series inductance, for constant output current.

As a result, the conditional equation (14-37) is satisfied over a wider range of  $R_i$ . Clearly, however, when a swinging choke is used, the ripple factor is no longer independent of the load.

Fig. 14-13. The curves give a measure of both the critical inductance and the output voltage.

**14-5. Multiple L-section Filters.** If it is desired to limit the ripple to a value that is less than that possible with a single *L*-section filter using commercially available elements, two or more *L*-section filters may be connected in cascade, as shown in Fig. 14-14. An approximate solution is possible by following the methods of Sec. 14-4. It is assumed, therefore, that the choke impedances are much larger than the reactances of the capacitors. Also, it is assumed that the reactance of the last capacitor is small compared with the resistance of the load. Under these assumptions, the impedance between *A*<sub>3</sub> and *B*<sub>3</sub> is *X*<sub>*c*2</sub>. The impedance between *A*<sub>2</sub> and *B*<sub>2</sub> is *X*<sub>*c*1</sub>, and the impedance between *A*<sub>1</sub> and *B*<sub>1</sub> is

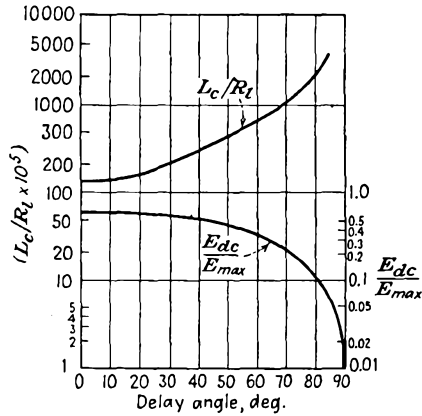


FIG. 14-13. Critical inductance and d-c output voltage as a function of the delay angle in a full-wave controlled rectifier.

*X*<sub>*L*1</sub>, approximately.

The a-c current *I*<sub>1</sub> is approximately

$$I_1 = \frac{\sqrt{2}}{3} E_{a-c} \frac{1}{X_{L1}}$$

The a-c potential across *C*<sub>1</sub> is approximately

$$E_{A_2B_2} = I_1 X_{C1}$$

The a-c current *I*<sub>2</sub> is approximately

$$I_2 = \frac{E_{A_2B_2}}{X_{L2}}$$

The a-c voltage across the load is approximately

$$I_2 X_{C2} = I_1 X_{C2} \frac{X_{C1}}{X_{L1}} = \frac{\sqrt{2}}{3} E_{d-c} \frac{X_{C1}}{X_{L1}} \frac{X_{C2}}{X_{L2}}$$

The ripple factor is given by the expression

$$r = \frac{\sqrt{2}}{3} \frac{X_{C1}}{X_{L1}} \frac{X_{C2}}{X_{L2}} \tag{14-38}$$

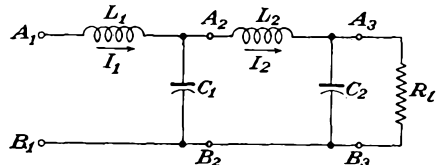


FIG. 14-14. A two-unit *L*-section filter.

A comparison of this expression with Eq. (14-34) indicates the generalization that should be made in obtaining an expression for the ripple of a cascaded filter of  $n$  sections. The expression would have the form

$$r = \frac{\sqrt{2}}{3} \frac{X_{C1}}{X_{L1}} \frac{X_{C2}}{X_{L2}} \dots \frac{X_{Cn}}{X_{Ln}} \tag{14-39}$$

If the sections are all similar, then Eq. (14-39) becomes

$$r = \frac{\sqrt{2}}{3} \left( \frac{X_C}{X_L} \right)^n = \frac{\sqrt{2}}{3} \frac{1}{(16\pi^2 f^2 LC)^n} \tag{14-40}$$

It follows from this that the required  $LC$  product for a specified ripple  $r$  is given by

$$LC = 1.76 \left( \frac{0.471}{r} \right)^{\frac{1}{n}} \tag{14-41}$$

Note also that, to the approximation that the impedance between  $A_2$  and  $B_2$  is simply  $X_{c1}$ , the critical inductance is given by Eq. (14-37), as for the single-section unit.

**14-6.  $\Pi$ -section Filter.** The use of a  $\Pi$ -section filter provides an output potential that approaches the peak value of the a-c potential of the source, the ripple components being very small. Such a filter is illustrated in Fig. 14-15. Although such filters do provide a higher d-c output potential than is possible with an  $L$ -section filter, the tube currents are peaked and the regulation is generally poor, these results being common with the simple capacitor filter.

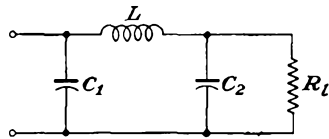


FIG. 14-15. A  $\Pi$ -section filter.

A study of the oscilloscope patterns at various points of such a filter shows that the action can be understood by considering the inductor and the second capacitor as an  $L$ -section filter that acts on the triangular output voltage wave from the first capacitor. The output potential is then approximately that from the input capacitor, the ripple contained in this output being reduced by the  $L$ -section filter. That is, the ripple factor of the  $\Pi$ -section filter is given approximately by

$$r_{\pi} = r_c r_L \tag{14-42}$$

where  $r_c$  is given by Eq. (14-29) and  $r_L$  is given by Eq. (14-34). This result is only approximate, since it assumes in effect that the ripple output from the capacitor filter is sinusoidal rather than triangular. A more careful calculation shows that Eq. (14-42) is slightly higher than that obtained by the complete calculation and so yields generally conservative results.

**14-7. Glow-tube Regulator.** The use of an electronic rectifier with an appropriate filter serves to provide a low-ripple source of d-c potential, the percentage of ripple present in the output depending upon the form of the filter that is used. Such rectifier systems, while generally satisfactory for many purposes, possess several shortcomings which may make them inadequate for certain services. The output voltage depends critically upon the input voltage to the rectifier, and a poorly regulated power system will be accompanied by a corresponding change in the output from

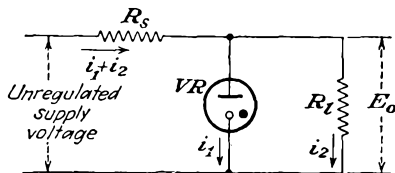


FIG. 14-16. Glow-tube voltage regulator.

the rectifier. Also, since the output impedance of the rectifier is usually quite high, the rectifier system will possess a poor regulation.

It is frequently necessary to construct a power supply the output potential of which is constant over wide ranges of input a-c voltage, so as to provide a constant output voltage

source from a poorly regulated power line. Or it may be necessary to maintain a constant output voltage for a varying output load. Electronic voltage regulators provide such a control device and are extensively used for such service.

The simplest form of voltage regulator makes use of the substantially constant voltage characteristic of a glow tube. A glow tube is a cold-cathode discharge tube which is characterized by a fairly high tube drop and a low current-carrying capacity (see Sec. 2-15). The voltage across the tube over the operating range is fairly constant and independent of the current. When connected in the circuit shown, the voltage across the load will be a constant and equal to the tube drop of the glow tube, over a range of currents. Specifically, if a VR-150/30 is used, the voltage across the load will be approximately 150 volts provided that the current through the tube does not exceed the rated 30 ma of the tube.

If a voltage is desired that is higher than that of a single glow tube, several tubes may be connected in series. This will provide a constant voltage source that is the sum of the tube drops of the tubes that are used. For example, the use of a VR-150 and a VR-105 in series will provide a constant 255-volt source.

The supply voltage must be greater than the breakdown voltage of the tubes in order to make operation possible. The difference between the supply voltage and the operating tube voltage drop will appear across the stabilizing resistor  $R_s$ .

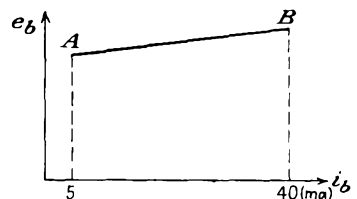


FIG. 14-17. A typical glow-tube volt-ampere characteristic.

An analysis of such a circuit is readily possible<sup>2</sup> if use is made of the practical fact that over the range of operation the volt-ampere characteristic of the regulator tube is linear. A typical characteristic has the form shown in Fig. 14-17. This characteristic may be expressed by an equation of the form

$$e = ai_1 + b \tag{14-43}$$

where 
$$a = \frac{e_B - e_A}{i_B - i_A} \quad \text{and} \quad b = e_A - ai_A \tag{14-44}$$

From the circuit diagram of Fig. 14-16 it follows that

$$E_i = (i_1 + i_2)R_s + E_b \tag{14-45}$$

Also,

$$E_b = E_o = Ri_2 = ai_1 + b \tag{14-46}$$

from which it follows that

and 
$$\left. \begin{aligned} i_1 &= \frac{E_o - b}{a} \\ i_2 &= \frac{E_o}{R_i} \end{aligned} \right\} \tag{14-47}$$

Combining these equations yields

$$E_i = \left( \frac{E_o - b}{a} + \frac{E_o}{R_i} \right) R_s + E_o$$

from which it follows that

$$E_o = \frac{aR_iE_i + bR_iR_s}{R_iR_s + aR_s + aR_i} \tag{14-48}$$

This is the expression for the regulated voltage as a function of the supply-voltage and circuit parameters.

In order to obtain an expression for the variation of the output voltage as the input voltage varies, Eq. (14-48) is differentiated. This gives for the ratio  $dE_i/dE_o$ , which is known as the stabilization ratio, the expression

$$G \equiv \frac{dE_i}{dE_o} = \frac{R_i(R_s + a) + aR_s}{aR_i} \tag{14-49}$$

Combining this with the expression for  $E_o$  gives

$$G = \frac{aE_i + bR_s}{aE_o} \tag{14-50}$$

This expression shows that for perfect regulation, *i.e.*, infinite stabilization ratio, the fraction  $dE_i/dE_o$  should be zero. For best stabilization features, both  $E_o$  and  $a$  should be small; and  $b$ ,  $E_i$ , and  $R_s$  should be large. Using typical values with a VR-75 tube, one finds

$$\begin{array}{llllll} E_i = 250 \text{ volts.} & R = \infty & R_s = 32.5^k & \Delta E_i = 20 & \Delta E_o = 0.15 \\ & = 3^k & = 5.85^k & = 20 & = 0.60 \end{array}$$

Such simple gas-tube regulators operate quite satisfactorily but are seriously limited in their usefulness owing to their limited flexibility, both because of their fixed potential ratings and the relatively low current-carrying capacity.

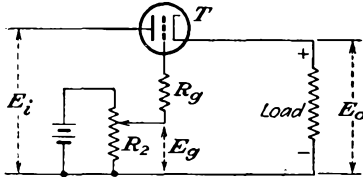


FIG. 14-18. A simple vacuum-tube voltage regulator.

One may employ the variable beam-resistance characteristic of a vacuum tube to maintain the output voltage from a power supply at a substantially constant level. The beam resistance, as previously defined, is  $r_b = E_b/I_b$  and is quite different from the plate resistance  $r_p$  of the tube. The circuit of such a simple voltage regulator is given in Fig. 14-18.

Assume that the voltage across the load is at the desired value. Under this condition, the cathode is positive relative to ground by a voltage  $E_o$ . The grid may be made positive relative to ground by a voltage  $E_g$  which is less than  $E_o$ . The potentiometer  $R_2$  is adjusted until the bias on the tube is such that the tube will pass load current. With this bias, the resistance of  $T$  is established at the desired value to reduce the rectifier output to the desired load voltage.

If the rectifier output voltage increases for whatever reason, the voltage at the cathode of  $T$  tends to increase. As  $E_o$  increases, the bias on the tube increases and the effective beam resistance of the tube becomes greater. Consequently the voltage drop across the tube becomes greater. If the circuit is properly designed, the increased voltage across  $T$  is approximately equal to the increase of voltage and the output potential remains substantially constant.

The practical form of the circuit will replace the battery by a glow tube. Such a circuit is shown in Fig. 14-19.

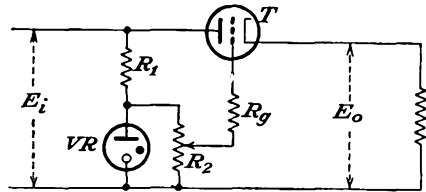


FIG. 14-19. A simple voltage-regulator circuit.

The output voltage from this regulator is not absolutely constant, since, for an increased input to the circuit, the voltage at the cathode of  $T$  must rise slightly if the regulator is to function. However, if the characteristics of tube  $T$  are carefully chosen, the rise of load voltage is not large.

It would be expected, of course, that vacuum tubes in which the beam resistance varied rapidly with small changes in bias would be most desirable for service in such regulators. Tubes possessing such a characteristic could probably be designed if there were no alternative approach. Actu-

ally such special tubes are not necessary, as it is quite possible to achieve the same ends by including a d-c amplifier in the circuit in such a way that slight changes in output potential are amplified before being applied degeneratively to  $T$ . These circuits are used extensively and a detailed analysis will be given below.

**14-9. Electronic Voltage Regulators—Basic Considerations.** The design of electronically regulated power supplies has become fairly well standardized. The elements of such a circuit are given in Fig. 14-20.

As discussed above, the operation of the circuit is essentially the following: The source of unregulated current from the rectifier and filter is applied across the input terminals of the regulator. The unregulated d-c current is fed through the series control tube, now designated  $T_2$  in the diagram, to the output circuit.

If the current requirements are too high for a single tube, a number of such tubes may be connected in parallel. A power triode is frequently used for this purpose, although a pentode or beam tetrode connected as a triode will serve equally well. Popular series control tubes include 6AS7G, 6B4, 6L6, 6V6, and 6Y6G.

These tubes will pass approximately 75 ma without seriously exceeding the plate dissipation of the tube. The regulating action is obtained by comparing a fixed fraction of the output voltage with a standard voltage source, such as a battery or a VR gas tube. Any difference between the two is applied degeneratively after amplification by a high-gain d-c amplifier to the control grid of the series current-control tube. The correction may be made nearly perfect by using a d-c amplifier of sufficient gain.

The design of a voltage regulator requires a knowledge of the characteristic curves of the control tube and also of the d-c amplifier tube. However, since small changes in voltage and current are ordinarily involved, the circuit operation may be analyzed in terms of the slope of the tube characteristics—specifically, in terms of the mutual conductance and the internal resistance of the tubes at the operating points. Several cases of interest will be examined separately.

*a. Varying Input Voltage— $R_3$  Connected to the Input Side of the Regulator.* Suppose that the output load remains constant but that the input voltage to the regulator varies, either because of the poor regulation of the input a-c supply voltage to the rectifier or because of the ripple in the output of the rectifier due to inadequate filtering. It follows from

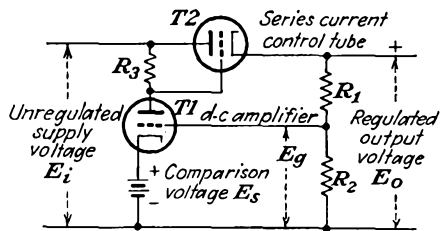


FIG. 14-20. A basic electronic regulator circuit.

an inspection of the circuit of Fig. 14-20 that the input voltage to the d-c amplifier is related to the output voltage by the relation

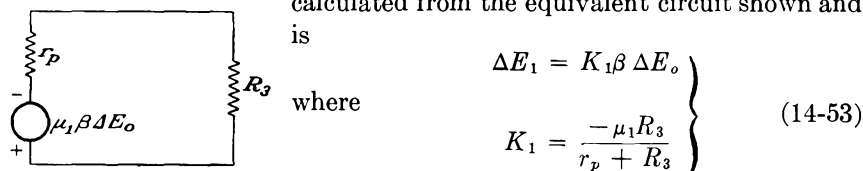
$$E_o = \frac{R_2}{R_1 + R_2} E_o = \beta E_o \tag{14-51}$$

This assumes that the current to the input of the d-c amplifier is negligible. This is a valid assumption, as the grid of the d-c amplifier is ordinarily maintained negative with respect to the cathode by an amount that will allow approximately normal tube current in the d-c amplifier.

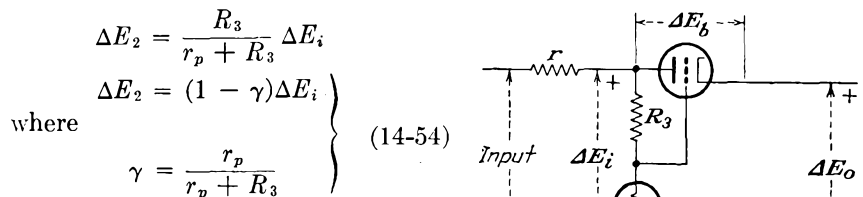
Suppose now that owing to a change  $\Delta E_i$  in the input a small change  $\Delta E_o$  appears in the output voltage. The corresponding change in the voltage appearing at the input to the d-c amplifier is

$$\Delta E_g = \beta \Delta E_o \tag{14-52}$$

Let  $K_1$  denote the gain of the d-c amplifier. The voltage appearing across the plate resistor  $R_3$ , which is also the plate-grid circuit of  $T_2$ , may be calculated from the equivalent circuit shown and is



However, when  $R_3$  is connected to the input side of the regulator, a second voltage appears in the circuit across  $R_3$ . This arises from the appearance of  $\Delta E_i$  across  $R_3$  and  $r_p$  (the tube). This voltage is evidently



The total voltage across  $R_3$  is

$$\Delta E = -\beta K_1 \Delta E_o + (1 - \gamma) \Delta E_i$$

The grid-cathode voltage of  $T_2$  is then

$$\begin{aligned} \Delta E_{gk} &= \Delta E_{pk} - \Delta E_{p0} \\ &= \Delta E_{pk} + \beta K_1 \Delta E_o - (1 - \gamma) \Delta E_i \end{aligned} \tag{14-55}$$

But by definition

$$-\mu \equiv \left( \frac{\partial E_b}{\partial E_c} \right)_I = \left( \frac{\Delta E_{pk}}{\Delta E_{gk}} \right)_I$$

Then

$$\Delta E_b = -\mu_2[\Delta E_b + \beta K_1 \Delta E_o - (1 - \gamma) \Delta E_i] \quad (14-56)$$

It follows from this that

$$\Delta E_b(1 + \mu_2) = -\beta K_1 \mu_2 \Delta E_o + (1 - \gamma) \mu_2 \Delta E_i$$

But as

$$\Delta E_b = \Delta E_i - \Delta E_o$$

then

$$(1 + \mu_2)(\Delta E_i - \Delta E_o) = -\beta K_1 \mu_2 \Delta E_o + (1 - \gamma) \mu_2 \Delta E_i \quad (14-57)$$

The voltage-stabilization ratio  $G$  is given by

$$G = \frac{\Delta E_i}{\Delta E_o} = \frac{1 + \mu_2 - \beta K_1 \mu_2}{1 + \gamma \mu_2} \quad (14-58)$$

which approximates, under normal conditions, to

$$G \doteq \frac{-\beta K_1 \mu_2}{1 + \gamma \mu_2} \quad (14-59)$$

The quantity  $G$  gives a measure of the effectiveness with which the regulator compensates for changes in voltage in the input. For a regulator with a single d-c amplifier stage,  $G$  may be of the order of 300 to 1,000. If an improved value for  $G$  is required in order to achieve an almost ripple-free output, it is necessary that the gain of the d-c amplifier be increased. This is most easily done by adding a second stage of d-c amplification. Such circuits will be considered below. With such circuits, a value of  $G$  of 25,000 is possible.

*b. Varying Input Voltage— $R_3$  Connected to the Output Side of the Regulator.* Somewhat improved results are theoretically possible if the plate resistor  $R_3$  of the d-c amplifier stage  $T1$  is connected to the output side of the regulator instead of the input side. That an improvement is possible follows from the fact that one may now assume that the plate voltage to which the amplifier  $T1$  is connected is substantially constant and that the output from this stage, *viz.*,

$$\Delta E = -\beta K_1 \Delta E_o$$

is the cathode-grid voltage applied to the series control tube  $T2$ . Consequently the net change in voltage appearing in the output is approximately

$$\Delta E_b = \Delta E_i - \Delta E_o = -\mu_2(\beta K_1 \Delta E_o)$$

and the voltage-stabilization ratio is now given by the relation

$$G = 1 - \mu_2 \beta K_1 \doteq = \mu_2 \beta K_1 \quad (14-60)$$

Owing to the denominator that appears in Eq. (14-59), the value of  $G$  appears to be higher in Eq. (14-60). Actually, however, the d-c amplifier

$T_1$  operates in a more linear manner under condition  $a$ , with somewhat higher gain  $K_1$ . Under normal circumstances the two connections yield about equal results, and both are used.

*c. Varying Load.* Suppose now that the change in output voltage results from a change in the load current because of the internal resistance of the supply. If this change in voltage is again denoted by  $\Delta E_o$ , then, as before, the voltage appearing at the grid of the current control tube is

$$\Delta E = -\beta K_1 \Delta E_o$$

If  $g_m$  denotes the mutual transconductance of the control tube, the resulting change in current through this tube due to a change in potential  $\Delta E_2$  at the grid is

$$\Delta I_p = g_m \Delta E_2$$

which is

$$\Delta I_p = -g_m \beta K_1 \Delta E_o \quad (14-61)$$

The ratio of the change in output voltage to the change in output current is denoted by  $R_o$  and is the effective internal resistance of the regulated power supply. This is given by

$$R_o \equiv \frac{\Delta E_o}{\Delta I_p} = \frac{1}{-g_m \beta K_1} \quad (14-62)$$

In a typical case, the effective internal resistance of the regulated supply can be as low as 0.5 ohm.

This calculation assumes, of course, that there is no change in the input applied potential with changes in output current or, equivalently, that the internal impedance of the unregulated power supply is low. This condition is not often met in practice, and due account must be taken of this factor. If the internal resistance of the unregulated driving source is denoted by  $r$ , then by Eqs. (14-60) and (14-62) the total effective internal resistance of the regulated power supply is given by

$$R = \frac{1}{-g_m \beta K_1} + \frac{r}{G} = \frac{1}{-g_m \beta K_1} \left( 1 + \frac{r}{r_{p2}} \right) \quad (14-63)$$

For a typical case  $r = 500$  ohms, and  $G = 1,000$ , so that the added resistance due to the regulation of the input source may be only about 0.5 ohm.

**14-10. Design Considerations.** If  $\Delta E_o$  denotes the change in output voltage, without regard to its cause, the change in current through the control tube is again given by Eq. (14-61). If the total resistance across the output side of the control circuit is denoted by  $R_l$ , the net change in output voltage is given by

$$(g_m \beta K_1 R_l - 1) \Delta E_o |_{\text{unreg}} = \Delta E_o |_{\text{reg}} \quad (14-64)$$

When voltage regulation occurs, the two quantities on the left just balance

each other and the initial change in voltage across the load is exactly compensated by the change in plate current. If the difference is positive, the initial change in output voltage is overcompensated; if the expression is negative, the circuit is undercompensated.

In view of the several adjustable factors that appear in this expression, they may ordinarily be so proportioned that the expression on the left becomes zero. The practical problem in the design of the circuit becomes that of determining the amplification factor  $\mu$ , which appears in the expression for the gain  $K_1$ , and in the determination of  $g_m$  of tube  $T_2$ . After this, the resistance values  $R_1$ ,  $R_2$ , and  $R_3$  may be chosen to satisfy the relation

$$g_m \frac{\mu R_3}{r_p + R_3} \frac{R_2}{R_1 + R_2} R_l = 1 \tag{14-65}$$

The value of  $\mu$  and  $g_m$  may be determined from the characteristic curves of the appropriate tubes when the applied grid and plate potentials are known. In the case of the d-c amplifier tube, the value of  $\mu$  is that at which the grid potential is

$$E_c = (\beta E_o - E_s)$$

and the plate potential is

$$E_b = E_i - E_s - I_p R_3$$

where  $I_p$  is the average tube current.

The value of the mutual conductance  $g_m$  of the control tube  $T_2$  is obtained in the same general way from the appropriate set of static-

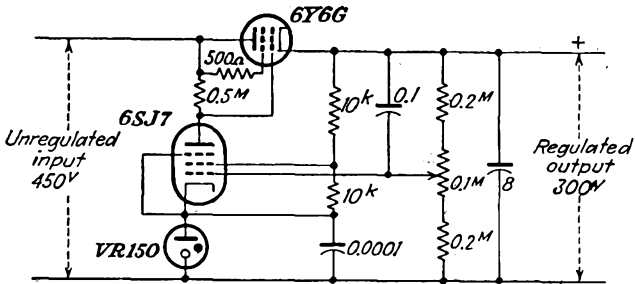


FIG. 14-21. An electronically regulated power supply.

characteristic curves of the tube used, where the total applied voltage is  $E_i - E_o$  and the applied grid voltage is  $E_i - E_o - I_p R_3$ , which depends on the operation of the d-c amplifier tube.

A typical circuit that yields satisfactory results over a wide range of input voltage and over a wide range of load current is given in Fig. 14-21.

Although the diagram of Fig. 14-20 shows a triode as the d-c amplifier, it is found more desirable to use a pentode in this position and this has

been done in the circuit of Fig. 14-21. The reason for this is that it frequently happens that the d-c regulation is not as good as one would expect when a triode is used, primarily because the grid impedance of a high-gain triode is quite low. The grid impedance should be high, especially if the full gain capabilities are to be realized. A 6SJ7 tube is

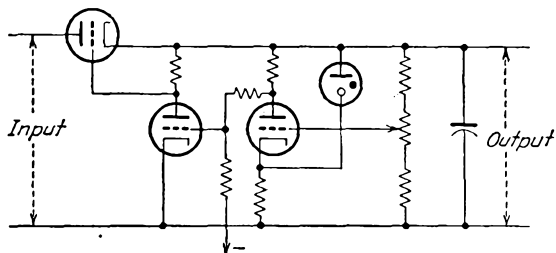


FIG. 14-22. An electronic voltage regulator employing a two-stage d-c amplifier.

superior in this respect and hence is frequently used. The 6Y6G pentode called for in Fig. 14-21 gives satisfactory results. The newer 6AS7G tube possesses some advantages over this, since it has a relatively high tube current rating (125 ma) with a relatively low tube drop. Also, the

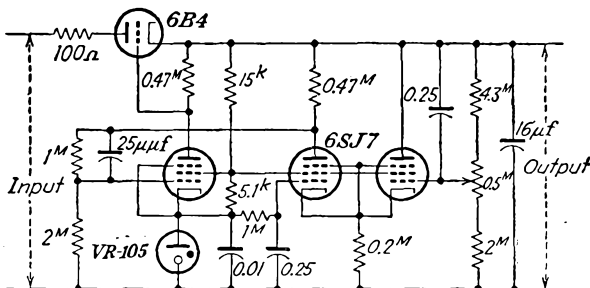


FIG. 14-23. A voltage regulator employing a difference amplifier.

heater-cathode insulation is sufficiently good to avoid the need for a separate filament heating transformer for this tube. The tube does have a rather low value of  $\mu$  ( $= 2.1$ ) which requires a rather large control voltage.

If a voltage regulator is required which is to provide a practically ripple-free output and an almost perfect regulation, it is necessary that the gain of the d-c amplifier be increased. This is most easily done by adding a second stage of d-c amplification to the regulator circuit. A variety of such circuits is possible, and several types are illustrated below. Figure 14-22 shows a simple two-stage resistance-coupled amplifier; Fig. 14-23 utilizes a difference amplifier; and Fig. 14-24 uses what is called a "cascode" amplifier.

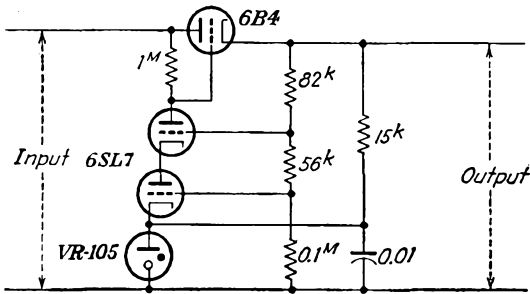


FIG. 14-24. A voltage regulator employing a "cascode" amplifier.

**14-11. Special Precautions.**<sup>3</sup> Although the principles of operation of the regulated power supply are straightforward, it frequently happens that the maximum performance will not be realized in practice. It is well to consider some of the reasons for this. The important factors to be examined closely are the degenerative d-c amplifier loop and the various sources of hum.

*a. The Degenerative D-C Amplifier Loop.* For satisfactory operation, the d-c amplifier must be degenerative at all frequencies for which the loop gain is greater than unity. If this condition is not met, the system will oscillate (refer to Sec. 5-9) and the regulation properties will be greatly affected. One of the best ways to ensure that the power supply will not break into oscillation is to limit the h-f response of the amplifier. This is best done by including a large capacitor across the output ( $8\ \mu\text{f}$  or  $16\ \mu\text{f}$ ). This will usually provide the necessary h-f cutoff and will still keep the power-supply impedance low at high frequencies. The  $0.1\text{-}\mu\text{f}$  capacitor from the grid of  $T_1$  to  $B+$  serves to prevent a phase lag at the grid of the d-c amplifier and also compensates somewhat for additional phase shift in the amplifier and increases  $K_1$  for frequencies above a cycle or two.

*Sources of Hum.* Among the sources of hum which give rise to a higher ripple in the output than is expected, and their possible cures, are the following:

1. Ripple from a-c heated filaments in the d-c amplifier. By grounding the center tap of the heater transformer and by choosing tubes with low heater-hum characteristics, the hum in the output voltage can be reduced to 4 or 5 mv rms or less.

2. Ripple from common leads. This may arise from coupling between the d-c supply and some a-c source, such as a filament supply. The use of the chassis as a common ground with grounds to various parts of the chassis may introduce this hum voltage. This effect is ordinarily small, perhaps several millivolts rms, except when the common coupling appears in the input of the d-c amplifier in the regulator, in which case it may be

appreciable. To avoid this difficulty, grounds should be separately returned to a single point.

3. Ripple from supply voltages. The screen voltage to the d-c amplifier must be ripple-free. This may require a filter at the screen terminal at the tube base.

4. Ripple in the comparison voltage source. It might be necessary to include a filter in the  $CR$  circuit for this purpose, in addition to the 0.0001- $\mu\text{f}$  condenser shown (which is to prevent any effects that might arise from the h-f plasma oscillations in the VR tube).

5. Induction loops. If coupling occurs between circuits by electrostatic or electromagnetic induction, it may be necessary to include a simple  $RC$  filter in the input circuit to the d-c amplifier and in the comparison-voltage circuit.

*Heater Supply.* When the heater of the d-c amplifier is fed from an unregulated source, changes in output with heater-voltage changes may be quite noticeable. This can be eliminated by operating the heaters from the regulated d-c supply.

#### REFERENCES

1. Overbeck, W. P., *Proc. IRE*, **27**, 655 (1939).
  2. Berg, W. R., *Electronics*, **20**, 136 (October, 1947).
  3. Lawson, J. L., *M.I.T. Radiation Lab. Internal Rept.*, unpublished.
- As general references, see
- Hunt, F. V., and R. W. Hickman, *Rev. Sci. Instruments*, **10**, 6 (1939).  
 Mautner, L., *Elec. Eng.*, **66**, 894 (1947).  
 Millman, J., and S. Seely, "Electronics," Chap. XIV, McGraw-Hill Book Company, Inc., New York, 1941.

#### PROBLEMS

**14-1.** It is planned to use a type 83 gas tube in a single-phase full-wave rectifier circuit with capacitor filter. The transformer voltage is 350 volts rms to center tap. The load consists of a 16- $\mu\text{f}$  condenser in parallel with a 2,500-ohm resistance. The tube drop and the transformer resistance and leakage reactance may be neglected.

- a. Calculate the cutout angle.
- b. Determine the cutin point.
- c. Calculate the peak tube current. Should the 83 tube be used? Compare the peak current per plate with that given (1 amp) in the tube manual.

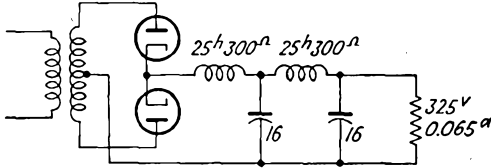
**14-2.** Given two 20-henry chokes, and two 16- $\mu\text{f}$  capacitors. Calculate the output voltage and ripple factors under the following conditions:

- a. The two chokes are connected in series with the load.
- b. The two capacitors are connected across the load.
- c. A single  $L$  filter, consisting of the two chokes in series and the two capacitors in parallel, is used.
- d. A double  $L$  filter, consisting of two sections, each of one choke and one capacitor, is used.

The load is 2,000 ohms, and a 375-0-375 transformer is used in a full-wave circuit. Assume a 25-volt drop occurs in the tubes.

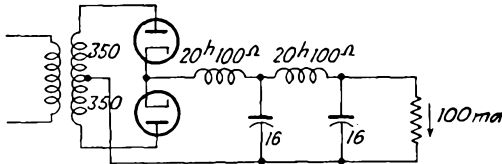
**14-3.** A power supply has the form shown in the diagram.

a. Determine the approximate secondary voltage of the power transformer.



b. What would be the ripple voltage if the power frequency is 60 cps; 400 cps?

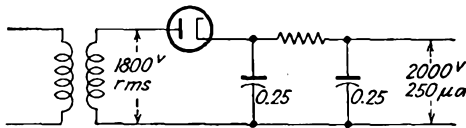
**14-4.** In the power supply shown in the figure,



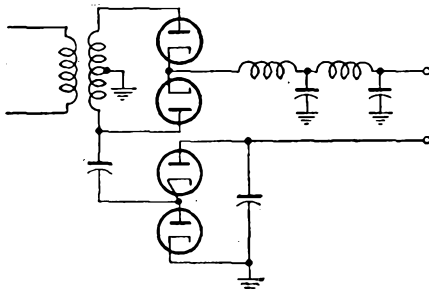
- a. What is the output d-c voltage?
- b. What is the ripple voltage in the output?
- c. What is the minimum load current below which current cutout in the filter occurs? What is the corresponding load voltage?

*Note:* Make allowance for tube drop, but assume a perfect transformer.

**14-5.** A typical circuit for the high-voltage supply for a cathode-ray tube is shown in the diagram. Estimate the output ripple voltage.

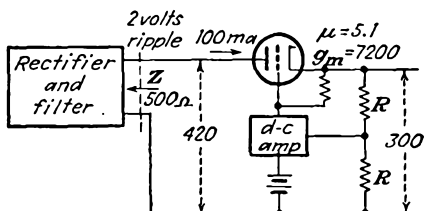


**14-6.** The circuit used (see the figure) is to supply two different voltages. If the transformer is 375-0-375, what are the output voltages?



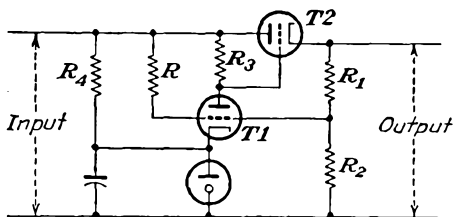
14-7. Given the electronically regulated power supply shown in the diagram.

a. What must be the gain of the d-c amplifier to reduce the output ripple to 8 mv?



b. What must be the gain of the d-c amplifier to reduce the output impedance to 1 ohm?

14-8. The addition of a resistor  $R$  to the electronic voltage regulator, as shown in the figure, improves the voltage-stabilization ratio. Express the required

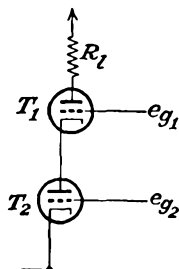


value of  $R$  in terms of the circuit parameters in order to achieve perfect stabilization.

14-9. Given the basic cascode circuit shown in the diagram, show that the total current through the tubes is

$$i = \frac{\mu_2(\mu_1 + 1)e_{o2} + \mu_1 e_{o1}}{r_{p1} + (\mu_1 + 1)r_{p2} + R_l}$$

Show that the over-all gain of this amplifier, when the grids are tied together



in so far as the a-c signal is concerned,  $e_{o1} = e_{o2} = e_o$ , is

$$K = \frac{\mu(\mu + 2)R_l}{(\mu + 2)r_p + R_l}$$



---

## CHAPTER 15

### AMPLITUDE MODULATION

**T**HERE are two major reasons for transmitting intelligence at a relatively high frequency level, (1) transmission by radiation is practicable at the high frequencies, and (2) it is possible to transmit a number of messages simultaneously without interference if the frequency level is different for each message. Of course, any complete system of conveying intelligence from one point to another must be capable of reproducing the intelligence, as represented by the amplitude or loudness, and the frequency, after transmission. The process of altering the frequency level of the intelligence is broadly known as *modulation*. The inverse process, in which the intelligence is extracted from the radiated wave, is known as *demodulation* or *detection*.

By definition<sup>1</sup> *modulation* is the process of producing a wave some characteristic of which varies as a function of the instantaneous value of another wave called the *modulating wave*. The modulating wave is usually the signal, the modulated wave being the h-f *carrier wave*, which has been altered in a manner to carry the intelligence.

Consider a wave which may be represented analytically by the expression

$$e = A \cos (\omega t + \theta) \quad (15-1)$$

where  $t$  is the time. If either  $A$ ,  $\omega$ , or  $\theta$  is varied according to some function of the instantaneous value of a modulating wave, then this expression will represent the modulated wave. It is possible, in fact, to produce a wave in which all three parameters vary simultaneously. However, in each of the modulating methods that are important practically, only one of these parameters is varied, and in commercial transmitters great care is taken to avoid the use of more than one type of modulation.

In *amplitude modulation* (a-m), the amplitude  $A$  is varied in accordance with the modulating wave, while  $\omega$  and  $\theta$  remain constant. In *frequency modulation* (f-m), the frequency  $\omega$  is varied, and both  $A$  and  $\theta$  remain constant. In *phase modulation* (p-m), the phase  $\theta$  is varied, while  $A$  and  $\omega$  remain constant. It should perhaps be mentioned that phase modulation is not of much practical importance in itself, but as will be shown

later, it may be used as an intermediate step in achieving frequency modulation.

**15-1. Characteristics of Amplitude Modulation.** As indicated, amplitude modulation is produced by varying the magnitude of the carrier in accordance with the amplitude and frequency of the modulating source. Let the signal voltage be designated as

$$e_m = E_m \cos \omega_m t \quad (15-2)$$

and let the unmodulated carrier be written as

$$e_c = E_c \cos (\omega_c t + \theta) \quad (15-3)$$

The carrier frequency  $\omega_c$  is usually much greater than the signal frequency  $\omega_m$  and is chosen at the designated frequency level desired for the transmission. The resulting modulated wave has the form

$$e = (E_c + k_a E_m \cos \omega_m t) \cos \omega_c t \quad (15-4)$$

The amplitude factor  $E_c + k_a E_m \cos \omega_m t$  expresses the sinusoidal variation of the amplitude of the wave, where the proportionality factor  $k_a$  determines the maximum variation in amplitude for a given modulating signal  $E_m$ . In this expression the arbitrary constant phase  $\theta$  has been chosen as zero, since it plays no part in the modulating process.

In examining this wave in detail, the expression is written in the form

$$e = E_c(1 + m_a \cos \omega_m t) \cos \omega_c t \quad (15-5)$$

which is then expanded to the form

$$e = E_c \cos \omega_c t + \frac{m_a E_c}{2} \cos (\omega_c + \omega_m) t + \frac{m_a E_c}{2} \cos (\omega_c - \omega_m) t \quad (15-6)$$

The factor  $m_a$  is known as the *modulation index*

$$m_a = \frac{k_a E_m}{E_c} \quad (15-7)$$

and  $100m_a$  is the *percentage modulation*. A sketch of Eq. (15-5) has the form shown in Fig. 15-1.

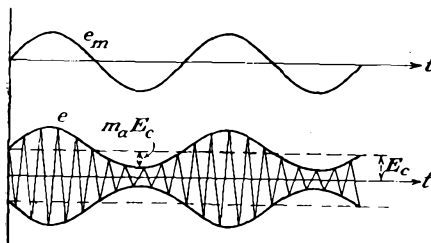


FIG. 15-1. The modulating signal and a modulated carrier.

The expanded expression of Eq. (15-6) indicates the frequency spectrum of the modulated wave. The first term is of carrier frequency  $\omega_c$ ; the second has the frequency  $\omega_c + \omega_m$  and is called the *upper side band*. Its frequency is equal to the sum of the carrier and the signal frequencies.

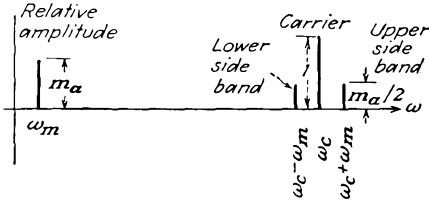


FIG. 15-2. Frequency spectrum of a sinusoidally modulated wave.

The third term has the frequency  $\omega_c - \omega_m$ , which is equal to the difference between the carrier and the signal frequency. This component is known as the *lower side band*. A plot of the frequency spectrum of the modulated wave is illustrated in Fig. 15-2.

It should be emphasized that the foregoing is not a mathematical fiction, as it is possible by means of appropriate filters to extract the frequencies in the spectrum. In fact, the features of transmission of intelligence with one or more of the frequencies in the spectrum suppressed will be examined below.

A simple sinor representation of Eq. (15-6) by means of a pair of rotating conjugate sinors in the complex plane is readily possible. A little thought will convince the reader that the three sinors in Fig. 15-3 represent the three terms of the equation, and that the resultant sinor does exhibit the properties of the a-m wave.

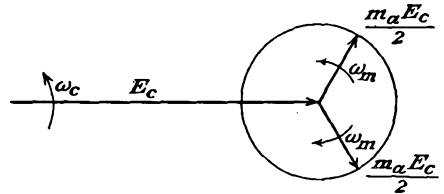


FIG. 15-3. The sinor representation of an a-m wave.

In general, the modulating signal is not sinusoidal but is a complex wave. Since, however, this complex wave may be represented by a Fourier series if the wave is periodic or by a Fourier integral if it is nonperiodic, the modulated carrier wave possesses a frequency spectrum which is more complex than that illustrated. But each frequency in the modulating signal produces a pair of side frequencies in the frequency spectrum. Then a signal with frequencies in the band  $g(\omega)$  will yield a frequency spectrum with a band of side bands  $\frac{1}{2}g(\omega_c + \omega)$  and  $\frac{1}{2}g(\omega_c - \omega)$ , symmetrically disposed about the carrier  $\omega_c$ . Such a spectrum would have the form illustrated in Fig. 15-4.

The frequency-shifting property of modulation is not limited to shifting an a-f wave to a higher position in the frequency spectrum. It is possible to shift an h-f signal up or down in the frequency scale, and both processes are important. Since such frequency shifting or frequency changing does

not involve directly the intelligence to be transmitted, frequency changing is classed, not as a modulation process, but rather as a detection process.

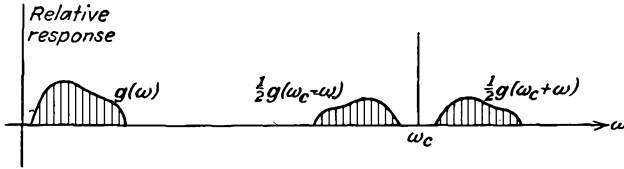


FIG. 15-4. The frequency spectrum of a complex wave.

**15-2. Square-law or Small-signal Modulation.** Amplitude modulation may be produced by impressing two sinusoidal voltages of different frequencies in a nonlinear circuit. The van der Bijl modulator is one of the earliest methods, although it is seldom used at the present time. This modulator depends for its operation on the curvature of the transfer characteristic. A circuit of this modulator is given in Fig. 15-5. The

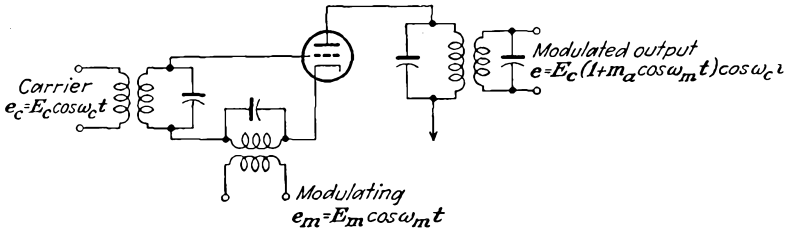


FIG. 15-5. The circuit of the van der Bijl modulator.

carrier and modulation-frequency voltages are both applied in the grid circuit of a triode or multigrid tube, and the modulated wave appears across the tank circuit in the plate circuit of the tube. The tank is tuned to the carrier frequency and must be sufficiently broad to include all the important side bands, usually about  $\pm 10$  kc for normal broadcast purposes; otherwise a distortion known as *side-band clipping* occurs.

The operation of the modulator is made clear in the sketches of Fig. 15-6.

To examine the modulation process analytically, it is supposed that the transfer curve is parabolic over the range of operation, so that the a-c plate current may be related to the input grid potential by the first two terms of the series expansion

$$i_p = a_1 e_g + a_2 e_g^2 \tag{15-8}$$

where  $a_1$  and  $a_2$  are constants. The excitation voltage  $e_g$  is of the form

$$e_g = E_m \cos \omega_m t + E_c \cos \omega_c t \tag{15-9}$$

and it follows, by combining this expression with Eq. (15-8), that the plate current is

$$i_p = a_1 E_m \cos \omega_m t + a_1 E_c \cos \omega_c t + a_2 E_m^2 \cos^2 \omega_m t + a_2 E_c^2 \cos^2 \omega_c t \\ + a_2 E_c E_m \cos (\omega_c + \omega_m)t + a_2 E_m E_c \cos (\omega_c - \omega_m)t$$

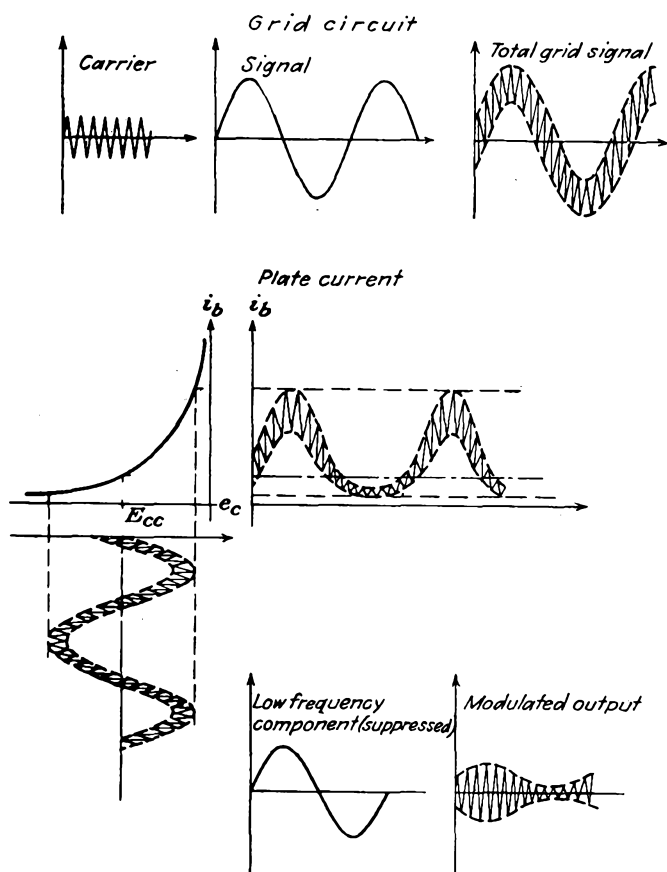


FIG. 15-6. The wave shapes at various points in the van der Bijl modulator.

This may be written as

$$i_p = a_1 E_c \cos \omega_c t + a_2 E_m E_c \cos (\omega_c + \omega_m)t + a_2 E_m E_c \cos (\omega_c - \omega_m)t \\ + a_1 E_m \cos \omega_m t + \frac{a_2 E_m^2}{2} + \frac{a_2 E_m^2}{2} \cos 2\omega_m t + \frac{a_2 E_c^2}{2} + \frac{a_2 E_c^2}{2} \cos 2\omega_c t \quad (15-10)$$

Assuming that  $\omega_c \gg \omega_m$  and also that those frequencies which are not in the neighborhood of  $\omega_c$  are eliminated by the use of tuned circuits or filters, the only voltages which appear across the output are

$$i_p = a_1 E_c \cos \omega_c t + a_2 E_m E_c \cos (\omega_c + \omega_m)t + a_2 E_m E_c \cos (\omega_c - \omega_m)t \quad (15-11)$$

This may be written in the form

$$i_p = a_1 E_c \left( 1 + \frac{2a_2 E_m}{a_1} \cos \omega_m t \right) \cos \omega_c t \quad (15-12)$$

from which it is seen that the modulation index is given by

$$m = \frac{2a_2 E_m}{a_1} \quad (15-13)$$

It should be noted that a circuit of the present type will operate satisfactorily if the signal voltages are applied in the plate and grid circuit, as tabulated.

<i>Grid circuit</i>	<i>Plate circuit</i>
$e_m + e_c$	
$e_m$	$e_m + e_c$
$e_c$	$e_c$
	$e_m$

The amount of modulated output available without appreciable distortion in such a modulator as here considered is not great, and the efficiency is low.

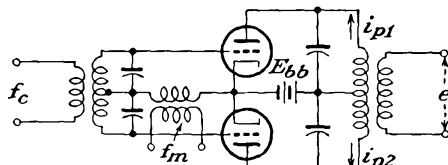


FIG. 15-7. A balanced modulator.

Owing to the fact that the plate circuit contains a parallel tuned rather than a pure resistance load, the foregoing analysis is not completely correct—this despite the fact that the load is purely resistive at or near resonance. By taking this matter into account, Carson<sup>2</sup> has shown that a substantial increase in output occurs with the substitution of the resonant load. However, other methods provide better modulation characteristics and have displaced the low-level method here discussed.

**15-3. Balanced Modulators.** The use of a balanced modulator,<sup>3</sup> which possesses an appearance somewhat like the push-pull amplifier, automatically eliminates either the carrier or the modulating frequency, as well as many of the intermodulation frequencies. The circuit of the balanced modulator is given in Fig. 15-7.

It is assumed that the two tubes are identical and that the circuit is symmetrical. The tube characteristics may be expressed by equations

of the form

$$\left. \begin{aligned} i_{p1} &= a_1 e_{g1} + a_2 e_{g1}^2 \\ i_{p2} &= a_1 e_{g2} + a_2 e_{g2}^2 \end{aligned} \right\} \quad (15-14)$$

But the input potentials have the form

$$\left. \begin{aligned} e_{g1} &= E_c \cos \omega_c t + E_m \cos \omega_m t \\ e_{g2} &= -E_c \cos \omega_c t + E_m \cos \omega_m t \end{aligned} \right\} \quad (15-15)$$

Then the currents in the plate circuits become

$$\left. \begin{aligned} i_{p1} &= a_1 E_c \cos \omega_c t + a_1 E_m \cos \omega_m t + a_2 E_c^2 \cos^2 \omega_c t \\ &\quad + a_2 E_m^2 \cos^2 \omega_m t + a_2 E_c E_m \cos (\omega_c + \omega_m) t \\ &\quad \quad \quad + a_2 E_c E_m \cos (\omega_c - \omega_m) t \\ i_{p2} &= -a_1 E_c \cos \omega_c t + a_1 E_m \cos \omega_m t + a_2 E_c^2 \cos^2 \omega_c t \\ &\quad + a_2 E_m^2 \cos^2 \omega_m t - a_2 E_c E_m \cos (\omega_c + \omega_m) t \\ &\quad \quad \quad - a_2 E_c E_m \cos (\omega_c - \omega_m) t \end{aligned} \right\} \quad (15-16)$$

But the voltage induced in the secondary of the coupling network is given approximately by

$$e \doteq j\omega M(i_{p1} - i_{p2}) \quad (15-17)$$

Then the output is of the form

$$e \doteq 2j\omega_c M a_1 E_c \cos \omega_c t + 2j\omega_c M a_2 E_c E_m [\cos (\omega_c + \omega_m) t + \cos (\omega_c - \omega_m) t]$$

which may be written as

$$e \doteq 2\omega_c M a_1 E_c \left( 1 + E_m \frac{a_2}{a_1} \sin \omega_m t \right) \sin \omega_c t \quad (15-18)$$

In certain applications it is found advantageous to use a balanced modulator in such a manner as to eliminate the carrier. This is readily accomplished by interchanging the sources  $f_m$  and  $f_c$  in the diagram. When this is done, the output contains frequencies  $\omega_c + \omega_m$  and  $\omega_c - \omega_m$ ,

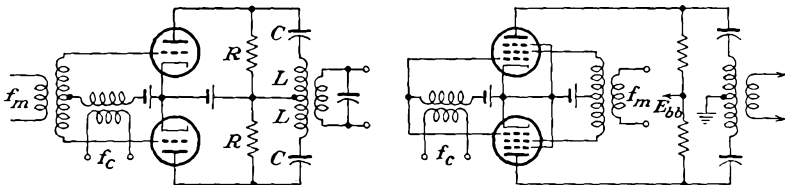


FIG. 15-8. Balanced modulators for producing suppressed carrier modulation.

with the carrier term  $\omega_c$  missing. Such modulated waves with carrier missing can be transmitted. The demodulation problem is more complicated than when the  $\omega_c$  term is present. This will be discussed in Chap. 16. Two circuits of balanced modulators which suppress the carrier are illustrated. In these circuits, the  $LC$  circuit is approximately

in resonance for all frequencies in the neighborhood of the carrier frequency  $\omega_c$ .

**15-4. Linear Modulation.** A somewhat different view of amplitude modulation from that above is possible. This point of view is very important if the carrier and modulating voltages are large or if the operation occurs near cutoff. Such a situation exists when a class C amplifier is modulated, whether this modulation is applied in the plate circuit, the grid circuit, the cathode circuit, or the suppressor circuit, if a tetrode or pentode is used. If a carrier voltage were introduced into the grid of a class C amplifier and if the modulating voltage were introduced into the plate circuit, then because  $\omega_c \gg \omega_m$  the variation in potential in the plate circuit caused by the signal could be considered to be the

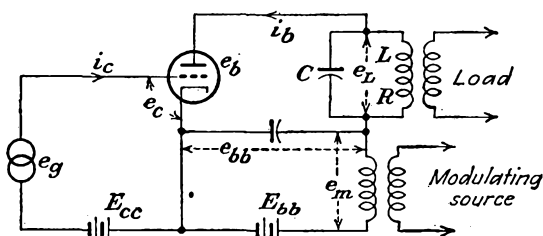


FIG. 15-9. A plate-modulated class C amplifier.

equivalent of a relatively slow change in plate supply potential. If the relationship between the output tank current is a linear function of the plate potential, for constant grid excitation, the output potential (which is a linear function of the tank current) would have the desired modulated characteristics.

With the proper design and adjustment, the modulation characteristic of a class C amplifier is such that 100 per cent modulation with distortion as low as 2 per cent in a plate-modulated amplifier and as low as 5 per cent in a linear grid amplifier may be attained. The distortion can be reduced below these values by the use of inverse feedback in the circuit.

**15-5. Plate-modulated Class C Amplifier.** The basic circuit of a plate-modulated class C amplifier is given in Fig. 15-9. It will be observed that it is essentially the circuit of the class C amplifier except for the introduction of the source of modulating voltage in the plate circuit. The modulation characteristic of such a plate-modulated amplifier is the plot of the tank current as a function of the plate supply voltage. The ideal plate-modulation characteristic is illustrated in Fig. 15-10a. Generally the situation is more nearly like that illustrated in Fig. 15-10b, which shows the effect of tank impedance. The more nearly straight the lines, the less the modulation distortion. A high value of tank impedance yields the smaller distortion, but the power output is also smaller.

If the frequency of the modulating signal is low compared with the carrier frequency, the impedance of the tank circuit at the modulating frequency will be negligible. Consequently the properties of the circuit are not appreciably affected by the modulating frequency, and the plate and tank currents will follow the characteristics shown even when  $e_{bb}$  varies at the modulation frequency.

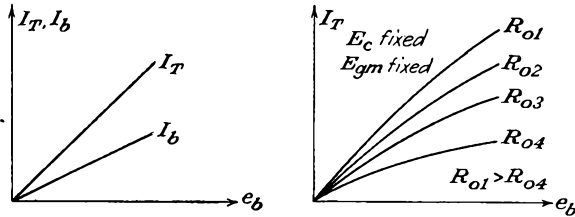


FIG. 15-10. (a) The ideal plate-modulation characteristic. (b) The modulation characteristics, showing the effects of load impedance.

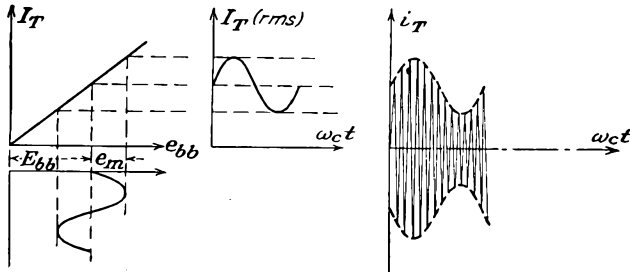


FIG. 15-11. The conditions during plate modulation.

Suppose therefore that the carrier voltage of angular frequency  $\omega_c$  is modulated by a modulating voltage of frequency  $\omega_m$ . The behavior of the circuit is that illustrated in Fig. 15-11.

To analyze the modulation process, it will be supposed that  $\omega_c \gg \omega_m$ . The grid-circuit potentials are, respectively,

$$\text{and } \left. \begin{aligned} e_g &= E_{gm} \cos \omega_c t \\ e_c &= E_{gm} \cos \omega_c t + E_{cc} \end{aligned} \right\} \quad (15-19)$$

If the modulating voltage in the plate circuit is written in the form

$$e_m = E_{mm} \cos \omega_m t \quad (15-20)$$

the resulting relatively slowly varying plate potential has the form

$$e_{bb} = E_{bb} + E_{mm} \cos \omega_m t \quad (15-21)$$

This may be written in the form

$$e_{bb} = E_{bb}(1 + m \cos \omega_m t) \quad (15-22)$$

where  $m$ , the modulation index, is given by the ratio

$$m = \frac{E_{mm}}{E_{bb}} \quad (15-23)$$

It should be noted from the curves of Fig. 15-10 that the rms tank current and the d-c plate current are related to the plate potential by expressions of the form

$$\left. \begin{aligned} I_T &= k_T e_{bb} \\ I_b &= k_b e_{bb} \end{aligned} \right\} \quad (15-24)$$

By combining Eqs. (15-24) with Eq. (15-22), it follows that

$$\left. \begin{aligned} I_T &= k_T E_{bb}(1 + m \cos \omega_m t) \\ I_b &= k_b E_{bb}(1 + m \cos \omega_m t) \end{aligned} \right\} \quad (15-25)$$

Also, corresponding to the rms tank current will be chosen the instantaneous tank current  $i_T$  to be of the form

$$i_T = \sqrt{2} I_T \sin \omega_c t \quad (15-26)$$

This may be expressed in the form

$$i_T = \sqrt{2} k_T E_{bb}(1 + m \cos \omega_m t) \sin \omega_c t \quad (15-27)$$

But the output voltage  $e_L$  that appears across the tank circuit is given with good approximation by

$$E_L = jX_L I_T = X_L I_T / 90^\circ \quad (15-28)$$

Therefore

$$\begin{aligned} e_L &= \sqrt{2} X_L I_T \sin(\omega_c t + 90) \\ &= \sqrt{2} X_L k_T E_{bb}(1 + m \cos \omega_m t) \cos \omega_c t \end{aligned} \quad (15-29)$$

The corresponding plate-cathode potential of the tube is

$$e_b = e_{bb} - e_L$$

which is

$$e_b = E_{bb}(1 + m \cos \omega_m t)(1 - \sqrt{2} X_L k_T \cos \omega_c t) \quad (15-30)$$

Also, from the fact that the plate current is given by

$$I_{p1} = \frac{E_L}{R_0} = j \frac{X_L I_T}{R_0} = j \frac{I_T}{Q} = \frac{I_T}{Q} / 90^\circ$$

the instantaneous plate current has the form

$$i_{p1} = \frac{\sqrt{2}}{Q} k_T E_{bb} (1 + m \cos \omega_m t) \cos \omega_c t \quad (15-31)$$

Likewise, it follows from the curve of Fig. 15-10 that

$$i_b = I_b(1 + m \cos \omega_m t) \quad (15-32)$$

The above information may be used to analyze the performance of the modulated amplifier.

The average power supplied by the d-c plate power source is

$$P_{bb} = \frac{1}{T} \int_0^T E_{bb} i_b dt \quad (15-33)$$

which is

$$P_{bb} = \frac{1}{T} \int_0^T E_{bb} I_b (1 + m \cos \omega_m t) dt$$

This integrates to

$$P_{bb} = E_{bb} I_b = k_b E_{bb}^2 \quad (15-34)$$

The power input by the modulating source is

$$P_m = \frac{1}{T} \int_0^T e_m i_b dt$$

This becomes

$$P_m = \frac{1}{T} \int_0^T E_{mm} \cos \omega_m t I_b (1 + m \cos \omega_m t) dt$$

which integrates to the form

$$P_m = E_{mm} I_b \frac{m}{2} = P_{bb} \frac{m^2}{2} \quad (15-35)$$

Clearly, for 100 per cent sinusoidal modulation, the modulating source must deliver one-half as much power as the d-c plate power supply. This requires, of course, that the modulating source must be an amplifier of large power capacity for a large power output.

The a-c power output at the tank circuit is given by the expression

$$P_L = \frac{1}{T} \int_0^T e_L i_{p1} dt = \frac{1}{T} \int_0^T R_0 i_{p1}^2 dt \quad (15-36)$$

This becomes

$$P_L = \frac{1}{T} \int_0^T 2R_0 \left( \frac{k_T E_{bb}}{Q} \right)^2 (1 + m \cos \omega_m t)^2 \cos^2 \omega_c t dt$$

which becomes, by performing the indicated integrations,

$$P_L = R_0 \left( \frac{k_T E_{bb}}{Q} \right)^2 \left( 1 + \frac{m^2}{4} + \frac{m^2}{4} \right)$$

This may be reduced to the form

$$P_L = \frac{R_0 k_T^2}{Q^2 k_b} P_{bb} \left( 1 + \frac{m^2}{2} \right) \quad (15-37)$$

It may be concluded from this that the d-c plate power supply furnishes

the power to produce the carrier wave and the modulated amplifier furnishes the power to produce the side bands in the output.

The plate-circuit efficiency of the modulated amplifier is given by the expression

$$\eta = \frac{P_L}{P_{bb} + P_m} \quad (15-38)$$

which becomes

$$\eta = \frac{R_0 k_T^2 P_{bb} (1 + m^2/2)}{Q^2 k_b P_{bb} (1 + m^2/2)}$$

or

$$\eta = \frac{R_0 k_T^2}{Q^2 k_b} \quad (15-39)$$

This result shows that the plate-circuit efficiency is independent of the degree of modulation. Therefore one may calculate the efficiency from considerations of the unmodulated amplifier as a simple class C device. To find an expression for the power dissipated in the plate of the tube, it is evident that

$$P_p = P_{bb} + P_m - P_L$$

which may be written in the form

$$P_p = P_{bb} (1 - \eta) \left( 1 + \frac{m^2}{2} \right) \quad (15-40)$$

Consider the results when the modulation index  $m$  is zero. The foregoing become, in this case,

$$\left. \begin{aligned} P_{bb} &= k_b E_{bb}^2 \\ P_m &= 0 \\ P_L &= \eta P_{bb} \\ P_p &= (1 - \eta) P_{bb} \\ \eta &= \frac{R_0 k_T^2}{Q^2 k_b} \end{aligned} \right\} \quad (15-41)$$

By comparing these expressions with the corresponding expressions when  $m$  is not zero, it is observed that the addition of modulation increases the plate dissipation. This requires that a given tube in being operated under modulated conditions must be operated with a reduced plate voltage and current if a specified maximum allowable plate dissipation is not to be exceeded.

In order to design the modulating amplifier, a knowledge of the effective impedance across the secondary terminals of the output transformer of this amplifier is needed. This will permit a specification of the turns ratio of the modulating transformer in order to reflect the optimum value of impedance into the plate circuit of the modulating tubes. This imped-

ance is readily obtained by observing that the plate impedance is substantially resistive and must be given by

$$R_m = \frac{E_m^2}{P_m} = \frac{E_{mm}^2/2}{E_{mm}I_b(m/2)} = \frac{E_{bb}}{I_b} = \frac{1}{k_b} = R_b \quad (15-42)$$

This shows that the effective impedance is independent of the modulation.

The plate-modulated amplifier is used extensively in radio transmitters. It has the advantage that modulation without excessive distortion is

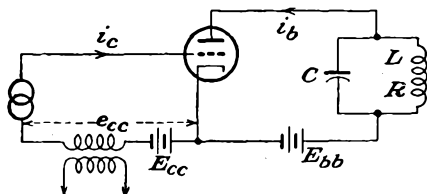


FIG. 15-12. A grid-bias modulated class C amplifier.

possible in practice by reasonably simple methods. Also, it operates at high efficiency and is relatively easy of adjustment. It has the disadvantage that a comparatively large amount of power at the modulating frequency is required. The resulting cost of the heavy and bulky modulating equipment is sometimes greater than that of other methods. It might be of interest to know that the two modulating transformers at the 500-kw radio station WLW weigh approximately 19 tons each and that an audio choke weighs 12 tons.<sup>4</sup>

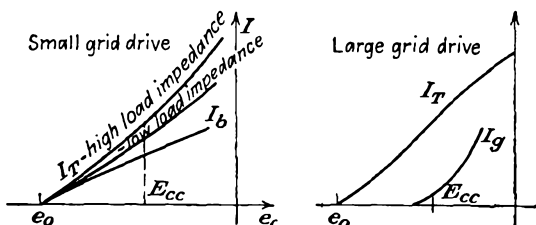


FIG. 15-13. Typical linearity curves of a grid-bias modulated class C amplifier under different conditions.

**15-6. Grid-bias Modulation.** Amplitude modulation may be accomplished by connecting the modulating source in series with the grid instead of in the plate circuit. The basic circuit of such a grid-bias modulated amplifier is illustrated in Fig. 15-12. Typical linearity curves of such an amplifier for several different conditions are illustrated in the curves of Fig. 15-13. The general character of the operation is illustrated graphically in Fig. 15-14.

To analyze the operation, the procedure is essentially parallel to that of Sec. 15-5 for the plate-modulated amplifier. It is assumed that the modulation characteristic is linear and that  $\omega_c \gg \omega_m$ . The carrier signal is chosen of the form

$$e_g = E_{gm} \cos \omega_c t \quad (15-43)$$

and the modulating voltage is of the form

$$e_m = E_{mm} \cos \omega_m t \tag{15-44}$$

The total grid-cathode potential has the form

$$e_c = E_{gm} \cos \omega_c t + E_{mm} \cos \omega_m t + E_{cc} \tag{15-45}$$

and the slowly varying grid supply source is given by

$$e_{cc} = E_{mm} \cos \omega_m t + E_{cc} \tag{15-46}$$

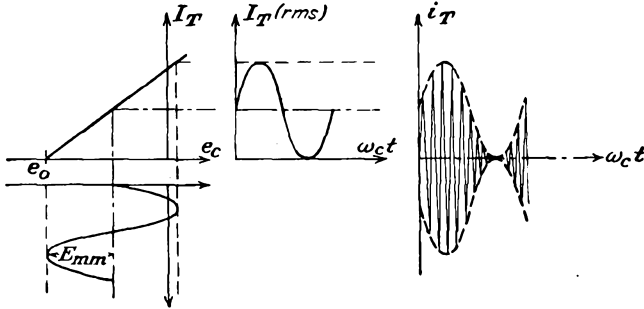


FIG. 15-14. Conditions for 100 per cent modulation in a grid-bias modulated class C amplifier.

Over the linear range of operation, the analytic form for the rms tank current is

$$I_T = k_T(e_{cc} - e_0) \tag{15-47}$$

Also, if the instantaneous value of the tank current is chosen as

$$i_T = \sqrt{2} I_T \sin \omega_c t$$

this may be written as

$$i_T = \sqrt{2} k_T(e_{cc} - e_0) \sin \omega_c t$$

or

$$i_T = \sqrt{2} k_T(E_{mm} \cos \omega_m t + E_{cc} - e_0) \sin \omega_c t \tag{15-48}$$

But when the modulation is zero, the tank current has the form

$$i_T = \sqrt{2} k_T(E_{cc} - e_0) \sin \omega_c t$$

which may be written as

$$\left. \begin{aligned} i_T &= I_{Tm} \sin \omega_c t \\ I_{Tm} &= \sqrt{2} k_T(E_{cc} - e_0) \end{aligned} \right\} \tag{15-49}$$

Note that, when the modulation exists, the value of the tank current at the peak of the modulating cycle is

$$I'_{Tm} = \sqrt{2} k_T(E_{mm} + E_{cc} - e_0) \tag{15-50}$$

The conditions are best examined graphically as in the accompanying

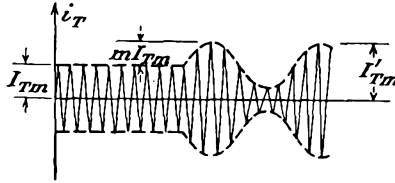


figure. Clearly, the degree of modulation is seen to be

$$m = \frac{I'_{Tm} - I_{Tm}}{I_{Tm}} \quad (15-51)$$

which may be written as

$$m = \frac{\sqrt{2}k_T(E_{mm} + E_{cc} - e_0) - \sqrt{2}k_T(E_{cc} - e_0)}{\sqrt{2}k_T(E_{cc} - e_0)}$$

which reduces to

$$m = \frac{E_{mm}}{E_{cc} - e_0} \quad (15-52)$$

By combining Eq. (15-52) with Eq. (15-48), the instantaneous tank current assumes the form

$$i_T = \sqrt{2}k_T[(E_{cc} - e_0)m \cos \omega_m t + (E_{cc} - e_0)] \sin \omega_c t$$

which is

$$i_T = \sqrt{2}k_T(E_{cc} - e_0)(1 + m \cos \omega_m t) \sin \omega_c t \quad (15-53)$$

In an entirely parallel way, it is possible to find for the plate current the expression

$$I_b = k_b(e_{cc} - e_0) \quad (15-54)$$

which may be written as

$$I_b = k_b(E_{cc} - e_0)(1 + m \cos \omega_m t) \quad (15-55)$$

The voltage across the tank circuit is

$$E_L = jX_L I_T$$

which is

$$E_L = jX_L k_T (E_{cc} - e_0)(1 + m \cos \omega_m t) \quad (15-56)$$

Therefore the instantaneous potential across the tank circuit is given by

$$e_L = \sqrt{2}X_L k_T (E_{cc} - e_0)(1 + m \cos \omega_m t) \sin(\omega_c t + 90)$$

or

$$e_L = \sqrt{2}X_L k_T (E_{cc} - e_0)(1 + m \cos \omega_m t) \cos \omega_c t \quad (15-57)$$

It is now possible to complete the analysis of the circuit.

Expressions for the various important values of power in the circuit are readily obtained. The power input to the plate circuit by the d-c plate supply is

$$P_{bb} = \frac{1}{T} \int_0^T E_{bb} i_b dt$$

This becomes, by Eq. (15-55),

$$P_{bb} = \frac{1}{T} \int_0^T E_{bb} k_b (E_{cc} - e_0) (1 + m \cos \omega_m t) dt$$

which integrates to

$$P_{bb} = E_{bb} k_b (E_{cc} - e_0) = E_{bb} I_b \quad (15-58)$$

Since this result shows no dependence on the modulation index  $m$ , it follows that the plate supply power is independent of the degree of modulation.

The power output at the tank circuit is given by

$$P_L = \frac{1}{T} \int_0^T e_L i_{p1} dt = \frac{1}{T} \int_0^T R_0 i_{p1}^2 dt$$

which becomes, by Eq. (15-53),

$$P_L = \frac{1}{T} \int_0^T \frac{2R_0 k_T^2}{Q^2} (E_{cc} - e_0)^2 (1 + m \cos \omega_m t)^2 \sin^2 \omega_c t dt$$

This integrates to

$$P_L = \frac{R_0 k_T^2}{Q^2} (E_{cc} - e_0)^2 \left(1 + \frac{m^2}{2}\right) = I_T^2 R \left(1 + \frac{m^2}{2}\right) \quad (15-59)$$

This shows that the r-f power increases with percentage modulation.

The plate-circuit efficiency of the modulated amplifier is given by

$$\eta = \frac{P_L}{P_{bb}} = \frac{(R_0 k_T^2 / Q^2) (E_{cc} - e_0)^2 (1 + m^2 / 2)}{E_{bb} k_b (E_{cc} - e_0)}$$

which becomes

$$\eta = \frac{R k_T^2}{k_b E_{bb}} (E_{cc} - e_0) \left(1 + \frac{m^2}{2}\right) \quad (15-60)$$

This expression shows that the plate efficiency increases as the modulation index increases. To realize the highest efficiency for a given modulation index ( $= 1$ ) it is necessary that the quantity  $E_{cc} - e_0$  be made as large as possible. This requires that the load impedance of the modulated amplifier be so adjusted that the peak amplitude of the output wave is only slightly less than the d-c plate supply.

The plate dissipation of the tube is given by the expression

$$P_p = P_{bb} - P_L$$

which is

$$P_p = k_b E_{bb}(E_{cc} - e_0) - Rk_T^2(E_{cc} - e_0)^2 \left(1 + \frac{m^2}{2}\right) \quad (15-61)$$

This may be written in the form

$$P_p = E_{bb}I_b - I_T^2 R \left(1 + \frac{m^2}{2}\right) \quad (15-62)$$

It should be noted that the plate dissipation decreases as the percentage modulation increases. Clearly, therefore, the plate dissipation is a maximum when the amplifier is unmodulated.

Grid-bias modulation has the advantage that only a small amount of l-f modulating power is required. However, the carrier power that is obtainable from the amplifier is approximately one-quarter of that from the same tube when operating as a simple class C amplifier. This is so because the peak power of the modulated amplifier corresponds to class C operation, and with a completely modulated wave the peak current is twice the unmodulated current and the corresponding peak power is four times the unmodulated, or carrier, power. Also, the plate efficiency during the unmodulated intervals is approximately one-half of the efficiency obtained with simple class C operation. This results from the fact that, if the amplifier is so adjusted that the plate voltage is small at the crest of the modulation cycle, then, when there is no modulation, the voltage across the load is halved. This results in a high voltage across the tube, with a corresponding large plate loss. As a result, the plate-circuit efficiency in the absence of modulation is of the order of 34 per cent. During 100 per cent modulation by a sinusoidal signal, the r-f power output increases by a factor of  $\frac{1}{2}$ , and the plate-circuit efficiency increases to approximately 51 per cent.

It is interesting to compare the operating features of a plate and a grid-bias modulated amplifier. These are

Grid-bias modulated amplifier:

Relatively low plate efficiency.

Low power output in proportion to the capabilities of the modulated tube.

Low grid-modulating power.

Plate-modulated amplifier:

Large power output in proportion to the power capabilities of the modulated tube.

Large modulator power.

In consequence, the over-all efficiency, considering both the modulating and the modulated tube capabilities, is roughly the same. The choice

between the two methods of modulation is largely one of convenience, since both methods of modulation will give sensibly 100 per cent modulated waves with essentially negligible distortion. The circuit adjustments are more difficult with grid-bias modulation, as they are sensitive to variations in the carrier exciting voltage, the plate supply voltage, and the magnitude of the tuned load impedance.

**15-7. Other Methods of Modulation of a Class C Amplifier.** A modulated output wave is produced if the modulating voltage is introduced in the cathode of the amplifier. Since in such a circuit the modulating voltage is effectively in both the plate and the grid circuits, the characteristics are a combination of those of the plate-modulated and the grid-bias modulated amplifiers. The plate efficiency and the modulating power requirements are intermediate between the corresponding requirements for the plate- and the grid-modulated amplifiers.

If a pentode is employed, the modulation voltage may be applied in the suppressor-grid circuit. The general characteristics of such a suppressor-grid modulated class C amplifier are similar to those for the control-grid modulation. However, adjustment of the amplifier is simpler. Fairly linear modulation up to 100 per cent may be obtained.

Modulation may be accomplished by injecting the modulation in the screen circuit of a tetrode or pentode. Some power is required from the modulating source, and 100 per cent modulation usually cannot be achieved without some distortion.

#### REFERENCES

As general references, see

- M.I.T. Staff, "Applied Electronics," Sec. 12-4 to 12-6, John Wiley & Sons, Inc., New York, 1943.
- Cruft Laboratory, War Training Staff, "Electronic Circuit and Tubes," Chap. XX, Secs. 15-18, 15-19, McGraw-Hill Book Company, Inc., New York, 1947.
- Standards on Transmitters and Antennas, Institute of Radio Engineers, 1933.
  - Carson, J. R., *Proc. IRE*, **9**, 243 (1921).
  - Peterson, E., and C. R. Keith, *Bell System Tech. J.*, **7**, 131 (1928).
  - Chambers, J. A., L. F. Jones, G. W. Fyler, R. H. Williamson, E. A. Leach, and J. A. Hutcheson, *Proc. IRE*, **22**, 1151 (1934).

#### PROBLEMS

**15-1.** The equation of a modulated wave is

$$e = (15 + 10 \sin 3,000t - 8 \cos 10,000t) \cos 2\pi \times 10^6 t$$

- What frequencies are contained in the modulated wave?
- What is the amplitude of each?

**15-2.** Carry out the analysis to show that amplitude modulation results in a square-law circuit when the carrier voltage is applied in the grid circuit and the modulating voltage is applied in the plate circuit.

15-3. Prove that the carrier term is missing in the balanced modulator of Fig. 15-8.

15-4. The balanced modulator of Fig. 15-8a is used for carrier suppression. In this circuit, the potentials applied are the following:

$$\begin{aligned} e_c &= E_c \cos \omega_c t \\ e_m &= E_m \cos \omega_m t \end{aligned}$$

with  $\omega_c \gg \omega_m$  and with  $E_m = 0.5E_c$ . Assume that the transconductance  $g_m$  varies linearly with grid voltage.

- a. Obtain an expression for the output voltage from the modulator.
- b. Plot the envelope of this potential.

15-5. Suppose that a band-pass filter is connected in the output of Prob. 15-4 of such characteristics that the lower side bands are eliminated.

- a. What is the expression for the resulting output?
- b. Plot the envelope of this wave.

15-6. An ideal diode for which  $r_p = 1,000$  ohms in the forward direction and  $r_p = \infty$  in the inverse direction is used as a modulator. There is applied to this circuit the two voltages

$$e = E_c \cos \omega_c t + E_m \cos \omega_m t$$

with  $\omega_c \gg \omega_m$  and with  $E_m = 0.5E_c$ .

- a. Determine the amplitude of the component of current of angular frequency  $(\omega_c - \omega_m)$ .
- b. Repeat for the component of frequency  $(\omega_c + \omega_m)$ .

15-7. Repeat Prob. 15-6 for the case where the single diode is replaced by four diodes connected in a bridge circuit.

15-8. A type 851 power triode operates with a bias of  $-300$  volts and with a peak r-f signal of 525 volts. The load impedance  $R_0 = 1,500$  ohms. Determine and plot the a-c plate potential across the tank as a function of the d-c plate supply voltage, for the following values of plate voltage:  $E_{bb} = 500, 1,500, 2,500, 3,500$  volts.

15-9. Repeat Prob. 15-8 for  $R_0 = 1,000$  ohms.

15-10. An 851 triode is used in a plate-modulated class C amplifier. It operates with a bias of  $-300$  volts, a peak r-f signal of 525 volts, and a plate supply  $E_{bb} = 2,000$  volts. When  $e_{bb} = E_{bb}$ , the peak plate swing is 1,750 volts. Determine the plate-current wave-forms at the values of  $e_{bb} = 1,000, 2,000, 3,000$  volts.

15-11. A type 891 r-f power triode has the following ratings as a class C oscillator for telegraphy:

D-c plate voltage.....	10,000 volts
D-c grid voltage.....	-2,000 volts
D-c plate current.....	1.45 amp
D-c grid current.....	0.105 amp
Grid driving power.....	310 watts
Power output.....	10 kw
Peak r-f grid voltage.....	2,900 volts

If the plate dissipation is the only limiting factor, determine the corresponding ratings of the tube for class C telephony, allowing for 100 per cent plate modulation. When plate-modulated 100 per cent, determine

- a. The audio power required.
- b. The impedance offered to the audio source.
- c. Power output.
- d. Plate-circuit efficiency.

15-12. An 852 transmitting triode has the following ratings as a plate-modulated r-f amplifier under carrier conditions that allow for 100 per cent modulation:

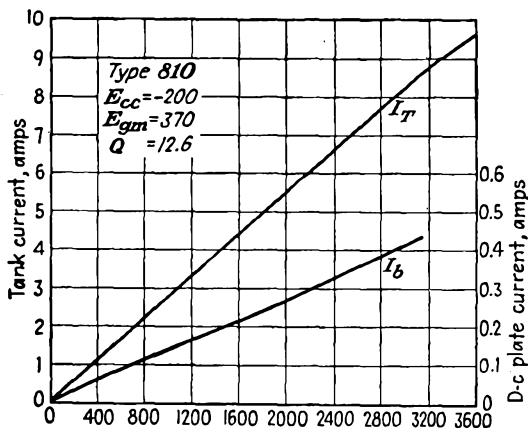
D-c plate voltage	2,000 volts
D-c grid voltage	-500 volts
D-c plate current	67 ma
D-c grid current	30 ma
Peak r-f grid voltage	750 volts
Grid driving power	23 watts
Power output	75 watts

The amplifier is sinusoidally plate-modulated 75 per cent. Determine

- a. Audio power required.
- b. Impedance offered to the audio source.
- c. Plate efficiency.
- d. Average plate dissipation.
- e. Grid dissipation at the tube terminal.

If the amplifier were unmodulated, what would be the maximum allowable r-f power output, assuming that the plate dissipation is the limiting factor, and that the plate-circuit efficiency remains constant?

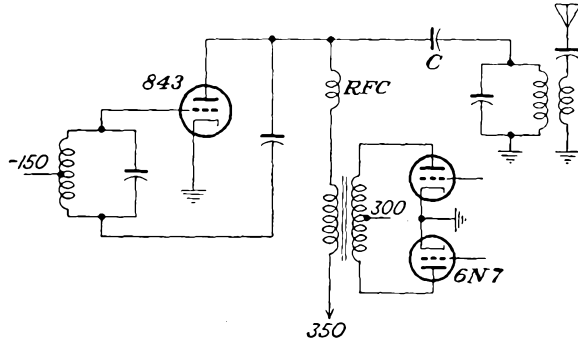
15-13. The results on a plate-modulated class C amplifier are given in the figure. Suppose that this modulated amplifier is operated at 1,600 volts d-c,



with 75 per cent modulation. Assume a constant plate efficiency of 60 per cent. Calculate the following:

- The power supplied by the d-c plate source.
- The power supplied by the audio source.
- The r-f carrier power.
- The r-f side-band power
- The resistance of the class C amplifier to the modulating source.
- The maximum and minimum instantaneous voltage between plate and cathode when the carrier is unmodulated.
- Repeat *f.* for  $m = 0.75$ .

**15-14.** The essential elements of a plate-modulated class C amplifier are



illustrated in the diagram. The tubes are operated under the following conditions:

843 tube:

$$\begin{aligned} f_c &= 1.2 \text{ megacycles} \\ E_{bb} &= 350 \text{ volts d-c} \\ I_b &= 30 \text{ ma d-c} \end{aligned}$$

6N7 tube:

$$\begin{aligned} E_{bb} &= 300 \text{ volts d-c} \\ \text{Effective plate-plate resistance} &= 8,000 \text{ ohms} \end{aligned}$$

Impedance of 843 tank circuit at 1.2 megacycles is 10,000 ohms.

Effective  $Q$  of 843 tank is 15.

The carrier output is to be 5 watts 100 per cent modulated.

Calculate the following:

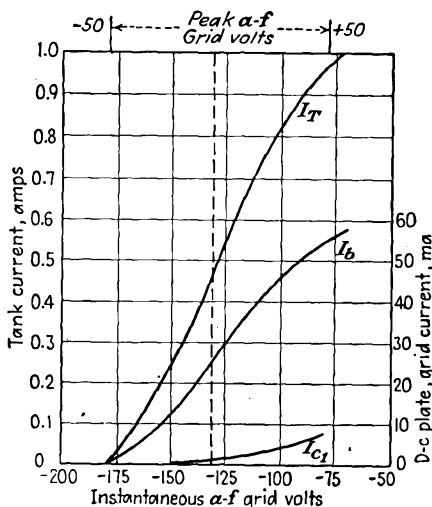
- The plate-circuit efficiency of the 843.
- The power required from the 6N7.
- The load impedance presented by the 843 to the secondary of the modulating transformer.
- The transformer ratio that should be used.
- If the output is to be down 1 db 5,000 cycles off resonance, what must the effective  $Q$  of the 843 tank circuit be?
- The value of  $C$ .
- The approximate value of the r-f choke  $RFC$ .
- With a loaded  $Q$  of 15, calculate the value of  $L$  and  $C$  of the 843 tank circuit.
- If the actual resistance in the 843 tank is 5 ohms, how much resistance is coupled into this tank from its load?
- What is the efficiency of power transfer from the tank to the load?

15-15. An 806 tube is to be used as the plate-modulated class C power amplifier of a transmitter. It operates from a 2,500-volt power supply. Carry out the design of this and the associated transformer-coupled class B modulator. The design must fulfill the following specifications:

- The plate dissipation is not to exceed 150 watts.
- The transmitter is to be plate-modulated 70 per cent.
- The distortion in the modulating envelope is not to exceed 10 per cent.
- The transmitter frequency is 2 megacycles.
- The grid bias may be obtained with grid leak, fixed bias, or a combination of both.
- Specify the plate supply voltage, grid bias, and excitation voltage.
- The output is to feed a 76-ohm antenna.
- Specify the primary inductance, secondary inductance, tuning condenser, and mutual inductance. Assume that the unloaded  $Q$  of the coils is 300 and that the loaded  $Q$  is 12.
- Give the modulation-transformer requirements.

Be sure that any assumptions that are made are clearly stated.

15-16. The characteristics of an 802 tube when used as a grid-bias modulated



Control-grid modulation characteristic—type 802:  
 $E_{bb} = 500$        $E_{cc} = -130$   
 $E_{cc2} = 200$       Peak r-f grid volts = 145

class C amplifier are given in the sketch. Calculate for  $m = 1.0$  the following:

- The power supplied by the d-c source.
- The r-f carrier power.
- The side-band power.
- The plate efficiency.

- e.* The plate dissipation.
- f.* The maximum and minimum instantaneous voltage between cathode and plate when the carrier is unmodulated.
- g.* Repeat *f.* for  $m = 0.75$ .
- h.* What is the amplitude of the a-f signal to achieve the desired degree of modulation?
- i.* What is the a-f driving power?
- j.* What is the grid-cathode power loss?

Choose  $R_L = 12.6$  ohms;  $Q = 26.5$ .

**15-17.** Consider a class C amplifier that is modulated 100 per cent. Assume the output power to be 1,000 watts. Assume reasonable values of plate-circuit efficiency for each of the tubes involved, and calculate (1) the total power required by the modulated tube, (2) the total power required by the modulator tubes, and (3) the over-all plate-circuit efficiency when the amplifier is

- a.* plate-modulated, using a class A modulator.
- b.* plate-modulated, using a class B modulator.
- c.* grid-bias modulated.

Repeat the calculations for zero per cent modulation.

---

## CHAPTER 16

### DEMODULATION

WHEN the radiated modulated carrier signal reaches the receiving point, the signal or intelligence must be extracted therefrom. The process by which the signal is recovered from the radiated wave is broadly known as *demodulation* or *detection*.

It is important that the processes of modulation and demodulation be clearly understood. As already discussed, in the process of modulation the signal frequencies, which are centered about the zero-frequency reference level, are shifted upward on the frequency scale so as to be centered about the carrier frequency  $\omega_c$ . This frequency shifting is accomplished by mixing the signal frequencies with the carrier frequency in appropriate circuits. In the process of demodulation the signal spectrum, which is centered about  $\omega_c$ , is shifted downward on the frequency scale so as to be centered about the zero frequency, thus returning it to its original frequency position. This frequency shifting is accomplished by mixing the signal-frequency group centered about  $\omega_c$  with the carrier frequency  $\omega_c$  in appropriate circuits. Clearly, both the modulating and the demodulating processes involve frequency shifting, and both shifts are by an amount  $\omega_c$ . However, in the modulating process the carrier is generated in one circuit, and this is combined with the audio signal in the modulator. In demodulation the required carrier wave is ordinarily contained in the incoming modulated carrier, and no separate carrier-generating circuit is generally necessary. Such a separate carrier-generating circuit is required in suppressed carrier transmission.

It is also customary to consider the elimination of the original carrier from the modulated signal and the substitution for it of a new carrier, as in frequency changing, as demodulation. In essence, therefore, frequency shifting in which the signal frequency does not play a direct part would be considered as demodulation.

**16-1. Square-law Detection.** Detection is possible when a modulated voltage is applied to the grid of a tube which is biased to the nonlinear portion of its transfer characteristic. This is made evident by an examination of Fig. 16-1. The output curve clearly shows the presence in the output of a component that varies at the modulating-frequency rate.

To examine the operation of the circuit analytically, it will be supposed

that the transfer curve is a simple square-law characteristic of the form

$$i_p = ae_g^2 \quad (16-1)$$

Suppose that the signal is an a-m wave of the form

$$e_g = E_c(1 + m \cos \omega_m t) \cos \omega_c t \quad (16-2)$$

Then the output current will contain the terms

$$\begin{aligned} i_p &= aE_c^2(1 + m \cos \omega_m t)^2 \cos^2 \omega_c t \\ &= \frac{aE_c^2}{2} (1 + m \cos \omega_m t)^2 (1 + \cos 2\omega_c t) \\ &= aE_c^2 \left[ \frac{1}{2} + m \cos \omega_m t + \frac{m^2}{4} + \frac{m^2}{4} \cos 2\omega_m t \right. \\ &\quad \left. + \frac{1}{2} \cos 2\omega_c t + \frac{m}{2} \cos (2\omega_c + \omega_m)t + \frac{m}{2} \cos (2\omega_c - \omega_m)t \right. \\ &\quad \left. + \frac{m^2}{2} \cos 2\omega_c t + \frac{m^2}{8} \cos (2\omega_c + 2\omega_m)t \right. \\ &\quad \left. + \frac{m^2}{8} \cos (2\omega_c - 2\omega_m)t \right] \quad (16-3) \end{aligned}$$

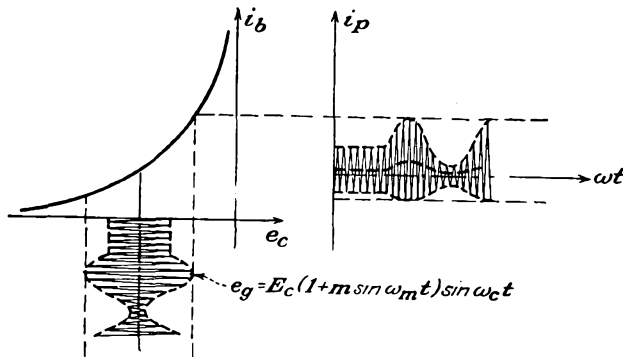


FIG. 16-1. Sketch showing the operation of a square-law detector.

Clearly, there will be included in the output a number of steady components, a term of modulating frequency, a number of components of frequencies equal to the sums and differences of the carrier and side frequencies, and a number of components of twice the carrier and side frequencies.

Suppose that a selective network is used which attenuates all components except those in the neighborhood of the modulating frequency  $\omega_m$ . The terms that appear in the output will then be

$$i_1 \doteq amE_c^2 \left( \cos \omega_m t + \frac{m}{4} \cos 2\omega_m t \right) \quad (16-4)$$

which consists of the desired term plus one of second harmonic of this frequency. If the second-harmonic amplitude is to be kept smaller than, say, 10 per cent of the fundamental, it is necessary that the modulation index be less than 0.4 for sinusoidal modulation. Despite this limitation, such detectors have been used extensively with generally satisfactory results, probably because the average modulation of the ordinary radio program is of the order of 40 per cent.

It is of interest and of significance in subsequent work to examine those terms in the neighborhood of the second harmonic of the carrier  $2\omega_c$ , although these results are not of importance at this particular point. The terms are

$$i_2 = \frac{aE_c^2}{2} \left[ \left( 1 + \frac{m^2}{2} \right) \cos 2\omega_c t + m \cos (2\omega_c + \omega_m)t + m \cos (2\omega_c - \omega_m)t + \frac{m^2}{4} \cos (2\omega_c + 2\omega_m)t + \frac{m^2}{4} \cos (2\omega_c - 2\omega_m)t \right] \quad (16-5)$$

If  $m$  is small, this equation can be written as

$$i_2 \doteq \frac{aE_c^2}{2} [\cos 2\omega_c t + m \cos (2\omega_c + \omega_m)t + m \cos (2\omega_c - \omega_m)t]$$

which is

$$i_2 = \frac{aE_c^2}{2} (1 + 2m \cos \omega_m t) \cos 2\omega_c t \quad (16-6)$$

Therefore, if one were to use a tuned circuit at the output of a square-law circuit which is tuned to  $2\omega_c$ , the output would be of second harmonic of the carrier but the modulation frequency would be unchanged. Frequency doublers of this type find extensive use in h-f operations.

**16-2. Diode Detection.** Diode detectors have almost completely supplanted other types of detectors in home radio-receiver use. They operate very satisfactorily, although the modulated input to the detector must be large—in excess of about 2 volts. Otherwise excessive distortion may result because of the nonlinear dynamic curve of the diode circuit. Since the diode detector possesses characteristics in common with ordinary rectification, it is possible to present a qualitative discussion of its operation on this basis.

There are two important types of operation of a diode detector. One is known as *average detection*, and the other is *envelope detection*. The circuit for average detection is illustrated in Fig. 16-2. Also illustrated in this figure is the character of input and output waves. It will be observed that this is just a simple diode rectifier without a filter in the output. The application of a modulated wave to the circuit yields an output the average value of which contains the modulating frequency.

It follows from simple rectifier theory that the output voltage is of the form

$$E_m = \frac{R}{\pi(R + r_p)} E_c(1 + m \cos \omega_m t) \quad (16-7)$$

The use of appropriate circuits permits the modulating-frequency component to be extracted from the output.

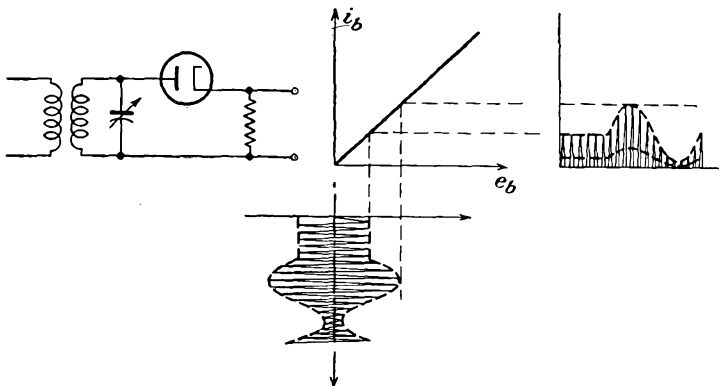


FIG. 16-2. The circuit and the operational characteristics of an average diode detector.

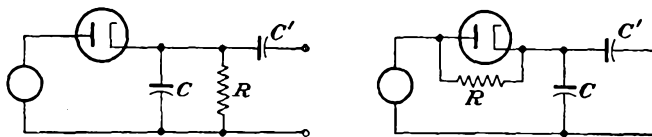


FIG. 16-3. Two circuits for envelope detection.

The circuit for envelope detection is illustrated in Fig. 16-3. It will be observed that these are essentially the circuits of a simple diode rectifier with a capacitor filter.

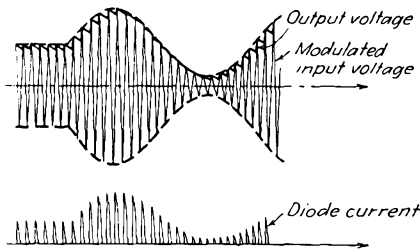


FIG. 16-4. Wave forms of the input voltage, output voltage, and plate current in a diode-detector circuit.

The operation of this circuit is substantially the same as that for the simple rectifier, with the additional fact that the a-c input voltage varies in amplitude. With the proper choice of the filter capacitor, the wave forms of the input voltage, the output voltage, and the tube current are roughly those shown in Fig. 16-4. Since the carrier frequency is much greater than the modulating

frequency, the jagged appearance of the above curves is considerably worse than is actually the case. In effect, therefore, the output voltage

of the detector follows closely the envelope of the modulated input wave and has the wave form of the modulating voltage.

**16-3. Analysis of Diode Detection.**<sup>1</sup> An analytic expression that gives certain of the properties of the diode detector is possible if several reasonable assumptions are made. In particular, it will be assumed that the d-c potential across the diode load, which arises from the tube current during the portion of the cycle when the input voltage exceeds the voltage across the output capacitor, will remain constant over the carrier-frequency cycle. It will also be assumed that the static characteristic of the diode is linear. The conditions that apply during one cycle of the impressed modulated r-f signal wave are as illustrated in Fig. 16-5.

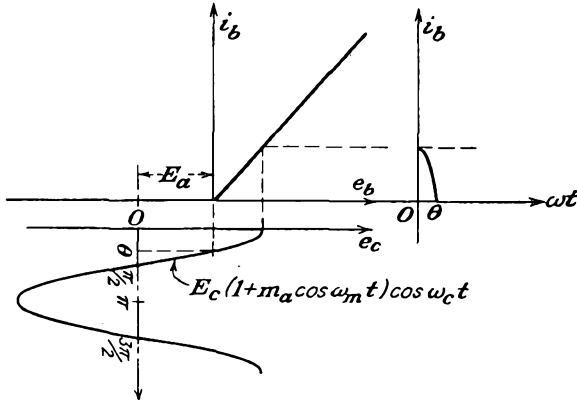


FIG. 16-5. The approximate action of a diode detector.

The equation of the assumed characteristic is

$$\left. \begin{aligned} i_b &= \frac{e_b}{r_p} = g_p e_b & e_b > 0 \\ i_b &= 0 & e_b < 0 \end{aligned} \right\} \quad (16-8)$$

But as the instantaneous voltage applied to the diode is given by the equation

$$\begin{aligned} e_b &= E_c(1 + m \cos \omega_m t) \cos \omega_c t - E_a \\ &= E' \cos \omega_c t - E_a \end{aligned} \quad (16-9)$$

the plate current will be of the form

$$\left. \begin{aligned} i_b &= g_p(E' \cos \omega_c t - E_a) & e_b > 0 \\ i_b &= 0 & e_b < 0 \end{aligned} \right\} \quad (16-10)$$

The shift from one equation to the other occurs at the angle  $\theta$ , which is such that

$$E' \cos \omega_c t_0 = E' \cos \theta = E_a \quad (16-11)$$

The instantaneous current  $i_b$  will contain a number of harmonic components, but those of interest are the d-c or average component and the a-c term at the driving frequency. The d-c component of  $i_b$  is given by

$$I_b = \frac{1}{2\pi} \int_0^{2\pi} i_b d\theta$$

which is, because of the symmetry that exists,

$$I_b = \frac{1}{\pi} \int_0^\theta i_b d\theta$$

This may be written as

$$I_b = \frac{1}{\pi} \int_0^\theta g_p(E' \cos \theta - E_a) d\theta \quad (16-12)$$

which becomes

$$I_b = \frac{g_p}{\pi} [E' \sin \theta - E_a \theta] \quad (16-13)$$

This becomes, by Eq. (16-11)

$$I_b = \frac{g_p}{\pi} E' (\sin \theta - \theta \cos \theta) \quad (16-14)$$

Also, it is initially assumed that

$$E_a = I_b R \quad (16-15)$$

By combining Eqs. (16-14) and (16-15), there results

$$I_b = \frac{E_a}{R} = \frac{E' \cos \theta}{R} = \frac{g_p E'}{\pi} (\sin \theta - \theta \cos \theta)$$

from which

$$\frac{r_p}{R} = \frac{1}{\pi} (\tan \theta - \theta) \quad (16-16)$$

This expression shows that there is a direct functional relationship between the operating angle  $\theta$  and the ratio of the plate resistance of the diode to the external resistance. An explicit expression for  $\theta$  as a function of  $r_p/R$  is very difficult, but the information may be given graphically.

The detection efficiency of a detector is defined as the ratio of the actual output voltage of modulation frequency  $E_m$  to the maximum possible value of this modulating voltage, *i.e.*, to the value of the envelope of the carrier. Analytically the detection efficiency is defined by the relation

$$\overline{E_m} = \overline{\eta m E_c} \quad (16-17)$$

To find an expression for  $\eta$ , it is noted that, when no capacitor is used

(average detection), the output voltage is

$$E_m = \frac{R}{\pi(R + r_p)} E_c(1 + m \cos \omega_m t)$$

which is, for  $R > r_p$

$$E_m \doteq \frac{E_c}{\pi} (1 + m \cos \omega_m t) \tag{16-18}$$

Evidently the maximum possible value would occur with  $C$  shunting  $R$  and would be

$$(E_m)_{\max} = E_c(1 + m \cos \omega_m t) \tag{16-19}$$

However, with  $C$  present, the output is actually given by Eq. (16-11), which is

$$E_a = E' \cos \theta = E_c(1 + m \cos \omega_m t) \cos \theta \tag{16-20}$$

Hence it follows, since

$$\eta = \frac{E_m}{(E_m)_{\max}}$$

that

$$\eta = \cos \theta \tag{16-21}$$

A plot of  $\eta$  as a function of  $r_p/R$  is contained in Fig. 16-6. It should be noted that, if  $R$  is large compared with  $r_p$ , then  $\eta$  is practically independent

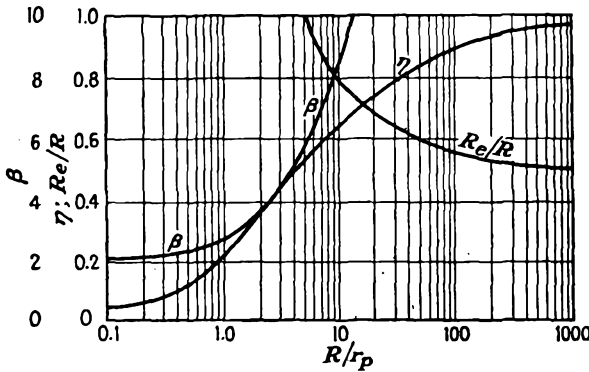


FIG. 16-6. Various important terms in the analysis of diode detectors.

of  $r_p$ . Consequently the detection efficiency of a diode is not appreciably influenced by the curvature of the characteristic.

Another quantity of importance in detector operation is the power absorbed by the detector, or the power loss in the diode circuit. To evaluate this requires a knowledge of the fundamental-frequency component of the current. The maximum value of the current is given by the Fourier coefficient

$$I_{p1m} = \frac{1}{\pi} \int_0^{2\pi} i_b \cos \omega t d(\omega t)$$

This becomes

$$I_{p1m} = \frac{2}{\pi} \int_0^\theta g_p(E' \cos \theta - E_a) \cos \theta d\theta \quad (16-22)$$

which integrates to

$$I_{p1m} = \frac{2g_p E'}{\pi} \left( \frac{\theta}{2} + \frac{1}{4} \sin 2\theta - \sin \theta \cos \theta \right)$$

or

$$I_{p1m} = \frac{g_p E'}{\pi} (\theta - \sin \theta \cos \theta) \quad (16-23)$$

The power input to the diode and its load is

$$P = \frac{1}{T} \int_0^T e i_b dt$$

$$P = \frac{E' I_{p1m}}{2} = \frac{g_p E'^2}{2} (\theta - \sin \theta \cos \theta) \quad (16-24)$$

The effective resistance of the diode circuit is defined by the relation

$$R_e \equiv \frac{E'^2}{2P} = \frac{\pi}{g_p(\theta - \sin \theta \cos \theta)} \quad (16-25)$$

which may be written as

$$\left. \begin{aligned} R_e &= r_p \beta \\ \beta &\equiv \frac{\pi}{(\theta - \sin \theta \cos \theta)} \end{aligned} \right\} \quad (16-26)$$

That is, the effective resistance in parallel with the capacitor due to the loss in the diode circuit is equal to  $\beta r_p$ . A plot of  $\beta$  is also contained in Fig. 16-6.

By combining Eqs. (16-26) with (16-16), an expression for the equivalent resistance that shunts the diode input circuit is possible. This is

$$\frac{R_e}{R} = \frac{R_e}{r_p} \frac{r_p}{R} = \frac{\tan \theta - \theta}{\theta - \sin \theta \cos \theta}$$

This expression is plotted as a function of  $R/r_p$  in Fig. 16-6.

For the case when  $\eta$  is high, the equivalent input resistance reduces to a simple form. Noting that, for  $\eta$  high,  $\theta$  is small,

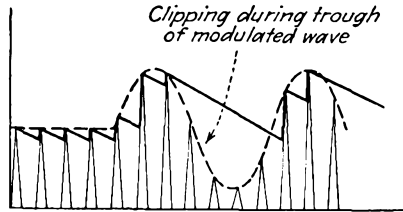
$$\sin \theta \doteq \theta - \frac{\theta^3}{6} \quad \cos \theta \doteq 1 - \frac{\theta^2}{2}$$

and

$$\frac{R_e}{R} = \frac{1}{\cos \theta} \left( \frac{\sin \theta - \theta \cos \theta}{\theta - \sin \theta \cos \theta} \right) \doteq \frac{1}{2\eta} \quad (16-27)$$

Hence the effective input resistance becomes  $R/2\eta$  for large  $\eta$  and hence is slightly greater than one-half the load resistance.

**16-4. Distortion in Diode Detectors.** There are two sources of distortion in a simple diode detector. One results from the curvature in the tube characteristic, making the efficiency of rectification vary according to the amplitude of the envelope. This source of distortion may be minimized by making the load resistance large compared with the diode plate resistance and by making the amplitude of the carrier amplitude applied to the diode reasonably large. Under practical conditions, when the detection efficiency exceeds 80 per cent, the distortion from this source is of the order of 2 per cent for a completely modulated wave. With small signals the distortion may reach as high as 25 per cent for a completely modulated wave when the signal voltage is a fraction of a volt.



The second source of distortion arises from the fact that the voltage across the capacitor in the output can die away only as fast as the charge can leak off through the load resistor. Hence, unless the time constant of this circuit is properly chosen, clipping may result during the troughs of the modulated signal.

FIG. 16-7. Diagonal clipping in a diode detector when the load-circuit time constant is too large.

If the h-f variations of the output voltage are to be small, the time constant of the load circuit  $RC$  must be large compared with the period of the carrier-frequency cycle. However, if this value is made too large, the output voltage cannot decay as rapidly as the envelope decreases, and clipping occurs. The conditions discussed are illustrated in Fig. 16-7.

To ascertain the maximum allowable value of the time constant, it should be noted that this value must be such as to permit the capacitor to discharge at the same rate as the decrease of the modulation envelope. This may be estimated in the following manner:<sup>2</sup> The most unfavorable condition occurs at the highest modulation frequency  $\omega_m$  that the detector is designed to handle and is that for which the equation of the envelope is

$$e = E_c(1 + m \cos \omega_m t) \tag{16-28}$$

At any particular time  $t = t_0$ , the value and the slope of the modulation envelope are

$$\left. \begin{aligned} e &= E_c(1 + m \cos \omega_m t_0) \\ \left(\frac{de}{dt}\right)_{t_0} &= -\omega_m m E_c \sin \omega_m t_0 \end{aligned} \right\} \tag{16-29}$$

If the voltage across the capacitor equals the modulation voltage at the time  $t = t_0$ ,

$$e_a = E_c(1 + m \cos \omega t_0) \tag{16-30}$$

and it decays thereafter according to the exponential expression

$$e_a = e_{a0} e^{-\frac{(t-t_0)}{RC}} \quad (16-31)$$

The initial rate of change is

$$\left(\frac{de_a}{dt}\right)_{t_0} = -\frac{1}{RC} e_a = -\frac{E_c}{RC} (1 + m \cos \omega_m t_0) \quad (16-32)$$

If the capacitor voltage is to be less than the value of the envelope for times  $t > t_0$ , the slope of  $e_a$  must be less than that of the envelope at  $t = t_0$ . This requires that

$$-\frac{E_c}{RC} (1 + m \cos \omega_m t_0) \geq -\omega_m m E_c \sin \omega_m t_0$$

or

$$\frac{1}{RC} \geq \omega_m \left( \frac{m \sin \omega_m t_0}{1 + m \cos \omega_m t_0} \right) \quad (16-33)$$

For the initial rate of decay of the capacitor voltage to be greater than the rate of decay of the envelope voltage, it is necessary that

$$\frac{1}{RC} > \omega_m \left( \frac{m \sin \omega_m t_0}{1 + m \cos \omega_m t_0} \right)$$

But the most severe condition on the  $RC$  constant is that for which the fraction is a maximum. To find this, consider the expression

$$\frac{d}{dt} \left( \frac{m \sin \omega_m t_0}{1 + m \cos \omega_m t_0} \right) = 0$$

This yields

$$\begin{aligned} \cos \omega_m t_0 &= -m \\ \sin \omega_m t_0 &= \sqrt{1 - m^2} \end{aligned}$$

from which

$$\frac{1}{RC} > \omega_m \frac{m}{\sqrt{1 - m^2}} \quad (16-34)$$

If this equation is satisfied, the output voltage follows the wave form of the envelope. According to this equation, as the modulation approaches 100 per cent, the required time constant approaches zero. Consequently, at 100 per cent modulation, the output voltage contains the carrier as well as the modulating frequency.

By taking into account a number of factors that were neglected in the above analysis, such as the impedance of the source supplying the modulated voltage, the results must be modified somewhat. Experimentally it has been found that the amount of harmonic generation is not excessive

for sound reproduction if

$$\frac{1}{RC} \geq \omega_m m \tag{16-35}$$

**16-5. Diodes with Complex Load Impedance.** It is generally found necessary to provide a filter to prevent any r-f voltage from reaching the output. A circuit that accomplishes this is illustrated in Fig. 16-8 and makes use of a simple  $\Pi$ -type resistance-capacitance filter. It is also common practice to use the d-c voltage that is developed across the diode load for automatic volume control. This necessitates the addition of impedance elements, as will be discussed below. The resulting modifications cause the impedance that the load offers to the modulation-frequency component of the output voltage to differ from, and in general be less than, the resistance that the diode circuit offers to the rectified d-c current. This results in a modification of the properties of the diode rectifier, and the results of Eq. (16-34) must be reexamined.

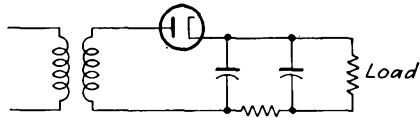


FIG. 16-8. Diode-detector circuit.

The conditional relation given in Eq. (16-34) is rearranged to the form

$$\frac{X}{R} \geq \frac{m}{\sqrt{1 - m^2}}$$

This may be expanded to

$$\frac{X^2}{R^2} \geq \frac{m^2}{1 - m^2}$$

or

$$\frac{R^2}{X^2} \leq \frac{1 - m^2}{m^2} = \frac{1}{m^2} - 1$$

from which

$$m^2 \leq \frac{1}{(R^2/X^2) + 1} = \frac{X^2}{R^2 + X^2} = \frac{X^2 R^2 / (R^2 + X^2)}{R^2}$$

or

$$m \leq \frac{XR / \sqrt{R^2 + X^2}}{R} = \frac{|\text{impedance of load to } \omega_m|}{\text{resistance of load to d-c}} \tag{16-36}$$

This shows the maximum degree of modulation that can be rectified without distortion. When the degree of modulation exceeds the value given by this expression, the negative peaks will be clipped.

**16-6. Rectification Characteristics.** It is clear from the discussion in Sec. 16-4 that the signal output from the diode detector consists of a d-c potential  $E_a$ , which is the average value of the rectified carrier signal and appears across the capacitor  $C$ , and an a-c term of modulating frequency, this being a measure of the amplitude of the envelope of the incoming

modulated carrier. Thus one might consider  $C$  as an effective by-pass for carrier-frequency currents, with two voltages across the output, a d-c term and an a-c term of modulation frequency. The quantitative relationships among the amplitude of the applied r-f voltage, the average rectified current, and the average anode voltage  $E_a$  are contained in the

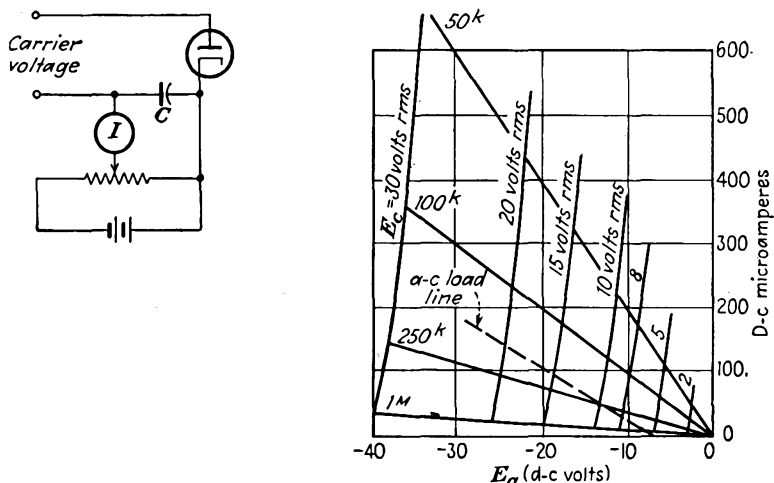


FIG. 16-9. The rectification characteristic of a 6H6 diode, and the circuit used for its determination.

rectification characteristic of the diode. A circuit for obtaining these curves and the results on a 6H6 are illustrated in Fig. 16-9. In the circuit shown, the a-c voltage  $E$  is maintained constant, while the bias voltage  $E_a$ , which simulates the drop across the load resistor, is varied, the rectified current being read by the microammeter.

Also indicated on this characteristic are the load lines from which one obtains the output voltage as the carrier voltage varies. Thus, by plotting the current as a function of time as the carrier amplitude varies because of the modulation, it is possible to determine both the output and the distortion.

In addition to the several static load lines, there is also shown an a-c load line, which represents a  $0.25^M$  static load that is shunted by a second  $0.25^M$  load. The effective value of the unmodulated signal is 10 volts. The resultant is the effective dynamic load into which the tube is working. In such a case, the load line will not in general pass through the point  $(0,0)$ , but may result in a curve such as that illustrated on the rectification characteristic. Consequently, if the operation is carried to the region of no current, severe distortion may result. The curves of

Fig. 16-10 show the character of the variation of distortion with per cent modulation.

**16-7. Automatic Volume Control.** The average amplitude of the modulated carrier wave that reaches the detector stage will depend upon a number of factors, including the field strength at the receiver of the station to which the receiver is tuned and the propagation conditions between the transmitter and receiver. It is desirable therefore to incorporate some means within the receiver for maintaining the average modulated carrier amplitude at the detector at a constant level so as to avoid the effects of fading. Such an automatic-volume-control (avc) circuit will automatically vary the gain of the r-f or i-f stages to yield a substantially constant level at the detector. Figure 16-11 shows a block diagram of a receiver incorporating automatic volume control.

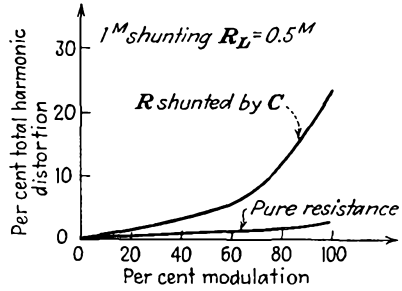


FIG. 16-10. Variation of distortion with per cent modulation. (From F. Langford Smith, "Radiotron Designer's Handbook," Chap. 18.)

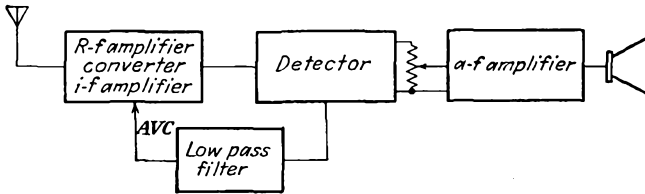


FIG. 16-11. Block diagram of a receiver incorporating automatic volume control.

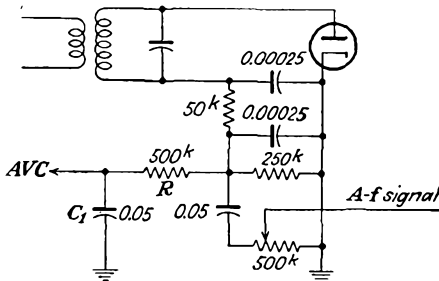


FIG. 16-12. A diode detector and automatic-volume-control circuit.

The details of a circuit in which a diode is used both as a linear detector and also to supply a d-c voltage for automatic-volume-control purposes is illustrated in Fig. 16-12. In this circuit the use of a separate isolating resistor and capacitor filter permits the extraction of a d-c potential that

is proportional to the average modulated carrier level. Also, the d-c voltage across the diode load resistor is blocked off by the use of a resistor and capacitor, the a-f component being made available for the following a-f amplification stages.

The time constant of the automatic-volume-control network  $RC_1$  is made long enough to average out the variations in carrier amplitude corresponding to the modulation, but short enough so that the automatic-volume-control voltage varies with the average amplitude of the carrier, dropping off as the carrier fades and increasing as the carrier becomes stronger. This voltage is used to vary the bias, and hence the transconductance of the r-f and i-f amplifier tubes, to maintain a substantially

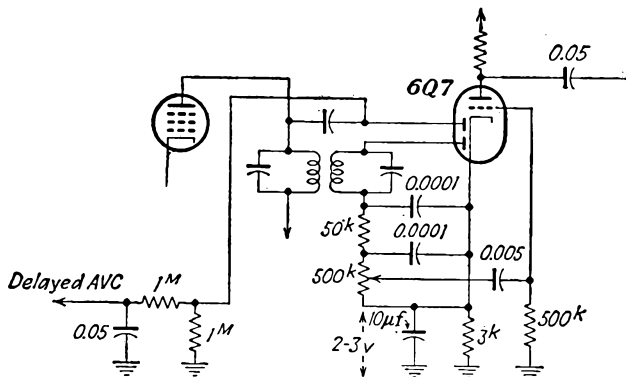


FIG. 16-13. A diode detector and delayed automatic-volume-control circuit.

constant level. In this way, fluctuations in the average amplitude of the modulated carrier delivered to the diode are greatly reduced. The r-f and i-f amplifier tubes that have automatic volume control applied to them should be of the remote-cutoff or variable-mu types; otherwise the system is very critical of adjustment, owing to the very marked sensitivity of transconductance with bias of the sharp-cutoff type of tubes.

If it is desired to have the automatic volume control operate only after the carrier strength reaches a specified minimum, so that the reception of weak signals will not be affected by the automatic-volume-control system, a *delayed* automatic-volume-control circuit may be used. A circuit with delayed automatic volume control is shown in Fig. 16-13. In this circuit the automatic-volume-control voltage is obtained from a separate diode. Also, the automatic-volume-control voltage is obtained from the output of the previous stage in order that a voltage—that across the cathode resistor of the triode element of the duo-diode triode—may be used as the reference level, below which no automatic volume control is applied.

**16-8. Single-side-band and Suppressed-carrier Demodulation.** It was pointed out in Sec. 15-3 that the output from a balanced modulator which was arranged to suppress the carrier contained the side bands of an amplitude-modulated carrier. The transmission of suppressed carrier signals is accomplished at high efficiency since the greater part of the power of an amplitude-modulated wave is in its carrier, and with its suppression a saving in power is effected. In the process of demodulation, it is required that the carrier be resupplied at negligible amplitude in the receiver. The requirement of generating a suitable carrier complicates the design of the receiver. As a result, suppressed-carrier transmission is not well adapted to radiobroadcasting.

The most difficult problem involved in resupplying the carrier is that of maintaining the proper phase relation between it and the side bands. Thus, unless the phase of the carrier is maintained at the zero difference required relative to the side bands [see Eq. (15-6)], it can be shown that the two signal components are out of phase with respect to each other, their difference in phase being a function of the difference between the phase of the original carrier and that resupplied by the receiver. The phase difference in the signal components will give rise to a serious distortion of the output.

If *single-side-band* demodulation is effected, and this requires only that one of the side bands be eliminated by a suitable filter network in the receiver before the carrier is resupplied, the problem is greatly simplified. Now the output from the demodulator depends only on the supplied carrier and the remaining side band and is independent of the phase of the carrier, thus eliminating the phase effects discussed above. The frequency of the resupplied carrier should be very nearly that of the original carrier; otherwise the signal frequency will not be translated to the proper zero position. However, a translation of several cycles from the zero is not particularly objectionable.

If the unwanted side band is eliminated at the transmitter rather than in the receiver, single-side-band transmission has the added advantage over conventional amplitude modulation in effecting an additional saving of radiated power and also a saving in band width required in the r-f spectrum. Single-side-band transmission makes it possible, without a sacrifice of audio fidelity, to space r-f channels twice as close as with standard amplitude modulation. Because of these advantages, this type of transmission is used extensively in point-to-point commercial communication.<sup>3</sup>

**16-9. Mixers and Converters.** A superheterodyne receiver incorporates a mixing element, a device in which the incoming modulated signal is combined with the signal from a local oscillator in order to shift the

carrier level from one frequency to another. The use of such a device permits the carrier level of any signal to be shifted to a preset i-f value and then to provide i-f amplification to bring the voltage level to the 10 volts or so desired at the input of the diode detector. The use of the superheterodyne is widespread because it provides a higher selectivity than a tuned r-f circuit, primarily because of the use of double-tuned amplifiers.

If a separate local or beating oscillator tube is used, the tube in which the combining is accomplished is called a *mixer*. If a multigrid tube is used to serve both as the local oscillator and the mixing element simultaneously, it is referred to as a *converter*. In both cases the effectiveness with which mixing is accomplished, *i.e.*, the ratio of the i-f current in the output to the signal-voltage input to the circuit, is an important quantity. This quantity is called the *conversion transconductance* and is, by definition,

$$g_c \equiv \frac{i_{i-f}}{E'} = \frac{\partial i_{b(i-f)}}{\partial e_{c(r-f)}} \quad (16-37)$$

It should be noted that this quantity is quite different from the mutual conductance of the tube.

**16-10. Square-law Conversion.** To examine certain of the aspects of the conversion process, it will be supposed that the output from the local oscillator is combined with the modulated carrier voltage, and this combined voltage is supposed impressed directly on the grid of a square-law tube. If the tube characteristic is represented by an expression of the form

$$i_p = ae_0^2 \quad (16-38)$$

then with the application of the voltage

$$e_0 = E_c(1 + m \cos \omega_m t) \sin \omega_c t + E_0 \sin \omega_0 t \quad (16-39)$$

the following terms will appear in the output:

$$\begin{aligned} i = a \left[ E_c^2 \sin^2 \omega_c t + E_0^2 \sin^2 \omega_0 t + \frac{m^2 E_c^2}{4} \sin^2 (\omega_c + \omega_m) t \right. \\ + \frac{m^2 E_c^2}{4} \sin^2 (\omega_c - \omega_m) t + 2E_c E_0 \sin \omega_c t \sin \omega_0 t \\ + mE_c^2 \sin \omega_c t \sin (\omega_c + \omega_m) t + mE_c^2 \sin \omega_c t \sin (\omega_c - \omega_m) t \\ + mE_c E_0 \sin \omega_0 t \sin (\omega_c + \omega_m) t + mE_c E_0 \sin \omega_0 t \sin (\omega_c - \omega_m) t \\ \left. + \frac{m^2 E_c^2}{2} \sin (\omega_c + \omega_m) t \sin (\omega_c - \omega_m) t \right] \quad (16-40) \end{aligned}$$

By the use of selective circuits, all terms will be eliminated except those having frequencies in the neighborhood of  $\omega_0 - \omega_c = \omega_i$ . Thus there will remain in the output the following:

$$i = a[E_c E_0 \cos \omega_i t + \frac{1}{2} m E_c E_0 \cos (\omega_i - \omega_m) t + \frac{1}{2} m E_c E_0 \cos (\omega_i + \omega_m) t] \tag{16-41}$$

which may be written as

$$i = a E_c E_0 (1 + m \cos \omega_m t) \cos \omega_i t \tag{16-42}$$

That is, the only signal that can get through the tuning coils which have been tuned to the i-f frequency and which have a band width sufficiently wide to accommodate the a-f spread, is essentially the modulation amplitude at the i-f frequency.

Because the tube which converts to the intermediate frequency often operates under square-law fixed-bias conditions, it is frequently called the "first detector." Actually it is a detector only in the sense that it permits obtaining output frequencies that are different from the input frequencies or, rather, that it shifts the frequency from the r-f level to the i-f level.

The problem of keeping the difference between the local oscillator and the input r-f frequencies constant as one varies the antenna tuning from a position corresponding to one end of the band (say 550 kc) to one corresponding to the other end of the band (say 1,600 kc) is not a simple matter if one wishes to adjust a single control. It requires careful construction of the variable capacitors and the choice of constants so that they "track" together. In general, perfect tracking is not possible over the entire band. Ordinarily provision is possible for ensuring perfect tracking at only three specific points. The errors over the intervening ranges are not great enough to throw the beat frequency out of the i-f pass band.

**16-11. Generalized Conversion Theory.**<sup>4</sup> In the foregoing discussion it was assumed that both the broadcast signal and the local oscillator signal were impressed on the grid of a square-law amplifier. Under these circumstances the conversion is distortionless. Owing to the interaction between the two circuits, electron coupling is ordinarily employed in modern practice, thus reducing this interaction. Consequently the only coupling is that through the electron stream.

Under the assumption that the signal voltage is small and that the local oscillator voltage is large, the signal electrode transconductance may be considered as a function of the oscillator voltage only. Then the signal electrode-plate transconductance  $g_m$  may be considered as varying periodically at the oscillator frequency. The situation is then somewhat as illustrated

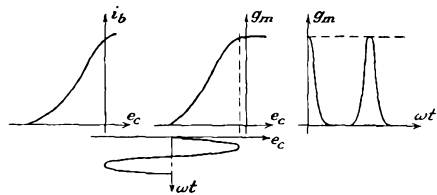


FIG. 16-14. Illustrating the variation of plate-grid transconductance of a converter tube with a large oscillator voltage on the grid.

in Fig. 16-14. Because of the periodic variation that occurs in  $g_m$ , this may be represented by a Fourier series of the form

$$g_m = \frac{b_0}{2} + b_1 \cos \omega_0 t + b_2 \cos 2 \omega_0 t + \dots \quad (16-43)$$

When a small signal is applied to the tube, the resulting a-c plate current has the form

$$i_p = g_m E' \cos \omega_c t \quad (16-44)$$

This may be written in the form

$$i_p = E' \cos \omega_c t \left( \frac{b_0}{2} + \sum_n b_n \cos n \omega_0 t \right)$$

or

$$i_p = \frac{b_0}{2} E' \cos \omega_c t + E' \left( b_1 \cos \omega_c t \cos \omega_0 t + \sum_{\substack{n \\ n \neq 1}} b_n \cos n \omega_0 t \cos \omega_c t \right) \quad (16-45)$$

For a circuit tuned to the frequency  $\omega_0 - \omega_c$ , the i-f frequency, the output is

$$i_{p(i-f)} = \frac{b_1}{2} E' \cos (\omega_0 - \omega_c) t = \frac{b_1}{2} E' \cos \omega_i t \quad (16-46)$$

whence the conversion transconductance is

$$g_c \equiv \frac{i_{p(i-f)}}{E'} = \frac{b_1}{2} \quad (16-47)$$

Upon combining this with the known form for  $b_1$ , there results

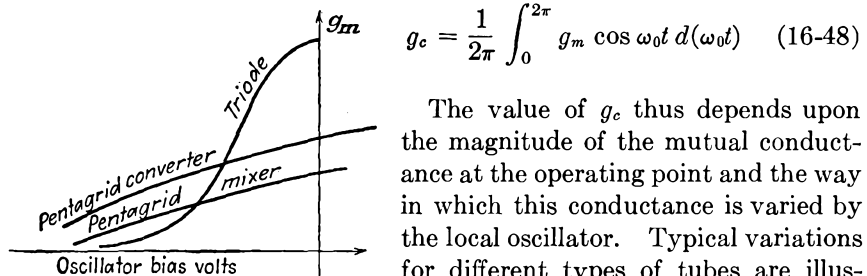


FIG. 16-15. Typical transconductance curves of different types of tubes.

$$g_c = \frac{1}{2\pi} \int_0^{2\pi} g_m \cos \omega_0 t d(\omega_0 t) \quad (16-48)$$

The value of  $g_c$  thus depends upon the magnitude of the mutual conductance at the operating point and the way in which this conductance is varied by the local oscillator. Typical variations for different types of tubes are illustrated in Fig. 16-15. With the oscillator bias near cutoff and with an oscillator amplitude to yield a high value of

instantaneous  $g_m$ , the value of  $g_c$  is approximately in the range from 0.25 to  $0.3g_{m\max}$ , the maximum value of  $g_m$  reached during the oscillator cycle.

If an exact determination of  $g_c$  for a specific tube is required, this can be accomplished by a numerical evaluation of the Fourier coefficient [Eq. (16-48)].

REFERENCES

1. Everitt, W. L., "Communication Engineering," 2d ed., pp. 427-433, McGraw-Hill Book Company, Inc., New York, 1937.
2. Terman, F. E., and N. R. Morgan, *Proc. IRE*, **18**, 2160 (1930).
3. Nichols, H. W., *Elec. Commun.*, **2**, 11 (1923).  
Oswald, A. A., *Proc. IRE*, **26**, 1431 (1938).
4. Peterson, E., and F. B. Llewellyn, *Proc. IRE*, **18**, 38 (1930).  
Herold, E. W., *Proc. IRE*, **30**, 84 (1942).  
Peterson, L. C., and F. B. Llewellyn, *Proc. IRE*, **33**, 458 (1945).

PROBLEMS

**16-1.** A sinusoidal voltage is applied to the average detector of Fig. 16-2, with  $R_l = 100k$ . Determine the variation of the rectified output voltage with applied signal.

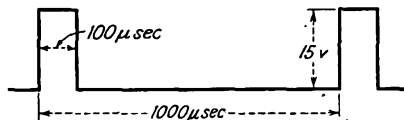
**16-2.** The envelope detector of Fig. 16-3 has  $R_l = 100k$  and  $C = 200 \mu\mu f$ . The impressed voltage is

$$e = 12 \cos 2\pi \times 1.5 \times 10^6 t + 1 \cos 2\pi \times 1.51 \times 10^6 t$$

Write an expression for the instantaneous voltage across  $C$ . Neglect tube drop in the diode.

**16-3.** A carrier is sinusoidally modulated 80 per cent by a 7.5-kc signal. The signal input to the envelope detector of Fig. 16-3 with  $R_l = 100k$  has a carrier component of 12 volts peak. What should be the maximum value of  $C$  for no distortion? Neglect the tube resistance.

**16-4.** The input to the detector of Prob. 16-3 with  $C = 100 \mu\mu f$ ,  $R_l = 100k$ ,



$R_o = 1M$ ,  $C' = \infty$  is a pulsed r-f signal, the carrier frequency being 5 megacycles. Sketch the wave form of the voltage across  $R_o$ .

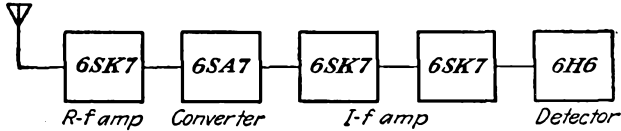
**16-5.** In the circuit of Fig. 16-3, the diode efficiency is 0.90. Calculate and plot as a function of the modulating frequency  $\omega_m$  the maximum degree of modulation of the input signal  $e$  for distortionless rectification.

**16-6.** Suppose that the d-c load resistance of a peak diode detector is  $250k$  and  $\eta = 0.90$ .

- a. Calculate and plot the maximum degree of modulation of a signal without negative peak clipping as a function of the ratio of a-c to d-c load impedances for ratios between 1 and 0.5.
- b. If the signal is 100 per cent modulated, plot the approximate distortion under these conditions.

**16-7.** Determine from the rectification characteristics of a 6H6 diode the largest permissible modulation without clipping if the d-c impedance of the load is  $100\text{ }\Omega$  and the modulation frequency impedance is  $50\text{ }\Omega$ . If the effective modulation is 70 per cent with a carrier of 10 volts rms, determine the approximate percentage distortion.

**16-8.** A superheterodyne as indicated in the diagram in block form gives for an unmodulated carrier-frequency signal of  $5\text{ }\mu\text{v}$  input to the r-f amplifier a detector



output of 5 volts. If automatic volume control is used on all tubes, what must the carrier level be to give a 5-volt output; a 10-volt output? Assume that the full d-c output voltage is used for automatic volume control.

**16-9.** A receiver is provided with a square-law detector, which is represented by the expression

$$i = ke^2$$

Calculate the form of the output, and specify whether or not an intelligible a-f signal results when the following are applied to the input:

- One side band is eliminated from the transmitted wave.
- The carrier is eliminated from the transmitted wave.
- One side band and the carrier are eliminated from the transmitted wave.

**16-10.** A single-side-band transmitted wave is applied to a square-law detector for which

$$i_p = 0.5(6 + e_g)^2 \quad \text{ma}$$

If the input consists of a supplied carrier of 2.5 volts peak and the side-band amplitude is 1 volt peak, calculate the signal current in the output.

**16-11.** A 6L7 pentagrid tube is used as a converter. A plot of the curve of plate-grid 1 transconductance as a function of grid 3 bias is sketched in the

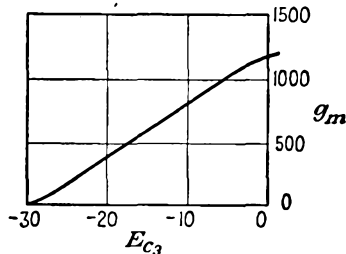


diagram for this problem. A beating oscillator signal of 24 volts peak, which causes a bias of  $-20$  volts to be developed, is applied to grid 3. The incoming signal of  $100\text{ }\mu\text{v}$  is applied to grid 1, which is maintained at a bias of  $-6$  volts. Calculate the conversion transconductance under these conditions.

---

## CHAPTER 17

### FREQUENCY MODULATION AND DETECTION

CHAPTER 15 was confined to a discussion of amplitude modulation (a-m), in which the amplitude of the transmitted wave is altered in a manner dictated by the amplitude and frequency characteristics of the signal. It was there pointed out that, in addition to such amplitude variations, it is possible to effect changes in the frequency or in the phase of the transmitted signal. In particular, however, if intelligence is to be transmitted, it is essential that the two features that characterize intelligence, *viz.*, amplitude or loudness, and frequency, must be available.

In frequency modulation (f-m) the transmitting frequency is varied by an amount depending on the signal amplitude, and the signal frequency determines the rate at which the variation takes place. In phase modulation (p-m) the phase of the transmitted wave is shifted by an amount that depends on the signal amplitude, and the rate at which this shift occurs is made proportional to the signal frequency. In general, any system that can transmit the two aspects of information required for the intelligence could serve as an acceptable system of communication. A variety of pulse systems have been devised which are satisfactory and which possess certain advantages over the a-m, f-m, and p-m systems. These are outside of the scope of this book and will not be discussed.

It should be particularly noted that the amplitude of the oscillations in the f-m system is not involved in the actual process of transmitting intelligence. Consequently, it is possible to make the system insensitive to any amplitude-modulated disturbances. This is a particularly desirable feature since atmospheric and man-made disturbances are largely amplitude-modulated. Owing to the difference in character between a-m and f-m signals, it is possible to separate and extract the signal from the interference.

**17-1. Basic Characteristics of Frequency Modulation.** To examine graphically the fundamental principles of frequency modulation, suppose that a telegraph dot and dash are applied to an a-m and to an f-m system. The results have the forms illustrated in Fig. 17-1. For the a-m system, the frequency of oscillation remains constant, but the amplitude is zero or a constant, depending upon the time in the cycle. In the f-m system,

the amplitude remains constant, but the frequency changes from a value  $f_2$  to a value  $f_1$  or  $f_3$  when the signal is applied.

If the applied signal is sinusoidal and of frequency  $f_m$ , the effect produced in an a-m system has the form illustrated in Fig. 17-2b and the effect produced in an f-m system has the form illustrated in Fig. 17-2c.

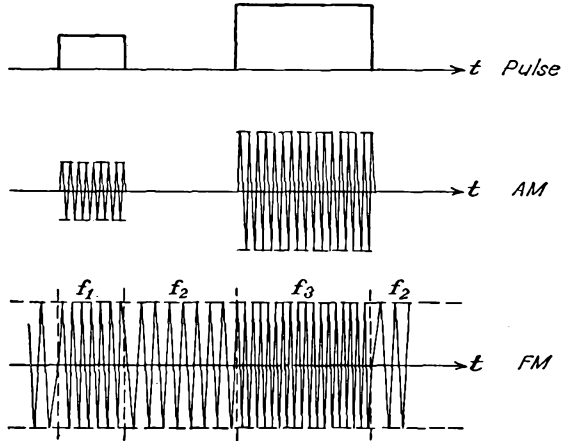


FIG. 17-1. The primary features of a-m and f-m waves.

**17-2. Instantaneous Phase and Frequency.** The general expression for an unmodulated carrier wave is given by

$$e_c = E_c \sin (\omega_c t + \theta) \tag{17-1}$$

In this expression the period of the wave is given by



$$T = \frac{1}{f} = \frac{2\pi}{\omega_c}$$

The quantity

$$\omega_c t + \theta = \varphi \tag{17-2}$$

is the total instantaneous "phase" of the function. If the phase is written as  $\varphi(t)$ , the value of the voltage at any instant is represented by the expression

$$e_c = E_c \sin \varphi(t) \tag{17-3}$$

But, clearly, the angular frequency is related to the phase by the expression

$$\omega = \frac{d\varphi}{dt} \tag{17-4}$$

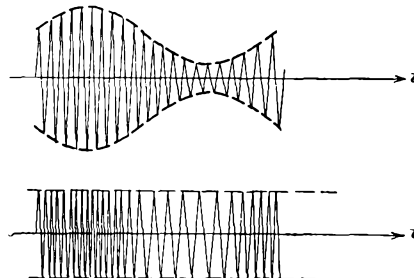


FIG. 17-2. The output of a sinusoidally modulated a-m and f-m transmitter.

This expression agrees with the usual definitions of frequency, and in the unmodulated case

$$\omega = \frac{d}{dt}(\omega_c t + \theta) = \omega_c$$

**17-3. Frequency Modulation (F-M).** Frequency modulation is produced by varying the instantaneous frequency of a carrier by an amount that is proportional to the amplitude of the modulating signal and at a rate that is proportional to the frequency of the modulating source. The amplitude of the carrier is assumed to remain constant in the process. That is, if the modulating signal has the form

$$e_m = E_m \cos \omega_m t \quad (17-5)$$

the f-m wave has an instantaneous frequency given by the expression

$$\omega(t) = \omega_c + k_f E_m \cos \omega_m t \quad (17-6)$$

The proportionality factor  $k_f$  determines the maximum variation in frequency for a given signal strength  $E_m$ .

To determine the expression for the f-m wave, use is made of Eq. (17-4). This requires that

$$\omega = \frac{d\varphi}{dt} = \omega_c + k_f E_m \cos \omega_m t$$

from which it follows that

$$\varphi(t) = \int_0^t \omega dt$$

which yields the expression

$$\varphi(t) = \omega_c t + k_f \frac{E_m}{\omega_m} \sin \omega_m t + \theta_0 \quad (17-7)$$

The initial phase  $\theta_0$  is neglected in what follows, for it plays no part in the modulating process. Thus, for the f-m wave,

$$e = E_c \sin \left( \omega_c t + k_f \frac{E_m}{\omega_m} \sin \omega_m t \right) \quad (17-8)$$

The instantaneous frequency of the f-m wave is

$$f = \frac{\omega}{2\pi} = f_c + k_f \frac{E_m}{2\pi} \sin \omega_m t \quad (17-9)$$

which has a maximum value of

$$f_{\max} = f_c + k_f \frac{E_m}{2\pi} \quad (17-10)$$

and a minimum value of

$$f_{\min} = f_c - k_f \frac{E_m}{2\pi} \quad (17-11)$$

The maximum swing of the frequency from its mean value is called the

frequency deviation and is denoted by  $f_d$ . It is

$$f_d \equiv f_{\max} - f_c = f_c - f_{\min} = k_f \frac{E_m}{2\pi} \quad (17-12)$$

By analogy with amplitude modulation, the *modulation index* is defined as

$$m_f \equiv \frac{f_d}{f_c} = \frac{\omega_d}{\omega_c} = k_f \frac{E_m}{\omega_c} \quad (17-13)$$

Also, the ratio of  $f_d$  to the modulating frequency  $f_m$  is called the *deviation ratio* and has the value

$$\delta \equiv \frac{f_d}{f_m} = \frac{\omega_d}{\omega_m} = m_f \frac{\omega_c}{\omega_m} = k_f \frac{E_m}{\omega_m} \quad (17-14)$$

In terms of these factors, the expression for the f-m wave assumes the form

$$e = E_c \sin (\omega_c t + \delta \sin \omega_m t) \quad (17-15)$$

**17-4. Frequency Spectrum of F-M Wave.** To examine the spectrum of the f-m wave, it is necessary to expand the expression [Eq. (17-15)] that represents the f-m wave. This is done as follows:

$$e = E_c [\sin \omega_c t \cos (\delta \sin \omega_m t) + \cos \omega_c t \sin (\delta \sin \omega_m t)] \quad (17-16)$$

Use is now made of the following expansions,

$$\left. \begin{aligned} \cos (\delta \sin \omega_m t) &= J_0(\delta) + 2 \sum_{n=1}^{\infty} J_{2n}(\delta) \cos 2n\omega_m t \\ \sin (\delta \sin \omega_m t) &= 2 \sum_{n=0}^{\infty} J_{2n+1}(\delta) \sin (2n+1)\omega_m t \end{aligned} \right\} \quad (17-17)$$

where the function  $J_n(\delta)$  is the Bessel function of the first kind and of order  $n$ . The f-m spectrum then becomes

$$e = E_c \sin \omega_c t [J_0(\delta) + 2J_2(\delta) \cos 2\omega_m t + 2J_4(\delta) \cos 4\omega_m t + \cdots] \\ + E_c \cos \omega_c t [2J_1(\delta) \sin \omega_m t + 2J_3(\delta) \sin 3\omega_m t + \cdots] \quad (17-18)$$

which may be written in the form

$$e = J_0(\delta) E_c \sin \omega_c t \\ + J_1(\delta) E_c [\sin (\omega_c + \omega_m) t - \sin (\omega_c - \omega_m) t] \\ + J_2(\delta) E_c [\sin (\omega_c + 2\omega_m) t + \sin (\omega_c - 2\omega_m) t] \\ + J_3(\delta) E_c [\sin (\omega_c + 3\omega_m) t - \sin (\omega_c - 3\omega_m) t] \\ + \cdots \quad (17-19)$$

where use has been made of the trigonometric expansions

$$\left. \begin{aligned} \sin x \cos y &= \frac{1}{2} [\sin (x+y) + \sin (x-y)] \\ \cos x \sin y &= \frac{1}{2} [\sin (x+y) - \sin (x-y)] \end{aligned} \right\} \quad (17-20)$$

The Bessel function  $J_n(\delta)$  is defined by the series

$$J_n(\delta) = \frac{\delta^n}{2^n n!} \left[ 1 - \frac{\delta^2}{2(2n+2)} + \frac{\delta^4}{2(4)(2n+2)(2n+4)} - \frac{\delta^6}{2(4)(6)(2n+2)(2n+4)(2n+6)} + \dots \right] \quad (17-21)$$

It follows from Eq. (17-19) that the spectrum of the f-m wave consists of a carrier and an infinite number of side bands all of whose amplitudes are various-order Bessel functions. Graphs of several of these functions are contained in Fig. 17-3. It will be noticed that  $J_0(\delta)$  has a root at

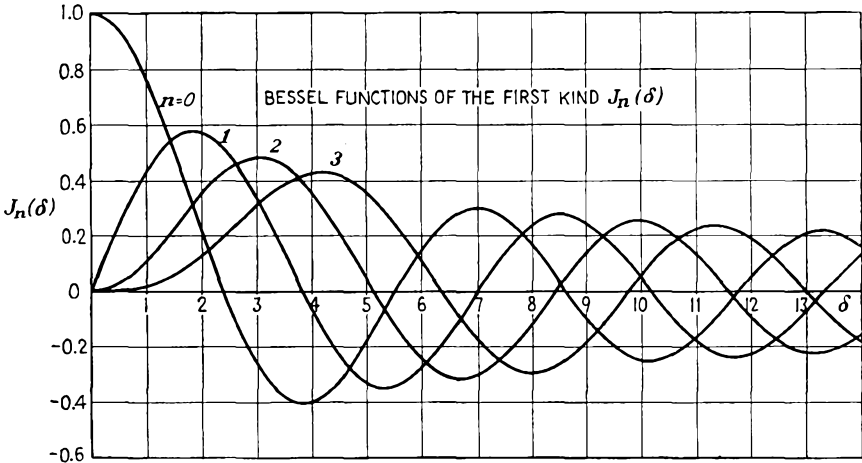


FIG. 17-3. Bessel functions of the first kind.

about 2.40. This means that the carrier will vanish when the frequency deviation is equal to 2.4 times the audio frequency. This fact provides a method for measuring the frequency deviation since the zero point of the carrier can be observed by a selective radio receiver.

A list of the roots of various Bessel functions is given in Table 17-1.

TABLE 17-1  
ROOTS OF  $J_n(\delta)$

$n = 0$	1	2	3	4	5
2.4048	3.832	5.135	6.379	7.586	8.780
5.520	7.016	8.417	9.760	11.064	12.339
8.654	10.173	11.620	13.017	14.373	15.700
11.792	13.323	14.796	16.224	17.616	18.982
14.931	16.470	17.960	19.410	20.827	22.220
18.071	19.616	21.117	22.583	24.018	25.431
21.212	22.760	24.270	25.749	27.200	28.628

It is instructive to examine a particular situation in some detail. Consider an r-f signal that is modulated  $\pm 75$  kc by an a-f signal of 7.5 kc. The corresponding deviation ratio is 10.0. The important Bessel function that occurs in the expression for such an f-m wave is  $J_n(10.0)$ . A plot of  $J_n(10.0)$  as a function of  $n$  is given in Fig. 17-4. Notice that the function falls off toward zero rapidly after the deviation 75 kc is passed but that the amplitudes are significant out to about  $14 \times 7.5 = 105$  kc.

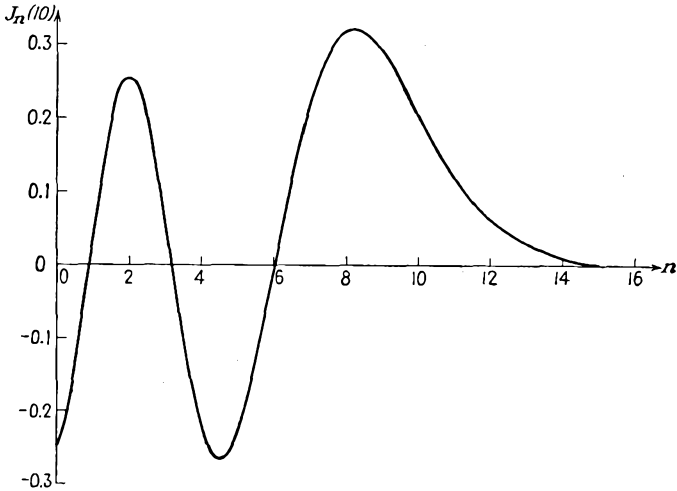


FIG. 17-4. A plot of  $J_n(10.0)$  as a function of  $n$ .

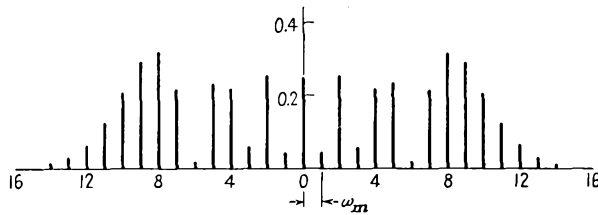


FIG. 17-5. The spectral distribution in an f-m wave with  $\delta = 10$ .

A plot of the spectrum corresponding to Eq. (17-19) is given in Fig. 17-5. Notice that this is just a plot of the spectral lines, without regard for sign, as dictated by the Bessel function plot of Fig. 17-4. The separation between individual side bands is 7.5 kc, the modulating frequency. It is evident from this plot that the total band width necessary to include all significant side-bands is 210 kc.

Two similar plots are also included. In Fig. 17-6 is illustrated a series of plots for constant modulating frequency  $f_m$  but for various values of frequency-deviation ratio  $\delta$ . The increasing number of side bands with

$\delta$  is clearly seen. Likewise, the disappearance of the carrier is plainly seen.

The plots of Fig. 17-7 show the spectra for a constant frequency deviation but for various modulation frequencies. It should be observed that the total band width required to include all significant side bands decreases somewhat with increasing deviation ratio. For a given frequency deviation  $f_d$ , except for the very small value of  $\delta$ , almost all significant side

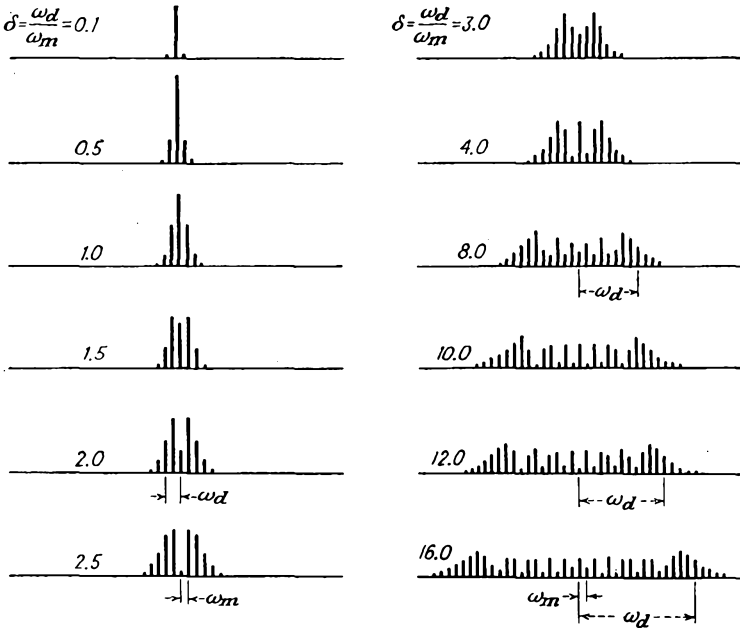


FIG. 17-6. The spectral distribution in an f-m wave for different values of  $\delta$ , different  $\omega_d$ , and fixed  $\omega_m$ .

bands are contained within the range  $f_d$ . The curve of Fig. 17-8 indicates the number of significant side bands (those with amplitudes exceeding 1 per cent of the largest side-band component) in an f-m spectrum for different values of  $n$  and  $\delta$ . In particular, if  $\delta = 5$ , then  $n$  must be about 8 for  $J_n(\delta)$  to be negligible compared with unity.

Some very important information is contained in Fig. 17-8. To appreciate this, consider the present Federal Communications Commission (FCC) regulations on frequency modulation. These regulations specify

Maximum frequency deviation,  $f_d = \pm 75$  kc.

Allowable band width,  $B = 200$  kc (including a 25-kc band at each end).

Frequency stability of carrier,  $\pm 2$  kc.

Remembering that the frequency deviation is related to the amplitude and frequency of the modulating voltage according to the relation

$$\omega_d = k_f E_m$$

then for that amplitude which provides a frequency deviation of 75 kc the band-width requirements increase with decreasing  $f_m$ . But from Fig.

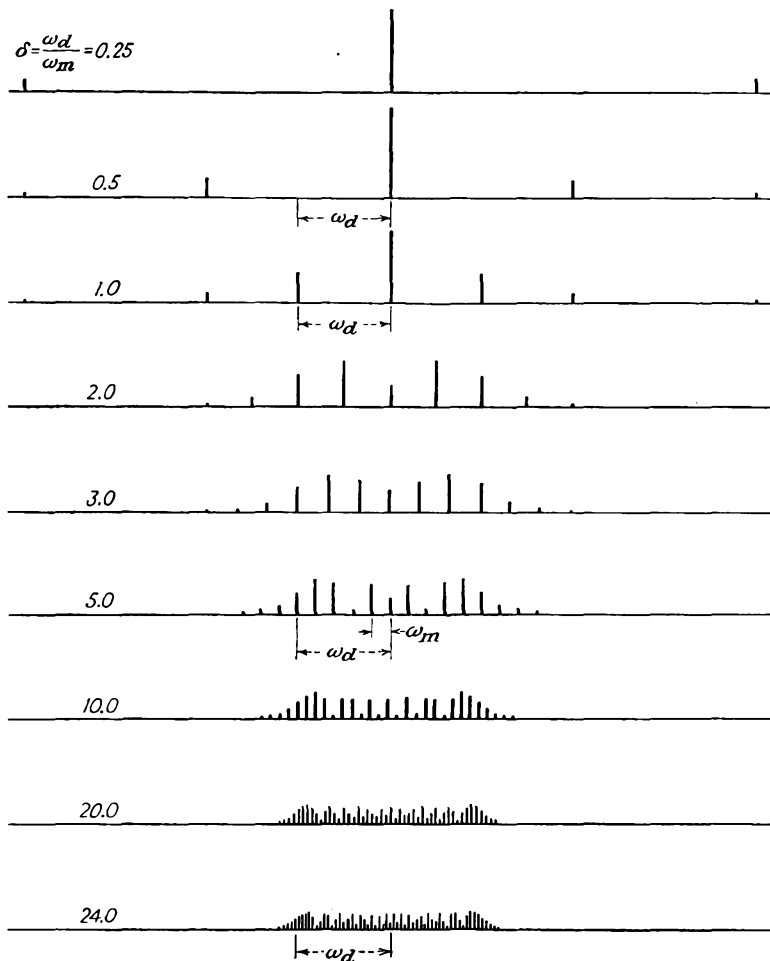


FIG. 17-7. The spectral distribution in an f-m wave for different values of  $\delta$ , fixed  $\omega_d$  and different  $\omega_m$ .

17-8 it is clear that all of the significant side bands or energy is contained within  $f_d$  for values of  $\delta = 10$  or higher. For  $\delta$  lower than 10, the number of side bands outside of  $f_d$  begins to increase rather seriously. This occurs for frequencies of 7.5 kc or higher. Note, however, that with ordinary

broadcasts the amplitude of the frequencies in the range of 7.5 kc and higher is considerably smaller than with the frequencies in the middle or lower registers. Clearly, therefore,  $E_m$  for these higher frequencies is smaller than for the mid-frequency band, and hence the total active  $f_a$  is materially less than the allowable 75 kc and the system is operating within a narrower band width than might otherwise be required. In fact, the band width is so much less than that allowed that it is found convenient to include weighting, or preemphasis, networks in the transmitter. These

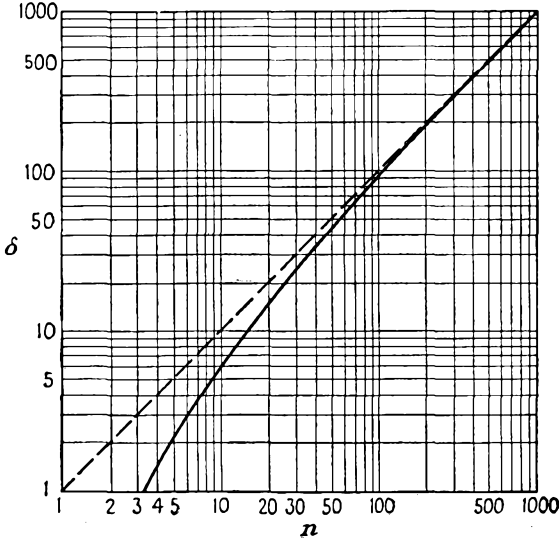


FIG. 17-8. Values of  $n$  for a given value of  $\delta$  to make  $J_n(\delta) < 0.01$ . Note that  $n$  may assume only integral values. (From L. Mautner, "Mathematics for Radio Engineers," Pitman Publishing Corp., New York, 1947.)

have such properties that they tend to accentuate the higher frequencies. In this way, the higher frequency components, which ordinarily do not contain much energy, are expanded beyond their natural level. This proves to be a desirable practice in that it tends to give an improved signal-noise ratio, for the noise generated within the tube circuits is uniformly distributed over the frequency band. Of course, for fidelity in reproduction, the receiver must have networks which deemphasize the incoming signal to yield the proper energy distribution. More will be said about this when the circuits for effecting preemphasis and deemphasis are discussed.

**17-5. Phase Modulation (P-M).** Phase modulation is produced by varying the instantaneous phase of the carrier at a rate that is proportional to the modulating frequency and by an amount that is proportional to the strength of this modulating signal. The amplitude of the carrier

remains unaltered in this process. If the modulating signal has the form

$$e_m = E_m \sin \omega_m t$$

the instantaneous phase of the wave is given by the expression

$$\theta = \theta_0 + k_p E_m \sin \omega_m t \quad (17-22)$$

where  $k_p$  is a proportionality factor that determines the maximum variation in phase for a given signal strength.

To find the analytic expression for the p-m wave, use is made of the fact that the instantaneous phase is given by

$$\varphi(t) = \omega_c t + \theta_0 + k_p E_m \sin \omega_m t \quad (17-23)$$

Equation (17-3) for the present case, when written in full, becomes

$$e = E_c \sin (\omega_c t + k_p E_m \sin \omega_m t) \quad (17-24)$$

The constant phase  $\theta_0$  is taken as zero, as it plays no part in the modulating process. This expression is written in the form

$$e = E_c \sin (\omega_c t + \theta_d \sin \omega_m t) \quad (17-25)$$

where the maximum deviation in phase is

$$\theta_d \equiv k_p E_m \quad (17-26)$$

A comparison of this expression with Eq. (17-15) for the f-m wave indicates that the two forms are identical. Consequently the entire discussion of the spectral distribution of the energy contained in an f-m wave can be extended to p-m waves. Therefore the frequency spectrum of a p-m wave having a maximum phase deviation of, say, 10 rad will be identical in form with the frequency spectrum of an f-m wave having a deviation ratio of 10.

There is one very significant difference between the f-m and the p-m waves, however. This difference is contained in the form of the phase deviation  $\theta_d$  and the deviation ratio  $\delta$  that appears in Eqs. (17-25) and (17-15), respectively. The differences lie in the definitions of  $\theta_d$  and  $\delta$ , namely

$$\begin{aligned} \theta_d &= k_p E_m && \text{for p-m waves} \\ \delta &= \frac{k_f E_m}{\omega_m} && \text{for f-m waves} \end{aligned}$$

Clearly, for p-m waves the phase deviation depends only on the amplitude of the modulating signal, and all modulating frequencies of equal  $E_m$  will possess equal values of  $\theta_d$ , independently of the frequency  $\omega_m$ . As a result, the spectral distribution will be the same in each case, although the separation of the spectral lines will depend on the modulating frequency. In particular, if it is supposed that the maximum phase deviation

tion of a particular wave is 5 rad, there will then be approximately 8 significant side-band components present. If the modulating frequency is 5 kc, then the band width is  $2 \times 8 \times 5,000 = 80,000$  cps. If the modulating frequency for the 5-rad maximum deviation is 50 cps, then the band width is  $2 \times 8 \times 50 = 800$  cps.

In the case of frequency modulation, if the value of  $E_m$  is such that the deviation ratio is  $\delta = 5$  for a modulating frequency of 5 kc, then for an equal  $E_m$  at 50 cps the corresponding deviation ratio is 500. The resulting spectral distribution in these two cases will be altogether different, there being 8 significant side bands for  $\delta = 5$ , and there being in

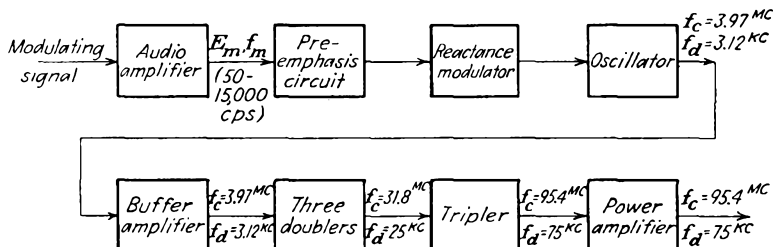


FIG. 17-9. A simple reactance-tube f-m transmitter.

excess of 500 significant side bands for  $\delta = 500$ . The band width is  $2 \times 8 \times 5,000 = 80$  kc under the first conditions and is approximately  $2 \times 500 \times 50 = 50$  kc in the second case.

Owing to the simple difference in form between  $\theta_d$  and  $\delta$ , it might appear that it should be possible to use p-m waves to produce f-m waves. This would be possible if one could arrange, by means of appropriate circuits, to cause the apparent phase deviation to vary inversely as the modulating frequency. Such circuits are possible, and the Armstrong method of producing frequency modulation operates on this principle. The details of this method will be discussed below.

**17-6. F-M Transmitters—Reactance-tube Types.** A variety of methods for the production of frequency modulation exist, although they do not all enjoy very great flexibility. In principle at least, the most direct way of producing an f-m wave is to alter the capacitance in the tank circuit of an oscillator. This might conceivably be done by incorporating a capacitor microphone as part of the tank capacitor in an oscillator circuit. A considerably more satisfactory method, and one which accomplishes the same result in substantially the same way, is to incorporate a *reactance tube* in the tank circuit. Such an electronic circuit produces a reactance, either inductive or capacitive depending upon its manner of connection, which may be varied by varying the potential on one grid of the tube.

The block diagram of a simple reactance-tube f-m transmitter is shown

in Fig. 17-9. The essential features of certain of the elements of the circuit are examined in some detail below. In particular, the operation of the reactance-tube circuit and the preemphasis circuit will be discussed.

**17-7. The Reactance Tube.** A simple reactance tube has features in common with the circuit of Fig. 8-18. A schematic diagram and its equivalent circuit are given in Fig. 17-10. It is desired to find the output

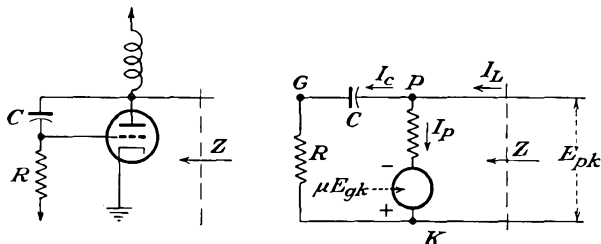


FIG. 17-10. The reactance tube and its equivalent circuit.

impedance of this circuit. This is readily accomplished. Note from the equivalent circuit the following relations:

$$\text{with } \left. \begin{aligned} I_c &= \frac{E_{pk}}{R - jX_c} \\ X_c &= \frac{1}{\omega C} \end{aligned} \right\} \quad (17-27)$$

Also, the grid potential is

$$E_g = RI_c = \frac{RE_{pk}}{R - jX_c} \quad (17-28)$$

The plate current is

$$I_p = \frac{E_{pk} + \mu E_g}{r_p} = \frac{E_{pk} + \mu E_g}{r_p}$$

which may be expressed as

$$I_p = \frac{E_{pk}}{r_p} + \frac{\mu}{r_p} \frac{RE_{pk}}{R - jX_c} \quad (17-29)$$

The total current is then

$$I = I_p + I_c = \frac{E_{pk}}{R - jX_c} + \frac{E_{pk}}{r_p} + g_m \frac{RE_{pk}}{R - jX_c} \quad (17-30)$$

The output admittance of the circuit is given by the relation

$$Y = \frac{I}{Z} = \frac{1}{E_{pk}} = \frac{1}{R - jX_c} + \frac{1}{r_p} + g_m \frac{R}{R - jX_c} \quad (17-31)$$

which may be expressed in the form

$$Y = \frac{1}{R - jX_c} + \frac{1}{r_p} + \frac{1}{\frac{1}{g_m} - j \frac{1}{g_m RC \omega}} \quad (17-32)$$

This expression indicates that, in so far as the output circuit of the reactance tube is concerned, it may be represented by the circuit of Fig. 17-11. Clearly, if the impedances  $r_p$  and  $R - jX_c$  are large compared with  $(1/g_m) - j(1/g_m RC\omega)$  and if  $1/\omega CR$  is large compared with unity, the output admittance becomes purely capacitive and arises from an equivalent capacitor  $g_m RC$ .

Since the output impedance of the reactance-tube circuit above may be made to appear as a pure capacitance  $g_m RC$ , then if the modulating signal is made to vary the  $g_m$  of the tube, and this is readily accomplished by applying the modulating signal to the grid of the tube, the effective capacitance will then change with changes in grid potential. The circuit of such a reactance-tube f-m oscillator is given in Fig. 17-12. Also

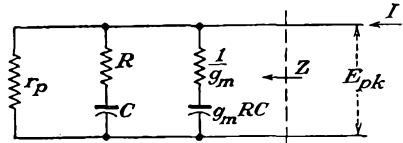


FIG. 17-11. The equivalent output circuit of a capacitive reactance tube.

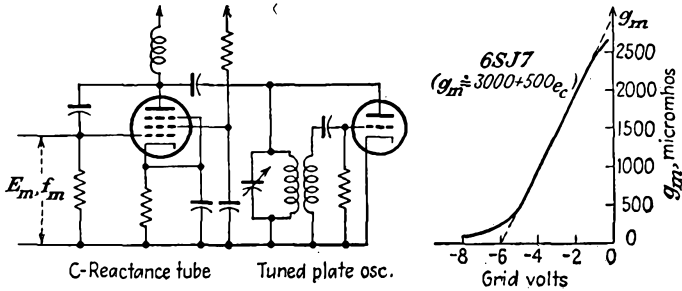


FIG. 17-12. A reactance-tube f-m oscillator, and the curve showing the variation of  $g_m$  with grid potential.

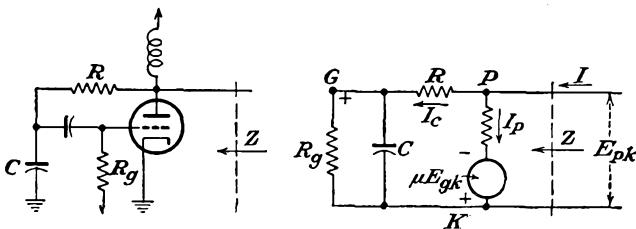


FIG. 17-13. An inductive reactance tube, and its equivalent circuit.

included is a curve showing the variation of  $g_m$  of the tube with changes in grid potential.

A reactance tube may be connected to yield an effective inductance, rather than an effective capacitance, across the output terminals. Such a circuit, with its electrical equivalent, is given in Fig. 17-13. By proceeding in the same general manner as for the capacitive reactance-tube

circuit, it can be shown that the equivalent output admittance has the form

$$Y = \frac{1}{R + \frac{R_g/j\omega C}{R_g + 1/j\omega C}} + \frac{1}{r_p} + \frac{1}{\frac{1}{g_m} + \frac{R}{g_m R_g} + j \frac{\omega CR}{g_m}} \quad (17-33)$$

for which an equivalent circuit exists.

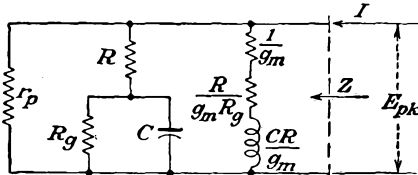


FIG. 17-14. The equivalent output circuit of an inductive reactance tube.

This equivalent circuit has the form illustrated in Fig. 17-14. By the proper choice of the various elements in the circuit, the circuit reduces to the simple form, comprising only an equivalent inductance  $CR/g_m$ .

A reactance-tube oscillator that incorporates an inductive reactance tube circuit as part of a Hartley oscillator is illustrated in Fig. 17-15. Also included is a graph showing the variation of  $g_m$  with changes in grid 3 potential.

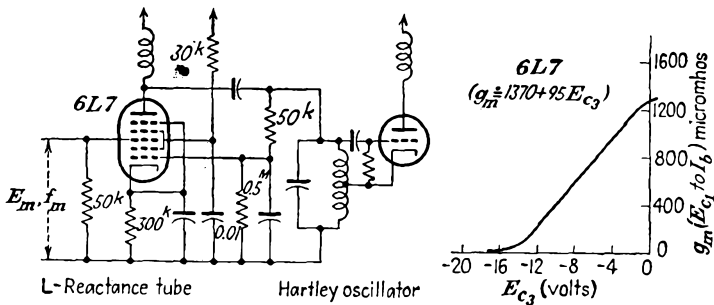


FIG. 17-15. An inductive-reactance-tube f-m oscillator, and the curve showing the variation of  $g_m$  with grid 3 potential of the reactance tube.

An approximate expression for the variation of the frequency of a reactance-tube oscillator as the voltage on the control electrode is varied is readily possible. The transconductance may be expressed analytically as a function of the potential of the control electrode. Note from the curve that

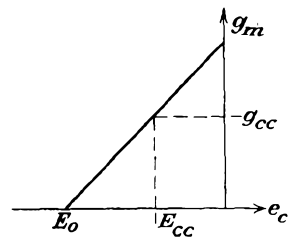
$$g_m = \frac{G_0}{E_0} e_c + G_0 \quad (17-34)$$

But since

$$\begin{aligned} e_c &= E_{cc} + e_m \\ &= E_{cc} + E_m \cos \omega m t \end{aligned} \quad (17-35)$$

then

$$g_m = G_0 \frac{E_{cc}}{E_0} + G_0 + \frac{G_0}{E_0} E_m \cos \omega m t \quad (17-36)$$



For the capacitive reactance-tube circuit, the effective output capacitance is

$$C_e \doteq g_m CR = G_0 CR \left( 1 + \frac{E_{cc}}{E_0} + \frac{E_m}{E_0} \cos \omega_m t \right) \quad (17-37)$$

If it is assumed that the frequency of oscillation of the oscillator is that of the tank circuit alone, then

$$f = \frac{1}{2\pi \sqrt{L_0(C_0 + C_e)}} \\ f = \frac{1}{2\pi \sqrt{L_0 C_0 + L_0 G_0 CR \left( 1 + \frac{E_{cc}}{E_0} + \frac{E_m}{E_0} \cos \omega_m t \right)}} \quad (17-38)$$

The carrier frequency is evidently the value of the frequency of the oscillator when the modulating signal voltage is zero. This is

$$f_c = \frac{1}{2\sqrt{L_0} \left[ C_0 + G_0 CR \left( 1 + \frac{E_{cc}}{E_0} \right) \right]} \quad (17-39)$$

The frequency ratio  $f/f_c$  is given by

$$\frac{f}{f_c} = \frac{1}{\sqrt{1 + \frac{L_0 G_0 CR E_m \cos \omega_m t}{L_0 [C_0 + G_0 CR (E_0 + E_{cc})]}}} \quad (17-40)$$

By expanding this expression by the binomial theorem and retaining only the first term in the expansion, since the total frequency shift is small, then

$$\frac{f}{f_c} \doteq 1 - \frac{1}{2} \frac{E_m \cos \omega_m t}{(C_0 E_0 / G_0 CR) + E_{cc} + E_0} \quad (17-41)$$

This expression may be written in the form

$$\left. \begin{aligned} f &= f_c (1 + m_f \cos \omega_m t) \\ \text{where the modulation index is} \\ m_f &= - \frac{1}{2} \frac{E_m}{(C_0 E_0 / G_0 CR) + E_{cc} + E_0} \end{aligned} \right\} \quad (17-42)$$

**17-8. Preemphasis Circuits.** As discussed in Sec. 17-4, there is a relatively small amount of energy contained in the h-f portion of the audio spectrum. As a result, the deviation at these high frequencies is far less than the maximum allowable value of 75 kc. The corresponding bandwidth requirement is correspondingly less than the allowable 150-kc total. In fact, the relative h-f amplitudes are so low that it is customary to include preemphasis networks in the circuit to accentuate the h-f

terms as against the lower frequency terms. In this way the relative signal strength at these higher frequencies is improved relative to tube and circuit noise, which has a uniform distribution over the entire audio spectrum. Of course, corresponding deemphasis must be incorporated in the receiver in order to bring the relative amplitudes of all frequencies to their proper levels.

Preemphasis circuits are chosen to satisfy the equation

$$\frac{e_0}{e_1} = \frac{1}{\sqrt{1 + (\omega_1/\omega)^2}} \quad (17-43)$$

The value of  $\omega_1$  was originally chosen to be  $1/\omega_1 = 100 \mu\text{sec}$ , but it is now taken as  $75 \mu\text{sec}$ . With such a preemphasis circuit the amplitude of a 2,100-cps signal is increased in the ratio  $\sqrt{2}/1$  over the normal level, and the relative amplitude of a 21-kc signal is increased in the ratio 10/1.

Either an  $RL$  or a  $CR$  circuit may be used to accomplish preemphasis. Two different circuits are illustrated in Fig. 17-16. In the  $RL$  circuit,

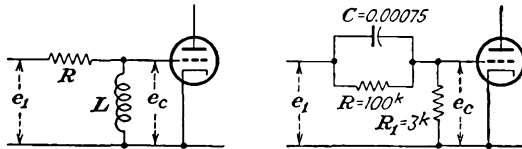


FIG. 17-16. Two different preemphasis circuits.

the voltage ratio  $e_c/e_1$  is readily found to be

$$\frac{e_c}{e_1} = \frac{j\omega L}{R + j\omega L} = \frac{1}{\sqrt{1 + (R/\omega L)^2}} \angle \tan^{-1}(-R/\omega L) \quad (17-44)$$

By writing  $\omega_1 = R/L$ , this becomes

$$\left| \frac{e_c}{e_1} \right| = \frac{1}{\sqrt{1 + (\omega_1/\omega)^2}} \quad (17-45)$$

Similarly, for the  $CR$  circuit, the mathematical development becomes

$$\frac{e_c}{e_1} = \frac{R_1}{R_1 + \frac{R}{R + 1/j\omega C}} \quad (17-46)$$

which is

$$\frac{e_c}{e_1} = \frac{R_1}{R_1 + \frac{R}{j\omega CR + 1}} \quad (17-47)$$

At the higher frequencies  $R \gg X_c$  or  $R \gg \frac{1}{j\omega C}$ . Eq. (17-47) then becomes

$$\frac{e_c}{e_1} = \frac{R_1}{R_1 + \frac{R}{j\omega CR_1}} = \frac{1}{1 + \frac{1}{j\omega CR_1}}$$

By writing  $\omega_1 = 1/CR_1$

$$\frac{e_c}{e_1} = \frac{1}{1 - j\omega_1/\omega} \quad (17-48)$$

or

$$\left| \frac{e_c}{e_1} \right| = \frac{1}{\sqrt{1 + (\omega_1/\omega)^2}} \quad (17-49)$$

**17-9. Frequency Stabilization of F-M Transmitters.** Just as in the case of the a-m transmitter, it is necessary that the average or carrier frequency of an f-m transmitter be maintained very nearly constant, even though the instantaneous frequency of the f-m transmitter varies with the modulating signal. When a reactance-tube modulator is used to modulate the carrier, the carrier cannot be crystal-controlled and the average frequency will depend to some extent on the temperature, the tube characteristics, and the various potentials. Slight drifts in the operating characteristics of the reactance tube or slight changes in any of the circuit elements will be accompanied by an appreciable change in the average frequency. It is possible to minimize the effects of the drift in the reactance-tube characteristics by employing two such tubes in a balanced connection. Nevertheless the stability is not sufficient without employing some type of stabilization to maintain the carrier frequency within the 2-kc deviation specified by the FCC regulations.

Two basically different methods of stabilizing a reactance-tube modulator are in present-day use. In both cases a standard reference frequency is provided by a crystal-controlled oscillator, and the fundamental or some subharmonic of the transmitter frequency is compared with this reference frequency. Deviations between the two serve to actuate control circuits which operate in such a manner as to reduce these deviations. The RCA and Federal schemes employ somewhat similar all-electronic methods to effect the frequency stabilization, and the Bell Laboratories method employs a frequency-sensitive servomechanism which drives a small motor to which is geared the tuning capacitor, the direction of rotation of the motor being determined by the relative frequency of the transmitter and the reference standard.

The RCA method of stabilizing a reactance-tube f-m modulator<sup>1</sup> is shown schematically in Fig. 17-17. In this circuit the frequency of the reference crystal differs from the center frequency of the f-m transmitter by some definite amount, say 1 megacycle. The two frequencies are mixed, and the difference frequency is applied to a discriminator (the operation of the discriminator will be discussed in Sec. 17-15). The d-c output from the discriminator, which is a direct measure of the difference frequency, is then applied to the grid of the reactance-tube modulator in

such a manner as to make the net control voltage equal to zero when the difference frequency is exactly 1 megacycle. Any frequency drifts can then be appreciably reduced. Clearly, the method cannot yield perfect stability, for unless there is a slight frequency difference, no control voltage is applied to the modulator. However, the improvement that results is sufficient to maintain the frequency stability within the FCC regulations.

The Federal center frequency-stabilization system is shown schematically in Fig. 17-18. In this system the frequencies of the crystal oscillator

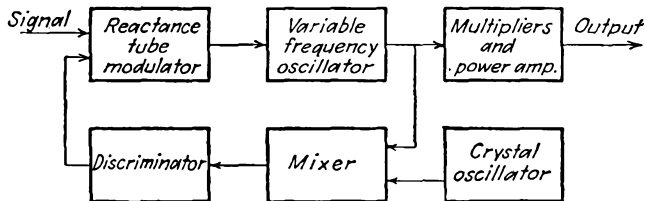


FIG. 17-17. RCA method of stabilizing a reactance-tube frequency modulator.

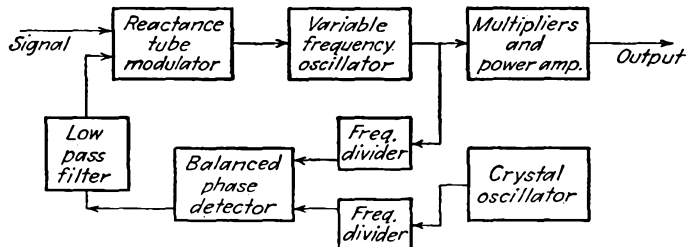


FIG. 17-18. The Federal center frequency-stabilization system.

and the master oscillator are each divided to a common frequency and are then combined in a balanced phase detector. The d-c output voltage, which is a measure of the phase difference between the two oscillators, is used to actuate the reactance-tube modulator in a manner to lock the oscillator mean frequency to that of the crystal reference frequency. This system maintains the center frequency constant within about 1 kc.

The schematic diagram of the Bell Laboratories method of stabilizing the frequency of an f-m transmitter<sup>2</sup> is illustrated in Fig. 17-19. Here the output is frequency-divided, and the resulting subharmonic is then modulated by the output of the crystal-controlled oscillator in such a manner as to produce two-phase beat currents. These currents are used to operate a small synchronous motor to which is geared a tuning capacitor, which is part of the f-m oscillator circuit. If the subharmonic remains in synchronism with the crystal reference, the motor does not move. If the carrier frequency drifts, the armature rotates, the direction

of rotation being set so as to readjust the carrier to the correct frequency. This method of stabilization proves to be very satisfactory and operates over a very wide range of drifts to yield satisfactory results.

**17-10. F-M Transmitters—Armstrong System.** The Armstrong phase-shift method of obtaining frequency modulation incorporates a crystal-controlled oscillator as a basic element of the system. Consequently this system has an intrinsic stability as good as that of its crystal, and no additional frequency stabilization is required.

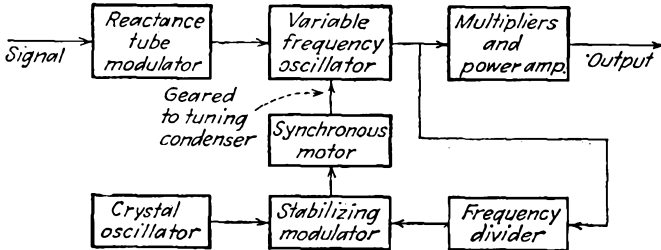


Fig. 17-19. The Bell Laboratories method of stabilizing a reactance-tube frequency modulator.

Before the specific features of this method of producing frequency modulation are examined, it is pertinent to examine the spectrum of p-m waves with small value of maximum phase deviation. For the particular case where  $\theta_d = 0.5$ , which is illustrated in Fig. 17-6, the significant terms depend on the following values of Bessel functions,

$$\begin{aligned} J_0(0.5) &= 0.9385 \\ J_1(0.5) &= 0.2423 \\ J_2(0.5) &= 0.0306 \\ J_n(0.5) &\doteq 0 \quad \text{for } n > 2 \end{aligned}$$

and the modulated wave has the explicit form

$$e = E_c \sin (\omega_c t + 0.5 \sin \omega_m t) \tag{17-50}$$

which is

$$e = 0.9385 E_c \sin \omega_c t + 0.2423 E_c [\sin (\omega_c + \omega_m) t - \sin (\omega_c - \omega_m) t] + 0.0306 E_c [\sin (\omega_c + 2\omega_m) t + \sin (\omega_c - 2\omega_m) t] \tag{17-51}$$

Note, however, that the second side-band components are quite small and that the expression may be written approximately as

$$e \doteq 0.9385 \left\{ E_c \sin \omega_c t + \frac{\theta_d}{2} [\sin (\omega_c + \omega_m) t - \sin (\omega_c - \omega_m) t] \right\} . \tag{17-52}$$

Clearly, this expression will be more accurate for values of  $\theta_d$  less than 0.5.

Now consider the corresponding a-m wave, having the form

$$e = E_c(1 + m_a \sin \omega_m t) \sin \omega_c t \quad (17-53)$$

which may be written as

$$e = E_c \sin \omega_c t + \frac{m_a}{2} [-\cos(\omega_c + \omega_m)t + \cos(\omega_c - \omega_m)t] \quad (17-54)$$

Note specifically that, if  $m_a = \theta_d$ , the only essential difference between the a-m and the p-m waves is in the relative phase of the carrier and the side bands. Evidently for small values of  $\theta_d$ , if the side bands of the a-m wave can be shifted by 90 deg with respect to the carrier, a p-m wave results. It is immaterial, of course, whether the phase of the carrier or the phase of the side bands is shifted in order to achieve the p-m waves.

The process here discussed can be given graphically in a manner that is quite illuminating. It was shown in Sec. 15-1 that amplitude modulation could be represented by means of a

FIG. 17-20. The sinor representation of an a-m wave.

sinor diagram. In this diagram, the carrier potential is represented by a fixed sinor, and the side-band components are represented by two sinors which rotate in opposite directions. This sinor representation is redrawn for convenience in Fig. 17-20. The resultant vector  $e$  represents the a-m wave at any instant.

A corresponding sinor representation of the process of p-m production is possible. Here, as shown in Eq. (17-52), the carrier must be shifted in phase by 90 deg relative to the side bands. The resultant sinor diagram then has the form shown in Fig. 17-21. It is evident from this diagram that a phase-modulated wave does result. Moreover, since  $\theta_d$  is chosen to be small, the amplitude variations that result in this process are very small. These variations can be eliminated by the use of amplitude limiters, although these are not found necessary.

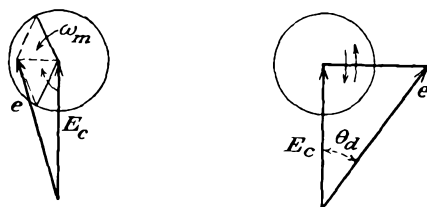


FIG. 17-21. The sinor representation of a p-m wave.

A block diagram of an Armstrong type f-m transmitter is given in Fig. 17-22. The essential features of the system are the following: A stabilized 200-kc primary-frequency oscillator is used to control the mean or carrier

frequency of the radiated wave. Part of this 200-kc signal is mixed in a balanced modulator with a signal representing a frequency-distorted version of the audio signal, the predistorted signal being such that the

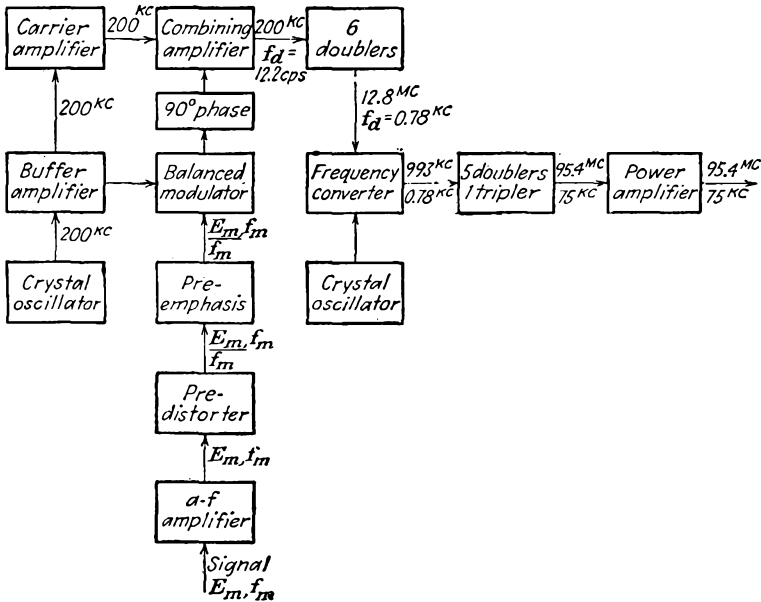


FIG. 17-22. Block diagram of an Armstrong f-m transmitter.

amplitude is made to vary inversely with its frequency. The output from the balanced modulator is the amplitude-modulated side bands with the carrier-frequency component missing. The modulation products are shifted through 90 deg in phase and are then combined with the carrier in the combining buffer amplifier. The result is an f-m wave, which has been achieved from the p-m wave, the phase deviation of which has been made to vary inversely with the modulating frequency. The resulting frequency modulation is multiplied in frequency until it is brought to the desired frequency level for final amplification and transmission.

**17-11. Pre-distorter Circuit.** The function of the predistorter circuit is to provide an output voltage the amplitude of which varies inversely with the frequency of the input voltage. A circuit which achieves the desired results is given in Fig. 17-23. The ratio of the output to the input voltage is given by

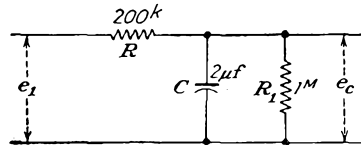


FIG. 17-23. A predistorter circuit.

$$\frac{e_c}{e_1} = \frac{\frac{R_1/j\omega C}{R_1 + 1/j\omega C}}{R + \frac{R_1/j\omega C}{R_1 + 1/j\omega C}} = \frac{\frac{R_1}{1 + j\omega CR_1}}{R + \frac{R_1}{1 + j\omega CR_1}} = \frac{1}{1 + R \frac{1 + j\omega CR}{R_1}} \quad (17-55)$$

or

$$\frac{e_c}{e_1} = \frac{1}{(1 + R/R_1) + j\omega CR} \quad (17-56)$$

This becomes, for the specific circuit constants indicated on the diagram,

$$\frac{e_c}{e_1} = \frac{1}{1.02 + j2.51f} \quad (17-57)$$

Note particularly that for all frequencies in excess of 50 cps the results are given within 1 per cent by the expression

$$\frac{e_c}{e_1} \doteq \frac{1}{j2.51f} \quad (17-58)$$

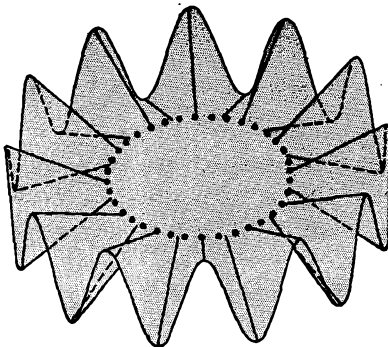
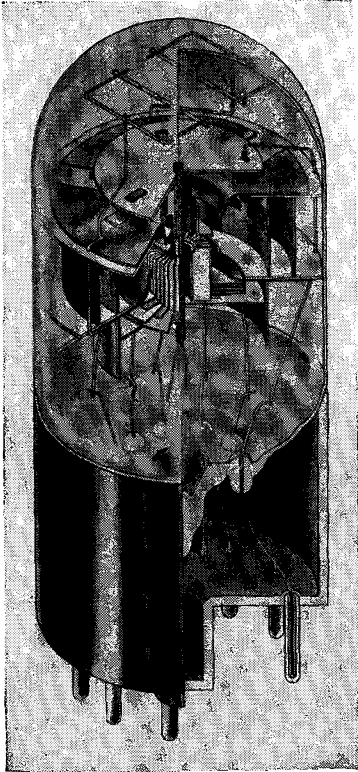


FIG. 17-24. The General Electric 2H21 phasitron.

**17-12. F-M Transmitters—The General Electric Phasitron.** A cutaway sketch of the General Electric GL-2H21 phasitron is shown in Fig. 17-24. It consists of a cathode, an electrostatic focus and deflection system, and an anode structure. The electrons that are drawn from the cathode surface to the anode assembly are acted on by the focus elements to form a tapered, thin-edged disk, whose axis is the cathode and whose focus is at anode 1 of the anode assembly. The deflection system consists of 36 rigidly mounted elements whose active portions lie in a radial plane below the electron disk and a solid neutral plane located above the disk. Every third deflector is connected together and to one phase of a three-phase excitation source. The three-phase voltage source comprises a crystal oscillator and phase-splitting network.

The action of the deflection system is such that portions of the electron disk are deflected above or below the normal plane by the magnetic field of the three-phase system to form a sinusoidal edge. The appearance of the disk is clearly illustrated in Fig. 17-24. The disk may be considered as rotating at a rate determined by the crystal oscillator.

Anode 1 is a cylinder with 24 holes punched alternately above and below the normal plane of the disk. Electrons striking the surface of the cylinder are collected by it, while those that pass through the holes are collected by the solid anode 2. Figure 17-25 shows a developed portion

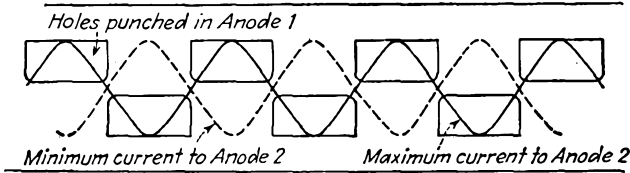


Fig. 17-25. A developed portion of anode 1.

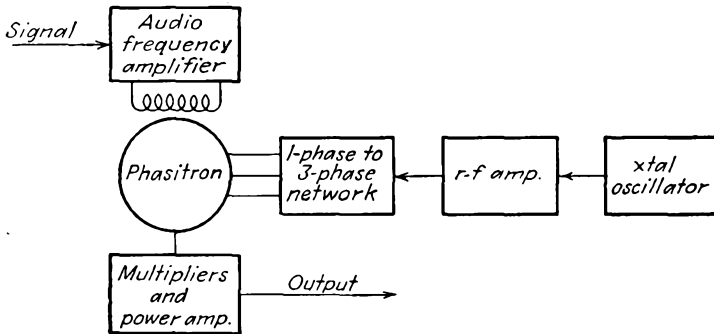


Fig. 17-26. The General Electric phasitron f-m transmitter.

of anode 1. The solid sine curve represents the edge of the electron disk at the time when the maximum number of electrons pass through the openings to anode 2. The dotted curve shows the situation one half cycle later, and almost no electrons pass through the openings to anode 2. If, therefore, the two anodes are connected to opposite ends of a resonant circuit, the circuit will be excited at the crystal driving frequency and in a time-phase sense that is determined by the phase of the anode-current pulses.

Frequency modulation of the resonant anode circuit is produced by phase modulation of the electron disk. This is accomplished by applying the audio signal to a solenoid which surrounds the phasitron. The axial magnetic field that is so produced causes the electron disk to be advanced or retarded about its axis relative to its zero signal position. Consequently the phase of the oscillator is shifted, with a resultant production

of phase-modulated waves. Moreover, since the magnetic field is produced by a solenoid which is essentially a pure reactance at audio frequencies, then, for a constant voltage input, the current, and hence the magnetic field that is produced, will vary inversely with the frequency of the impressed voltage. Clearly, therefore, the output from the oscillator is an f-m wave.

A schematic diagram of the phasitron f-m transmitter is given in Fig. 17-26.

**17-13. F-M Receivers.** The basic circuit of an f-m receiver is somewhat similar to that of an a-m receiver of the superheterodyne type. However, there are a number of significant differences in the two receivers. The required band width in the f-m receiver is larger than that for a-m reception, which requires that the frequency converter and the r-f and

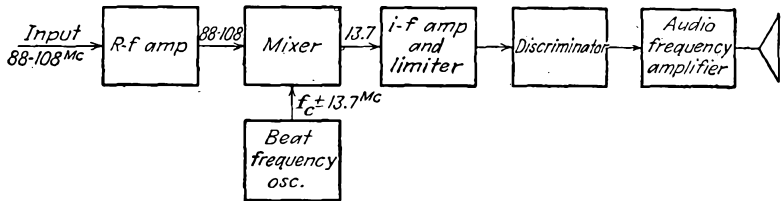


FIG. 17-27. Block diagram of a typical f-m receiver.

the i-f amplifiers must be designed for this broader band width. Also, the last i-f stage of the f-m receiver is operated as a limiter, thus eliminating any fluctuations in the amplitude of the i-f carrier, however produced. The other outstanding difference is in the circuit used to demodulate the f-m carrier. The f-m discriminator that is used to convert from frequency modulation to amplitude modulation does not appear in an a-m receiver, and also the detector, while it uses conventional diode circuits, operates somewhat differently in the f-m circuit. The operation of this will be examined below.

A block diagram of a typical f-m receiver is shown in Fig. 17-27. Such a receiver must provide a high r-f gain in order to permit high sensitivity with amplitude limitation. Also, it is necessary to use a relatively high i-f frequency in order to permit the necessary 225-kc band width. In addition, the high intermediate frequency has the feature that the image signals fall outside of the tuning range. In particular, in the block diagram shown for use in the range from 88 to 108 megacycles, the image frequencies lie in the band 115.4 to 135.4 megacycles.

**17-14. The Limiter.** It is the function of the limiter to remove any amplitude modulation that might exist in the signal. These fluctuations in the amplitude of the i-f carrier might have been produced either by variations in the transmitting conditions or by man-made or natural

static. Such a circuit, which usually operates on the nonlinear portion of its characteristic, provides an output voltage that is sensibly independent of the amplitude of the input voltage. Such limiter action is easily secured by operating the plate of a tube at a very low plate potential; by using a high series-grid resistor, by using a low screen potential, or by a combination of these three. Other limiters are discussed in Chap. 7.

As ordinarily used, the last i-f stage of the f-m receiver is usually operated at low screen and low plate potential, in a circuit of the type illustrated. The general character of the gain curve is also included.

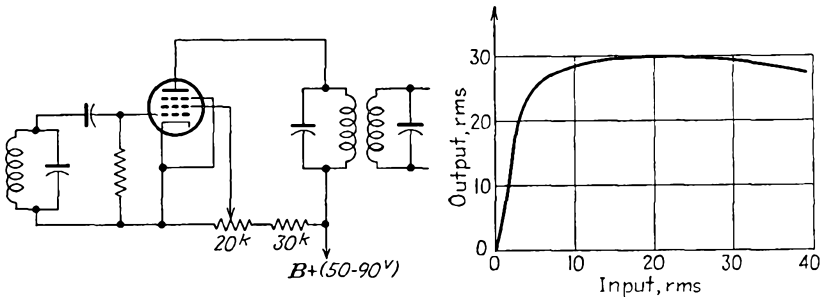


FIG. 17-28. The circuit of a limiter, and the general character of the results.

Such a circuit as that illustrated will saturate at about 10 volts input to the grid, and at this point the stage has a gain of approximately unity.

**17-15. The Discriminator.** In demodulating an f-m wave, the method generally used is first to convert from frequency modulation to amplitude modulation and then demodulate the amplitude modulation by conventional methods. The circuit that is used to make this conversion is known as a *discriminator*. A variety of such circuits are possible, and several will be considered in some detail.

The simplest form of discriminator comprises an ordinary resonant circuit that is tuned to a frequency that differs somewhat from the average frequency of the f-m carrier. The action is made clear by reference to the diagram of Fig. 17-29. Clearly, as the carrier frequency fluctuates, the current in the detuned circuit varies, increasing as the impressed frequency approaches the resonant frequency of the circuit, and decreasing as the impressed frequency departs from the resonant frequency. The output from such a circuit is an a-m wave. However, since the side of the simple resonance curve is not linear, the amplitude-modulated output is distorted.

The linearity can be greatly improved by using two “off-tuned” or “stagger-tuned” circuits instead of one and then choosing the difference between the two outputs. Such a stagger-tuned discriminator circuit<sup>3</sup> is illustrated in Fig. 17-30. In this discriminator, the input *A* is tuned to

the carrier frequency  $f_c$ , circuit  $B$  is tuned to a frequency that is somewhat higher than  $f_c$ , and circuit  $C$  is tuned to a frequency that is somewhat lower than  $f_c$ . The a-m output from such a circuit is without appreciable distortion, owing to the linear resulting characteristic around the point

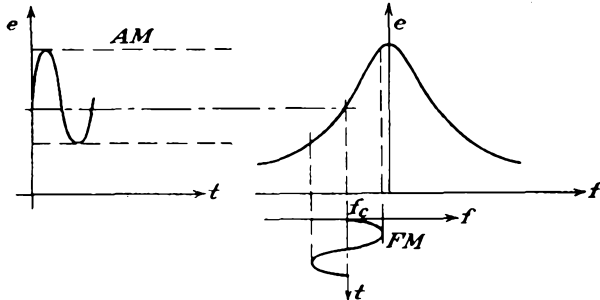


FIG. 17-29. A simple antiresonant circuit operating as a discriminator.

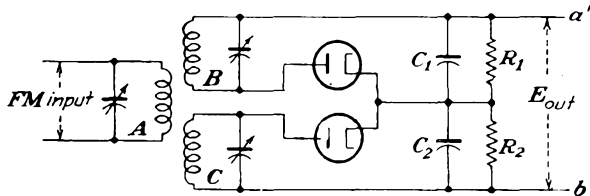


FIG. 17-30. A discriminator employing two stagger-tuned circuits.

$f_c$ . Such circuits suffer from the fact that reception is possible at three points, corresponding to each outer portion of the resonant curves and also to the center or desired linear operating region. The response from such a circuit is illustrated in Fig. 17-31.

As seen in the diagram, the output from each circuit is passed through a diode detector of the envelope or peak detection type. The capacitors

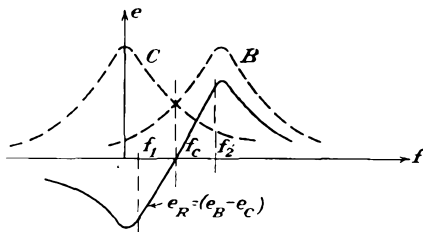


FIG. 17-31. The a-m output from the discriminator of Fig. 17-30.

$C_1$  and  $C_2$  are equal and have negligible reactance at the carrier frequency. The resistors  $R_1$  and  $R_2$  are equal and are quite large. The d-c potential across  $C_1R_1$  is a measure of the amplitude of the output from circuit  $B$ , and the d-c potential across  $C_2R_2$  is a measure of the amplitude of the output from circuit  $C$ . Also, the total

output across  $a'b'$  is then a measure of the difference between the outputs from circuits  $B$  and  $C$  and has a form like the resultant curve  $e_R$  of Fig. 17-31. By careful adjustment of the circuit constants, and if the fre-

quency deviation is limited to the range between  $f_2$  and  $f_1$ , the rectified voltage is an approximately linear function of the impressed frequency.

Another commonly used type of discriminator circuit<sup>4</sup> is shown in Fig. 17-32. It is possible to show that this circuit is substantially a stagger-

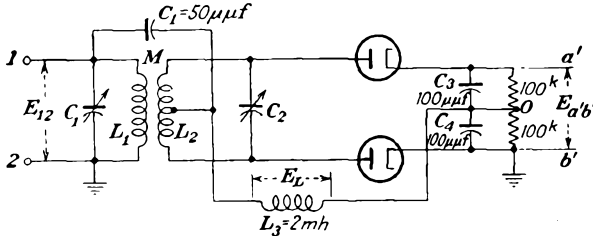


FIG. 17-32. A center-tuned discriminator circuit.

tuned pair<sup>5</sup> and that the results illustrated in Fig. 17-31 also apply for this case.

A limited analytic solution of the operation of the center-tuned discriminator circuit is possible. Consider the circuit comprising  $C_1L_3C_4$ . At the i-f frequency, assumed to be 4.3 megacycles in this circuit,

$$X_{C1} = \frac{10^{12}}{2\pi \times 4.3 \times 10^6 \times 50} = 800 \text{ ohms}$$

$$X_{C4} = 400 \text{ ohms}$$

$$X_{L3} = 2\pi \times 4.3 \times 10^6 \times 2 \times 10^{-3} = 50^k$$

The voltage across  $L_3$  is then

$$E_L \doteq \frac{jX_{L3}E_{12}}{jX_{L3} - j(X_{C1} + X_{C4})} \doteq E_{12} \tag{17-59}$$

Consider now the mutually coupled circuit. If the mutual inductance is small, the impedance coupled into the primary circuit is small and approximately

$$I \doteq \frac{E_{12}}{R_1 + jX_{L1}}$$

which becomes, for high- $Q$  coils,

$$I \doteq \frac{E_{12}}{jX_{L1}} \tag{17-60}$$

The voltage induced in the secondary is then

$$E_{sec} = \pm j\omega MI = \pm \frac{M}{L_1} E_{12} \tag{17-61}$$

If the loading effects of the diode rectifiers are neglected, then

$$E_{ab} = \frac{-jX_{C2}}{R_2 + jX_{L2} - jX_{C2}} = \mp \frac{jX_{C2}(M/L_1)}{R_2 + jX_2} E_{12} \quad (17-62)$$

where

$$X_2 = \omega L_2 - \frac{1}{\omega C_2}$$

Note now that the output d-c potential  $E_{a'o}$  is proportional to the peak of the envelope of  $E_{ao}$ , and correspondingly the output voltage  $E_{b'o}$  is proportional to the peak of the envelope of  $E_{bo}$ . The total output d-c potential is

$$E_{a'b'} = E_{a'o} + E_{b'o} = E_{a'o} - E_{b'o} \quad (17-63)$$

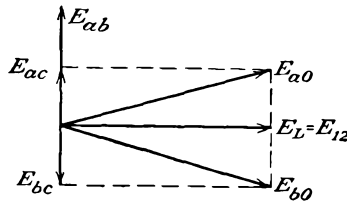
However, the a-c envelopes can be represented in terms of the potentials  $E_{ab}$  and  $E_{12}$ , namely,

$$\left. \begin{aligned} E_{ao} &= E_{ac} + E_L = E_{ac} + E_{12} = \frac{E_{ab}}{2} + E_{12} \\ E_{bo} &= E_{bc} + E_L = -E_{cb} + E_{12} = \frac{-E_{ab}}{2} + E_{12} \end{aligned} \right\} \quad (17-64)$$

Consider the situation when the instantaneous frequency equals the carrier frequency. At this frequency, the secondary circuit is resonant, and the quantity  $X_2$  is zero. The voltage  $E_{ab}$  is then given by the following expression, obtained from Eqs. (17-62). The positive sign is chosen arbitrarily.

$$E_{ab} = j \left( \frac{X_{C2} M}{R_2 L_1} \right) E_{12} = j \left( \frac{M}{\omega C_2 L_1} \right) E_{12} Y / 0 \quad (17-65)$$

The voltages  $E_{ao}$  and  $E_{bo}$  then have the amplitudes and phase somewhat as illustrated in the accompanying sinor diagram. Note that since



$$|E_{ao}| = |E_{bo}|$$

and

$$E_{a'o} = E_{b'o}$$

then

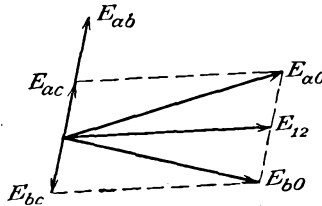
$$E_{a'b'} = 0$$

When the instantaneous frequency is greater than the carrier frequency, the secondary reactance  $X_2$  is positive and Eqs. (17-62) may be written

in the form

$$E_{ab} = j \left( \frac{M}{\omega C_2 L_1} \right) E_{12} \frac{1}{R_2 + jX_2} = j \left( \frac{M}{\omega C_2 L_1} \right) E_{12} Y / -\theta \quad (17-66)$$

The corresponding sinor diagram has the form shown.



Here, since

$$| E_{a0} | > | E_{b0} |$$

then

$$E_{a'o} > E_{b'o}$$

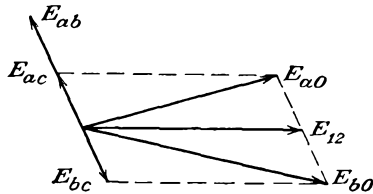
and it follows that

$$E_{a'b'} \text{ is positive}$$

When the instantaneous frequency is less than the carrier frequency,  $X_2$  is negative and Eqs. (17-62) become

$$E_{ab} = j \left( \frac{M}{\omega C_2 L_1} \right) E_{12} \frac{1}{R_2 - jX_2} = j \left( \frac{M}{\omega C_2 L_1} \right) E_{12} Y / \theta \quad (17-67)$$

The corresponding sinor diagram in this case is as shown. In this case



$$| E_{a0} | < | E_{b0} |$$

and

$$E_{a'o} < E_{b'o}$$

so that

$$E_{a'b'} \text{ is negative}$$

The above gives a good representation of the action of such a centered discriminator over the linear range. Owing to the approximations that have been made, it does not represent too well the action over the entire range.

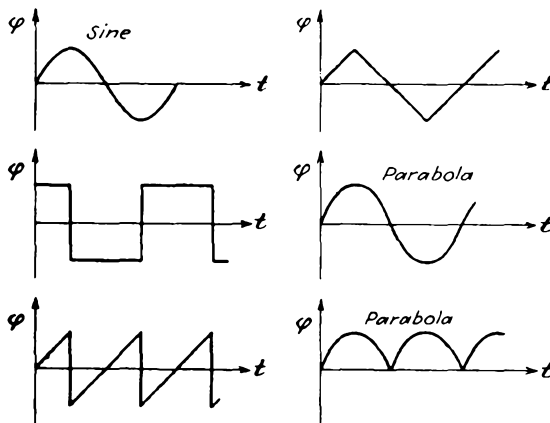
#### REFERENCES

1. Crosby, M. G., *RCA Rev.*, **5**, 89 (1940).
2. Morrison, J. F., *Proc. IRE*, **28**, 444 (1940).

3. Travis, C., *Proc. IRE*, **23**, 1125 (1935).
4. Foster, D. F., and S. W. Seeley, *Proc. IRE*, **25**, 289 (1937).
5. Arguimbau, L. B., "Vacuum Tube Circuits," pp. 486-494, John Wiley & Sons, Inc., New York, 1948.
- Sturley, K. R., *Wireless Eng.*, **21**, 72 (1944).

### PROBLEMS

**17-1.** Determine and plot the instantaneous frequency corresponding to each of the phase functions in the figure.



**17-2.** A 100-megacycle f-m signal is modulated  $\pm 75$  kc at a 400-cps rate. Write an expression for the instantaneous voltage if the signal amplitude is 10 volts and if both the frequency and instantaneous magnitude are a maximum at  $t = 0$  sec.

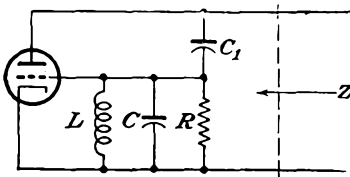
**17-3.** A wave is frequency-modulated at an audio rate of 5,000 cps. If the frequency deviation  $f_d$  is 75 kc, plot the spectrum of the wave, including all significant side-band components.

**17-4.** *a.* The amplitude of a 15-kc wave causes a 75-kc frequency deviation of an f-m wave. Plot the spectrum, and calculate the band width required to pass all side bands of appreciable magnitude.

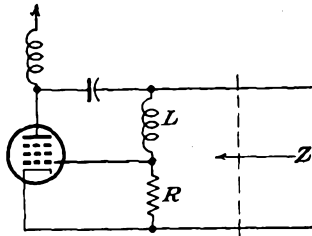
*b.* Suppose that the amplitude is altered to give deviation ratios of 3 and 1. Repeat part *a* for these two cases.

*c.* From these results, estimate the value of the deviation ratio that may be used to be within the FCC limitations of  $\pm 75$ -kc-frequency band spread.

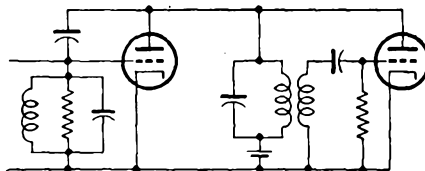
**17-5.** Consider the reactance-tube circuit shown in the diagram. Show that by choosing  $L$  properly  $Z$  is capacitive and is given by  $C/g_m R$  without approximation. Compare with Eq. (17-32).



17-6. Given the reactance-tube circuit in the figure. Show that, if the reactance of  $C$  is negligible at the operating frequency and if  $\omega L \gg R$ , the effective input impedance results from an inductance  $L/g_m R$ .



17-7. Consider the reactance tube and oscillator shown in the diagram for this problem. The oscillator is to operate at 5 megacycles with a frequency deviation

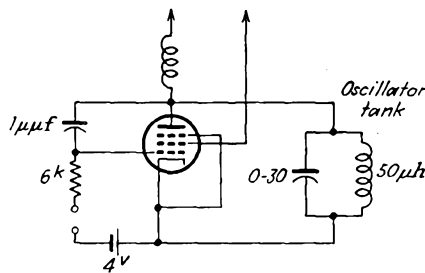


of  $\pm 10$  kc. What change in  $g_m$  is required to achieve the desired frequency modulation?

17-8. Assume that between the limits of  $-2$  and  $-6$  volts the  $g_m-e_{c1}$  characteristic of a 6SJ7 tube may be represented by the expression

$$g_m = 3,000 + 500e_c \quad \mu\text{mhos}$$

This tube is connected as a reactance modulator, as illustrated in the figure. It is desired to have a center or carrier frequency of 5 megacycles and a frequency



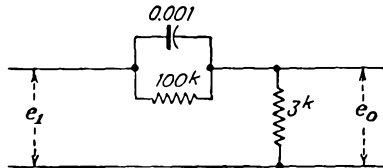
deviation of 7.5 kc. Determine the correct setting of the oscillator tank capacitor and the required modulating voltage.

17-9. Carry out the analysis to show that Eq. (17-33) does give the equivalent output admittance of the inductive reactance circuit.

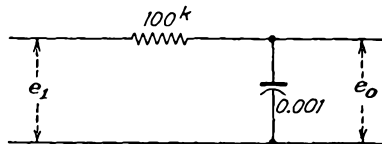
17-10. Obtain an approximate expression for the variation of the frequency of an f-m oscillator as the voltage on the grid of an inductive reactance tube is

varied. Proceed in a manner analogous to that employed in the text in obtaining the corresponding expression for a capacitive reactance tube.

**17-11.** Calculate and plot the voltage ratio for the preemphasis or accentuator circuit, shown in the diagram, as a function of frequency. Plot the curve on semilog paper.



**17-12.** Calculate and plot the voltage ratio for the deemphasis circuit, shown in the accompanying figure, as a function of frequency. Plot the curve on semi-log paper.



**17-13.** Determine the maximum frequency deviation possible with the Armstrong system of Fig. 17-22 if the distortion is to be less than 6 per cent. The phase varies at a 60-cps rate.

**17-14.** What must be the ratio of side-band to carrier voltages in the Armstrong system to produce a frequency deviation of  $\pm 12.2$  cps at the audio frequency of 400 cps?

**17-15.** Show by an analysis similar to that which leads to Eq. (16-6) for the a-m case that the output of a frequency doubler to which an f-m signal is applied is the f-m signal centered about the second harmonic of the carrier.

**17-16.** An f-m wave of the form given by Eq. (17-15) is combined with a large sine wave  $E_c \sin \omega_c t$ . Show that, if both waves are applied to a rectifier, the output will contain the f-m wave shifted in the frequency scale.

**17-17.** An antiresonant circuit consists of a capacitance of  $65 \mu\text{f}$  and an inductance of 0.4 mh and 16 ohms. It is to be used to receive a wave having a frequency modulation of 1.5 kc. What should be the value of the carrier frequency? Estimate the percentage modulation of the output.

**17-18.** Suppose that a discriminator as shown in Fig. 17-30 comprises two circuits which have band widths of 200 kc and are tuned approximately to 4.7 megacycles. Plot the resultant discriminator characteristic for the following separation of the resonant peaks: 150, 200, 250, 300 kc.

## CHAPTER 18

### RELAXATION OSCILLATORS

**I**N ADDITION to the feed-back and negative-resistance oscillators that are discussed in Chap. 12, there is a class of oscillators that is referred to as *relaxation* oscillators. This type of oscillator, like the feed-back oscillator, is provided with a feed-back loop. However, in the case of the feed-back oscillator the amount of feedback is usually so adjusted that a substantially sinusoidal output voltage results. In the relaxation circuits, the feed-back voltage is very large—so large, in fact, that the tube is driven

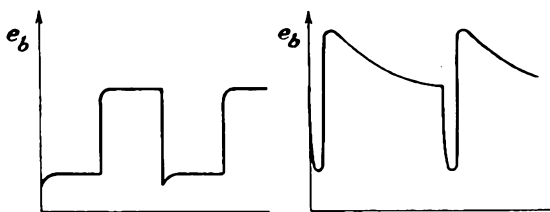


FIG. 18-1. The output-voltage wave forms in the multivibrator and in the blocking oscillator.

beyond cutoff. The tube remains cut off for a time determined by the time constant of the elements in the grid circuit, after which the grid recovers control of the circuit. Because of this operation, a seriously distorted output results. But as such a distorted wave is rich in harmonics, it may be used as a harmonic source. More often, however, these waves serve to provide wave shapes that possess direct applications.

Among the important relaxation oscillators are the multivibrator, a device that provides a sensibly square wave in the output, and the blocking oscillator, a device that provides relatively narrow pulses. The general character of the wave shapes at the output of these circuits is illustrated in Fig. 18-1.

Owing to the nonsinusoidal wave forms present in the circuit and the fact that cutoff exists for an appreciable portion of the cycle, the mathematical analysis of the general feed-back circuit is no longer applicable to a description of the operation of relaxation oscillators. In fact, owing to the cutoff that occurs, a substantially transient analysis must be made. Details of the operation of several types of circuits will be given below.

**18-1. Plate-Coupled Multivibrator.** The multivibrator was first described by Abraham and Bloch<sup>1</sup> in 1918. The circuit is shown in Fig. 18-2. It will be observed that this circuit is essentially that of a simple two-stage resistance-capacitance coupled amplifier, with the output of the second stage coupled through a capacitor to the grid of the first tube. As a result, any signal on the grid of the first stage will be amplified by the two-stage  $RC$  amplifier, and the output signal is in phase with the input signal on the grid of the first stage. Because the output of the second stage is of the proper polarity to reinforce the input signal, positive feedback results and oscillations can take place.

The operation of the circuit is substantially the following. When the anode current in one of the tubes, say  $T1$ , is increasing because of a positive-going signal on the grid, a negative signal is being applied to the grid of the second tube  $T2$ . As a result, the current in  $T2$  is reduced, and the output signal is positive. This positive signal, which is coupled back to  $T1$ , causes the grid of  $T1$  to become more positive, thus increasing the anode current of  $T1$  still further. This effect is cumulative—the current in  $T1$  reaches a maximum, while the potential of the grid of  $T2$  is driven so far negatively, almost instantaneously, that the current in  $T2$  is cut

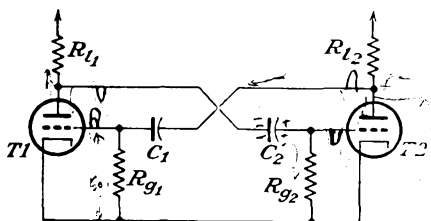


FIG. 18-2. A free-running plate-coupled multivibrator.

off. With  $T2$  still cut off, the charge on capacitor  $C_2$  leaks away through the resistor  $R_{g2}$ , and at some point the potential of the grid of  $T2$  becomes such that the tube will again begin to conduct. This results in a negative output signal being applied to the grid of  $T1$ . The current in  $T1$  decreases, and the start of a cumulative

chain, which results in  $T1$  being cut off and  $T2$  reaching the state of maximum conduction, is initiated. Evidently there are two unstable limiting conditions that occur. In one of these  $T1$  is cut off and  $T2$  is fully conducting, and in the other the roles of  $T1$  and  $T2$  are interchanged.

**18-2. Detailed Explanation of Operation.**<sup>2</sup> Consider the circuit from the instant when the cumulative action discussed above has caused the grid of  $T2$  to be driven beyond cutoff. The circuit of Fig. 18-2 is redrawn for convenience. Just before the switching occurs, the voltage across the capacitor  $C_1$  is  $E_1$  and is given by

$$E_1 = E_{b2} - E_{01} \quad (18-1)$$

where  $E_{b2}$  is the drop across tube  $T2$  when it is conducting and  $E_{01}$  is the cutoff potential of  $T1$  and the grid potential of  $T1$  at which current will just begin to flow in  $T1$ .

When  $T2$  is cut off, this tube is effectively removed from the action of the circuit and remains out of the circuit until the grid potential has recovered to the cutoff value  $E_{02}$ , when the tube will again begin to draw current. During the cutoff period, there will be no plate current through the plate resistor  $R_{12}$ , and this plate will assume the potential of the

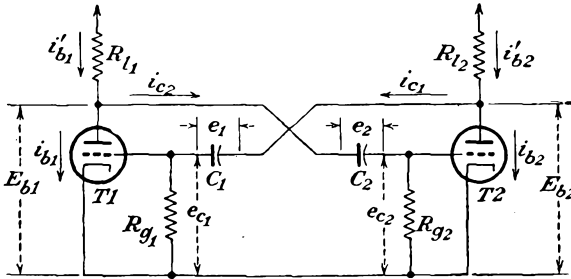


FIG. 18-3. The plate-coupled multivibrator, with voltages and currents labeled.

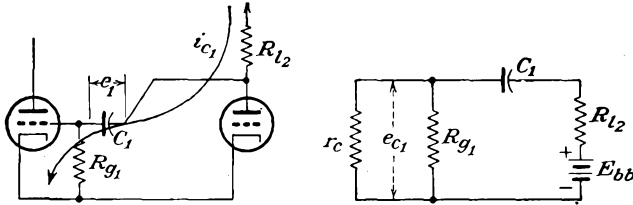


FIG. 18-4. The charging path, and the equivalent circuit for charging capacitor  $C_1$ .

B-supply source  $E_{bb}$ . Hence, during the cutoff period of  $T2$ , the capacitor  $C_1$  begins to charge toward  $E_{bb}$ . Since the charge on  $C_1$  cannot change instantaneously, the sudden rise in plate voltage will appear on the grid of  $T1$ . Thus  $T1$  is caused to conduct its maximum plate current. But as the grid of  $T1$  becomes positive with respect to the cathode, grid current will flow. Thus  $C_1$  begins to charge toward  $E_{bb}$  through the path shown in Fig. 18-4. In fact, since the resistance  $r_c$  of the internal grid-cathode path is smaller than the resistor  $R_{g1}$ , capacitor  $C_1$  will charge mainly through this path.

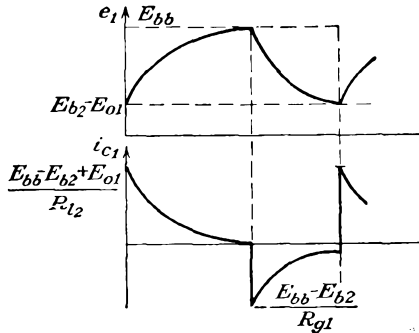


FIG. 18-5. The wave shapes of the current through and the potential across capacitor  $C_1$  during its charging period.

Since  $r_c$  of the internal grid-cathode path during conduction is small compared with  $R_{g1}$  and, in fact, is also small compared with  $R_{12}$ , the charging time constant is approximately  $C_1 R_{12}$ . During the charging process

the potential  $e_1$  across the capacitor  $C_1$  will vary between  $-E_{b2} - E_{01}$  and  $E_{bb}$ , where  $E_{b2}$  is the voltage across  $T_2$  when this tube is conducting. The voltage and current conditions have the forms illustrated in Figs. 18-5 and are governed approximately by the equations

$$e_1 \doteq E_{bb} - (E_{bb} - E_{b2} + E_{01})e^{-\frac{t}{R_{12}C_1}} \quad (18-2)$$

and

$$i_{C_1} \doteq \frac{E_{bb} - E_{b2} + E_{01}}{R_{12}} e^{-\frac{t}{R_{12}C_1}} \quad (18-3)$$

The process illustrated in Fig. 18-5 continues in the manner illustrated until the switching action occurs. At this time  $T_1$  stops conducting, and  $T_2$  begins to conduct. The discharge path of  $C_1$  and the equivalent electrical circuit are given in Fig. 18-6. At the instant that discharge of  $C_1$

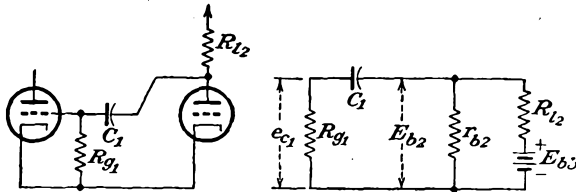


FIG. 18-6. The discharge path, and the equivalent circuit for the discharge of capacitor  $C_1$ .

begins, the voltage across  $C_1$  is essentially  $E_{bb}$ .  $C_1$  begins to discharge toward  $E_{b2} - E_{01}$  in the circuit shown. But in this circuit  $R_{l2}$  is shunted by  $r_{b2}$ , the beam resistance of the tube. Ordinarily  $r_{b2}$  is small compared with  $R_{g1}$ , and the controlling equations for the current and voltage are approximately

$$e_1 \doteq (E_{b2} - E_{01}) + (E_{bb} - E_{b2} + E_{01})e^{-\frac{t}{R_{g1}C_1}} \quad (18-4)$$

and

$$i_{C_1} \doteq \frac{E_{bb} - E_{b2} + E_{01}}{R_{g1}} e^{-\frac{t}{R_{g1}C_1}} \quad (18-5)$$

Clearly, the current builds up until it reaches the value  $+E_{01}/R_{g1}$ , at which time the potential on the grid of  $T_1$  is  $E_{01}$  and the cumulative action once again occurs. The cycle of operation is thus completed, and the circuit is ready to repeat its cycle.

The wave forms of the potentials and currents at various points of the circuit are given in Fig. 18-7. The corresponding results for the second tube are of the same form, but will be shifted  $t_1$  sec along the time axis.

**18-3. Frequency of Oscillation.** The period of oscillation of the multi-vibrator is readily found. It follows from Eq. (18-5), since  $T_1$  is off for

the time required for  $e_1$  to increase from  $E_{bb} - E_{b2}$  to  $E_{01}$  along the exponential curve, that

$$E_{01} = -(E_{bb} - E_{b2})e^{-\frac{t}{R_{01}C_1}}$$

from which

$$t_1 = R_{01}C_1 \log_e \frac{E_{bb} - E_{b2}}{-E_{01}} \quad (18-6)$$

Similarly, for  $T_2$ , the results are

$$t_2 = R_{02}C_2 \log_e \frac{E_{bb} - E_{b1}}{-E_{02}} \quad (18-7)$$

The period of the complete oscillation, neglecting the switching time, is

$$T = t_1 + t_2 = R_{01}C_1 \log_e \frac{E_{bb} - E_{b2}}{-E_{01}} + R_{02}C_2 \log_e \frac{E_{bb} - E_{b1}}{-E_{02}} \quad (18-8)$$

If the two tubes have identical characteristics, then

$$\begin{aligned} E_{b1} &= E_{b2} = E_2 \\ E_{01} &= E_{02} = E_0 \end{aligned}$$

and Eq. (18-8) becomes

$$T = (R_{01}C_1 + R_{02}C_2) \log_e \frac{E_{bb} - E_b}{-E_0} \quad (18-9)$$

If, also,

$$R_{01} = R_{02} = R_0 \quad C_1 = C_2 = C$$

Eq. (18-9) reduces to

$$T = 2R_0C \log_e \frac{E_{bb} - E_b}{-E_0} \quad (18-10)$$

The expressions given by Eqs. (18-8) to (18-10) apply to multivibrators having a low repetition frequency, since they do not take stray capacitances into account. At the higher repetition frequencies, the following more precise equation should be employed instead of Eq. (18-8):<sup>3</sup>

$$T = (C_1 + C_{k01})R_{01} \log_e \left( \frac{E_{bb} - E_{b2}}{-E_{01}} \frac{C_1}{C_1 + C_{k01}} \right) + (C_2 + C_{k02})R_{02} \log_e \left( \frac{E_{bb} - E_{b1}}{-E_{02}} \frac{C_2}{C_2 + C_{k02}} \right) \quad (18-11)$$

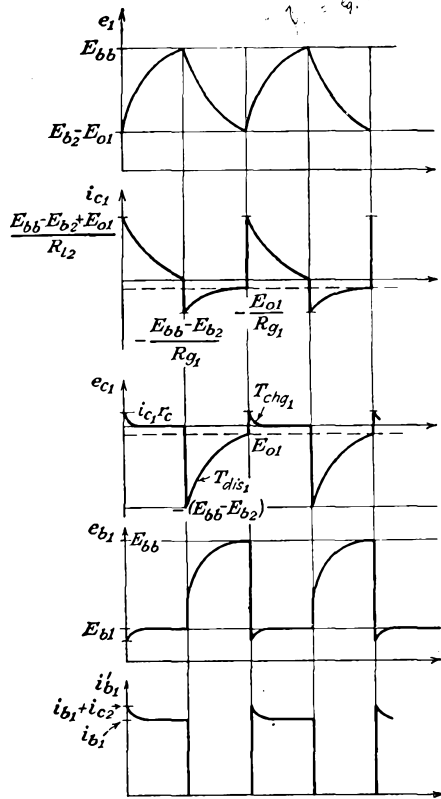


FIG. 18-7. The potential and current wave forms at various points in a symmetrical multivibrator.

This expression is also subject to limitations and should not be used for extremely high repetition frequencies, except perhaps as an approximation.

An approximate value for the period of oscillation of the multivibrator is frequently found in the literature. If one assumes that the period is that determined only by the time constants of the discharge circuits of  $C_1$  and  $C_2$  without regard for the potential levels between which the discharges occur, the period of the oscillation is approximately

$$T \doteq C_1 R_{\sigma 1} + C_2 R_{\sigma 2} \quad (18-12)$$

This result is in error, of course, and frequently an empirical constant is used to give the frequency of operation. The frequency is given by

$$f \doteq \frac{1}{N(C_1 R_{\sigma 1} + C_2 R_{\sigma 2})} \quad (18-13)$$

where  $N$ , the correction factor given in Eq. (18-13), is about 2 for frequency operation below 500 cps and rises to about 4 at 10,000 cps.

**18-4. Biased Multivibrators.**<sup>3</sup> If the time duration of the output wave of a multivibrator is important, switching of the nonconducting

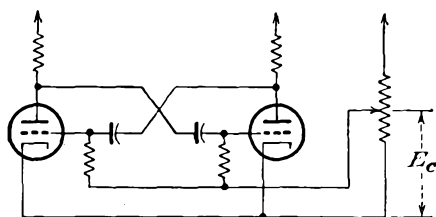


FIG. 18-8. A biased multivibrator to reduce the time jitter of the trailing edge.

tube, which determines the trailing edge, is critical. Switching occurs when the exponential grid voltage discharge curve intersects the tube cutoff curve. If this intersection is sharp, the time at which the trailing edge occurs is correspondingly well defined. If the intersection is gradual, the point of intersection will depend

to a greater or lesser degree on the variations of tube constants and voltages. To ensure a sharp intersection, it is usual to employ a positive bias on the tubes. Such a circuit is illustrated in Fig. 18-8. The expression for the period of such a modified circuit becomes

$$T = C_1 R_{\sigma 1} \log_e \frac{E_{bb} - E_{b2} + E_c}{-E_{o1} + E_c} + C_2 R_{\sigma 2} \log_e \frac{E_{bb} - E_{b1} + E_c}{-E_{o2} + E_c} \quad (18-14)$$

For normal operations, it is found that the frequency of oscillation may be varied over wide limits in an almost linear manner by controlling  $E_c$ . The linearity between frequency of oscillation and control voltage  $E_c$  can be improved by including resistors  $R_k$  in each cathode,<sup>4</sup> the value of these being determined experimentally.

The effect of the application of the positive bias is best illustrated graphically,<sup>5</sup> and Fig. 18-9 shows the wave form  $e_{c1}$  on the grid of  $T_1$ .

The equivalent circuits for the charging of  $C_1$  and the discharging of  $C_2$ , corresponding to those shown in Figs. 18-4 and 18-6, now become as shown in Fig. 18-10.

If it is desired to operate the biased multivibrator at a fixed frequency,  $E_c$  should be made as high as possible, *e.g.*, equal to  $E_{bb}$ . If the values of  $E_b$  and  $E_0$  are negligible in comparison with  $E_{bb}$ , the period then approximates to

$$T \doteq (C_1 R_{g1} + C_2 R_{g2}) \log_e 2 \quad (18-15)$$

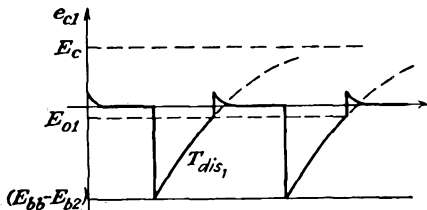


FIG. 18-9. Wave form of  $e_{c1}$  for the circuit of Fig. 18-8.

If the positive bias is applied to a single tube only, as in the circuit of Fig. 18-11, the expression for the period becomes

$$T = C_1 R_{g1} \log_e \frac{E_{bb} - E_{b2}}{-E_{01}} + C_2 R_{g2} \log_e \frac{2E_{bb} - E_{b1}}{E_{bb} - E_{02}} \quad (18-16)$$

This shows that the period has changed because the time required for the

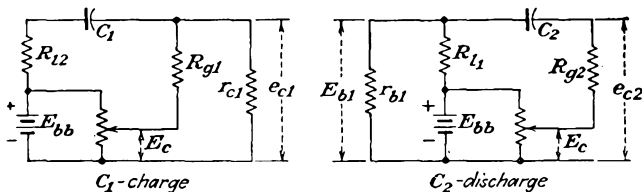


FIG. 18-10. Equivalent circuits for the charge of  $C_1$  and the discharge of  $C_2$  in Fig. 18-8.

grid recovery of  $T_2$  has been decreased, the recovery time for  $T_1$  remaining unchanged. This means that the wave forms for the recovery of the two tubes are not of equal time duration,

and an unsymmetrical or unbalanced condition results. Of course, an unsymmetrical wave form is easily obtained with the previously discussed circuits by changing the grid-circuit time constants of one circuit and not of the other. One should not attempt to achieve a markedly unbalanced condition of time in the multi-

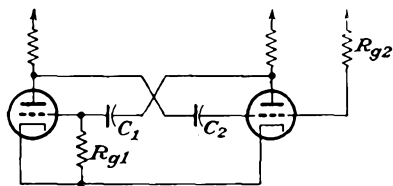


FIG. 18-11. Multivibrator with one grid returned to the plate supply voltage.

vibrator, since if the time constant  $C_2 R_{g2}$  were made too different from  $C_1 R_{g1}$ , the trailing edge of the long-time-constant tube might become unstable.

The wave form of  $e_{c2}$  of this circuit is given in Fig. 18-12. The equivalent circuits governing the charge and discharge of the capacitors are those of Fig. 18-10, with  $E_c$  in the discharge circuit replaced by  $E_{bb}$ .

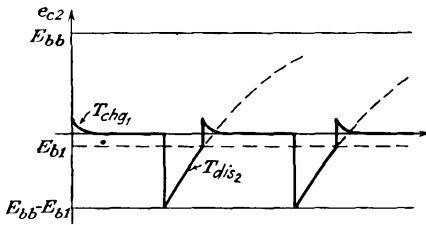


FIG. 18-12. Wave form of  $e_{c2}$  for the circuit of Fig. 18-11.

**18-5. Cathode-coupled Multivibrator.** The circuit of a cathode-coupled multivibrator is given in Fig. 18-13. The operation of this circuit is somewhat different from the plate-coupled circuit of Fig. 18-2. To understand the action of this circuit, suppose that it

is initially without plate voltage. There will be no charge on  $C$ , and the grids of both  $T1$  and  $T2$  will be at ground potential. When the supply potential is suddenly applied, both tubes will start to conduct and the plates of  $T1$  and  $T2$  will begin to fall in potential. But since the voltage across  $C$  cannot change instantaneously, the drop in potential that takes place at

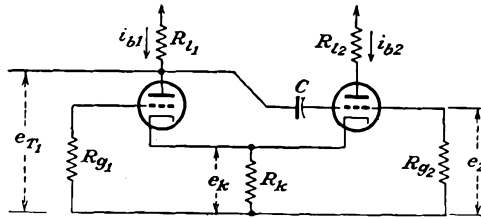


FIG. 18-13. A cathode-coupled multivibrator using direct coupling.

the plate of  $T1$  is coupled to the grid of  $T2$ , tending to cause  $T2$  to cut off. This tendency is also accentuated by the tube currents which flow through the cathode resistor  $R_k$ , which raises the cathode potential of both tubes. But, with the current  $i_{b2}$  tending to decrease,  $i_{b1}$  will increase, resulting in a larger negative potential to the grid of  $T2$  and also a larger positive potential to the cathode of  $T2$ , and  $T2$  will rapidly reach cutoff.

$T2$  is held beyond cutoff during the time required for  $C$  to discharge along an exponential curve and reach the cutoff potential of the tube. The equivalent circuit of the discharge is given in Fig. 18-14. When this cutoff potential is reached,  $T2$  will begin to conduct. This current through  $R_k$  will tend to raise the cathode potential of  $T1$ , and the current  $i_{b1}$  will begin to decrease. As a result, the plate

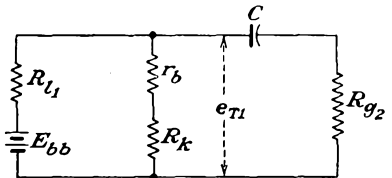


FIG. 18-14. The equivalent circuit for discharge of  $C$  of Fig. 18-13.

potential of  $T1$  will increase, resulting in a positive signal to the grid of  $T2$ , and the cumulative cycle will continue until  $T1$  is cut off and  $T2$  is conducting its maximum current.

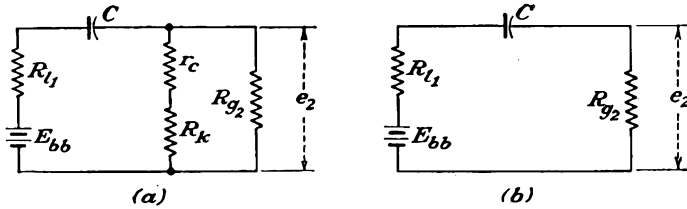


FIG. 18-15. The equivalent charging circuits of  $C$ : (a) applies during the time that grid current is drawn; (b) applies for the remainder of the time interval.

The grid of  $T2$  is driven highly positive, resulting in a large plate current, which causes the voltage across  $R_k$  to rise quickly. However, because grid current is drawn, the capacitor  $C$  charges relatively quickly for a time, until the potential  $e_{c2}$  and  $e_k$  are the same, and thereafter charging continues at a slower rate.

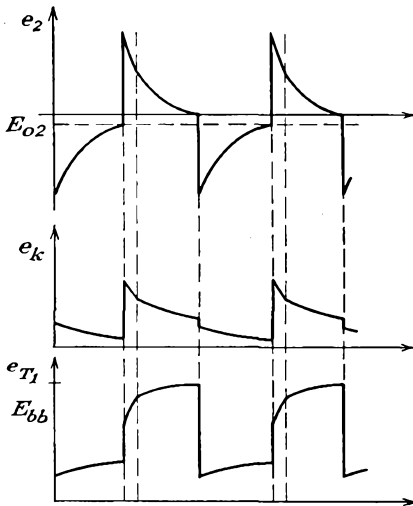


FIG. 18-16. Wave forms in a cathode-coupled multivibrator with direct coupling.

The equivalent charging circuits are shown in Fig. 18-15. As  $C$  charges, the bias on  $T2$  decreases, causing  $i_{b2}$  to decrease. This in turn causes  $e_k$  to decrease. The grid of  $T1$  is held constant at ground potential so that this tube remains cut off as

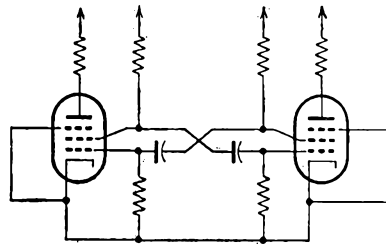


FIG. 18-17. An electron-coupled multivibrator.

long as  $e_k$  is positive relative to ground by more than cutoff voltage. When  $e_k$  drops to  $E_{01}$ ,  $T1$  begins to conduct and the cycle reverses.

The wave forms at several points in the circuit (see Fig. 18-16) illustrate the operation.

**18-6. Pentodes in Multivibrator Circuits.** One may use pentodes in a multivibrator circuit, as illustrated in Fig. 18-17. It will be observed that the circuit is essentially a conventional plate-coupled multivibrator,

the cathode, control grid, and screen grid serving as the triode for the switching action. Since the load resistors are connected to the anodes, which are shielded from the switching circuit by the suppressor grid, load changes will not materially affect the oscillatory circuit and the frequency is reasonably independent of the load.

**18-7. Design Considerations.** In addition to the choice of constants to yield the desired repetition frequency, a number of other factors must be considered in designing a multivibrator circuit. If the wave shape of the output is important, it is necessary to examine the factors which affect the steepness of the rapid shifts of potential. If a rapid rise of voltage is desired, one may have to employ design factors that are common to the design of video amplifiers. Thus it is necessary to employ low values of plate resistance and to use tubes with low shunt capacitance. With reasonable care in the choice of these values, it is not difficult to design a multivibrator circuit which can reach its full rise of potential in  $1 \mu\text{sec}$ , using low-current receiving types of tubes. If more rapid action is required, heavier current tubes must be used. For example, the full rise may be obtained in  $0.2 \mu\text{sec}$ , using a 6AG7 tube.

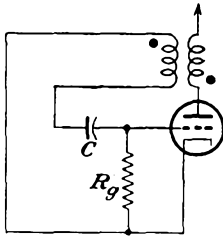


FIG. 18-18. A simple blocking oscillator.

**18-8. The Blocking Oscillator.**<sup>4</sup> Suppose that the second stage of a free-running multivibrator is replaced by a transformer which is so connected that regenerative feedback results. Such a circuit has the properties that the tube can be made to conduct hard for a short period of time and then turned off for a relatively long interval before it goes through its cycle. The circuit of such an oscillator is given in Fig. 18-18.

The operation of the circuit is substantially the following: Suppose that the grid is only slightly negative. The tube will conduct, and the voltage of the anode will begin to fall. This changing potential, which appears across the transformer in the plate circuit, will be accompanied by a changing potential in the grid winding of the transformer. The phase of the transformer connection is such that the potential of the grid becomes positive, thus increasing the plate current. This is a regenerative action, which continues until the grid draws current, thus charging the capacitor  $C$  to a voltage  $\frac{1}{C} \int_0^{\tau} i_g dt$ , where  $\tau$  is the duration of the charging time, the current through  $R_g$  being neglected. The charging ceases when the plate potential falls so low that the plate circuit can no longer drive the low impedance reflected from the grid circuit.

At this time there is no longer any voltage induced in the grid winding

of the transformer, and the voltage on  $C$  begins to discharge. The discharge of  $C$  causes the grid-cathode voltage to decrease. This results in a decreasing plate current and hence a rising plate potential. The resulting voltage in the grid winding causes the grid to go more negative, thus initiating the cumulative action that causes the tube to cut off.

Now, however, with the tube cut off, the charge on the capacitor can leak off only through the grid resistor  $R_g$ , resulting in an exponential rise toward ground with a time constant approximately equal to  $R_g C$ . This rise continues until the grid potential reaches the cutoff potential of the tube, when the cycle will repeat itself.

The wave forms at various points in the circuit are shown in Fig. 18-19.

The total repetition period of such a blocking oscillator is seen to be

$$T = \tau + R_g C \log_e \frac{E}{-E_0} \quad (18-17)$$

where  $\tau$  is the duration of the pulse and  $E$  is the potential to which the capacitor is charged during the pulse.

The transformer in the circuit may be connected in a number of ways. Thus, in addition to the connection of Fig. 18-18, the transformer windings can be in the grid and cathode line and also in the plate and cathode lines (see Prob. 18-6).

Precisely the same considerations concerning the possibility of jitter of the trailing edge of the output pulse applies for the blocking oscillator as for the multivibrator, and the biased blocking oscillator achieves the same results in the same way as the biased multivibrator. Consequently, if the jitter is to be kept to a minimum, a biased blocking oscillator should be used. The diagram of such a circuit is given in Fig. 18-20. The recurrence period of this device will be given by the expression

$$T = \tau + RC \log_e \frac{E_c + E}{E_c - E_0} \quad (18-18)$$

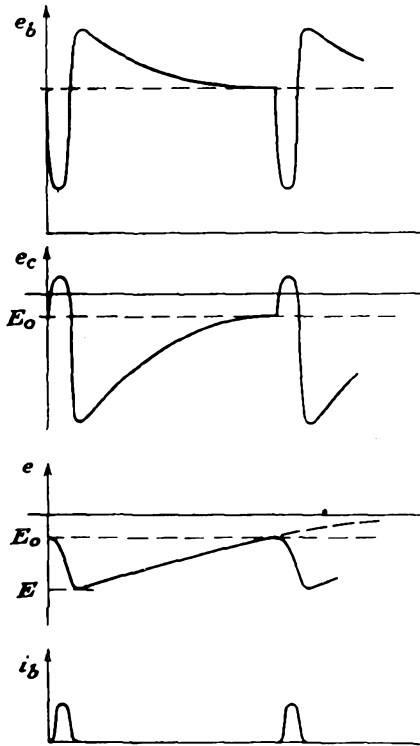


FIG. 18-19. The wave forms in a single-swing blocking oscillator.

The duration of the pulse, *i.e.*, the length of the conducting period  $\tau$ , depends upon the capacitor  $C$  and upon the characteristics of the transformer. For a given transformer,  $C$  is the most important circuit element, larger values of  $C$  being accompanied by longer pulses. For example, a certain transformer, when used in the circuit of Fig. 18-20, yielded pulses which could be varied from approximately 0.2 to 20  $\mu\text{sec}$  by changing the size of the capacitor  $C$ .

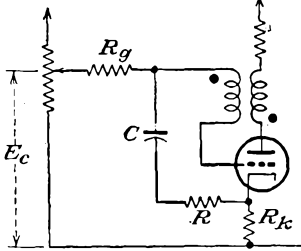


FIG. 18-20. A biased blocking oscillator.

**18-9. Van der Pol Relaxation Oscillator.**

One of the earliest forms of single-tube relaxation oscillators was described by van der Pol in 1926.<sup>5</sup> The circuit of such an oscillator is given in Fig. 18-21. It consists of a tetrode in which the control grid and the screen grid are capacitively coupled, the control grid being maintained positive by means of a high resistance coupling to  $E_{bb}$ . However, since these oscillators ordinarily incorporate a pentode rather than a tetrode, the pentode-type oscillator will be discussed here.

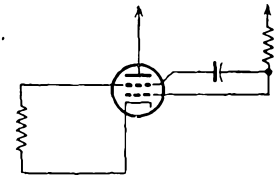


FIG. 18-21. The van der Pol oscillator.

The circuit of the pentode-type relaxation oscillator is given in Fig. 18-22. This circuit depends for its operation on the fact that a change of potential on the suppressor grid is accompanied by an amplified change of potential without phase reversal on the screen grid. To see that this is so, consider for the moment that capacitor  $C$  is removed, and suppose that the tube is in a quiescent state. The situation is then as illustrated in Fig. 18-23.

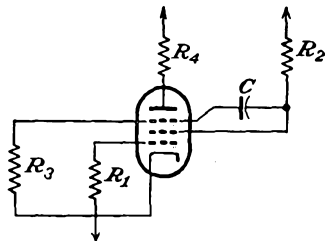


FIG. 18-22. A pentode van der Pol relaxation oscillator.

Suppose that a negative signal is applied to the suppressor grid of such amplitude that the anode current is interrupted. As a result, the total space current will be collected by the screen grid, with a consequent decrease in screen potential, owing to the screen resistor. In fact, if it is considered that the control-grid potential establishes the total space current, the effect of a signal on the suppressor grid is to control, in a nonlinear manner, the division of the space current between the anode and the screen grid, although a more positive suppressor grid results in a decreased screen current and hence a more positive screen-grid poten-

tial. That is, the suppressor-signal and the screen-potential variations are in the same phase. Thus, if the gain of the circuit is greater than unity and if feedback is arranged between the output circuit (the screen) and the input circuit (the suppressor), the device becomes an oscillator and is almost equivalent to a multivibrator.

Refer now to the circuit of Fig. 18-22, and suppose that, at the instant that the suppressor is positive, the anode is taking current. As a result, the anode potential is falling, and the screen potential is rising, owing to the reduced screen current. The rising screen potential, which is coupled to the suppressor through the capacitor  $C$ , is accompanied by a rising suppressor-grid potential, since the capacitor voltage cannot change instantaneously. This is a cumulative action that continues until the maximum current is drawn by the anode. When this condition is reached, a charging current immediately starts flowing into the capacitor through the combination of  $R_2$  in parallel with the screen-cathode path resistance and the combination of  $R_3$  in parallel with the suppressor-cathode path resistance, assuming that a suppressor-grid current flows.

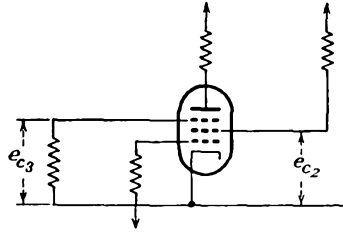


FIG. 18-23. To illustrate the principle of operation of the pentode type of van der Pol relaxation oscillator.

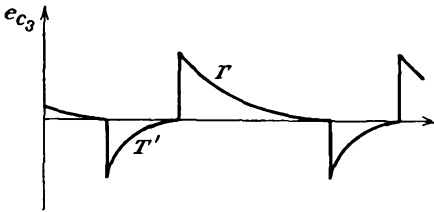


FIG. 18-24. Typical wave form of the suppressor voltage in a pentode van der Pol relaxation oscillator.

flows in the screen circuit. The capacitor charging current now flows through  $R_3$  and the combination of  $R_2$  in parallel with the screen-cathode path resistance, and the potential of the suppressor begins to rise. This brings the action to the point at which the considerations began, and the cycle repeats.

A typical wave form of the suppressor voltage is given in Fig. 18-24. The wave is unsymmetrical because during one portion of the cycle the time constant  $T$  is given by  $C \left( R_3 + \frac{R_2 r_2}{R_2 + r_2} \right)$ , where  $r_2$  is the average screen-cathode resistance; and during the second portion of the cycle the

As the voltage across the capacitor rises, the suppressor voltage falls. This results in a falling screen potential, and at a critical value the anode current begins to fall, with a resulting increase in screen current. This causes a cumulative effect which continues rapidly until the anode current is cut off and maximum current

time constant  $T'$  is given by  $C \left( \frac{R_2 r'_3}{R_3 + r'_3} + \frac{R_2 r'_2}{R_2 + r'_2} \right)$ , where  $r'_2$  and  $r'_3$  are the average screen-cathode and the average suppressor-cathode resistances during the charging period. Evidently, the larger that  $C$  and  $R_2$  are made, the lower is the frequency of oscillation.

**18-10. Synchronized Relaxation Oscillators.** Synchronization in multivibrators may be of two general classes according to the character of the operation. The lightly synchronized multivibrator is free-running, and its frequency is "corrected" by the application of a synchronizing

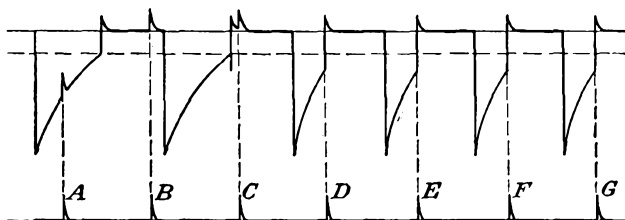


FIG. 18-25. Synchronizing a multivibrator with positive pulses.

voltage. The heavily synchronized multivibrator operates with one or both tubes so heavily biased that the circuit is inactive until a comparatively strong synchronizing or triggering voltage is applied. Furthermore, the presence of the heavy bias causes the circuit to come to rest after it has passed through one complete cycle. Such circuits are frequently referred to as *gate*, *one-shot*, or *univibrator* circuits. Only the lightly synchronized multivibrators will be discussed here, Chap. 19 being devoted to a study of gate circuits, among others.

In the lightly synchronized multivibrator, the inherent poor frequency stability of the system is overcome by "driving" the multivibrator with a synchronizing voltage. This forces the period of the multivibrator to be exactly the same period as the synchronizing frequency or a multiple or submultiple of it. The synchronizing wave form may be of almost any shape, although a pulse or a sine-wave potential is generally used.

Actually the discussion to follow applies for any of the free-running relaxation oscillators and is not confined to multivibrator circuits.

**18-11. Synchronization by Positive Pulses.** Figure 18-25 illustrates the effect of applying positive pulses to one grid of a free-running multivibrator. This diagram shows the conditions before synchronization occurs and the transition stages until synchronization becomes complete. Note that the pulse *A* has no effect because it does not raise the grid recovery voltage above the cutoff potential of the tube and that pulses *B* and *C* have no effect because they are applied to the grid of the conducting tube and grid clipping occurs. Pulse *D* is of sufficient amplitude to

raise the grid above the cutoff potential, and as a result the tubes are switched as the current begins to flow in the tube that was formerly cut off.

Suppose that the frequency of the triggering pulses is considerably higher than the natural frequency of the multivibrator. The situation is then as illustrated in Fig. 18-26. Thus, if trigger *A* causes the multivibrator to switch, triggers *B* and *C* occur at times when the tube is conducting. Since the grid is already positive, these pulses have no effect

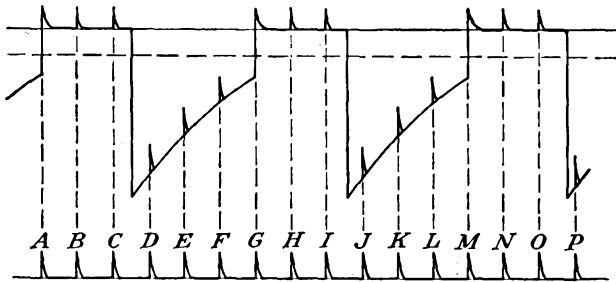


FIG. 18-26. Synchronization with pulses of higher frequency than the natural period of the multivibrator.

on the conduction. Triggers *D*, *E*, *F* are applied to the nonconducting tube, but they are not large enough to cause conduction. Trigger *G* does carry the grid voltage above the cutoff point of the tube, and conduction occurs. In this example, every sixth pulse switches the multivibrator, and hence the repetition frequency of the multivibrator is one-sixth of the frequency of the trigger pulses.

In multivibrators, if accurate frequency division is desired, the division per stage should be relatively low, say 10 or less. If accurate division is not required, a single stage may be used for a division of 100 or more. Also, for best results, the peak of one pulse should rise above the base of the next pulse on the grid recovery curve by about 20 per cent of its height.

**18-12. Synchronization by Negative Pulses.** Multivibrators may be synchronized by means of negative pulses. The situation is then somewhat as shown in Fig. 18-27. To understand the operation in this case, it is necessary to remember only that the application of a negative pulse to the grid of the nonconducting tube will have no effect, as the grid is already negative and beyond cutoff. However, a negative trigger applied to the conducting tube will result in the application of a positive pulse to the nonconducting tube, owing to the amplifier action of the conducting tube. If the resulting positive pulse is large enough, this will initiate the regenerative effect, with the subsequent switching.

**18-13. Sine-wave Synchronization.** The condition when a sine wave is used for synchronization is not unlike that for synchronization by

pulses, although the addition of a sine-wave synchronizing voltage to the grid recovery does change the grid-voltage wave form, somewhat as shown in Fig. 18-28.

The operation of the circuit is substantially the following: When  $T1$  is conducting during the time from  $A$  to  $B$ , grid limiting occurs and the potential  $e_{c1}$  remains substantially constant. When the synchronizing voltage falls below zero and starts to decrease the voltage on the grid, the

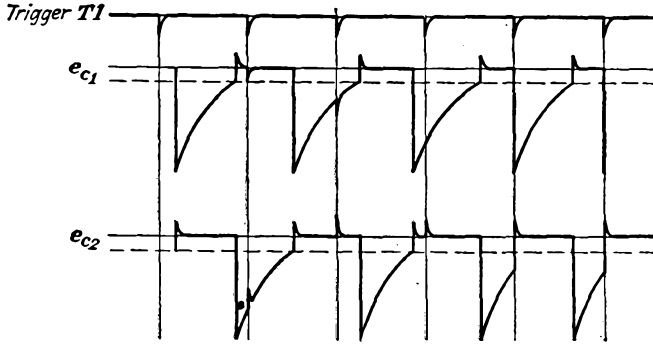


FIG. 18-27. Synchronization with negative pulses.

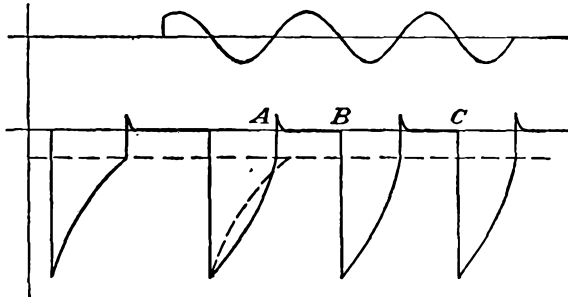


FIG. 18-28. Synchronization with sine-wave voltage.

multivibrator regenerative action causes  $T1$  to cut off. As this occurs at the same point  $B, C, D, \dots$  in each cycle of the synchronizing voltage, the multivibrator is forced to operate at the synchronizing frequency. Evidently, however, this action exists only when the synchronizing frequency is higher than the natural frequency of the multivibrator.

Synchronization by means of a sine-wave potential injected in the cathode circuit of one tube is possible. It is essential that the internal impedance of the synchronizing voltage source must be low in order that the tube current through this impedance does not seriously alter the shape of the wave. The operation of such a synchronized circuit is illustrated graphically in Fig. 18-29. If one supposes that the grid-ground potential is not affected by the presence of the sine-wave synchronizing

voltage but that the grid-cathode potential contains this sinusoidal component of voltage, then one may consider that the effective cutoff potential of the tube varies sinusoidally about the normal value in phase with the synchronizing voltage.

At the instant when the synchronizing voltage is suddenly applied at point *A*, it is supposed that *T1* is conducting. The synchronizing voltage causes the cathode to rise, so that conduction of *T1* is decreased. This

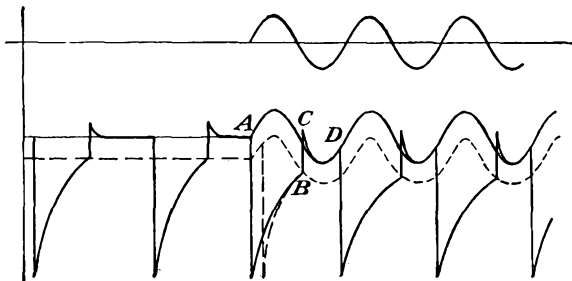


FIG. 18-29. Wave forms of a multivibrator synchronized by a sine wave in the cathode circuit.

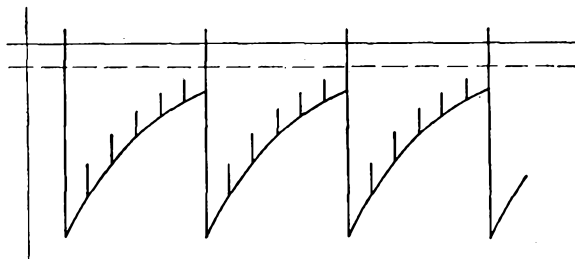


FIG. 18-30. The grid-voltage wave form of a blocking oscillator synchronized with positive pulses.

leads to the regenerative action, and the tube is quickly cut off. This switching action will cause the tube to stop conducting at a time earlier than would be the case for the free-running multivibrator. The voltage  $e_{c1}$  will follow its normal exponential curve until it intersects the cutoff curve, which has the assumed sinusoidal form, and switching takes place at the point *B*. If it is assumed that during conduction the grid-cathode potential remains constant at some small positive value, which is given, in fact, by  $i_{qr}r_c$ , the presence of added negative potential on the cathode will cause the grid voltage to follow the cathode potential and the potential follows the curve *CD*. When the cathode voltage begins to rise, conduction in *T1* is decreased and the regenerative action again takes place.

**18-14. Synchronization of Blocking Oscillators.** Blocking oscillators may be synchronized with either sine waves or pulses applied to the grid,

in much the same manner as for synchronizing multivibrators. For example, Fig. 18-30 illustrates the grid-voltage wave form of a six-count divider. As for the multivibrator synchronization, the trigger heights should be such that the peak of one pulse rises above the base of the next pulse by about 20 per cent of its height. A smaller trigger might allow the divider to fire unsynchronously between triggers. An excessively large trigger may introduce instability due to variations in trigger heights. Also, for accurate frequency division with a blocking oscillator, as for the multivibrator, the division per stage should be relatively low, also 10 or less.

### REFERENCES

1. Abraham, H., and E. Bloch, *Ministère de la guerre Pub.* 27, April, 1918.  
Abraham, H., and E. Bloch, *Ann. Phys.*, **12**, 237 (1919).
  2. Vecchiacchi, F., *Alta frequenza*, **9**, 745 (1940).
  3. Puckle, O. S., "Time Bases," John Wiley & Sons, Inc., New York, 1943.
  4. Benjamin, R., *J.IEE*, **93**, 1159 (1946).  
Cruft Laboratory, War Training Staff, "Electron Circuit and Tubes," pp. 804-809, McGraw-Hill Book Company, Inc., New York, 1947.
  5. van der Pol, B., *Phil. Mag.*, **2**, 978 (1926).
- As general references, see  
Reich, H. J., "Theory and Application of Electron Tubes," New York, McGraw-Hill Book Company, Inc., 2d ed., 1944.  
M.I.T. Radar School Staff, "Principles of Radar," McGraw-Hill Book Company, Inc., 2d ed., New York, 1947.

### PROBLEMS

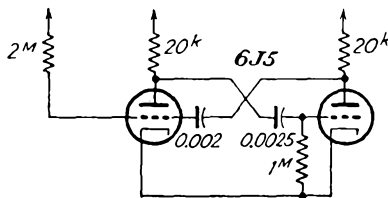
*Note:* In the following problems, if necessary, assume that  $r_c$  for each tube is 500 ohms. If it is necessary to determine the value of  $r_b$  when  $e_c = 0$ , refer to the plate characteristics of the tube. The cutoff grid voltage of each tube may also be obtained from the plate characteristics.

- ✓ **18-1.** Determine the frequency of oscillation of a plate-coupled multivibrator using 6J5 tubes for which

$$R_{g1} = R_{g2} = 500^* \quad C_1 = C_2 = 0.01 \mu\text{f} \quad R_{i1} = R_{i2} = 30^* \quad E_{bb} = 300^v$$

- 18-2.** Repeat Prob. 18-1 when the grids are returned to a positive supply. Plot the frequency as  $E_{cc}$  is varied from 0 to  $E_{bb}$ .

- 18-3.** Given the biased multivibrator shown in the diagram.



- a. Calculate the discharge time constants of the capacitors.
- b. Calculate the peak value of each grid voltage. Assume the grid voltage of the conducting tube to be zero in these calculations.  $E_{bb} = 300$  volts.
- c. Calculate the cutoff periods of each section of the tube.
- d. Calculate the repetition frequency of the multivibrator.

✓ **18-4.** Design a free-running balanced multivibrator to operate at 1,000 cps. Assume the following:  $R_i = 10^6$ ,  $R_o = 500^6$ , 6J5 tubes,  $E_{bb} = 200$  volts.

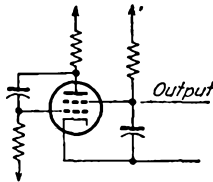
✓ **18-5.** Design a free-running unbalanced multivibrator to operate at 5,000 cps, with one half cycle three times as long as the other. Use  $R_o = 500^6$ ,  $R_i = 10^6$ , 6J5 tubes, and  $E_{bb} = 250$  volts.

**18-6.** Sketch blocking-oscillator circuits with the transformer windings in

- a. Grid and cathode circuits.
- b. Plate and cathode circuits.

Be sure to indicate the transformer winding directions with appropriately placed dots.

**18-7.** Discuss the operation of the tetrode relaxation oscillator shown in the figure.\*



**18-8.** A balanced multivibrator is operated at 1,000 cps. The constants are those of Prob. 18-1 except for the values of  $C_1$  and  $C_2$ . It is to be synchronized by injecting a positive pulse on the grid. What must be the amplitude of the synchronizing pulse if the frequency is 1,100 cps?

**18-9.** Repeat Prob. 18-8 if the pulse-recurrence frequency is 5,600 cps.

**18-10.** Sketch a curve of the grid potential of one tube of a balanced multivibrator that is being synchronized by a sine-wave voltage injected in the grid circuit. The synchronizing voltage is in the frequency ratio of 5:1 with the multivibrator frequency.

**18-11.** Discuss the possibility of synchronizing a multivibrator with a positive pulse, the recurrence frequency of which is a submultiple of the free-running frequency of the multivibrator.

\*Black, D. H., *Elec. Commun.*, 18, 50 (1939).

## CHAPTER 19

### HEAVILY BIASED RELAXATION CIRCUITS

THESE are two important heavily biased relaxation circuits. One type is known as *gate*, *one-shot*, or *univibrator* circuits, the other general class being known as *trigger* or *flip-flop* circuits. The gate circuit operates with one or both tubes so heavily biased that the circuit is inactive until a comparatively strong synchronizing or triggering voltage is applied. This strong signal causes the circuit to change from its stable limiting

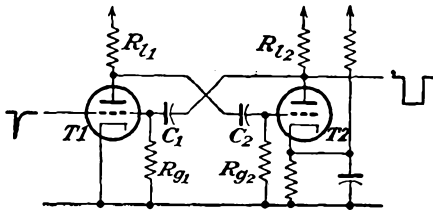


FIG. 19-1. A gate circuit with two a-c couplings.

condition to an unstable limiting condition, and after a definite time interval that is determined by the circuit constants the circuit returns to the stable state, where it will remain until it is again triggered. The trigger, or flip-flop, circuit is quite like the gate circuit except that for fixed values of applied voltage there are two

stable conditions of equilibrium. The currents and voltages in such circuits can be made to change abruptly from one set of stable values to a second set of stable values, or back again, although independent disturbances are required for each switching action.

**19-1. A-C Coupled Gate.** Refer to the diagram of Fig. 19-1, which is essentially a multivibrator of the conventional plate-coupled type, but with one tube biased to or beyond cutoff by the application of a fixed positive potential to the cathode of tube  $T2$ . In this circuit  $T1$  is normally conducting, and  $T2$  is normally cut off, thus requiring that the synchronizing or triggering pulse must be negative-going. Likewise, the duration of this negative-going pulse should be less than the time of the unstable portion of the cycle. If it is required to operate the circuit with a positive pulse, it should be applied to the grid of  $T2$ , although in this case the pulse amplitude must be larger than when it is applied to  $T1$ .

The analysis of such a circuit follows the same general method as that used in analyzing the free-running multivibrator. The result of such an analysis leads to the following expression for the time duration of the pulse:

$$t = C_1 R_{g1} \log_e \frac{E_{bb} - E_{b2}}{-E_{01}} \tag{19-1}$$

An alternative circuit to that of Fig. 19-1, but one which is normally triggered with a positive pulse, is given in Fig. 19-2. The time duration of the output square wave is found to be

$$t = C_2 R_{g2} \log_e \frac{E_{bb} - E_{b1}}{E_{02}} \tag{19-2}$$

**19-2. D-C Coupled Gate.** The circuit of a d-c coupled gate is given in Fig. 19-3. It will be noted that this circuit is only a slight rearrangement of the circuit of Fig. 19-2.

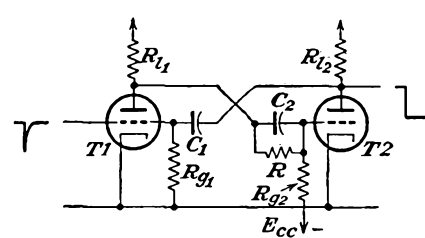


FIG. 19-3. A d-c coupled gate.

In this circuit tube *T2* is biased at or beyond cutoff by the application of a negative potential to the grid. This fixed bias is obtained from the voltage divider comprising  $R_{11}$ ,  $R$ , and  $R_{g2}$ , which is connected between  $E_{bb}$  and  $E_{cc}$ . Also, in order to ensure that *T1* is normally in the conducting stage,  $R_{g1}$ , which is shown connected to ground, may be connected to  $E_{bb}$ .

The capacitor  $C_2$ , which might appear to be unnecessary at first glance, actually serves a twofold purpose. It serves to decrease the switching time from *T1* to *T2*, and also it serves to increase the reliability of operation of the circuit. To examine this matter, it is necessary to consider the effects of the several interelectrode tube capacitances. Thus the tube capacitance  $C_{pk}$  in *T2* tends to prevent the grid-cathode voltage from changing rapidly. The capacitance  $C_{gp}$  which couples the grid with the plate of the tube tends to cause the grid voltage to vary in a direction to oppose the effective switching from *T1* to *T2*. The capacitance  $C_{kp}$  tends to prevent the plate potential from changing.

Another factor to be considered arises from the voltage-divider action of the coupling and biasing resistors  $R$  and  $R_{g2}$ . Without  $C_2$  in the circuit, the change in grid voltage is  $R_{g2}/(R + R_{g2})$  of the change in the plate potential of *T1*, and this ratio is normally about  $1/2$ . In fact, the action of the interelectrode capacitances is to reduce the change in grid voltage considerably below this value of  $1/2$ .

The presence of  $C_2$ , which is usually of the order of 50  $\mu\mu\text{f}$  and which is

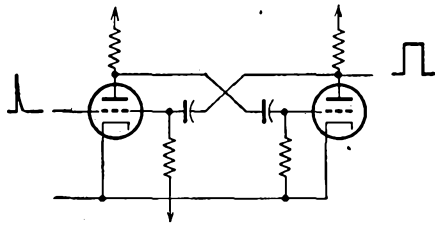
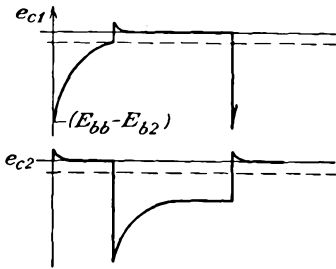


FIG. 19-2. A gate circuit that is roughly comparable with that of Fig. 19-1 except for the polarity of the triggering pulse.

therefore appreciably higher than the tube capacitances, forces the grid of *T2* to respond more quickly to the changes in the *T1* plate potential. This



is because any change in potential of the plate results in a nearly equal instantaneous change of the voltage of the grid. Furthermore, with *C*<sub>2</sub> shunting the coupling resistor *R*, the full value of the voltage appears on the grid, the resistor *R* being effectively short-circuited for these short-period changes.

FIG. 19-4. The grid potentials of the d-c coupled gate.

The shapes of the grid potentials at each of the tubes are illustrated in Fig. 19-4. The time duration of the gate

from the circuit is given by

$$t = C_1 R_{g1} \log_e \frac{E_{bb} - E_{b2}}{-E_{01}} \tag{19-3}$$

**19-3. The Cathode-coupled Gate.** The cathode-coupled gate is essentially the cathode-coupled multivibrator which is so arranged that one tube is normally biased beyond cutoff. A comparison of the circuit of Fig. 19-5 with that of Fig. 18-13 shows that these are almost the same, except that *R*<sub>g2</sub> in the circuit of Fig. 19-5 is connected from the grid to the cathode of *T2* instead of from grid to ground. In this circuit, *T1* will be nonconducting, and *T2* will normally be in the conducting state.

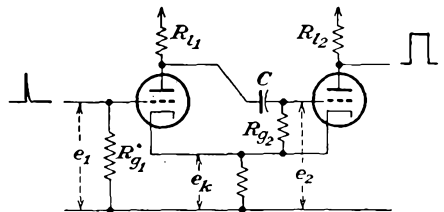


FIG. 19-5. A cathode-coupled gate.

Consequently a positive triggering pulse applied to the grid of *T1* is required in order to activate the circuit.

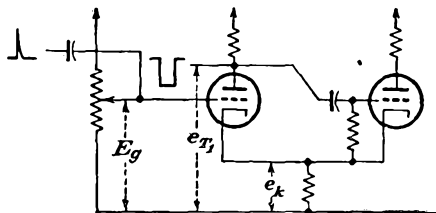


FIG. 19-6. A cathode-coupled gate with the grid of *T1* tied to a positive bias *E*<sub>g</sub>.

As ordinarily used, the grid of *T1* is returned to a positive potential, rather than to ground. With this change, it is found that the pulse width *t* is directly proportional to the d-c potential *E*<sub>g</sub> to a high degree of accuracy over a wide range of variation of this d-c potential. Such a

modified circuit is illustrated in Fig. 19-6. A detailed analysis of the operation of this circuit follows.

The d-c bias voltage *E*<sub>g</sub> is kept low enough so that tube *T2* is nominally

conducting. The current through this tube is given by the relation

$$I_{b2} = \frac{E_{bb}}{R_{l2} + r_{b2} + R_k} \tag{19-4}$$

and the cathode-ground potential  $E_{k2}$  is then simply

$$E_{k2} = I_{b2}R_k \tag{19-5}$$

Consequently, the voltage across the capacitor, assuming that the grid-cathode potential of  $T2$  during conduction is zero, is

$$E_2 = E_{bb} - E_{k2} \tag{19-6}$$

When the circuit is triggered,  $T1$  conducts and  $T2$  is turned off. The current through  $T1$  is given by the relation

$$I_{b1} = \frac{E_{bb}}{R_{l1} + r_{b1} + R_k} \tag{19-7}$$

and the cathode-ground potential  $E_{k1}$  is

$$E_{k1} = I_{b1}R_k \tag{19-8}$$

Clearly, when the circuit is triggered, the plate of tube  $T1$  falls from  $E_{bb}$  to  $E_{bb} - I_{b1}R_{l1}$ , and the point  $K$  changes from  $E_{k2}$  to  $E_{k1}$ . Because of this, the voltage across the capacitor  $C$  will tend to change from the value given in Eq. (19-6) to the value

$$E_1 = (E_{bb} - I_{b1}R_{l1}) - E_{k1} = E_{T1} - E_{k1} = E_{b1} \tag{19-9}$$

The capacitor potential changes by an amount

$$\Delta E = E_2 - E_1 = E_{bb} - E_{T1} - E_{k2} + E_{k1} \tag{19-10}$$

Of this, the fraction  $e_{c2}$  initially appears across the grid of  $T2$ , where

$$e_{c2} = (E_{bb} - E_{T1} - E_{k2} + E_{k1}) \frac{R_{g2}}{R' + R_{g2}} \tag{19-11}$$

and where  $R'$  is the parallel combination of  $r_{b1}$  and  $R_{l1} + R_k$ . The potential will then approach zero along an exponential curve, and  $T2$  will again begin to conduct when  $e_{c2} = E_{02}$  in the circuit of Fig. 19-7. This occurs at the time when

$$-E_{02} = e_{c2}e^{-\frac{t}{CR_{g2}}} \tag{19-12}$$

approximately. This expression assumes that  $R_{g2}$  is large compared with the parallel combination of  $r_{b1}$  and  $R_{l1} + R_k$ . Solving for the time  $t$  yields

$$t = CR_{g2} \log_e \left( \frac{E_{bb} - E_{T1} - E_{k2} + E_{k1}}{-E_{02}} \frac{R_{g2}}{R' + R_{g2}} \right)$$

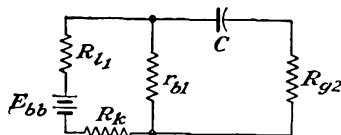


FIG. 19-7. The discharge circuit of the capacitor  $C$ .



to the input will cause the tube to cut off, the time of cutoff being controlled by  $C_1$ ,  $R_2$ , and  $E_{bb}$ . During the triggering pulse, the capacitor

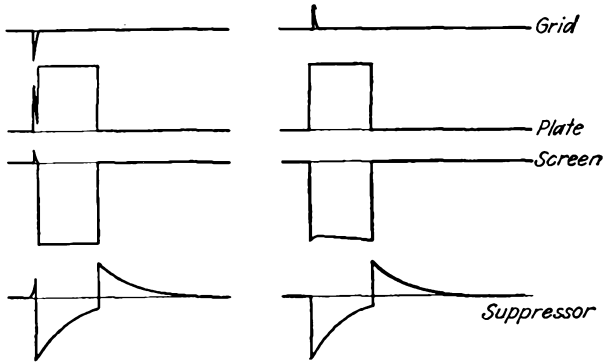


FIG. 19-11. The wave forms of a pentode gate when triggered with negative and with positive pulses.

$C_1$  is discharged through  $T_2$ , and recharging takes place through  $R_2$ , since at the end of the pulse  $T_2$  will be cut off. The grid and plate wave forms are somewhat as illustrated in Fig. 19-13.

**19-5. Trigger or Flip-flop Circuits.** The trigger circuit is not unlike the gate circuit except that, for fixed values of applied voltage, there are two stable conditions of

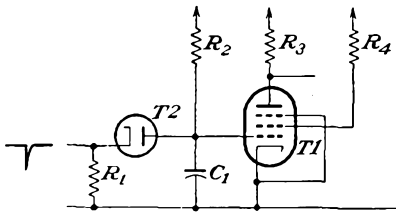


FIG. 19-12. A positive-bias pentode gate circuit.

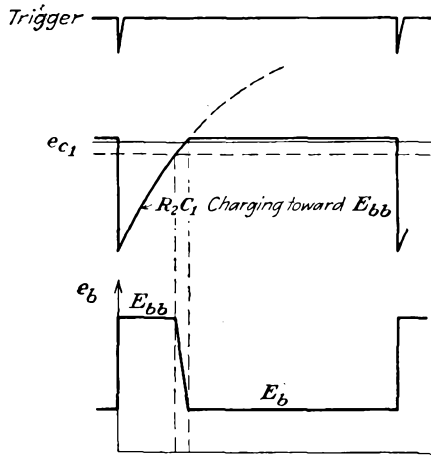


FIG. 19-13. The grid and plate wave forms in the pentode gate circuit of Fig. 19-12.

equilibrium. The currents and voltages in such a circuit can be made to change abruptly from one set of stable values to a second set of stable values, or back again, although independent disturbances are required for each switching action.

Refer to the circuit of Fig. 19-14, which was first discussed by Eccles and Jordan in 1919.<sup>2</sup> Observe that this circuit is like the multivibrator, although direct coupling exists between the plate of  $T_1$  and the grid of

$T2$  and between the plate of  $T2$  and the grid of  $T1$ . Likewise, the grids are normally maintained negative by the voltage divider and the negative C-supply voltage.

Suppose that  $T1$  is conducting and  $T2$  is cut off. The d-c potentials on the grids of the tubes are then, respectively, approximately zero on  $T1$ , owing to grid clipping, and  $-E_{cc} + \frac{R_{g2}}{R_2 + R_{g2}} (E_{cc} + E_{b1})$  on  $T2$ . These must be such that  $e_{c1}$  is slightly positive and  $e_{c2}$  is negative. If now a positive signal is applied to both grids simultaneously, there will be no appreciable action in  $T1$  but  $T2$  will begin to conduct. This will reduce

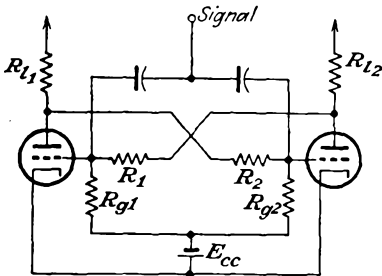


FIG. 19-14. The Eccles-Jordan trigger circuit.

the grid potential on  $T1$ , which reduces the tube current, setting off a regenerative action that continues until  $T1$  ceases to conduct and  $T2$  is fully conducting. The transfer is effected in precisely the same manner as that discussed for other multivibrator circuits. The circuit will remain in this new stable condition until another positive pulse is applied.

Negative trigger pulses may also be used to effect the switching. In this case the negative trigger acts on the conducting tube, causing a sudden decrease in the plate current and a corresponding rise in the plate voltage. This rise is passed to the tube that is cut off, resulting in a flow of current in its plate circuit, which initiates the switching action.

A practical form of the trigger circuit is illustrated in Fig. 19-15. Note the use of capacitors  $C_1$  and  $C_2$  across the coupling resistors  $R_1$  and  $R_2$ .

These are used to overcome the effects of the presence of the tube capacitances and also to increase the reliability of operation, precisely as for the action of the capacitor in the d-c coupled gate circuit of Fig. 19-3. Since two pulses are required to cause the circuit to complete its cycle, *viz.*, for each tube to pass from the non-conducting state to the conducting state

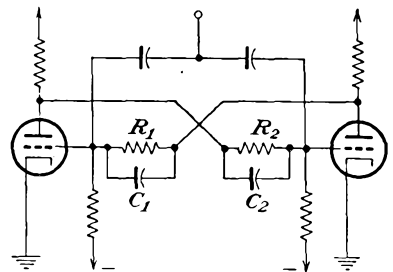


FIG. 19-15. A "scale-of-2" circuit.

and then back again, the output from a differentiating circuit connected to either plate will consist of a series of positive and negative pulses, the rate of each being one-half that of the triggering group. Thus, if either the positive or the negative output pulses are selected, there will be

one-half as many as the primary triggering source. This accounts for the name, *scale-of-2* circuit. Circuits of this type are used very extensively in scaling down the number of pulses produced in nuclear-physics reactions. Ordinarily such scaling circuits are connected in cascade to produce *scale-of-4*, *scale-of-8*, *scale-of-16*, etc., outputs. This permits a high-speed pulse source to be measured on a low-speed mechanical recorder.

A circuit of the Eccles-Jordan type may be used to form gates, one edge of which is controlled by one circuit, the other edge of which is controlled by a second circuit. In this case, the grids are fed from separate sources, one source switching the circuit on, the other switching it off.

A number of variants of this basic circuit have been published. Reich<sup>3</sup> replaced the triodes by pentodes. In this case the grids are free for the application of the initiating signals, the suppressor grids serving the same function as the triode grids. The circuit is shown in Fig. 19-16. Here the application of a positive voltage to the control grid of the nonconducting tube cannot cause conduction to begin, owing to the high negative voltage on the suppressor grid, which prevents plate current from flowing. The application of a negative voltage to the control grid of the conducting tube reduces its current and triggers the circuit. If a short-duration negative pulse is applied to the control grids of both tubes simultaneously, both tubes will be cut off. However, the coupling capacitors cause the

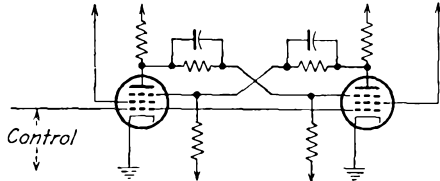


FIG. 19-16. Eccles-Jordan type of trigger circuit using pentodes.

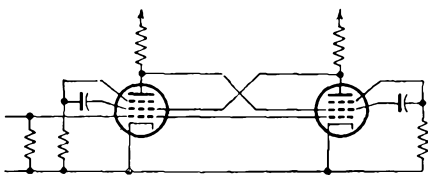


FIG. 19-17. An alternative form of trigger circuit using pentodes.

the suppressor of the tube which was conducting to be more negative than that of the other tube, and as a result the current transfers to the other tube at the end of the triggering pulse. The size of the capacitors should be such that the time taken for them to charge or to discharge from one equilibrium value of voltage to the other values is large compared with the duration of the triggering pulse but small compared with the time between successive pulses.

An alternative circuit that operates satisfactorily was suggested by Regener.<sup>4</sup> The circuit is shown in Fig. 19-17.

A cathode-coupled *scale-of-2* circuit was suggested by Scal.<sup>5</sup> The circuit is shown in Fig. 19-18. It will be observed that this circuit bears

the same relation to the cathode-coupled multivibrator that the circuit of Fig. 19-15 bears to the plate-coupled multivibrator.

**19-6. Single-tube Pentode Trigger Circuit.** It was first pointed out by Reich<sup>3</sup> that, by replacing with a resistor the coupling capacitor between the screen and the suppressor grids of the pentode relaxation oscillator of Fig. 18-22, the result is a trigger circuit. This circuit is illustrated in Fig. 19-19.

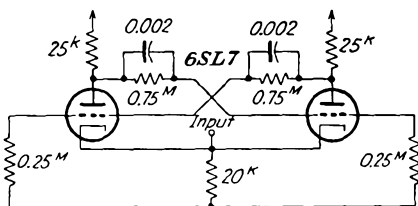


FIG. 19-18. A cathode-coupled scale-of-2 circuit.

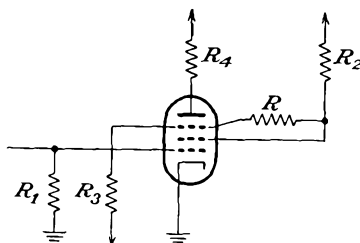


FIG. 19-19. A single pentode trigger circuit.

A physical explanation of the operation of the circuit is possible. Suppose that the tube is initially in such a condition that the current to the plate is zero when the current to the screen is a maximum. If the resistors  $R$  and  $R_3$  and the suppressor bias are properly chosen, the suppressor potential is sufficiently low to maintain no plate current and the tube remains in the zero-plate-current state.

Suppose now that a positive triggering pulse is applied to the control grid which is sufficiently positive to cause plate current to flow. As a result, the screen current will begin to fall, and the screen and also the suppressor potential will begin to rise. This causes the plate potential to tend to increase, resulting in a cumulative action which continues until the maximum possible plate current flows. At this point, the screen is almost at  $E_{bt}$ , the suppressor potential is slightly positive, owing to the suppressor-grid current when the potential is positive, and the plate continues to draw current. The tube thus remains in the conducting state.

To turn the tube off will require the application of a second positive triggering pulse. With an increase of tube current, the screen will collect more electrons, lowering the screen potential. This lowers the suppressor potential, which then begins to control the anode current. With a decreased anode current, the screen current increases and the cumulative action begins, which ends when the anode current is zero.

**19-7. Scaling Circuits.** In addition to the scaling circuits which may be constructed by forming a cascaded group of scale-of-2<sup>6</sup> circuits, the result being scale-of-4, -8, -16, -32, -64, etc., circuits are possible to yield scale-of-5,<sup>7</sup> scale-of-6,<sup>8</sup> scale-of-10,<sup>9</sup> and others. Some of these scalars use

the basic trigger circuit but provide for forced resetting at the count of, say, 10. Others make use of what is known as a *ring circuit*. Since decade scalers are used extensively, it might be well to consider the operation of such typical circuits.

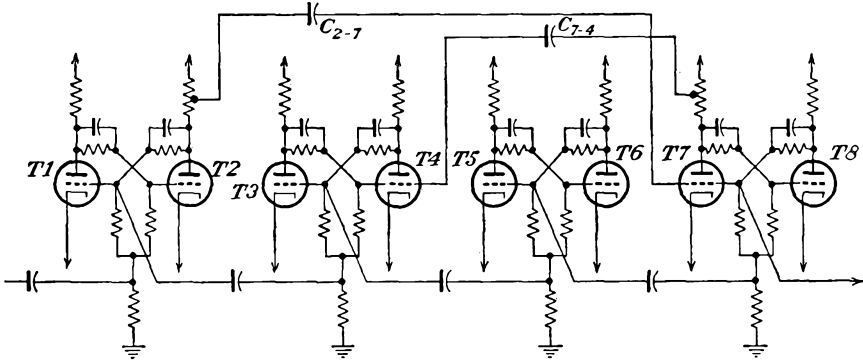


FIG. 19-20. A decade scaler consisting of conventional trigger circuits with forced recycling at the count of 10.

A representative type of decade scaler which consists of four conventional trigger circuits but which provides for forced recycling at the count of 10 is illustrated in Fig. 19-20.<sup>9</sup> This circuit will operate in a conventional manner for the first nine pulses of a pulse train, assuming that the initial reset causes all even-numbered tubes, T<sub>2</sub>, T<sub>4</sub>, T<sub>6</sub>, T<sub>8</sub>, to be conducting. Table 19-1 shows the sequence of tube operation with successive pulses. If now provision is made after the ninth pulse to force T<sub>4</sub> to

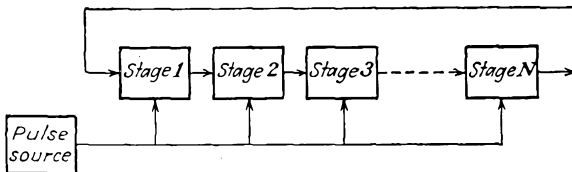


FIG. 19-21. Block diagram of a conventional ring counter.

remain conducting and also to cause T<sub>8</sub> to become conducting, then the scaler will have been recycled, with T<sub>2</sub>, T<sub>4</sub>, T<sub>6</sub>, T<sub>8</sub> conducting after the tenth pulse. It is the function of the feedback from a tap on R<sub>i</sub> associated with T<sub>2</sub> through capacitor C<sub>2-7</sub> to force T<sub>7</sub> to go out and T<sub>8</sub> to become conducting. Also, in a similar manner, the feedback obtained from R<sub>i</sub> associated with T<sub>7</sub> through capacitor C<sub>7-4</sub> forces T<sub>4</sub> to remain conducting.

A block diagram showing the general features of a ring counter which is capable of operating with as many as 50 stages is given in Fig. 19-21. The pulses are fed continuously into each stage, which is some form of

trigger circuit with two input channels. This tends to keep all the stages in one of their two stable conditions, which might be termed the normal state. If some pulse causes stage 1 to flip into its other state, the next pulse will flop stage 1 back to normal. This change of state causes a pulse which flips stage 2 to its odd state, to be returned to normal by the next input pulse. Thus the odd state advances systematically down the string of states, moving one stage with each regular input pulse.

TABLE 19-1  
SEQUENCE OF TUBE OPERATIONS IN A DECADE SCALER

Pulse	Conducting tubes							
	T1	T2	T3	T4	T5	T6	T7	T8
0		x		x		x		x
1	x			x		x		x
2		x	x			x		x
3	x		x			x		x
4		x		x	x			x
5	x			x	x			x
6		x	x		x			x
7	x		x		x			x
8		x		x		x	x	
9	x			x		x	x	
10		x	x			x	x	

Clearly, the pulse from each preceding stage, which serves to flip a given stage over from its normal state, will arrive at the stage almost simultaneously with the regular input pulse which tends to keep the stage in its normal state. If the regular input pulses are short enough and if the time constants of the stages are long enough, then the flipping-action pulse may be delayed until the regular input pulse has passed and satisfactory operation is possible. The diagram of a scale-of-5 ring circuit employing pentodes is given in Fig. 19-22.<sup>7</sup>

**19-8. Linear Delay Circuits.** Certain radar applications among others require circuits to generate pulses, the width of which is directly propor-

tional to a d-c potential, to a high degree of accuracy, and over a wide range of variation of this d-c potential. Such a circuit as this will make possible the generation of a marker or triggering pulse at an accurately known instant after it was initiated. Although a tremendous effort was expended in the investigations of circuits to fulfill these requirements, only a few circuits have been found which are even moderately satisfactory.

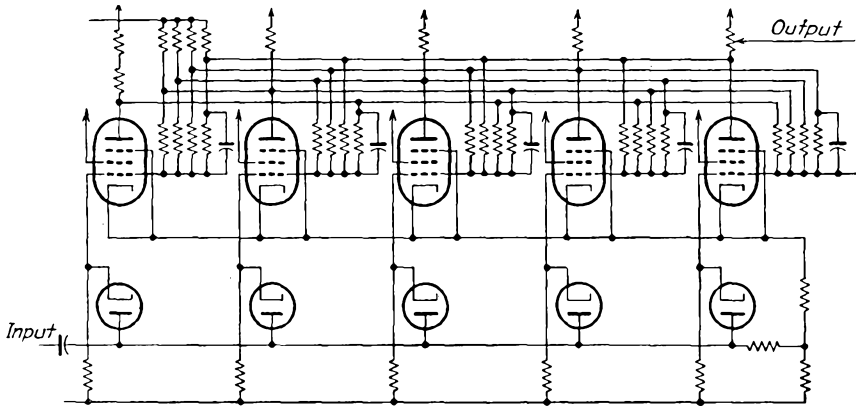


FIG. 19-22. The General Electric scale-of-5 ring circuit.

Among the circuits to be studied which do possess the desired characteristics are: (a) the linear delay multivibrator, (b) the sanatron, (c) the phantatron, and (d) the linear-sweep delay circuit.

The essential element of the *linear delay multivibrator* is the cathode-coupled delay multivibrator of Fig. 19-8. To see that the time duration of the gate is directly proportional to the bias voltage  $E_o$ , Eq. (19-14) is examined in some detail. This expression is rewritten for convenience.

$$t \doteq CR_{g2} \log_e \frac{2E_{bb} - E_{T1} - E_{k2}}{E_{bb} - E_{k1} - E_{o2}} \tag{19-15}$$

First it is noted from the tube characteristics of a typical triode, say the 6SN7, that the plate current can be related to the plate and grid potentials by a relation of the form

$$I_b = \frac{1}{k} (E_b + \mu E_c) \tag{19-16}$$

where  $E_b$  is the plate-cathode potential and  $E_c$  is the grid-cathode potential. That is, except in the region of very small currents, the linear set of curves is a fair representation of the normal space-charge curves of the tube. It follows from this expression that

$$E_b = kI_b - \mu E_c \tag{19-17}$$

Also, it follows from Fig. 19-8 that

$$E_b + I_b(R_{l1} + R_k) = E_{bb} \quad (19-18)$$

By combining Eqs. (19-17) and (19-18) there results

$$I_b = \frac{E_{bb} + \mu E_c}{R_{l1} + R_k + k} \quad (19-19)$$

Also from the figure

$$E_g = E_c + I_b R_k \quad (19-20)$$

It then follows from Eqs. (19-19) and (19-20) that

$$I_b = \frac{E_{bb} + \mu E_g}{R_{l1} + (\mu + 1)R_k + k} \quad (19-21)$$

These expressions are combined with Eq. (19-15) to yield

$$t = CR_{g2} \log_e \frac{E_{bb} + I_b R_{l1} - E_{k2}}{E_{bb} - I_b R_k - E_{02}}$$

$$t = CR_{g2} \log_e \left\{ \frac{[R_{l1} + (\mu + 1)R_k + k](E_{bb} - E_{k2}) + R_{l1}E_{bb} + \mu E_g R_{l1}}{[R_{l1} + (\mu + 1)R_k + k](E_{bb} - E_{02}) - R_k E_{bb} - \mu E_g R_k} \right\} \quad (19-22)$$

This may be written in the form

$$t = CR_{g2} \log_e \frac{a + bE_g}{c - dE_g} \quad (19-23)$$

where

$$\left. \begin{aligned} a &= [R_{l1} + (\mu + 1)R_k + k](E_{bb} - E_{k2}) + R_{l1}E_{bb} \\ b &= \mu R_{l1} \\ c &= [R_{l1} + (\mu + 1)R_k + k](E_{bb} - E_{02}) - R_k E_{bb} \\ d &= \mu R_k \end{aligned} \right\} \quad (19-24)$$

Now expand Eq. (19-23) to the form

$$t = CR_{g2} \left[ \log_e \frac{a}{c} + \log_e \left( 1 + \frac{b}{a} E_g \right) - \log_e \left( 1 - \frac{d}{c} E_g \right) \right] \quad (19-25)$$

But over the range for which

$$\frac{b}{a} E_g < 1 \quad \frac{d}{c} E_g < 1 \quad (19-26)$$

the logarithm may be expanded and only the first term in the expansion retained. The expression for  $t$  then becomes

$$t \doteq CR_{g2} \left( \log_e \frac{a}{c} + \frac{b}{a} E_g + \frac{d}{c} E_g \right)$$

or finally

$$t = CR_{g2} \left[ \log_e \frac{a}{c} + \left( \frac{b}{a} + \frac{d}{c} \right) E_g \right] \quad (19-27)$$

A circuit that was used extensively at the M.I.T. Radiation Laboratory for producing a marker pulse is illustrated in Fig. 19-23. This circuit yields an output pulse the delay of which is directly proportional to the d-c potential applied to the grid of  $T1$  within  $\pm 0.25$  per cent over the

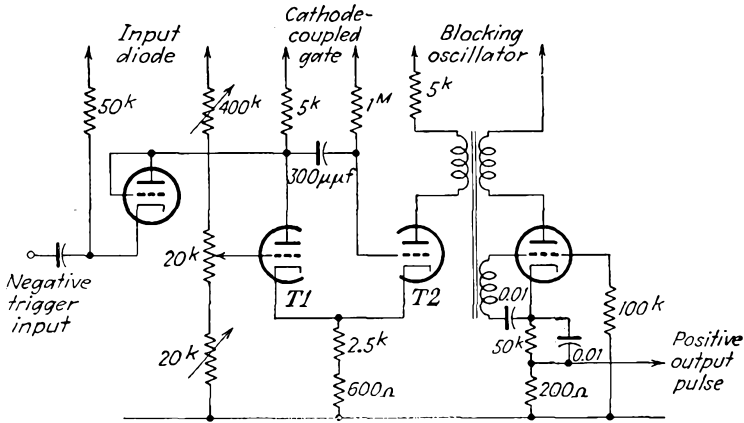


FIG. 19-23. A linear delay multivibrator which triggers a blocking oscillator to produce a sharp pulse.

range from about 8 to 150  $\mu$ sec. Other characteristics of this circuit will be given below.

**19-9. Miller Integrating Delay Circuits.**<sup>1</sup> The sanatron and phantatron delay circuits are two of a variety of linear delay circuits which have been designed around the so-called *Miller integrating circuit*. This cir-

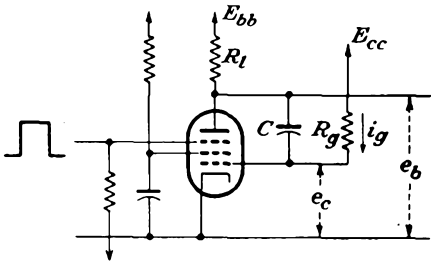


FIG. 19-24. The basic Miller integrating circuit.

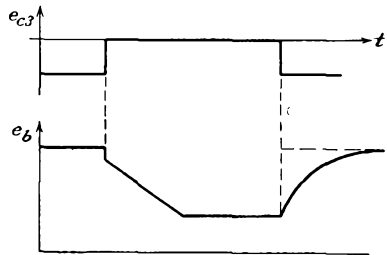


FIG. 19-25. The suppressor and plate potential of the Miller integrating circuit of Fig. 19-24.

cuit, which is illustrated in Fig. 19-24, makes use of the fact that the potential of the plate  $e_b$  will fall linearly with time when the plate is made conducting by applying a positive-going gate to the suppressor. The general character of the output is illustrated in Fig. 19-25.

To examine the action of the circuit analytically, it is noted that the

current  $i_g$  is given by

$$i_g = (E_{cc} - e_c)Y_g \quad (19-28)$$

and the output voltage is related to the grid potential by the expression,

$$e_b = Ke_c \quad (19-29)$$

where  $K$  is the gain of the tube. It is assumed that the grid current in the tube remains substantially constant, and any changes occur across the capacitor  $C$ . It then follows that

$$e_b = e_c - \frac{1}{Cp} i_g \quad (19-30)$$

By combining Eqs. (19-28), (19-29), and (19-30), there is obtained

$$e_b = \frac{e_b}{K} - \frac{Y_g}{C} \frac{1}{p} \left( E_{cc} - \frac{e_b}{K} \right)$$

which is

$$e_b \left( 1 - \frac{1}{K} \right) - \frac{Y_g}{CK} \frac{1}{p} e_b = - \frac{Y_g}{C} \frac{1}{p} E_{cc}$$

or

$$\frac{C(K-1)}{Y_g} p e_b - e_b = -KE_{cc} \quad (19-31)$$

By writing, for convenience,

$$-b = \frac{Y_g}{C(K-1)} \quad (19-32)$$

then

$$\left( \frac{p}{b} + 1 \right) e_b = KE_{cc} \quad (19-33)$$

This is the controlling differential equation that relates the plate potential with the input potential.

The solution of this differential equation, subject to the initial conditions

$$e_b = E_{bb} \quad \text{when } t = 0$$

is the expression

$$e_b = KE_{cc} + (E_{bb} - KE_{cc})e^{-bt} \quad (19-34)$$

Ordinarily the bias supply potential  $E_{cc}$  is the plate supply potential  $E_{bb}$ , in which case the expression, Eq. (19-34), assumes the form

$$e_b = KE_{bb} + (1 - K)E_{bb}e^{-bt} \quad (19-35)$$

But for the conditions of operation this expression may be expanded and only the lower-order terms retained. This yields

$$e_b = KE_{bb}(1 - K)E_{bb} \left[ 1 - bt + \frac{(bt)^2}{2!} - \dots \right]$$

or approximately

$$e_b \doteq E_{bb}[1 - (1 - K)bt] \tag{19-36}$$

But

$$(1 - K)b = - \frac{(1 - K)}{CR_o(K - 1)} = + \frac{1}{R_oC}$$

and Eq. (19-36) reduces to the form

$$e_b = E_{bb} \left( 1 - \frac{1}{R_oC} t \right) \tag{19-37}$$

Some measure of the linearity is possible by examining the ratio of the second order to the first order term in the above expansion. The percentage deviation from the linear is

$$\text{Per cent deviation} = \frac{\frac{1}{2}(bt)^2}{bt} 100 = 50bt \tag{19-38}$$

For a circuit for which the linear time is to extend for 100  $\mu\text{sec}$ , the deviation becomes

$$50bt = \frac{100 \times 10^{-6} \times 50}{3 \times 10^6 \times 100 \times 10^{-12} \times 200} \doteq 0.1\%$$

The initial potential drop that appears in the plate potential does not appear in these equations but represents the contribution to the initial plate current by the charging current required to charge the tube and wiring capacitances.

If the circuit is modified as illustrated in Fig. 19-26, a control is possible to the upper and lower potential limits between which the linear saw tooth traverses. In this circuit, if the potential of the plate is higher than  $E_1$ , the diode  $T2$  will conduct. In this way the plate of  $T1$  is tied to  $E_1$ . Likewise, when the plate potential is falling with the application of the gate to the suppressor grid of  $T1$ , diode  $T3$  will be non-conducting until the plate potential falls to  $E_2$ , when the diode  $T3$  will fix the lower potential of the plate fall to  $E_2$ .

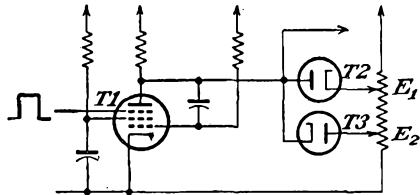


FIG. 19-26. A Miller integrator with controlled limits.

The linear saw-tooth wave from the Miller integrating circuit is then used in a comparator circuit. In this circuit a comparison is effected between the potential, and hence the corresponding setting of a poten-

tiometer, with that of any desired position on the linear saw tooth. The output, which appears as the movable edge of the gate, is directly proportional to the potential on the linear potentiometer, and hence to the position of the potentiometer shaft. Such a *voltage comparator* circuit is illustrated in Fig. 19-27. Note that the saw-tooth voltage from the Miller integrator is fed directly to the grid of one tube, the second tube being connected to the movable arm of the linear potentiometer.

The circuit resembles the cathode-coupled gate, and its operation depends on two cumulative actions taking place when certain conditions are realized. Suppose that the potential at the slider of the ranging

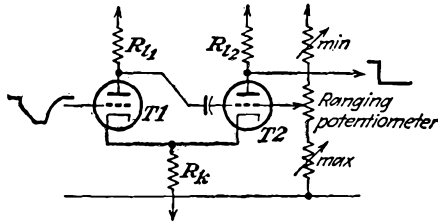


FIG. 19-27. A voltage comparator circuit.

potentiometer is about  $\frac{1}{2}E_{bb}$ . At the instant that the Miller integrator is activated by the application of the positive gate to the suppressor grid, the potential of the grid of  $T1$  will be  $E_{bb}$ , the potential of the grid of  $T2$  will be  $\frac{1}{2}E_{bb}$ , and  $T1$  will be conducting. This state of the comparator circuit continues while the grid of  $T1$  falls with the saw tooth, until it approaches the potential of the grid of  $T2$ . The circuit now becomes unstable, and a flip action takes place, with  $T1$  becoming nonconducting and  $T2$  beginning to conduct. Clearly, as the potential of the slider is reduced, the flip action takes place at an increasing time after the start of the initial event. The time delay between them will be proportional to the angular position of the shaft of the ranging potentiometer. The corresponding action which returns the circuit to its initial state takes place at the equivalent potential on the exponential rise when the Miller circuit capacitor is recharging.

The amplitudes of the voltage steps that appear at the anodes of  $T1$  and  $T2$  depend on the amount of current that is transferred from  $T1$  to  $T2$  at the instant of the flip action. This current depends on the setting of the potentiometer slider, but the variation may be reduced considerably by returning the cathode resistor to a negative supply. The two adjustable resistors at each end of the ranging potentiometer are to permit the voltage across the ranging potentiometer to be adjusted during calibration.

**19-10. The Sanatron.**<sup>1</sup> A circuit which incorporates a pentode gate circuit for producing the positive gate for starting the integrator, and the

Miller integrator circuit, the output of which would then be used to feed a voltage comparator circuit, is called a *sanatron*. The complete circuit

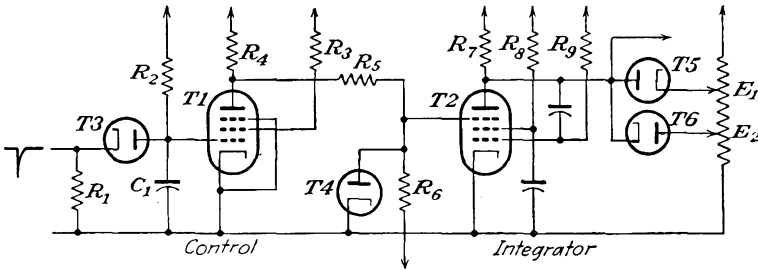


FIG. 19-28. The sanatron delay circuit.

is given in Fig. 19-28. The significant wave forms at several points in this circuit are given in Fig. 19-29.

**19-11. The Phantatron.** The phantatron combines the Miller integrator and the trigger properties of the sanatron in a single tube.

The schematic diagram is given in Fig. 19-30, and the significant wave forms at several points in the circuit are given in Fig. 19-31. Owing to the mutual effects that exist during the course of its operation, the phantatron in the

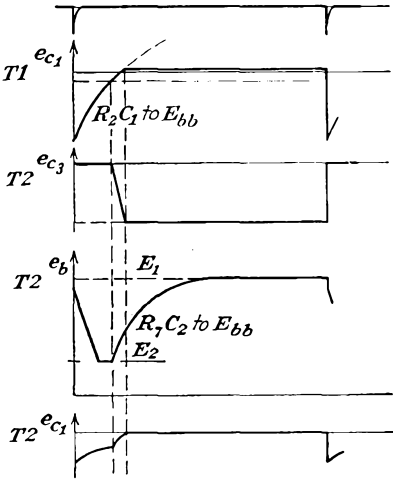


FIG. 19-29. The potentials at various points of the sanatron.

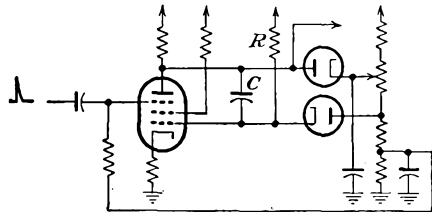


FIG. 19-30. The phantatron delay circuit.

form shown is somewhat inferior to the sanatron. It is for this reason that during the Second World War the British, who devised both circuits, preferred the sanatron.

The American version of the phantatron is designed around the 6SA7 heptode, which, owing to the mutual shielding between significant elements, proved to be entirely satisfactory. One version of the circuit is given in Fig. 19-32.

A second variation of the basic circuit is given in Fig. 19-33. This circuit employs a cathode follower to restore the 6SA7 to the quiescent

state quickly by helping to restore the plate voltage to the starting condition at the end of the operating period. In fact, the circuit of Fig. 19-33 yields an output pulse the delay of which is directly proportional to the

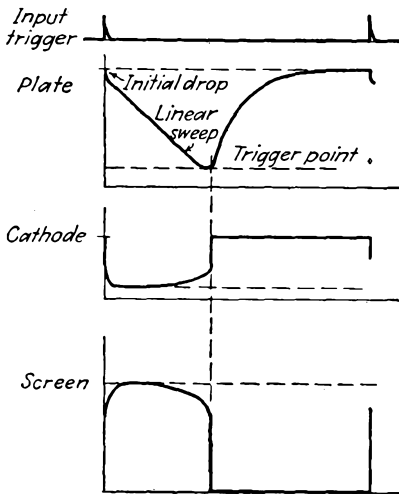


FIG. 19-31. The potentials at various points of the phantastron.

d-c potential applied to the control diode within  $\pm 0.1$  per cent over the range from about 8 to 150  $\mu$ sec.

**19-12. The Linear-sweep Delay.** The linear-sweep delay circuit incorporates a feed-back linearizing circuit to achieve a linear saw-tooth wave. This particular circuit will be discussed in some detail in Chap. 20. A comparison is then effected between the potential, and hence the setting of a potentiometer, with that of any desired position on the linear saw tooth. Although the voltage comparison is accomplished in a different manner from that in the sanatron, the net result is a comparable delay circuit.

The essential elements of the linear sweep may be discussed by reference to the circuit of Fig. 19-34. In this circuit  $T1$  is normally conducting, and the potential across the capacitor is  $E_{b1}$ . With  $T2$  absent and with the application of a negative gate to the grid of  $T1$ , the capacitor will

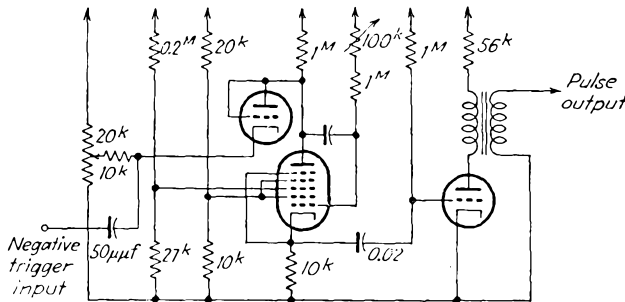


FIG. 19-32. One version of the phantastron built around the 6SA7.

begin to charge from  $E_{b1}$  toward  $E_{bb}$  along an exponential curve, with a time constant  $R_{11}C$ . With  $T2$  connected as shown and with the application of the negative gate to cut  $T1$  off, then as the potential across the capacitor increases, the feedback through the cathode follower  $T2$  which is applied to the circuit through which the capacitor charges will cause

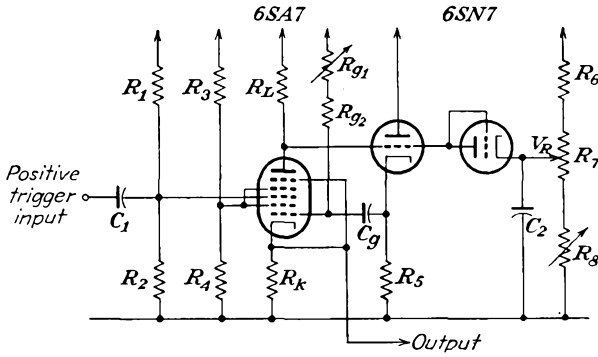


FIG. 19-33. A second version of the phantastron delay circuit.

the point *A* to increase. In effect, therefore, the capacitor, instead of charging to a constant potential  $E_{bb}$ , charges toward a continually increasing potential. As a result, instead of the charging curve being exponential, it is very nearly linear, the extent of the linearity being determined by how nearly unity the gain of the cathode follower is.

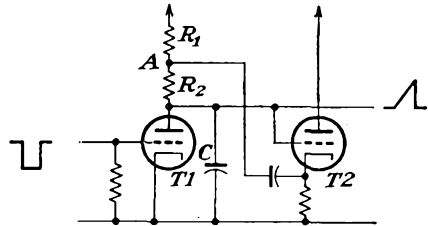


FIG. 19-34. A linear saw-tooth generator.

The circuit of the linear-sweep delay is shown in Fig. 19-35. In this circuit, *T1* and *T2* are connected as a simple cathode-coupled gate, the negative square wave thus generated being applied to the grid of *T3*. The time duration of this square wave is the maximum length of the

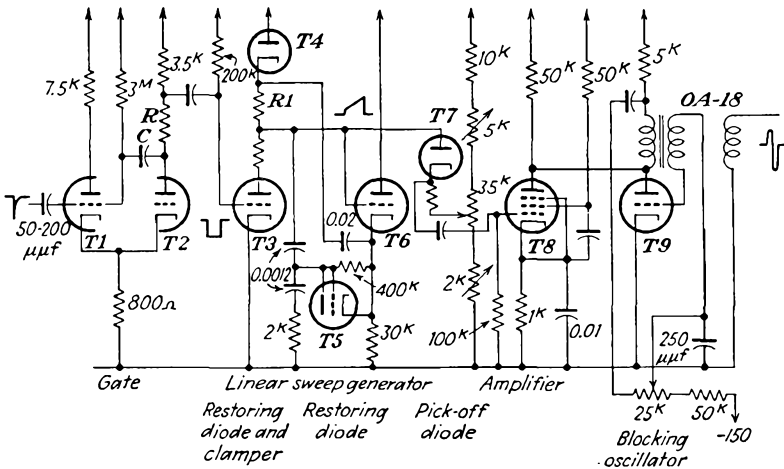


FIG. 19-35. A 150- $\mu$ sec linear-sweep delay circuit.

delay desired. This negative square wave is applied to the linear sawtooth circuit, comprising  $T3$  and  $T6$ .  $T4$  helps restore the sweep quickly to the quiescent condition. The  $2^k$  resistor to ground causes a rapid rise at the beginning of the saw tooth, making it a trapezoidal wave. This is necessary in order to make the sweep start rapidly enough to overcome circuit capacitance. Often this resistor may be omitted. The  $400^k$  resistor and  $T5$  are placed in the circuit as an additional sweep correction to produce linearity.  $T7$  is called the *pick-off* diode because it begins to conduct at a point on the sweep determined by the selection of its cathode voltage with the adjustment of the  $35^k$  potentiometer. This is essentially the voltage comparator in the circuit. When  $T7$  begins to conduct, its output is amplified by  $T8$ , whose plate output triggers  $T9$ , the blocking oscillator tube.

Table 19-2, taken from *M.I.T. Radiation Laboratory Report T-18*, shows a comparison of the features of the cathode-coupled delay multivibrator (Fig. 19-23), the phantastron circuit (Fig. 19-33), and the linear-sweep delay circuit (Fig. 19-35). These data are tentative. The percentage change in range indicated is the maximum change of the maximum observed at any point in the cycle.

TABLE 19-2  
COMPARISON OF THREE DELAY CIRCUITS FOR 150  $\mu$ SEC MAXIMUM DURATION

Subject	Delay multivibrator	Phantastron	Linear sweep
Duration vs. voltage. . . . .	0.25 % from about 8 to 150 $\mu$ sec	0.1 % from 8 to 150 $\mu$ sec	0.1 % from 5 to 150 $\mu$ sec
10 % change in $E_{bb}$ about 250 volts	$\pm 0.5$ % change in time duration	$\mp 0.15$ % change in duration	$\pm 0.15$ % change in duration
Temperature coefficient (% change in duration $7^\circ\text{C}$ ) . . . . .	$-0.005$ %/ $^\circ\text{C}$	$-0.002$ %/ $^\circ\text{C}$	$\pm 0.003$ %/ $^\circ\text{C}$
Number of tube envelopes . . . . .	2½	3	5
Max over-all sensitivity to all tubes . . . . .	$\pm 10$ % change	$\pm 5$ %	$\pm 1$ %

**19-13. Pulse Generators.** It is ordinarily not possible to distinguish between a narrow gate and a pulse, particularly since the two may be generated in the same manner. A sharp distinction is hardly necessary, but one might perhaps distinguish between them on the basis of the ultimate purpose of the signal. Another distinguishing feature might be based on the time duration of the signal. There are, however, certain

methods available for generating very narrow pulses with reasonably sharp rise and fall which are not suitable for generating wider gates. It is not always necessary that the pulse be rectangular, although certain applications require such a pulse. Several methods for generating such narrow rectangular pulses will be considered. These methods fall into two general classes. In one, tube circuits are employed, and these may be gas-filled or vacuum tubes, with provision for damping to keep the pulse narrow and rectangular. In another type, artificial transmission or pulse-forming lines are used to control the duration of the pulse and also to effect a rectangular shape.

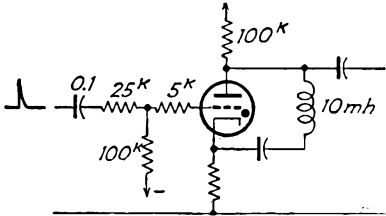


FIG. 19-36. A thyatron pulse generator with an oscillatory extinguishing circuit.

A simple circuit for generating pulses incorporates an oscillatory circuit between the plate and cathode of a thyatron. Such a circuit is given in Fig. 19-36. It is the function of the oscillatory circuit when shock-excited to cause the plate potential to fall below that required to maintain the discharge of the thyatron, once it has been fired. The pulses so gen-

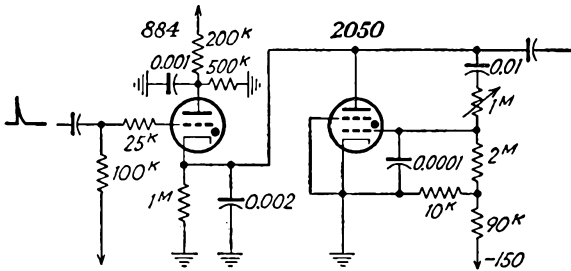


FIG. 19-37. A thyatron pulse generator with thyatron clipper.

erated are not rectangular in shape but are acceptable for some types of service.

The circuit of Fig. 19-37 shows a circuit for generating narrow rectangular pulses ranging from less than 1  $\mu$ sec duration to perhaps 10 or 20  $\mu$ sec duration. In this circuit an 884 thyatron with its ionization time of approximately  $10^{-8}$  sec is used to generate the pulse, the trailing edge of which is controlled by a second thyatron. The output pulse from such a circuit has relatively sharp sides.

Suppose that the 884 has been triggered by the application of a positive triggering pulse to the grid. This causes the 884 to conduct, and the potential that appears across the 0.001- $\mu$ f capacitor from plate to ground, less the drop in the 884 appears across the cathode resistor, capacitor,

and the 2050 clipper thyatron. Note that the  $200^k$  plate resistor and the  $1^M$  cathode resistor are so large that a continuous discharge through the 884 cannot be sustained, and that the energy of the pulse must be supplied from the  $0.001\text{-}\mu\text{f}$  capacitor. Clearly, for different pulse lengths, different sizes of plate-ground capacitors will be required.

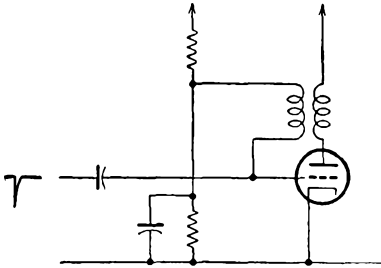


FIG. 19-38. A triggered blocking oscillator for pulse generation.

Once the 884 has been fired, the potential on the plate of the 2050 increases to some positive value, and if the energy in the pulse is small compared with that on the plate capacitor, the 2050 plate potential remains relatively constant. Owing to the  $RC$

circuits between the plate and the control grid and the grid and the cathode of the 2050, there will be a time delay before the grid-cathode potential increases from the normally nonconducting value of  $-15$  volts, determined by the voltage divider between the  $-150$ -volt source and ground, to the approximately zero potential required for the tube to fire. The time duration is controlled by the adjustable  $1^M$  resistor in the circuit. Once the 2050 fires, the cathode of the 884 is effectively short-circuited to ground, thus terminating the output pulse. Of course, the 2050 continues to conduct until enough of the charge has leaked off the capacitor in the 884 circuit for the potential across the 2050 to fall below that required for maintaining the discharge.

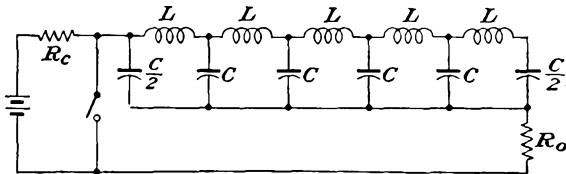


FIG. 19-39. The basic circuit incorporating a pulse-forming line.

The use of a blocking oscillator which is biased to be off normally and which is triggered as desired will yield pulses which are sometimes suitable for some services. Such a circuit which provides for an adjustable pulse width is given in Fig. 19-38.

**19-14. Line-controlled Pulse Generators.** The use of artificial transmission lines in the formation of short rectangular pulses has become widespread in recent years. The basic circuit is shown in Fig. 19-39. The line is considered to consist of a sufficient number of sections so that it closely approximates a continuous transmission line. One end of the

line is open-circuited; a resistance  $R_0$  equal to the characteristic impedance of the line  $Z_0 = \sqrt{L/C}$  is connected across the other end. The line is initially charged by means of the battery, and hence all capacitors are charged to full battery potential. When the switch is closed, one half of the battery voltage appears across the terminating resistance  $R_0$  and the remaining half of the voltage traverses the line as a voltage wave. The wave front is delayed  $t = \sqrt{LC}$  sec for each section through which it passes. As it progresses down the line, the voltage wave removes one-half of the voltage present across the line. When it reaches the end of the line, the wave encounters the open circuit and is reflected without change of polarity. The remaining voltage on the line is then progressively removed as the wave returns toward the starting point. When the wave front reaches the starting point, it cancels the voltage across the resistance  $R_0$  and the entire system comes to rest. In traversing the line forward and backward, the occupied time is

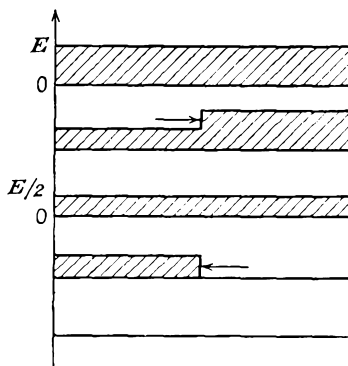


FIG. 19-40. The traveling voltage wave on an open-circuited transmission line that is originally charged and is being discharged.

$$t = 2N \sqrt{LC} \quad \text{sec} \tag{19-39}$$

where  $N$  is the number of sections.

The sequence of events is illustrated in the block diagram of Fig. 19-40, which shows the voltage distribution on the line at various times during the existence of the running wave. As a result of the sequence of actions, a voltage pulse appears across the resistor  $R_0$ . When the switch is closed, the voltage instantaneously assumes one-half of the applied voltage; this voltage persists until the voltage wave has traversed the line and returned to  $R_0$ , and it thereupon drops to zero suddenly.

The circuit provides a very simple method of forming a rectangular pulse of controllable length, provided that the pulse length is short enough to be obtained in an artificial line of practical dimensions. The practical difficulty that might be encountered in such a pulse-forming circuit is the number of sections required to approximate a continuous transmission line. Each section introduces a small deviation in the flat top of the pulse. If the top is to be essentially flat, a large number of sections should be used.

The Guillemin line is a network which simulates the section of a transmission line which is open-circuited at the far end. A circuit of this line

is given in Fig. 19-41. This network is a closer approximation to the continuous transmission line than a simple line of an equal number of sections. Several typical line-controlled pulse circuits are given below.

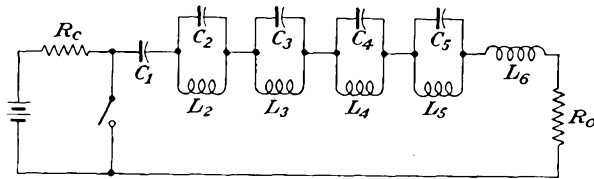


FIG. 19-41. The general characteristics of a pulse-forming circuit employing a Guillemin line.

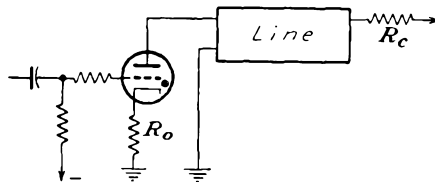


FIG. 19-42. A line-controlled thyatron pulse generator.

Figure 19-42 is essentially the circuit of Fig. 19-36, except that the pulse duration is controlled by the "length" of the line in the plate circuit, the thyatron being extinguished when the plate potential falls to zero.

In the circuit of Fig. 19-43 a line is added to the grid circuit of a blocking oscillator to control the duration of the pulse. In this circuit the

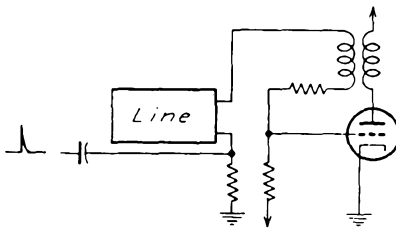


FIG. 19-43. A line-controlled blocking oscillator.

triggering pulse is applied to the artificial line and is followed immediately thereafter by the beginning of the rectangular wave. The wave of voltage traverses to the open end of the line and then is reflected back without change of sign. When the wave front reaches the input end, the positive grid voltage is removed from the line, reducing the input potential

to zero. This causes the grid-cathode potential to be driven below cutoff, thus yielding a sharp pulse in the output of the circuit.

A delay line may also be used as the cathode impedance in an amplifier tube, as shown in Fig. 19-44. The operation of this circuit is essentially the following: The sharp rise at the beginning of the applied gate to the grid is accompanied by a corresponding sharp increase in the plate current. This causes a cathode-ground voltage wave, which then proceeds

down the transmission line, which is essentially open-circuited, as the terminating resistance  $R_k$  is made much higher than the characteristic impedance of the line.  $R_k$  serves only to complete the d-c path from cathode to ground. The voltage wave is reflected from the open end and retraces its path back along the line. This reflected voltage at the input end adds to the applied voltage to cause the cathode-ground potential to reach a value of nearly twice the initial voltage. This increase in the cathode-ground voltage is enough to cause the tube to cut off, thus terminating the pulse.

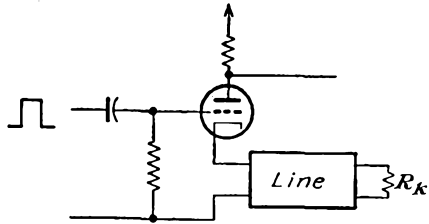


FIG. 19-44. A pulse generator with the line in the cathode circuit.

**REFERENCES**

1. Williams, F. C., and N. F. Moody, *J. IEE*, **93**, 1188 (1946).
2. Eccles, W. H., and F. W. Jordan, *Radio Rev.*, **1**, 143 (1919).
3. Reich, H. J., *Rev. Sci. Instruments*, **9**, 222 (1938).
4. Regener, V. H., *Rev. Sci. Instruments*, **17**, 180 (1946).
5. Scal, R. K. F., *Electronics*, **20**, 150 (September, 1947).
6. Sharpless, T. K., *Electronics*, **21**, 122 (March, 1948).
7. General Electric Co., Decade Scaling Unit, Type YYZ-1.
8. Langberg, E. L., *Rev. Sci. Instruments*, **18**, 796 (1947).
9. Potter, J. T., *Electronics*, **17**, 110 (June, 1944).
10. Close, R. N., and M. T. Lebenbaum, *Electronics*, **21**, 100 (April, 1948).

As a general reference, see Chance, B., *et al.*, *Waveforms*, Vol. 21, M.I.T. Radiation Laboratory Series, McGraw-Hill Book Company, Inc., New York, 1949.

**PROBLEMS**

**19-1.** A 6SN7 tube is to be used to produce a positive rectangular gate of 108  $\mu$ sec duration. The pulse repetition frequency is 400 per second. The gate is driven by a negative trigger pulse, and the positive gate is to begin at the time that the trigger is applied.

- a. Draw the circuit for such a gate. Indicate on the circuit the terminals to which the negative trigger is applied, the terminals from which the gate is taken, and the circuit elements which determine the length of the gate.
- b. One grid should be returned to B+, and the other to ground. Give reasons.
- c. Calculate the coupling capacitor connected to the grid of tube T1. Use the following data:

	Section 1 Grid to B+	Section 2 Grid to ground
$E_{bb}$ .....	300	300
$R_g$ .....	$0.5^M$	$1^M$
$R_l$ .....	$20^k$	$30^k$
$\mu$ .....	20	20
Static $r_c$ .....	500 ohms	500 ohms
Static $r_b$ when $e_c = 0$ .....	$10^k$	$10^k$

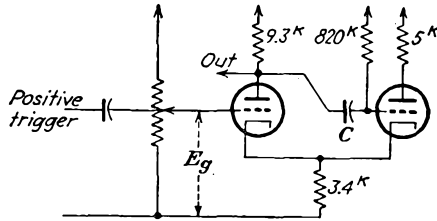
**19-2.** *a.* Calculate the recharging time constant of the capacitor  $C$  in the cathode-coupled delay gate.

*b.* To what values does  $e_{c2}$  jump when the circuit recovers, *i.e.*, what is the value of  $e_{c2}$  at point *A* of Fig. 19-9?

*c.* What is the value of  $e_{b1}$  at point *B*?

**19-3.** Carry out the analysis that leads to Eq. (19-14) for the duration of the gate of Fig. 19-8.

**19-4.** The circuit shown in the diagram is to be designed to give a pulse output



of 100  $\mu$ sec width. Assume the following:

6SN7 tube;  $E_{bb} = 250$  volts

$r_c = 1^k$  when  $e_c = 0$  or positive

$r_b = 10^k$  when  $e_c = 0$  or positive

$E_0 = -10$  volts

Trigger prf = 400 cps

*a.* For operation under these conditions, what limits are imposed on the values that  $E_g$  might assume?

*b.* Calculate the value of the coupling capacitor  $C$ .

**19-5.** The circuit of Fig. 19-23 uses a 6SN7 tube and is supplied from a 300-volt regulated supply. Suppose that the bias voltage  $E_g$  can be varied over the limits from 20 to 65 volts.

*a.* Are the approximations in Eqs. (19-26) satisfied over this voltage range?

*b.* Calculate the duration of the gate at each limiting value. The plate current is related to the voltages by the approximate expression

$$I_b = 9.1 \times 10^{-5}(E_b + 20E_c) \quad \text{amp} \quad \pm 10\%$$

**19-6.** The variable resistor of the pulse circuit of Fig. 19-37 is set at 0.5 $\mu$ . Estimate the duration of the pulse generated by the circuit.  $E_{bb} = 300$  volts.

**19-7.** The fundamental problem in the design of a tuned pulse-forming network is to determine a network composed of but few circuit elements which will respond with a closely rectangular wave of current when excited with a unit voltage. Show that the rectangular wave may be represented by a Fourier series, the first five terms of which have the form:

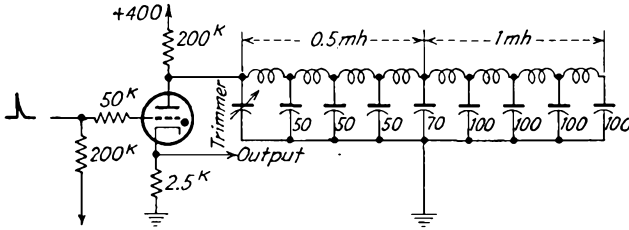
$$f(t) = a_1 \sin \omega t + a_3 \sin 3\omega t + a_5 \sin 5\omega t + a_7 \sin 7\omega t + a_9 \sin 9\omega t$$

Calculate the values of the coefficients  $a_n$ . Plot the resulting curve represented by these results, and compare with the results for which

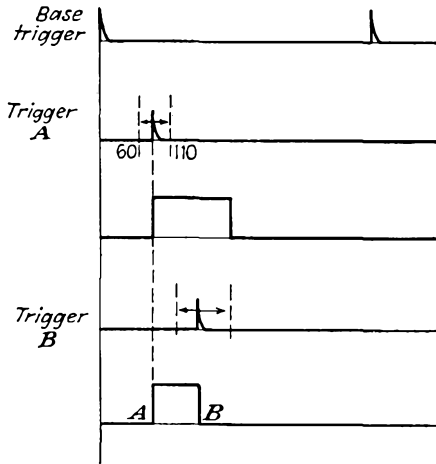
$$a_1 = 1.2575 \quad a_3 = 0.3725 \quad a_5 = 0.1735$$

$$a_7 = 0.08315 \quad a_9 = 0.02777$$

19-8. The diagram for this problem shows a circuit of the pulse-forming stage of a pulse modulator. Calculate the width and amplitude of the generated pulse.



19-9. It is required to design a circuit which will provide the several outputs as shown on the accompanying time diagram.



- Draw a block diagram of a circuit that will satisfy the requirements.
- Show the complete circuit diagram. Do not evaluate the circuit elements to be used.

All times are given in microseconds.

## CHAPTER 20

### SWEEP GENERATORS

THE function of the sweep circuit as applied to a cathode-ray tube is to cause the luminous spot that results from the impact of the electron beam on the fluorescent screen phosphor to move across the screen with a known velocity, whether it be constant or whether it be varying in some definite way with respect to time. The proper selection of the form of the sweep is most important, since otherwise a relatively simple investigation may prove to be almost impossible. If, for example, it is desired to examine the shape of a periodically recurring wave, a sweep circuit that is proportional to the time would normally be desired. Such a linear sweep might not be appropriate in some application where a sweep that is proportional to some other quantity might be indicated.

The problems that arise in producing sweep circuits for electrostatic cathode-ray tubes are quite different from those in producing the sweep circuits for electromagnetic-type tubes. This chapter will consider the problems that arise in the generation of sweeps for electrostatic-type tubes; the next chapter will consider the problems arising in the generation of magnetic and other sweeps.

**20-1. Simple Saw-tooth Sweep.** One of the most common sweep requirements is for a repetitive trace along a straight line. Owing to the dimensional limitations of the cathode-ray tube screen, the wave form

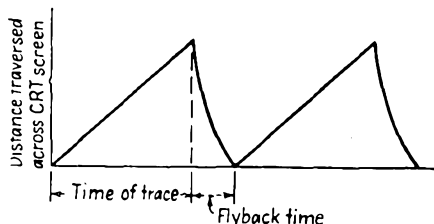


FIG. 20-1. A simple saw-tooth sweep.

required to produce it is of the saw-tooth form, as shown in Fig. 20-1. The wave form illustrated is the ideal, since it varies linearly with time, but following standard practice, no attempt is made to linearize the fly-back portion of the wave. With the wave form shown, the electron spot moves across the tube face with a uniform velocity and with a speed depending upon the slope of the curve. The spot is caused to return to the starting point very rapidly, and ordinarily it is not seen or, at worst, its brilliancy is much reduced over that of the writing portion of the cycle.

The ideal saw tooth illustrated is not easily obtained by direct means.

and various methods have been employed to linearize or to compensate nonlinear waves. The details of such circuits will be examined below.

**20-2. Capacitive Sweep Circuits.** Many of the more common circuits employ the changing potential across a capacitor upon the application of a constant source of potential through a resistor. These circuits usually employ separate charging and discharging circuits in order that the retrace, or fly-back, time may be made much shorter than the writing time. Ordinarily the charging circuit is permitted to function continuously, the rapid discharge being accomplished by a rapidly acting switching circuit. The equivalent form of such a circuit is shown in Fig. 20-2.

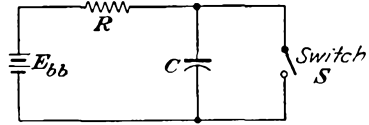


FIG. 20-2. The elements of a switching circuit for producing a saw-tooth wave.

The potential across the capacitor in the circuit shown follows the form

$$e_c = E_{bb}(1 - e^{-\frac{t}{RC}}) \tag{20-1}$$

where  $E_{bb}$  is the voltage applied to the  $RC$  combination,  $t$  is the time in seconds,  $C$  is the capacitance of the capacitor in farads, and  $R$  is the resistance in ohms. For a short time after the application of the voltage

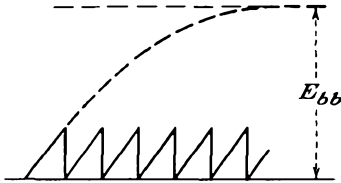


FIG. 20-3. Achieving a linear saw tooth from an  $RC$  circuit.

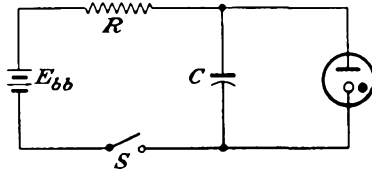


FIG. 20-4. A saw-tooth generator using a glow discharge tube.

$E_{bb}$ , the voltage increases across the capacitor will be reasonably linear with time. For example, for a time equal to one-fifth the time constant of the circuit, the voltage increase will be linear within about 5 per cent. If the switching is properly timed, a reasonably satisfactory wave, of the form illustrated in Fig. 20-3, is possible.

One of the earliest and probably one of the simplest capacitive saw-tooth generators utilizes a glow discharge tube as the switch in the circuit of Fig. 20-2. The circuit of this saw-tooth generator is given in Fig. 20-4. Suppose that the capacitor is initially uncharged when the switch  $S$  is closed. The voltage across the capacitor will increase according to Eq. (20-1). When  $e_c$  equals the breakdown potential of the glow tube  $E_d$ , charge will flow through the tube. This discharge is accompanied by a rapidly falling capacitor potential, because charge is being drained

from the capacitor. When the potential across the capacitor falls below the extinction potential  $E_e$  of the glow tube, the discharge ceases. The discharge current is high since it is limited only by the resistance and inductance of the leads that connect the capacitor to the glow tube, and the discharge time is very small.

Once the tube becomes extinguished, the capacitor immediately begins to recharge. When the potential across the capacitor again reaches the discharge  $E_d$ , the tube will again break down and conduction will continue until the capacitor voltage again falls to  $E_e$ , when the process repeats itself. This process is periodic and results in oscillations that have a period  $T$  equal to the time required for the capacitor to charge from the potential  $E_e$  to  $E_d$  and then discharge to  $E_e$ . The expression governing the process is found from Eq. (20-1) to be

$$T = RC \log_e \frac{E_{bb} - E_e}{E_{bb} - E_d} \quad (20-2)$$

The amplitude of the oscillation equals the voltage difference  $E_d - E_e$ .

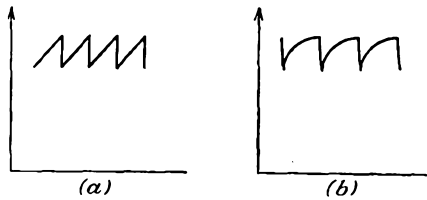


FIG. 20-5. The wave shape of the output in a simple glow-tube sweep generator. Curve (a) is for a supply voltage of 600 volts; curve (b) is for a supply voltage of 135 volts. The amplitude of oscillation is the same in both cases.

Such simple glow-tube circuits may be used for frequencies of 1 cycle every few minutes to frequencies well up in the a-f range.

The wave shape of the resulting saw tooth is dependent upon the magnitude of the supply source  $E_{bb}$ . The use of a VR-90, for which  $E_d$  equals approximately 120 volts and for which  $E_e$  equals 85 volts approximately, and a 600-volt supply yields a wave that is approximately triangular, as

shown in Fig. 20-5a. The same circuit when used on a 135-volt supply yields the curved wave form of Fig. 20-5b.

**20-3. Thyatron Sweep Generators.** Two obvious shortcomings of the simple glow-tube sweep generator are that high voltages must be used in order to obtain relatively linear saw-tooth waves and that the amplitude of the output wave is relatively small. The use of a thyatron as a switch allows reasonable flexibility in control of the period of oscillation and also in the amplitude of the saw-tooth wave so generated. The cir-

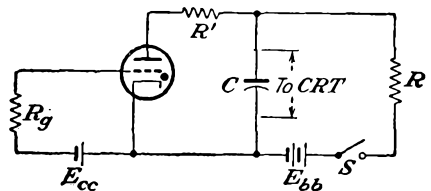


FIG. 20-6. A saw-tooth generator employing a thyatron.

cuit of a saw-tooth voltage generator employing an 884 thyratron in such a relaxation circuit is given in Fig. 20-6. In this circuit  $R_p$  is a protective resistor in the grid circuit, and  $R'$  is a protective resistor in the plate circuit.  $R'$  is a current-limiting resistor that is made as small as possible consistent with the tube-current rating in order that the capacitor may discharge very quickly through the tube.

To understand the operation of the circuit, reference must be made to the critical grid curve of the thyratron, which is given in Fig. 20-7. Suppose that the battery potentials are set at  $E_{cc} = -20$  and  $E_{bb} = 250$  volts. Also suppose that the capacitor is initially uncharged. After the switch  $S$  is closed, the voltage across the capacitor will increase exponentially according to Eq. (20-1). This charging process will continue until the voltage across the capacitor reaches approximately 160 volts. At this time the tube will break down. Charge will leak off the capacitor very rapidly, and the tube will stop conducting when the cathode-anode potential falls below about 16 volts, the arc-maintaining voltage of the tube. The capacitor will again begin to charge through

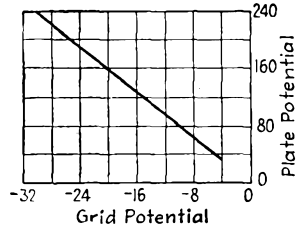


FIG. 20-7. Typical critical grid characteristic of an 884 argon-filled thyratron.

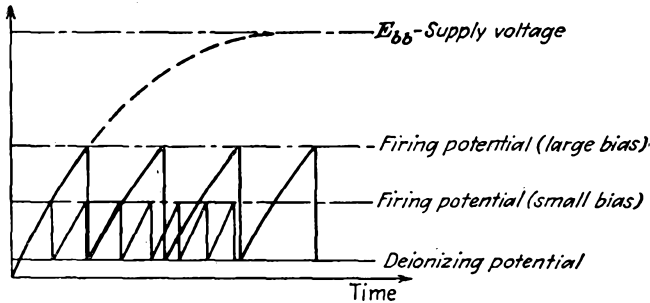


FIG. 20-8. The change of amplitude and frequency of a thyratron saw-tooth generator by change of grid bias.

the local  $RC$  circuit, and the entire process will repeat itself. The period of oscillation can be adjusted by varying  $R$ ,  $C$ , or the voltages  $E_{cc}$  or  $E_{bb}$ . Certain of these results are made evident from an inspection of Fig. 20-8.

The oscillations of a gas-tube generator are not very stable in frequency. The thyratron oscillator can be synchronized with a given frequency by injecting a small voltage of the desired frequency on the grid, in precisely the same way as synchronization is achieved for a multi-vibrator or blocking oscillator (see Chap. 18). The entire synchroni-

zation process is illustrated in Fig. 20-9. The operation is essentially the following: The natural period of the oscillator is adjusted to be slightly less than that of the synchronizing voltage. The natural action is shown dotted in the figure. Without the synchronizing voltage, the tube would fire at point A. The presence of the synchronizing voltage on the grid

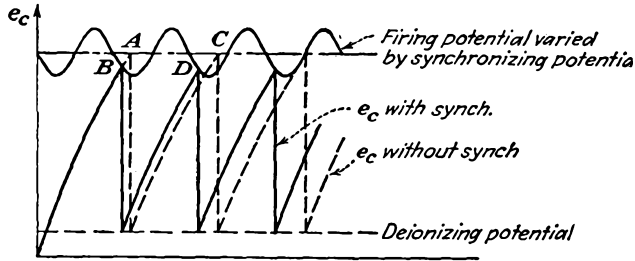


FIG. 20-9. Synchronizing a thyatron saw-tooth generator with a sine wave.

causes the firing point to vary in accordance with the grid signal. At some time during the synchronizing cycle the firing potential will be low, so that the tube fires at point B. On the next cycle the voltage across the capacitor reaches the firing point at D. The period, or time per cycle, is thus reduced from AC to BD, and the oscillator is now synchronized, or locked, to the frequency of the injected voltage. In a similar manner it may be synchronized to a submultiple or multiple of the synchronizing voltage.

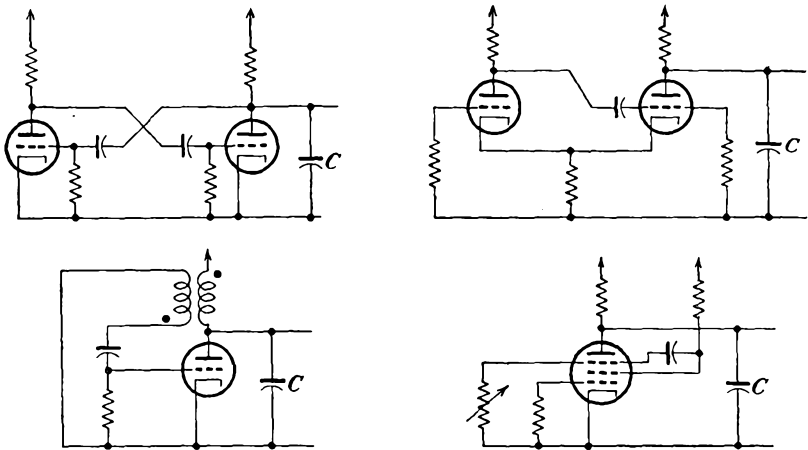


FIG. 20-10. Free-running vacuum-tube sweep generators.

**20-4. Free-running Vacuum-tube Circuits.** The thyatrons of the previous circuits may be replaced by vacuum tubes with substantially the same operation. However, since a vacuum tube as such is neither self-triggering nor self-extinguishing, circuits must be employed which

accomplish this action. The use of a hard-tube relaxation-oscillator circuit serves the purpose very well, and such circuits are used extensively. Four such circuits are illustrated in Fig. 20-10. One circuit employs a conventional plate-coupled multivibrator; one employs a cathode-coupled multivibrator; the third employs a blocking-oscillator circuit; and the fourth employs a pentode relaxation oscillator. These circuits may be synchronized by injecting a synchronizing voltage into the grid or into the cathode circuits, as already discussed in connection with the several oscillator circuits. Hence all the properties of the gas-tube relaxation circuits are also possessed by these relaxation circuits.

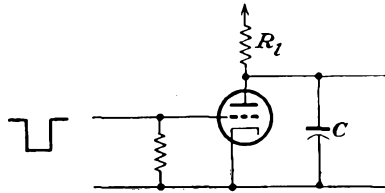


FIG. 20-11. A hard-tube sweep circuit.

**20-5. Triggered Sweep Circuits.** The use of a vacuum tube as a switch allows a very accurate timing of the start of the sweep voltage, since there is substantially no delay between the application of a signal

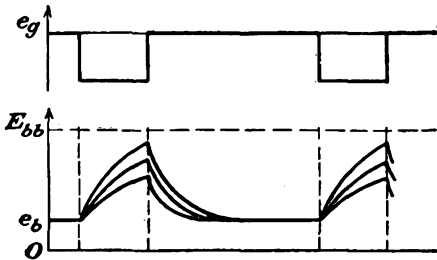


FIG. 20-12. The voltage across the capacitor  $C$  in the circuit of Fig. 20-11.

on the grid and the consequent effect in the plate circuit. In particular, refer to the circuit of Fig. 20-11. In this circuit, the grid is so biased that the tube is conducting when no square wave is applied to the grid. The potential across the capacitor  $C$  is then  $E_b$ , the drop across the tube. With the application of the negative gate, the tube ceases to conduct, and the

voltage across  $C$  begins to increase toward  $E_{bb}$  through the plate-load resistor  $R_l$ . Then, depending on the width of the gate and the constants of the circuit, the saw-tooth will follow one of the paths shown in Fig. 20-12.

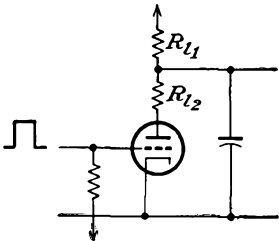


FIG. 20-13. A negatively biased saw-tooth generator.

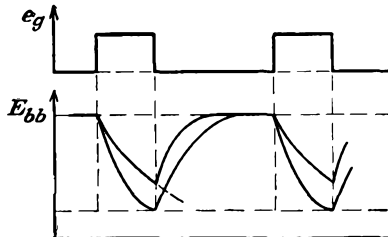


FIG. 20-14. The output-voltage wave form from the sweep generator of Fig. 20-13.

If the tube is normally biased negatively so that no current flows through it, then upon the application of a positive gate the potential across the capacitor will fall from the value  $E_{bb}$  to the value determined by the drop across the tube  $E_b$  and the drop across the resistor  $R_{L2}$ , if one is used to limit the current through the tube. The generator circuit is given in Fig. 20-13, and the general character of the discharge curves is illustrated in Fig. 20-14.

**20-6. Linearizing Saw-tooth Waves.** When a linear-sweep voltage is necessary, the most direct recourse is to employ a high potential toward which the capacitor is charging and then to use only the lower portion of the charging curve. An alternative and somewhat more satisfactory method is to replace the charging resistor by a constant-current device, such as a pentode or other constant-current generator, and charge the capacitor through this. For the majority of cases, the degree of linearity obtainable with such a constant-current generator is usually sufficient. Other methods of linearizing saw-tooth generators do exist, and these generally employ one or another of the following methods of obtaining the desired

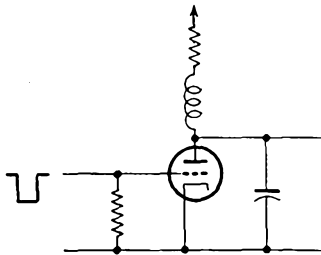


FIG. 20-15. Linearization of a saw-tooth wave by using a high charging voltage, obtained by interrupting the current in a large inductor.

compensation: (a) the inverse curvature of a vacuum-tube characteristic; (b) an auxiliary time-constant circuit; (c) feed-back methods. Each of these methods will be considered below.

*Charging to a High Voltage.* As already pointed out, the use of a fraction of the charging curve will yield a substantially linear voltage increase, particularly if the capacitor is charging to a high potential. It is not necessary that a high d-c potential source be available, and the circuit of Fig. 20-15 illustrates the method of generating a high voltage by interrupting the current in a large choke (of the order of 500 henrys). Such circuits have long flyback times and are limited to circuits having a small duty cycle (the ratio of the duration of the sweep to the sweep recurrence period).

*Use of Constant-current Generators.* The use of a constant-current generator in place of the ordinary charging resistor allows a very satis-

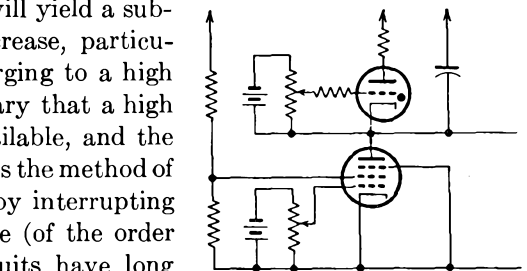


FIG. 20-16. A thyatron saw-tooth generator with a pentode charging circuit.

factory linear saw-tooth voltage to be generated. With such a device, the capacitor charging current passes through the constant-current generator, and the capacitor potential increases linearly with time. Figure 20-16 illustrates the circuit of a thyratron generator with a pentode

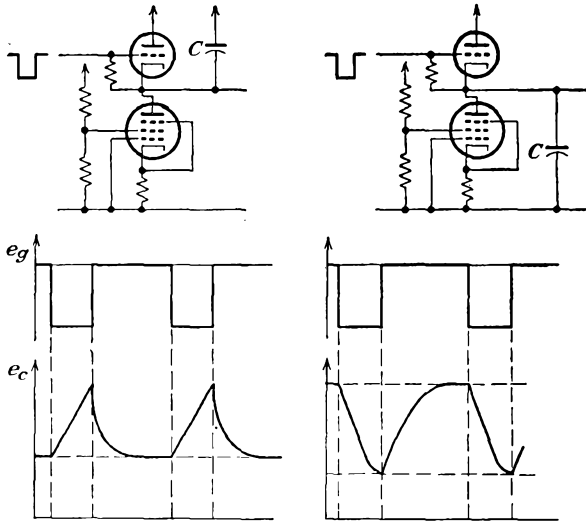


FIG. 20-17. Positive- and negative-going linear saw-tooth generators employing pentode constant-current generators for linearization.

as the constant-current generator. With such a circuit, the frequency may be varied by changing the bias of the pentode, since this controls the tube current and hence the charging rate of the capacitor.

The circuits of Fig. 20-17 show the connections and the wave forms expected from a vacuum-tube circuit employing pentode charging. For a circuit that incorporates a triode as a constant-current generator see the figure of Prob. 20-7.

A slightly modified circuit provides pentode charging with adjustable feedback. In this way, any curvature that might still remain in the saw tooth can be compensated by controlling the feedback. This circuit is illustrated in Fig. 20-18. A variation of this circuit was suggested by Bedford. His arrangement is given in Fig. 20-19.

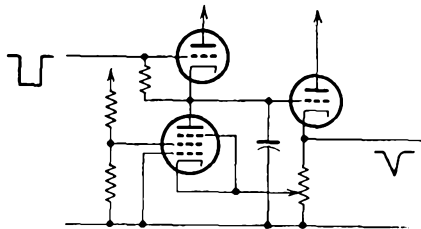


FIG. 20-18. A saw-tooth generator incorporating pentode charging with adjustable feedback.

*Linearization by Means of Inverse Curvature.* These methods compensate to a certain degree for the curvature of the charging characteristic by inserting a device having a similar but inverse characteristic. An arrangement which is often adopted is to amplify the potential across the capacitor by means of a tube in such a way that the curvature of the tube characteristic is employed as a linearizing means. It is fortunate in this respect that the curvature of a part of the transfer curve of the

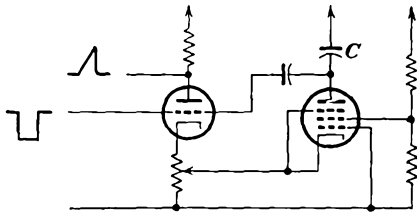


FIG. 20-19. An alternative circuit that provides a combination of pentode charging and feedback to linearize the saw tooth.

tube approximates the inverse of an exponential characteristic. Such a circuit is illustrated in Fig. 20-20. In this circuit the output potential is amplified by a second tube which is operated with such a bias that the nonlinear operation compensates the nonlinear input. The added capacitor  $C_2$  is to maintain the anode potential reasonably constant during the discharge period of  $C_1$ .

*Linearization by Means of an Auxiliary Time-constant Circuit.* A simple method that yields fairly satisfactory results modifies the exponential wave form across the capacitor by the addition of an integrating circuit.<sup>1</sup> The essentials of the circuit are illustrated in Fig. 20-21. In this circuit, the charging capacitor consists of two parts  $C_1$  and  $C_2$  in series. These are charged together, through the resistance  $R_1$ , and discharge through the tube.

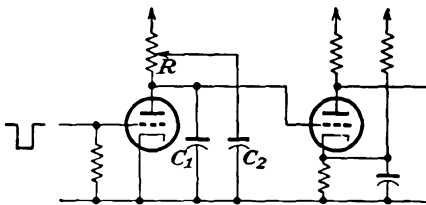


FIG. 20-20. A circuit for linearizing a saw tooth by employing the curved characteristic of a vacuum-tube amplifier.

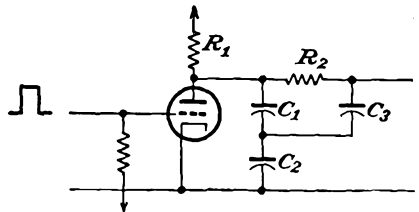


FIG. 20-21. A circuit that employs an integrating network in the output to linearize the saw-tooth wave.

Assume that the capacitors  $C_1$  and  $C_2$  have just been charged. The capacitor  $C_3$  will be at a potential less than that across  $C_1$ , as  $C_3$  charges through  $R_2$ . The potential of  $C_3$  depends on the time constant  $C_3R_2$  and the length of time that  $C_3$  is charging through  $R_2$ . When the gate is applied to the grid,  $C_1$  and  $C_2$  begin to discharge, while the potential across  $C_3$  falls more slowly owing to the large time constant  $C_3R_2$ . When  $C_1$  and  $C_2$  are discharged and the tube is again nonconducting,  $C_3$  will

retain a considerable charge.  $C_1$  and  $C_2$  now start to charge once more, but  $C_1$  receives charge from two sources, the B+ supply through  $R_1$  and from  $C_3$  through  $R_2$ .  $C_3$  supplies charge to  $C_1$  until the potentials are equalized, and  $C_3$  charges thereafter from  $C_1$ . As a result, the potential across  $C_1$  and  $C_2$  is exponential, while that across  $C_3$  is approximately parabolic. If  $C_2$  and  $C_3$  are properly chosen, the output is approximately linear.

*Linearization by Means of Feed-back Arrangements.* Feedback may be applied at two points in a saw-tooth generator for improving the linearity of the output. The effect that results from the stray capacitances of the leads and the plates of the cathode-ray tube can be minimized by feeding the output from the cathode of a cathode-follower stage. The other effect arises because the potential across the charging capacitor is exponential as it approaches the fixed charging potential. This can be compensated by introducing a compensating potential in the charging circuit to counterbalance the potential of the capacitor. A circuit that accomplishes this result is illustrated in Fig. 20-22.

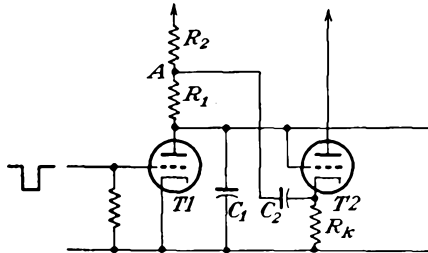


FIG. 20-22. A linear saw-tooth generator employing a cathode follower for feedback.

In this circuit,  $T1$  is normally conducting, and the potential across the capacitor is  $E_{b1}$ . With  $T2$  absent and with the application of a negative gate to the grid of  $T1$ , the capacitor will begin to charge from  $E_{b1}$  toward  $E_{bb}$  along an exponential curve, with a time constant  $(R_1 + R_2)C_1$ . With  $T2$  connected as shown and with the application of the negative gate to cut  $T1$  off, as the potential of  $C_1$  increases the potential at  $R_k$  increases, and if the gain of the cathode follower is unity, the two potentials are exactly equal. Consequently, by the application of the output of the cathode follower into the circuit in such a way that the voltage across the capacitor is just balanced by the cathode-follower output, the net effect is a linear output. The capacitance of  $C_2$  is made sufficiently large so that the potential across it remains steady, and it is kept charged from the B+ supply through  $R_2$ .

It should be noted that the charge leaking off  $C_2$  through  $R_1$  and  $R_2$  must be replaced during the recycling time, and since the time constant of the circuit must be large compared with  $T$ , this requires an appreciable time. Unless the recycling time is long compared with the duty time, a d-c shift will result. Moreover, the presence of  $R_2$  reduces the feedback gain. The use of a diode in place of  $R_2$  avoids these difficulties, as it

cuts off during the duty interval but closes to give a low impedance during recycling. Such a circuit is illustrated in Fig. 20-23.

The extent to which the resulting saw tooth is linear depends upon how closely the gain of the cathode follower approaches unity. In effect, therefore, the circuit is such that the capacitor, instead of charging to a constant potential  $E_{bb}$ , charges toward a continually increasing potential, the extent of the increase being such as to compensate very nearly for the potential across the capacitor. Thus the current through the circuit remains constant, with a consequent linear potential across  $C_1$ .

Of course, if amplification is provided before applying the output across the capacitor  $C_1$  to the grid of the cathode follower, it is then possible to get almost any degree of compensation. Such a circuit would have the form illustrated in Fig. 20-24.

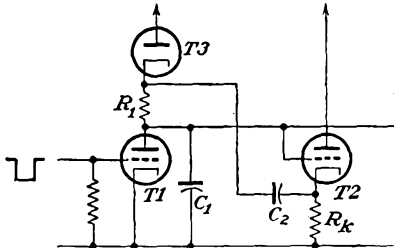


FIG. 20-23. The use of a diode in the plate circuit to reduce any d-c shift and to maintain the feed-back gain.

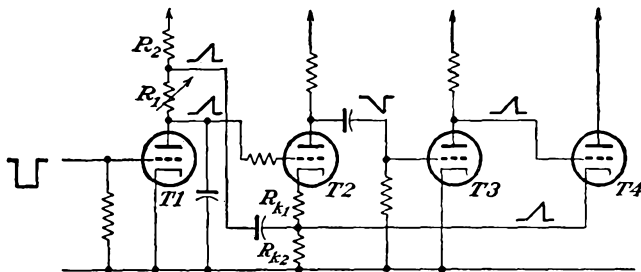


FIG. 20-24. A linear saw-tooth generator with amplification before the application of feedback through a cathode follower.

It is a disadvantage of the above circuits that the grid of the cathode follower is driven negatively during the flyback period. Because of the various stray capacitances across the output circuit, these will tend to delay the fall of the cathode potential, and the cathode follower may momentarily cut off, with a consequent poor flyback. For those applications in which the duty cycle is small, the results with the circuit of Fig. 20-23 are highly satisfactory. This circuit is used in the linear delay gate and was discussed in Sec. 19-14.

**20-7. Push-pull Deflection.** By tying one of each pair of deflecting plates in a cathode-ray tube to the second anode, the total number of external leads is reduced by two. On the other hand, when this is done, both defocusing and trapezium distortion will result.<sup>2</sup> Consequently, in

those cases where these effects cannot be tolerated, it is necessary to connect the anode potential to the mid-point of a high resistor across each pair of plates and apply the deflecting potential across the plates. Using the connection illustrated in Fig. 20-25 provides the opportunity for using push-pull deflection. This is particularly desirable in that a number of advantages are gained. These are improved linearity of the trace, improved deflection sensitivity, and avoiding the need for clamping circuits.

Actually, the use of push-pull deflection with one of the pair of deflecting plates being connected directly to the saw-tooth generator, the other being fed from an inverting amplifier of unity gain, results in a sacrifice in linearity and in flyback speed.

However, it is possible to arrange the circuit so that the distortion introduced by the tube approximately cancels out the effect of an exponential curvature in the wave form of the saw tooth. It is essential that the gain of the amplifier remain unity—otherwise some distortion will result but this is not difficult to achieve if the amplifier is provided with negative feedback.

The improved deflection sensitivity results because the instantaneous deflecting potential difference with push-pull deflection is twice what it is with a single-sided, or unbalanced, deflection.

Clamping circuits are unnecessary because the average ordinate of one wave is equal and opposite to that of the other wave, and the effects are in such a direction as to cancel each other.

Five important methods of obtaining push-pull deflection potentials from a single input wave are available. These are

1. A single-tube phase-reversing stage which may or may not provide more than unity gain. This may be subdivided into

- a. Those circuits in which the input saw-tooth wave form is sensibly linear and the tube distortion is arranged to be a minimum.
- b. Those circuits in which the input wave form is exponential and the amplifier characteristic is employed also for compensation of the input curvature.

2. A single-tube push-pull, or paraphase, amplifier.

3. A two-tube push-pull amplifier which has been modified to handle the peculiarities of a saw-tooth wave form. This may be subdivided into

- a. A standard form of push-pull amplifier.
- b. A cathode-coupled push-pull, or paraphase, amplifier.

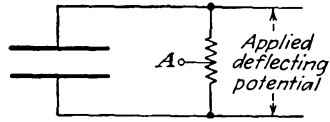


FIG. 20-25. The connection to the deflecting plates in a cathode-ray tube to reduce defocusing and trapezium distortion.

4. Split saw teeth.

5. The use of two equivalent saw teeth operating in phase opposition.

It is not possible to state which of these methods is the most satisfactory, since each possesses certain merits. For most purposes, type 2, the single-tube paraphase circuit, where no amplification is required, and type 3b, the cathode-coupled paraphase amplifier, where amplification is required in addition to the provision of a push-pull output, will ordinarily provide satisfactory results. The use of 4 and 5 usually permit deflection voltages with a minimum of distortion.

*Single-tube Phase-reversing Amplifier.* Any vacuum tube used as a conventional plate-coupled amplifier provides an output voltage that is

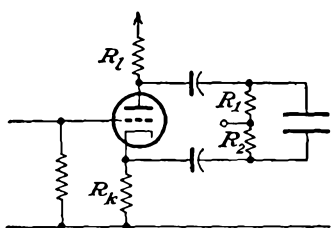


FIG. 20-26. A single-tube paraphase amplifier.

opposite in polarity to the input voltage.

However, since the gain of such a stage is ordinarily greater than unity, some means must be found to reduce the amplification. One common method of reducing the gain is to introduce sufficient negative feedback; the anode follower, discussed in Sec. 6-7, would be suitable for this service.

However, it is quite likely that the phase difference between input and output potentials might differ slightly, particularly at the higher frequencies, where stray capacitances become important.

A second way to reduce the gain of the simple amplifier circuit to unity is to use a voltage divider in the input circuit to reduce the amplitude of the grid signal by an amount equal to the gain of the amplifier. If the wave form which is to be inverted contains many harmonics, special care must be taken to compensate the voltage divider for the shunting effect of the stray capacitances associated with it.

*Single-tube Paraphase Amplifier.* A combination of amplifier and phase inverter to provide a push-pull output from a single input wave is known as a *phase splitter* or *paraphase amplifier*. A single-tube paraphase amplifier in which the plate resistor is divided equally between the plate and cathode circuits is the simplest form of paraphase amplifier and was examined in Sec. 9-11 (page 187). The circuit of this amplifier is redrawn for convenience in Fig. 20-26.

An important feature of this circuit is to be noted. This arises from the presence of stray capacitances between the cathode and ground. If a positive-going trace is applied to the grid, this capacitance will charge slowly during the trace, and when the grid is brought down sharply at the end of the trace, the tube current decreases and hence during the flyback time the capacitance must discharge through the cathode resistor,

a relatively long time-constant circuit. If, on the other hand, a negative-going saw tooth is applied to the grid, the cathode-ground capacitance will charge slowly and during the retrace time the tube current will be large; as a result the cathode potential is enabled to change rapidly, and the flyback is not impaired.

Another point to be observed is that the tube behaves as a cathode follower sufficiently to prevent the output at the cathode from being appreciably influenced by the value of the cathode load impedance. The presence of  $R_k$  increases the effective impedance of the tube as seen from the anode, so that the anode current is almost independent of the anode circuit. The output potential at the anode is directly dependent upon the value of  $R_l$  in parallel with the deflecting-plate leak resistor  $R_1$  and the total stray capacitance associated with the anode and the deflecting plates. It is for this reason that the stray capacitances across  $R_1$  and  $R_2$  must be equalized. This balancing arrangement prevents the flyback from overshooting the start of the trace.

*Two-tube Paraphase Amplifiers.* These paraphase amplifier circuits are discussed in some detail in Sec. 9-11 (page 187), and reference should be made to this section for details.

*Cathode-coupled Push-pull Amplifier.* The cathode-coupled paraphase amplifier is discussed in some detail in Sec. 6-9 (page 117) as the difference amplifier. This paraphase amplifier has many desirable features which recommend it as a satisfactory solution of the paraphase problem. The circuit is redrawn in convenient form in Fig. 20-27.

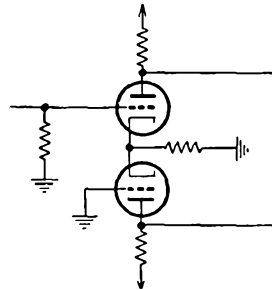


FIG. 20-27. A cathode-coupled paraphase amplifier.

The attractive features of this circuit are the following:

1. Low distortion and relatively small value of grid current when overloaded.
2. Freedom from any tendency to self-oscillation.
3. Permits d-c connections at the input and output.
4. Permits providing shift, astigmatism correction, and balance controls.
5. Permits sweep expansion.

Figure 20-28 shows a circuit in which a cathode-coupled paraphase amplifier is arranged to provide sweep expansion and other controls.

*Split Saw Teeth.* It is sometimes desirable to avoid the necessity for amplification and phase inversion by generating a saw-tooth wave form having sufficient amplitude to allow half the output voltage to be applied

to each deflecting plate. The principle involved is indicated in Fig. 20-29a. Here the two charging resistors have a capacitor between them, although one might equally well use two equal charging capacitors with the charging resistor between them. The output provides equal poten-

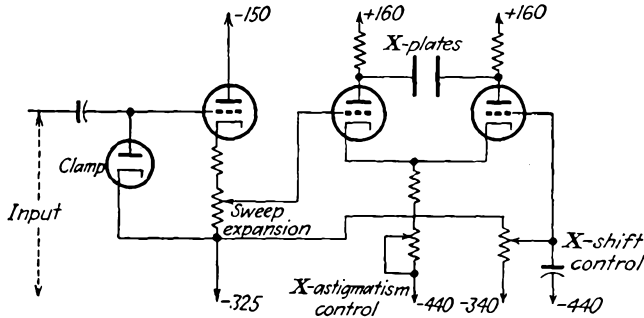


FIG. 20-28. A cathode-coupled paraphase amplifier with sweep expansion.

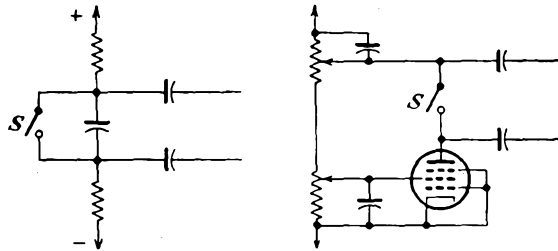


FIG. 20-29. A split saw-tooth generator. (a) employs a single capacitor and two resistors. (b) employs two capacitors and one charging device.

tials of opposite phase. The discharging device is indicated by the switch *S*. Figure 20-29b shows a practical circuit for obtaining a split saw tooth from two capacitors and one charging device.

*Saw Teeth in Phase Opposition.* In Fig. 20-30 is shown a circuit which comprises two saw-tooth generators, one of which is connected in the

reverse sense to the other. In this circuit a single discharging device may be employed, but the plate supply would be larger than would be necessary if separate discharging devices are employed. The resistors  $R_1$  and  $R_2$  may be replaced by constant-current devices. The switch *S* which represents the discharging device is used to bring the capacitors to the same potential. Since  $R_1$  and  $R_2$  are equal, this potential is half that

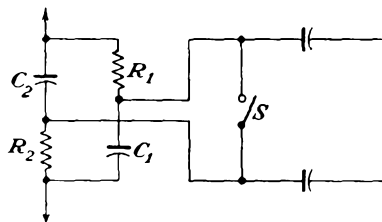


FIG. 20-30. Saw teeth operating in push-pull.

of the plate source. When the switch  $S$  is opened, one plate is driven in the positive direction and the other plate is driven in the negative direction.

The circuit of Fig. 20-31 is one in which the elements are so arranged as to provide a push-pull output in which the whole of the available supply potential may be made to appear across each of the capacitors  $C_1$  and  $C_2$ .

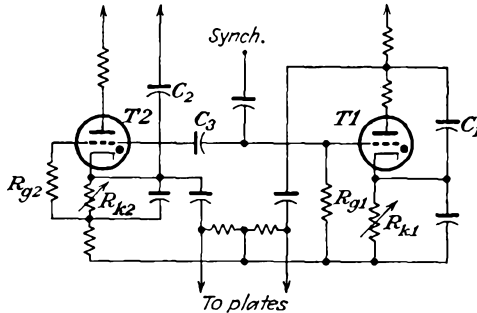


FIG. 20-31. Two thyatron saw-tooth generators operating in push-pull.

In this circuit the two thyratrons  $T1$  and  $T2$  are connected across the capacitors  $C_1$  and  $C_2$ , respectively, and the bias potentials applied to their grids are determined by the adjustment of the resistors  $R_{k1}$  and  $R_{k2}$ . The potentials across these resistors remain constant.

When the capacitors  $C_1$  and  $C_2$  are being charged, the potential of the anode of  $T2$  remains fixed, while those of the cathode and grid rapidly become more negative with respect to the anode. Since the grids of the two thyratrons are joined together through  $C_3$  and the discharge current of  $C_3$  passes through  $R_{g1}$ , the grid-cathode bias of  $T1$  is greater than that due to the potential drop across  $R_1$ . For this reason  $R_1$  must be adjusted to provide a smaller bias potential than is the case with  $R_2$ , since otherwise there will be a time lag between striking of  $T1$  and  $T2$ . The object is to obtain simultaneous striking, and this is best achieved by making the potentials at the two grids equal at the instant immediately prior to striking by accurate adjustment of  $R_1$ .

**REFERENCES**

As a general reference, see  
 Puckle, O. S., "Time Bases," John Wiley & Sons, Inc., New York, 1943.  
 1. Hawkins, G. F., *Wireless World*, **5**, 425 (1939).  
 2. Millman, J., and S. Seely, "Electronics," Sec. 3-10, McGraw-Hill Book Company Inc., New York, 1941.

**PROBLEMS**

**20-1.** An 884 thyatron is used in the saw-tooth generator of Fig. 20-6. The parameters are adjusted to be

$$E_{bb} = 300 \text{ volts} \quad E_{cc} = -20 \text{ volts} \quad C = 0.003 \mu\text{f} \quad R = 10^6 \text{ ohms}$$

- Calculate the frequency of oscillation.
- Calculate the amplitude of the generated waves.
- Plot the wave shape of the generated waves. Assume that the flyback time is zero.

**20-2.** Design a thyratron relaxation saw-tooth generator to yield a substantially linear saw tooth having a peak amplitude of 25 volts, with a recurrence frequency of 1,000 cps. Specify reasonable values of  $E_{bb}$ ,  $E_{cc}$ ,  $R$  and  $C$ , and give reasons for your choice.

**20-3.** Derive an equation for the potential across capacitor  $C$  in the circuit of Fig. 20-11:

- During the time that the gate is applied.
- After the gating period.
- Sketch these results.

**20-4.** The parameters in the simple sweep circuit of Fig. 20-11 are the following, for tube 6SN7:

$$R_t = 75\text{k} \quad C = 0.005 \mu\text{f} \quad E_{bb} = 300 \text{ volts} \quad \text{prf} = 1,000 \text{ cps}$$

The input negative gate has an amplitude of 50 volts, and a duration of 150  $\mu\text{sec}$ .

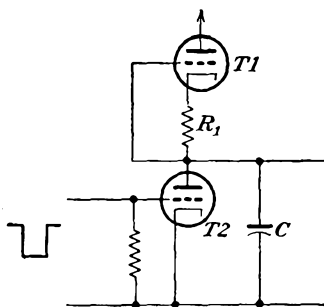
- Calculate and plot curves of the form illustrated in Fig. 20-12.
- Repeat *a* for  $R_t = 50\text{k}$ .

**20-5.** Set up and solve the differential equation that controls

- The charge to capacitor  $C$  of Fig. 20-17*a* when the negative cutoff gate is applied.
- The discharge of capacitor  $C$  at the end of the gate period.

**20-6.** The circuit of Fig. 20-17*b* is to be used in a saw-tooth generator circuit. The triode is a 6J5, and the pentode is a 6SJ7. A linear saw tooth with a 100-volt excursion is required, the duration of which is 250  $\mu\text{sec}$ . The recurrence frequency is 1,000 cps. The available plate-supply source  $E_{bb} = 300$  volts. Specify all elements of the circuit.

**20-7.** *a.* Find expressions for the potential across  $C$  during the charge and discharge portions of the cycle of the circuit in the figure for this problem.



Assume that the beam resistance of  $T_2$  is  $r$ , when the tube conducts and is infinite when the gate is applied.

b. Plot the results of part a.

c. On this same curve sheet, plot the results of Prob. 20-3, assuming the same value of  $C$  and that  $R_i = R_1$ .

**20-8.** Derive an expression for the output potential from the circuit of Fig. 20-21 when a positive pulse is applied to the grid. The tube is normally biased beyond cutoff. What should be the relation among the circuit elements for an approximately linear output?

**20-9.** The circuit shown in the diagram is essentially the feed-back circuit of

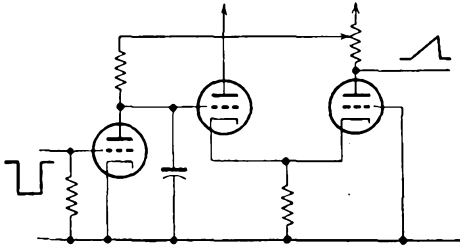
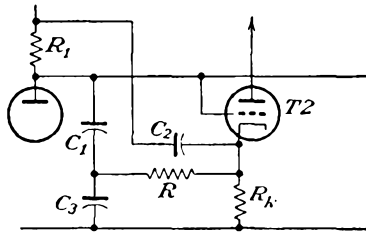


Fig. 20-22. Discuss the advantages of this arrangement over that of Fig. 20-22.

**20-10.** Derive an expression for the voltage across capacitor  $C_1$  in Fig. 20-22.

**20-11.** If the circuit of Fig. 20-22 is modified as shown in the accompanying diagram, and assuming that the cathode of  $T_2$  rises linearly at a constant rate  $K_1$ ,

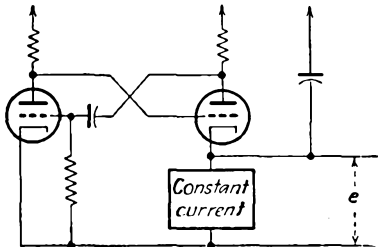


show that the voltage that appears across  $C_3$  during the saw tooth is given by

$$e_3 = K_1 t + K_1 R C_3 (e^{-\frac{t}{R C_3}} - 1)$$

Neglect the effect of charging  $C_2$  from the main source.

**20-12.** Discuss the operation of the following circuit, suggested by Puckle.



## CHAPTER 21

### SPECIAL SWEEP GENERATORS

IT MAY be shown that the deflection of the electron beam in an electromagnetically deflected cathode-ray tube is proportional to the field strength of the deflecting field. The field strength is proportional to the current passing through the deflecting coil, if saturation is avoided. Consequently, if it is desired to deflect the electron beam linearly with time, the current through the coil must be increased linearly with time. When the end of the sweep is reached, the electron beam must be returned to its starting point quickly. It will be seen below that achieving a linear current through a deflecting coil (a series  $RL$  circuit) is a difficult task; in general, one seeks to achieve satisfactory results, even though these may leave something to be desired.

**21-1. Sweep Generators for Electromagnetic Deflection.** There are four general methods in use for obtaining a linear current through a deflecting yoke. They make use of (a) the initial portion of the exponential charge of current through the yoke when a step voltage is impressed on the series  $RL$  circuit, (b) the initial change of current in an inductance during an oscillation when the current in a parallel  $RLC$  circuit is varied suddenly, (c) the increase of current in an inductance due to the application of a trapezoidal voltage of properly chosen dimensions, and (d) the use of feedback in a way to provide for linearity. Each of these methods will be examined below.

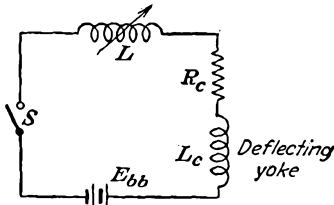


FIG. 21-1. A simple circuit for producing a saw-tooth current.

In this circuit it is supposed that no current is initially flowing in the deflecting-yoke circuit. When the switch  $S$  is closed, the current will begin to rise exponentially according to the equation

$$i = \frac{E_{bb}}{R_c} (1 - e^{-\frac{R_c t}{L + L_c}}) \quad (21-1)$$

The rate of rise of current is given by

$$\frac{di}{dt} = \frac{E_{bb}}{L + L_c} \tag{21-2}$$

and hence the sweep speed may be varied by adjusting the magnitude of the inductance in the circuit.

To return the sweep to the initial condition, the switch  $S$  is opened. When this is done, however, the current tends to oscillate owing to the oscillatory circuit consisting of the yoke inductance and the distributed capacitance of the yoke. In order to damp out these oscillations, it is sometimes necessary to connect a resistor or a damping diode across the deflecting yoke.

An electronic circuit that is based on these principles is illustrated in Fig. 21-2. In this circuit, the tube is normally biased beyond cutoff, and hence no current is flowing in the deflecting-coil circuit. At the time that the sweep is to be produced, a positive pulse is applied to the grid of the tube. The purpose of the resistor and diode that are connected across the deflection coil is to damp out the oscillations that are excited at the end of the sweep. The diode serves to disconnect the damping resistor during the rise of current. When the driver tube is cut off at the end of the positive pulse, a reversal of potential across the inductance results, which will make the diode conduct and permit current to flow through the damping resistor.

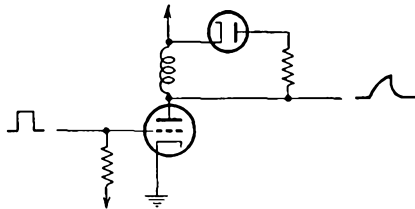


FIG. 21-2. A circuit for generating a sweep current by impressing a rectangular pulse on an  $RL$  circuit.

*Initial Part of Oscillation.* When an attempt is made to interrupt the current in a circuit consisting of a coil shunted by a capacitor, an oscillatory current is produced in the tuned circuit. The first part of the first

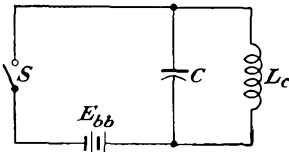


FIG. 21-3. A circuit for obtaining an oscillating current in a deflecting coil.

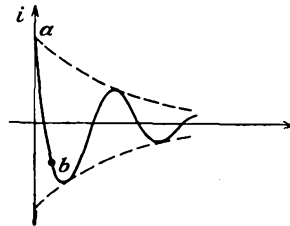


FIG. 21-4. The current in the deflecting coil in the circuit of Fig. 21-3.

cycle of the oscillation of the current is reasonably linear and may be used as a sweep current. The elements of the circuit are illustrated in Fig. 21-3.

The shape of the current in the coil is somewhat as illustrated in Fig. 21-4. The rate of change of current in the interval from  $a$  to  $b$  depends

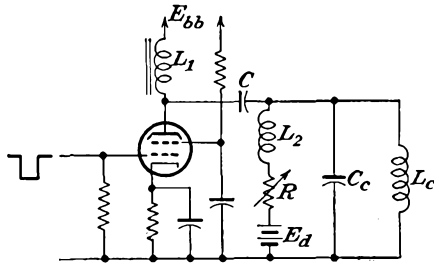


FIG. 21-5. An oscillatory sweep-current circuit with arrangements for adjusting the zero position of the sweep.

upon the resonant frequency of the deflecting-coil inductance, and the shunt capacitance, and the amplitude of the initial current. Of course, if different values of shunt capacitance are used, different resonant frequencies result, whence the sweep speeds (considering the region from  $a$  to  $b$  to be the effective portion of the oscillation) may be varied. Likewise, the amplitude of the oscillation

will depend upon the magnitude of the d-c current in the coil before it is interrupted.

A sweep circuit that employs such an oscillatory circuit is given in Fig. 21-5. In this circuit the deflecting coil is coupled to the plate circuit of a current-amplifier stage by means of a large capacitor  $C$ . The inductors  $L_1$  and  $L_2$  are very large and hence serve to isolate the a-c oscillatory current from the zero-position circuit and the plate supply  $E_{bb}$  and thus confine the current to the deflecting-yoke circuit. However, the bias battery  $E_d$  sends a steady current through resistor  $R$ , inductor  $L_2$ , and the deflecting coil for the purpose of centering the spot.

In this circuit the application of the pulse to the amplifier tube causes the current in the deflecting-coil circuit to decrease and oscillate about one level, and the removal of the pulse causes the current to oscillate about the d-c value determined by the local circuit containing  $E_d$ . The shape of the curve is somewhat as illustrated in Fig. 21-6. The second oscillation is damped more rapidly than the first because the beam resistance of the tube is in parallel with the circuit during this portion of the cycle.



FIG. 21-6. The current in the deflecting-coil circuit when a pulse is applied to the grid of the current tube in Fig. 21-5.

*Linear Current by Trapezoidal Voltage.* Both the foregoing methods for obtaining a linear-sweep current utilize a small essentially linear portion of a nonlinear function. It is possible to find a voltage wave form which, when applied to the inductive circuit of the deflecting coil, will yield a current that is linear with time. To examine the required voltage wave shape, refer to Fig. 21-7.

For a linear current having the form

$$i = kt \tag{21-3}$$

the voltage across the deflecting coil must be

$$e = L \frac{di}{dt} + Ri \tag{21-4}$$

which requires, for the linear current, that the voltage have the form

$$e = Lk + Rkt \tag{21-5}$$

This has the form illustrated in Fig. 21-8.

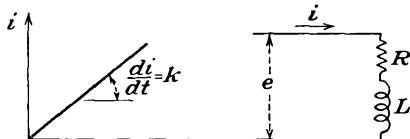


FIG. 21-7. A linear deflecting current.

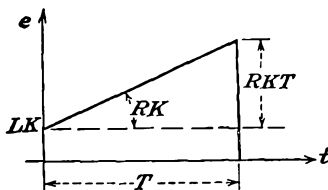


FIG. 21-8. The voltage wave to produce a saw-tooth current in an  $RL$  circuit.

A circuit which is capable of developing a trapezoidal voltage wave form is shown in Fig. 21-9. The switch  $S$  that is connected across  $R_c$  and  $C$  permits the capacitor to be charged and discharged. When the switch is opened, the current in this circuit increases according to the relation

$$i = \frac{E_{bb}}{R_L + R_c} e^{-\frac{t}{(R_L + R_c)C}} \tag{21-6}$$

The output voltage of the circuit is

$$e = E_{bb} - iR_L$$

or

$$e = E_{bb} - \frac{E_{bb}R_L}{R_L + R_c} e^{-\frac{t}{(R_L + R_c)C}} \tag{21-7}$$

The slope of the voltage is

$$\frac{de}{dt} = \frac{E_{bb}R_L}{(R_L + R_c)^2C} e^{-\frac{t}{(R_L + R_c)C}} \tag{21-8}$$

At the initial time,  $t = 0$ ,

$$\left(\frac{de}{dt}\right)_0 = E_{bb} \frac{R_L}{(R_L + R_c)^2C} \tag{21-9}$$

and

$$(e)_0 = E_{bb} \frac{R_c}{R_L + R_c}$$

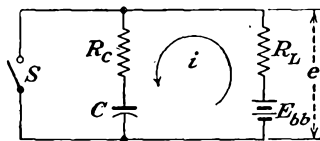


FIG. 21-9. A circuit for generating a trapezoidal wave.

If the time constant  $(R_L + R_c)C$  is large compared with the sweep time  $T$ , so that only a reasonably linear portion of the exponential curve is used, the output voltage will be a sufficiently good trapezoidal voltage wave having the properties shown in Fig. 21-10.

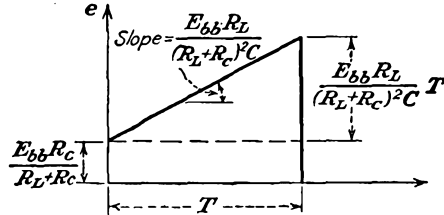


FIG. 21-10. Trapezoidal voltage and the relation to the circuit constants.

An electronic circuit that incorporates the foregoing features for producing a linear saw-tooth current through the deflecting coil is given in Fig. 21-11. It will be observed that tube  $T1$  serves as the switch of

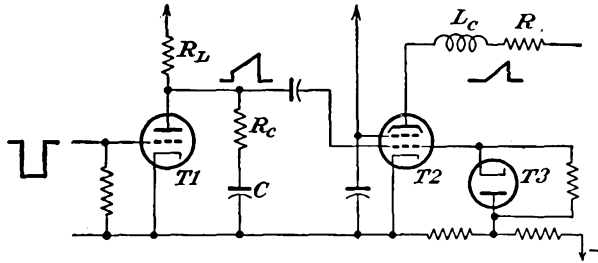


FIG. 21-11. A circuit for generating a saw-tooth current wave for electromagnetic deflection.

Fig. 21-9, the output trapezoidal wave being applied to the grid of a current amplifier tube  $T2$ . A biased clamp  $T3$  is used to set the reference level.

It would be possible to deduce the features of the voltage that must be applied to the grid of the driver or current amplifier tube in Fig. 21-11 in order to give the desired saw-tooth current in the deflecting yoke. However, this will require a knowledge of the tube parameters. Since these will not be constant, owing to the fact that the tube is nominally biased beyond cutoff, and will conduct only on the application of the grid driving potential, such an expression is only approximate, at best. More accurate results are possible by direct recourse to the plate characteristics of the tube, and deducing therefrom the requisite grid signal. This will require a knowledge of the yoke current and the features of the voltage across the yoke, as well as the grid clamping potential. This grid signal may, in fact, be nontrapezoidal.

A variation of the circuit of Fig. 21-11 that does not require a clamp is shown in Fig. 21-12.

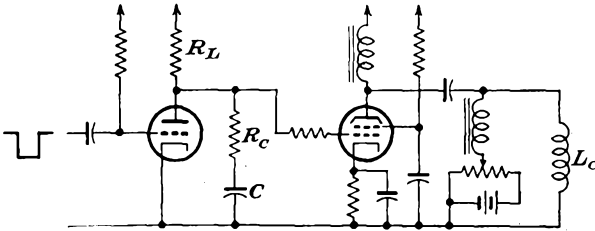


FIG. 21-12. A saw-tooth current generator that provides for d-c restoration by means of a separate circuit.

There are two factors which tend to influence adversely the considerations given above, *viz.*, the distributed capacitance of the coil, and the capacitance of the circuit wiring. Since the voltage across a capacitor in a series  $RC$  circuit cannot change suddenly, the distributed capacitance at the input to the current or driver stage will reduce the steepness of the

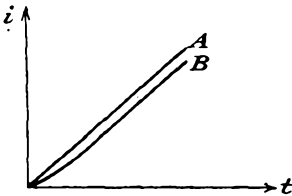


FIG. 21-13. The effect of distributed capacitance in retarding the start of a sweep current.



FIG. 21-14. The use of a narrow spike to aid in starting a linear-sweep current.

initial jump of the trapezoidal voltage, making the trapezoid tend to approach a saw tooth. The application of such a voltage to the  $RL$  circuit through the current tube is a current which increases slowly at first, as shown in Fig. 21-13, and gradually becomes linear with time. Frequently one applies a sharp spike at the beginning of the sweep to help overcome this effect. Such a wave has the form shown in Fig. 21-14.

The effect of the distributed capacitance of the deflecting-coil circuit, which may be considered to appear as a capacitance across the coil, is to produce an oscillatory circuit. The rapid change of current passing through the coil at the time of the return trace will ordinarily shock-excite the coil into oscillation. But since it is necessary to provide some means of dissi-

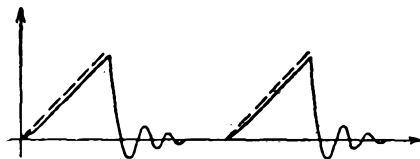


FIG. 21-15. The wave form of the current in the deflecting coil.

pating the energy in the electromagnetic field of the coil so that the current can fall to zero in a short time, a resistor is often connected in parallel with the deflecting coil. This resistor serves to damp the oscillations produced by the shock excitation. The complete curve is generally of the form illustrated in Fig. 21-15.

*Feed-back Circuits.* Although the circuit methods described under Exponential Rise of Current have been used extensively for magnetic sweep-current generation, the present-day methods generally incorporate feedback in the circuit as a means for linearizing the current wave. That is, the circuit is so arranged that the application of a linear voltage saw tooth to the grid of the input amplifier tube will result in a linear saw-tooth current through the deflecting yoke.

Consider the circuit of such a feed-back sweep amplifier shown in Fig. 21-16. The input saw tooth to this amplifier may be generated by a

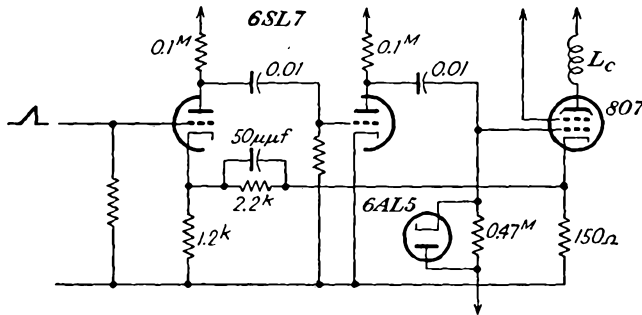


FIG. 21-16. A feed-back sweep-current amplifier.

simple  $RC$  sweep generator, since only a small input signal is required, and for most purposes the resulting linearity in using a small portion of the wave is adequate. This input is passed through two voltage-amplifying stages and is then applied to the grid of the current-amplifier tube. If the total current through the current tube differs from a linear variation, there will be a difference in potential between the cathode of the input stage and an appropriately chosen sample of the output current stage. Owing to the feedback between the output and the input stages, the effective signal will vary in a manner to yield a linear current in the output. Note also in the figure that the grid of the output stage is d-c restored to a value beyond cutoff.

An improved circuit is shown in Fig. 21-17. In this improved circuit, the sampled output current is amplified before being fed back to the input.

There are two features of the above circuits that should be discussed. In the first place, the sampling of the output current is done by means of the potential drop across the cathode resistor. Evidently, therefore, it is the total current that is being sampled, and not the current through

the deflecting yoke. Of course, if the fraction of the total current that flows through the deflecting yoke remains constant as the current increases, then there will be no error resulting from this manner of sampling.

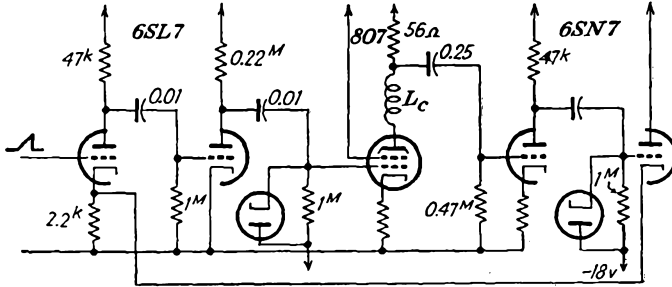


FIG. 21-17. An improved version of the amplifier of Fig. 21-16.

A second feature is one which is important in certain types of application. It will be noted from Figs. 21-16 and 21-17 that the deflecting yoke is in the plate lead of the current-amplifier tube. Likewise, with the clamping tube that is provided, the position of the cathode-ray beam at the start of the sweep will be independent of sweep amplitude or sweep speed. This is a very desirable characteristic in a radar indicator, since it avoids the requirement for a centering voltage, which will depend on the sweep speed.

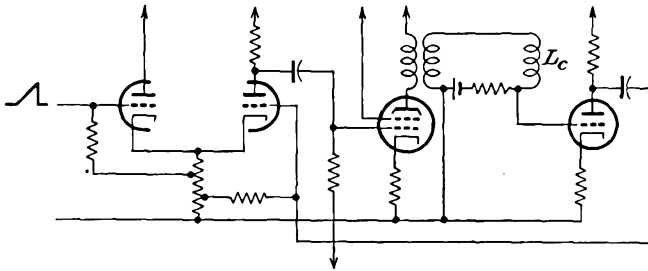


FIG. 21-18. A feed-back amplifier with an a-c coupled output.

If provision must be made for controlling the position of the start of the sweep, the yoke may be a-c coupled to the current amplifier by means of a transformer and by providing a separate source for effecting the desired displacements. The elements of a circuit that permits this type of operation are given in Fig. 21-18. In this circuit the current in the deflecting yoke is sampled, amplified, and combined with the input saw tooth in a difference amplifier. The output from such an amplifier is a very satisfactory linear current wave.

**21-2. Circular-sweep Generator.** In certain applications it is found desirable to employ other than a linear sweep of the cathode-ray beam across the face of the tube. In some instances the beam may be deflected across the tube face according to some prescribed function of time, not necessarily linear. In other cases the cathode-ray beam may be caused to describe a circular path, a spiral path, a rotating radial path, or, in fact, any of a wide variety of paths. Several of such sweep generators will be studied.

An elliptical or circular sweep of the electron beam can be readily accomplished by making use of the fact that the application of sinusoidal

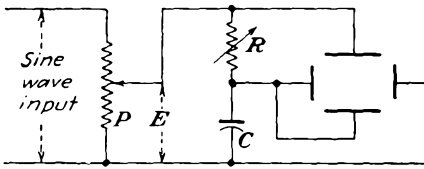


FIG. 21-19. Phase-shifting circuit for producing an elliptical or circular trace.

voltages which differ in time phase by 90 deg to the two sets of deflecting plates of the cathode-ray tube which are 90 deg apart in space will generate an ellipse, if the vertical deflection is different from the horizontal deflection, or will generate a circle, if the two

deflections are the same. The amplitude of the voltages must be slightly different in general in generating a circular sweep in order to take into account the different deflection sensitivities of the deflecting plates, owing to their different distances from the screen.

The simplest circuit for obtaining the necessary two voltages which are 90 deg apart in time phase is illustrated in Fig. 21-19. The circle diagram of this circuit is given in Fig. 21-20, and it will be seen that, for a fixed

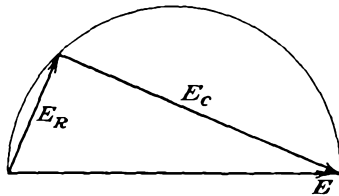


FIG. 21-20. The circle diagram of the phase-shifting network of Fig. 21-19.

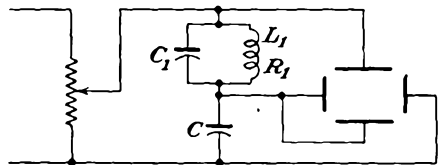


FIG. 21-21. An improved simple phase-shifting circuit.

value of  $C$ , the degree of ellipticity, which depends upon the relative voltage across  $R$  and  $C$ , is controlled by controlling the value of  $R$ . The potentiometer  $P$  controls the amplitude of the sine-wave voltage that is applied to the phase-shifting circuit. If this voltage is large, the voltages across both  $R$  and  $C$  will also be large. Consequently, the circle traced on the screen will be of large diameter.

If the source of voltage for the sweep generator contains appreciable harmonics, the trace cannot be made circular. A modification of the circuit of Fig. 21-19 is possible which will avoid most of the errors arising

from this cause. It consists in replacing the resistance of the circuit by a parallel circuit that is tuned to the frequency of the supply source. The circuit then has the form illustrated in Fig. 21-21. At the supply frequency, the impedance of the parallel circuit is equivalent to a pure resistance of value  $L_1/C_1R_1$ , where  $R_1$  is the effective resistance of the induct. With this circuit, the parallel branch impedance is capacitive for the harmonic frequencies, and so the variation of this impedance with frequency is substantially the same as that for the capacitor  $C$ , with

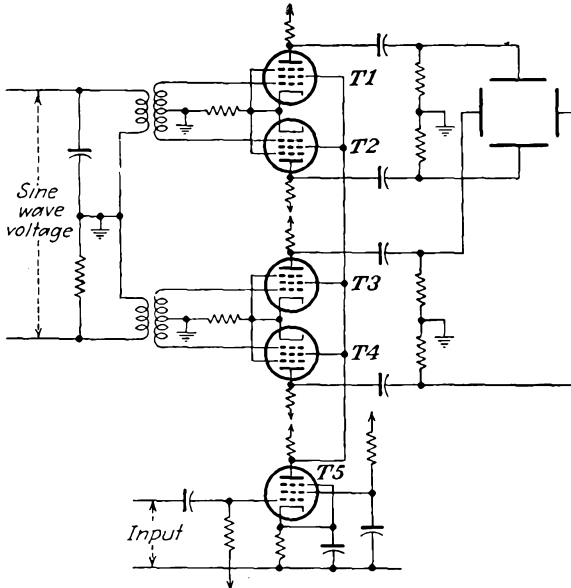


FIG. 21-22. A circular-sweep generator circuit.

the result that the amplitudes of the harmonic potentials applied to the two deflector plates are substantially reduced and the circularity of the trace is not seriously impaired.

The main advantages of such a circular trace are the ease of generation, the increase in the length of trace possible on a given cathode-ray tube face, and the avoidance of flyback. A disadvantage is that such sweeps are ordinarily used with tubes which require the presence of a central electrode to which the signal is applied in order to obtain a deflection of the trace. However, it will be shown that the use of such special tubes is not required since it is possible to obtain a radial deflection without the use of the central electrode.

The disadvantage of these generators is that the omission of push-pull sweep deflection results in trapezium distortion unless the tube is specially designed to reduce this. The effect of the distortion is readily avoided

through the use of the somewhat more elaborate circuit illustrated in Fig. 21-22. This circuit, which is based on the same principles as above, provides a greater flexibility.

In this circuit the values of  $C$  and  $R$  are chosen so that a circular sweep will be generated at the frequency of the applied voltage. Push-pull deflection is provided in order to reduce trapezium distortion. The gain of the four amplifier tubes is controlled by the voltage on the screen grids, which is controlled by the voltage at the plate of  $T_5$ , a quantity that is set by the setting of the bias potentiometer in the grid circuit of this tube.

If no signal is applied to the grid of  $T_5$ , the voltage at its plate will be constant and a circle will be generated. However, if a signal is applied to the grid of  $T_5$ , the voltage at the plate will be changed in accordance with the shape of the input signal, assuming that there is no distortion. This will cause the diameter of the circle to change in accordance with the applied signal, whence the signal is made to appear on the beam. Such a pattern may have the form illustrated in Fig. 21-23a.

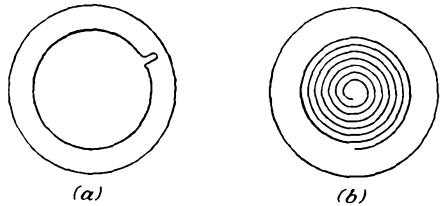


FIG. 21-23. A circular and a spiral trace possible with the circuit of Fig. 21-22.

To obtain the spiral trace illustrated in Fig. 21-23b, it is necessary only to apply a saw tooth to the input of  $T_5$ , the frequency of which is a submultiple of the frequency of the applied sine wave. In particular, suppose that the applied sine-wave voltage is 1,000 cps and that a saw-tooth voltage of 200 cps is applied to the grid of  $T_5$ . The gain of the amplifier tubes will be varied continuously during the 5 cycles of the sine wave. As the gain increases from zero to the maximum, the spot rotates on a circle of ever-increasing diameter, returning to the center during the flyback period of the saw tooth. If the saw tooth is not a submultiple of the sine wave, the spiral will revolve.

By substituting current-amplifier tubes for the voltage-amplifier tubes in the push-pull circuit and replacing the electrostatic deflecting system by an electromagnetic deflecting yoke, the foregoing discussion is valid for the electromagnetic type of tube.

**21-3. Rotating Radial Sweep.** A radial linear sweep which can be rotated with uniform angular velocity is extensively used in radar applications. Such an indicating system is known as a plan position indicator (PPI) since, in its operation, the rotation is synchronized with the scanning of the radar system, the resulting display being in effect a plan view of the scanned area. A number of methods have been used to generate such a display.

The simplest method of producing the plan-position-indicator sweep incorporates the magnetic deflecting yoke which produces the nominal linear deflection in a mechanical assembly which can be rotated physically. The physical rotation of the mechanical assembly can be synchronized with the primary driving source either by means of rigid mechanical couplings or by means of a servomechanism, a device which permits accurate follow-up of driven and driver systems by purely electrical interconnection.

A second method that has been extensively used utilizes a so-called *two-phase selsyn transformer*. Such a device consists of two stator

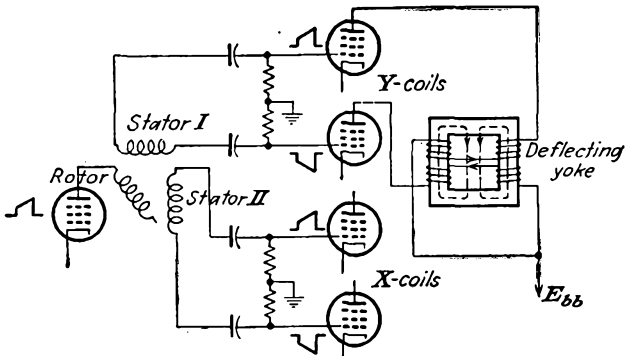


FIG. 21-24. A selsyn transformer circuit for producing a rotating radial sweep.

windings which are placed at right angles to each other and which are excited from a single-phase movable rotor. The application of, say, a trapezoidal wave form (which would theoretically provide a linear-sweep current) to the primary will yield two output voltages which are in time phase but the amplitudes of which vary respectively as the sine and cosine of the angle of the rotor or primary with respect to the secondary windings. These outputs when amplified and applied to two deflecting coils at right angles to each other will produce a display of the type here considered. That this is so follows readily from the fact that the horizontal and vertical magnetic fields are proportional to

$$B_x = \phi(t) \cos \varphi$$

$$B_y = \phi(t) \sin \varphi$$

from which it follows that

$$B = \sqrt{B_x^2 + B_y^2} = \phi(t)$$

That is, the resulting field, and hence the deflection, at any angle  $\varphi$  is constant in amplitude and of the form to produce a linear saw-tooth current wave. Of course, the requirements imposed on the selsyn trans-

former is that it faithfully reproduce in the output circuit the wave shape of the input wave.

The main elements of such a circuit are given in Fig. 21-24.

#### REFERENCES

As general references, see

Puckle, O. S., "Time Bases," John Wiley & Sons, Inc., New York, 1943.

Soller, J. T., M. A. Starr, and G. E. Valley, Jr. "Cathode Ray Tube Displays," M.I.T. Radiation Laboratory Series, Vol. 22, McGraw-Hill Book Company, Inc., New York, 1948.

#### PROBLEMS

**21-1.** The deflecting yoke of a magnetic cathode-ray tube has an inductance of 8.9 mh and a resistance of 15 ohms. It is connected in the circuit of Fig. 21-3. The initial current in the coil is 80 ma when  $S$  is opened. Calculate and plot the current through the coil when  $C = 0.01, 0.1$  and  $1 \mu\text{f}$ , respectively. Estimate the range over which a linear current within 5 per cent exists.

**21-2.** The deflecting yoke of Prob. 21-1 is connected in the circuit of Fig. 21-11. Tube  $T1$  is a 6J5,  $T2$  is a 6V6,  $E_{cb} = 300$ . The clamp sets the grid bias of  $T2$  at  $-50$  volts. If the current wave through the yoke is to vary linearly from 0 to 80 ma in  $60 \mu\text{sec}$ ,

- a.* Specify the trapezoidal wave that must be applied to the grid of  $T2$ .
- b.* Specify a set of constants of the circuit of  $T1$  to yield such a trapezoidal wave.

---

## CHAPTER 22

### ELECTRONIC INSTRUMENTS

A NUMBER of instruments have been developed which incorporate vacuum tubes as an integral part of these devices. These instruments possess certain advantages over the standard electromechanical varieties. In particular, most of the vacuum-tube types of instruments possess relatively high input impedance and also may be used over a very wide range of frequencies. These instruments are divided into the following general classes: voltmeters, ammeters, power meters, frequency meters, and phasemeters.

Perhaps the most versatile of all electronic instruments is the cathode-ray oscilloscope, which may be used as a voltmeter, ammeter, frequency meter, and phasemeter, depending upon the manner of its connection in a test circuit. The applications to these various services will be discussed below in the appropriate section.

**22-1. Electronic Voltmeters.** *The Oscilloscope.* The applicability of the oscilloscope as a voltmeter arises from the fact that the deflection sensitivity of the cathode-ray tube, for a given accelerating potential, is a constant and the deflection of the cathode-ray beam on the screen is directly proportional to the applied deflecting potential. Thus, by setting the gain of the amplifiers associated with the oscilloscope at some convenient value, the peak of any applied potential may be compared with a calibrating potential.

Such devices are very flexible but are usually limited to the lower frequencies, owing to the frequency distortion that occurs in the amplifiers at the higher frequencies. If connection is made directly to the plates of the tube, this frequency limitation is avoided and the tube may be used to the very high frequencies. However, as the deflection sensitivity is usually low, of the order of 40 volts/in. on a 5-in. tube with an applied accelerating potential of 2,000 volts, such a voltmeter would be limited to the higher potentials, in the range from 5 to 150 volts. For higher voltages, a potential divider might be used. Lower voltages cannot be measured, except with the aid of amplifiers, and with their consequent frequency limitations.

*Vacuum-tube Voltmeters.* The vacuum-tube voltmeter provides a convenient method for the accurate measurement across high-impedance

sources of both d-c and also a-c voltages up to very high frequencies. The use of the conventional type of tube usually limits the operation to frequencies below about 1.5 megacycles. For frequencies higher than this, the grid-circuit loading, resulting from the input capacitances of the tube and the electron transit time, usually becomes sufficiently serious to influence the operation. Where the loading effects are permissible, the use of suitable standard receiving-type tube is permissible to frequencies of approximately 20 megacycles without serious calibration errors.

For the measurement of voltages having frequencies above 1.5 megacycles, to perhaps 30 megacycles, Acorn type tubes in a special probe construction may be used without introducing appreciable loading. With such a probe construction, the lead impedance is reduced to zero by allowing direct connection to be made from the voltage source to the grid of the tube. Also, the shunting effect of the grid resistor is made negligible either by neglecting it entirely or by using resistors of low self-capacitance in series to provide from 5 to 10 megohms across the grid to cathode.

A wider range of operation, perhaps to 100 megacycles or higher, is possible by the use of the Acorn type diode rectifier. Such a circuit provides a low input capacitance and low transit time, and although a high efficiency of rectification is possible and a high average impedance may be obtained when the load is of the order of 50 megohms, the input impedance during the peak of the positive half cycle of the applied voltage decreases. Also, the reading is dependent on the impedance of the source, which results in a reduction of the applied voltage at the terminals of the voltmeter. If the tube diode is replaced by one of the present-day crystals, the range of a vacuum-tube voltmeter is extended somewhat, to perhaps as high as 500 megacycles.

All a-c voltmeters are essentially rectifiers, employing diode, grid-circuit, or plate-circuit rectification. They may be grouped according to the value of the wave form of the applied voltage to which their readings are proportional, as rms, average, peak, or logarithmic. A number of circuits that are currently in use will be discussed.

*RMS voltmeters.* The response of this type of voltmeter is proportional

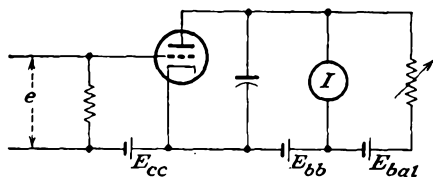


FIG. 22-1. The basic circuit of a vacuum-tube voltmeter.

to the rms value of the applied voltage. To achieve such a response, the rectifier that is used must have a square-law relation between the applied input voltage and the mean rectified current. Such voltmeters may therefore be used to measure the rms values of

voltages, regardless of what the wave form may be.

The basic circuit of such an instrument is given in Fig. 22-1, which is essentially a conventional thermionic vacuum-tube circuit, except that an auxiliary d-c circuit is applied across the indicating milliammeter in the plate circuit in order to balance out the steady component of the tube current when the input voltage is zero. In this way, the milliammeter reads the average rectified current that results when the a-c voltage is applied to the input terminals.

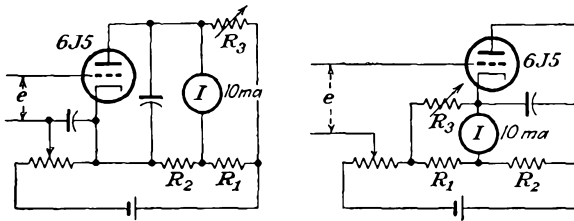


FIG. 22-2. Vacuum-tube voltmeters with balanced output.

It is possible to arrange the circuit in such a way that the tube forms one arm of a balanced Wheatstone bridge. In this way, the static operating current may be balanced out without the need for a separate d-c source. Two such circuits are illustrated in Figs. 22-2. In these circuits, to achieve good sensitivity, the resistor  $R_3$  must be made large in comparison with the meter resistance.

A characteristic which is closely square law for a limited range of applied voltage, and this is usually less than about 1 volt peak, may be obtained by operating a triode or a pentode on the curved portion of the characteristic curve. To ensure that the negative peak of the applied voltage will not approach too closely to the cutoff bias of the tube, the static plate current must be slightly greater than twice the increment of plate current required to produce full-scale deflection of the indicating meter. The situation is best understood by referring to Fig. 22-3, which illustrates the operation of the above circuits.

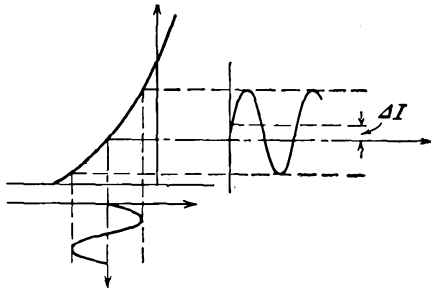


FIG. 22-3. Illustrating the operation of an rms voltmeter.

Values of applied voltage higher than 1 volt peak may be measured without affecting the square-law property of the voltmeter by using a voltage divider across the source of voltage and applying a known small fraction of the total voltage to the input terminals. When this is done, however, the desirable property of very high input impedance is lost.

In general, also, the calibration of this type of instrument is dependent upon the tube maintaining its square-law characteristic. As a result, frequent calibration is usually necessary.

*Average-reading voltmeters.* The response of an average-reading voltmeter is proportional to the average value of the input voltage. To achieve such a response, there must be a linear relation between the applied input voltage and the mean rectified current of the rectifier that is used. But as the mean rectified current is proportional to the mean of the positive excursions of the applied voltage, the instrument is dependent on the wave form of the input voltage.

The rectifier that is employed may be either a simple diode rectifier without a shunt capacitor, a diode bridge circuit, or a biased triode or

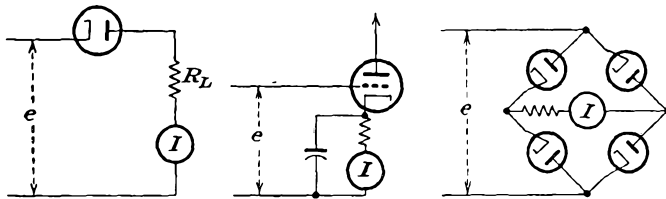


FIG. 22-4. The circuits of several average-reading vacuum-tube voltmeters.

pentode that is operated from approximately cutoff over the linear portion of the dynamic curve. Owing to the fact that the dynamic curve is nonlinear at low voltage levels, a substantially linear response is obtained only for relatively large values of applied voltage. The linearity may be considerably improved by using a large load resistor in the diode circuit or by the use of a high plate resistor and negative feedback in the case of triodes or pentodes. Several circuits of such average-reading voltmeters are given in Fig. 22-4.

Since the reading of these voltmeters is dependent upon the wave form of the input voltage wave, then when the applied voltage is not a sine wave or other symmetrical wave form, a reversal of the polarity of the input wave will, except for the bridge circuit, change the reading of the instrument. This effect is known as *turnover*.

*Peak-reading voltmeters.* The response of a peak-reading voltmeter is proportional to the peak value of the applied voltage and is, therefore, independent of the wave form when it is calibrated in peak volts. Peak-reading voltmeters may be calibrated to read rms values for sinusoidal voltages, which then correspond to 0.707 of the peak value. A number of peak-reading voltmeters are possible. They include diode, grid-leak, feed-back, and slide-back types.

The *diode peak voltmeter* provides one of the most convenient and accurate methods of measuring peak voltages, especially at radio frequencies.

It consists of a conventional diode rectifier provided with a capacitor input filter. The capacitance that shunts the load resistance is so chosen that the time constant of the circuit is large compared with the period of the applied voltage. A nonlinearity exists for low input voltages which causes an error, but the indication is linear for voltages above about 10 volts. The circuits of two such voltmeters are shown in Fig. 22-5.

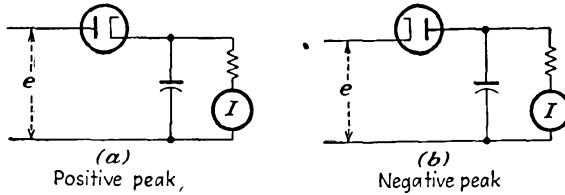


FIG. 22-5. Peak-reading voltmeters.

The shortcoming of these voltmeters is that the input impedance during the conducting portion of the cycle is different from that during the non-conducting portion of the cycle. This difference arises from the fact that the diode consumes power during the conducting portion of the cycle. This effect is precisely that discussed in Sec. 16-3, where it was shown that the effective input resistance to the diode  $R_e = R/2\eta$  and is approximately  $R/2$ , where  $R$  is the load resistance. Ordinarily  $R$  is so large that voltage

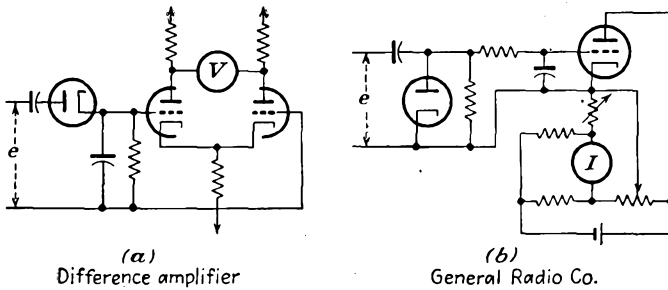


FIG. 22-6. Diode peak voltmeters with d-c amplifier.

fluctuations which might result from such a changing load impedance are negligible.

When the rectified current through the load resistance is too small to be measured conveniently by a d-c microammeter, the voltage developed across the load resistance may be applied to the input of a d-c amplifier. Several such circuits are illustrated in Fig. 22-6. In circuit *a*, a difference amplifier with  $e_2 = 0$  is used as the d-c amplifier. In circuit *b*, a single tube balanced amplifier is used.

The *grid-leak peak voltmeter* consists of a grid-circuit rectifier employing either a triode or a pentode. Rectification occurs in the grid-cathode

circuit in the same manner as in a diode, and grid current flows over the positive half cycle of the applied voltage. The input impedance is substantially the same as that of the diode peak-reading voltmeter.

A *negative feed-back peak voltmeter* consists essentially of a self-biased tube which operates from approximately cutoff over the linear portion of the dynamic curve. To maintain the tube almost at cutoff for all except the peak portions of the cycle, the bias resistor must be shunted by a capacitor which is adequate for essentially class B operation. As a result, the plate current flows only at the positive peaks of the applied voltage. The indications on this type of voltmeter are dependent on the wave form. Since the grid is not driven positive over any portion of the cycle of the applied voltage, the input impedance of the voltmeter is high.

The circuit connections of such a voltmeter for use with either a 6J7 or a 954 Acorn tube, depending upon the frequency range required, are shown in Fig. 22-7. The 6J7 is satisfactory for use to several megacycles, but where the voltmeter is intended for use across high-impedance tuned circuits at frequencies as high as 10 megacycles, and in cases where the input capacitance must be kept small, the 954 is used. Note that the tube is connected as a triode, with the suppressor connected to the cathode.

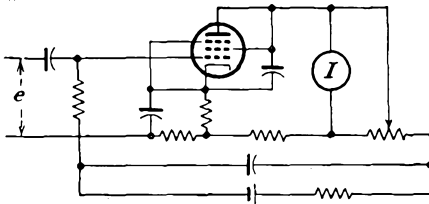


FIG. 22-7. A negative feed-back peak voltmeter.

This instrument may be used to measure d-c voltages by omitting the blocking capacitor in the input, although a separate calibration must be used.

The *slide-back voltmeter* consists essentially of a threshold indicator, this threshold being indicated by a d-c voltmeter when the d-c voltage is made equal to the peak value of the applied potential. The circuit of the instrument is illustrated in Fig. 22-8. The triode or pentode is operated at a very low value of plate current, and the bias is read on the d-c voltmeter. The voltage to be measured is then applied to the input terminals, and the grid bias is increased until the plate current is reduced to its initial value. The peak of the applied voltage is then equal to the increase of grid bias, as obtained from the d-c readings.

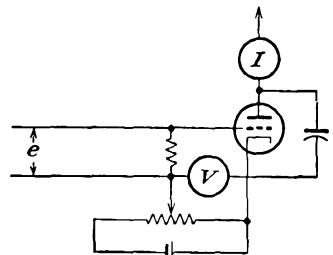


FIG. 22-8. A slide-back peak voltmeter.

This type of voltmeter is true peak-reading, and owing to the method of operation it is self-calibrating. It is completely independent of varia-

tions in operating voltages and tube characteristics. Moreover, it has a very high input impedance and operates over a very wide range of voltages simply by changing the slide-back voltage. Because of the method of operation, such voltmeters are restricted to steady sources of potential.

*Logarithmic voltmeter.* A voltmeter with a logarithmic scale is possible by using a variable-mu tube in which the amplification factor is an exponential function of the grid voltage. Thus for such a tube circuit

$$\frac{e_2}{e} = Ae^{aE_c} \tag{22-1}$$

where  $a$  and  $A$  are constants and  $E_c$  is the d-c bias on the tube.

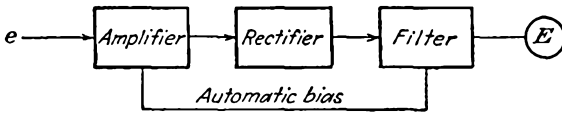


FIG. 22-9. Block diagram of a logarithmic voltmeter.

In this voltmeter, the output is maintained constant by rectifying and filtering the output and using the resulting d-c voltage to bias the amplifier tube. That is, with  $e_2$  constant,

$$E_c = K - \frac{1}{a} \log_e e$$

But since

$$db = 20 \log_{10} \frac{e_2}{e} = K' - 8.69 \log_e e$$

then

$$db = K' - 8.69a(K - E_c)$$

or

$$db = k + mE_c \tag{22-2}$$

where  $K$ ,  $K'$ ,  $k$ , and  $m$  are constants. A block diagram of this circuit appears in Fig. 22-9.

In another type of instrument, illustrated in Fig. 22-10, use is made of the fact that the average diode current varies logarithmically with the input voltage to the variable-mu pentode, over a large range of input voltage.

*D-c voltmeters.* Most of the circuits considered as a-c voltmeters will operate to give a meter deflection for an input d-c potential applied directly to the grid of the tube. However, since rectification is not required for such an

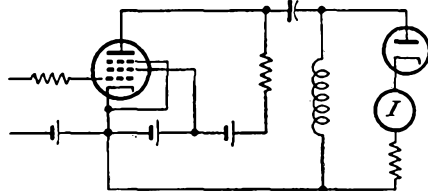


FIG. 22-10. A logarithmic voltmeter.

instrument, the tubes might be used for amplification and also to provide a very high input impedance.

The circuit of Fig. 22-11 is one which possesses a very high input impedance. The indicating instrument is a low-resistance milliammeter, having a resistance  $R_m$ . An analysis of the equivalent circuit shows that the meter current is

$$I_m = \frac{\mu R E}{[R + r_p + (\mu + 1)R_k](2R + R_m) - 2R} \quad (22-3)$$

where  $E$  is the d-c potential being measured. However, for a pentode

$$r_p \gg R \gg R_m \quad \mu \gg 1 \quad R_k \gg \frac{1}{g_m}$$

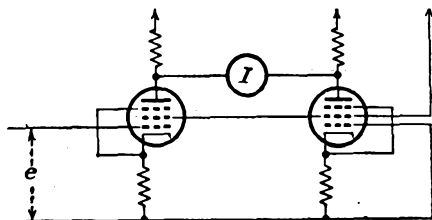


FIG. 22-11. A high-impedance d-c voltmeter.

and the current through the milliammeter is given by

$$I_m = \frac{E}{2R_k} \quad (22-4)$$

This shows that a linear relation exists between the applied potential and the reading of the indicating instrument.

A voltmeter employing triodes, which utilizes a high-resistance voltmeter as the indicating instrument, may be built using the simple difference amplifier. The circuit of such an instrument is given in Fig. 22-12. As shown in Sec. 6-9, the potential difference across the high-resistance indicating instrument is given by

$$E = \frac{\mu R}{2(r_p + R)} e \quad (22-5)$$

**22-2. Electronic Ammeters.** The oscilloscope may be used to measure currents, although an indirect method must be adopted. In this measurement, the current to be measured is passed through a calibrated resistor, the resulting voltage across the resistor being given on the oscilloscope screen. The current may then be calculated from the known voltage and resistance. However, owing to the fact that the input impedance of the oscilloscope is only moderately high, the oscilloscope is limited to the measurement of relatively high

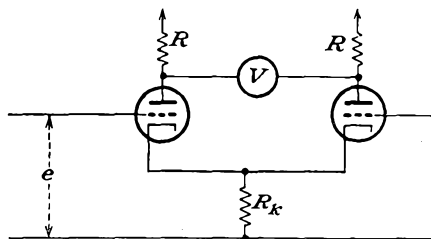


FIG. 22-12. A d-c voltmeter employing triodes.

currents, of the order of that possible with good-quality d-c instruments, say  $0.1 \mu\text{amp}$ .

*Electrometer Tubes.* The amplification properties of a vacuum tube may be used to amplify extremely small currents, which are then indicated on a sensitive galvanometer. In order to measure these small currents, it is essential that the grid current of the tube be very small compared with the currents to be measured. Normal tubes, if selected for quality, and if operated at reduced electrode voltages, are satisfactory over rather wide limits. Special tubes with unusually small values of grid current are available. These include, among others,

General Electric Co. FP-54	$I_g \sim 10^{-15}$ amp
Victoreen Inst. Co. VX-41	$I_g \sim 10^{-15}$ amp
Raytheon Mfg. Co. CX-570A	$I_g \sim 10^{-14}$ amp

A circuit utilizing a General Electric FP-54 electrometer tube and operating from a 12-volt storage battery is given in Fig. 22-13. Even though the FP-54 tube is a low-grid-current type, great care must be

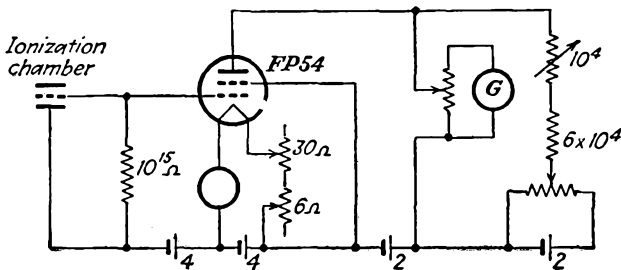


FIG. 22-13. An electrometer circuit using an FP-54 tube.

exercised in keeping leakage and surface currents to a minimum if high sensitivity and dependable operation are desired. This is frequently accomplished by incorporating the entire circuit in a suitable probe type of construction, which is shielded electrostatically and which is kept dry by the use of a drying agent. Also, the grid current is kept small by driving the circuit at low potential from batteries, the circuit being kept in continuous operation for long periods of time in order to reduce tube drift. With the simple circuit shown, the indicating instrument being a sensitive wall galvanometer, currents of the order of  $10^{-14}$  amp may be reliably measured.

**22-3. Phasemeters.** *Lissajous Patterns.* A Lissajous pattern is the figure created on an oscilloscope screen when sine-wave voltages are applied to both the horizontal and vertical deflecting plates. If the frequencies of these two component voltages are the same but differ in phase, the resulting pattern is a measure of the phase difference between the two waves.

To see that this is so, suppose that the voltage across the horizontal deflecting plates of the oscilloscope is denoted as

$$E_x = E_1 \sin(\omega t + \theta_1)$$

and that across the vertical deflecting plates is given by

$$E_y = E_2 \sin(\omega t + \theta_2)$$

Then

$$\frac{E_x}{E_1} = \sin \omega t \cos \theta_1 + \cos \omega t \sin \theta_1 \quad (22-6)$$

and

$$\frac{E_y}{E_2} = \sin \omega t \cos \theta_2 + \cos \omega t \sin \theta_2 \quad (22-7)$$

Now eliminate the time factor  $\omega t$ . To do this, multiply the first equation by  $\cos \theta_2$ , and subtract the second, multiplied by  $\cos \theta_1$ . This gives

$$\frac{E_x}{E_1} \cos \theta_2 - \frac{E_y}{E_2} \cos \theta_1 = \cos \omega t (\sin \theta_1 \cos \theta_2 - \cos \theta_1 \sin \theta_2)$$

Similarly, multiplying the first by  $\sin \theta_2$  and the second by  $\sin \theta_1$  and subtracting, there results

$$\frac{E_x}{E_1} \sin \theta_2 - \frac{E_y}{E_2} \sin \theta_1 = \sin \omega t (\cos \theta_1 \sin \theta_2 - \sin \theta_1 \cos \theta_2)$$

Squaring and adding these equations gives

$$\frac{E_x^2}{E_1^2} + \frac{E_y^2}{E_2^2} - \frac{2E_x E_y}{E_1 E_2} \cos(\theta_1 - \theta_2) = \sin^2(\theta_1 - \theta_2) \quad (22-8)$$

This is the equation of an ellipse whose principal axes coincide with the coordinate axes when  $\theta_1 - \theta_2 = \pi/2$ . Hence, in most cases, the result is an ellipse, the orientation of which depends upon the phase difference between the two waves. The results have the form illustrated in Fig. 22-14.

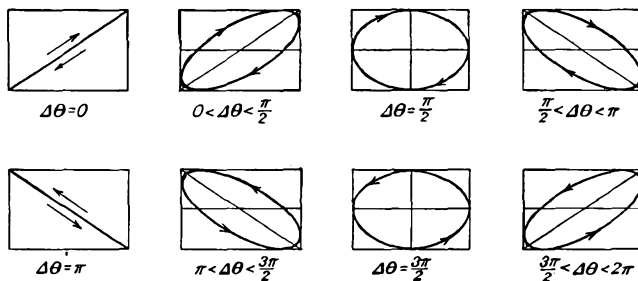


FIG. 22-14. Lissajous patterns showing the effect of the phase difference of two sources.

If the amplitudes of the voltage applied to the vertical and horizontal deflecting plates are equal, then the pattern at the phases  $\Delta\theta = \pi/2$  and  $3\pi/2$  will be circular. For the measurement of phase, it is customary to set the two amplitudes equal to each other, although this is not necessary.

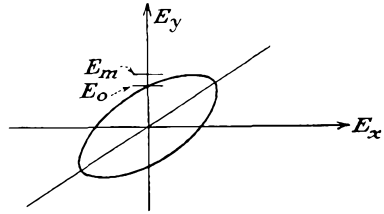


FIG. 22-15. To measure the phase difference between two voltages by means of the Lissajous pattern.

The experimental procedure necessary for measuring the phase difference between the two voltages is quite direct and consists in measuring the two distances  $E_0$  and  $E_m$  illustrated in Fig. 22-15. The distance  $E_0$  is evidently the value of  $E_y$  when  $E_x$  is zero. This requires that

$$E_0 = E_2 \sin (\theta_1 - \theta_2)$$

Likewise, the value of  $E_m$  is the maximum value of  $E_y$  and from Eq. (22-7) is given by

$$E_m = E_2$$

Solving these expressions simultaneously yields

$$\sin (\theta_1 - \theta_2) = \frac{E_0}{E_m} \tag{22-9}$$

*Electronic Phasemeter.* The elements of a simple electronic phasemeter are illustrated in Fig. 22-16. It will be observed that the circuit comprises in essence two diode peak-reading voltmeters which have been

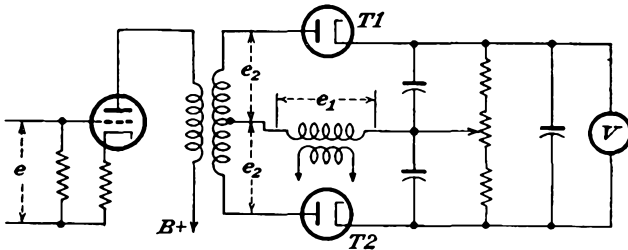


FIG. 22-16. An electronic phasemeter.

differentially connected. With no input signal, the voltages appearing across the input of each diode-voltmeter circuit arise only from the impressed reference voltage. When the circuit is balanced, a zero reading appears on the zero-center high-resistance voltmeter. This high-resistance voltmeter might be a d-c vacuum-tube voltmeter with a zero-center indicating instrument.

If now a voltage of preset amplitude is impressed across the input, the

potential at one anode decreases and becomes, say,  $e_1 - e_2$ , while the potential at the other anode increases and becomes  $e_1 + e_2$ . As a result, the output potentials will no longer be the same, and a reading will appear on the output voltmeter. The extent of the change will depend directly upon the phase of the input voltage with respect to the reference potential, being a maximum in one direction for zero phase difference, and being a maximum in the other direction for 180 deg phase difference, there being a calculable phase difference for every intermediate reading. The mathematical analysis parallels that of the f-m discriminator and follows below.

Suppose that the voltages  $e_1$  and  $e_2$  are

$$e_1 = E_s \sin \omega t \quad (22-10)$$

and

$$e_2 = E_s \cos (\omega t + \varphi) = E_s \sin \left( \omega t + \frac{\pi}{2} + \varphi \right) \quad (22-11)$$

The a-c potential that appears in the circuit diode  $T1$  is

$$e_a = e_1 + e_2$$

and that in the circuit of  $T2$  is

$$e_b = e_1 - e_2$$

But  $e_a$  may be written explicitly as

$$e_a = E_s \sin \omega t + E_s \cos (\omega t + \varphi)$$

which reduces to

$$e_a = 2E_s \cos \frac{1}{2} \left( \varphi + \frac{\pi}{2} \right) \sin \left[ \omega t + \frac{1}{2} \left( \varphi + \frac{\pi}{2} \right) \right]$$

Similarly

$$e_b = -2E_s \sin \frac{1}{2} \left( \varphi + \frac{\pi}{2} \right) \cos \left[ \omega t + \frac{1}{2} \left( \varphi + \frac{\pi}{2} \right) \right]$$

The corresponding d-c output potentials are then given by

$$\left. \begin{aligned} E_a &= 2\eta E_s \cos \frac{1}{2} \left( \varphi + \frac{\pi}{2} \right) \\ E_b &= 2\eta E_s \sin \frac{1}{2} \left( \varphi + \frac{\pi}{2} \right) \end{aligned} \right\} \quad (22-12)$$

where  $\eta$  is the detector efficiency (see Sec. 16-3). The corresponding indicating-voltmeter reading is then

$$E = E_a - E_b = 2\eta E_s \left[ \left| \cos \frac{1}{2} \left( \varphi + \frac{\pi}{2} \right) \right| - \left| \sin \frac{1}{2} \left( \varphi + \frac{\pi}{2} \right) \right| \right] \quad (22-13)$$

The result has the form illustrated in Fig. 22-17.

A somewhat similar type of phasemeter is possible using triodes.<sup>1</sup> A circuit is shown in Fig. 22-18. It is supposed that the two voltages  $e_1$  and  $e_2$  are of equal frequency and of constant amplitude. The equal voltages appearing across the secondaries of the input transformers are connected in series opposition so that, when the input voltages are in phase, the voltage across  $ab$  is zero. When the input potentials are slightly out of phase, a small voltage appears across  $ab$  the magnitude of which is proportional to the phase angle. For small angles this voltage may be considered to be 90 deg out of phase with either input.

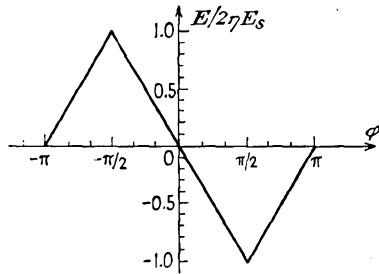


FIG. 22-17. The output of the phasemeter of Fig. 22-16.

The phase-shifting network causes a voltage  $e'$  which is 90 deg out of phase with  $e$ , the voltage across  $ab$ , to appear across  $cd$ . This voltage is applied across the grid resistor  $R$  and excites the grids of tubes  $T1$  and  $T2$ , which are connected in push-pull. Owing to the initial 90-deg phase shift and the added 90-deg shift, then for an a-c potential applied to the plates

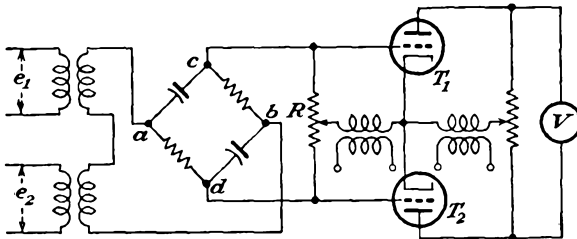


FIG. 22-18. A double-triode phasemeter.

the grid voltage of one tube is in phase with its plate, whereas the grid potential of the other is in phase opposition with the plate. As a result, one tube conducts, while the other is cut off, either because of a highly negative grid or because of a negative plate. The conduction causes the zero center instrument to deflect according to which tube conducts.

The instrument must be zero-set initially with no signal on the grids, whence the unidirectional pulses of plate current through the tubes divide equally through the plate resistor, so that zero resultant voltage appears across the d-c instrument. In this instrument, since  $e'$  is proportional to  $\theta$  for small angles, the magnitude of the voltage across the d-c instrument is proportional to  $\theta$ .

Should either  $e_1$  or  $e_2$  drop below or exceed normal rated voltage, the difference voltage  $ab$  increases in length and rotates. This sinor may

be resolved into two components, one of which is in phase with  $e$ , and will be effective in producing the voltage across the indicating instrument. The other component, which is 90 deg out of phase with  $e$ , will not appreciably effect the accuracy of the instrument.

**22-4. Wattmeters.** The circuit of an electronic wattmeter is given in Fig. 22-19. In this circuit, the resistors  $R_2$  are equal and sufficiently small

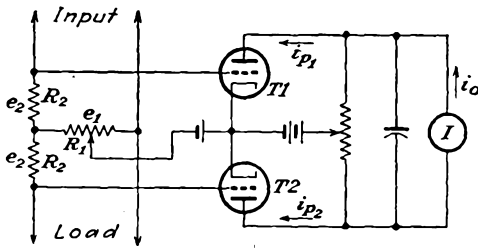


FIG. 22-19. An electronic wattmeter.

so that the voltage drop across them does not appreciably reduce the load voltage. The resistor  $R_1$  is high in order to prevent appreciable power loss.

To examine the operation, it is supposed that the first two terms of the series expansion adequately represent the dynamic characteristics of the tubes. Thus

$$i_{p1} = a_1(e_1 + e_2) + a_2(e_1 + e_2)^2 \tag{22-14}$$

and

$$i_{p2} = a_1(e_1 - e_2) + a_2(e_1 - e_2)^2 \tag{22-15}$$

The output meter reads the difference between  $i_{p1}$  and  $i_{p2}$ . Hence

$$i_0 \sim i_{p1} - i_{p2} = 2a_1e_2 + 4a_2e_1e_2 \tag{22-16}$$

But with

$$\left. \begin{aligned} ke_1 &= kE_m \cos \omega t \\ e_2 &= R_2 I = R_2 I_m \cos (\omega t + \theta) \end{aligned} \right\} \tag{22-17}$$

and since the indicating instrument reads the average, then

$$\begin{aligned} I_0 &= \frac{1}{T} \int_0^T i_0 dt \\ &= \frac{2a_1}{T} \int_0^T R_2 I_m \cos (\omega t + \theta) dt + \frac{4a_2 R_2 E_m I_m k}{T} \int_0^T \cos \omega t \cos (\omega t + \theta) dt \end{aligned}$$

so that finally

$$I_0 = 2ka_2 R_2 E_m I_m \cos \theta \tag{22-18}$$

If the load contains harmonics, it can be shown that the reading of the d-c meter is proportional to the total load.

**22-5. Frequency Meters. Lissajous Patterns.** If the component voltages that are applied to the horizontal and vertical deflecting plates of an oscilloscope differ in frequency, as well as in phase, the pattern that results is far more complicated than the simple ellipse that has already been considered. If the frequencies are in a constant ratio with each other, the

resulting patterns permit a comparison of the ratio of these frequencies. If one of these frequencies is known, the method permits a comparison of the unknown frequency with the given standard.

Suppose that a voltage  $E_x = E \sin \omega_1 t$  is applied to the horizontal

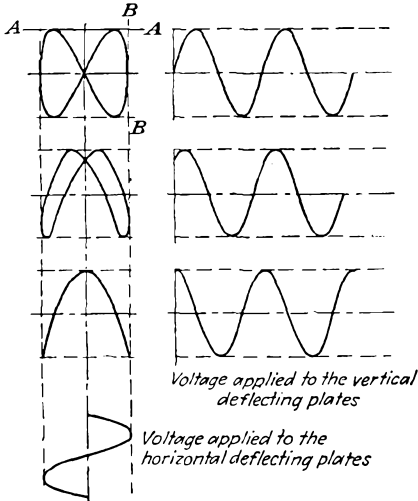


FIG. 22-20. Lissajous figure for 1:2 frequency ratio.

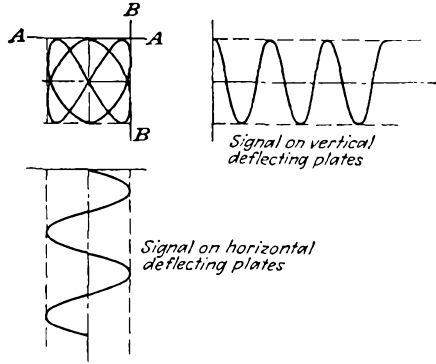


FIG. 22-21. Lissajous pattern for 2:3 frequency ratio.

plates and a voltage  $E_y = E \sin (\omega_2 t + \theta)$  is applied to the vertical plates. If the frequencies are in the ratio  $\omega_2/\omega_1 = 2$ , the form of the resulting patterns is readily calculated. The construction is illustrated in Fig. 22-20. In a similar way, if the frequencies are in the ratio 2:3, the Lissajous pattern assumes the form shown in Fig. 22-21.

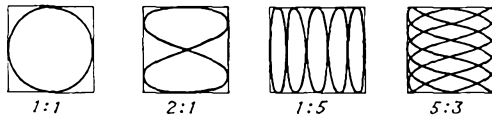


FIG. 22-22. A number of Lissajous patterns.

A feature that is common to all Lissajous figures is that the horizontal line  $AA$  and the vertical line  $BB$  are tangent to the pattern at a number of points, the number depending, respectively, on the frequency applied to the vertical and to the horizontal deflecting plates. Thus the frequency ratio

$$\frac{\omega_h}{\omega_v} = \frac{\text{no. of points at which the figure is tangent to the vertical line}}{\text{no. of points at which the figure is tangent to a horizontal line}}$$

A number of Lissajous patterns are contained in Fig. 22-22.

*Electronic Frequency Meters.* The circuit of such an electronic device is given in Fig. 22-23. The input causes periodic switching from  $T1$  to

T2. When the current begins to flow in  $T1$ , the potential across  $R_{k1}$

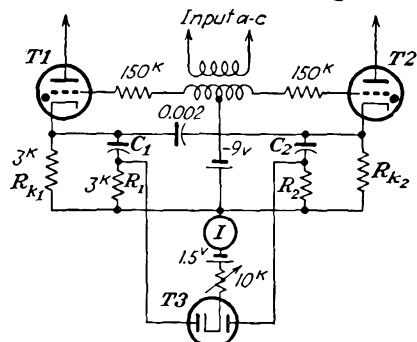


FIG. 22-23. An electronic frequency meter.

causes  $C_1$  to charge through the parallel paths  $R_1$  and one plate of the rectifier  $T3$ . The average diode current is indicated by the meter in series with the diode cathode. The diode current is proportional to the frequency, over the range for which  $C_1$  and  $C_2$  charge "fully" in less than the time of one half cycle of the impressed voltage. For the circuit shown, the calibration of the instrument is linear to approximately 7,000 cps.

### REFERENCES

As general references, see

Reich, H. J., "Theory and Application of Electron Tubes," McGraw-Hill Book Company, Inc., New York, 2d ed., 1944.

Langford-Smith, F., "Radiotron Designer's Handbook," Amalgamated Wireless Valve Co., 1941.

1. Mikelson, W., *Gen. Elec. Rev.*, **41**, 557 (1938).

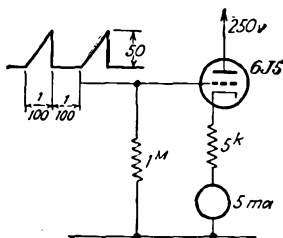
### PROBLEMS

22-1. The plate current in a 6SK7 tube with  $E_{cc2} = 100$ ,  $E_{bb} = 250$ , is approx:

$$I_b = 18e^{0.20E_c} \quad \text{ma}$$

This tube is used in a Ballantine voltmeter circuit. An a-c potential of 18 volts peak is applied. What must be the shift in bias potential if the voltmeter is to read correctly?

22-2. The voltage applied to the input of an average-reading vacuum-tube voltmeter has the form shown in the figure.



- a. What is the zero input reading of the d-c milliammeter?
- b. Calculate the reading when the signal is applied.
- c. If the input voltage were sinusoidal with the same peak amplitude, what would be the corresponding reading?

22-3. Show the connections for employing the multiplying circuit of Fig. 8-11 as an electronic wattmeter.

---

## APPENDIX A

### MILLMAN THEOREM

THE usual methods for the solution of the currents in or the potential differences across the elements of a network involve a direct application of Kirchhoff's laws. This involves setting up the mesh currents and then equating the sum of the potentials around any closed loop equal to zero. The number of independent loops that must be chosen must equal the number of unknown currents to be found. The resulting algebraic equations are then solved, ordinarily by using determinants, for the desired unknown quantities. If a large number of branches are involved, the resultant solution may become quite laborious. A network theorem suggested by Millman\* will frequently materially reduce the amount of work involved in effecting the solution.

Consider a general network of the form illustrated in Fig. A-1. The impedances  $Z_1$ ,  $Z_2$ , and  $Z_3$  terminate in the common junction  $O'$ . The

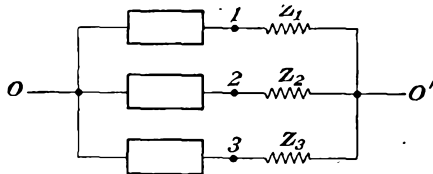


FIG. A-1. A general network for deriving the Millman theorem.

opposite ends of these impedances are numbered 1, 2, and 3. The point  $O$  is any other point in the network. It is not necessary to know the network interconnections between the points  $O$ , 1, 2, and 3. The network theorem states that the potential difference  $E_{00'}$  between points  $O$  and  $O'$  is given by

$$E_{00'} = \frac{E_{01}Y_1 + E_{02}Y_2 + E_{03}Y_3}{Y_1 + Y_2 + Y_3} \quad (\text{A-1})$$

where  $E_{0s}$  ( $s = 1, 2$ , or  $3$ ) is the potential difference between point  $O$  and the  $s$ th impedance and where  $Y_s = 1/Z_s$  is the admittance corresponding to the  $s$ th impedance. Note specifically that no requirements are imposed on the character of the element connected between points  $O$  and

\* Millman, J., *Proc. IRE*, **28**, 413 (1940).

$s$  and between which there exists the potential difference  $E_{0s}$ . The proof of the theorem follows.

The potential difference across impedance  $Z_1$  is

$$E_{10'} = E_{10} + E_{00'} = E_{00'} - E_{01}$$

The current through this impedance is, therefore,

$$I_{10'} = \frac{E_{10'}}{Z_1} = (E_{00'} - E_{01})Y_1$$

Similarly, the currents in the other two branches are given by

$$I_{20'} = \frac{E_{20'}}{Z_2} = (E_{00'} - E_{02})Y_2$$

and

$$I_{30'} = \frac{E_{30'}}{Z_3} = (E_{00'} - E_{03})Y_3$$

But from Kirchhoff's point law, the sum of the three currents  $I_{10'}$ ,  $I_{20'}$ ,  $I_{30'}$ , meeting at the point  $O'$ , must be zero. Then

$$(E_{00'} - E_{01})Y_1 + (E_{00'} - E_{02})Y_2 + (E_{00'} - E_{03})Y_3 = 0$$

from which Eq. (A-1) is readily obtained.

This result is not restricted to three impedances, as shown in Fig. A-1, but may be extended to any number  $n$  terminating in the common junction  $O'$ . The generalized result is

$$E_{00'} = \frac{\sum_{s=1}^n E_{0s} Y_s}{\sum Y_s} \quad (\text{A-2})$$

where the summation  $\sum_{s=1}^n$  denotes the summation of the  $n$  terms.

## APPENDIX B

### PLATE CHARACTERISTICS OF RECEIVING-TYPE TUBES

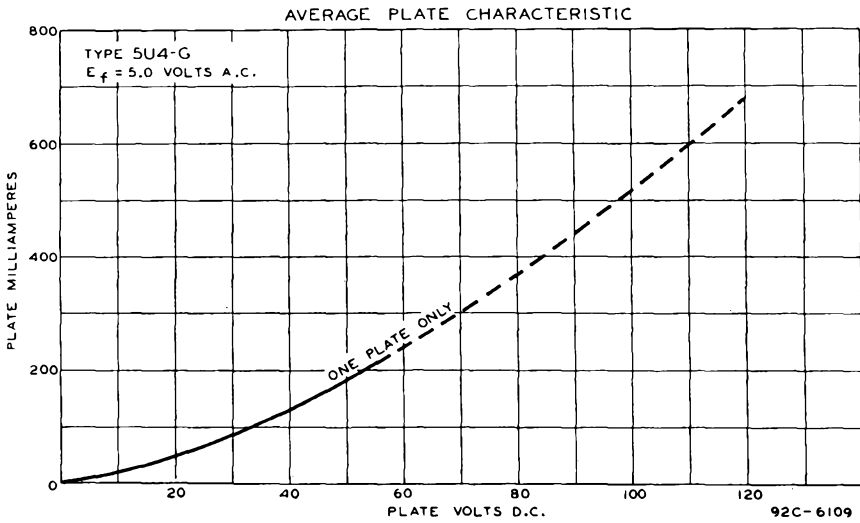


FIG. B-1. 5U4-G diode.

## AVERAGE PLATE CHARACTERISTICS

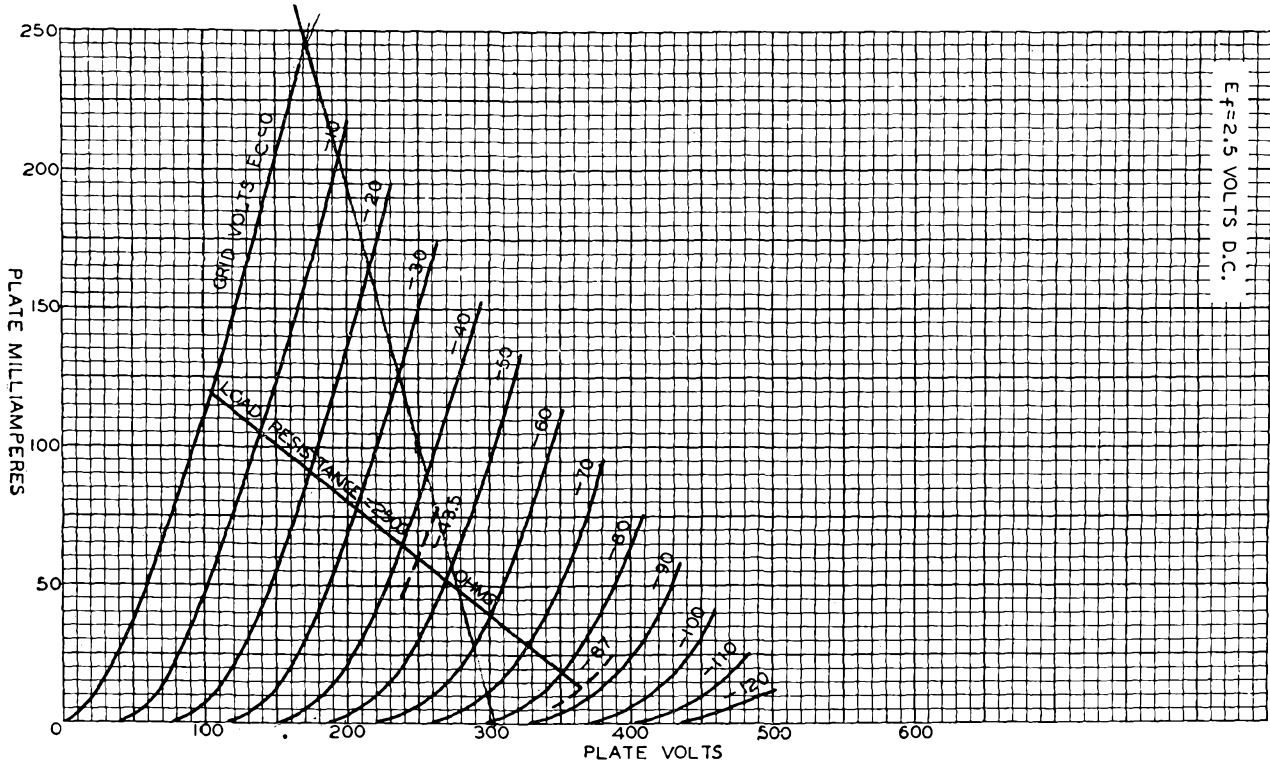


FIG. B-2. 2A3 triode.

Class A amplifier:  $E_b = 250$  volts,  $E_c = -45$  volts,  $I_b = 60$  ma,  $\mu = 4.2$ ,  $r_p = 800$  ohms,  $g_m = 5,250$   $\mu$ mhos.  
 Interelectrode capacitances:  $C_1 = 7$   $\mu$ f,  $C_2 = 5$   $\mu$ f,  $C_3 = 16$   $\mu$ f.

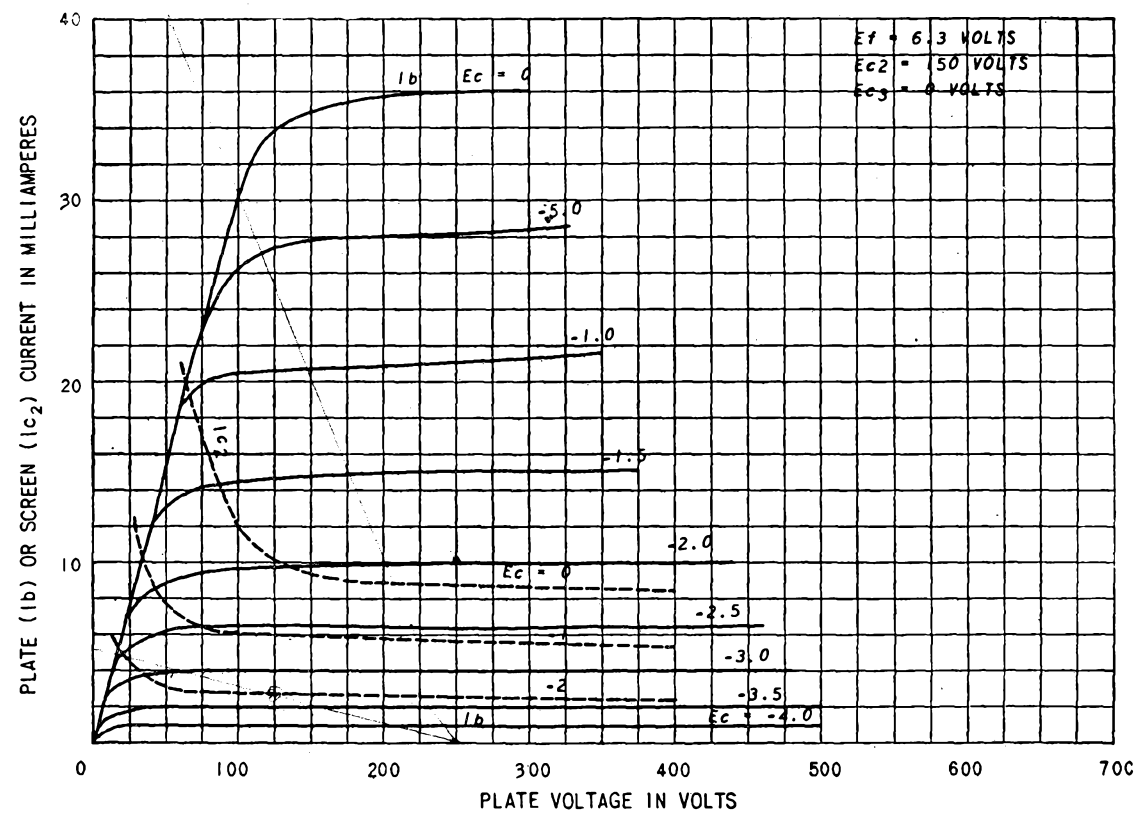


FIG. B-3. 6AC7 pentode.

Class A amplifier:  $E_b = 300$  volts,  $E_{c2} = 150$  volts,  $E_c = -2$  volts,  $I_b = 10$  ma,  $I_{c2} = 2.5$  ma,  $r_p = 1$  megohm approx,  $g_m = 9,000 \mu\text{mhos}$ . Interelectrode capacitances:  $C_1 = 11 \mu\mu\text{f}$ ,  $C_2 = 5 \mu\mu\text{f}$ ,  $C_3 = .015 \mu\mu\text{f}$ .

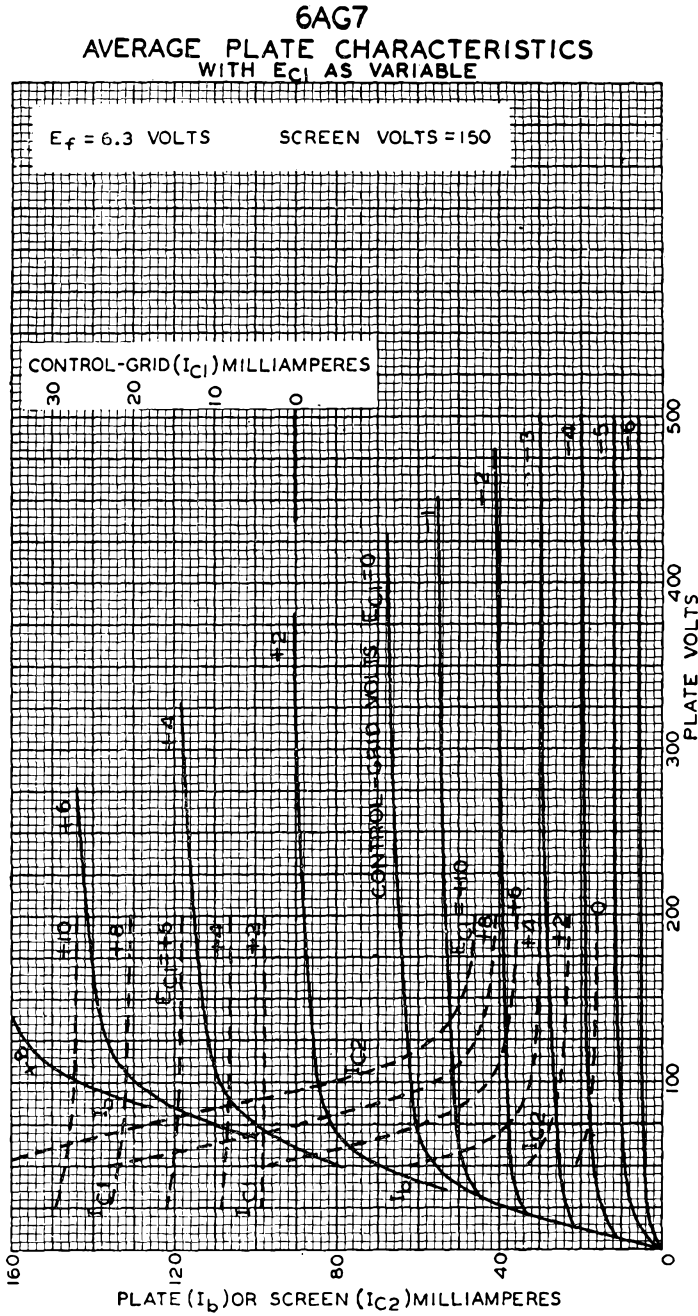


FIG. B-4. 6AG7 pentode.

Class A amplifier:  $E_b = 300$  volts,  $E_{c2} = 150$  volts,  $E_c = -3$  volts,  $I_b = 30$  ma,  $I_{c2} = 7$  ma,  $r_p = 0.13$  megohm approx,  $\mu_m = 11,000$   $\mu$ mhos.

Interelectrode capacitances:  $C_1 = 13$   $\mu$ mf,  $C_2 = 7.5$   $\mu$ mf,  $C_3 = 0.06$   $\mu$ mf.

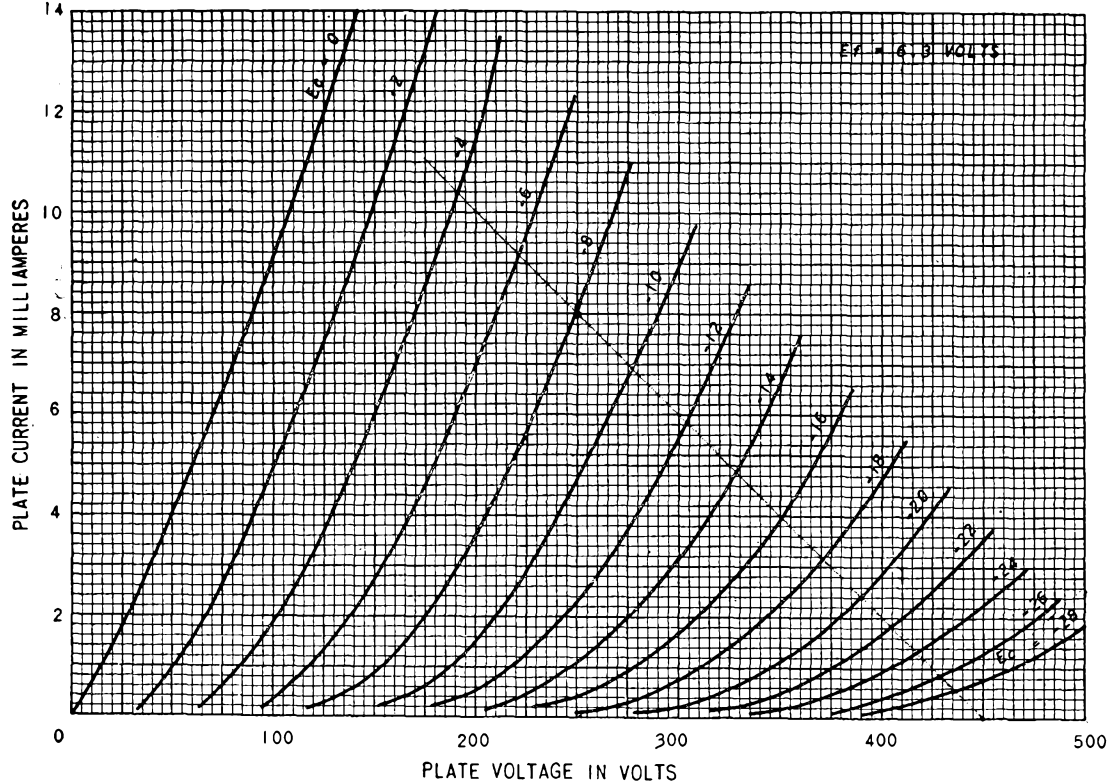


FIG. B-5. 6C5 triode.

Class A amplifier:  $E_b = 250$  volts,  $E_c = -8$  volts,  $I_b = 8$  ma,  $\mu = 20$ ,  $r_p = 10,000$  ohms,  $g_m = 2,000$   $\mu$ hos. Interelectrode capacitances:  $C_1 = 3$   $\mu$ mf,  $C_2 = 11$   $\mu$ mf,  $C_3 = 2.0$   $\mu$ mf.

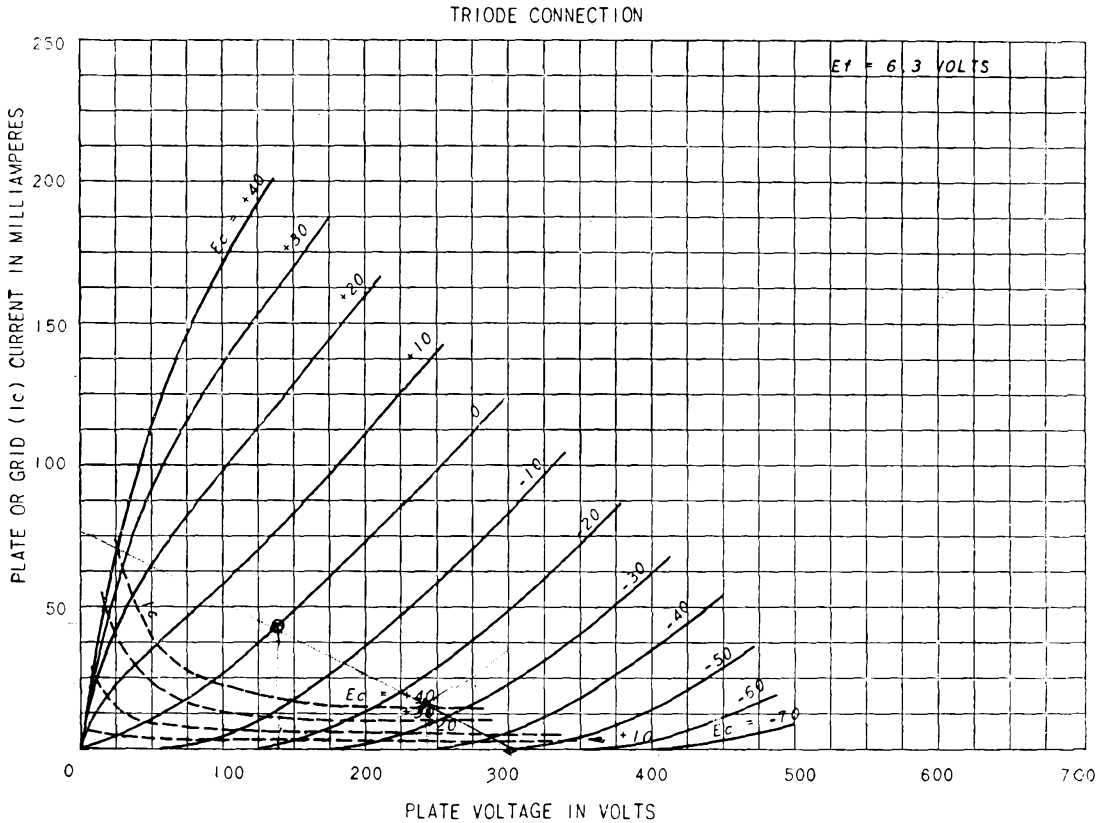
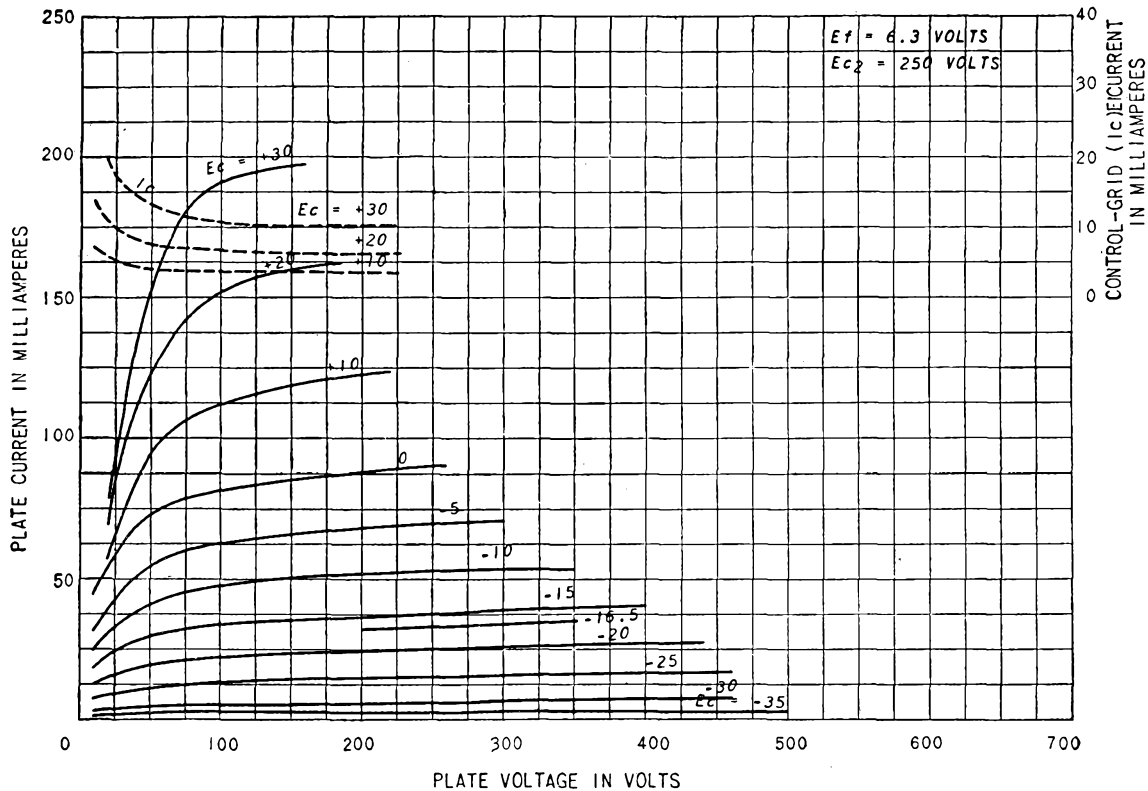


Fig. B-6. 6F6 triode (screen connected to plate).

Class A amplifier:  $E_b = 250$  volts,  $E_c = -20$  volts,  $I_b = 31$  ma,  $\mu = 6.8$ ,  $r_p = 2,600$  ohms,  $g_m = 2,600 \mu\text{mhos}$ .

PENTODE CONNECTION

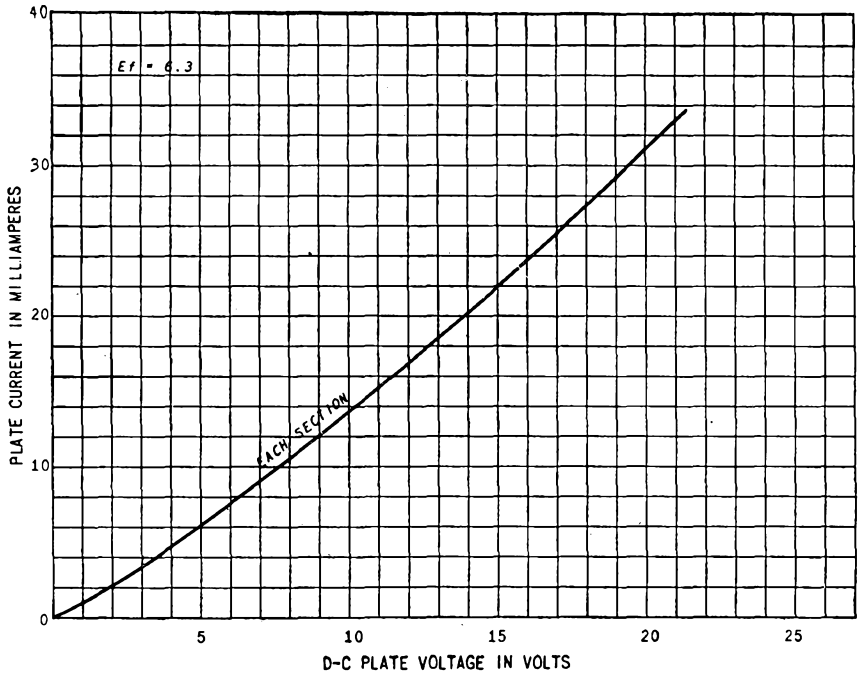


App. B]

PLATE CHARACTERISTICS

FIG. B-7. 6F6 pentode.

Class A amplifier:  $E_b = 250$  volts,  $E_{c2} = 250$  volts,  $E_c = -16.5$  volts,  $I_b = 34$  ma,  $r_p = 80,000$  ohms approx,  $g_m = 2,500$   $\mu$ mhos. Interelectrode capacitances:  $C_1 = 6.5$   $\mu$  $\mu$ f,  $C_2 = 13$   $\mu$  $\mu$ f,  $C_3 = 0.2$   $\mu$  $\mu$ f.



D-C PLATE VOLTAGE IN VOLTS  
FIG. B-8. 6H6 diode.

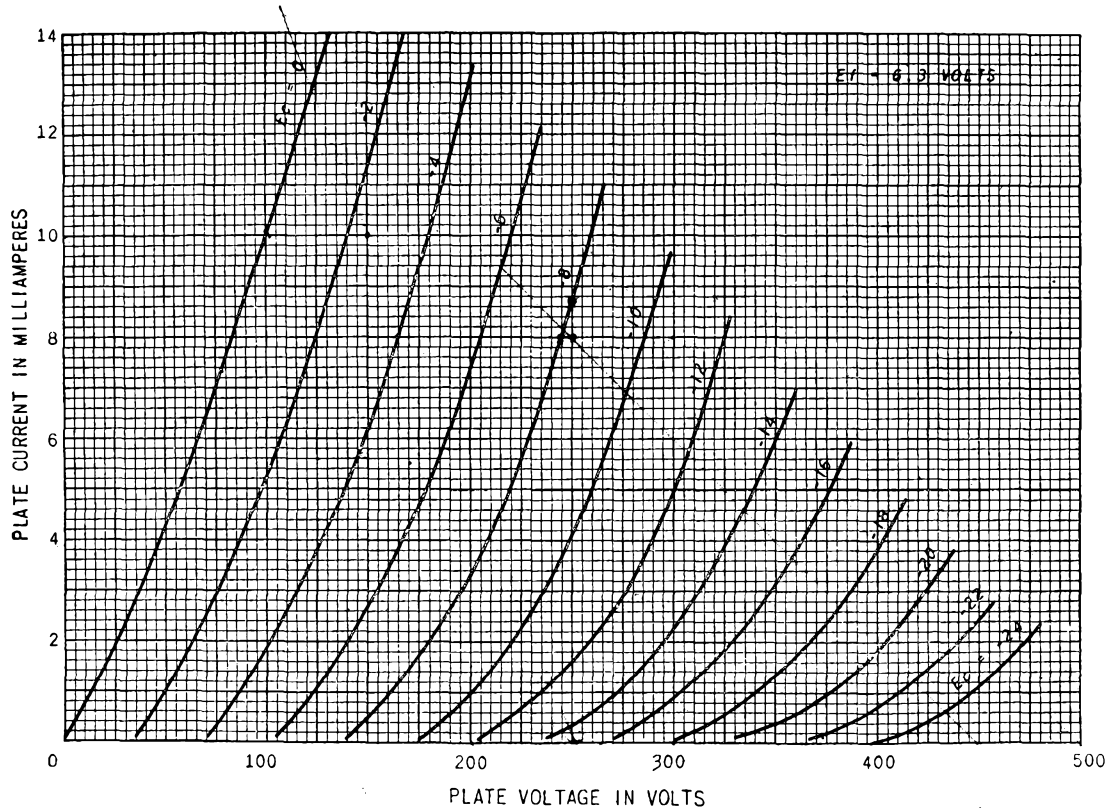


FIG. B-9. 6J5 triode.

Class A amplifier:  $E_b = 250$  volts,  $E_c = -8$  volts,  $I_b = 9$  ma,  $\mu = 20$ ,  $r_p = 7,700$  ohms,  $g_m = 2,600$   $\mu$ mhos.  
 Interelectrode capacitances:  $C_1 = 3.4$   $\mu$ mf,  $C_2 = 3.6$   $\mu$ mf,  $C_3 = 3.4$   $\mu$ mf.

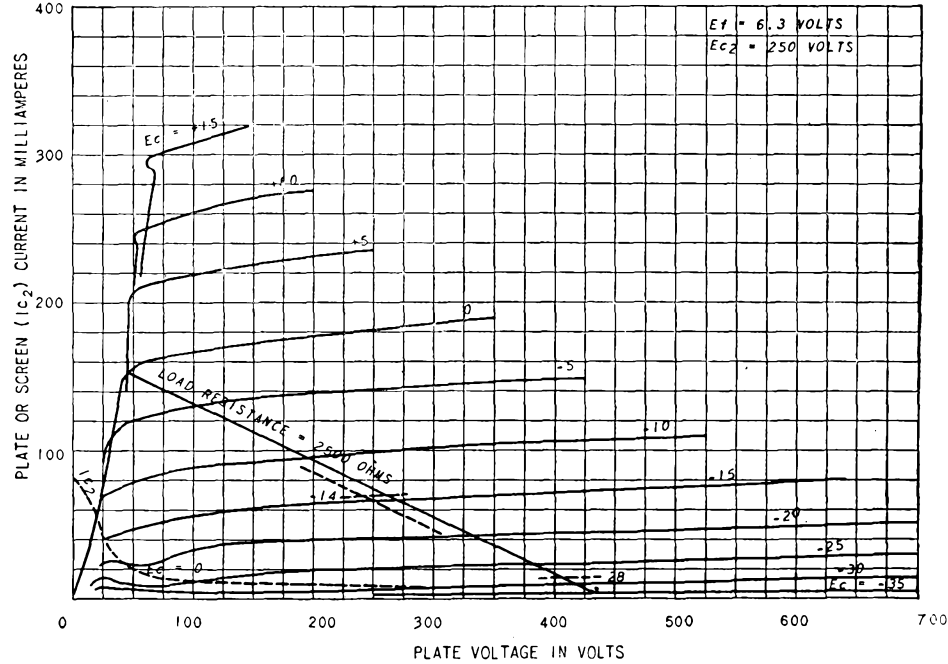


FIG. B-10. 6L6 beam tube.

Class A amplifier:  $E_b = 350$  volts,  $E_{c2} = 250$  volts,  $E_c = -18$  volts,  $I_b = 54$  ma,  $I_{c2} = 2.5$  ma,  $r_p = 33,000$  ohms approx,  $g_m = 5,200 \mu\text{mhos}$ .  
 Interelectrode capacitances:  $C_1 = 10 \mu\text{mf}$ ,  $C_2 = 12 \mu\text{mf}$ ,  $C_3 = 0.4 \mu\text{mf}$ .

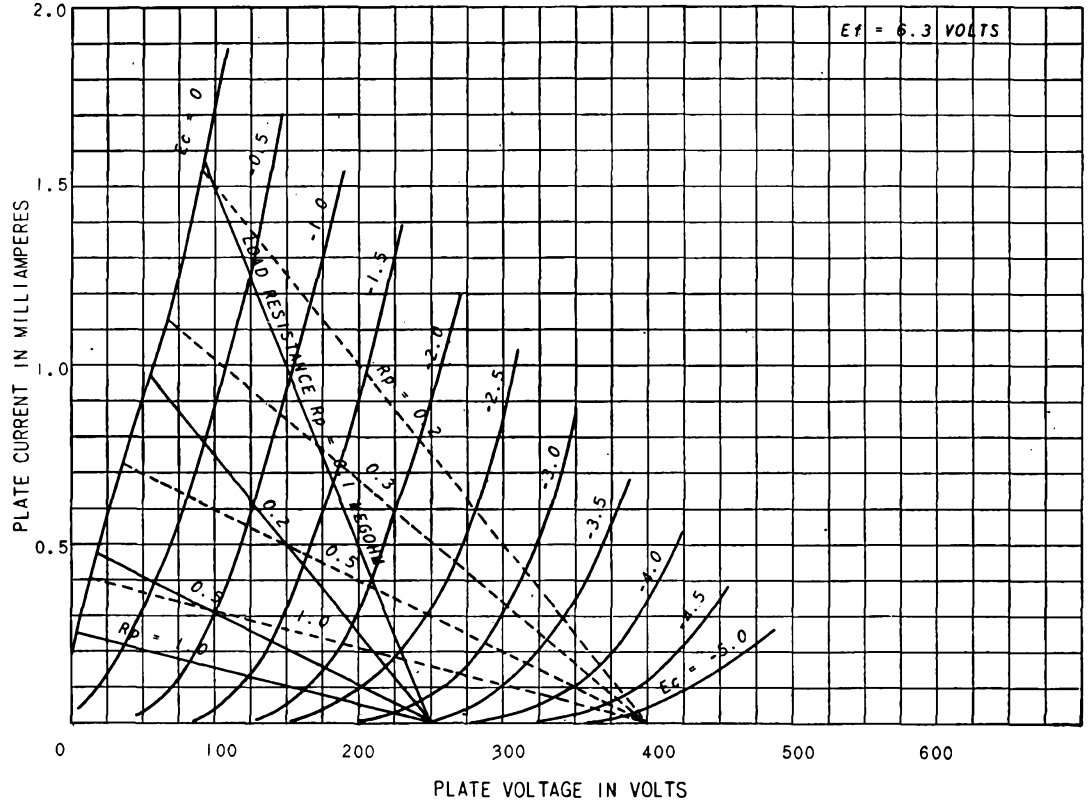


FIG. B-11. 6SF5 triode.

Class A amplifier:  $E_b = 250$  volts,  $E_c = -2$  volts,  $I_b = 0.9$  ma,  $\mu = 100$ ,  $r_p = 66,000$  ohms,  $g_m = 1,500 \mu\text{mhos}$ . Interelectrode capacitances:  $C_1 = 4.0 \mu\text{f}$ ,  $C_2 = 3.6 \mu\text{f}$ ,  $C_3 = 2.4 \mu\text{f}$ .

## AVERAGE PLATE CHARACTERISTICS

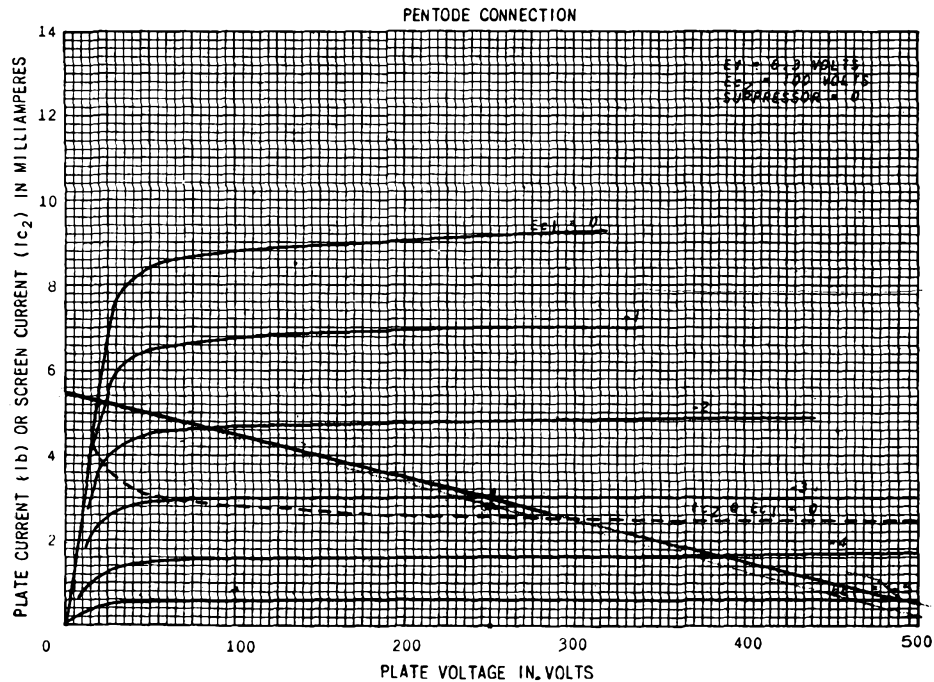


FIG. B-12. 6SJ7 pentode.

Class A amplifier:  $E_b = 250$ ,  $E_{c_2} = 100$  volts,  $E_c = -3$  volts,  $I_b = 3$  ma,  $I_{c_2} = 0.8$  ma,  $r_p = 1.0$  megohm approx;  $g_m = 1,650$   $\mu$ hos.

Interelectrode capacitances:  $C_1 = 6.0$   $\mu$ mf,  $C_2 = 7.0$   $\mu$ mf,  $C_3 = .005$   $\mu$ mf.

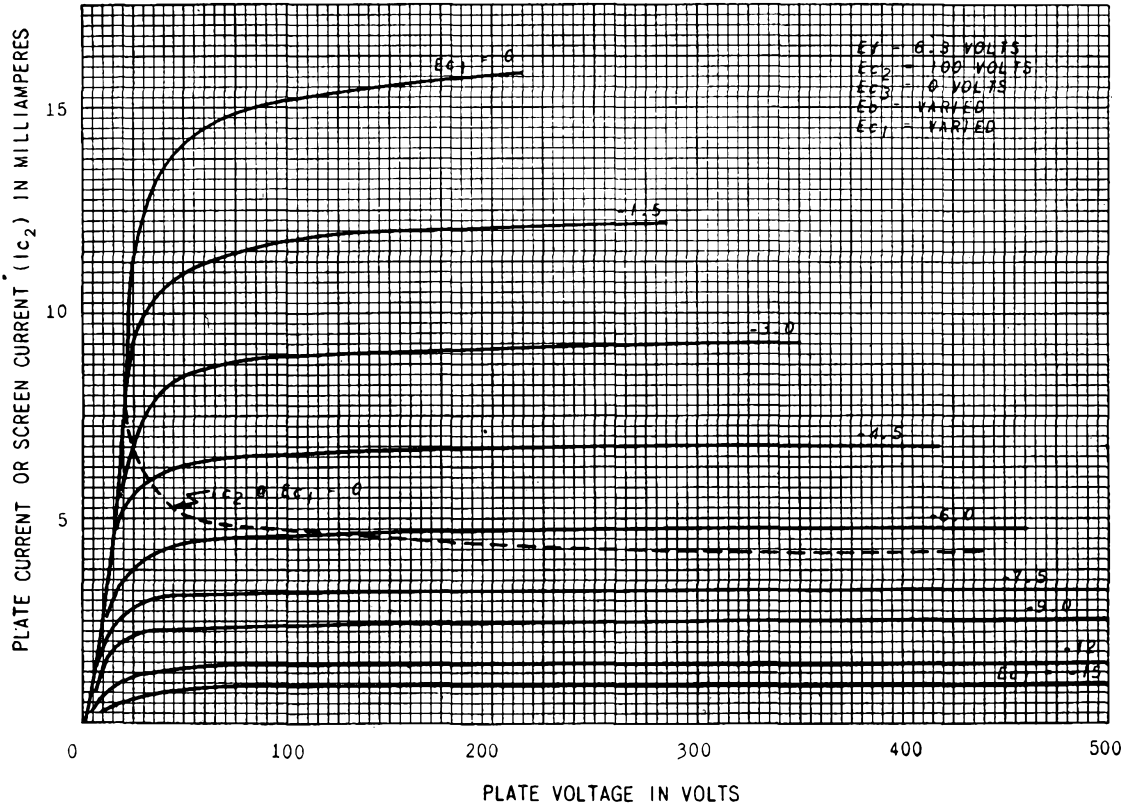


Fig. B-13. 6SK7 variable-mu pentode.

Class A amplifier:  $E_b = 250$  volts,  $E_{c2} = 100$  volts,  $E_c = -3$  volts,  $I_b = 9.2$  ma,  $I_{c2} = 2.6$  ma,  $r_p = 0.8$  megohm approx,  $g_m = 2,000$   $\mu$ mhos. Interelectrode capacitances:  $C_1 = 6.0$   $\mu$ mf,  $C_2 = 7.0$   $\mu$ mf,  $C_3 = .003$   $\mu$ mf.

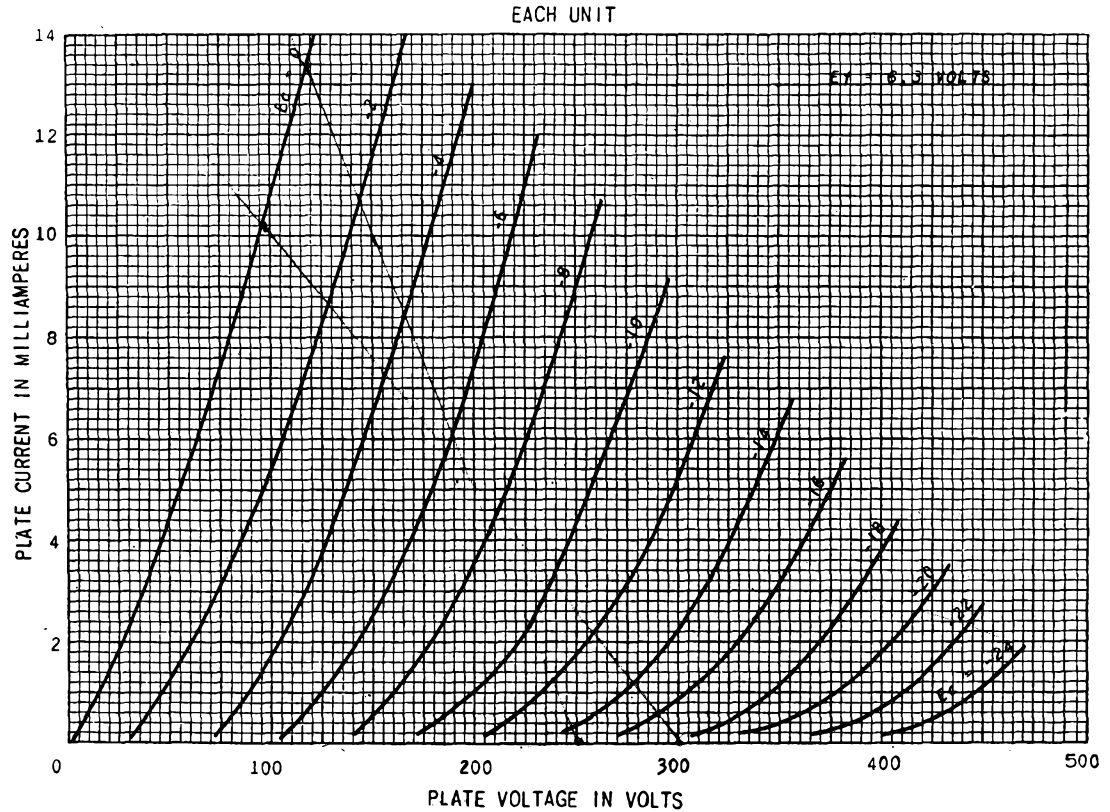


FIG. B-14. 6SN7-GT dual-triode.

Class A amplifier:  $E_b = 250$  volts,  $E_c = -8$  volts,  $I_b = 9$  ma,  $\mu = 20$ ,  $r_p = 7,700$  ohms,  $g_m = 2,600$   $\mu$ hos. Interelectrode capacitances: Unit 1:  $C_1 = 3.2 \mu\text{mf}$ ,  $C_2 = 3.4 \mu\text{mf}$ ,  $C_3 = 4 \mu\text{mf}$ . Unit 2:  $C_1 = 3.8 \mu\text{mf}$ ,  $C_2 = 2.6 \mu\text{mf}$ ,  $C_3 = 4 \mu\text{mf}$ .

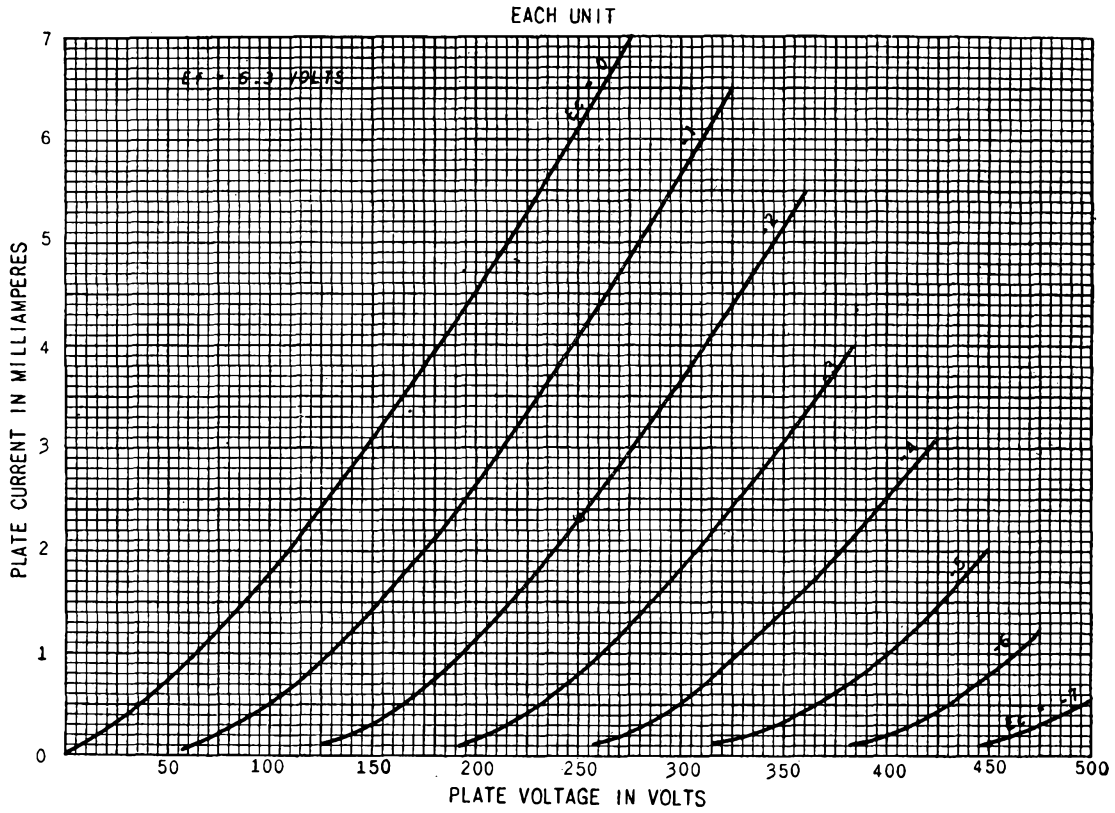


FIG. B-15. 6SL7-GT dual triode.

Class A amplifier:  $E_b = 250$  volts,  $E_c = -2$  volts,  $I_b = 2.3$  ma,  $\mu = 70$ ,  $r_p = 44,000$  ohms,  $g_m = 1,600$   $\mu$ mhos.  
 Interelectrode capacitances: Unit 1:  $C_1 = 3.0$   $\mu$ mf,  $C_2 = 3.8$   $\mu$ mf,  $C_3 = 2.8$   $\mu$ mf. Unit 2:  $C_1 = 3.4$   $\mu$ mf,  $C_2 = 3.2$   $\mu$ mf,  $C_3 = 2.8$   $\mu$ mf.

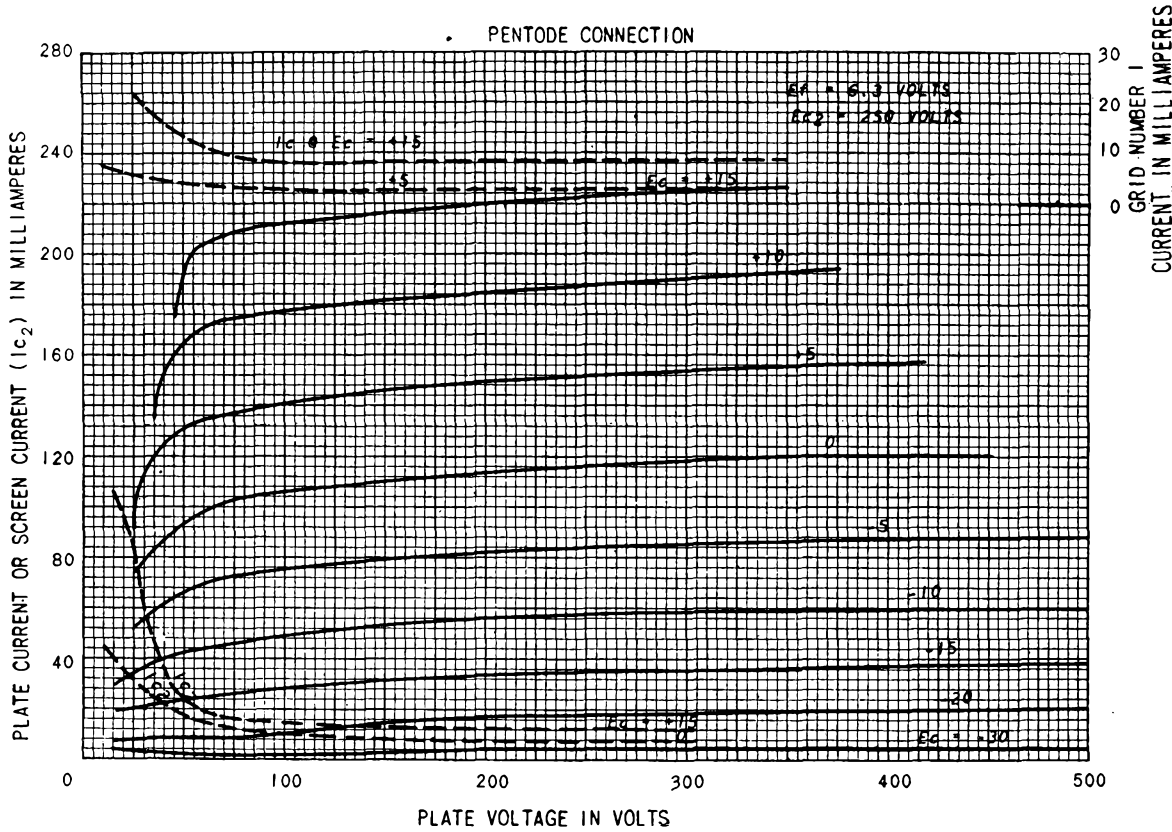


FIG. B-16. 6V6 beam tube.

Class A amplifier:  $E_b = 250$  volts,  $E_{c2} = 250$  volts,  $E_c = -12.5$  volts,  $I_b = 45$  ma,  $I_{c2} = 4.5$  ma,  $r_p = 52,000$  ohms approx,  $g_m = 4,100 \mu\text{hos}$ . Interelectrode capacitances:  $C_1 = 10 \mu\text{mf}$ ,  $C_2 = 11 \mu\text{mf}$ ,  $C_3 = 0.3 \mu\text{mf}$ .

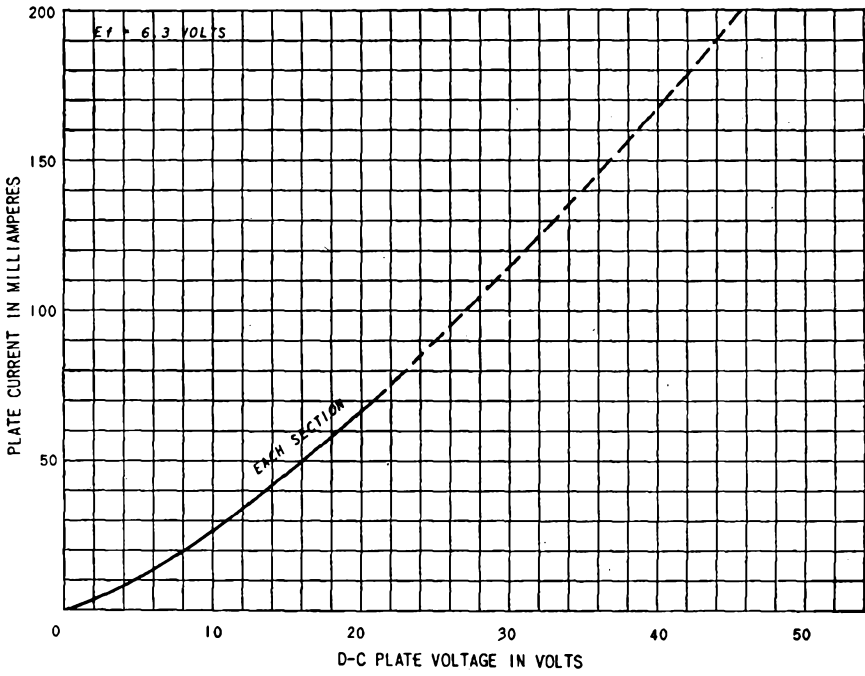


FIG. B-17. 6X5 triode.

CHARACTERISTICS OF TRANSMITTING TUBES

APPENDIX C

( $E_f = 7.5$  VOLTS D-C)

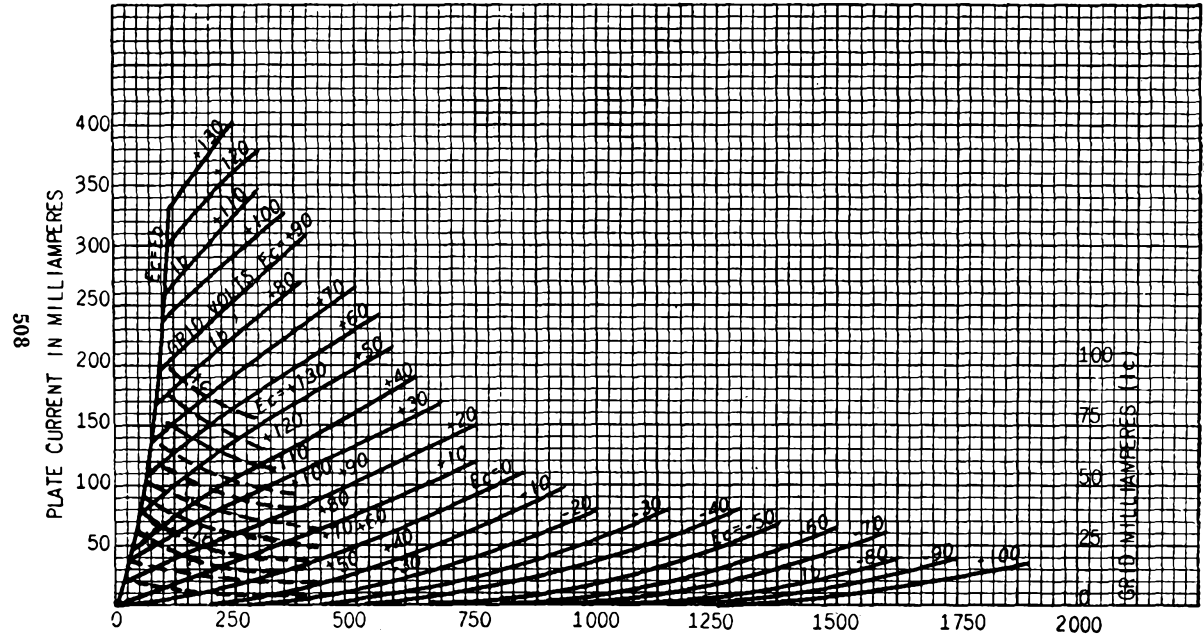


PLATE VOLTAGE IN VOLTS

Fig. C-1. 800 triode.

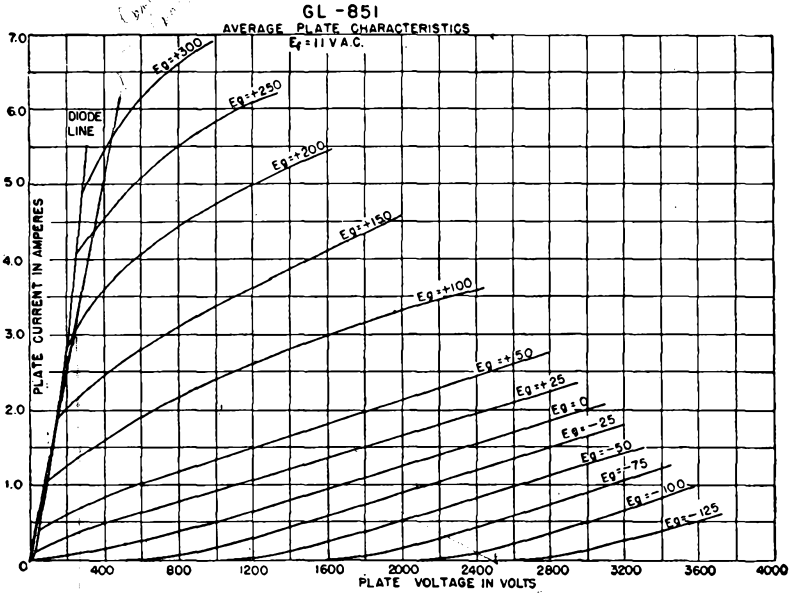


FIG. C-2. 851 triode.

b b



---

APPENDIX D  
TABLE OF BESSEL FUNCTIONS OF THE FIRST KIND

$n$	$J_n(1)$	$J_n(2)$	$J_n(3)$	$J_n(4)$	$J_n(5)$	$J_n(6)$	$J_n(7)$	$J_n(8)$	$J_n(9)$	$J_n(10)$	$J_n(11)$	$J_n(12)$	$J_n(13)$	$J_n(14)$	$J_n(15)$	$J_n(16)$	$J_n(17)$	$J_n(18)$	$J_n(19)$	$J_n(20)$
0	+0.7652	+0.2239	-0.2601	-0.3971	-0.1776	+0.1506	+0.3001	+0.1717	-0.0903	-0.2459	-0.1712	+0.0477	+0.2069	+0.1711	-0.0142	-0.1749	-0.1699	-0.0134	+0.1466	+0.1670
1	+0.4400	+0.5767	+0.3391	-0.0660	-0.3276	-0.2767	-0.0047	+0.2346	+0.2453	+0.0435	-0.1768	-0.2234	-0.0703	+0.1334	+0.2051	+0.0904	-0.0977	-0.1880	-0.1057	+0.0668
2	+0.1149	+0.3528	+0.4861	+0.3641	+0.0466	-0.2429	-0.3014	-0.1130	+0.1448	+0.2546	+0.1390	-0.0849	-0.2177	-0.1520	+0.0416	+0.1862	+0.1584	-0.0075	-0.1578	-0.1603
3	+0.0025	+0.1289	+0.3091	+0.4302	+0.3648	+0.1148	-0.1676	-0.2911	-0.1809	+0.0584	+0.2273	+0.1951	+0.0033	-0.1768	-0.1940	-0.0439	+0.1349	+0.1863	+0.0725	-0.0989
4	+0.0002	+0.0340	+0.1320	+0.2811	+0.3912	+0.3576	+0.1578	-0.1054	-0.2655	-0.2196	-0.0150	+0.1825	+0.2193	+0.0762	-0.1192	-0.2026	-0.1107	+0.0696	+0.1806	+0.1307
5		+0.0070	+0.0430	+0.1321	+0.2611	+0.3621	+0.3479	+0.1858	-0.0550	-0.2341	-0.2383	-0.0735	+0.1316	+0.2204	+0.1305	-0.0575	-0.1870	-0.1554	+0.0036	+0.1512
6		+0.0012	+0.0114	+0.0491	+0.1311	+0.2458	+0.3392	+0.3376	+0.2043	-0.0145	-0.2016	-0.2437	-0.1180	+0.0812	+0.2061	+0.1667	+0.0007	-0.1560	-0.1788	-0.0550
7		0.0002	+0.0025	+0.0152	+0.0534	+0.1296	+0.2336	+0.3206	+0.3275	+0.2167	+0.0184	-0.1703	-0.2406	-0.1508	+0.0345	+0.1825	+0.1875	+0.0514	-0.1165	-0.1842
8			+0.0005	+0.0040	+0.0184	+0.0565	+0.1280	+0.2235	+0.3051	+0.3179	+0.2250	+0.0451	-0.1410	-0.2320	-0.1740	-0.0070	+0.1537	+0.1959	+0.0929	-0.0739
9				+0.0004	+0.0055	+0.0212	+0.0589	+0.1263	+0.2149	+0.2919	+0.3089	+0.2304	+0.0670	-0.1143	-0.2200	-0.1895	-0.0429	+0.1228	+0.1947	+0.1251
10				+0.0002	+0.0015	+0.0070	+0.0235	+0.0608	+0.1247	+0.2075	+0.2804	+0.3005	+0.2338	+0.0850	-0.0901	-0.2062	-0.1991	-0.0732	+0.0916	+0.1865
11					+0.0004	+0.0020	+0.0083	+0.0256	+0.0622	+0.1231	+0.2010	+0.2704	+0.2927	+0.2357	+0.0999	-0.0682	-0.1914	-0.2041	-0.0984	+0.0614
12						+0.0005	+0.0027	+0.0096	+0.0274	+0.0634	+0.1216	+0.1953	+0.2615	+0.2855	+0.2367	+0.1124	-0.0486	-0.1762	-0.2055	-0.1190
13						+0.0001	+0.0008	+0.0033	+0.0108	+0.0290	+0.0643	+0.1201	+0.1901	+0.2536	+0.2787	+0.2368	+0.1228	-0.0309	-0.1612	-0.2041
14							+0.0002	+0.0010	+0.0039	+0.0120	+0.0304	+0.0650	+0.1188	+0.1855	+0.2464	+0.2724	+0.2364	+0.1316	-0.0151	-0.1464
15								+0.0003	+0.0013	+0.0045	+0.0130	+0.0316	+0.0656	+0.1174	+0.1813	+0.2399	+0.2666	+0.2356	+0.1389	-0.0008
16									+0.0004	+0.0016	+0.0051	+0.0140	+0.0327	+0.0661	+0.1162	+0.1775	+0.2340	+0.2611	+0.2345	+0.1452
17									+0.0001	+0.0005	+0.0019	+0.0057	+0.0149	+0.0337	+0.0665	+0.1150	+0.1739	+0.2286	+0.2559	+0.2331
18									0.0002	+0.0006	+0.0021	+0.0063	+0.0158	+0.0346	+0.0669	+0.1138	+0.1706	+0.2235	+0.2511	
19										+0.0002	+0.0008	+0.0025	+0.0068	+0.0166	+0.0354	+0.0671	+0.1127	+0.1676	+0.2189	
20											+0.0009	+0.0028	+0.0074	+0.0173	+0.0362	+0.0673	+0.1116	+0.1647		
21												+0.0003	+0.0010	+0.0030	+0.0079	+0.0180	+0.0369	+0.0674	+0.1106	
22												+0.0001	+0.0004	+0.0012	+0.0034	+0.0084	+0.0187	+0.0375	+0.0676	
23													+0.0001	+0.0004	+0.0004	+0.0013	+0.0036	+0.0089	+0.0193	+0.0381
24															+0.0005	+0.0015	+0.0039	+0.0094	+0.0199	

---

## INDEX

### A

- A supply, 64
- Abnormal glow discharge, 28
- Ammeters, electronic, 480
  - electrometer tubes, 481
- Amplification, voltage (*see* Amplifier, voltage-gain)
- Amplification factor, measurement of, 45
  - numerical values for several tubes, 492*ff.*
  - tetrode, 23
  - triode, 17
- Amplifier, audio-frequency, anode-follower, 108*ff.*
  - comparison with cathode follower, 111
  - gain, 109
  - input admittance, 110
  - output impedance, 109
- broad-band, anode-follower (*see* Amplifier, anode-follower)
- cathode-follower (*see* Amplifier, cathode-follower)
- compensated, high-frequency, 95*ff.*
- low-frequency, 101*ff.*
- direct-coupled (*see* Amplifier, direct-coupled)
- cascode, 314
- cathode-coupled, 113*ff.*
- cathode-follower, 102*ff.*
  - comparison with anode follower, 111
  - double, 120
  - gain, 104
  - input admittance, 107
  - output impedance, 107
- class A, beam power tubes in, 176
  - cascade, 68*ff.*
    - voltage gain of, 70
  - definition of, 53
  - degenerative (*see* Feedback)
  - distortion in, 169
  - dynamic characteristic of, 42
- Amplifier, class A, equivalent circuit for, 43*ff.*
  - (*See also* Equivalent circuit, linear class A)
  - grid-bias voltage in, 39
    - (*See also* Self-bias in amplifiers)
  - grid signal voltage in, 39
  - inductance-capacitance coupled (*see* Inductance-capacitance coupled amplifier)
  - input admittance of, 60*ff.*
  - inverse-feedback (*see* Feedback)
  - load line for, 41
  - load resistance for maximum power output from, 168
  - maximum power output from, 168, 173
  - output transformer in, 170
  - parallel operation in, 178
  - pentode in, 176
  - phase relations in, 42
  - plate dissipation, 174
  - plate efficiency of, 174
  - power output from, 168
  - push-pull (*see* Push-pull amplifier)
  - quiescent operating point for, 41
  - radio-frequency (*see* Tuned amplifiers)
  - resistance-capacitance coupled (*see* Resistance-capacitance coupled amplifier)
  - self-bias in (*see* Self-bias in amplifiers)
  - single-stage, 39*ff.*
  - tetrode in, 21*ff.*
  - transformer-coupled (*see* Transformer-coupled amplifiers)
  - tuned (*see* Tuned amplifiers)
  - voltage gain of (*see* Amplifier, voltage-gain)
- class AB, definition, 53
  - push-pull (*see* Push-pull amplifier)
- class B, definition, 53

- Amplifier, class B, push-pull (*see* Push-pull amplifier)
- tuned (*see* Tuned amplifiers, class B power)
- class C, definition, 53
- tuned (*see* Tuned amplifiers, class C power)
- compensated (*see* Amplifier, broad-band)
- computing (*see* Electronic computer circuits)
- degeneration in (*see* Feedback)
- difference (*see* Amplifier, cathode-coupled; Amplifier, direct-coupled)
- direct-coupled, 111*ff.*
- battery-coupled, 111
  - cathode-coupled, 113*ff.*
  - resistance-coupled, 112
  - series balanced, 121
- double-tuned (*see* Tuned amplifiers)
- driver stage for (*see* Push-pull amplifier)
- dynamic characteristic of, construction from static, 42
- equations of, 48
  - push-pull (*see* Push-pull amplifier, class A, composite dynamic characteristic of)
- in feed-back oscillator, 258
- feedback in (*see* Feedback)
- frequency characteristics of, 74
- frequency classification, 54
- frequency distortion (*see* Frequency distortion)
- frequency response of (*see* Frequency distortion)
- extension of (*see* Amplifier, broad-band)
- gain (*see* Amplifier, voltage-gain)
- graphical analysis of output, 41
- grid-base voltage of, 40
- (*See also* Self-bias)
- grid signal voltage in, 40
- grounded-grid, 122
- harmonic distortion in (*see* Nonlinear distortion)
- interelectrode capacitances in, 58
- intermediate-frequency (*see* Tuned amplifiers, class A)
- internal impedance of, effect of feedback on, 86*ff.*
- Amplifier, inverse-feedback (*see* Feedback)
- back)
  - inverted, 122
  - limiters (*see* Limiter, amplitude)
  - linear, class B (*see* Tuned amplifiers, class B power)
    - conditions for, 43, 216
  - load line for, 41
  - maximal flatness in (*see* Tuned amplifiers, class A, double-tuned)
  - modulated (*see* Modulator, amplitude, amplifier as)
  - for modulated wave (*see* Tuned amplifier, class B power)
  - narrow-band (*see* Tuned amplifiers)
  - oscillations in, 89
  - output impedance, anode follower, 109
    - cathode follower, 107
    - effect of feedback on, 88
  - output transformer in, 170
  - output wave form, 42
  - parallel or shunt-feed, 76
  - path of operation in, 41, 217, 223
  - phase characteristic of, 74
  - phase-inverter, 187
  - phase relations in, 42
  - plate-circuit efficiency (*see* Plate-circuit efficiency)
  - plate-current components, 42, 49
  - plate dissipation (*see* Plate dissipation)
  - plate-modulated (*see* Modulator, amplitude, amplifier as)
  - power, 167*ff.*
    - (*See also* Push-pull amplifier; Tuned amplifier, class B power; Tuned amplifier, class C power)
  - power supply in, common, 64
  - push-pull (*see* Push-pull amplifier)
  - quiescent operating point for, 41
  - radio frequency (Tuned amplifiers)
  - regenerative (*see* Feedback)
  - resistance-capacitance coupled (*see* Resistance-Capacitance coupled amplifier)
  - resistance coupled (*see* Amplifier, direct-coupled).
  - shunt feed in, 170
  - stagger-tuned (*see* Tuned amplifiers; class A, stagger-tuned)
  - transformer-coupled (*see* Transformer-coupled amplifiers)

Amplifier, tuned (*see* Tuned amplifiers)  
   video (*see* Amplifier, broad-band)  
   voltage-gain, db gain, 56  
     effect of feedback on, 83  
     inductance-coupled, 76  
     interelectrode capacitances, effect of,  
       59  
     multistage amplifier, 70  
     resistance-capacitance coupling, 71  
     resistance coupling, 113  
     resistance load, 56  
     transformer coupling, 76  
     tuned, double-tuned, 200  
       single-tuned, direct coupling, 194  
       transformer coupling, 197  
 Amplitude distortion (*see* Nonlinear distortion)  
 Amplitude modulation (*see* Modulation, amplitude)  
 Angstrom unit, 5  
 Anode fall, 28  
 Anode follower (*see* Amplifier, anode-follower)  
 Arc, anode fall, 28  
   cathode fall, 27  
   cathode spot, 27  
   externally heated, 30  
   high-pressure, 31  
   initiation, grid control (*see* Thyratrons)  
   ignitor rod (*see* Ignitron rectifier)  
   mercury pool (*see* Mercury-arc rectifier)  
 Arc back in mercury rectifiers, 36  
 Argon, in high-pressure diodes, 31  
   in phototubes, 7  
   in thyratrons, 33  
 Automatic amplitude control, oscillators with, 258  
 Automatic volume control, 355

## B

B supply, 64  
 Backfire, 36  
 Balanced modulators (*see* Modulator, amplitude, balanced)  
 Band width, tuned amplifiers, 194, 195, 197  
   reduction in cascade stages, 205, 206  
   untuned amplifiers, 74, 95  
 Barkhausen criterion for oscillators, 247

Beam power tubes, 25  
 Beam resistance of tube, 133  
 Beat-frequency oscillator, 357  
 Beating (*see* Converter)  
 Bel, 55  
 Bessel functions, 367, 511  
 Bias, grid, 53  
   impedance, effect of, in amplifiers, 85  
 Bias control of thyratrons, 286  
 Bias phase control of thyratrons, 287  
 Bleeder resistance, 303  
 Blocking, oscillator (*see* Oscillators, relaxation, blocking)  
   in oscillators, 250  
 Blocking capacitor, 69  
 Bombardment by positive ions, 7, 28  
 Breakdown, gas tubes, 27  
   mercury-arc tubes, 28  
 Breakdown potential, 27  
 Bridge measurements of triode coefficients, 45  
 Bridge rectifier, 279  
 By-pass capacitor, 64

## C

C supply, 64  
 Capacitance, interelectrode, numerical values for several tubes, 492ff.  
   pentodes, 63  
   tetodes, 62  
   triodes, 58  
 Capacitor filters (*see* Filter, rectifier, capacitor)  
 Carrier suppression, 325  
 Carrier wave, disappearance of, in frequency modulation, 369  
   suppression of, 325  
 Cathode, directly heated, 4  
   indirectly heated, 4  
   inward-radiating, 4  
   mercury as, 28  
   oxide-coated, disintegration, 31  
     emission, 3  
     work function, 3  
   photoelectric, 4  
   power for heating, 64  
   thermionic (*see* Thermionic cathodes; Thermionic emission)  
   thoriated-tungsten, 3

- Cathode, tungsten, 3
- Cathode efficiency, 3
- Cathode fall, arc, 28  
glow discharge, 28
- Cathode follower (*see* Amplifier, cathode-follower)
- Cathode modulation (*see* Modulation, cathode)
- Cathode-ray tube, electrostatic deflection in, 442  
magnetic deflection in, 460  
sweep circuits for (*see* Sweep generators, for cathode-ray tubes)  
tracing speed of beam in, 442
- Characteristic tube curves, FG-27 (thyatron), 33  
FG-33 (thyatron), 33  
FG 98 (shield-grid thyatron), 34  
PJ 22 (vacuum photocell), 5  
PJ 23 (gas photocell), 6  
RCA OA4G (cold-cathode triode), 30  
2A3 (power triode), 492  
5U4 (double diode), 491  
6AC7 (television pentode), 493  
6AG7 (power pentode), 494  
6C5 (voltage triode), 495  
6F6 (power tube), 496, 497  
6H6 (duo diode), 498  
6J5 (voltage triode), 499  
6L6 (beam power tetrode), 500  
6SF5 (voltage triode), 501  
6SJ7 (voltage pentode), 502  
6SK7 (voltage supercontrol pentode), 503  
6SL7 (voltage duo-triode), 505  
6SN7 (voltage duo-triode), 504  
6V6 (beam power tetrode), 506  
6X5 (duo-diode), 507  
800 (transmitting triode), 508  
851 (transmitting triode), 509  
866 (mercury diode), 36  
884, 885 (thyatron), 33  
889A (transmitting triode), 19, 20
- Child's law, 11  
(*See also* Space-charge limited current)
- Choke input filters (*see* Filter, rectifier)
- Clamping circuit, continuously acting, 133  
switched, double-sided, 139  
single-sided, 139
- Class A amplifiers (*see* Amplifier, class A)
- Class B, C, amplifiers (*see* Push-pull amplifier; Tuned amplifiers, class B power; Tuned amplifiers, class C power)
- Class C modulated amplifier (*see* Modulator, amplitude, amplifier as)
- Clipping, circuit (*see* Limiter)  
side-band, in modulators, 323
- Cloud, electron (*see* Space charge)
- Coefficient, coupling, 201
- Coil,  $Q$  of, 194
- Cold-cathode triodes, 30
- Collisions, in arc tubes, 28  
ionizing, 7  
by positive ions, 7
- Colpitts oscillator, 253
- Compensated amplifiers (*see* Amplifiers, broad-band)
- Composite characteristics, push-pull, dynamic, 184  
static, 181
- Computer circuits (*see* Electronic computer circuits)
- Condensed mercury temperature and vapor pressure, 30
- Conductance, mutual, 17
- Conduction, gaseous, 27*ff.*  
(*See also* Arc)
- Constant-current characteristic, 20, 225
- Constants, multielectrode tube, 23  
triodes, 18
- Controlled rectifiers, applications of, 281  
filter for, 304  
ignitron, 288  
thyatrons, average current, 283  
bias control, 286  
bias phase control, 287  
on-off control, 287  
phase-shift control, 285  
circuits, 286  
circle diagram of, 286  
voltage across tube, 284
- Conversion, theory, general, 259  
transconductance, 358  
square-law, 358
- Converter, pentagrid, 360
- Counter circuits (*see* Trigger circuits)
- Coupling, amplifier, impedance, 75  
resistance, 68

- Coupling, amplifier, resistance-capacitance, 112  
 transformer, 76  
 coefficient, critical, 201  
 transitional, 203  
 networks, design of, 214
- Critical grid control curves, 33
- Critical inductance, filters, 302
- Crystal oscillators (*see* Oscillators, crystal)
- Current density, 11
- Current feedback (*see* Feedback, current)
- Current-source equivalent circuit, 47
- Current-voltage locus, push-pull amplifier, 181  
 resistance load, 41
- Cutin, capacitor input filter, 297  
 inductance filter, 294  
 thyatron, 281
- Cutout, capacitor input filters, 297  
 controlled rectifiers, 282  
 inductance filter, 294  
 L-section filters, 302
- Cylinders, space charge limited current (*see* Space-charge limited current)
- D
- D-c amplifier (*see* Amplifier, direct-coupled)
- D-c restorer, 134  
 (*See also* Clamping circuit)
- Decibel gain, 55
- Decoupling filters in amplifiers, 65
- Deflection in cathode-ray tubes (*see* Sweep generators)
- Degenerative feedback (*see* Feedback, negative)
- Deionization, 36
- Delay, avc systems, 356  
 generation of time, 424*ff.*  
 linear delay multivibrator, 425  
 linear-sweep delay, 432  
 Miller integrating methods, 427  
 phantatron, 431  
 sanatron, 430  
 (*See also* Gate circuits)
- Delay distortion, 54
- Demodulation, 343*ff.*  
 definition of, 343  
 (*See also* Detection)
- Demodulator, definition of, 343  
 (*See also* Demodulation; Detection; Detector; Modulation)
- Detection, for amplitude-modulated waves, 343*ff.*  
 conversion, 357  
 definition of, 343  
 diode (*see* Detection, linear)  
 for frequency-modulated waves, 387  
 linear, 345  
 a-c to d-c impedance in, 353  
 distortion in, 351  
 effect of load on, 353  
 input impedance of, 350  
 rectification characteristic, 353  
 single-side-band, 357  
 square-law, 343  
 distortion in, 344  
 with triode, 343  
 suppressed-carrier, 357
- Detector, diode, 345  
 first (*see* Converter)  
 linear, 345  
 square-law, 343  
 (*See also* Demodulation; Detection)
- Deviation, frequency, in frequency modulation, 366
- Deviation ratio in frequency modulation, 366
- Difference amplifier, 113*ff.*, 146*ff.*  
 cascode type, 121, 147  
 cathode-coupled, 113, 146
- Differentiation, circuits, 128*ff.*  
 amplifiers, 161
- Diode, characteristics, operating, 12, 35  
 clipper, 123*ff.*  
 cylindrical, 12  
 detector, 345  
 discriminator, 387  
 high-pressure gas, 31  
 high-vacuum, as clamper, 133*ff.*  
 hot-cathode gas, 30  
 phasemeter, 483  
 plane parallel, 9  
 ratings, 12  
 as rectifiers (*see* Rectifiers)  
 square-law modulation with, 323  
 static characteristics, 11  
 voltmeter, 476
- Discharge, electrical, in gases (*see* Electrical discharge in gases)

- Discriminator for frequency modulation, 387
- Disintegration of cathodes, 31
- Disintegration voltage, 31
- Dissipation (*see* Plate dissipation)
- Distortion, amplitude (*see* Nonlinear distortion)
- in class A amplifiers, 54, 169
- causes of, 54
- permissible maximum, 171
- for push-pull operation, 185
- delay, 54
- feed-back effect on, 84
- frequency (*see* Frequency distortion)
- harmonic (*see* Nonlinear distortion)
- in linear detectors, 354
- in modulation, 337
- nonlinear (*see* Nonlinear distortion)
- phase, 54
- in square-law detection, 345
- Distributed capacitance, 79
- Doubler, frequency, 243
- voltage, 280
- Driver stage (*see* Push-pull amplifier, driver stages for)
- Dushman's equation, 2
- Dynamic characteristics, class A, 48
- construction of, 43
- general power series representation, 48
- nonlinear distortion, 48, 54
- parabolic, 48
- push-pull, 184
- rectifier, 272
- resistance load, 43
- Dynatron, 262
- oscillator (*see* Oscillators, negative-resistance)
- E
- Eccles-Jordan trigger circuit (*see* Trigger circuits, Eccles-Jordan)
- Efficiency, cathode, 3
- plate-circuit (*see* Plate-circuit efficiency)
- rectification, 274
- tuned circuit transfer, 216
- Electric arc (*see* Arc)
- Electrical discharge in gases, 27*ff.*
- arc (*see* Arc)
- breakdown, 27
- Electrical discharge in gases, glow (*see* Glow discharge)
- Electrometer (*see* Ammeters, electronic tubes for, 481)
- Electron, secondary (*see* Secondary emission)
- Electron-coupled oscillator (*see* Oscillators, electron-coupled)
- Electron-current density, drift, 11
- Electron emission, bombardment, 7
- photoelectric (*see* Photoelectric emission)
- secondary (*see* Secondary emission)
- thermionic (*see* Thermionic emission)
- Electron tubes (*see* Diode; Pentode; Tetrode; Thyratrons; Triode)
- classification of, 9*ff.*
- Electronic computer circuits, 146*ff.*
- adding, 148
- difference, 146
- difference of squares, 153
- differentiating, 129, 161
- dividing, 154
- integrating, 129, 158
- multiplying, 152
- square root, 154
- squaring, 150
- Electronic instruments, ammeter (*see* Ammeters, electronic)
- frequency (*see* Frequency meter)
- phase (*see* Phasemeter)
- power (*see* Wattmeter)
- voltmeter (*see* Vacuum-tube voltmeter)
- Electrostatic deflection in cathode-ray tubes (*see* Cathode-ray tube)
- Emission, electron (*see* Electron emission)
- Equivalent circuit, linear class A, 43*ff.*
- analytical derivation of, 43
- applicability, 44
- current source, 47
- interelectrode capacitance, effect of, 58
- pentode, 63
- push-pull, 180
- tetrode, 62
- voltage source, 43
- Excitation voltage, in amplifiers, a-c d-c components, 40
- multistage, 70
- push-pull, 178
- thyratrons, 282

## F

- Feedback, in amplifiers, 81*ff.*  
 effect of, on distortion, 84  
   on output impedance, 88  
 gain, 83  
 negative, 81  
 positive, 81  
 circuits, 85*ff.*, 155  
 compound, 87  
 current, 85  
 and stability in amplifiers, 89  
   criterion for oscillation, 90  
   (See also Oscillators, feed-back)  
 voltage, 86
- Feed-back factor, 82
- Feed-back oscillators (see Oscillators, feed-back)
- Feed-back ratio, complex, 246
- Field emission, 7
- Filament (see Thermionic cathodes)
- Filament voltage, 64
- Filter, capacitor input, 296  
   cutin in, 297  
   cutout in, 297  
   effect on inverse peak voltage, 300  
   peak tube current with, 297  
   ripple, 300  
 choke input, 293  
   cutout in, 294  
   ripple, 295  
 controlled rectifier, 304  
 decoupling, in amplifiers, 65  
 L-section, 300  
   bleeder resistance, 303  
   critical inductance, 302  
   cutout, 302  
   ripple, 301  
   swinging choke, 303  
 multiple L-section, 304  
 pi-section, 305
- Flash-back voltage, 36
- Focusing electrodes in beam tubes, 26
- Forward voltage rating, rectifiers, 36
- Fourier series, amplifier output, push-pull, 179  
   single tube, 49  
 rectifier output, single-phase, full-wave, 293  
   half-wave, 293
- Frequencies, half-power, 72, 74, 195  
   mid-frequency range, 71  
   side band, in amplitude-modulated wave, 322  
   in frequency-modulated wave, 366  
   video, 95
- Frequency, angular, instantaneous, 364  
 carrier, 321  
 division, blocking oscillator, 412  
   multivibrator, 409  
   scaling circuits, 420  
 mid-band, 71  
 modulation (see Modulation, frequency)  
 threshold, 5
- Frequency characteristic, 74, 80  
 with inverse feedback, 81
- Frequency conversion, 358
- Frequency converter tubes, 360
- Frequency distortion, description, 54  
 inductance-capacitance coupled amplifier, 76  
 resistance-capacitance coupled, 74  
 transformer-coupled, 80  
 tuned power, 213*ff.*  
 tuned voltage, 192*ff.*  
 video, 98
- Frequency doubler, 243
- Frequency measurement, with oscilloscope, 486  
 frequency meter (see Frequency meter, electronic)
- Frequency meter, electronic, 487
- Frequency-modulated oscillator (see Oscillators, frequency-modulated)
- Frequency modulation (see Modulation, frequency)
- Frequency modulation detection (see Detection, for frequency-modulated waves)
- Frequency modulation receivers (see Receiver, frequency modulation)
- Frequency response, 74  
 extension of, in amplifiers, 95*ff.*
- Frequency stability of oscillators (see Oscillators, stabilization)
- Frequency translation (see Detection; Modulation)
- Full-wave rectification (see Rectifiers)

## G

- Gain, voltage (*see* Amplifier, voltage-gain)
- Gain-band width product, 206
- Gas amplification, mechanism, 7
  - phototube, 6
- Gas diodes, 30
- Gas phototubes, 6
- Gaseous conduction (*see* Electrical discharge in gases)
- Gate circuits, a-c coupled, 414
  - cathode-coupled, 416
  - d-c coupled, 415
  - pentode, 418
 (*See also* Delay, generation of time)
- Glow discharge, 27
- Glow tubes, diodes, 29
  - triodes, 30
- Graphical determination of Fourier components, 49
- Grid, control, definition of, 14
  - cold-cathode triode, 30
  - grid control curves, 16
  - in high-vacuum tubes, control of current, 14
    - heating of, 15, 218
    - nonuniform, 25
  - screen, 18,
  - suppressor, 24
  - in thyatron, 32
- Grid-bias modulation (*see* Modulation, grid-bias)
- Grid-bias voltage, 64
  - self-bias, 64
- Grid control curves, thyatron, 33
- Grid current, causes, of, 15, 218
  - class B amplifier, 218
  - class C amplifier, 226
  - electrometer, effects in, 480
  - oscillators, 249
  - thyatrons, 34
- Grid driving power, class C amplifiers, 230
- Grid glow tube, 30
- Grid leak and capacitor bias voltage, 249
  - build up of, 249
  - effect on oscillator stability of, 250
- Grid-plate transconductance, 17
- Grid voltage, bias, 64
  - (*See also* Self-bias)

- Grid voltage, cutoff, 53, 216
- Grounded-grid amplifier (*see* Amplifier, grounded-grid)

## H

- Harmonic distortion (*see* Nonlinear distortion)
- Harmonic generation, in linear detector, 355
  - in modulation, 327
  - multivibrator, 395
  - in square-law detection, 345
- Harmonics (*see* Fourier series; Nonlinear distortion)
- Hartley oscillator (*see* Oscillators, feedback)
- Heat-shielded cathodes, 4
- Heptode, 25
- Hexode, 25
- High field emission, 7
- High-level modulation (*see* Modulation, high-level)
- High-pressure arcs, 31

## I

- Ignitor rod, 34
- Ignitron rectifier, 35
- Image force, 2
- Impedance matching, 168
  - by transformer, 170
- Impedance-stabilized oscillator (*see* Oscillators, stabilization of, impedance)
- Inductance, for filters, 293
  - critical in L-section filters, 302
  - leakage, 79
  - primary of transformer, 77
  - swinging choke, 303
- Inductance-capacitance coupled amplifier, 75
- Input admittance, pentode, 63
  - tetrode, 62
  - triodes, 60
- Input capacitance of amplifiers, 70
  - effect on operation, 73
- Input resistance of triodes, 61
  - negative, conditions for, 61
- Input volts (*see* Excitation voltage)

- Instantaneous amplitude, 320  
 Instantaneous angular frequency, 320, 364  
 Instantaneous phase, 320, 364  
 Insulation stress in transformers, 274, 277, 280  
 Integrating amplifier, 158, 427  
 Integrating circuits, 128  
 Interelectrode capacitance, 58*ff.*  
   in the cathode follower, 103  
   effect of, on input admittance, 60  
   equivalent circuit including, 59  
   numerical values for several tubes, 492*ff.*  
   pentode, 63  
   reduction of, by screen grid, 21  
   tetrode, 62  
 Intermediate frequency, 358  
 Inverse feedback (*see* Feedback, in amplifiers, negative)  
 Inverse peak voltage rating, bridge circuit, 280  
   single-phase, full-wave circuit, 277  
   single-phase, half-wave circuit, 274  
   with capacitor input filter, 300  
   voltage doubler, 280  
 Inverted amplifier, 122  
 Inward radiating cathodes, 4  
 Ionization, description, 7  
   by electron bombardment, 7  
   in gas phototubes, 6  
   photoelectric, 7  
   in plasmas, 28  
   by positive ions, 7, 28  
 Ionization time, 36  
 Ions, 7  
   function in gaseous conduction, 27  
   in glow discharge cathode fall space, 28  
   in plasma, 28
- K
- Kinetic energy, electrons and electron velocity, 11  
 Konal metal, 3
- L
- L-section filter, 300  
 Langmuir-Child's law, 11  
   (*See also* Space-charge limited current)
- Leakage reactance (*see* Reactance, transformer, leakage)  
 Limiter, amplitude, 123*ff.*  
   diode, 123  
   in frequency modulation receivers, 286  
   grid, 126  
   plate, 127  
 Line-controlled pulse generator (*see* Pulse generation, line-controlled)  
 Linear amplifier, class A, 48  
   class B, 216  
 Linear delay circuits (*see* Delay, generation of time)  
 Linear detector (*see* Detector, linear)  
 Lissajous pattern, for measurement of frequency, 486  
   for measurement of phase, 482  
 Load line, nonlinear in push-pull amplifier, 185  
   pentode amplifier circuit, 176  
   rectifier, single-phase, half-wave, 272  
   triode amplifier circuit, 41  
 Load resistance, choice in pentodes, 176  
   class A amplifier, 41  
   maximum power output, 168, 173  
   matching, 170  
   push-pull amplifier, 181  
 Local oscillators (*see* Converter; Mixer)  
 Low-level modulation (*see* Modulation, low-level)
- M
- Magnetic deflection in cathode-ray tubes, 460  
 Master oscillator (*see* Oscillators, master)  
 Maximal flatness, 98  
 Maximum power output, class A amplifier, 168, 172  
   push-pull connection, 186  
   from linear modulator, 330  
   undistorted, 172  
 Mercury, vapor pressure of, 30  
 Mercury-arc rectifier, arc back, 36  
   arc drop, 27  
   cathode disintegration, 31  
   evaporation of mercury, 30  
   flash-back voltage, as function of temperature, 36  
   ratings of, average current, 35  
   forward voltage, 35

- Mercury-arc rectifier, ratings of, inverse voltage, 35  
 surge current, 36  
 vapor pressure in, 30  
 (*See also* Rectifiers; Thyratrons; Controlled rectifiers)
- Metals, image force, 2  
 secondary emission, 6  
 thermionic emission, 2  
 work function, 3
- Miller integrating circuit, 427
- Millman network theorem, 489
- Misch metal, 29
- Mixer, 357
- Mixing (*see* Conversion)
- Modulated wave, components of, amplitude-modulated, 322  
 frequency-modulated, 366  
 envelope of, 323
- Modulation, amplitude, 320*ff.*  
 definition of, 320  
 expression for, 320  
 frequency spectrum for, 322  
 linear, 327  
 modulation characteristic for, 327  
 side bands in, 322  
 sinor representation of, 322  
 square-law, 323
- angular, 364  
 instantaneous frequency, 364  
 carrier suppression of, 325  
 cathode, 337  
 defined, 320  
 frequency, 363*ff.*  
 characteristics of, 364  
 comparison with phase modulation, 372  
 definition of, 363  
 deviation ratio for, 366  
 expression for, 366  
 frequency deviation in, 366  
 narrow band, 381  
 spectrum of, 366  
 wide band, 373
- frequency translation by, 320  
 grid-bias, 332  
 advantages of, 336  
 high-level, 327  
 index, 321  
 low-level, 325
- Modulation, percentage, 321  
 phase, 371*ff.*  
 comparison with frequency modulation, 372  
 definition of, 371  
 expression for, 372  
 plate, 327  
 advantages of, 332  
 process of, 320  
 side bands in, 322  
 single side band, 357  
 sinor representation of, 322  
 square-law, 323  
 suppressor grid, 337  
 transformer for, 331  
 types of, 321  
 van der Bijl, 323
- Modulation characteristics, 328
- Modulation factor, 321
- Modulation frequency, 321
- Modulator, amplitude, 320*ff.*  
 amplifier as, 327  
 balanced, 325  
 van der Bijl, 323  
 frequency, 363*ff.*  
 Armstrong method, 381  
 phasitron, 384  
 reactance tube, 373  
 phase, 371  
 single side band, 357  
 suppressed carrier, 326, 357  
 (*See also* Modulation)
- Multielectrode tubes, 18*ff.*  
 (*See also* Beam power tubes; Pentode; Tetrode; Thyratrons, shield-grid)
- Multiple L-section filters, 304
- Multiplication in high-vacuum tubes, 152  
 frequency, 243  
 voltage, 280
- Multiplier, circuits for frequency, 243  
 voltage, 280
- Multistage amplifiers, 68*ff.*, 204
- Multivibrators (*see* Oscillators, relaxation)  
 one-shot (*see* Gate circuits)
- Mutual characteristics, 17
- Mutual conductance, 17  
 measurement of, 46  
 numerical values of several tubes, 492*ff.*

## N

- Negative feedback (*see* Feedback, in amplifiers, negative)
- Negative input resistance of amplifiers, 61, 262
- Negative plate resistance in tetrodes, 22, 263
- Negative-resistance oscillator (*see* Oscillators, negative-resistance)
- Negative-transconductance oscillator (*see* Oscillators, transitron)
- Network theorem, Millman, 489
- Neutralization, electron space charge, 29 in amplifiers, 239
- Nonlinear circuit element as modulator, 343
  - as rectifier, 271*ff.*
- Nonlinear distortion, description, 48*ff.*, 54
  - distortion factor, 50
  - effect of feedback on, 84
  - five-point schedule, 50
  - general dynamic curve, 48
  - grid current, cause of, 126
  - parabolic dynamic curve, 50
  - push-pull amplifiers, 185
- Nonlinearity and oscillator stability, 246
- Normal current density, 28
- Normal glow discharge, 28

## O

- On-off control of thyratrons, 287
- Operating point, 41
- Oscillation, in amplifiers, 82
  - Barkhausen criterion for, 246
  - Nyquist criterion for, 90
- Oscillators, 244*ff.*
  - amplitude stability of, 258
  - automatic amplitude control of, 258, 261
  - basic circuits, 253
  - class A, 258
  - classification of, 244
  - Colpitts, 253
  - crystal-controlled, 256
    - circuits for, 257, 269
    - equivalent circuit of, 257
    - stability of, 258

- Oscillators, dynatron, 262
  - electron-coupled, 254
  - feed-back, 244*ff.*
    - self-excitation in, 244
  - Franklin, 267
  - frequency-modulated, 373*ff.*
  - frequency stability of, 254
  - grid bias in, 249
  - Hartley, 253
  - intermittent operation of, 250
  - local (*see* Converter, Mixer)
  - master, 254
  - multivibrator, 396
  - negative-resistance, 262
  - negative-transconductance, 263
  - nonlinearity and stabilization, 247
  - phase-shift, 262
  - power, 251
  - relaxation, 395*ff.*
    - blocking, 404
    - synchronization of, 411
  - gas diode, 443
  - gas triode, 444
  - multivibrator, 296
    - biased plate coupled, 400
    - cathode-coupled, 402
    - pentodes in, 403
    - period of, 399
    - plate-coupled, 396
    - pentode, van der Pol, 406
    - synchronization of, sine wave, 409
    - pulse, 408
  - resistance-capacitance tuned, 259
  - resistance-stabilized, 255
  - self-starting of, 248
  - square-wave, 396
  - stabilization of, amplitude, 254
    - impedance, 255
    - resistance, 255
  - transitron, 264
  - tuned-grid, 253
  - tuned-grid-tuned-plate, 253
  - tuned-plate, 250
    - frequency of oscillation in, 252
    - self-excitation in, 251
    - sinor diagram for, 252
- Wien bridge, 261
- Oscilloscope as frequency meter, 486
  - as phase meter, 481
  - as voltmeter, 473

- Output impedance, 88  
 anode follower, 109  
 cathode follower, 107  
 effect of feedback on, 89
- Output voltage of amplifier (*see* Amplifier, voltage-gain)
- Oxide-coated cathodes, 4  
 disintegration, 31  
 work function, 3
- P
- Parallel feed amplifiers, 170
- Paraphase amplifiers, 187
- Peak inverse voltage rating (*see* Inverse peak voltage rating)
- Peaking circuits, 128*ff*
- Pentode, 24*ff*.  
 in class A amplifier, 176  
 in class B a-f amplifier, 184  
 distortion in, 25  
 equivalent circuit for, 63  
 input admittance of, 63  
 interelectrode capacitances in, 63  
 load resistance for, 177  
 modulation with, 337  
 plate characteristics of, 24  
 power, 176  
 remote cutoff, 25  
 in tuned amplifier, 192  
 voltage gain with, 63
- Phase characteristic, 74
- Phase distortion, 54
- Phase inverter, 187
- Phase modulation (*see* Modulation, phase)
- Phase relations, amplifier, 42, 74  
 thyratron, 285
- Phase-shift characteristics of tuned amplifier, 196
- Phase-shift control, ignitron, 288
- Phase-shift distortion (*see* Phase distortion)
- Phasemeter, electronic, 483
- Photocells (*see* Phototubes)
- Photoelectric emission, 4*ff*.  
 gas amplification, 6
- Phototubes, vacuum, 5  
 gas-filled, 6  
 volt-ampere curve, 5
- Pi-section filters, 305
- Piezoelectric crystals in oscillators, 256
- Plasma, description of, 28
- Plate characteristics, 492*ff*.  
 (*See also* Characteristic tube curves)
- Plate-circuit efficiency, amplifier, class A, 174  
 class B, tuned, 221  
 untuned  
 class C, tuned, 229
- Plate current, average value of, 226  
 total differential of, 17
- Plate dissipation, 174  
 in class C amplifier, 229  
 during modulation, 331, 335  
 permissible, 222  
 in tuned class B amplifier, 221  
 late efficiency, amplifier, class A, 174  
 series-fed, 175  
 shunt-fed, 176  
 tuned class B, 221  
 tuned class C, and operating angle, 233
- Plate modulation (*see* Modulation, plate)
- Plate resistance, diode, 273  
 measurement of, 46  
 negative, in tetrodes, 22, 263  
 numerical values of several tubes, 492*ff*.  
 push-pull amplifiers, 186  
 tetrode, 23  
 triodes, 17, 47  
 variable nature of, 18
- Plate-plate resistance, 186
- Polar diagram of feed-back amplifier, 89
- Positive feedback, 81
- Positive ion bombardment, 7, 28
- Positive ion current, 7, 27
- Positive ions (*see* Ions)
- Potential, breakdown (sparking), 28
- Potential distribution, 10, 27  
 glow discharge, 27  
 parallel-plane diode, space-charge flow, 10  
 in plasma, 27
- Power, rectifier, output, 273  
 input, 274  
 maximum (*see* Maximum power output)
- Power amplifiers (*see* Amplifier, power)
- Power oscillator (*see* Oscillators, power)
- Power sensitivity, 55
- Power series, 48

- Power supply, voltage-regulated, 306*ff.*  
 glow-tube, 306  
 series vacuum-tube, 308  
 electronically regulated, 309  
 output resistance, 312  
 stabilization ratio, 311
- PPI presentation, 470
- Predistorter in frequency modulation, 383
- Preemphasis of high frequencies, 377
- Pressure, mercury, as function of temperature, 30
- Pulse generation, 434*ff.*  
 by differentiation (*see* Peaking circuits)  
 with gas tubes, 435  
 line-controlled, 436
- Push-pull amplifier, class A, 178*ff.*  
 circuit, 178  
 composite dynamic characteristic of, 184  
 composite static-characteristic curves, 181  
 distortion in, 185  
 equivalent circuit, 180  
 harmonics in, 185  
 plate-plate resistance, 180  
 power output, 185  
 class B, 186  
 driver stages for, 187  
 single-tube paraphase, 187  
 two-tube paraphase, 117, 187
- Q
- Q point, 41
- Quadrupler, voltage, 281
- Quiescent point, 41
- R
- Radio communication, amplitude modulation, 320  
 frequency modulation, 386  
 modulation essential for, 320  
 single side band, 357
- Radio frequency amplifiers (*see* Tuned amplifiers)
- Reactance, primary, effect on amplifier operation, 77  
 transformer, leakage, effect on amplifier operation, 79
- Reactance tube, 373
- Receiver, automatic volume control in, 355  
 band width in  
 for amplitude-modulated waves, 212  
 for frequency-modulated waves, 386  
 frequency modulation, 386  
 discriminator, 387  
 limiter, 386  
 selectivity of, 192, 206  
 single side band, 357  
 superheterodyne, 362  
 tracking of, 359  
 volume control in, 355
- Recombination, ions, 28
- Rectification, definition of, 271
- Rectification characteristics, 353
- Rectifier filters (*see* Filter, rectifier)
- Rectifier meter, 280
- Rectifiers, circuits, bridge, 279  
 full-wave single-phase, 276  
 gas tubes, 277  
 half-wave, single-phase, 271  
 voltage-doubling, 280  
 voltage-quadrupling, 281  
 controlled types (*see* Controlled rectifiers)
- Rectigon tube, 31
- Reflected resistance, 170
- Regeneration, in amplifiers (*see* Feedback, positive)
- Regulation, voltage (*see* Power supply)
- Regulators, electronic (*see* Power supply, electronically regulated)  
 glow-tube, 306
- Relaxation oscillator (*see* Oscillators, relaxation)
- Remote-cutoff tubes, 25
- Resistance, bleeder, 303  
 grid, for high-vacuum tubes, 39  
 input, of tubes, 61  
 load (*see* Load resistance)  
 negative (*see* Dynatron)  
 plate (*see* Plate resistance)  
 multielectrode tubes, 21  
 numerical values for several tubes, 492*ff.*  
 triode, 18  
 plate-plate (*see* Push-pull amplifier; Plate-plate resistance)  
 reflected, 170

- Resistance-capacitance coupled amplifier, 68*ff.*  
 applicability of, 68  
 feedback in, 88  
 frequency characteristic, 74  
 gain of, high-frequency, 73  
 low-frequency, 71  
 mid-frequency, 71  
 half-power frequency, 72, 73  
 extending (*see* Amplifier, broad-band, compensated)  
 universal amplification curve, 74
- Resistance-capacitance tuned oscillator (*see* Oscillators, resistance-capacitance tuned)
- Resistance-coupled amplifiers, 112  
 (*See also* Amplifier, direct-coupled, resistance-coupled)
- Resistance-stabilized oscillator (*see* Oscillators, stabilization of, resistance)
- Resonance, parallel, 194  
 transformer-coupled circuit, 196  
 universal resonance curve, 196
- Ripple factor, capacitor filter, 300  
 definition, 275  
 with electronic regulators, 315  
 full-wave circuit, 277  
 half-wave circuit, gas tube, 279  
 vacuum tube, 276  
 inductance filter, full-wave, 295  
 half-wave, 294  
 L-section filter, 301  
 multiple L-section filter, 305  
 pi-section filter, 305
- S
- Saturation, in phototubes, 4  
 in screen-grid tubes, 21  
 space charge limited current, 11  
 temperature limited current, 2  
 tungsten filament, 3
- Saw-tooth generators (*see* Sweep generators)
- Scaler circuits, with trigger circuits, 422  
 ring counter circuits, 423
- Schedule method in Fourier analysis, 49
- Screen grid in tubes, 18
- Screen-grid tubes (*see* Tetrode)
- Screen supply voltage, 65
- Second harmonic, in rectifiers (*see* Ripple factor)  
 in tubes (*see* Nonlinear distortion)
- Secondary emission, 6  
 by ion bombardment, 6  
 suppression, in beam tubes, 27  
 in pentodes, 24  
 in tetrodes, 22
- Self-bias in amplifiers, 64  
 feedback through, 64  
 in push-pull amplifiers, 179
- Semigraphical analysis, class B and class C amplifiers, 223
- Series, Fourier (*see* Fourier series)  
 power (*see* Power series)  
 Taylor (*see* Taylor series)
- Shield-grid thyatrons, 34
- Shunt-feed amplifiers, 76
- Shunt peaking in amplifiers (*see* Amplifier, broad-band, compensated)
- Side bands, amplitude modulation, 322  
 separation of, from carrier, 357  
 frequency modulation, 366
- Side frequencies, detection of (*see* Detection)  
 for frequency modulation, 366  
 receivers for (*see* Receiver)  
 separation of carrier from, 325
- Signal voltage (*see* Excitation voltage)
- Sources of electrons, 1  
 (*See also* Electron emission)
- Space charge, cloud, 9  
 in glow discharge, 28  
 limitation of current by (*see* Space-charge limited current)  
 in plasma, 28  
 positive ions neutralize, 29
- Space-charge flow (*see* Space-charge limited current)
- Space-charge limited current, factors influencing, 11  
 parallel planes, current between, 9*ff.*  
 three-halves-power dependence, 11
- Sparking potential, 27
- Square-law modulation (*see* Modulation, square-law)
- Stability of oscillators, amplitude, 254  
 frequency, 379  
 reactance-tube, 379
- Stabilization of amplifiers by feedback, 88
- Stage, driver, 187

- Stagger-tuned amplifier (*see* Tuned amplifiers, stagger-tuned)
- Starter probe, 34
- Static characteristics (*see* Plate characteristics)
- Supercontrol tubes, 25
- Superheterodyne (*see* Receiver, superheterodyne)
- Suppression of carrier wave, 325
- Suppressor grid modulation, 337
- Surge current rating, 12
- Sweep generators, for cathode-ray tubes,
  - capacitive, 443
  - characteristics of, 442
  - electrostatic deflection, 442*ff.*
  - free-running, synchronization of, 445
  - thyratrons in, 444
  - vacuum tubes in, 446
- linearizing methods, auxiliary time constant, 450
- constant-current generator, 448
  - feedback, 451
  - high-voltage charging, 448
  - inverse curvature, 450
- push-pull, 452*ff.*
- (*See also* Push-pull amplifier, driver stages for)
- triggered, 447
- circular, 468
- electromagnetic deflection, 460*ff.*
- characteristics of, 460
  - effects of distributed capacitance in, 465
- linearizing methods, exponential, 460
- feedback, 466
  - oscillatory, 461
  - trapezoidal, 462
- rotating radial (PPI), 470
- Swinging chokes for filters, 303
- Synchronization of blocking oscillators, 411
- multivibrators, 408
- T
- Tank circuits for tuned power amplifier, 214
- Taylor series, for triode, 151
- (*See also* Power series)
- Temperature, anodes in diodes, 36, 174
- arc cathodes, 31
  - glass envelope of tubes, 13
  - mercury pressure, 30
  - rating of diodes, 12, 35
  - thermionic cathodes, 3
- Temperature limited current, 11
- Tetrode, 18
- (*See also* Beam power tubes)
- coefficients of, 23
  - disadvantages of, 24
  - equivalent circuit for, 62
  - gas (*see* Thyratrons, shield-grid)
  - input admittance, 62
  - interelectrode capacitances in, 62
  - modulation with, 337
  - mutual conductance of, 23
  - negative resistance in, 22
  - plate characteristic of, 22
  - screen-grid, 22
  - secondary emission, 22
- Thermionic cathodes, carbonization, 3
- directly heated, 4
  - efficiency, 3
  - heat-shielded, 4
  - indirectly heated, 4
  - oxide-coated, 3
- (*See also* Oxide-coated cathodes)
- temperature of, 3
  - thoriated-tungsten, 3
- Thermionic emission, 2*ff.*
- constants of ( $A_0$ ,  $b_0$ ,  $E_w$ ), 2
  - Dushman equation of, 2
  - efficiency of, 3
  - power for heating cathodes, 64
  - saturation, 2
  - work function, 3
- (*See also* Work function)
- Third harmonic (*see* Nonlinear distortion)
- Thoriated-tungsten cathodes, 3
- Three-halves-power law (*see* Space-charge limited current)
- Threshold frequency, 5
- Threshold wave length, 5
- Thyratrons, 32*ff.*
- argon-filled, 33
  - cathode for, 4
- (*See also* Oxide-coated cathodes)
- cathode-ray oscilloscope sweep circuit, use in, 444

- Thyratrons, control of average current, 282  
 critical grid control curves, 32  
 cutin, 281  
 deionization time, 36  
 filters for use with, 304  
 grid glow tube, 30  
 ignitron controlled by, 289  
 ionization time of, 36  
 mercury vapor pressure in, 30  
 positive control tubes, 33  
 pulse generators, use in, 435  
   line-controlled, 438  
 shield-grid, 34  
 tube drop, 282
- Time, deionization, 36
- Time delay, generation of (*see* Delay, generation of time)  
 in amplifiers, 54
- Transconductance, grid-plate (*see* Mutual conductance)
- Transfer characteristic (*see* Mutual characteristics)
- Transformer, interstage, 76  
 capacitances in, 77  
 output, push-pull, 180  
 r-f air core, 192
- Transformer-coupled amplifiers, 76*ff.*  
 gain, high-frequency, 79  
   low-frequency, 78  
   mid-frequency, 77  
 impedance matching, 170  
 push-pull amplifier, 178  
 tuned, in amplifiers (*see* Tuned amplifiers, class A, single-tuned, transformer coupled)
- Transformer insulation stress, full-wave rectifier, 277  
 half-wave rectifier, 274
- Transformers as impedance matching devices, 170
- Translation, frequency, by modulation (*see* Modulation, frequency translation by)
- Transmission line, pulse generators, 436
- Transmitters, amplitude-modulated, 340  
 frequency-modulated, 373, 381  
   using phase-shift modulators, 381  
   using reactance-tube modulators, 373  
 stabilization of, 379
- Trapezium distortion in cathode-ray tubes, 453
- Trigger circuits, 419*ff.*  
 Eccles-Jordan, 419  
 pentode, 422  
 scale-of-two, 420  
 pentodes in, 421
- Triode, gas (*see* Thyratrons)  
 vacuum, 14*ff.*  
 amplification factor (*see* Amplification factor)  
 characteristic curves (*see* Characteristic tube curves)  
 coefficients of, 18  
 grid current in, 15  
   (*See also* Grid current)  
 grid heating in, 231  
 input admittance of, 60  
 interelectrode capacitances in, 58  
 mutual characteristics, 16  
 mutual conductance (*see* Mutual conductance)  
 plate characteristics, 16  
 plate resistance of, 17  
 space charge in, 15  
 square-law detection with, 343  
 square-law modulation with, 323  
 Taylor series for, 17
- Tube constants, multielectrode tubes, 23  
 relation among, 24  
 triodes, 18
- Tube drop, in arcs, 28  
 in glow tubes, 28
- Tubes (*see* Characteristic tube curves)
- Tuned amplifiers, class A, 192*ff.*  
 coupling in, 192  
 distortion in, 192  
 double-tuned, 199*ff.*  
   band width, 204  
   cascade, 205  
     band-width reduction, 206  
   gain, 200  
   gain-band-width product, 206  
   maximal flatness in, 201  
   transitional coupling in, 203  
 single-tuned, 192*ff.*  
 cascade, 204  
   band-width reduction factor, 205  
 direct-coupled, 193  
   band width, 195

- Tuned amplifiers, class A, single-tuned,  
 direct-coupled, gain, 194  
 gain-band-width product, 206  
 transformer-coupled, 196  
 band width, 198  
 gain, 197  
 optimum coupling in, 197  
 stagger-tuned, 207*ff.*  
 comparison with double-tuned,  
 208
- class B power, 216*ff.*  
 analysis tabulation for, 229  
 analytical treatment of, 219  
 applications of, 213  
 optimum conditions in, 222  
 phase relations in, 218  
 semigraphical analysis for, 229
- class C power, 223*ff.*  
 analysis tabulation for, 229  
 approximate analytical solution, 234  
 cathode-modulated, 337  
 conditions in, for high efficiency, 233  
 design considerations for, 231  
 grid-bias modulated, 332  
 grid current in, 226  
 grid driving power in, 230  
 plate current in, 226  
 plate dissipation in, 230  
 plate efficiency of, 229  
 plate modulation of, 327  
 Q of load for, 213  
 semigraphical analysis for, 223
- neutralization, grid, 239  
 plate, 239
- Tuned circuits, class B and class C ampli-  
 fiers, 213  
 half-power frequencies in, 196  
 in oscillators, 248  
 single-tuned, direct-coupled, 193  
 single-tuned, transformer-coupled, 196  
 double-tuned, 199
- Tuned-grid oscillator (*see* Oscillators,  
 tuned-grid)
- Tuned-grid-tuned-plate oscillator (*see*  
 Oscillators, tuned-grid-tuned plate)
- Tuned-plate oscillator (*see* Oscillators,  
 tuned-plate)
- Tuned power amplifier (*see* Tuned ampli-  
 fiers, class B power; Tuned amplifier,  
 class C power)
- Tungar tubes, 31
- Tungsten, filaments, 3  
 work function, 3
- U
- Universal resonance curve, 196
- V
- Vacuum-tube voltmeter, 473*ff.*  
 average, 476  
 d-c, 479  
 logarithmic, 479  
 peak, diode, 476  
 grid leak, 477  
 negative feedback, 478  
 slide back, 478  
 rms, 474
- Van der Bijl modulation, 323
- Variable-mu tube, 25
- Video amplifier (*see* Amplifier, broad-  
 band, compensated)
- Volt-ampere characteristics (*see* Char-  
 acteristic tube curves)
- Voltage, disintegration, 31
- Voltage comparator, 430, 434
- Voltage-doubling rectifier, 280
- Voltage gain, cascade amplifier, 70  
 decibels of, 56  
 with feedback, 83  
 (*See also* Amplifier, voltage-gain)
- Voltage-quadrupling rectifier, 281
- Voltage-regulated power supplies (*see*  
 Power supply, voltage-regulated)
- Voltage-source equivalent circuit, 43
- Voltmeter, vacuum-tube (*see* Vacuum-  
 tube voltmeter)
- W
- Wattmeter, electronic, 488
- Wave length, threshold, 5
- Wide-band amplifiers (*see* Amplifier,  
 broad-band; Tuned amplifiers)
- Work function, 2  
 definition, 2  
 Dushman equation involving, 2  
 oxide-coated cathodes, 3  
 photoelectric emission, 5  
 table of values, 3  
 thoriated tungsten, 3  
 tungsten, 3

